

Alice Johnson

# Synthesis and Properties of Novel Organogold Complexes: Ylide, Allenyl, N-Heterocyclic Carbene and Propargyl Derivatives

Departamento  
Química Orgánica

Director/es  
Gimeno Floría, M<sup>a</sup> Concepción

<http://zaguan.unizar.es/collection/Tesis>



Reconocimiento – NoComercial – SinObraDerivada (by-nc-nd): No se permite un uso comercial de la obra original ni la generación de obras derivadas.

© Universidad de Zaragoza  
Servicio de Publicaciones

ISSN 2254-7606



**Universidad**  
Zaragoza

Tesis Doctoral

SYNTHESIS AND PROPERTIES OF NOVEL  
ORGANO GOLD COMPLEXES: YLIDE, ALLENYL, N-  
HETEROCYCLIC CARBENE AND PROPARGYL  
DERIVATIVES

Autor

Alice Johnson

Director/es

Gimeno Floría, M<sup>a</sup> Concepción

**UNIVERSIDAD DE ZARAGOZA**

Química Orgánica

2018





Universidad de Zaragoza  
Departamento de Química Inorgánica

**SYNTHESIS AND PROPERTIES OF  
NOVEL ORGANOGOLD COMPLEXES:  
YLIDE, ALLENYL, N-HETEROCYCLIC CARBENE  
AND PROPARGYL DERIVATIVES**

Memoria Presentada para acceder al título de Doctor por

**Alice Johnson**

Zaragoza, 2017



***María Concepción Gimeno Floría***, Profesor de Investigación de Organismo Público de Investigación (Consejo Superior de Investigaciones Científicas) en el Instituto Universitario de Investigación mixto de Síntesis Química y Catálisis Homogénea (ISQCH)

HACE CONSTAR:

Que la presente memoria titulada “*Synthesis and Properties of Novel Organogold Complexes: Ylide, Allenyl, N-Heterocyclic Carbene and Propargyl Derivatives*” ha sido desarrollado en el Departamento de Química Inorgánica de la Facultad de Ciencias de la Universidad de Zaragoza, y autoriza su presentación para que sea calificada como Tesis Doctoral.

Zaragoza, 7 de noviembre de 2017

Fdo. Prof. M. Concepción Gimeno



**Parts of this thesis have been published in the following journal articles:**

“Axially Chiral Allenyl Gold Complexes”

A. Johnson, M. Concepción Gimeno, A. Laguna

*J. Am. Chem. Soc.*, 2014, **136**, 12812–12815.

“An efficient and sustainable synthesis of NHC gold complexes”

A. Johnson, M. Concepción Gimeno

*Chem. Commun.*, 2016, **52**, 9664-9667.

“Synthesis of Propargyl-Functionalized NHC Gold Complexes”

A. Johnson, M. Concepción Gimeno

*Organometallics*, 2017, **36**, 1278-1286.



# Resumen

La investigación presentada en esta tesis doctoral se centra en la síntesis de complejos organometálicos de oro(I) y oro(III) con ligandos iluro de fosforo, alenilo, carbeno N-heterocíclico y propargilo y, también en el estudio de algunas propiedades de los compuestos como la luminiscencia y la actividad biológica.

Se describe la síntesis de derivados de oro(I) y de oro(III) a partir de la sal de fosfonio, cloruro de cianometiltrifenilfosfonio. Estos incluyen complejos mononucleares en los que la sal de fosfonio se ha desprotonado una vez para formar el iluro, permitiendo la coordinación a un centro metálico, y complejos polinucleares en los que la sal de fosfonio se desprotona dos veces para dar la unidad ildiuro que puede formar puente entre dos centros metálicos. También se describen complejos heterometálicos en los que hay un centro metálico adicional coordinado al átomo de nitrógeno del grupo nitrilo, que incluyen dos ejemplos luminiscentes que presentan emisiones fosforescentes a 77 K. Varios de los complejos muestran actividad antiproliferativa en la línea celular de cáncer de pulmón A549.

El bromuro de trifenilpropargilfosfonio sufre a una isomerización prototrópica al tautómero alenilo en disolución en varios disolventes, sin embargo, no se observa un tautomerismo análogo en las sales de amonio funcionalizadas con propargilo. Se describe la síntesis de complejos de oro con ligandos alenilo sin precedentes derivados del bromuro de trifenilpropargilfosfonio en el que se observa una regioselectividad que depende del estado de oxidación del oro. En los complejos de oro(I) se observa una coordinación del átomo de carbono  $\alpha$  al centro de oro, mientras que en los derivados de oro(III) una coordinación del átomo de carbono  $\gamma$  al centro metálico da lugar a complejos con una quiralidad axial inusual. También se describen derivados de oro(I) de sales de amonio funcionalizadas con propargilo, sin embargo, en estos complejos, la unidad de propargilo se mantiene y la coordinación al centro de oro se produce a través del átomo de carbono alquino terminal. Los complejos resultantes muestran actividad antiproliferativa en células A549. Los intentos de preparar un derivado de oro(I) de una sal de sulfonio funcionalizada con propargilo produjeron una mezcla de los complejos propargilo y alenilo de oro.

Se describe un nuevo método para la síntesis general de complejos de oro(I) NHC. La reacción de sales de imidazolio, con diferentes requerimientos estéricos y electrónicos, con derivados de  $[\text{AuX}(\text{tht})]$  (tht = tetrahidrotiofeno), en presencia de  $\text{NBu}_4$  (acac), al aire y a temperatura ambiente produce la especie de oro NHC con buenos rendimientos y tiempos de reacción muy cortos. Una serie de complejos de NHC oro(I) funcionalizados con propargilo se han sintetizado mediante este método, que incluyen los derivados  $[\text{AuBr}(\text{NHC})]$ ,  $[\text{Au}(\text{NHC})_2]\text{Br}$ ,  $[\text{Au}(\text{C}_6\text{F}_5)(\text{NHC})]$  y  $[\text{Au}(\text{NHC})(\text{PR}_3)]\text{BF}_4$ , y muchos ejemplos se han caracterizado por estudios de difracción de rayos-X de monocristal. Todos los complejos muestran actividad antiproliferativa en células A549, siendo los derivados de fosfina los más potentes. Estos complejos son también luminiscentes y presentan emisiones fosforescentes a temperatura ambiente y a 77 K.

Se describe la síntesis de complejos de propargilo oro(I) fosfina por dos métodos diferentes. Los complejos se han caracterizado estructuralmente por difracción de rayos-X de monocristal y en todos los casos se observa la coordinación del carbono alquino terminal de la unidad de propargilo al oro. También se describe un derivado heterometálico luminiscente dinuclear de oro(I) y cobre(I) que presenta emisiones fosforescentes a temperatura ambiente y a 77 K. Los complejos son activos en células A549 con el derivado heterometálico dinuclear mostrando la mejor actividad antiproliferativa.



# Abstract

The research presented in this PhD thesis concerns the synthesis of organometallic complexes of gold(I) and gold(III) with phosphorus ylide, allenyl, *N*-heterocyclic carbene and propargyl ligands. The luminescence and biological properties of the complexes are also reported.

The synthesis of gold(I) and gold(III) derivatives of the phosphonium salt, cyanomethyltriphenylphosphonium chloride, is described. These include mononuclear complexes in which the phosphonium salt has been deprotonated once to form the ylide, allowing coordination to one metal centre, and polynuclear complexes in which the phosphonium salt is deprotonated twice to give the ylide unit which can bridge two metal centres. Heterometallic complexes bearing an additional metal centre at the nitrogen atom of the nitrile group are also described, including two luminescent examples which exhibit phosphorescent emissions at 77 K. Several of the complexes exhibit antiproliferative activity in cancer cell line A549.

Triphenylpropargylphosphonium bromide undergoes a prototropic isomerisation to the allenyl tautomer in solution in several solvents, however, an analogous tautomerism is not observed in propargyl functionalised ammonium salts. The synthesis of unprecedented allenyl gold complexes derived from triphenylpropargylphosphonium bromide is described in which a regioselectivity is observed depending on the oxidation state of gold. In the gold(I) complexes a coordination of the  $\alpha$ -carbon atom to the gold centre is observed, whereas in the gold(III) derivatives a coordination of the  $\gamma$ -carbon atom to the metal centre results in highly unusual axially chiral complexes. Gold(I) derivatives of propargyl functionalised ammonium salts are also described, however in these complexes the propargyl unit is maintained and coordination to the gold centre occurs through the terminal alkyne carbon atom. The resulting complexes exhibit antiproliferative activity in A549 cells. Attempts to prepare a gold(I) derivative of a propargyl functionalised sulfonium salt led to a mixture of the propargyl and allenyl complexes.

A new method for the general synthesis of NHC gold(I) complexes is described. The reaction of imidazolium salts, of different steric and electronic requirements, with  $[\text{AuX}(\text{tht})]$  (tht =

tetrahydrothiophene) derivatives, in the presence of  $\text{NBu}_4(\text{acac})$ , in air and at room temperature leads to the NHC gold species in good yields and with very short reaction times. A series of propargyl functionalised NHC gold(I) complexes have been synthesised by this method, including  $[\text{AuBr}(\text{NHC})]$ ,  $[\text{Au}(\text{NHC})_2]\text{Br}$ ,  $[\text{Au}(\text{C}_6\text{F}_5)(\text{NHC})]$  and  $[\text{Au}(\text{NHC})(\text{PR}_3)]\text{BF}_4$  derivatives, and many examples have been characterised by single crystal X-ray diffraction studies. All of the complexes show antiproliferative activity in A549 cells with the phosphine derivatives being the most potent. These complexes are also luminescent, exhibiting phosphorescent emission at room temperature and at 77 K.

The synthesis of propargyl gold(I) phosphine complexes by two different methods is reported. The complexes were structurally characterised by single crystal X-ray diffraction and in all cases coordination of the terminal alkyne carbon of the propargyl unit to gold is observed. A luminescent heterometallic dinuclear gold(I) copper(I) derivative is also described which exhibits phosphorescent emissions at room temperature and at 77 K. The complexes were active in A549 cells with the dinuclear heterometallic derivative showing the best antiproliferative activity.

# Contents

Resumen.....	7
Abstract.....	9
Abbreviations.....	15
<b>Chapter 1 – General Introduction.....</b>	<b>19</b>
1.1. Gold.....	19
1.1.1. Relativistic Effects .....	19
1.1.2. History.....	23
1.2. Organogold Complexes .....	24
1.2.1. Basic Concepts.....	24
1.2.2. Early Work on Organogold Complexes.....	27
1.2.3. Organogold Complexes with Bridging Carbon Ligands .....	30
1.2.4. Recent Developments in Organogold Chemistry .....	32
1.3. Applications of Organogold Complexes.....	53
1.4. Objectives .....	54
1.4.1. Phosphorus Ylide Gold Complexes .....	54
1.4.2. Allenyl Gold Complexes.....	55
1.4.3. NHC Gold Complexes .....	56
1.4.4. Propargyl Gold Complexes.....	58
<b>Chapter 2 – Phosphorus Ylide Complexes .....</b>	<b>59</b>
2.1. Introduction.....	59
2.1.1. Basic Concepts.....	59
2.1.2. Phosphorus Ylides as Ligands .....	63
2.1.3. History.....	65
2.1.4. Triphenylphosphoniumcyanomethylide .....	69

## Contents

---

2.2. Synthesis of Starting Reagents.....	73
2.2.1. (Cyanomethyl)triphenylphosphonium Triflate .....	73
2.2.2. Triphenylphosphoniumcyanomethylide .....	74
2.3. Synthesis of Mononuclear Ylide Complexes.....	76
2.3.1. Neutral Gold(I) and Gold(III) Complexes .....	76
2.3.2. Cationic Complexes .....	83
2.3.3. Bis-Ylide Complexes .....	93
2.4. Synthesis of Polynuclear Yldiide Complexes.....	97
2.4.1. Anionic Complexes.....	97
2.4.2. Neutral Complexes.....	102
2.4.3. Cationic Complexes .....	105
2.4.4. Heterometallic Complexes with N Coordination.....	115
2.5. Luminescence .....	121
2.6. Biological Activity.....	123
2.7. Conclusions.....	128
2.8. Experimental.....	130
<b>Chapter 3 – Allenyl Gold Complexes .....</b>	<b>151</b>
3.1. Introduction.....	151
3.1.1. Allenes – Structure and Axial Chirality.....	151
3.1.2. History.....	152
3.1.3. Tautomerism in Allenyl Metal Complexes.....	158
3.1.4. Triphenylpropargyl Phosphonium Bromide .....	159
3.2. Propargyl Phosphonium Salts .....	162
3.2.1. Triphenylpropargylphosphonium bromide isomerism in solution .....	162
3.2.2. Triphenylpropargylphosphonium triflate.....	162
3.3. Allenyl Gold Complexes from Triphenylpropargylphosphonium Salts .....	166

---

3.3.1. Synthesis of Allenyl Gold Complexes .....	166
3.3.2. Influence of Steric and Electronic Properties .....	172
3.4. Propargyl Functionalised 1,1-Bis(diphenylphosphino)methane Derivatives .....	185
3.5. Propargyl Functionalised Ammonium Salt Derivatives .....	192
3.6. Propargyl Functionalised Sulfonium Salt Derivatives.....	197
3.7. Biological Activity.....	199
3.8. Conclusions.....	201
3.9. Experimental.....	203
<b>Chapter 4 – NHC Gold Complexes .....</b>	<b>221</b>
4.1. Introduction.....	221
4.1.1. Basic Concepts.....	221
4.1.2. History.....	224
4.1.3. Applications of NHC Gold Complexes .....	227
4.1.4. Synthetic Methods for the Preparation of NHC Gold Complexes.....	233
4.2. Synthesis of NHC Gold Complexes using Tetrabutylammonium Acetylacetonate ...	237
4.2.1. Synthesis of Tetrabutylammonium Acetylacetonate .....	237
4.2.2. Synthesis of NHC Gold Complexes using Tetrabutylammonium Acetylacetonate .....	238
4.3. Synthesis of Propargyl Functionalised Imidazolium Salts .....	245
4.4. Synthesis of Propargyl Functionalised NHC Gold Complexes .....	247
4.4.1. Synthesis of Bromo Derivatives .....	247
4.4.2. Synthesis of Bis-NHC Complexes.....	249
4.4.3. Synthesis of Pentafluorophenyl Derivatives .....	252
4.4.4. Synthesis of NHC Gold Phosphine Derivatives .....	254
4.4.5. Gold(III) Derivatives .....	264
4.4.6. Di-NHC Complexes.....	265

## Contents

---

4.5. Functionalisation of the Propargyl Unit.....	271
4.5.1. Dinuclear NHC Gold JohnPhos Derivatives.....	271
4.5.2. Formation of Trimers.....	273
4.5.3. Propargyl-Allenyl Tautomerism .....	276
4.6. Biological Activity.....	279
4.7. Luminescence .....	282
4.8. Conclusions.....	287
4.9. Experimental.....	289
<b>Chapter 5 – Propargyl Gold Complexes.....</b>	<b>333</b>
5.1. Introduction.....	333
5.1.1. History of Gold in Medicine .....	334
5.1.2. Mechanism of Action of Anti-Cancer Gold(I) Complexes.....	338
5.1.3. Alkynyl Gold(I) Phosphine Complexes with Anti-Cancer Activity.....	340
5.2. Synthesis of Propargyl Functionalised Ligands.....	345
5.3. Synthesis of Propargyl Gold(I) Phosphine Complexes .....	348
5.3.1. Derivatives with Nitrogen Substrates .....	348
5.3.2. Derivatives with Oxygen and Sulfur Substrates .....	355
5.3.3. Synthesis of a Heterometallic Dinuclear Complex .....	359
5.4. Biological Activity.....	363
5.5. Conclusions.....	366
5.6. Experimental.....	368
General Conclusions .....	377
Conclusiones Generales .....	381
References.....	384

## Abbreviations

Å	Angstrom
acac	Acetylacetonate
ADC	Acyclic Diamino Carbene
APT	Attached Proton Test
Bu	Butyl
BuLi	Butyllithium
CAAC	Cyclic Alkyl Amino Carbene
calcd.	Calculated
cod	Cyclooctadiene
Cy	Cyclohexane
CyJohnPhos	2-(Dicyclohexylphosphino)biphenyl
d	Doublet
DAPTA	3,7-Diacetyl-1,3,7-triaza-5-phosphabicyclo[3.3.1]nonane
DMEM	Dulbecco's Modified Eagle's Medium
DMSO	Dimethyl sulfoxide
DNA	Deoxyribonucleic acid
dppe	1,2-Bis(diphenylphosphino)ethane
dppf	1,1'-Bis(diphenylphosphino)ferrocene
dppm	1,1-Bis(diphenylphosphino)methane
δ	Chemical Shift
ESI	Electrospray Ionisation
Et	Ethyl
FAD	Flavin Adenine Dinucleotide
FT	Fourier Transformed
g	Grams
h	Hours
HMBC	Heteronuclear Multiple Bond Correlation
HRMS	High Resolution Mass Spectrometry
HSQC	Heteronuclear Single Quantum Correlation
IC <sub>50</sub>	Half Maximal Inhibitory Concentration

## Abbreviations

---

IMes	1,3-Bis(2,4,6-trimethylphenyl)imidazol-2-ylidene
IPr	1,3-Bis(2,6-diisopropylphenyl)imidazol-2-ylidene
<i>i</i> Pr	Isopropyl
IR	Infrared
JohnPhos	2-(Di- <i>tert</i> -butylphosphino)biphenyl
L	Neutral ligand
<i>m</i>	<i>meta</i>
m	Multiplet
MALDI	Matrix-Assisted Laser Desorption/Ionisation
Me	Methyl
Mes	Mesityl
min	Minutes
ml	Millilitres
μl	Microlitres
mmol	Millimoles
MTT	3-(4,5-Dimethylthiazol-2-yl)-2,5-diphenyltetrazolium bromide
NADPH	Nicotinamide Adenine Dinucleotide Phosphate
NaHMDS	Sodium bis(trimethylsilyl)amide
NHC	<i>N</i> -Heterocyclic Carbene
NMR	Nuclear Magnetic Resonance
<i>o</i>	<i>ortho</i>
<i>p</i>	<i>para</i>
Ph	Phenyl
ppm	Parts per million
Pr	Propyl
PTA	1,3,5-Triaza-7-phosphaadamantane
Py	Pyridyl
RT	Room Temperature
s	Singlet
t	Triplet
<i>t</i> Bu	<i>tert</i> -Butyl
THF	Tetrahydrofuran



## Abbreviations

---

tht	Tetrahydrothiophene
tmbn	2,4,6-Trimethoxybenzonitrile
TrippyPhos	1-[2-[Bis(tert-butyl)phosphino]phenyl]-3,5-diphenyl-1H-pyrazole
XantPhos	4,5-Bis(diphenylphosphino)-9,9-dimethylxanthene
Z	Atomic number



# Chapter 1 – General Introduction

## 1.1. Gold

Gold, one of the noble metals, has fascinated people of all cultures and civilisations for millennia.<sup>1</sup> Although it is not known when this metal was first discovered by humans, flakes of gold have been found in Palaeolithic caves dating back as far as 40 000 BC. Its glowing yellow colour and resistance to corrosion led to gold becoming a symbol of immortality and power in many ancient cultures and its attractive properties such as high durability and malleability have meant that it has been highly valued throughout history.<sup>2</sup> The extensive chemistry of gold has only relatively recently started to receive attention and has led to this metal, in the form of complexes, finding application in fields as diverse as luminescence, medicine and catalysis. The ever-increasing number of novel complexes with exciting and unusual properties ensures that gold remains an important element to this day.

### 1.1.1. Relativistic Effects

The name ‘gold’ is thought to be derived from the Germanic or Old English ‘*ghel*’ or ‘*geolu*’ meaning ‘yellow’, and the Latin name ‘*aurum*’ from which its chemical symbol, Au, is derived translates to ‘shining dawn’, reflecting one of the most dominant characteristics of this metal, its yellow colour.<sup>3</sup> This unusual mellow hue along with the immunity of gold to tarnishing and corrosion are all a result of a phenomenon known as special relativity, the significance of which in the chemistry of gold was first noted by Pitzer<sup>4</sup> and Pyykkö and Desclaux<sup>5</sup> almost 40 years ago.

Einstein’s Theory of Special Relativity states that the mass of any moving object changes as its velocity changes according to Equation 1.1, where  $m_{rel}$  is the relativistic mass,  $m$  is the rest mass,  $v$  is the velocity and  $c$  is the vacuum speed of light.

$$m_{rel} = \frac{m}{\sqrt{1 - \left(\frac{v}{c}\right)^2}} \quad (1.1)$$

In most ordinary conditions, the term  $\left(\frac{v}{c}\right)^2$  is so small that the resultant change in mass is insignificant, however, when the velocity of an object approaches the speed of light, this change in mass can have important consequences. In the case of gold, the intense electrostatic attraction experienced by the s electrons as a result of the 79 protons in the nucleus results in an increase in their velocity to near enough to the speed of light to cause a substantial relativistic increase in their mass. This increase in mass causes a relativistic contraction of the orbit since the radius of an orbit with constant angular momentum will shrink proportionately as mass increases. The ratio of the relativistic radius,  $r_{rel}$ , to the normal radius,  $r_{non-rel}$ , is given by Equation 1.2.

$$\frac{r_{rel}}{r_{non-rel}} = \sqrt{1 - \left(\frac{v}{c}\right)^2} \quad (1.2)$$

The contraction of the orbital radii mainly affects the s electrons, even those in outer shells, since their probability density remains close to the nucleus. This effect occurs in several heavy metals but is most pronounced for gold with a contraction of  $\sim 18\%$  (Figure 1.1).

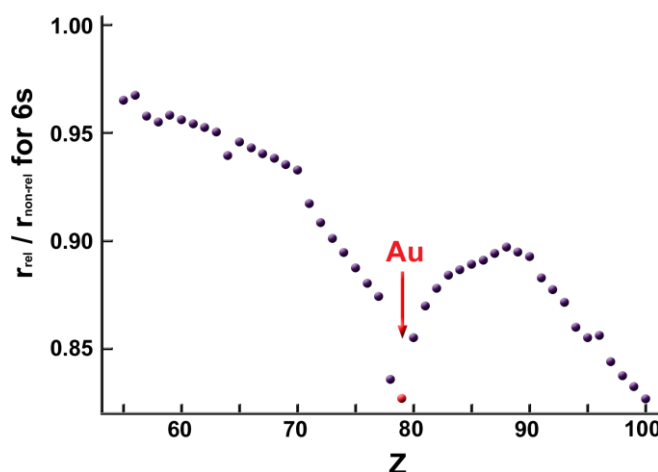


**Figure 1.1.** Ratio of relativistic radius of the 6s electrons to their non-relativistic radius as a function of atomic number for elements Cs ( $Z = 55$ ) to Fm ( $Z = 100$ ) (Adapted from *Acc. Chem. Res.*, 1979, **12**, 226, Copyright (1979) American Chemical Society).<sup>5</sup>

The outermost d electrons are somewhat shielded from the nucleus by the s electrons, and the d orbitals therefore actually experience a slight expansion. The energy levels of the outermost 6s orbital are consequently shifted closer towards the 5d orbitals (Figure 1.2).

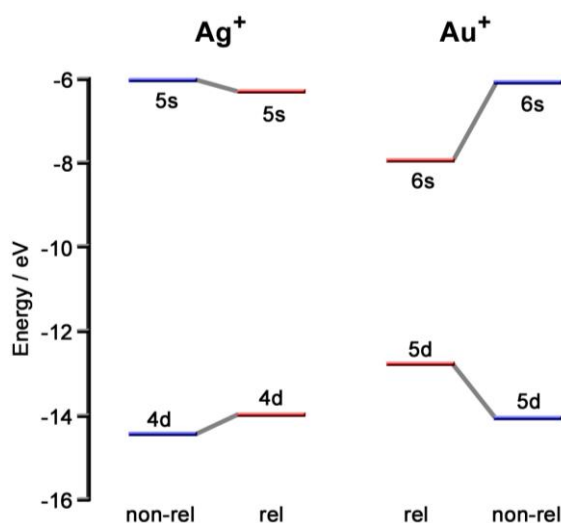


**Figure 1.2.** Calculated relativistic and non-relativistic (n-1)d and ns orbital energies for Ag (n = 5) and Au (n = 6). Relativistic d-orbital energies are the weighted average of the  $d_{3/2}$  and  $d_{5/2}$  spin-orbit components (Adapted from *Acc. Chem. Res.*, 1979, **12**, 226, Copyright (1979) American Chemical Society).<sup>5</sup>

These relativistic effects have several significant effects in the chemistry of gold and consequently many of the usual periodic trends do not hold true for the coinage metals triad.

Although gold and silver have virtually identical metallic radii in close packed cubic lattices (the lattice constants are 4.0862 Å (Ag) and 4.07825 Å (Au),<sup>6</sup> and the nearest-neighbour interatomic distances are 2.889 Å (Ag-Ag) and 2.884 Å (Au-Au) for coordination number 12),<sup>7</sup> the covalent radius of gold(I) is anomalously small and has been reported by Schmidbaur to be around 0.09 Å smaller than that of silver when comparing crystal structures of the complexes  $[M(\text{PMes})_2]\text{BF}_4$  (M = Cu, Ag, Au). For two coordinate M(I) complexes the radii were estimated to be 1.13 Å for copper, 1.33 Å for silver and 1.25 Å for gold.<sup>8</sup> The usual periodic trend would be for the radius to increase down a group.

The usual trend of increasingly stable high oxidation state on descending the group does not hold true for the group 11 metals; for copper the +2 oxidation state dominates, whereas silver is usually found in the +1 oxidation state and for gold oxidation states +1 and +3 are most common. The relative ease with which gold can be oxidised to gold(III) with respect to the other coinage metals, can be explained by the small 5d-6s orbital separation since two electrons can more easily be removed from the expanded 5d orbital. Silver(III) and copper(III), on the other hand, are very rare but are accessible with highly oxidising fluoride ligands e.g.  $[\text{AgF}_4]^-$

or  $[\text{CuF}_6]^{3-}$ .<sup>9</sup> The stabilisation of the 6s orbital in gold can also explain the formation of the gold(-I) oxidation state<sup>10</sup> which is unknown for copper and silver.

Gold(I) complexes are predominantly linear, two-coordinate, diamagnetic, 14 electron species whereas copper(I) and silver(I) generally adopt three or four-coordinate trigonal planar or tetrahedral geometries. The tendency for gold(I) to adopt a linear geometry is a result of the relativistic contraction of the 6s orbital and the resulting large 6s-6p separation. Molecular orbital calculations generally suggest that the bonding in gold(I) species involves mainly the 6s and  $5d_{z^2}$  which combine to form the  $\psi_1$  and  $\psi_2$  hybrid orbitals. The electron pair originally in the  $5d_{z^2}$  will occupy  $\psi_1$  away from the two ligands considered to lie along the z axis. The  $\psi_2$  orbital will combine further with the  $6p_z$  to give a further two bonding orbitals  $\psi_3$  and  $\psi_4$  with empty lobes pointing along the z axis which can accept pairs of electrons from two ligands, and hence a linear coordination is favoured (Figure 1.3).<sup>11</sup> Gold(III) complexes are typically four-coordinate, diamagnetic, 16 electron species and adopt a square planar geometry.

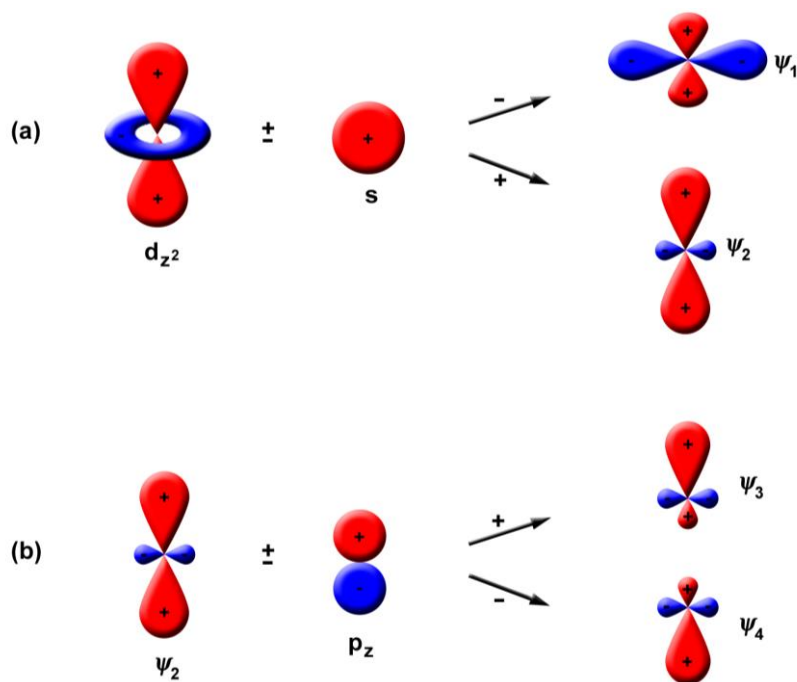


**Figure 1.3.** Mixing of atomic orbitals to give hybrid orbitals capable of linear coordination (Adapted from J. E. Huheey, *Inorganic Chemistry*, Harper and Row, London, 1975).<sup>11</sup>

One of the most significant consequences of relativity in the chemistry of gold is the formation of gold-gold interactions. This phenomenon was first noted in the 1980s when based on

## 1.1. Gold

---

increasing evidence from crystal structure data it was noted that in many cases gold(I) centres appear to be drawn together to sub van der Waals Au...Au distances in the range 2.8-3.5 Å.<sup>12-16</sup> The lower limit of this range is smaller than the interatomic distance in metallic gold and the upper limit is still shorter than the estimated sum of two van der Waals radii of a gold atom (3.65 Å). The binding energy of these interactions has been estimated base on several systems to be in the range 5-15 kcal mol<sup>-1</sup> and hence comparable to typical hydrogen bonds.<sup>14-16</sup> Classical theories of chemical bonding cannot explain such short Au...Au interactions since it would normally be expected that two Au(I) centres with equal charge and closed 5d<sup>10</sup> configuration would repel one another on close contact.<sup>17,18</sup> However, taking into account the relativistic effects, the attractive Au...Au contacts can be interpreted as the donation of electron density from the expanded filled 5d orbitals on one metal centre to the empty p orbital on another. These interactions are one of the most significant intermolecular forces in gold chemistry and the phenomenon has been named “aurophilicity” by Schmidbaur.<sup>19</sup> It should be noted that this phenomenon is not exclusive to gold and “metallophilicity” has also been observed for the neighbouring elements in the periodic table,<sup>20-24</sup> however the effect is by far the most pronounced in gold due to the steric accessibility of the metal atoms as a result of the two-coordinate linear geometry.

One final consequence of the relativistic effects in gold is the unusual colour of the metal. For the majority of metals, the absorption of light, primarily due to the 5d to 6s transition has an energy corresponding to ultraviolet light, hence frequencies in the visible band are not absorbed and are all reflected equally, meaning that these metals are observed as “silvery”. In gold, however, the contraction of the 6s orbital means that the 5d-6s energy gap is lowered to around 2.4 eV and light in the visible blue range is strongly absorbed. All other frequencies in the spectrum, the reds and greens, are reflected, combining to give the golden yellowish colour that has attracted humans to gold since ancient times.

### 1.1.2. History

It is believed gold was first smelted by the ancient Egyptians around 3600 BC<sup>25</sup> and from then on it has found use in a wide variety of applications. The earliest examples of gold jewellery date back to 2600 BC in Mesopotamia,<sup>26</sup> and gold coins from around 700 BC have been found in Turkey, marking the first use of gold in currency.<sup>27</sup> Specimens of gold dental fillings from

as early as 600 BC have been found in Italy<sup>28</sup> and it is known that colloidal gold has been used since ancient Roman times to colour glass intense shades of yellow, red or mauve.<sup>29</sup> The history of gold has by far been dominated by the metallic form of this element, and its high resistance to oxidation, a consequence of relativistic effects and the tighter binding of the 6s electron, meant that for many years it was believed to be completely unreactive.

The first chemical reactions of gold were reported towards the end of the eighteenth century by Scheele<sup>30</sup> when he found that metallic gold could be dissolved in cyanide solutions to give what we now know to be salts of  $[\text{Au}(\text{CN})_2]^-$ , however throughout the following century the main focus was on the use of this reaction for electroplating or mining processes and little interest was shown in gold chemistry. The first attempts to prepare organogold complexes were made over 150 years ago by Frankland and Duppa<sup>31</sup> at what was really the beginning of organometallic chemistry, although it was many years before the existence of such complexes was proven<sup>32</sup> and many more before the number of practical applications was realised. In the long history of this element, the organometallic chemistry of gold only really started to receive attention in the last 40 years and with an ever-increasing number of practical applications as well as simpler and more facile routes for the synthesis of organogold complexes, the field of organogold chemistry has grown at a phenomenal pace. Novel organometallic complexes of gold are constantly being found with properties that can be utilised in a number of different fields, highlighting the richness of organogold chemistry.

## 1.2. Organogold Complexes

### 1.2.1. Basic Concepts

Organogold complexes are defined as those in which an organic group is linked directly to gold through at least one carbon atom, either in the form of an Au-C  $\sigma$ -bond or through  $\pi$ -bonding. The majority of organogold complexes involve gold in the +1 or +3 oxidation states, however since the 1980s an increasing number of gold(II) complexes have also been reported. Gold is unusual among the transition metals in that, even in the +1 oxidation state, it shows reluctance to form stable  $\pi$ -complexes with alkenes, alkynes or aromatic hydrocarbons and therefore its organometallic chemistry is dominated by complexes with Au-C  $\sigma$ -bonds.



Simple alkyls and aryls  $\text{AuR}$  or  $\text{AuR}_3$  are electron deficient and generally unstable and highly reactive. The only stable examples of such compounds are those in which the nature of the R group allows polymerisation or oligomerisation by coordination to neighbouring gold atoms and coordinative saturation is achieved, such as the pentanuclear mesityl gold(I) complex (Figure 1.4), the first isolated example of a homoleptic aryl gold(I) complex. Carbon atoms bridge the gold atoms resulting in three-centre, two-electron bonds.<sup>33</sup>

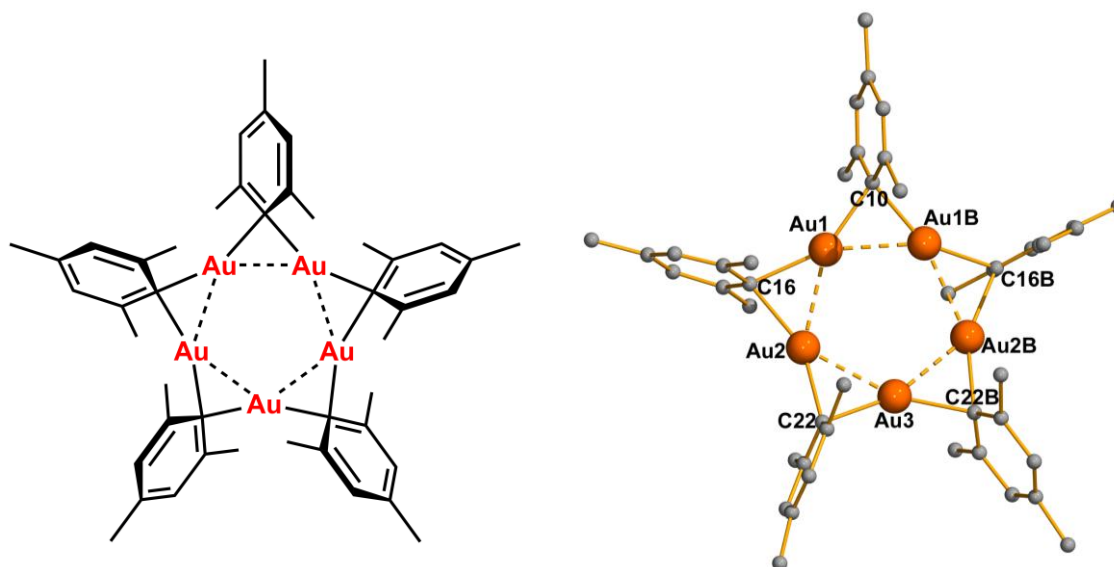


**Figure 1.4.** Molecular structure of  $(\text{AuMesityl})_5$  determined by single crystal X-ray diffraction. Hydrogen atoms are omitted for clarity. Selected bond lengths [Å] and angles [°]: Au(1)-C(10) 2.13(3), Au(1)-C(16) 2.20(2), Au(2)-C(16) 2.19(2), Au(2)-C(22) 2.12(2), Au(3)-C(22) 2.18(2), Au(1)-Au(2) 2.697(3), Au(2)-Au(3) 2.7081(29), Au(1)-Au(1B) 2.692(4), C(10)-Au(1)-C(16) 150.4(6), C(16)-Au(2)-C(22) 152.9(8), C(22)-Au(3)-C(22B) 148.3(7), Au(1)-C(10)-Au(1B) 78.2(1), Au(1)-C(22)-Au(2) 75.9(7), Au(2)-C(22)-Au(3) 78.1(8).

Alkynyl gold(I) complexes are one of the principle examples of stable gold compounds with empirical formula  $\text{AuR}$ , since the triple bond can occupy the free coordination site on an adjacent gold atom thus removing the electron deficiency and giving oligomeric or polymeric structures (Figure 1.5).

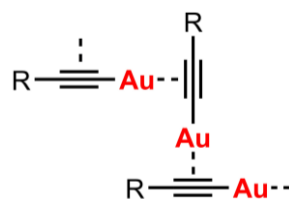


**Figure 1.5.** Alkynyl gold(I) polymer.

The alkynyl gold(I) complex  $[\text{Au}(\text{C}\equiv\text{C}'\text{Bu})]_n$  was for many years assumed to have a tetrameric structure,<sup>34</sup> however successful determination of the crystal structure by Mingos in the mid-1990s revealed far more complex catenane structure involving both  $\sigma$ - and  $\pi$ -bound gold atoms (Figure 1.6).<sup>35</sup>

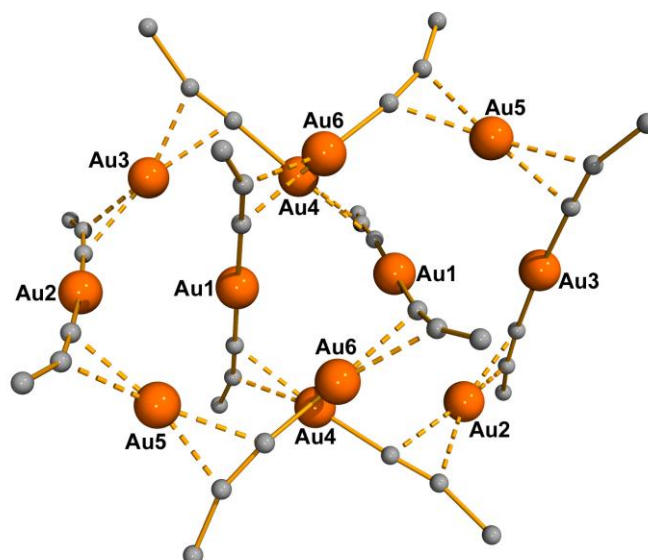


**Figure 1.6.** Molecular structure of  $[\text{Au}(\text{C}\equiv\text{C}'\text{Bu})]_n$  determined by single crystal X-ray diffraction. *Tert*-butyl groups are omitted for clarity.<sup>35</sup>

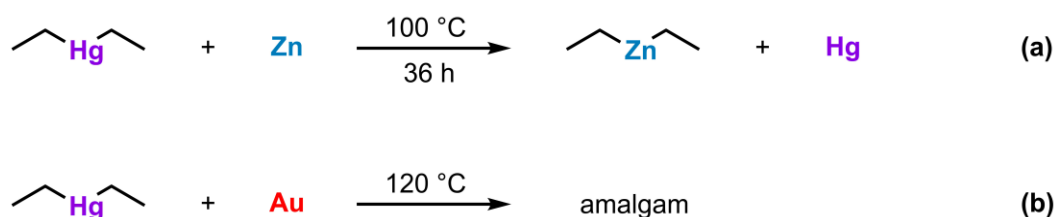
When additional anionic or neutral ligands are present to make up the normal coordination numbers of 2 for gold(I) and 4 for gold(III), organogold complexes of all possible stoichiometries are known, with one or two R groups for gold(I) and one to four R groups for gold(III). Three coordinate trigonal planar organometallic complexes of gold(I) have also been characterised but are not as numerous.<sup>36,37</sup>

For the majority of organogold compounds the R groups are considered as carbanions acting as conventional mononegative, two-electron ligands, however, recently attempts have been made to prepare novel organogold compounds with neutral carbene type ligands and higher Au-C bond orders. Organic ligands are among the softest ligands known due to their high polarisability and consequently they transfer a lot of electron density to the gold atom, demonstrated by Mössbauer spectroscopic data.<sup>38,39</sup> This results in a high *trans* influence and hence gold complexes in which the R groups are mutually *trans* are generally of lower stability. In Au(III) complexes soft ligands generally adopt a position *cis* to the R group. Complexes

$[\text{AuR}_2]^-$  and  $[\text{AuR}_4]^-$  are usually highly reactive although derivatives of the harder perfluoro-organic groups  $-\text{CF}_3$  and  $-\text{C}_6\text{F}_5$  show greater stability.<sup>40,41</sup>

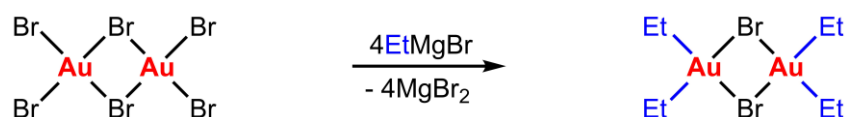
### 1.2.2. Early Work on Organogold Complexes

The first reported attempts to prepare organogold compounds were made in 1864 by Frankland and Duppa during the very early stages of organometallic chemistry. They had successfully prepared a series of organozinc reagents by transmetallation reactions with zinc metal and organomercury compounds (Scheme 1.1) and went on to attempt the same reactions with other metals. The reaction of gold leaves with diethylmercury was unsuccessful giving only an amalgam and no organogold compound was isolated.<sup>31</sup> Since there was little interest in organogold chemistry at that time, further attempts were not made and attention was focussed on the organometallic chemistry of other metals.



**Scheme 1.1.** Synthesis of diethylzinc from diethylmercury and zinc metal (a) and attempted formation of diethylgold (b).

The existence of organogold complexes was conclusively demonstrated by the pioneering work of Gibson at the beginning of the twentieth century. He carried out reactions of gold(III) bromide and chloride with Grignard reagents to give dialkyl gold(III) complexes<sup>32</sup> (Scheme 1.2).

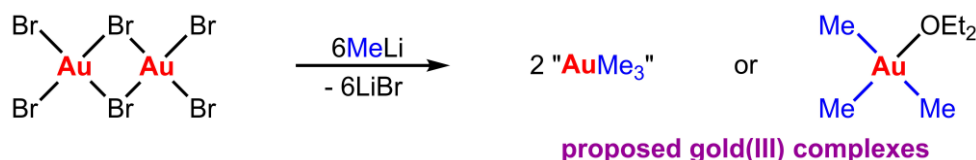


**Scheme 1.2.** Synthesis of bromo(diethyl)gold(III).

Isolation was difficult due to the instability of the complexes, and the lack of characterisation techniques at that time meant that the dimeric structure of such complexes was not realised

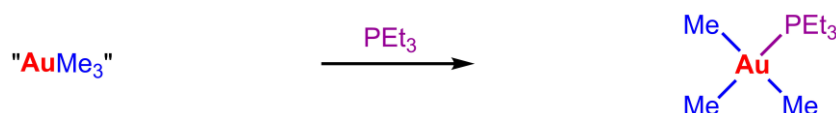
until 1930, some 23 years later. This was again achieved by Gibson when following experiments to determine the molecular weight by a cryoscopic method in benzene he found the compound to have double the predicted molecular weight and hence concluded it should more correctly be written as a dimer.<sup>42</sup> He also stated that all gold(III) complexes must be four-coordinate to be stable.<sup>43</sup>

Gilman went on to further develop the work of Gibson by using the more reactive organolithium reagents in place of the Grignard reagents to form what he believed to be the very unstable trimethyl gold (Scheme 1.3).<sup>44</sup> The reaction was carried out at  $-65\text{ }^{\circ}\text{C}$  with decomposition observed at temperatures above  $-35\text{ }^{\circ}\text{C}$  meaning that characterisation was again difficult. Despite previous reports by Gibson claiming that three-coordinate gold(III) complexes would be impossible to form, Gilman believed that he had successfully prepared the first  $\text{AuR}_3$  type compound, although he did also propose a possible coordination of diethyl ether to give a four-coordinate structure. It is probable that what actually formed in this reaction was the lithium salt  $\text{Li}[\text{AuBrMe}_3]$  since a bromide ion will readily bind to gold(III).



**Scheme 1.3.** Synthesis of “ $\text{AuMe}_3$ ” proposed by Gilman.<sup>44</sup>

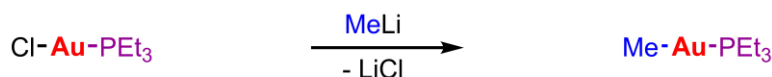
Further important developments of this work on organogold chemistry were made by Coates in the 1960s with the preparation of stable alkyl gold(III) derivatives by the addition of tertiary phosphine ligands (Scheme 1.4).<sup>45</sup>



**Scheme 1.4.** Synthesis of  $[\text{AuMe}_3(\text{PEt}_3)]$

Coates was also able to prepare the first alkyl gold(I) complexes using the same stabilising phosphine ligands (Scheme 1.5).<sup>45</sup>

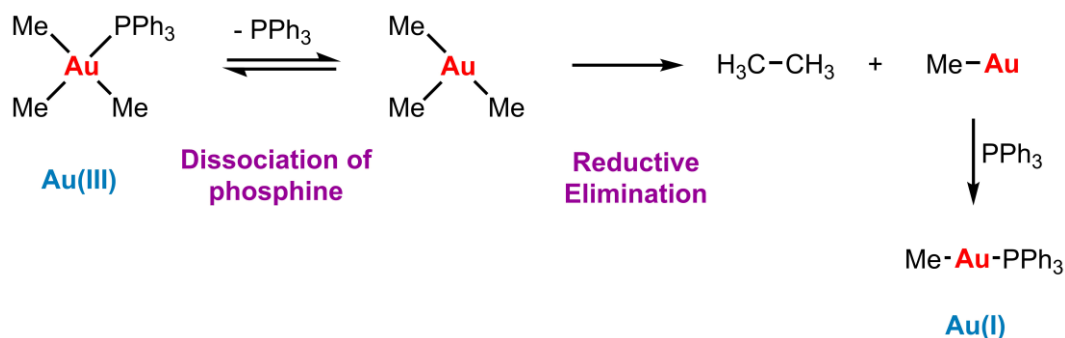
## 1.2. Organogold Complexes



**Scheme 1.5.** Synthesis of the first alkyl gold(I) complex.

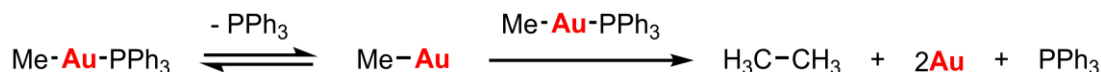
It was believed that the great stability of these compounds arises from the formation of a  $d_{\pi}-d_{\pi}$  bond between gold and phosphorus and that such  $\pi$ -bonding ligands would be necessary for the formation of thermally stable organogold complexes. This was later proven not to be the case as exemplified by the work of Usón and Laguna in which the complexes  $\text{NBu}_4[\text{Au}(\text{C}_6\text{F}_5)_2]$  and  $\text{NBu}_4[\text{Au}(\text{C}_6\text{F}_5)_4]$ , which do not possess any  $\pi$ -bonding ligands, were prepared and isolated as air and moisture stable crystalline solids.<sup>46</sup>

The stability of organogold(III) compounds was later explained by Kochi by analysis of the decomposition pathways.  $[\text{AuMe}_3(\text{PPh}_3)]$  decomposes by first dissociation of the phosphine ligand and subsequent reductive elimination of ethane (Scheme 1.6).<sup>47</sup>



**Scheme 1.6.** Decomposition pathway for  $[\text{AuMe}_3(\text{PPh}_3)]$ .

The decomposition of the methyl gold(I) complex was described to proceed in a similar manner, again the first step being the dissociation of the phosphine (Scheme 1.7).<sup>48</sup>



**Scheme 1.7.** Decomposition pathway for  $[\text{AuMe}(\text{PPh}_3)]$ .

It was therefore concluded that the thermal stability of an organogold complex with formula  $[\text{AuMe}_3\text{L}]$  or  $[\text{AuMeL}]$  depends solely on the strength of the Au-L bond. In the case of the phosphine derivatives the strong Au-P bond is not easily cleaved and hence very stable

compounds may be prepared. The anions  $[\text{Au}(\text{C}_6\text{F}_5)_2]^-$  and  $[\text{Au}(\text{C}_6\text{F}_5)_4]^-$  are thermally stable due to the strength of the gold-carbon bond.

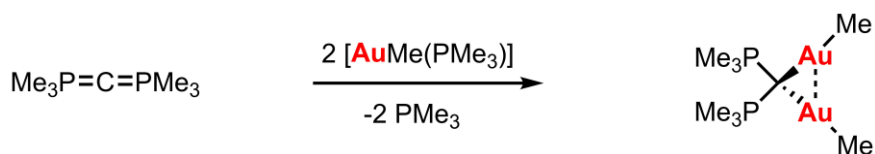
### 1.2.3. Organogold Complexes with Bridging Carbon Ligands

Early gold chemistry focussed on the preparation of complexes in which the organic ligand binds to a single gold atom, and polygold derivatives were initially rare. Multiple auration of carbon was first achieved in the 1970s in which ferrocenylgold(I) and arylgold(I) complexes with three-centre, two-electron  $\text{CAu}_2$  units were prepared and characterised by Nesmeyanov and co-workers, indicating that aggregation of gold atoms at a carbon centre is surprisingly facile (Figure 1.7).<sup>49</sup>



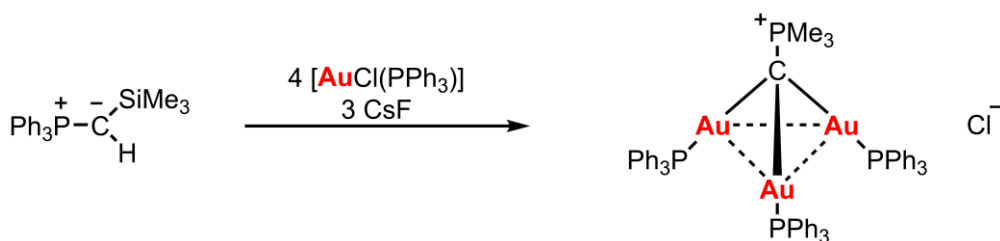
**Figure 1.7.** First examples of complexes with diaurated carbon atoms.

Schmidbaur went on to prepare the first example of a complex with two gold atoms bound to a tetrahedral carbon atom by reaction of a carbodiphosphorane (or “bis-ylide”) with  $[\text{AuMe}(\text{PMe}_3)]$  (Scheme 1.8). The resulting complex was air-sensitive but thermally stable up to 80 °C and was characterised by NMR spectroscopy.<sup>50</sup>



**Scheme 1.8.** Synthesis of first dinuclear gold complex with two gold atoms bound to a tetrahedral carbon atom.

The first tri-gold substituted carbon was reported by Schmidbaur in the late 1980s. Reaction of a silylated ylide precursor with  $[\text{AuCl}(\text{PPh}_3)]$  in the presence of caesium fluoride led to the formation of the trigold phosphonium salt (Scheme 1.9) in which the  $\text{R}_3\text{-P}$  unit caps a triangle of gold atoms.<sup>51</sup>



**Scheme 1.9.** Synthesis of first complex with triaurated carbon atom.

It was later found that complete auration and even hyperauration of carbon with up to six Au-C  $\sigma$ -bonds was possible. Reaction of polyborylmethanes with  $[\text{AuCl}(\text{PR}_3)]$  leads to the tetra-,<sup>52</sup> penta-<sup>53</sup> and hexagold<sup>19</sup> methane compounds or cations. In fact, tetragold methanes are only obtained when very bulky phosphine groups are used, and with smaller ligands penta- or hexauration occurs to give electron deficient trigonal bipyramidal or octahedral structures, respectively (Figure 1.8).

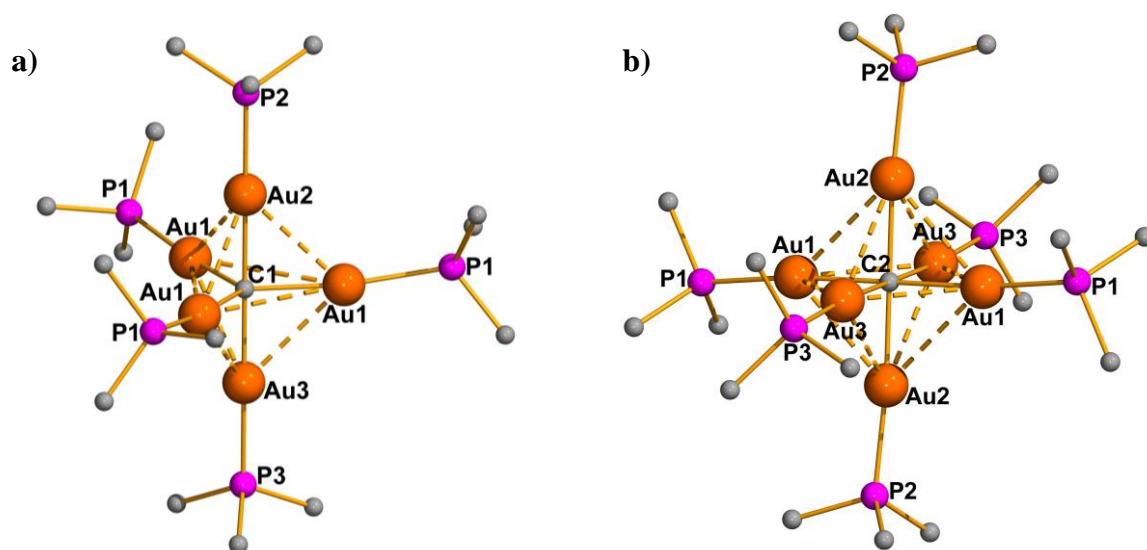


**Figure 1.8.** Molecular structures of trigonal bipyramidal organogold complex (a) and octahedral organogold complex (b) determined by single crystal X-ray diffraction. Hydrogen atoms and phenyl groups are omitted for clarity.

The driving force for the formation of such polynuclear gold compounds is the formation of multiple aurophilic interactions which stabilise the structures.<sup>13</sup>

### 1.2.4. Recent Developments in Organogold Chemistry

The recent upsurge in interest in organogold chemistry as a result of the increasing applications of gold complexes, particularly within homogeneous catalysis, has led to significant developments within the last decade. Many novel organogold complexes have been prepared, either in the hunt for new catalysts, to help better understand catalytic mechanisms or in attempts to find complexes with unique and unusual structures and properties.

#### 1.2.4.1. Gold(III) Complexes

Many organogold(III) complexes are now known but most are relatively unstable and undergo reductive elimination reactions to give carbon-carbon coupling products and gold(I) species. Recent interest has therefore focussed on the development of organogold(III) complexes of higher stability.

Cyclometallated gold(III) complexes bearing a tridentate  $(C^N^C)^{2-}$  2,6-diphenylpyridyl ligand were introduced by Che and co-workers in their search for luminescent gold(III) derivatives.<sup>54</sup> Many similar cyclometallated gold(III) complexes, such as those bearing 2-2'-2''-terpyridine or 6'-phenyl-2-2'-bipyridine  $(C^N^N)$  ligands have been known for several years and are relatively stable (Figure 1.9).<sup>55-57</sup> However, the cyclometallated gold(III) derivatives bearing the 2,6-diphenylpyridyl ligand feature two robust gold-carbon bonds and the strong  $\sigma$ -donor capacity of the ligand renders the gold(III) centre more electron rich, enhancing the stability of the complexes towards reductive elimination.<sup>58</sup>

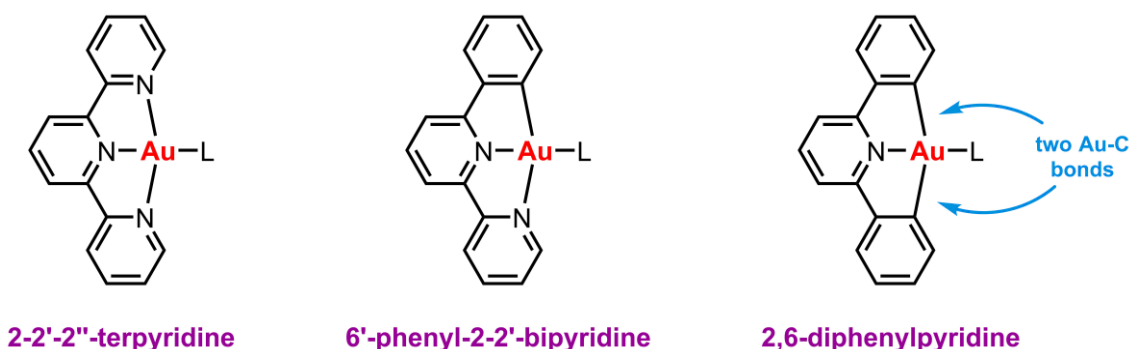
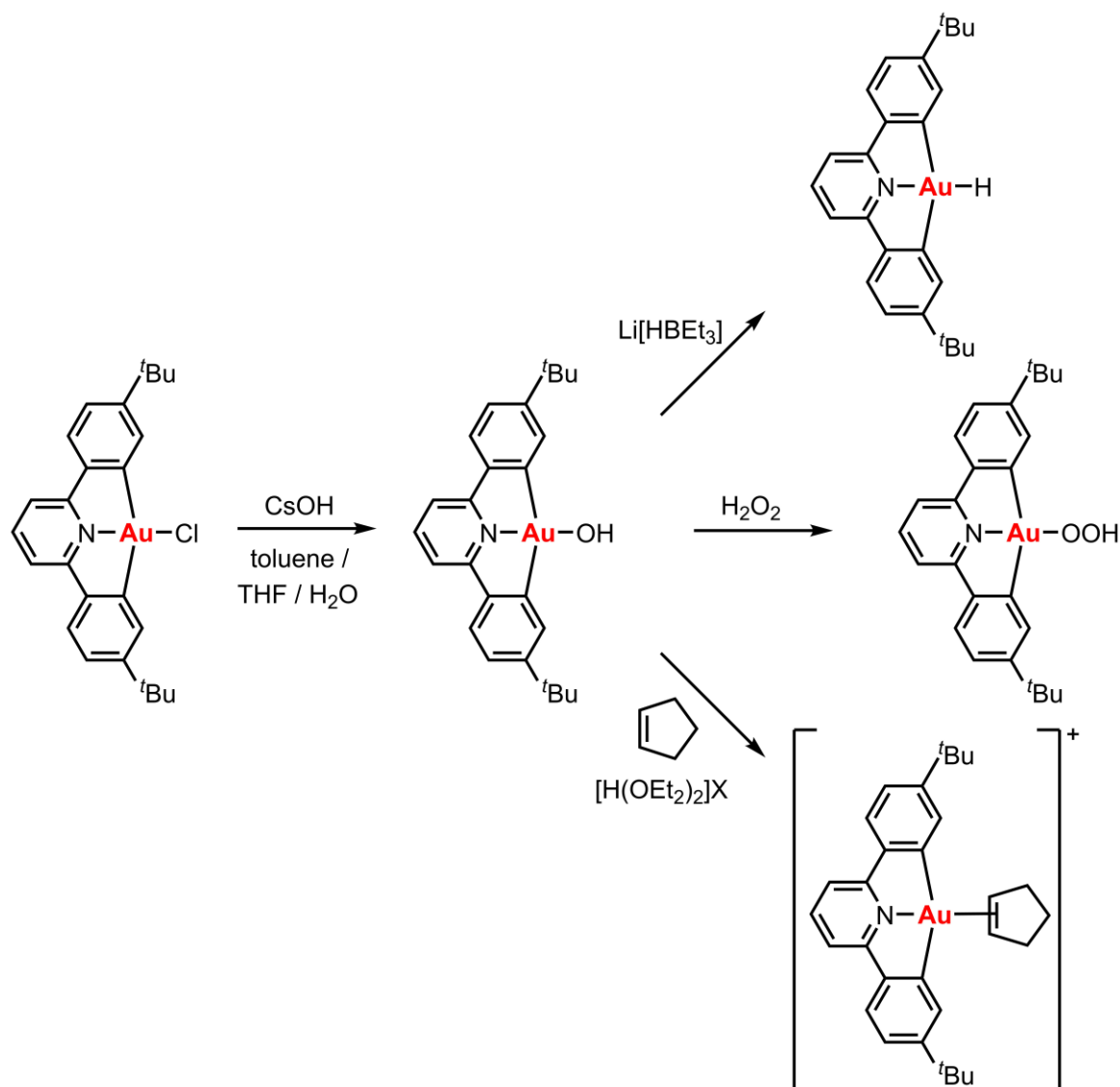


**Figure 1.9.** Cyclometallated gold(III) complexes.



## 1.2. Organogold Complexes

The group of Bochmann took advantage of the high thermal stability of these cyclometallated 2,6-diphenylpyridine gold(III) derivatives in order to prepare a series of novel organogold(III) complexes (Scheme 1.10).



**Scheme 1.10.** Synthetic routes to gold(III) hydride, superoxide and alkene complexes.

Initially the chloro derivative was prepared in which the chloride ligand may readily be substituted allowing synthesis of the hydroxide complex.<sup>59</sup> A number of other gold(III) hydroxides are known,<sup>60-62</sup> however, their reactivity has not been extensively studied. Bochmann and co-workers were able to successfully react the [(C<sup>^</sup>N<sup>^</sup>C)\*AuOH] complex with LiHB(Et)<sub>3</sub> to form the first example of an isolable and thermally stable organogold(III) hydride complex.<sup>63</sup> Following this, they went on to prepare several other novel organogold(III)

complexes including the first gold(III) superoxide<sup>64</sup> and the long sought after gold(III)  $\pi$ -alkene complexes.<sup>65</sup> Gold(III)  $\pi$ -alkene complexes are analogous to the platinum complex Zeise's Salt (Figure 1.10), reported in 1827,<sup>66</sup> however, despite the isoelectronic relationship between Pt(II) and Au(III), the gold adducts have been considerably more challenging to prepare.

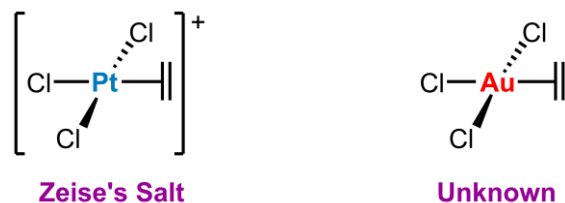


**Figure 1.10.** Zeise's Salt and hypothetical gold(III) analogue.

Che and co-workers were also able to take advantage of the stabilising 2,6-diphenylpyridine ligand to prepare the first example of a gold(III) allenylidene complex (Figure 1.11). They found it to be phosphorescent, with intense bright yellow emission in the solid state, and also to exhibit efficient cytotoxic activity in HeLa cells.<sup>67</sup>

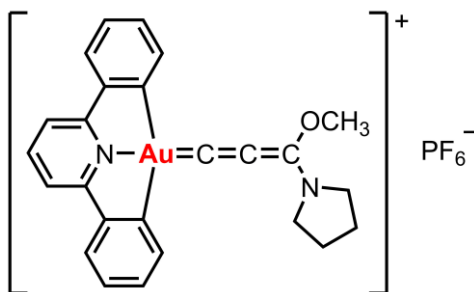
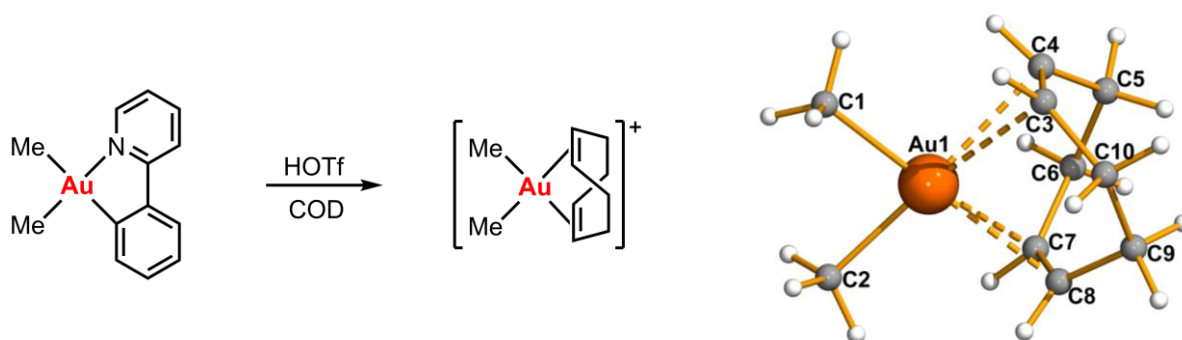


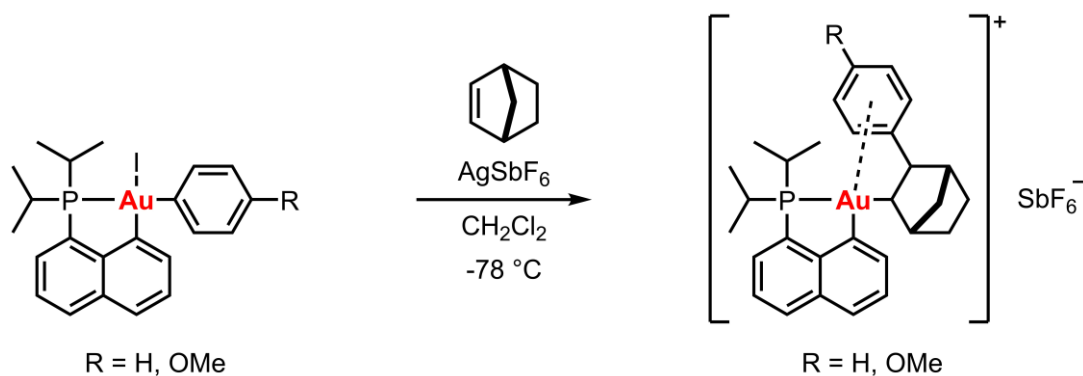
**Figure 1.11.** First gold(III) allenylidene complex.

Another significant recent contribution to organogold(III) chemistry comes from the group of Tilset with the isolation of a gold(III) complex of 1,5-cyclooctadiene from a cyclometallated gold(III) precursor (Scheme 1.11).<sup>68</sup> This is the first example of a gold(III) complex bearing two olefinic groups whereas platinum(II) analogues have been known for several decades.<sup>69</sup>



**Scheme 1.11.** Synthesis of gold(III) cod complex and molecular structure determined by single crystal X-ray diffraction. Selected bond lengths [Å]: Au(1)-C(3) 2.3712, Au(1)-C(4) 2.4149, Au(1)-C(7) 2.3620, Au(1)-C(8) 2.4064.

The first gold(III) arene complexes were reported by the group of Bourissou in 2017 and were prepared by the insertion of olefins into gold-aryl bonds (Scheme 1.12). The  $\eta^2$ -coordination of the phenyl ring was demonstrated spectroscopically and crystallographically, allowing important information on the interactions between arenes and gold(III) species to be obtained in the context of the gold-catalysed functionalisation of aromatic C-H bonds.<sup>70</sup>



**Scheme 1.12.** Formation of gold(III) norbornyl complexes by insertion of norbornene into the Au(III)-Ar bond.

#### 1.2.4.2. Gold(I) Complexes

One of the most significant developments in organogold(I) chemistry has been the preparation of singlet carbene derivatives (Figure 1.12). Although first prepared in the 1970s and 1980s by the groups of Bonati and Mighetti,<sup>71,72</sup> acyclic diamino carbene (ADC) and *N*-heterocyclic carbene (NHC) complexes of gold(I) were initially of little interest. The recent development of more facile syntheses as well as the discovery of the potential of such complexes to act as catalysts or precatalysts has led to a huge increase in their research. More recently

cyclic(amino)(alkyl)carbenes (CAAC), another type of singlet carbene, have attracted attention due to having an even greater nucleophilic character than NHCs and ADCs and hence they can form some very robust complexes of gold(I).<sup>73,74</sup>

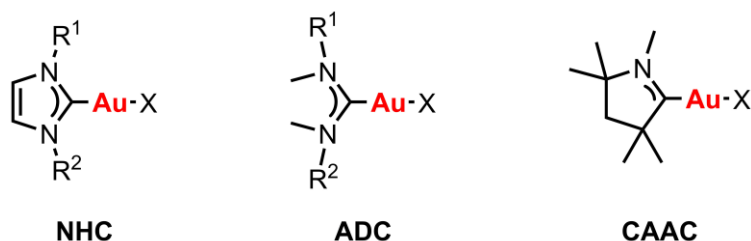


**Figure 1.12.** Singlet carbene gold(I) complexes.

The stabilising influence of these carbene ligands on gold(I) complexes is comparable to that of phosphines, and the steric and electronic properties of the complexes can be altered with relative ease by variation of the substituents of the carbene ligand. The use of very bulky NHC ligands has allowed the isolation of the first gold(I) hydride (Figure 1.13(a))<sup>75</sup> and fluoride (Figure 1.13(b)),<sup>76</sup> both of which had been elusive targets in preparative chemistry.<sup>2</sup>

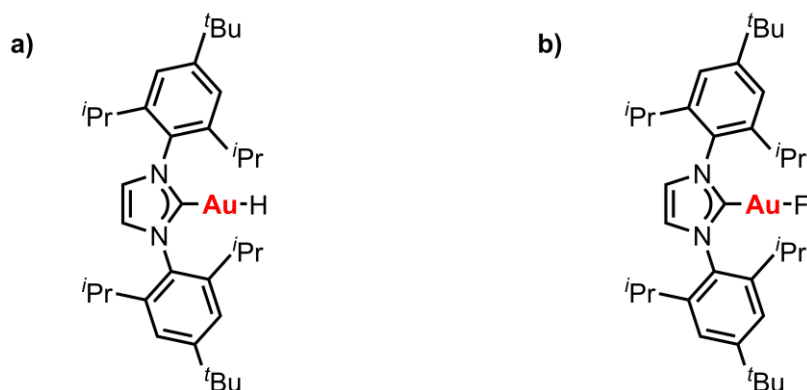


**Figure 1.13.** First gold(I) hydride (a) and fluoride (b) complex.

#### 1.2.4.2.1. Catalytic Intermediates – $\sigma$ complexes

Although homogeneous gold catalysis is now a well-developed field, there is still considerable uncertainty regarding the mechanisms involved in many processes. The recent isolation of several novel organogold(I) complexes which are intermediates in catalytic cycles has allowed further understanding to be gained. Examples are shown in Figure 1.14.

## 1.2. Organogold Complexes

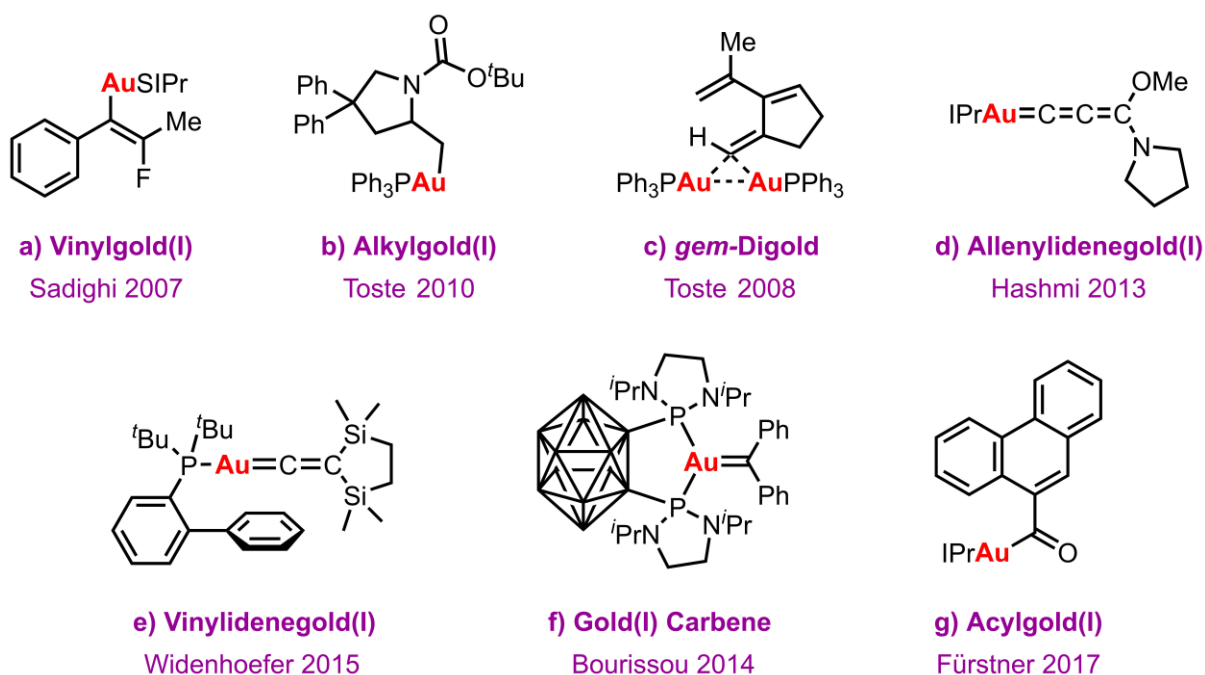
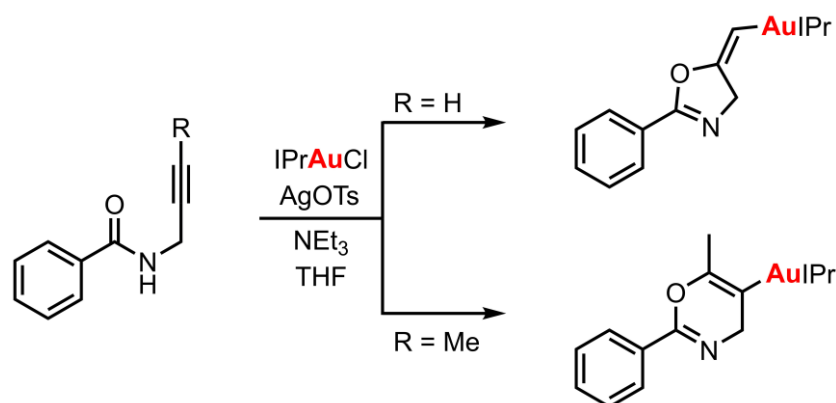


**Figure 1.14.** Recently isolated organogold(I) complexes.

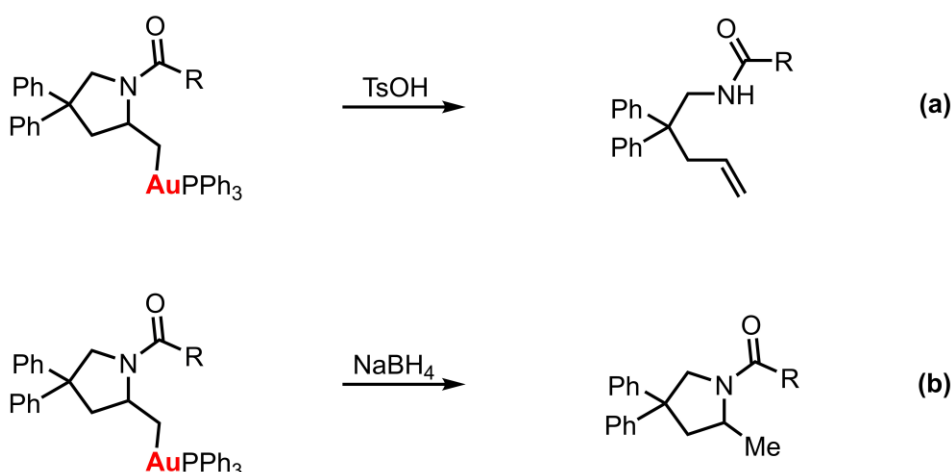
Vinyl gold(I) complexes were suggested as intermediates in the first reports of homogeneous gold catalysis, in the cleavage reactions of bicyclo[1.1.0]butanes, over 40 years ago,<sup>77</sup> and are now considered key intermediates in many gold-catalysed reactions. However, it was not until 2007 that the first example was isolated and crystallised by Sadighi and co-workers (Figure 1.14(a)). The crystal structure allowed the *trans* arrangement of gold and fluorine to be confirmed in the intermediate, allowing a key step in the catalytic cycle of the hydrofluorination of alkynes to be determined.<sup>78</sup>

A more general access to vinyl gold(I) complexes was later introduced by Hashmi and co-workers by suppression of the protodeauration step of the catalytic cycle, in the gold-catalysed cycloisomerisation of propargylamides, by addition of a base (Scheme 1.13).<sup>79,80</sup>



**Scheme 1.13.** Synthesis of vinylgold(I) complexes (IPr = 1,3-bis(2,6-diisopropylphenyl)imidazole-2-ylidene)

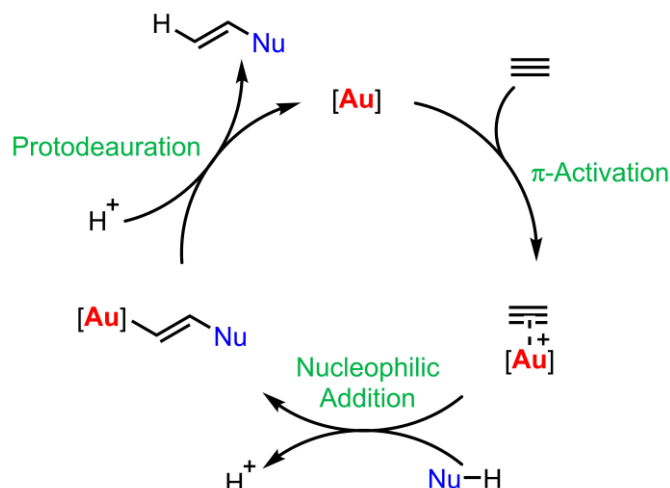
The first alkylgold(I) intermediate to be isolated and characterised by single crystal X-ray diffraction was achieved by the group of Toste in 2010 (Figure 1.14(b)). Aminoaurated complexes were isolated using the same method of suppression of protodeauration previously established by Hashmi and co-workers for the isolation of vinylgold intermediates, by addition of excess triethylamine to the reaction. Surprisingly the protodeauration of these alkylgold(I) complexes, which had previously been proposed in the mechanism of gold-catalysed hydroamination of alkenes, was unsuccessful and upon treatment with acid the complexes reverted back to the starting aminoalkenes. However, addition of sodium tetraborohydride did give the desired cyclic amine products (Scheme 1.14).<sup>81</sup>



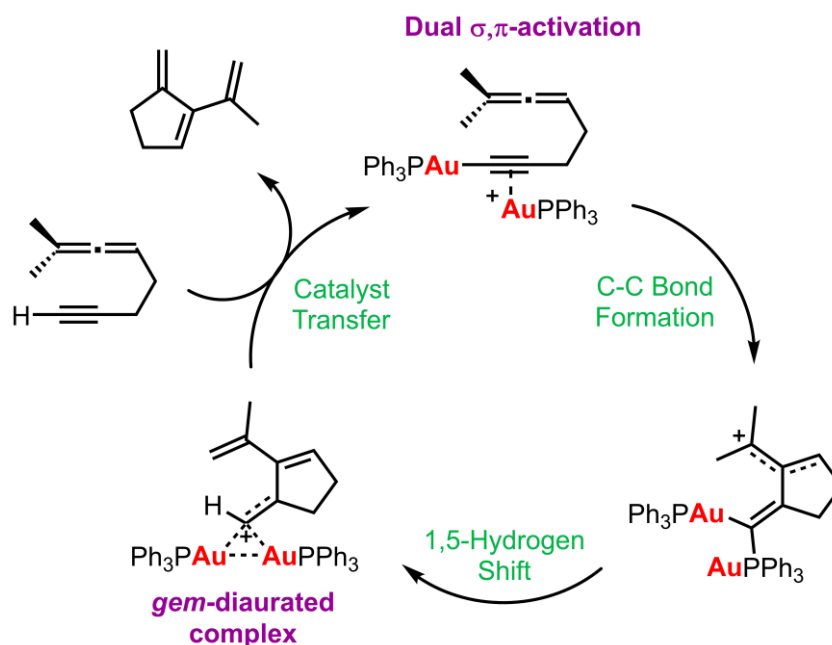
**Scheme 1.14.** Attempted protodeauration of alkylgold(I) complexes (a), and reaction of alkylgold(I) complexes with NaBH<sub>4</sub> (b).

## 1.2. Organogold Complexes

Geminally diaurated complexes have been known since the 1970s,<sup>49</sup> however they were initially only considered curiosities and it was not until 2008 when Toste and co-workers suggested a *gem*-digold complex as a catalytic intermediate (Figure 1.14(c)) that a resurgence in interest began. Gold-catalysed transformations involving terminal alkynes had always previously been assumed to proceed via  $\pi$ -activation by just one gold centre (Scheme 1.15).



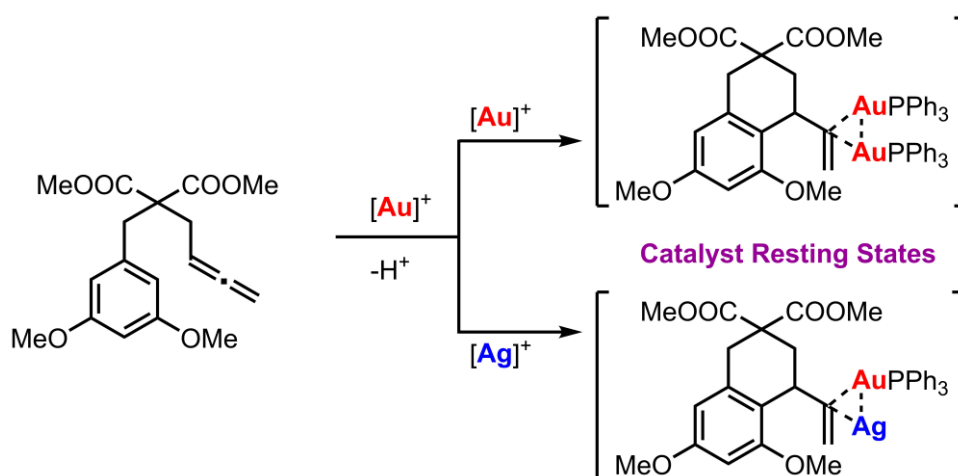
**Scheme 1.15.** General mechanism for a gold-catalysed reaction involving a terminal alkyne.



**Scheme 1.16.** Mechanistic proposal involving dual  $\sigma, \pi$ -activation and the formation of *gem*-diaurated species.

Toste and co-workers reported the first evidence of dual  $\sigma,\pi$ -activation by a gold catalyst. Computational studies supported by experimental data suggested the most plausible mechanism to involve the formation of a *gem*-diaurated species which would react with a new substrate molecule to release the final product (Scheme 1.16).<sup>82</sup> This work raised many questions about the mechanisms by which gold complexes catalyse organic transformations involving terminal alkynes.

In 2009 Gagné and co-workers reported the isolation of a geminally diaurated intermediate in the gold(I) catalysed intramolecular hydroarylation of an allene.<sup>83</sup> They suggested that this digold species could be a catalyst resting state rather than a reactive species in the catalytic cycle. The same group also reported that depending on the silver to gold ratio in the catalytic reaction an alternative hetero geminally dimetallated species could be the resting state (Scheme 1.17).<sup>84</sup>



**Scheme 1.17.** Formation of *gem*-dimetallated catalyst resting states.

Whilst the digold complex was proposed to have three-centre two-electron bonding, the heterometallic species would be dominated by the stronger Au-C bond, similar to the structurally characterised related Au-Ag complex published by the group of Laguna in 1994 (Figure 1.15).<sup>85</sup>



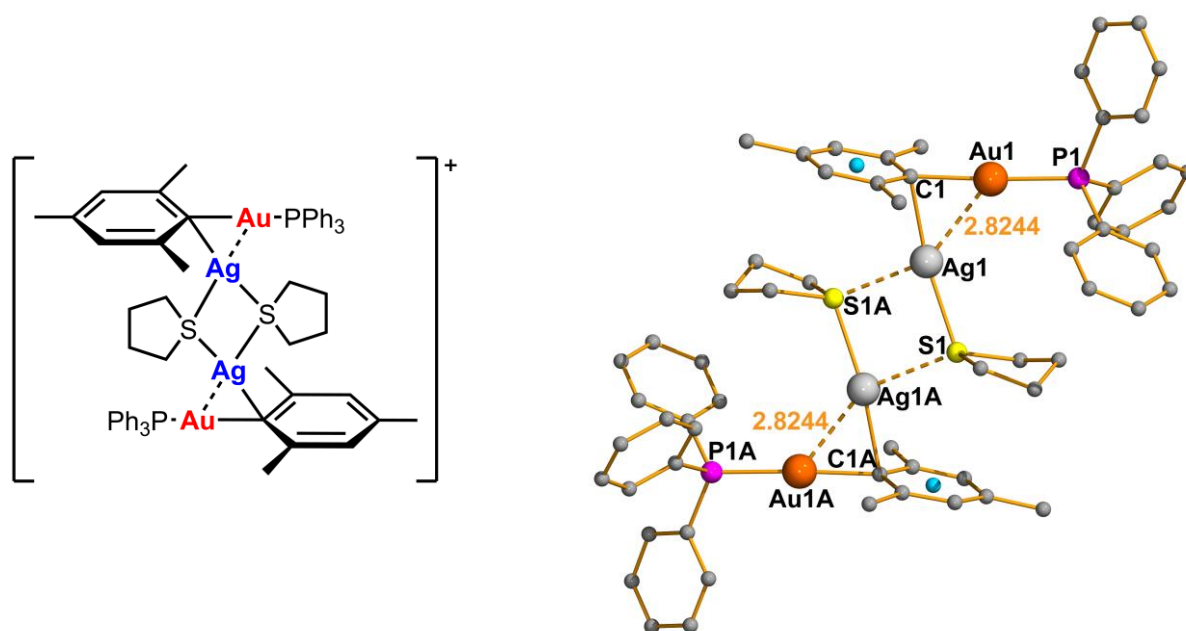


**Figure 1.15.** Molecular structure of geminally dimetallated mesityl complex  $[(\text{PPh}_3)\text{Au}(\mu\text{-Mes})\text{Ag}(\text{tht})]_2^+$  determined by single crystal X-ray diffraction. Hydrogen atoms are omitted for clarity. Selected bond lengths [Å] and angles [°]: C(1)-Au(1) 2.085(4), C(1)-Ag(1) 2.327(4), Au(1)-P(1) 2.289(1), Au(1)-Ag(1) 2.8244(6), Ag(1)-S(1) 2.477(1), Ag(1)-S(1A) 2.839(1), C(1)-Au(1)-P(1) 177.3(1), C(1)-Ag(1)-S(1) 160.0(1), centroid-C(1)-Au(1) 170.10, centroid-C(1)-Ag(1) 110.50.

Gagné's work showed that even if reactants were untouched by the silver cations, they could still have a huge influence on gold-catalysed reactions by intercepting key organogold intermediates to form heteronuclear complexes with different reactivity. This could be one explanation for the “silver effect” in gold catalysis.<sup>86</sup>

Work published by the group of Fürstner in 2010 allowed further insight into the role of geminally diaurated complexes in catalysis to be gained. They developed an efficient synthesis for such complexes from a vinyl borane and  $[\text{Au}(\text{NTf}_2)(\text{PPh}_3)]$  and were able to structurally characterise two examples by single crystal X-ray diffraction analysis. They found that the nature of the bond between the two gold centres and the olefin can either be a three-centre two-electron system, or two regular Au-C  $\sigma$ -bonds flanked by a stabilised cationic centre (Figure 1.16). They also found *gem*-diaurated species to be quite resistant to protodeauration, suggesting that the protodeauration step in catalytic cycles must proceed through a vinyl intermediate (Scheme 1.18).<sup>87</sup>

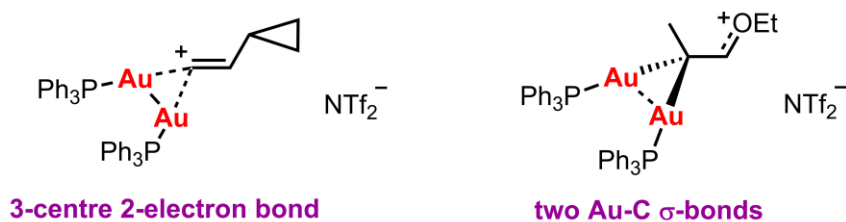
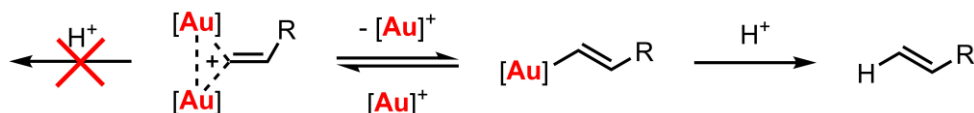


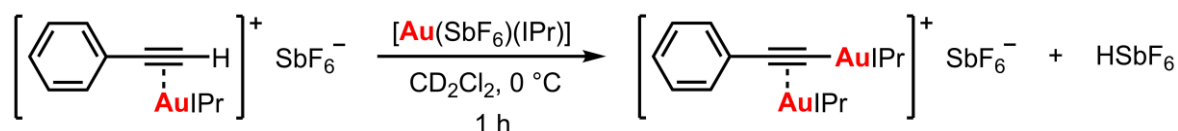
**Figure 1.16.** Possible bonding situations in geminally diaurated complexes.



**Scheme 1.18.** Conclusions from Fürstner's studies on protodeauration of geminally diaurated complexes.

The increased interest in geminally diaurated complex led to new methods for their preparation to be developed by the groups of Gray<sup>88</sup> and Nolan<sup>89</sup>, although there was speculation as to the involvement of such diaurated species in catalytic cycles. The lack of mechanistic insights also led to many groups to study  $\sigma,\pi$ -digold acetylides based on the original mechanistic proposal by Toste. Such species are not uncommon in organometallic chemistry and have been reviewed by Schmidbaur,<sup>90</sup> however, the suggested reactivity, in which they are precursors to the geminally diaurated species in catalytic cycles, was new.

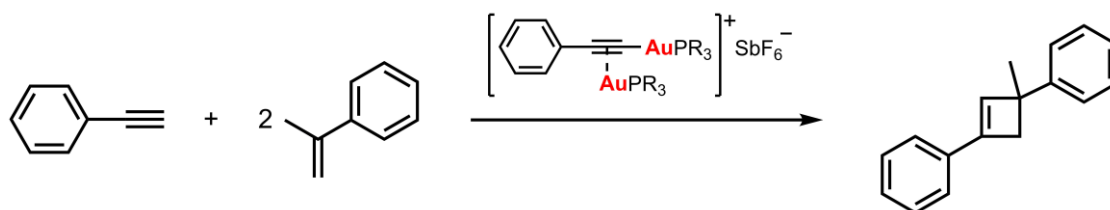
Widenhoefer and co-workers found that  $[\text{Au}(\text{IPr})]^+$  could form a  $\pi$ -complex with phenylacetylene at low temperatures which converts to a  $\sigma,\pi$ -digold acetylide at temperatures above  $-20\text{ }^\circ\text{C}$  (Scheme 1.19). The ease with which such species formed in the absence of a base led them to suggest that they may be generated in catalytic reactions involving terminal alkynes although their role in the catalytic cycle was uncertain.<sup>91</sup>



**Scheme 1.19.** Formation of  $\sigma,\pi$ -digold acetylide reported by Widenhoefer.

In the same year the group of Corma synthesised a series of  $\sigma,\pi$ -digold acetylides<sup>92</sup> and found them to possess good catalytic activity in the intermolecular alkene/alkyne [2+2] cycloaddition developed by Echavarren (Scheme 1.20).<sup>93</sup>

## 1.2. Organogold Complexes



**Scheme 1.20.** [2+2] Cycloaddition catalysed by  $\sigma,\pi$ -digold acetylides.

Another interesting recent example, although unrelated to homogeneous catalysis, is the  $\sigma,\pi$ -digold acetylide complex published by the group of Laguna in 2012. The  $\pi$ -coordinated gold bears two phosphine ligands and the structure of the complex which was determined by X-ray diffraction analysis shows a very unusual unsymmetrical coordination of the alkyne and the presence of gold-gold interactions (Figure 1.17).<sup>94</sup>

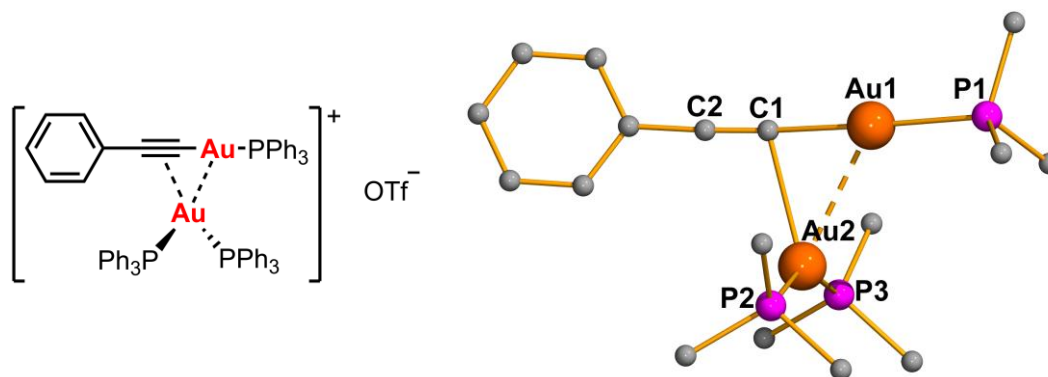
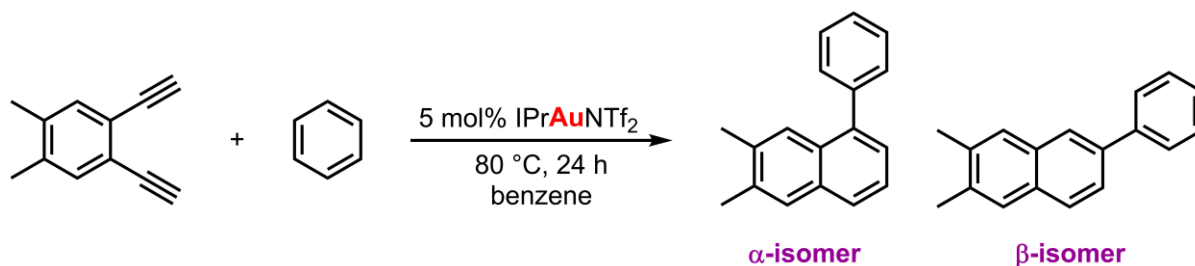


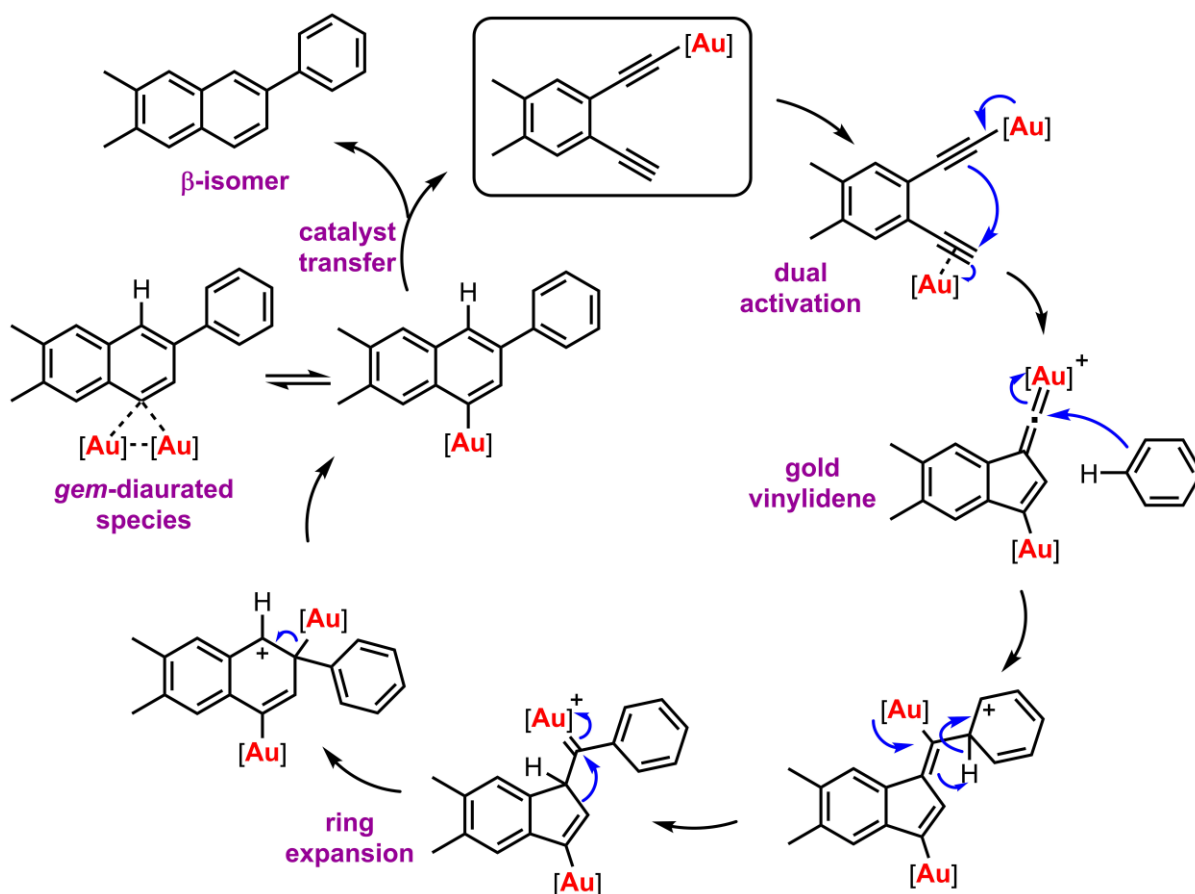
**Figure 1.17.** Molecular structure of  $\sigma,\pi$ -digold acetylide complex determined by single crystal X-ray diffraction. Hydrogen atoms and  $\text{PPh}_3$  phenyl rings are omitted for clarity. Selected bond lengths [Å]: Au(1)-Au(2) 2.9165(5), Au(1)-C(1) 2.033(5), Au(2)-C(1) 2.602(6), Au(2)-C(2) 3.134(6).

Following on from the work of Toste, Hashmi and co-workers carried out extensive studies on the dual activation of diynes to give *gem*-diaurated intermediates and developed a novel type of gold-catalysed transformation that requires dual activation of the substrate by the gold catalyst.<sup>95</sup> Studies of the cycloaddition between a diyne and benzene found that two different products formed with the  $\beta$ -isomer favoured in the presence of basic additives (Scheme 1.21).



**Scheme 1.21.** Gold-catalysed cycloaddition reaction between diyne and benzene.

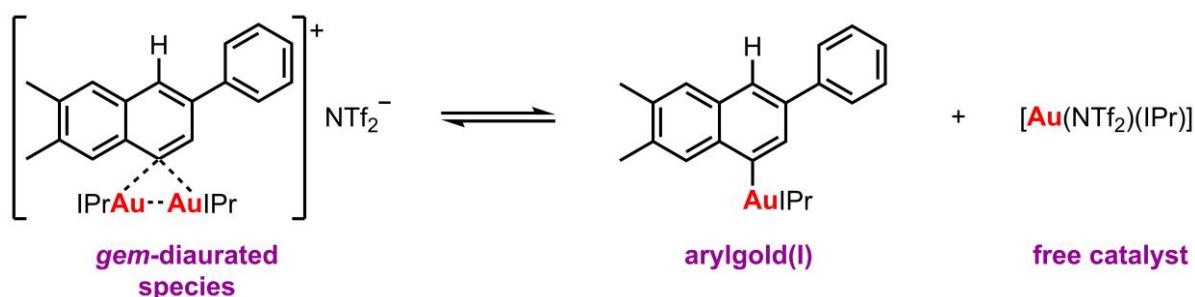
While the formation of the  $\alpha$ -isomer can be explained by the standard  $\pi$ -activation of the substrate by gold(I) and subsequent nucleophilic attack, the formation of the  $\beta$ -isomer must proceed through dual  $\sigma, \pi$ -activation. The catalytic cycle proposed by Hashmi involves initial formation of a gold(I) acetylide species which subsequently undergoes  $\pi$ -activation by a second  $[\text{Au}]^+$  unit at the other triple bond (dual activation) to activate the system for nucleophilic attack in the  $\beta$ -position (Scheme 1.22).



**Scheme 1.22.** Catalytic cycle proposed by Hashmi ( $[\text{Au}] = [\text{Au}(\text{SbF}_6)(\text{IPr})]$ ).

## 1.2. Organogold Complexes

In attempts to gain further insight into the mechanism the *gem*-diaurated species was isolated. Employing this as the catalyst led to formation of the  $\beta$ -isomer in high yields. Further investigations revealed an equilibrium between this *gem*-diaurated species and the arylgold(I) complex and free catalyst at high temperatures (Scheme 1.23) and for this reason the reaction proceeds. It was therefore concluded that the *gem*-diaurated complex is an excellent “off-cycle” or “reservoir” catalyst for this transformation.



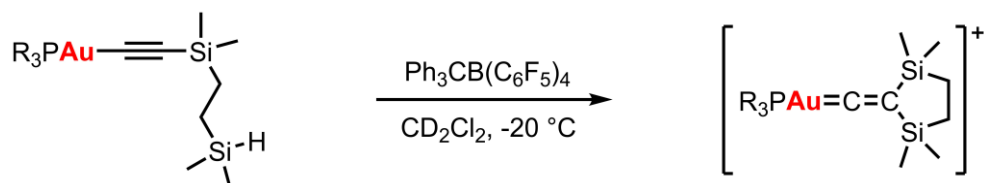
**Scheme 1.23.** Equilibrium between *gem*-diaurated complex and arylgold(I) complex and free catalyst.

Many more reports of dual gold catalysis have been published in the last two years and novel digold catalysts have been designed to enable the dual activation of the substrates. Very recently dual catalysis with one gold and one copper complex has been described as an alternative, more cost-effective method for the hydroxyphenylation of alkynes.<sup>96</sup>

Gold vinylidenes ( $\text{Au}=\text{C}=\text{CR}_2$ ) were suggested in the catalytic cycle for dual gold catalysis proposed by Hashmi in 2012 and were also independently suggested by the group of Zhang<sup>97</sup> in the same year, however neither group was able to successfully isolate any examples. In 2013, the group of Hashmi did successfully isolate the first higher cumulene of gold(I), a gold allenylidene (Figure 1.14(d)), which although not itself a catalytic intermediate could provide important bonding information. The nature of the ligands present had a huge influence on the Au-C bond: strong  $\pi$ -acidic ligands were found to compete for electron density on gold and weaken the Au-C bond, while strong  $\pi$ -donors shortened the Au-C bond, however, no significant Au-C double bond character could be confirmed.<sup>98</sup>

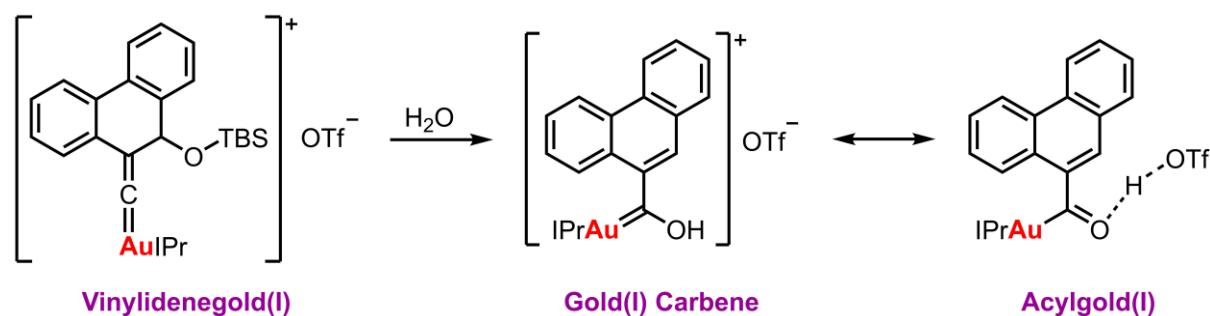
In 2015, Widenhoefer was able to isolate the first gold vinylidene (Figure 1.14(e)) by carrying out a hydride abstraction reaction with a (disilyl)ethylacetylide complex (Scheme 1.24). Although the complex was unstable at temperatures above -20 °C, they were able to fully

characterise it by NMR spectroscopy at  $-80\text{ }^{\circ}\text{C}$ .<sup>99</sup> This is to date the only species of its kind to be characterised by NMR spectroscopy.



**Scheme 1.24.** Synthesis of gold ( $\beta,\beta$ -disilyl)vinylidene complex.

Recently, the group of Fürstner studied the fate of gold vinylidene complexes finding that they can rearrange into gold carbenes (Scheme 1.25). In their studies they were able to isolate and characterise by X-ray diffraction the first example of an acylgold(I) species (Figure 1.14(g)).<sup>100</sup>



**Scheme 1.25.** Conversion of vinylidenegold(I) complex into acylgold(I) complex.

Gold(I) carbenes are suggested as intermediates in many catalytic cycles and also have a broad reactivity. They therefore have attracted significant interest. A huge effort has been made into gaining insight into the nature of the Au-C bond, and there has been debate as to whether such species are more carbocation-like or carbene-like.<sup>101-103</sup> In 2014, Fürstner and co-workers were able to isolate the first gold(I) carbene complex with no heteroatom stabilisation, a species closely related to gold-carbene intermediates in gold(I) catalysed reactions (Figure 1.18).<sup>104</sup> However, the strong electron donating character of the 4-methoxy substituent stabilises the carbene centre and there is little back-donation from gold. In the same year the group of Straub successfully prepared a gold carbene complex with significant Au-C double bond character by using a sterically demanding IPr ligand. The Au-CMe<sub>2</sub> distance was found to be 2.014(6) Å.<sup>105</sup> The group of Bourissou went on to synthesise and structurally characterise a gold(I) diphenylcarbene complex with a *o*-carborane diphosphine ligand (Figure 1.14(f)). The bending

induced by the diphosphine raises the energy of the gold  $d_{xz}$  orbital which increases significantly the  $\pi$ -back-donation. This complex has the shortest Au-C bond to date at just 1.984(4) Å.<sup>106</sup>

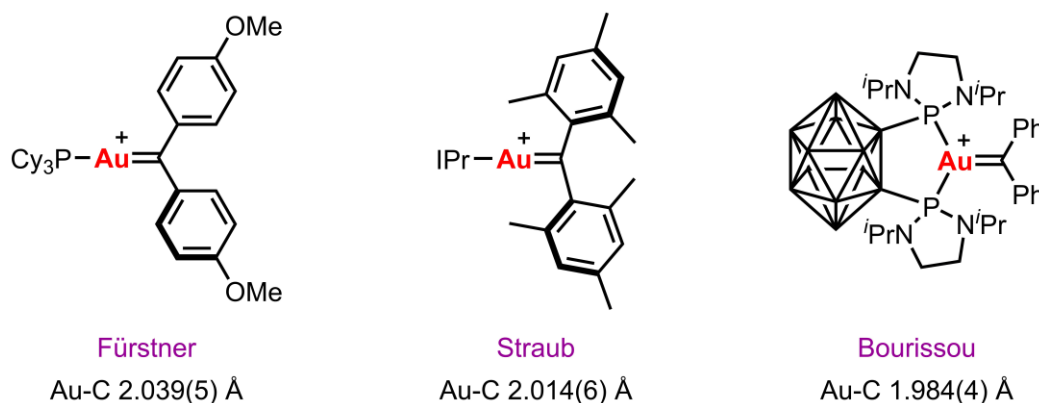
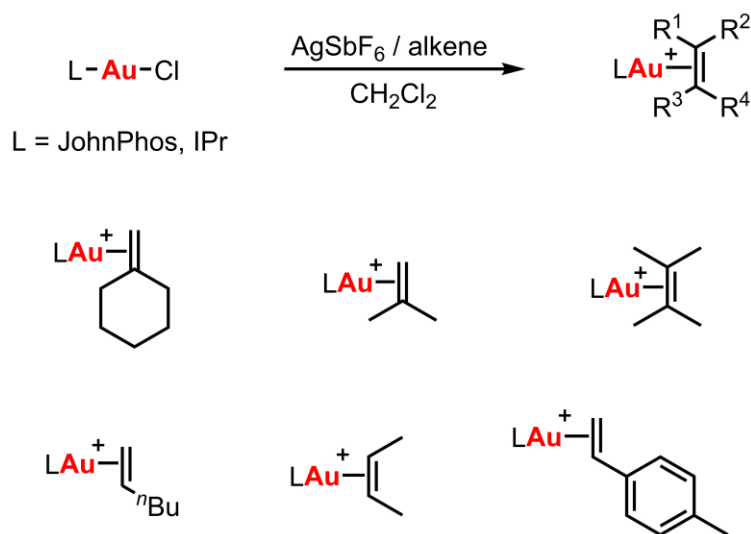


**Figure 1.18.** Characterised gold(I) carbene species and corresponding Au-C bond lengths.

#### 1.2.4.2.2. Catalytic Intermediates – $\pi$ complexes

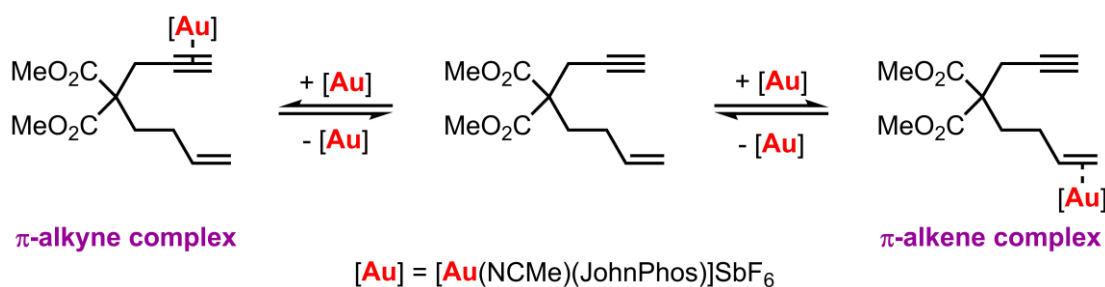
The vast majority of gold(I) catalysed reactions involve activation of a C-C multiple bond by  $\pi$ -coordination to gold(I). The isolation of such complexes is therefore of interest to gain a better understanding of catalytic mechanisms.

Gold(I)  $\pi$ -alkene complexes were first described by Chalk in 1964 with the preparation of the gold(I) cyclooctadiene complex which was characterised by elemental analysis and infrared spectroscopy.<sup>107</sup> The first example to be characterised by X-ray crystallography was [AuCl(cis-cyclooctane)], prepared by Weiss in 1987.<sup>108</sup> Many gold(I)  $\pi$ -alkene complexes have very poor thermal stability in solution and hence well characterised examples are scarce. In 2009 Widenhoefer made significant progress by introducing a general approach for the synthesis of  $\pi$ -alkene complexes by halide abstraction from a chloro-gold(I) JohnPhos or IPr complex using AgSbF<sub>6</sub> and subsequent addition of alkene (Scheme 1.26).<sup>109,110</sup> The  $\pi$ -alkene complexes which formed were stable and several examples were characterised by X-ray diffraction. The analogous reaction with [AuCl(PPh<sub>3</sub>)] did give the alkene complexes at low temperatures but they were unstable above -20 °C and the formation of the bis-phosphine complex [Au(PPh<sub>3</sub>)<sub>2</sub>] was observed.<sup>111</sup> The same methodology with the JohnPhos and IPr ligands also allowed the isolation and structural characterisation of the first gold(I)  $\pi$ -allene complex.<sup>112</sup>



**Scheme 1.26.** Gold(I)  $\pi$ -alkene complexes prepared by Widenhoefer.

Gold is generally known for its high affinity to C-C triple bonds rather than double bonds, previously assumed to be a result of the higher electron density of the bond attracting the highly electrophilic gold(I). An interesting study into the  $\pi$ -bonding situation in an enyne at 223 K, a temperature at which the catalytic cyclisation reaction is avoided, found the presence of two distinct  $\pi$ -complexes (Scheme 1.27).<sup>113</sup> Spectra show a close 1:1 ratio of the gold complexes, however the catalytic reaction always proceeds via the  $\pi$ -alkyne complex. Electrophilic and nucleophilic attacks are more thermodynamically favoured for alkynes and hence the alkynophilicity of gold(I) in catalytic reactions is more a result of the reactivity of the  $\pi$ -complex than the preference in coordination.



**Scheme 1.27.** Equilibrium between gold  $\pi$ -alkyne and gold  $\pi$ -alkene complexes in enyne.

The first examples of gold(I)  $\pi$ -alkyne complexes to be characterised by X-ray diffraction were reported in 1998. These complexes were prepared by the reaction of  $[\text{AuCl}(\text{tht})]$  with the cycloheptynes 3,3,6,6-tetramethyl-1-thiacyclohept-4-yne-1,1-dioxide and 3,3,6,6-tetramethyl-



1-thiacyclohept-4-yne and in both cases a trigonal planar geometry about the gold centre was observed (Figure 1.19).<sup>114</sup>

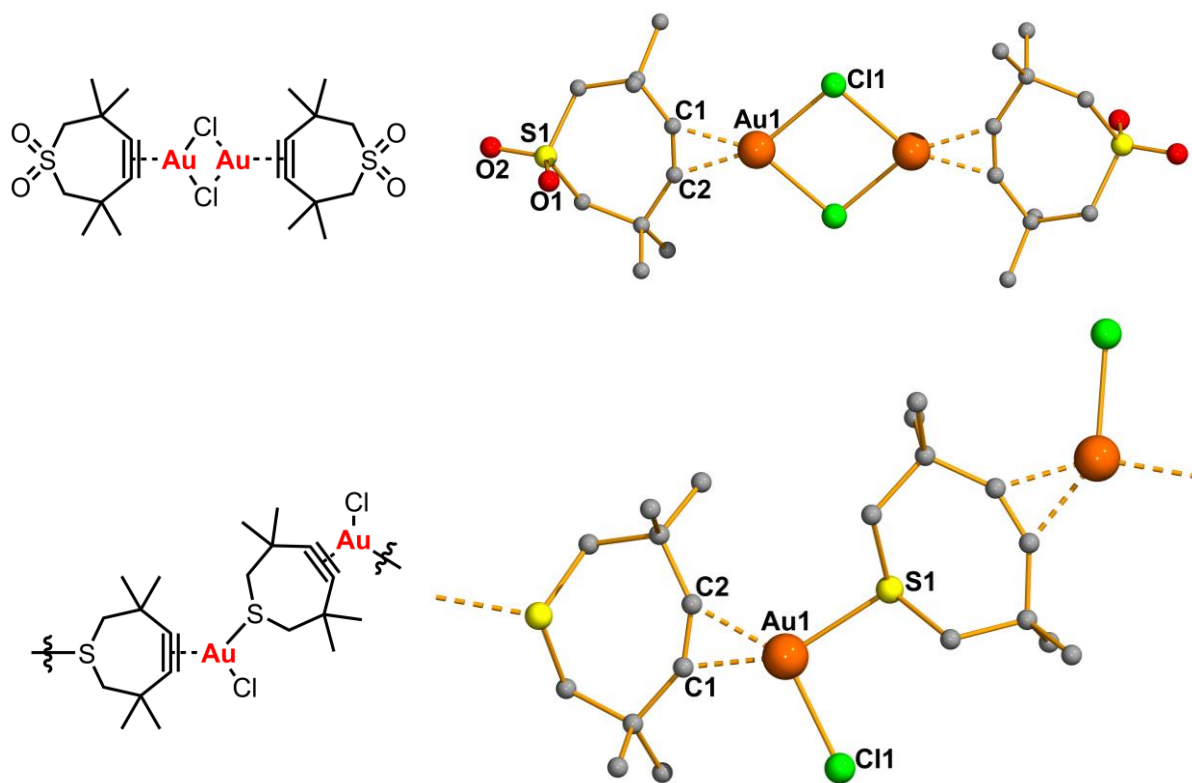
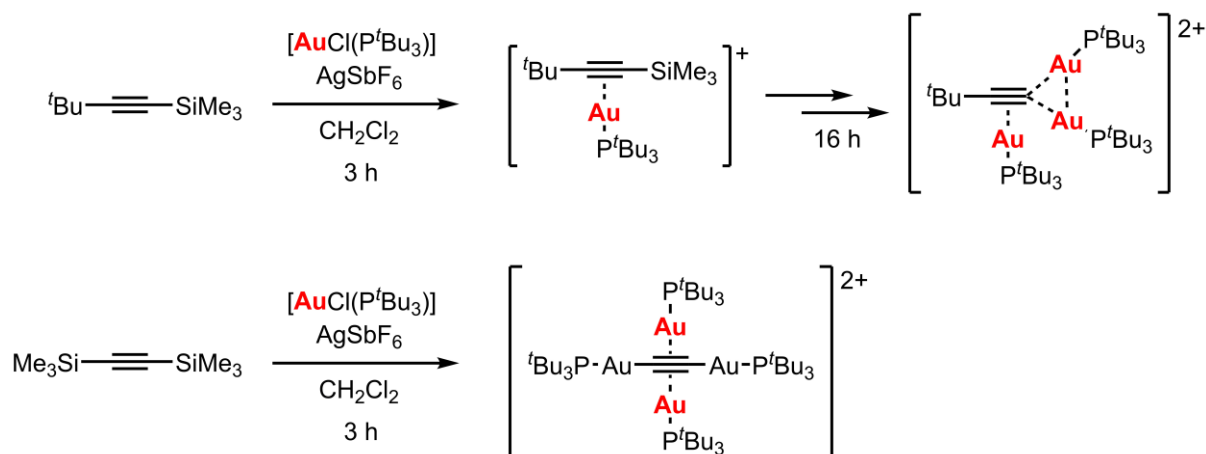


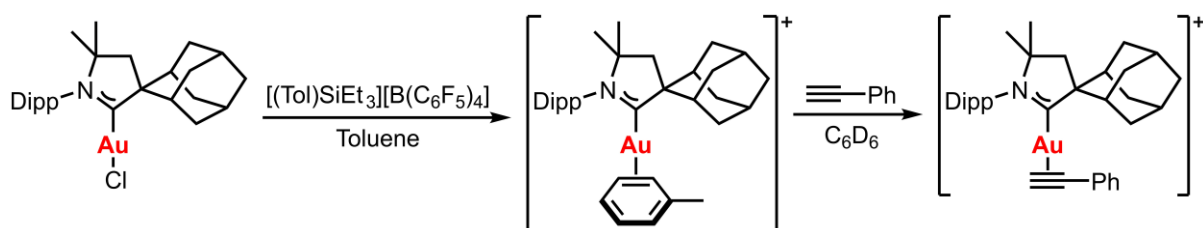
**Figure. 1.19.** Molecular structures of gold  $\pi$ -alkyne complexes.

Non-cyclic  $\pi$ -alkyne gold(I) complexes have been reported but are generally unstable and decompose rapidly at room temperature. Some interesting examples were prepared by the group of Russell using TMS-protected alkynes and  $[\text{AuCl}(\text{P}^t\text{Bu}_3)]$ , with  $\text{AgSbF}_6$  as a halide abstractor. With short reaction times the mono-gold  $\pi$ -alkyne complex was obtained, as expected, however, increasing the reaction time led to desilylation and a triaurated species. When a doubly silylated alkyne was employed the tetra-aurated alkyne bearing two  $\sigma$ -coordinated and two  $\pi$ -coordinated gold centres was obtained (Scheme 1.28). The complexes were successfully characterised by single crystal X-ray diffraction, although the authors did note that it is likely that a different structure exists in solution since only one peak is observed in the  $^{31}\text{P}\{^1\text{H}\}$  NMR spectrum, even at low temperatures.<sup>115</sup>



**Scheme 1.28.** Synthesis of mono, tri and tetra-aurated alkyne species.

In 2007, Bertrand and co-workers were able to successfully prove the formation of a gold(I) terminal alkyne complex in a catalytic cycle. Using the very strongly  $\sigma$ -donating CAAC ligand they first prepared a catalytically active toluene derivative by reaction of the chloro gold(I) complex with a silylium-like salt,  $[(\text{Tol})\text{SiEt}_3][\text{B}(\text{C}_6\text{F}_5)_4]$ . The product was fully characterised by X-ray diffraction and was found to catalyse the cross-coupling reaction of enamines with terminal alkynes to give allene products. Addition of phenylacetylene in the absence of enamine afforded the alkyne complex (Scheme 1.29), which was successfully characterised by NMR spectroscopy. This is one of very few examples of a terminal alkyne  $\pi$ -bound to gold(I).<sup>116</sup>



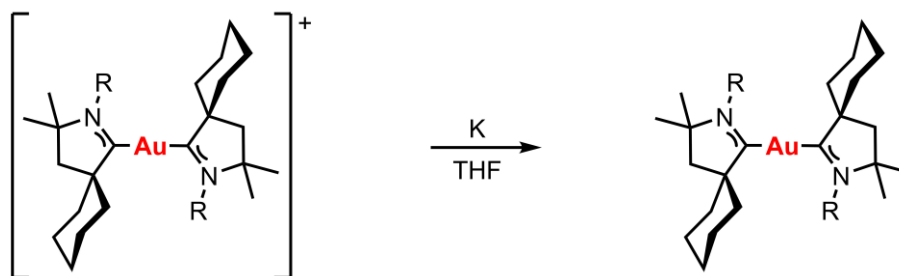
**Scheme 1.29.** Synthesis of a gold(I) complex bearing  $\pi$ -bound terminal alkyne.

#### 1.2.4.3. Gold(0) Complexes

In 2013 the group of Bertrand made a significant discovery in the field of organogold chemistry by the successful isolation of the first organogold complex with gold in oxidation state 0. Reduction of the cationic bis-CAAC gold(I) precursor using potassium in THF gave the paramagnetic product in which gold is a radical with electronic configuration  $5d^{10}6s^1$

## 1.2. Organogold Complexes

(Scheme 1.30). ESR spectroscopy and crystal structure analysis confirmed the identity of the gold(0) complex (Figure 1.20).



**Scheme 1.30.** Synthesis of a gold(0) complex.

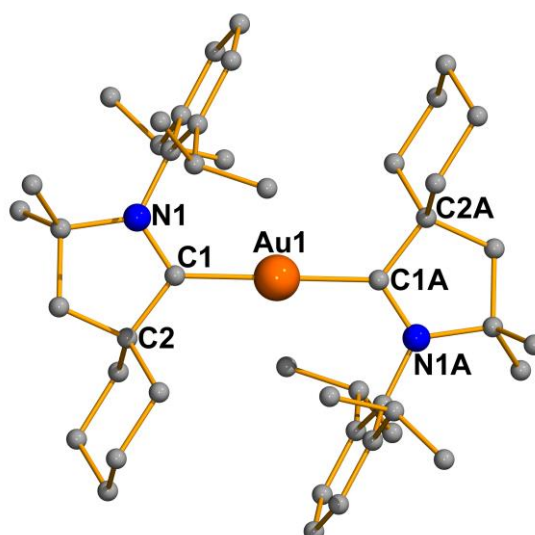
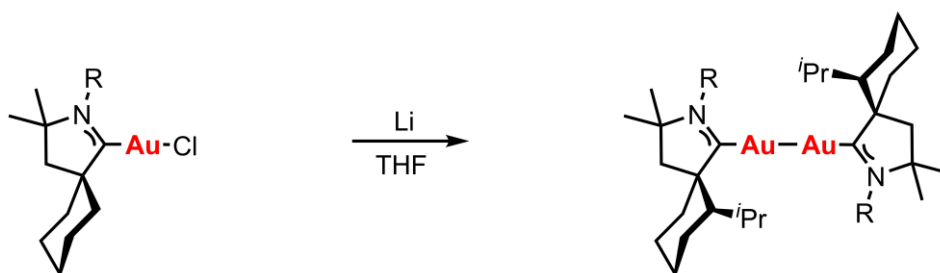


**Figure 1.20.** Molecular structure of gold(0) complex determined by single crystal X-ray diffraction. Hydrogen atoms are omitted for clarity. Selected bond lengths [Å] and angles [°]: Au(1)-C(1) 1.991, N(1)-C(1) 1.344(2), C(1)-C(2) 1.519(4), C(1)-Au(1)-C(1A) 180.0.

Using the same ligand, the group was also able to prepare the first authentic complex of the neutral digold molecule, Au<sub>2</sub>, previously only known as a component of gold vapour. In this case reduction of the chloro gold(I) complex with lithium in THF gave the product (Scheme 1.31) which was again successfully characterised by X-ray diffraction (Figure 1.21). A quasi-linear C-Au-Au-C arrangement is observed which is isolobal to dihydrogen, H-H.



**Scheme 1.31.** Synthesis of the first complex of neutral Au<sub>2</sub> molecule.

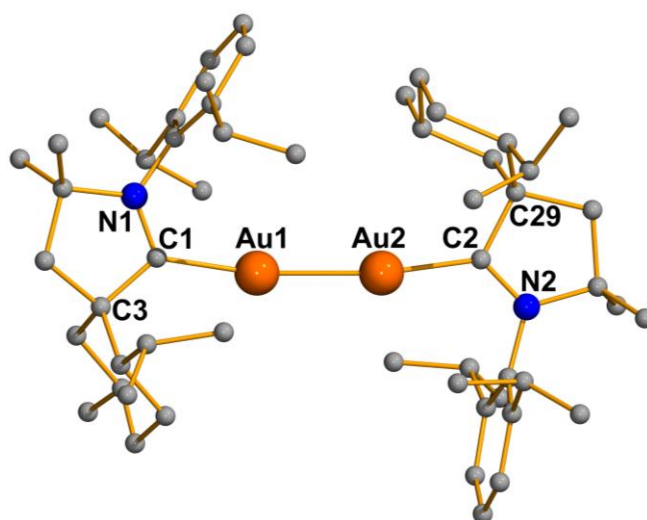


**Figure 1.21.** Molecular structure of the first complex of Au<sub>2</sub> determined by single crystal X-ray diffraction. Hydrogen atoms are omitted for clarity. Selected bond lengths [Å] and angles [°]: Au(1)-Au(2) 2.542(1), Au(1)-C(1) 2.101(8), Au(2)-C(2) 2.043(9), N(1)-C(1) 1.316(9), C(1)-C(3) 1.52(1), N(2)-C(2) 1.33(1), C(2)-C(29) 1.53(1), C(1)-Au(1)-Au(2) 170.6(2), Au(1)-Au(2)-C(2) 172.3(3).

### 1.3. Applications of Organogold Complexes

Many early studies into the organometallic chemistry of gold had the simple aim of gaining further understanding of the fundamental coordination chemistry of this metal. Early organogold complexes were considered laboratory curiosities with little potential for any useful application. More recently, however, organogold complexes have found potential use in a huge variety of different applications as a result of their photophysical, biological and catalytic properties. Many of the most recent developments in organogold chemistry have arisen in the search for new complexes with enhanced properties for specific applications. The most important applications of organogold complexes are summarised in Figure 1.22.

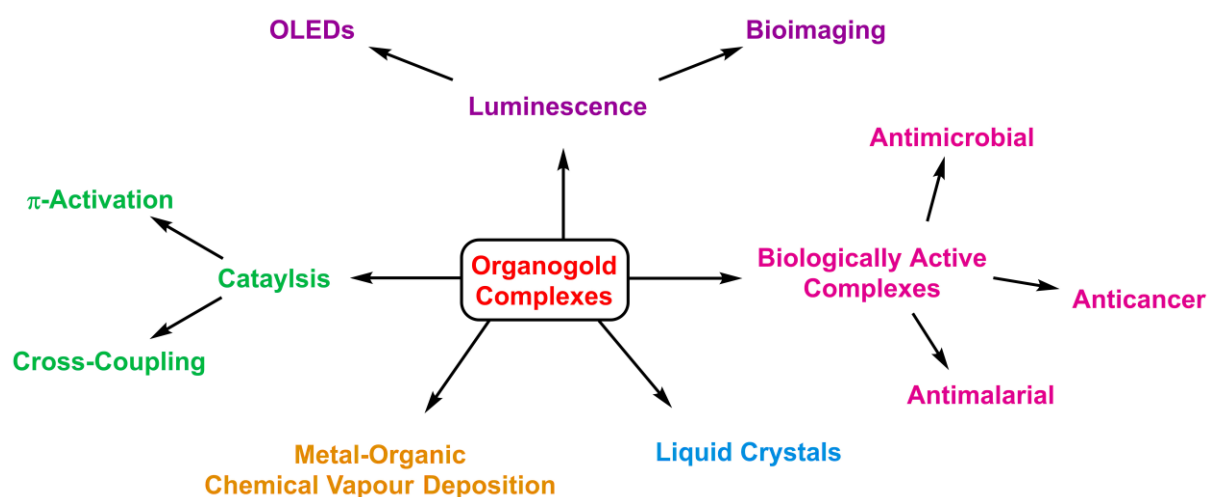


**Figure 1.22.** Applications of organogold complexes.

The huge number of different application shows just how versatile organogold complexes are and highlights the need for further research in this area.

## 1.4. Objectives

The main objective of this PhD thesis was to prepare novel organogold complexes which, in addition to providing further insight into the structure and bonding in coordination complexes of gold, could also possess properties such as luminescence or biological activity. Phosphorus ylide, allenyl, NHC and propargyl derivatives of gold were chosen as suitable synthetic targets. The objectives for each chapter are outlined below.

### 1.4.1. Phosphorus Ylide Gold Complexes

Phosphorus ylides complexes of gold are known to be highly stable and the coordination chemistry of many simple phosphorus ylides with gold has been widely studied. However, complexes of gold with the cyano-functionalised ylide triphenylphosphoniumcyanomethylide have been little explored.<sup>117</sup> This ylide could potentially have a very rich coordination chemistry with gold since there exists the possibility for coordination through not only the ylide  $\alpha$ -carbon, but also the nitrogen of the nitrile group (Figure 1.23).

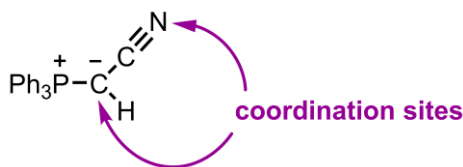
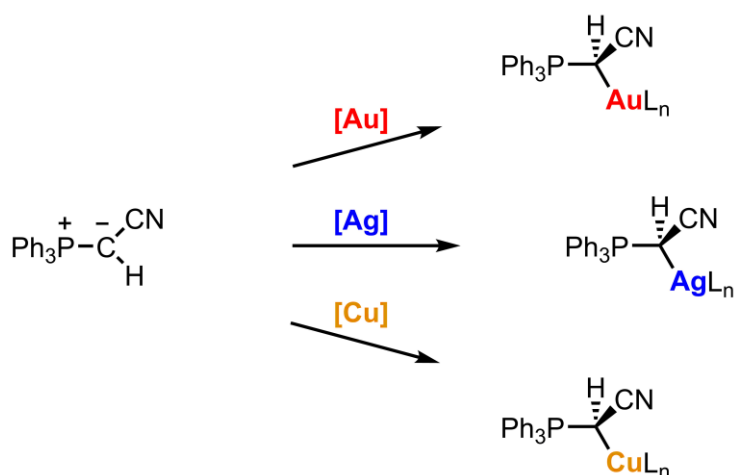


**Figure 1.23.** Coordination sites of triphenylphosphoniumcyanomethylide.

Our first objective was to explore the coordination chemistry of triphenylphosphoniumcyanomethylide with gold by preparing simple mononuclear complexes of both gold(I) and gold(III) with different anionic and neutral ligands at the gold centre. The preparation of derivatives of the other coinage metals, copper and silver, would allow comparisons to be made between the coordination chemistry of these elements (Scheme 1.32).



**Scheme 1.32.** Preparation of complexes of the coinage metals with triphenylphosphoniumcyanomethylide.

Triphenylphosphoniumcyanomethylide can be further deprotonated to give the ylide unit which can act as a bridging ligand between two metal centres (Scheme 1.33). Polynuclear gold derivatives are of interest since complexes in which gold atoms are in close proximity often exhibit luminescence. An additional objective was therefore to prepare dinuclear or polynuclear derivatives of the ylide with gold and the other coinage metals and to explore their luminescence.



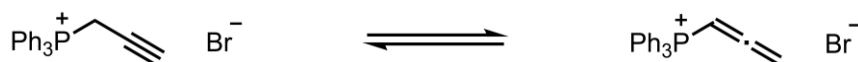
**Scheme 1.33.** Dinuclear derivatives of triphenylphosphoniumcyanomethyliide.

Despite their high stability and generally high solubility, the potential biological activity of phosphorus ylide gold complexes has not previously been studied. Our final objective in this area was to study the anticancer properties of the phosphorus ylide gold complexes.

### 1.4.2. Allenyl Gold Complexes

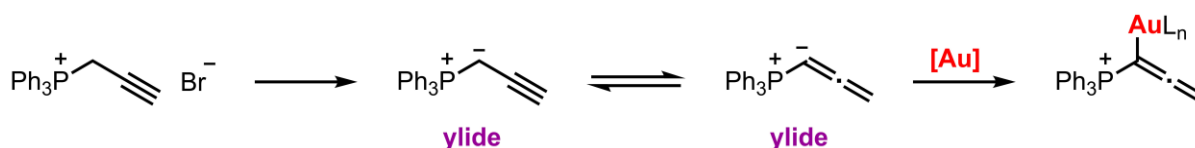
The phosphonium salt triphenylpropargylphosphonium bromide is known to readily tautomerise to the allenyl form in solution in different solvents and in the presence of a base (Scheme 1.34).<sup>118,119</sup> This phosphonium salt is also the precursor to a phosphorus ylide and hence has the potential for the preparation of stable derivatives of gold. Allenyl gold derivatives

are unknown in the literature and hence their potential synthesis from triphenylpropargylphosphonium bromide is of interest.



**Scheme 1.34.** Tautomerisation of triphenylpropargylphosphonium bromide to the allenyl form.

Our first objective was to explore the coordination chemistry of the ylide triphenylphosphoniumpropargylide or its allenyl tautomer with gold with the aim of preparing the first allenyl derivatives of gold(I) and gold(III) (Scheme 1.35).



**Scheme 1.35.** Synthesis of allenyl gold complexes from triphenylpropargylphosphonium bromide.

Our second objective was to explore the importance of the heteroatom in the tautomerisation of this phosphonium salt. Therefore, we aimed to prepare propargyl functionalised ammonium and sulfonium salts and explore their coordination chemistry with gold (Figure 1.24).



**Figure 1.24.** Propargyl functionalised phosphonium, ammonium and sulfonium salts.

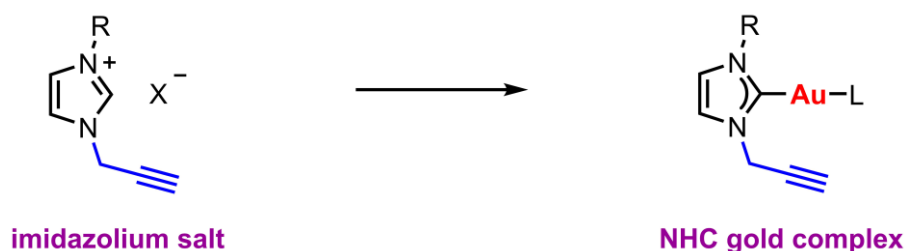
### 1.4.3. NHC Gold Complexes

NHC gold complexes are of ever-increasing interest for their potential use in homogeneous gold catalysis as well as for their luminescence and biological properties. Many synthetic methods for the preparation of these complexes are known, the most straightforward involve starting from the corresponding imidazolium salts. A huge range of complexes are possible due to the variety of substituents which can be introduced at the nitrogen atoms. Propargyl- and allenyl- functionalised NHC gold complexes, however, are unknown.



## 1.4. Objectives

Continuing our study into propargyl-allenyl tautomerism, we aimed to prepare propargyl functionalised imidazolium salts and their corresponding NHC gold complexes (Scheme 1.36). Since the propargyl side-arm is sterically small, the previously reported methods for the synthesis of NHC gold complexes from imidazolium salts are not suitable. Therefore, our first objective was to find a suitable synthetic method for the synthesis of the propargyl functionalised NHC gold complexes.



**Scheme 1.36.** Synthesis of propargyl functionalised NHC gold complexes.

NHC gold phosphine complexes are rare in the literature, but could potentially possess interesting photophysical properties due to the presence of two strongly  $\sigma$ -donating ligands. Cationic bis-NHC complexes are known to have potent anticancer activity<sup>120</sup> and hence cationic NHC gold phosphine complexes could show similar biological activity since phosphines and NHCs are comparable. We therefore aimed to prepare gold phosphine derivatives of our propargyl functionalised NHCs and study their luminescence and anticancer activity (Figure 1.25).

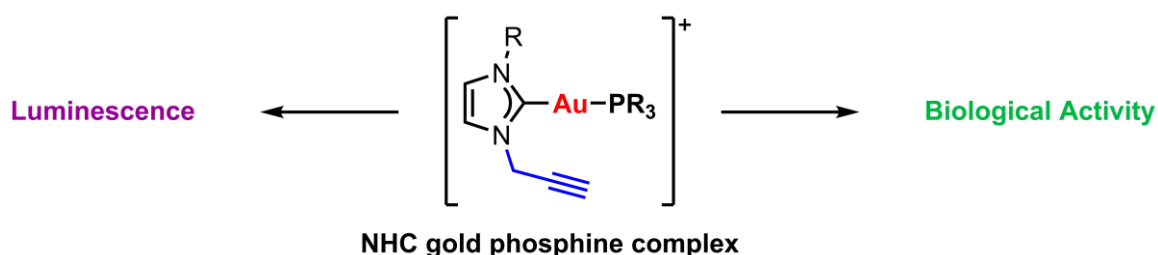
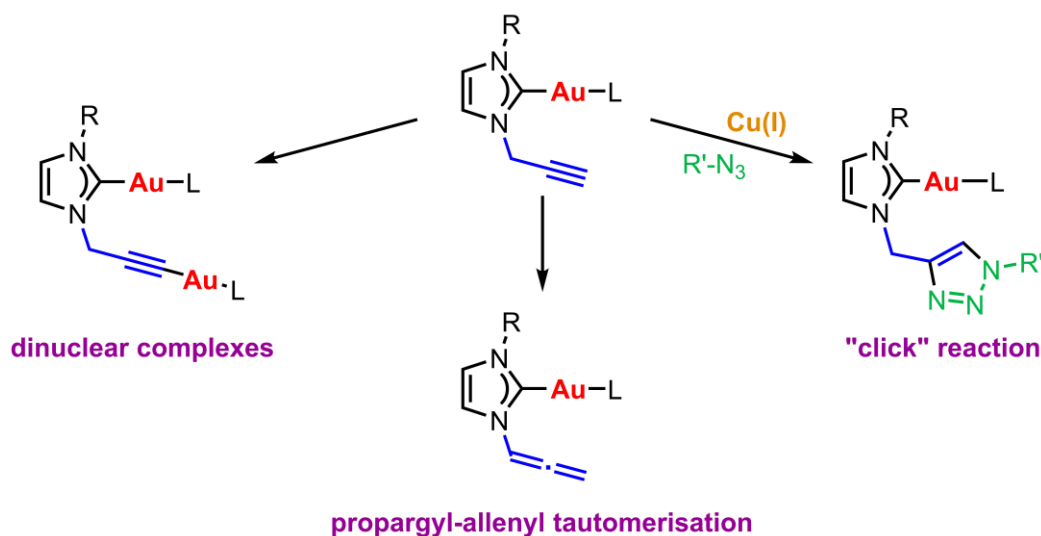


**Figure 1.25.** Propargyl functionalised NHC gold phosphine complexes.

Another objective was to explore the potential functionalisation of the propargyl side-arm. This could provide an additional coordination site for the preparation of dinuclear or polynuclear complexes. However, it could also undergo tautomerisation to the allene or participate in a copper catalysed “click” reaction with an azide (Scheme 1.37).



**Scheme 1.37.** Functionalisation of the propargyl side-arm.

#### 1.4.4. Propargyl Gold Complexes

Alkynyl gold complexes have recently been found to show promising anticancer activity.<sup>121-123</sup> Due to the ease of synthesis of both the substrates and the corresponding gold complexes, we aimed to prepare a series of propargyl gold phosphine complexes, where gold is bound at the terminal alkyne. In order to explore the effect of the heteroatom on the activity of the complex, we chose to compare propargylamines, propargylethers and propargylsulfides (Figure 1.26). In these cases, the lack of positive charge at the heteroatom would disfavour deprotonation at the  $\alpha$ -carbon atom and therefore tautomerism to the allene would be extremely unlikely.

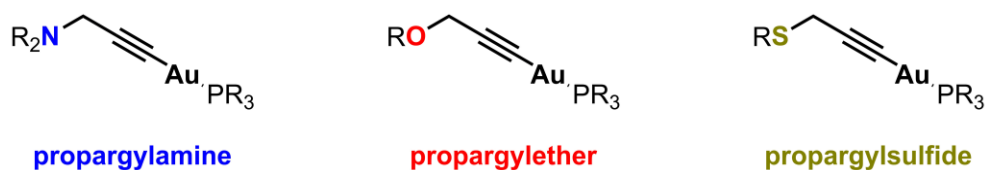


**Figure 1.26.** Propargylamine, propargylether and propargylsulfide gold phosphine complexes.

Our first objective was to prepare the mononuclear propargyl gold phosphine derivatives and study their anticancer activity with the aim of observing any effect caused by changing the heteroatom in the substrate or the nature of the phosphine bound to the gold centre. We then aimed to prepare dinuclear derivatives which could potentially have enhanced anticancer activity due to the presence of two metal centres.

# Chapter 2 – Phosphorus Ylide Complexes

## 2.1. Introduction

Phosphorus ylides are today classed amongst some of the most important reagents in organic chemistry, finding use in the synthesis of a wide variety of fundamental biologically active compounds, pharmaceuticals and natural products.<sup>124-126</sup> These zwitterionic species were first discovered over 100 years ago,<sup>127</sup> however it is only really in the last 50 years that the true synthetic potential of these compounds has been realised and there has been rapid growth in this field.<sup>124</sup>

The application of phosphorus ylides as ligands in organometallic chemistry is an active area of research. This is due not only to the outstanding potential of ylides to form transition metal-carbon bonds, but also the range of possible bonding modes and incredible versatility of these compounds.<sup>128</sup> The steric and electronic requirements of ylides can be tuned and it is possible to design ylides with several potential donor atoms allowing polynuclear species to be synthesised.<sup>129</sup> The enormous variety of oxidation levels, coordination numbers and complex geometries characteristic of metals, along with the bonding features of phosphorus ylides give rise to incredible possibilities in this branch of coordination chemistry.

Complexes of gold with phosphorus ylides initially sparked interest because of their possible application in the treatment of arthritis and use in catalysis.<sup>130,131</sup> Subsequent studies found that ylide-gold complexes are particularly stable towards oxidation and hydrolysis, a feature which is uncommon in the organometallic chemistry of gold<sup>132</sup> and one which led a considerable amount of attention to be given to this area. Despite this, there are still many areas of the field of phosphorus ylide-gold chemistry, such as the synthesis of gold derivatives of functionalised phosphorus ylides, that have until now been relatively untouched.

### 2.1.1. Basic Concepts

The most widely accepted definition of an ylide is “*a substance in which a carbanion is attached directly to a heteroatom carrying a substantial degree of positive charge and in which*

the positive charge is created by the sigma bonding of substituents to the heteroatom".<sup>128</sup> Ylides with a variety of different heteroatoms are known, including nitrogen,<sup>133,134</sup> oxygen,<sup>135</sup> sulfur<sup>136</sup> and arsenic.<sup>137</sup> However, phosphorus ylides are by far the most widely used and extensively studied.<sup>128</sup>

Phosphorus ylides can be described by two canonical structures: ylide and ylene (Figure 2.1).

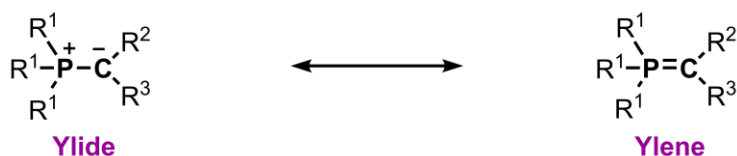


**Figure 2.1.** Canonical forms of phosphorus ylides

The ylide form is a zwitterion, reflecting the highly polar nature of the phosphorus-carbon bond, whereas the ylene or phosphorane canonical form comprises a double bond between the carbon and the phosphorus atoms and no formal charges are present. Many theoretical calculations have shown that the highest occupied molecular orbital of most ylides is strongly localised on the ylide carbon and it is therefore the polar ylide canonical structure which makes the major contribution to the ground state of phosphorus ylides and the contribution of the ylene form is minimal.<sup>138</sup>

Phosphorus ylides may also be classified according to the nature of the substituents at the ylide  $\alpha$ -carbon atom. The presence of groups which allow the delocalisation of the negative charge from the carbanionic centre confer stability to the ylide and reduce its basicity. Three main types of ylide exist: “stabilised” in which there is at least one strong electron withdrawing group on the  $\alpha$ -carbon, stabilising the formal negative charge; “semi-stabilised” in which the presence of at least one moderately conjugating group such as an alkenyl or aryl substituent has a stabilising effect; “non-stabilised” which usually have only alkyl substituents or hydrogen on the  $\alpha$ -carbon (Figure 2.2).<sup>139</sup> Stabilised ylides are weak bases and are generally unreactive towards moisture and oxygen. Consequently, they can often be prepared under ambient conditions and stored for weeks or months without decomposition. Non-stabilised ylides, however, are far more reactive and often have to be generated *in situ* under inert atmosphere to avoid undesired reactions with oxygen or moisture.

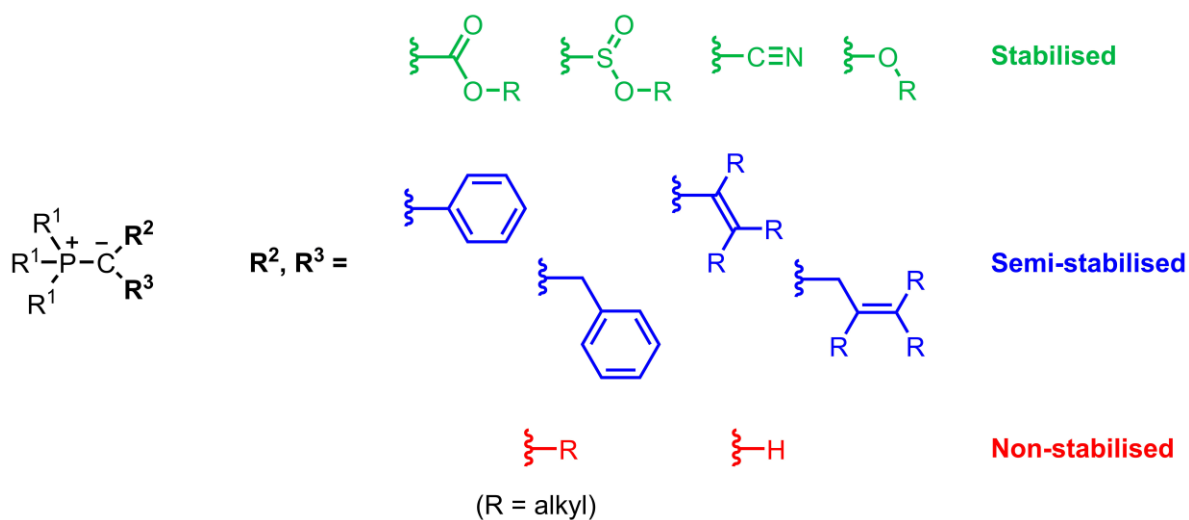


**Figure 2.2.** Types of ylides

Many stabilised and non-stabilised ylides have been structurally characterised by single crystal X-ray diffraction, such as the non-stabilised ylide, triphenylphosphoniumisopropylide (Figure 2.3(a)),<sup>140</sup> and the ester stabilised ylide (Figure 2.3(b)),<sup>141</sup> allowing important bonding information to be obtained.

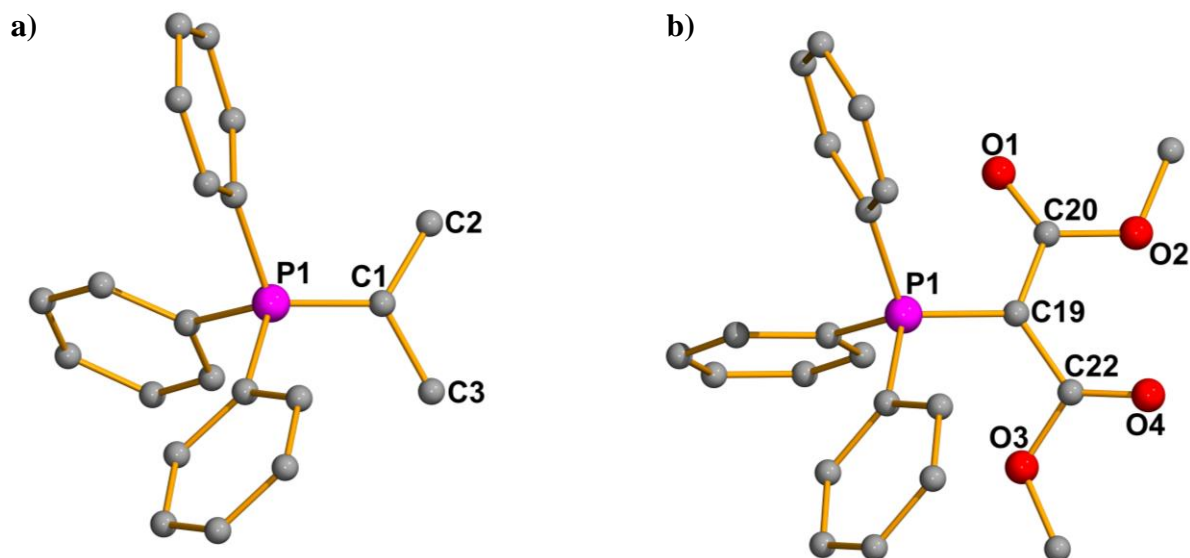


**Figure 2.3.** Molecular structures of complexes non-stabilised ylide (a) and stabilised ylide (b) determined by single crystal X-ray diffraction. Selected bond lengths [Å] and angles [°]: a: P(1)-C(1) 1.678(2), C(1)-C(2) 1.503(2), C(1)-C(3) 1.508(3), P(1)-C(1)-C(2) 122.1(1), P(1)-C(1)-C(3) 120.1(1), C(2)-C(1)-C(3) 114.1(2); b: P(1)-C(19) 1.745(2), C(19)-C(20) 1.438(3), C(19)-C(22) 1.457(3), P(1)-C(19)-C(20) 115.6(1), P(1)-C(19)-C(22) 120.1(2).

Stabilised ylides feature a trigonal planar carbanion, whereas non-stabilised ylides can have a slightly pyramidal structure. The P-C<sub>ylide</sub> bond in phosphorus ylides is typically in the range 1.63-1.75 Å, somewhat shorter than a classical P-C single bond (1.87 Å).<sup>142</sup> This would suggest a degree of double bond character; however, calculations have found there to be very little resistance to rotation about the P-C<sub>ylide</sub> bond. Comparison of the simplest ylides of phosphorus, oxygen, nitrogen and sulfur found the barrier for rotation for the phosphonium ylide H<sub>3</sub>P-CH<sub>2</sub> to be 0.24 kcal mol<sup>-1</sup>, compared to 5.6 kcal mol<sup>-1</sup> for H<sub>2</sub>O-CH<sub>2</sub>, 2.3 kcal mol<sup>-1</sup> for H<sub>3</sub>N-CH<sub>3</sub> and 21.2 kcal mol<sup>-1</sup> for H<sub>2</sub>S-CH<sub>2</sub>.<sup>143</sup> This is particularly surprising since nitrogen ylides are found to have C-N distances in the range typical for a C-N single bond.

Phosphorus ylides are generally more stable than the ylides of other elements. This was initially believed to be a result of an interaction of the lone pair of electrons in the ylide  $\alpha$ -carbon p-orbital with the empty d-orbitals on the phosphorus atom (Figure 2.4).<sup>144</sup> Ylides of nitrogen would not have this interaction since the d-orbitals on nitrogen are far too high in energy to participate in bonding and hence it could explain their lower stability compared to the phosphorus analogues. However, theoretical studies suggest very little participation of the phosphorus d-orbitals in the P-C<sub>ylide</sub> bond and other theories about the nature of the ylide bond in phosphorus ylides are now favoured.<sup>145,146</sup>

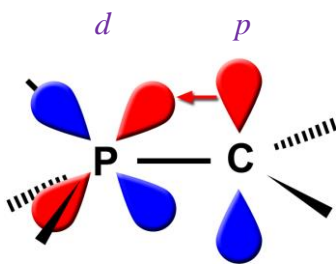


**Figure 2.4.**  $\pi$ -bond formed by back donation from carbon p-orbital to phosphorus d-orbital.

In 1977, Bernardi and co-workers suggested an alternative model for the bonding in phosphorus ylides in which the double bond is again formed by a  $\sigma$ -bond from phosphorus to carbon and a  $\pi$ -back-bond from carbon to phosphorus, but in this case the carbon p-orbital interacts with the  $\sigma^*$  LUMO orbital of the phosphine (Figure 2.5(a)). This type of interaction would also be possible in the perpendicular orientation (Figure 2.5(b)) and hence could explain the low barrier to rotation in phosphorus ylides.<sup>147</sup> Although phosphorus ylides were one of the

first types of compounds to have their bonding described in this way, this bonding description, termed negative hyperconjugation, is now relatively common.<sup>148-151</sup>

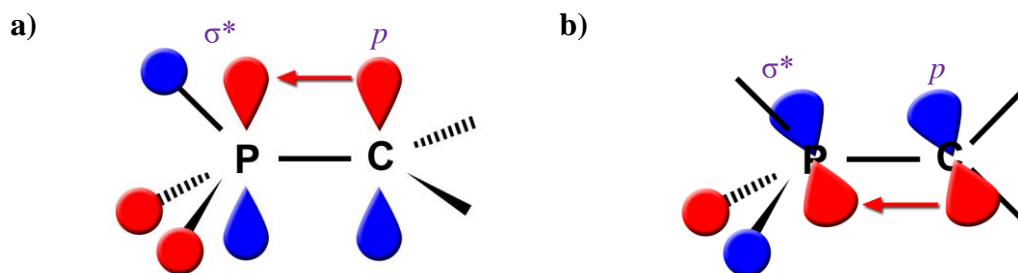


**Figure 2.5.**  $\pi$ -bond formed by back donation from carbon p-orbital to phosphine  $\sigma^*$  antibonding orbital in two different orientations.

Another explanation for the bonding in phosphorus ylides suggests that rather than the existence of a  $\sigma$ -bond and  $\pi$ -back-bond, there are actually two electron pairs in two  $\Omega$  bonds or “banana bonds” (Figure 2.6). This bonding description was given by Dixon in the early 1980s and would explain the shorter P-C<sub>ylide</sub> bond length compared to a normal P-C single bond.<sup>152</sup> However, this model clearly suggests that the P-C bond has a significant degree of double bond character and the low barrier for rotation about the P-C bond cannot be well explained.

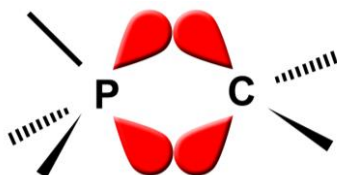


**Figure 2.6.** Banana bonding model for the bonding in phosphorus ylides.

One final explanation for the short P-C bond in ylides is a simple electrostatic shortening in which a coulombic attraction between the positively charged phosphorus and the negatively charged carbon atom results in a reduction in bond length.<sup>146</sup>

### 2.1.2. Phosphorus Ylides as Ligands

The excess negative charge on the ylide carbon atom results in ylides having high Brønsted basicity, donor activity and nucleophilicity; properties which make them very good ligands.<sup>132</sup> Even stabilised ylides, despite being less nucleophilic, will readily coordinate to transition metals. Phosphorus ylides generally act as  $\sigma$ -carbon ligands with very little back-bonding. A

variety of different coordination possibilities exist, which can be classified into three main types (Figure 2.7). These are: complexes in which the phosphorus ylides occur as simple monodentate terminal ligands (A), those in which the ylide is a bridging group (B) and those in which the ylide acts as a chelating moiety (C).

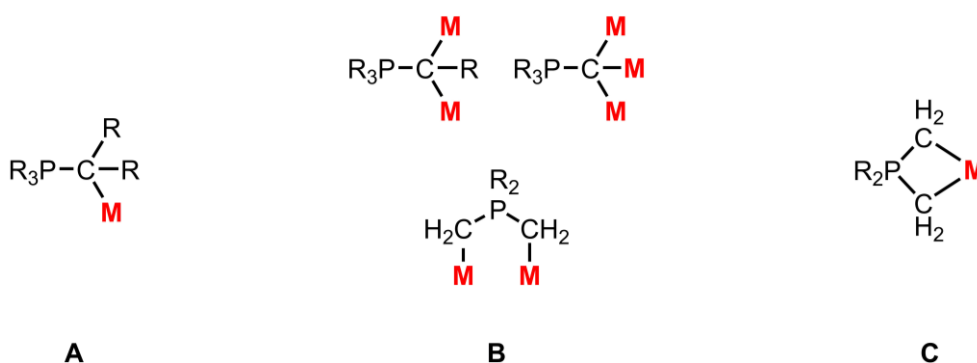
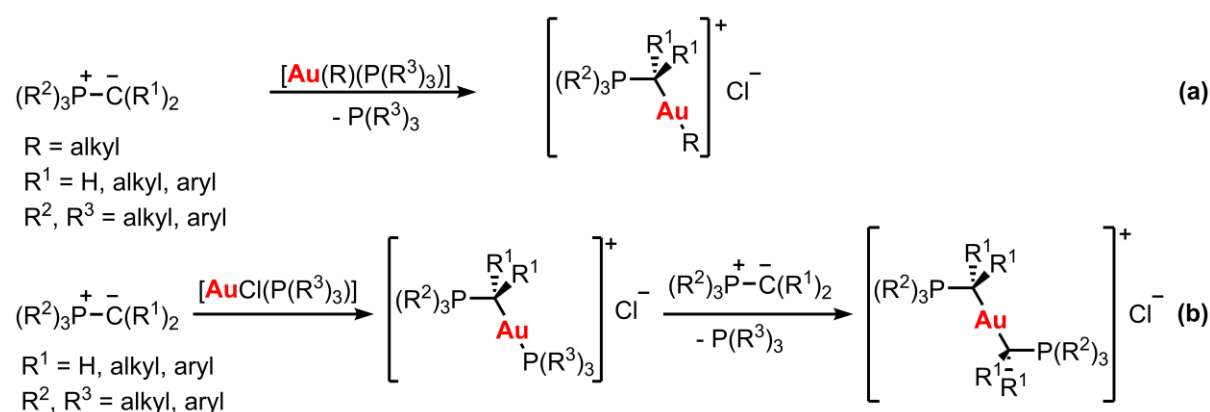


Figure 2.7. Phosphorus ylide coordination possibilities.

The exceptional donor character of phosphorus ylides with respect to practically all metals is often sufficient to drive all other ligands out of the coordination sphere.<sup>132</sup> Thus, alkylgold(I) monoylide derivatives are readily prepared by the reaction of alkylgold(I) phosphine complexes with phosphorus ylides, liberating phosphine (Scheme 2.1(a)),<sup>153</sup> and bis-ylide gold(I) complexes may be formed in a two-step process using phosphinegold(I) halides. In this case initial reaction with the ylide gives the isolable monoylide gold(I) phosphine species, following displacement of the chloride ligand from the coordination sphere of gold, and this species can be converted into the bis-ylide species by addition of excess ylide and displacement of the phosphine (Scheme 2.1(b)).<sup>154</sup>

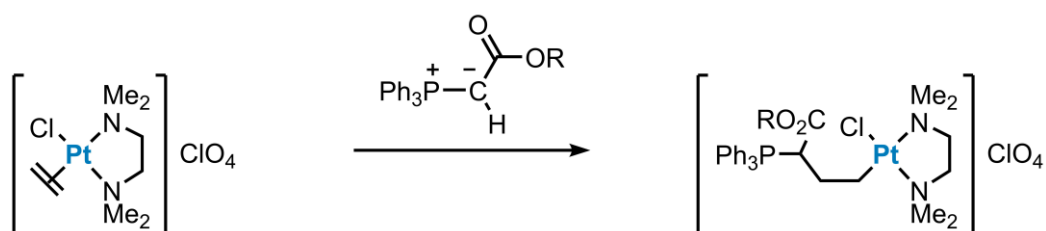


**Scheme 2.1.** Synthesis of alkylgold(I) ylide complexes (a) and bis-ylide gold(I) complexes (b).



## 2.1. Introduction

Exceptions to such ligand displacement reactions can occur when there exists the possibility for ylide attack at one of the ligands already present at the metal centre, for example in the nucleophilic attack on an alkene-platinum(II) complex by a carbonyl-stabilised ylide (Scheme 2.2).<sup>155</sup>

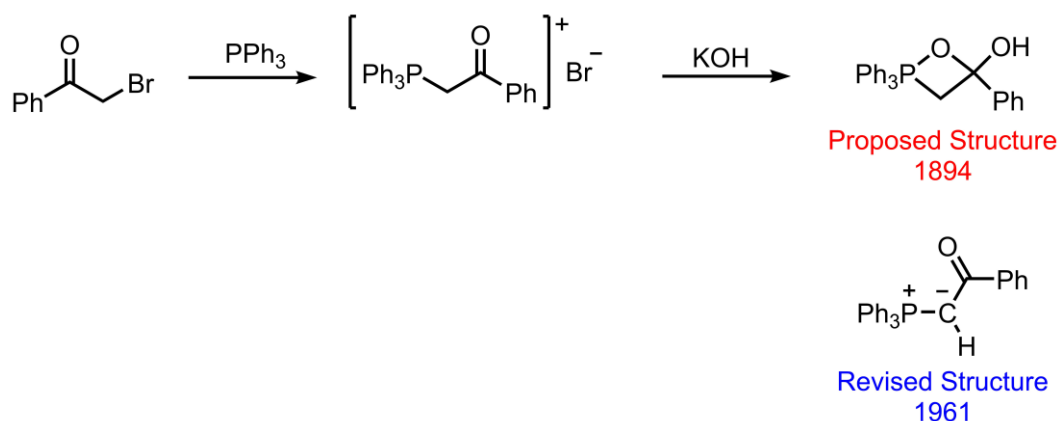


**Scheme 2.2.** Nucleophilic attack by carbonyl-stabilised phosphorus ylide

The great potential of phosphorus ylides with respect to the formation of transition metal-carbon bonds is due to the presence of the phosphonium group which blocks a major decomposition pathway:  $\beta$ -H elimination. This allows phosphorus ylides to form relatively stable coordination complexes in comparison with simple alkyls. In fact, phosphorus ylide gold complexes are particularly stable towards oxidation and hydrolysis and are among the most thermally stable organometallic complexes of gold.

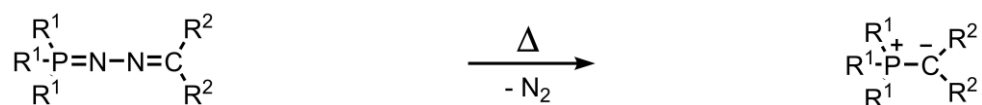
### 2.1.3. History

The first example of a phosphorus ylide was prepared in 1894 by Michaelis and co-workers. Addition of triphenylphosphine to 2-bromoacetophenone led to the formation of the phosphonium bromide salt and subsequent addition of potassium hydroxide gave the ylide<sup>127</sup> (Scheme 2.3). However, the lack of characterisation techniques available at that time led Michaelis to incorrectly propose a structure with a pentavalent phosphorus atom due to the formation of a phosphorus-oxygen bond and it was not until 65 years later, in 1961, that the correct structure was determined by Aksnes,<sup>156</sup> Ramirez and Dershowitz.<sup>157</sup> This, along with the fact that no reactions were carried out with the ylides meant that the significance of the pioneering work carried out by Michaelis was not recognised for many years.



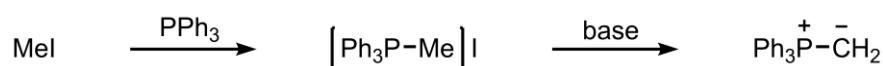
**Scheme 2.3.** Synthesis of the first phosphorus ylide.

In 1919, it was shown by Staudinger and co-workers that heating phosphazenes causes a thermal decomposition, evolving nitrogen and producing a phosphorus ylide (Scheme 2.4).<sup>158</sup> Little work was done at the time into studying the reactions of the phosphorus ylides and in the subsequent years, development of this work and further study of phosphorus ylides was minimal.



**Scheme 2.4.** Thermal decomposition of phosphazene.

The breakthrough for phosphorus ylides came in 1949 with a serendipitous discovery by Wittig whilst attempting to prepare pentavalent phosphorus compounds. Wittig showed that phosphonium salts could readily be generated by an  $\text{S}_{\text{N}}2$  reaction of a trialkyl- or triarylphosphine with an alkyl halide, and that subsequent reaction with strong base yields the corresponding ylide (Scheme 2.5).<sup>159</sup>

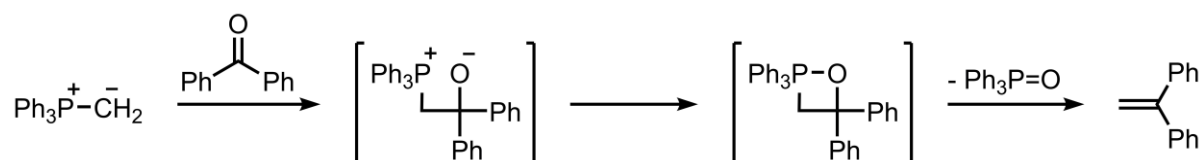


**Scheme 2.5.** Synthesis of phosphorus ylide carried out by Wittig.

Wittig went on to carry out the reaction of triphenylphosphoniummethyllide with benzophenone (Scheme 2.6), showing that the reaction of a phosphorus ylide with an aldehyde or ketone will form an alkene product.<sup>160</sup> Very quickly was this new method for the preparation of alkenes, now known as the “Wittig reaction”, shown to be widely applicable in organic synthesis due

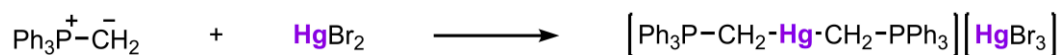
## 2.1. Introduction

to high selectivity and the fact it can proceed without isomerisation or rearrangement. Wittig was later awarded a Nobel Prize as recognition of the great importance of his work and a renewed interest in phosphorus ylides led to rapid progression in this field of chemistry. However, despite importance of phosphorus ylides in organic chemistry, the great potential for ylides within inorganic and organometallic chemistry was overlooked for several years.



**Scheme 2.6.** Reaction of triphenylphosphoniummethylide with benzophenone.

In 1961 Seyferth and Grim synthesised the first examples of transition metal-ylide coordination complexes through nucleophilic displacement reactions with metal halides. Reaction of triphenylphosphonium methylide with mercury(II) bromide led to the formation of a cationic bis-ylide complex (Scheme 2.7) which was isolated as a stable solid and characterised by elemental analysis.<sup>161</sup>



**Scheme 2.7.** Reaction of phosphorus ylide with metal halide

The first phosphorus ylide transition metal complex to be structurally characterised by single crystal X-ray diffraction was the nickel complex tricyclohexylphosphoniummethylidenickel tricarbonyl (Figure 2.8), reported in 1972 by Barnett and Krüger. This provided the first structural evidence that phosphorus ylides bond to metals through the  $\alpha$ -carbon atom. The P-C<sub>ylide</sub> bond distance, 1.743(8) Å, was found to be in the range for a typical stabilised ylide, and shorter than that for a typical carbon-carbon single bond.<sup>162</sup>

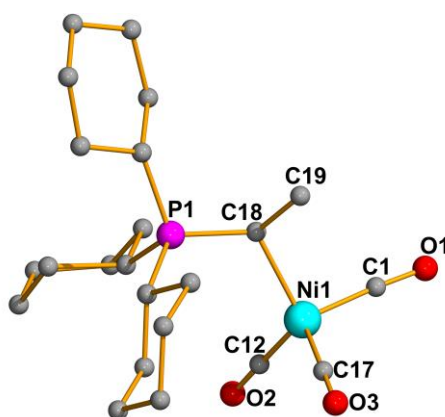
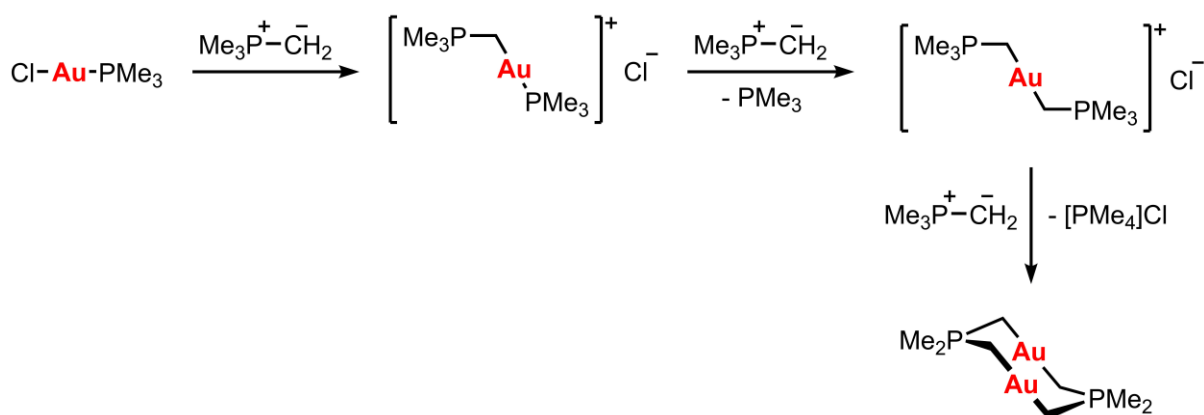


**Figure 2.8.** Molecular structure of tricyclohexylphosphoniummethylenickel tricarbonyl determined by single crystal X-ray diffraction. Selected bond lengths [Å] and angles [°]: P(1)-C(18) 1.743(8), C(18)-C(19) 1.558(3), C(18)-Ni(1) 2.0960, Ni(1)-C(1) 1.7426, Ni(1)-C(12) 1.7416, Ni(1)-C(17) 1.7762, C(1)-O(1) 1.1600, C(12)-O(2) 1.1373, C(17)-O(3) 1.1361, P(1)-C(18)-C(19) 114.26, P(1)-C(18)-Ni(1) 118.23, C(19)-C(18)-Ni(1) 111.35.

The first phosphorus ylide gold complexes were prepared by Schmidbaur in 1973. The reaction of chloro(trimethylphosphine) gold(I) with trimethylphosphoniummethide was carried out to produce a phosphonium-gold chloride. Further reaction with the ylide resulted in the formation of a bis-ylide-gold derivative and even further addition led to the formation of the dinuclear ylide-gold complex (Scheme 2.8).<sup>163</sup>

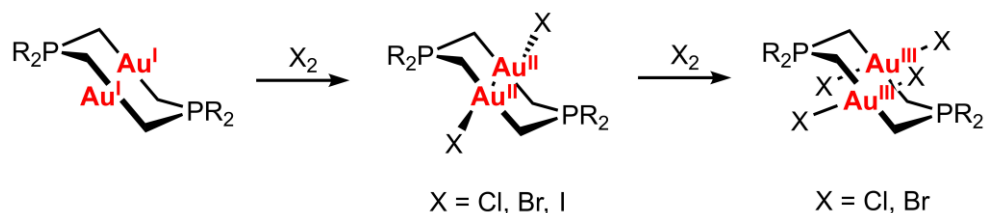


**Scheme 2.8.** Synthesis of the first phosphorus ylide gold complex.

Dinuclear gold complexes with bridging ylide ligands are of particular interest because the close proximity of the gold atoms favours oxidative addition reactions in which metal-metal bonds can be formed and cleaved. Dimers containing two gold(I) centres may be oxidised by the addition of halogens to give gold(II) and subsequently gold(III) (Scheme 2.9). Mixed valence dimers containing one gold(I) centre and one gold(III) centre are also possible.

## 2.1. Introduction

Examples of each oxidation state have successfully been characterised by single crystal X-ray diffraction (Figure 2.9).<sup>164-166</sup> The gold(II) derivative (Figure 2.9(b)) was the first example of a phosphorus ylide gold complex to be structurally characterised.<sup>166</sup>



**Scheme 2.9.** Dinuclear complexes of gold with bis(ylide)  $[R_2P(CH_2)_2]^+$ .

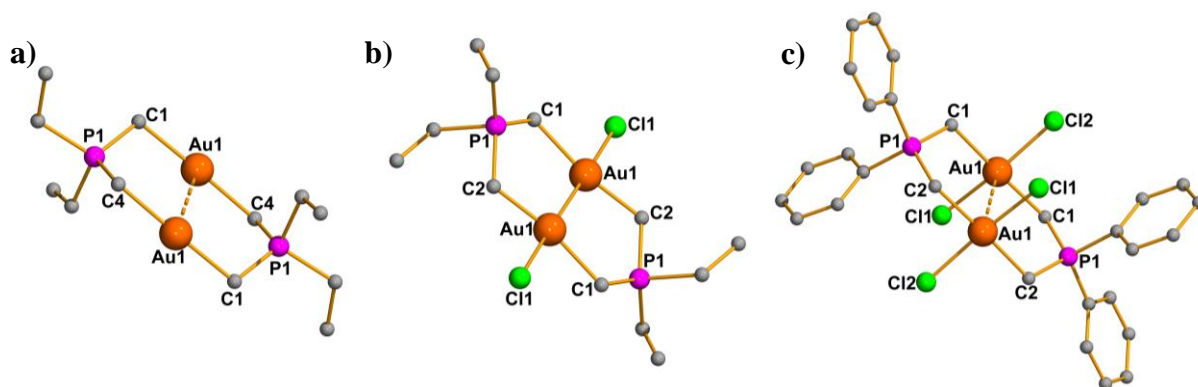


**Figure 2.9.** Molecular structure of ylide gold complexes determined by single crystal X-ray diffraction. Selected bond lengths [ $\text{\AA}$ ] and angles [ $^\circ$ ] **a**: P(1)-C(1) 1.761, P(1)-C(4) 1.83, C(1)-Au(1) 2.09, C(4)-Au(1) 2.10, Au(1)-Au(1)' 3.02, C(1)-Au(1)-C(4) 178.68; **b**: P(1)-C(1) 1.724, P(1)-C(2) 1.779, C(1)-Au(1) 2.051, C(2)-Au(1) 1.946, Au(1)-Cl(1) 2.382, Au(1)-Au(1)' 2.594, C(1)-Au(1)-C(2) 169.39, Cl(1)-Au(1)-Au(1)' 176.93; **c**: P(1)-C(1) 1.83(3), P(1)-C(2) 1.81(3), C(1)-Au(1) 2.12(3), C(2)-Au(1) 2.10(2), Au(1)-Cl(1) 2.273(7), Au(1)-Cl(2) 2.301(7), Au(1)-Au(1)' 3.088, C(1)-Au(1)-C(2) 178(1), Cl(1)-Au(1)-Cl(2) 168.5(3).

### 2.1.4. Triphenylphosphoniumcyanomethylide

Triphenylphosphoniumcyanomethylide is an example of a stabilised phosphorus ylide. The stability arises from the fact the electron density may be delocalised onto the nitrogen atom, resulting in three resonance forms (Figure 2.10).

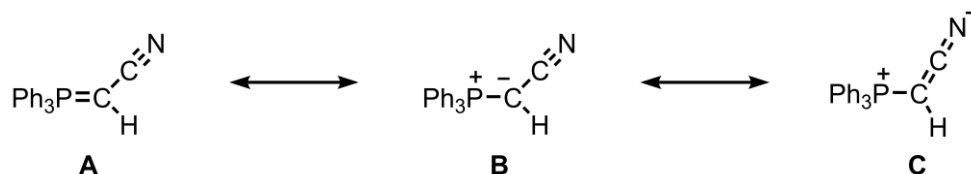


**Figure 2.10.** Resonance forms of triphenylphosphoniumcyanomethylide.

This delocalisation of electron density results in an ambidentate behaviour since the ylide may coordinate to metals through the carbon or the nitrogen atom. In fact, a variety of different coordination geometries are possible (Figure 2.11). As well as the typical C-coordination, **a**, there is the possibility for an end-on N-coordination with the nitrile group, **b**, or an angular N-coordination, **c**.<sup>167</sup>

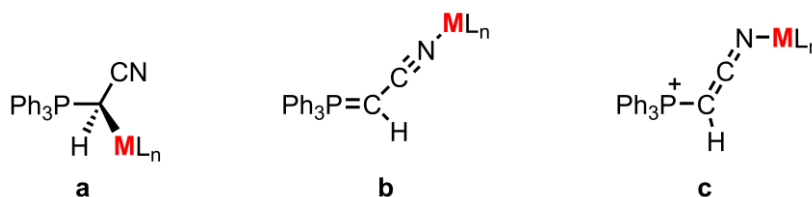


**Figure 2.11.** Coordination modes of triphenylphosphoniumcyanomethylide.

The ylide may be further deprotonated to form the yldiide species which can act as a bridging ligand allowing the synthesis of dinuclear complexes, and even trinuclear complexes via an additional N-coordination (Figure 2.12).

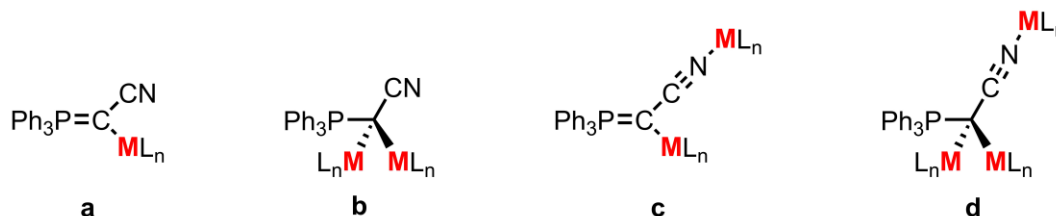
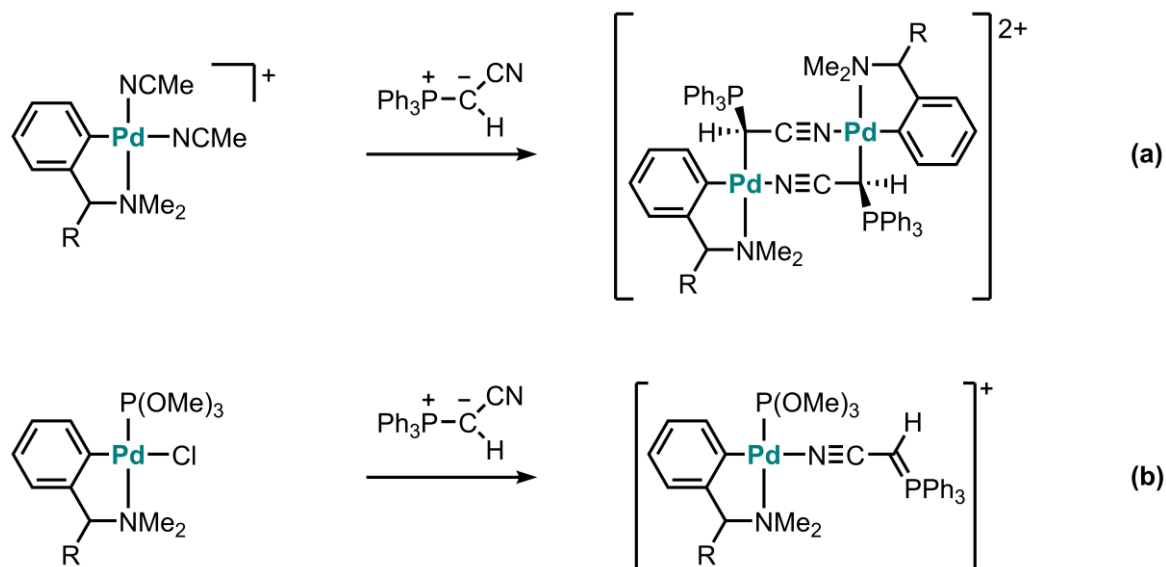


**Figure 2.12.** Coordination modes of triphenylphosphoniumcyanomethyldiide.

The coordination chemistry of triphenylphosphoniumcyanomethylide was first reported in 1997 with the preparation of palladium complexes. The authors reported two different coordination modes depending on the starting complex used. Reaction of the orthometallated palladium complex bearing two acetonitrile ligands led to the formation of a dinuclear complex in which the ylide coordinates to one palladium centre through the  $\alpha$ -carbon atom and to another through the nitrogen of the nitrile group (Scheme 2.10(a)). However, if the orthometallated palladium complex bearing a triphenylphosphite and a chloride ligand is reacted with the ylide, a complex bearing the ylide coordinated only through the nitrogen of the ylide is observed (Scheme 2.10(b)). This complex was successfully characterised by single

## 2.1. Introduction

crystal X-ray diffraction with the nitrogen coordination of the ylide clearly shown (Figure 2.13).<sup>167</sup>



**Scheme 2.10.** Synthesis of palladium derivatives of triphenylphosphoniumcyanomethylide with C-coordination (a) and N-coordination (b).

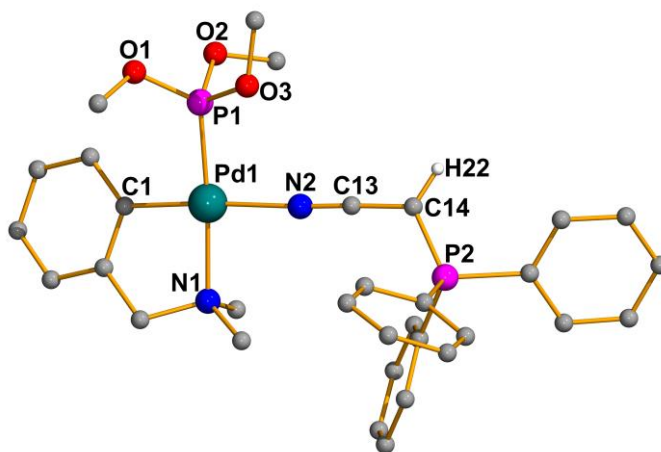
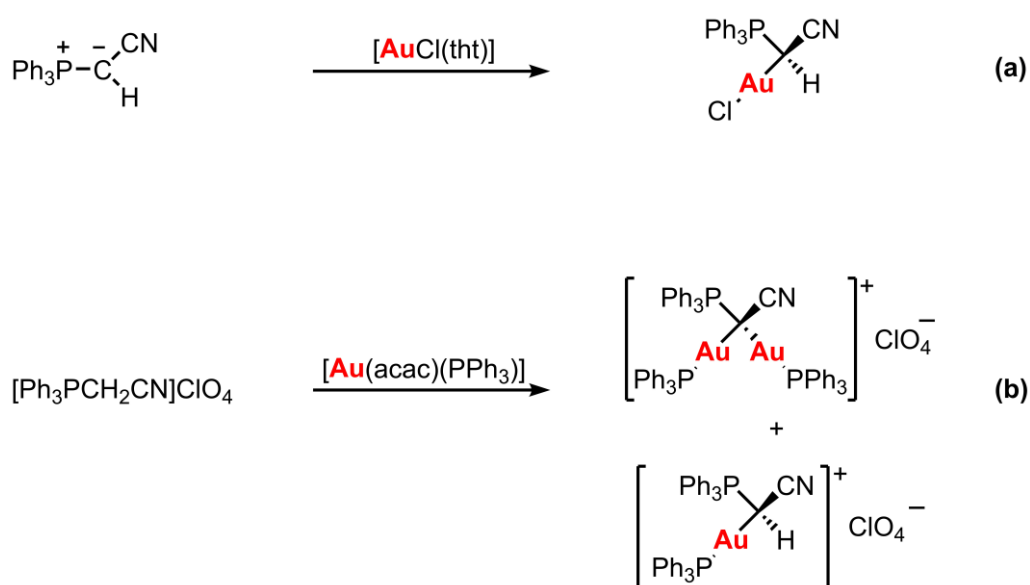


**Figure 2.13.** Molecular structure of triphenylphosphoniumcyanomethylide complex determined by single crystal X-ray diffraction. Selected bond lengths [Å] and angles [°]: Pd(1)-C(1) 2.003(4), Pd(1)-P(1) 2.2070(9), Pd(1)-N(1) 2.133(3), Pd(1)-N(2) 2.076(3), N(2)-C(13) 1.155(4), C(13)-C(14) 1.379(5), P(2)-C(14) 1.709(4), C(1)-Pd(1)-N(2) 170.2(1), P(1)-Pd(1)-N(1) 175.80(9), Pd(1)-N(2)-C(13) 177.1(3), N(2)-C(13)-C(14) 177.7(4), C(13)-C(14)-P(2) 118.4(3).

Coordination complexes of triphenylphosphoniumcyanomethylide with gold are of interest because there exists the possibility of coordinating multiple gold atoms and the aurophilic

interactions that will arise from the close proximity of the gold atoms could give interesting optical properties such as luminescence.

Despite being a weak nucleophile, triphenylphosphoniumcyanomethylide has been shown to readily displace the labile tetrahydrothiophene ligand from  $[\text{AuCl}(\text{tht})]$  (Scheme 2.11(a)). The authors also reported that the phosphonium salt precursor can be deprotonated by the acetylacetonato ligand from  $[\text{Au}(\text{acac})(\text{PPh}_3)]$ , generating the ylide ligand *in situ*. However, attempts to carry out this reaction to form an ylide gold complex resulted in a mixture of the phosphonium salt, the mononuclear derivative and the dinuclear complex (Scheme 2.11(b)).<sup>117</sup>



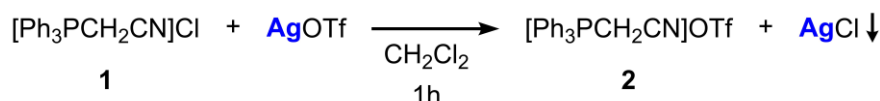
**Scheme 2.11.** Synthesis of triphenylphosphoniumcyanomethylide gold derivatives.



## 2.2. Synthesis of Starting Reagents

### 2.2.1. (Cyanomethyl)triphenylphosphonium Triflate

For the preparation of ylide gold complexes, the use of a phosphonium salt with a weakly coordinating or non-coordinating anion rather than a halide is often more desirable to remove the possibility for the formation of any undesired chloro-gold products, hence giving cleaner reactions. (Cyanomethyl)triphenylphosphonium triflate, **2**, can readily be prepared from the commercial chloride salt, **1**, by reaction with silver triflate in dichloromethane (Scheme 2.12). The precipitation of silver chloride drives this anion exchange reaction, leaving (cyanomethyl)triphenylphosphonium triflate in solution which may be isolated as a solid by removal of solvent.



**Scheme 2.12.** Synthesis of (cyanomethyl)triphenylphosphonium triflate, **2**.

In the  $^1\text{H}$  NMR spectrum of the phosphonium triflate salt the  $\text{C}_\alpha\text{H}_2$  protons are observed as a doublet at 5.05 ppm with a coupling constant  $^2J_{\text{HP}} = 15.1$  Hz due to coupling with the phosphorus atom. The position of this doublet is significantly less shifted than in the analogous chloride salt where it appears as a doublet at around 6.13 ppm.<sup>168</sup> This phenomenon has previously been observed for other phosphonium salts when a halide anion is exchanged for a larger weakly coordinating anion and can be explained by a loss of hydrogen bonding.<sup>169</sup> In the crystal structure of (cyanomethyl)triphenylphosphonium chloride intermolecular  $\text{C-H}\cdots\text{Cl}$  hydrogen bonds link the molecules and may be responsible for the stabilisation of the structure (Figure 2.14).<sup>170</sup> These contacts cause a significant deshielding of the  $\text{C}_\alpha\text{H}_2$  protons. In the triflate salt, however, these hydrogen bonds are not present and hence in the  $^1\text{H}$  NMR spectrum the  $\text{C}_\alpha\text{H}_2$  appear at a lower chemical shift.

The successful formation of the triflate salt can also be confirmed by  $^{19}\text{F}$  NMR spectroscopy in which a singlet at -78 ppm due to the triflate anion is observed as the only signal in the spectrum.

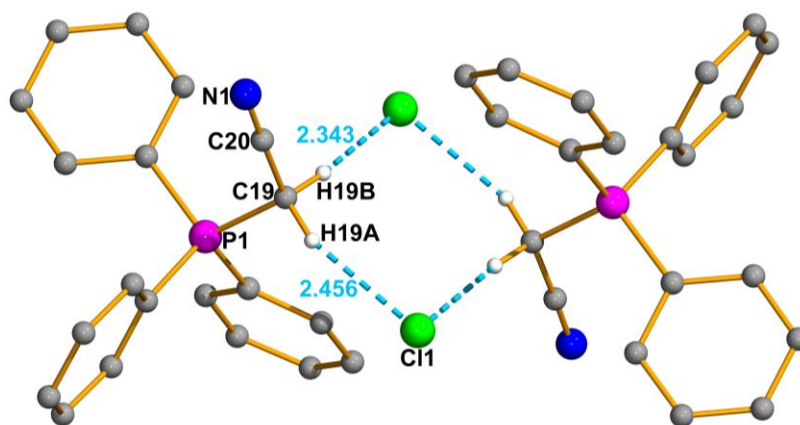
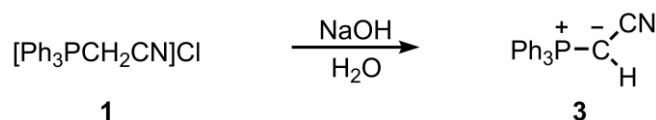


**Figure 2.14.** Molecular structure of (cyanomethyl)triphenylphosphonium chloride determined by single crystal X-ray diffraction with hydrogen bonds shown as dashed lines. Phenyl hydrogen atoms are omitted for clarity. Selected bond lengths [Å] and angles [°]: P(1)-C(19) 1.8046(17), C(19)-C(20) 1.445(3), C(20)-N(1) 1.133(3), Cl(1)-H(19A) 2.456, Cl(1)-H(19B) 2.343.<sup>170</sup>

### 2.2.2. Triphenylphosphoniumcyanomethylide

Gold-ylide complexes can also be prepared by reaction of a gold precursor with the free ylide. Many non-stabilised ylides are highly reactive and may not be isolated or stored for periods of time. Triphenylphosphoniumcyanomethylide, however, is stabilised by the delocalisation of electron density onto the nitrogen atom of the cyano group and may be stored under ambient conditions for weeks without decomposition, therefore making it a convenient starting reagent for the synthesis of complexes. It was prepared by a modification of the procedure first reported by Trippett and Walker in 1959<sup>171</sup> (Scheme 2.13). (Cyanomethyl)triphenylphosphonium chloride, **1**, was dissolved in deionised water and the solution made alkaline by the addition of dilute sodium hydroxide solution, resulting in the precipitation of a white solid.



**Scheme 2.13.** Synthesis of triphenylphosphoniumcyanomethylide.

Phosphorus NMR studies of this crude product showed the presence of considerable amounts of triphenylphosphine oxide, however, recrystallisation from toluene allowed the ylide, **3**, to be obtained cleanly (Figure 2.15).

## 2.2. Synthesis of Starting Reagents

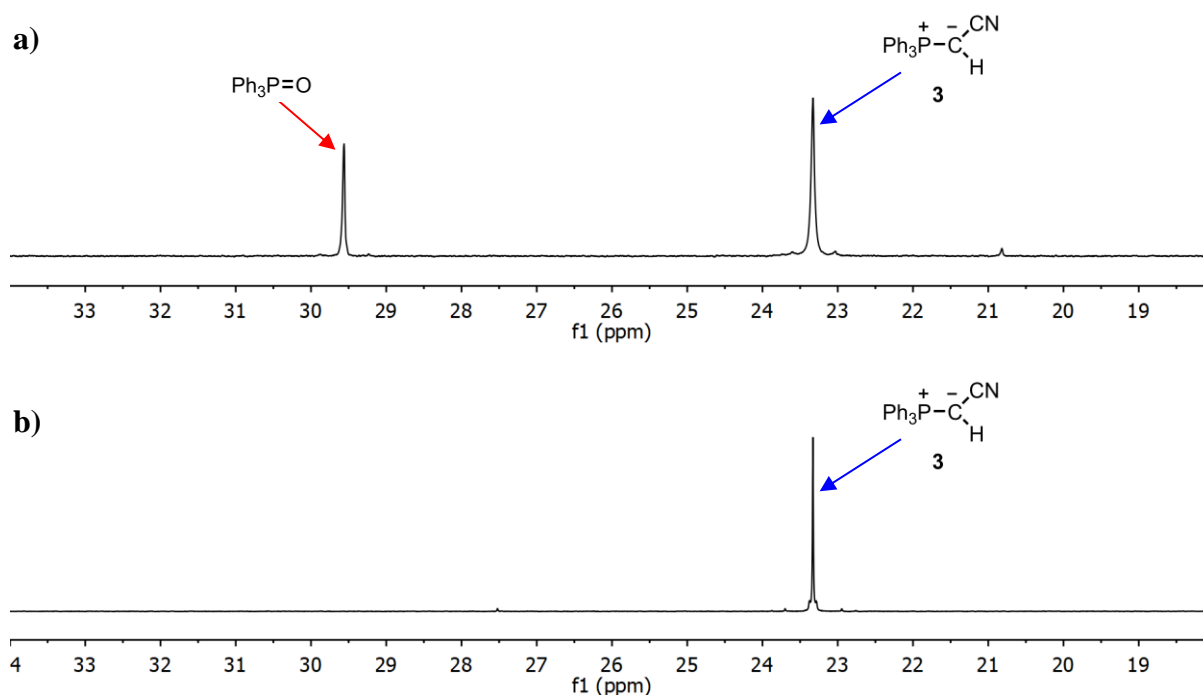


**Figure 2.15.**  $^{31}\text{P}\{^1\text{H}\}$  NMR spectra in  $\text{CDCl}_3$  of crude product (**a**) and product following recrystallisation in toluene (**b**).

**Table 2.1.** Infrared absorption frequencies

Compound	$\nu(\text{C}\equiv\text{N})$ ( $\text{cm}^{-1}$ )
<b>1</b>	2231
<b>2</b>	2250
<b>3</b>	2136

The infrared absorption frequency for the  $\text{C}\equiv\text{N}$  bond of the free ylide, **3**, is considerably lower than for the phosphonium chloride and triflate salts, **1** and **2** (Table 2.1). This is due to the fact the free ylide exists as three resonance forms and hence the  $\text{C}\equiv\text{N}$  will have significantly less triple bond character. Such resonance is not possible in the phosphonium salts.

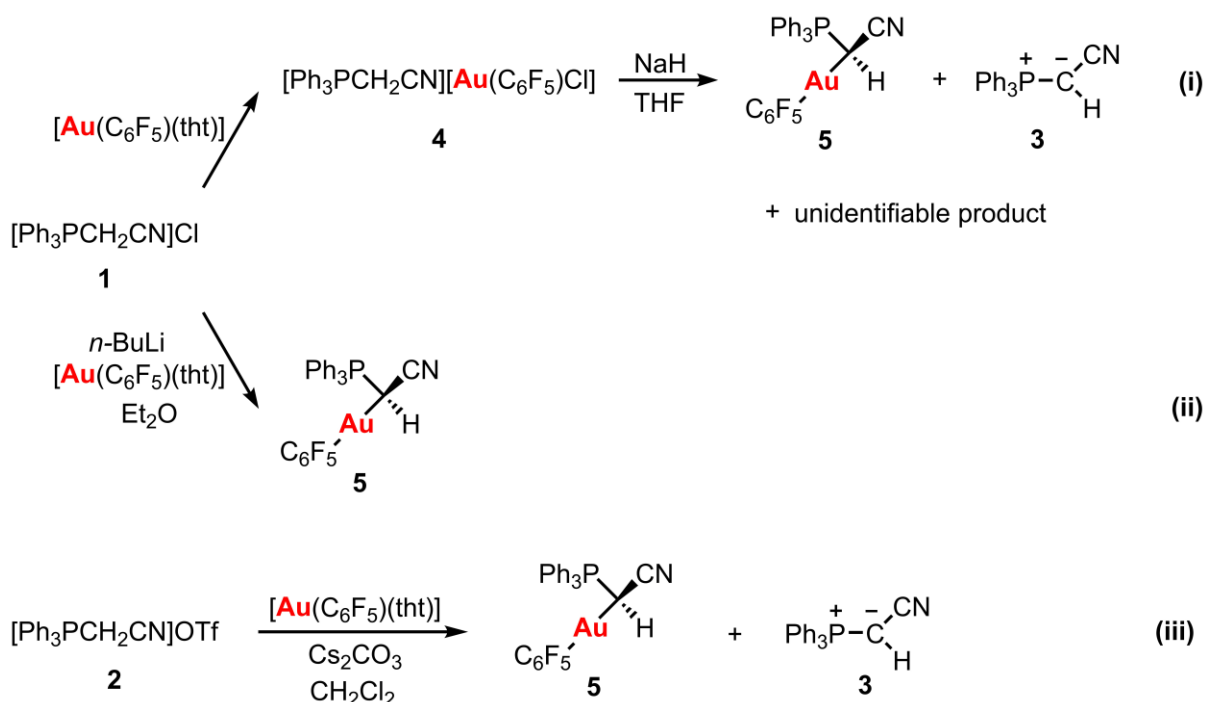
Despite the weaker nucleophilic character of triphenylphosphonium cyanomethylide compared to non-stabilised phosphorus ylides, it still has a strong enough coordination capacity to displace other ligands from the coordination sphere of the coinage metals which can lead to the formation of some very stable and interesting complexes.

## 2.3. Synthesis of Mononuclear Ylide Complexes

### 2.3.1. Neutral Gold(I) and Gold(III) Complexes

The synthesis of pentafluorophenyl gold derivatives of triphenylphosphoniumcyanomethylide was of particular interest because of their predicted high stability. The pentafluorophenyl group as a ligand confers great thermodynamic and kinetic stability on gold complexes because of the strong electron withdrawing effect of the C<sub>6</sub>F<sub>5</sub> group and the fact that the Au-C bond is relatively resistant to cleavage by mild acids. The C<sub>6</sub>F<sub>5</sub> group can also impart crystallinity on gold complexes.<sup>172</sup>

Several different synthetic routes were attempted to prepare pentafluorophenyl[cyano(triphenylphosphonio)methyl] gold(I), **5** (Scheme 2.14).



**Scheme 2.14.** Syntheses of complex **1**.

Since a method with fewer synthetic steps is preferable, initial attempts were made starting from the commercially available phosphonium chloride salt, **1**. The first (Scheme 2.14(i)) was a one pot reaction in which addition of a stoichiometric amount of pentafluorophenyl(tetrahydrothiophene) gold(I), [Au(C<sub>6</sub>F<sub>5</sub>)(tht)], to the phosphonium salt led

### 2.3. Synthesis of Mononuclear Ylide Complexes

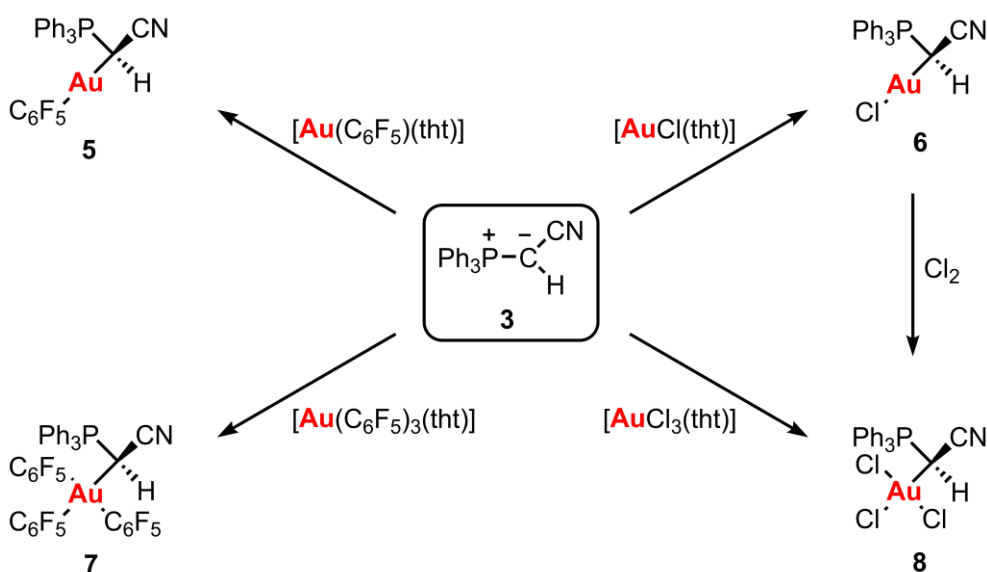
---

to the formation of phosphonium aurate salt, **4**, cleanly, which could be isolated in a high yield, 81%, and fully characterised. The  $^1\text{H}$  NMR spectrum clearly shows the presence of the  $\text{CH}_2$  protons as a doublet at 5.07 ppm ( $^3J_{\text{HP}} = 14.8$  Hz), and an infrared absorption at  $316\text{ cm}^{-1}$  confirms the presence of the newly formed Au-Cl bond. Subsequent reaction of salt **4** with NaH was attempted in order to mono-deprotonate the  $\text{CH}_2$  and allow coordination to  $\text{Au}(\text{C}_6\text{F}_5)$ , with the chloride removed as NaCl. Although the desired complex did form, this reaction was not clean and considerable amounts of free ylide, **3**, were obtained along with another unidentifiable product which could not be separated and hence an alternative route was required.

Reaction of (cyanomethyl)triphenylphosphonium chloride, **1**, with a stoichiometric amount of *n*-butyllithium in diethyl ether and subsequent addition of a stoichiometric amount of  $[\text{Au}(\text{C}_6\text{F}_5)(\text{tht})]$  did give the desired complex, **5** (Scheme 2.14(ii)). Recrystallisation from dichloromethane to remove lithium salts allowed the pure product to be obtained with a reasonable yield of 69%. This route essentially involves the formation of the free ylide, although it is never isolated, and subsequent displacement of the labile tetrahydrothiophene from  $[\text{Au}(\text{C}_6\text{F}_5)(\text{tht})]$ . Although complex **5** was obtained cleanly, the fact that an inert argon atmosphere is required and the need for recrystallisation to remove lithium salts formed as side products make this route undesirable.

The third route was the stoichiometric reaction of the phosphonium triflate salt, **2**, with  $[\text{Au}(\text{C}_6\text{F}_5)(\text{tht})]$  in dichloromethane in the presence of excess caesium carbonate which gave a mixture of complex **5** and the free ylide, **3** (Scheme 2.14(iii)). These could readily be separated due to the solubility of complex **5** in diethyl ether, which following recrystallisation was obtained in a yield of 63%. In this case no intermediate aurate salt is formed in the reaction as the triflate anion has only a very weak coordination capacity with gold and is not able to displace the tetrahydrothiophene ligand from  $[\text{Au}(\text{C}_6\text{F}_5)(\text{tht})]$ . Instead, the caesium carbonate base deprotonates the phosphonium salt to form the ylide which then reacts with  $[\text{Au}(\text{C}_6\text{F}_5)(\text{tht})]$ , displacing tht to form complex **5**. This route does not require the use of an argon atmosphere nor anhydrous solvents, however, although the desired complex could readily be separated from unwanted side products, the final yield was not particularly high.

Since triphenylphosphoniumcyanomethylide, **3**, may readily be prepared and is stable enough to be isolated and stored, reactions were attempted using this free ylide as a starting reagent (Scheme 2.15), rather than generating it *in situ* from the phosphonium salt, with the aim of achieving the desired products more cleanly. The reaction of the free ylide with  $[\text{Au}(\text{C}_6\text{F}_5)(\text{tht})]$  in dichloromethane gave complex **5** in an excellent yield of 97%. The only side product in this case is tetrahydrothiophene which is a volatile liquid and is removed during the reaction work up.



**Scheme 2.15.** Synthesis of neutral ylide gold complexes **5** – **8**.

The use of triphenylphosphoniumcyanomethylide to displace the labile tetrahydrothiophene ligand from the gold(I) complex chloro(tetrahydrothiophene)gold(I),  $[\text{AuCl}(\text{tht})]$ , to form the chloro-gold ylide complex **6** was first reported in 1999,<sup>117</sup> however the synthetic method was limited to the formation of this one complex and the molecular structure was not determined by X-ray diffraction methods. This complex is of interest since the chloride ligand may readily be displaced by other groups to form new complexes, therefore making it a convenient entry point for the formation of new triphenylphosphoniumcyanomethylide gold(I) derivatives. Knowledge of the crystal structure could also provide further understanding of the stability and reactivity of such complexes and therefore the synthesis of complex **6** was also attempted. Two gold(III) derivatives, **7** and **8**, were also prepared by the same method and obtained in yields of 96% and 90%, respectively. These are the first reported gold(III) derivatives of this particular ylide. In all cases the reaction of **3** and  $[\text{AuX}(\text{tht})]$  or  $[\text{AuX}_3(\text{tht})]$  in a 1:1 molar ratio in dichloromethane at room temperature gave the complex (**5–8**) after just 1 hour reaction time.

### 2.3. Synthesis of Mononuclear Ylide Complexes

The reactions proceeded cleanly with the desired complexes forming uniquely and in high yield. All of the complexes were air stable solids that could be handled and stored under ambient conditions. Complex **8** could also be prepared by the oxidation of complex **6** with chlorine.

**Table 2.2** Selected NMR Peaks for Complexes **5-8** in CD<sub>2</sub>Cl<sub>2</sub>.

Complex	<sup>1</sup> H NMR C <sub>α</sub> -H (ppm)	<sup>31</sup> P{ <sup>1</sup> H} NMR (ppm)
<b>5</b>	3.33	27.28
<b>6</b>	3.59	25.89
<b>7</b>	2.36	24.60
<b>8</b>	5.09	24.87

Complexes **5-8** show similar <sup>1</sup>H NMR spectra since all display peaks arising from the ylide unit: the C<sub>α</sub>-H proton and aromatic protons from the Ph groups. In all cases the C<sub>α</sub>-H signal is observed as a doublet due to coupling with the phosphorus atom. Comparing the chemical shift of this doublet in the two gold(I) derivatives, **5** and **6**, we find that it appears at higher chemical shift in the chloro complex but the difference is only slight (Table 2.2). However, comparing the two gold(III) complexes, **7** and **8**, a significant difference is observed, with the C-H appearing at 5.09 ppm in the <sup>1</sup>H NMR spectrum of the trichloro derivative, **8**, compared to 2.27 ppm for the pentafluorophenyl derivative, **7**. This is due to the presence of Cl...H contacts causing a deshielding of the proton in the chloro derivatives. The <sup>31</sup>P{<sup>1</sup>H} NMR spectra of complexes **5-8** show a single sharp peak due to the ylide phosphorus atom.

For complexes **5** and **7** <sup>19</sup>F NMR studies were also carried out with characteristic spectra for the Au(C<sub>6</sub>F<sub>5</sub>) and Au(C<sub>6</sub>F<sub>5</sub>)<sub>3</sub> units observed. For the gold(I) derivative, complex **5**, the *para* fluorine atoms, F<sub>p</sub>, are observed as a triplet (Figure 2.17(a)) with <sup>3</sup>J<sub>FF</sub> = 20.1 Hz as a result of coupling to the two meta fluorine atoms, whilst signals due to the *ortho*, F<sub>o</sub>, and *meta*, F<sub>m</sub>, fluorine atoms are observed as more complex multiplets. For the gold(III) derivative, complex **7**, the <sup>19</sup>F NMR spectrum is slightly more complex with six signals observed (Figure 2.17(b)). This is because the two pentafluorophenyl groups *trans* to one and other are equivalent and can also rotate freely, hence giving three signals, one for each of F<sub>o</sub>', F<sub>m</sub>' and F<sub>p</sub>' (see Figure 2.16). The C<sub>6</sub>F<sub>5</sub> group *trans* to the ylide is inequivalent and hence a further three signals are observed for F<sub>o</sub>, F<sub>m</sub> and F<sub>p</sub>.

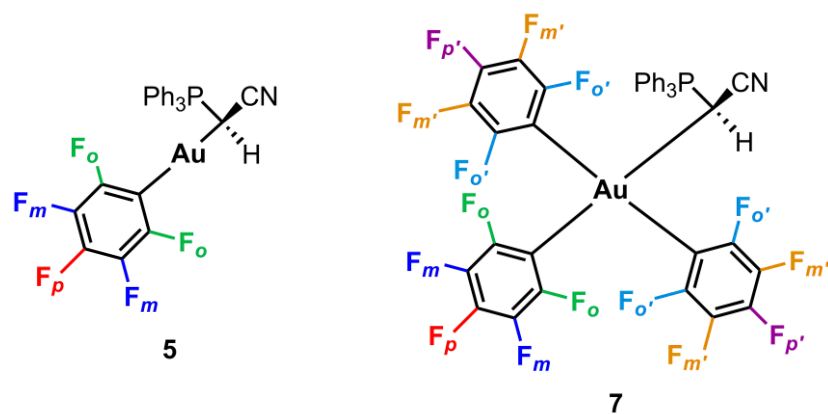


**Figure 2.16.** Complexes **5** and **7** with pentafluorophenyl F atoms labelled.

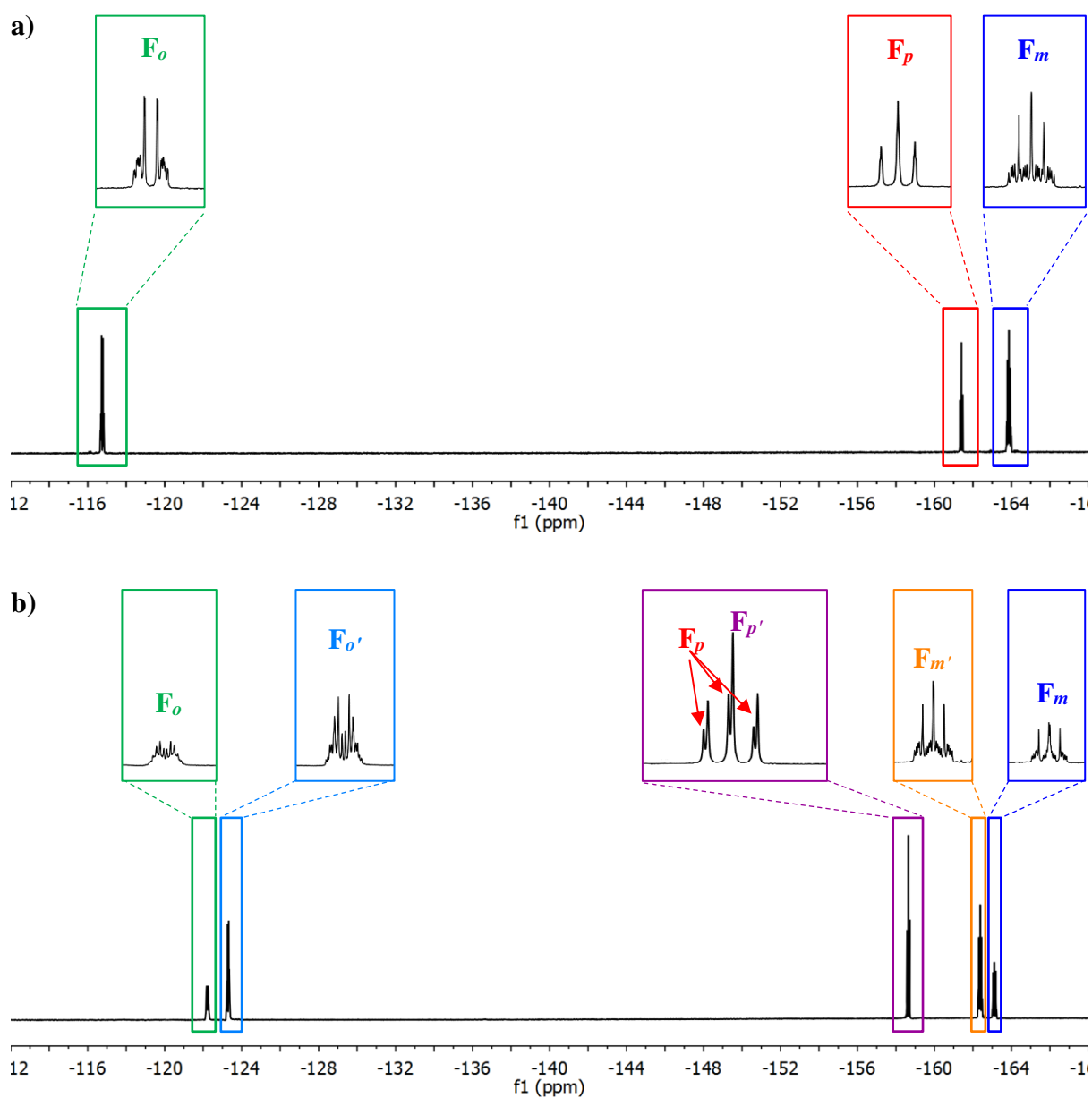


**Figure 2.17.**  $^{19}\text{F}$  NMR spectra of complexes **5** (a) and **7** (b).



### 2.3. Synthesis of Mononuclear Ylide Complexes

**Table 2.3.** Infrared absorption frequencies

Complex	$\nu(\text{C}\equiv\text{N})$ ( $\text{cm}^{-1}$ )	$\nu(\text{Au-Cl})$ ( $\text{cm}^{-1}$ )
<b>4</b>	2255	316
<b>5</b>	2201	-
<b>6</b>	2202	325
<b>7</b>	2227	-
<b>8</b>	2228	315, 342, 360

The infrared absorption frequencies of the  $\text{C}\equiv\text{N}$  bond in the complexes can also be compared (Table 2.3). The phosphonium aurate salt, **4**, has an absorption frequency comparable to the phosphonium chloride and triflate salts (see Table 2.1), as would be expected since no change in triple bond character of the  $\text{C}\equiv\text{N}$  occurs. Coordination of the ylide to gold in complexes **5-8** results in an increase in the absorption frequency of the  $\text{C}\equiv\text{N}$  compared to the free ylide, indicating the greater triple bond character in these complexes. The values are, however, slightly lower than in the phosphonium salts likely because of the inductive effects caused by the high electrophilicity of gold. Complexes **6** and **8** and salt **4** also show bands corresponding to the Au-Cl bond. For the gold(I) complex, **6**, this is a single absorption band at  $325\text{ cm}^{-1}$ . The gold(III) complex, **8**, exhibits bands at  $315\text{ cm}^{-1}$  corresponding to  $\nu(\text{Au-Cl})$  for the chloride *trans* to the ylide and  $360\text{ cm}^{-1}$  for the asymmetric stretch  $\nu_{\text{asim}}(\text{Cl-Au-Cl})$ . A weaker band at  $342\text{ cm}^{-1}$  is a result of the symmetric stretch  $\nu_{\text{sim}}(\text{Cl-Au-Cl})$ .

The molecular structures of complexes **5-8** were determined by single crystal X-ray diffraction. In all cases crystals were obtained by the slow diffusion of *n*-pentane into a solution of the complex in dichloromethane. The molecular structures are shown in Figure 2.18. The unit cell of the structure of complex **7** featured two molecules and unfortunately one of these was badly disordered and could not be resolved and hence no structural parameters can be obtained. However, coordination of the ylidic carbon to the gold(III) centre can clearly be seen. Complex **6** was a twin crystal.

In both complexes **5** and **6** a linear coordination about the gold centre can clearly be seen with angles very close to  $180^\circ$  ( $\text{C}(1)\text{-Au}(1)\text{-C}(7)$   $177.16(11)^\circ$  for **5** and  $\text{Cl}(1)\text{-Au}(1)\text{-C}(1)$   $177.64^\circ$  for **6**). In complex **5** the gold-carbon bond to the pentafluorophenyl ligand ( $\text{Au}(1)\text{-C}(1)$   $2.014(3)\text{ \AA}$ ) is slightly shorter than the gold-carbon bond to the ylide ligand

(Au(1)-C(7) 2.099(3) Å) which could indicate that the gold-pentafluorophenyl bond is stronger. For complexes **7** and **8** a square planar geometry is observed about the gold centre. For complex **8** the Au-Cl bond *trans* to the ylide carbon is slightly longer than the other two Au-Cl bonds, likely due to the strong *trans* effect of the strongly  $\sigma$ -donating ylide ligand.

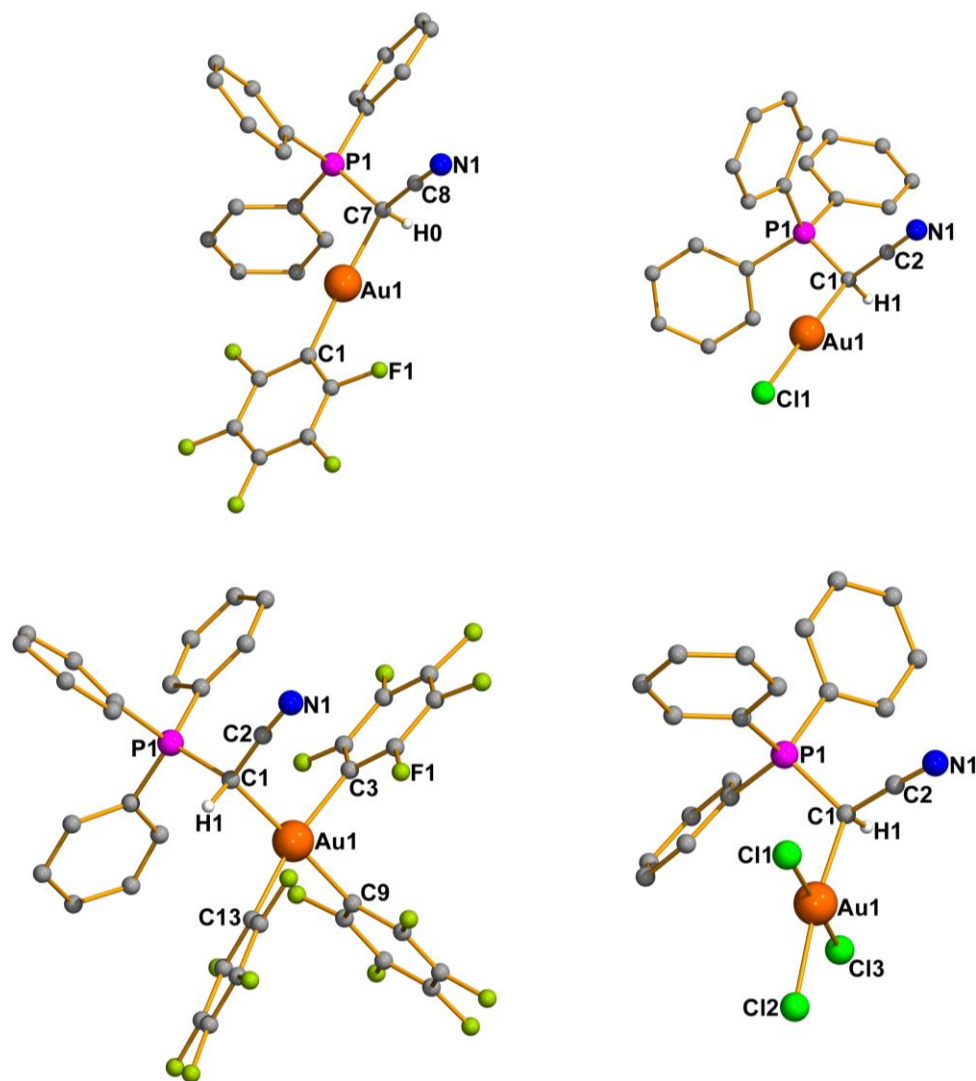
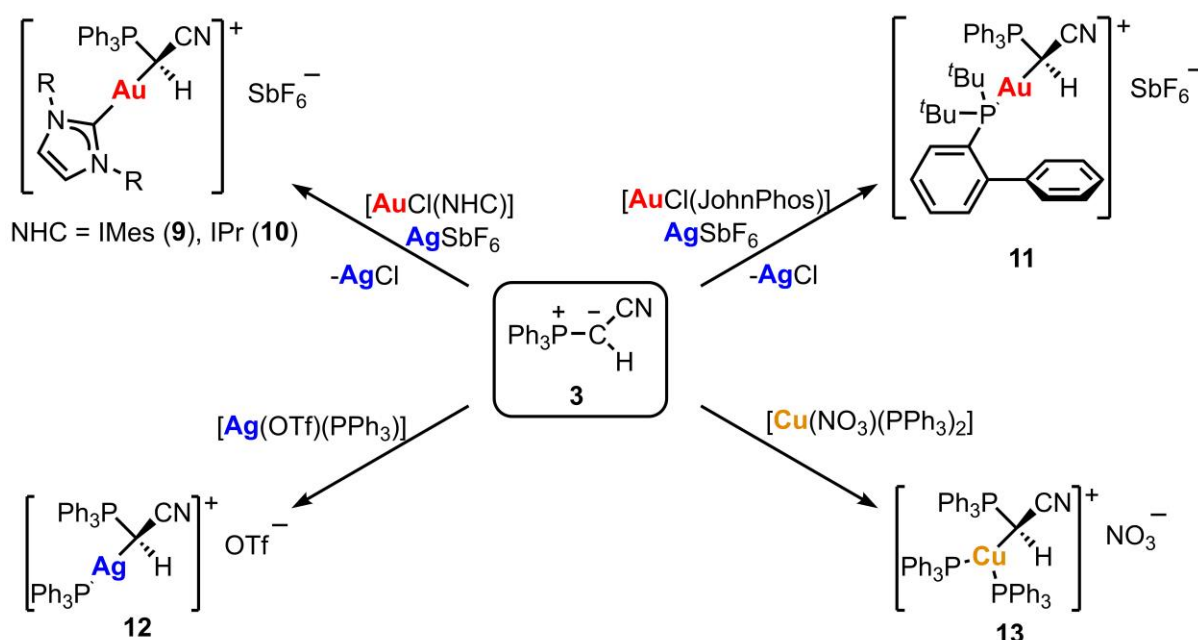


**Figure 2.18.** Molecular structures of **5-8** determined by single crystal X-ray diffraction. Hydrogen atoms, except the one at the ylidic carbon atom, are omitted for clarity. Selected bond lengths [Å] and angles [°] **5**: Au(1)-C(1) 2.014(3), Au(1)-C(7) 2.099(3), C(7)-C(8) 1.450(4), C(7)-P(1) 1.785(3), C(8)-N(1) 1.146(4), C(1)-Au(1)-C(7) 177.16(11), C(7)-C(8)-N(1) 176.7(4); **6**: Au(1)-Cl(1) 2.2870, Au(1)-C(1) 2.0487, C(1)-P(1) 1.7923, C(1)-C(2) 1.4531, C(2)-N(1) 1.1440, Cl(1)-Au(1)-C(1) 177.64, C(1)-C(2)-N(1) 178.59; **8**: Au(1)-Cl(1) 2.252(3), Au(1)-Cl(2) 2.310(1), Au(1)-Cl(3) 2.254(2), Au(1)-C(1) 2.083(4), C(1)-P(1) 1.821(3), C(1)-C(2) 1.447(8), C(2)-N(1) 1.136(9), Cl(1)-Au(1)-Cl(3) 177.20(8), Cl(2)-Au(1)-C(1) 173.1(1), C(1)-C(2)-N(1) 177.1(6).

## 2.3.2. Cationic Complexes

Cationic gold(I) derivatives of triphenylphosphoniocyanomethylide, complexes **9-11**, were prepared by reaction of the free ylide, **3**, with a gold precursor of the form  $[\text{AuCl}(\text{L})]$  in the presence of a silver salt (Scheme 2.16). Since **3** is not a strong nucleophile the silver salt helps drive the reaction by abstracting the chloride ligand from the gold(I) precursor and allowing the ylide to coordinate to gold. For the silver and copper triphenylphosphine derivative, complexes **12** and **13**, the ylide displaces the weakly bound anion from the corresponding precursor,  $[\text{Ag}(\text{OTf})(\text{PPh}_3)]$  or  $[\text{Cu}(\text{NO}_3)(\text{PPh}_3)_2]$ .



**Scheme 2.16.** Synthesis of cationic ylide complexes **9-13**.

These reactions were carried out in conditions analogous to those for the neutral complexes i.e. dichloromethane as solvent, 1 hour reaction time, room temperature. Since in the synthesis of complexes **9-12** silver salts were used, the reactions were protected from light to avoid any decomposition. The silver chloride formed as a by-product in the formation of complexes **9-11** could readily be removed by filtration of the reaction solution through celite.

Complexes **9** and **10** were both very stable white solids. Their  $^1\text{H}$  NMR spectra are comparable in that in both cases the  $\text{C}_\alpha\text{-H}$  proton appears as a doublet, at 3.05 ppm ( $^2J_{\text{HP}} = 13.5$  Hz) and 3.04 ppm ( $^2J_{\text{HP}} = 14.3$  Hz) respectively, and in both cases a single peak is observed in the

$^{31}\text{P}\{^1\text{H}\}$  NMR spectrum at 28.1 ppm and 28.7 ppm. The absorption frequencies for the  $\text{C}\equiv\text{N}$  in the infrared spectrum appear at  $2211\text{ cm}^{-1}$  for complex **9** and  $2214\text{ cm}^{-1}$  for complex **10**, evidence of the similar sigma donor capacity of these two NHCs.

Complex **10** was successfully characterised by single crystal X-ray diffraction. Suitable crystals were grown by the slow diffusion of *n*-hexane into a solution of the complex in dichloromethane. In this complex a slight deviation from linear coordination about gold ( $\text{C}(21)\text{-Au}(1)\text{-C}(1)$   $171.48(13)^\circ$ ) is observed in the molecular structure (Figure 2.19) due to the bulkiness of the NHC ligand and the hindrance with the triphenylphosphine group of the ylide. The gold-carbon bond to the NHC ligand ( $\text{Au}(1)\text{-C}(21)$   $2.012(3)\text{ \AA}$ ) is shorter than the gold-carbon bond to the ylide ligand ( $\text{Au}(1)\text{-C}(1)$   $2.098(3)\text{ \AA}$ ), likely due to the stronger sigma donor capacity of the NHC ligand which will form a stronger bond to gold compared to the ylide ligand.

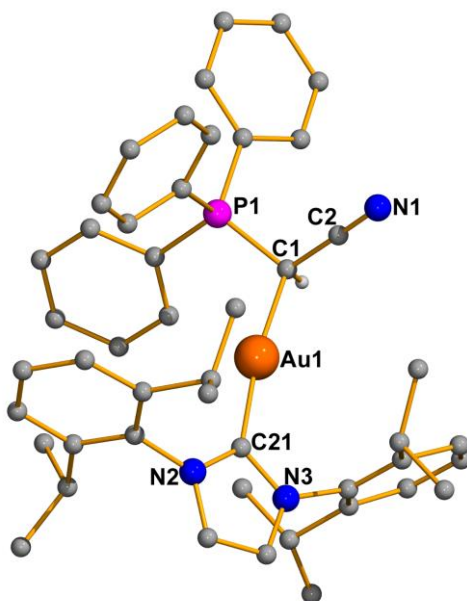


**Figure 2.19.** Molecular structure of **10** determined by single crystal X-ray diffraction. Anions and hydrogen atoms, except the one at C1, are omitted for clarity. Selected bond lengths [ $\text{\AA}$ ] and angles [ $^\circ$ ]:  $\text{Au}(1)\text{-C}(1)$   $2.098(3)$ ,  $\text{Au}(1)\text{-C}(21)$   $2.012(3)$ ,  $\text{C}(1)\text{-C}(2)$   $1.446(5)$ ,  $\text{N}(1)\text{-C}(2)$   $1.145(5)$ ,  $\text{P}(1)\text{-C}(1)$   $1.783(3)$ ,  $\text{C}(21)\text{-Au}(1)\text{-C}(1)$   $171.48(13)$ .

Complex **11** was also formed as a highly stable white solid. In this case in the  $^1\text{H}$  NMR spectrum the  $\text{C}_\alpha\text{-H}$  is observed as a doublet of doublets due to coupling with both the ylide phosphorus and the phosphorus of the JohnPhos ligand with  $^2J_{\text{HP}} = 12.2\text{ Hz}$  and  $^3J_{\text{HP}} = 7.5\text{ Hz}$ ,

### 2.3. Synthesis of Mononuclear Ylide Complexes

respectively (Figure 2.20(a)). Likewise, in the  $^{13}\text{C}$  APT spectrum the signal due to the ylide carbon atom is observed as a doublet of doublets with  $^1J_{\text{CP}} = 68.6$  Hz and  $^2J_{\text{CP}} = 53.7$  Hz (Figure 2.20(b)). The  $^{31}\text{P}\{^1\text{H}\}$  NMR spectrum shows the phosphorus-phosphorus coupling with two doublets observed at 64.31 ppm (JohnPhos P) and 26.94 ppm (ylide P) with  $^3J_{\text{PP}} = 8.4$  Hz (Figure 2.20(c)).

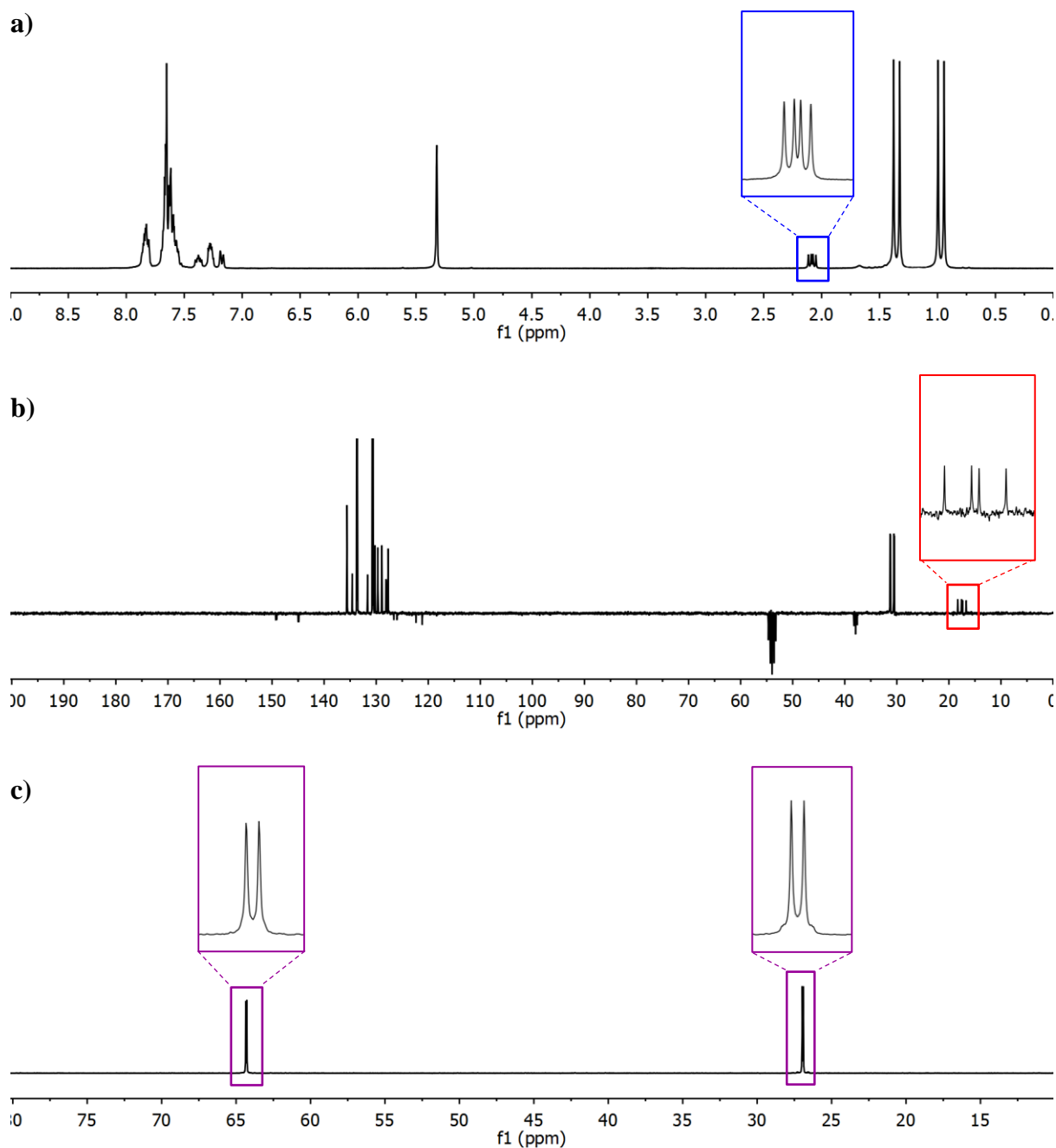


**Figure 2.20.**  $^1\text{H}$  NMR spectrum (a),  $^{13}\text{C}$  APT spectrum (b) and  $^{31}\text{P}\{^1\text{H}\}$  NMR spectrum (c) for complex 7 in  $\text{CD}_2\text{Cl}_2$ .

Complex **11** was structurally characterised by single crystal X-ray diffraction (Figure 2.21). Suitable crystals were grown by the slow diffusion of *n*-hexane into a solution of the complex in dichloromethane. The expected linear coordination about the gold centre is observed with the P(2)-Au(1)-C(2) angle of 175.5(3)°. The gold-carbon bond to the ylide, Au(1)-C(2) 2.096(8) Å, is very similar to that for complex **10** (2.098(3) Å) which bears the NHC ligand, highlighting the similarity of the phosphine and NHC bonds to gold.

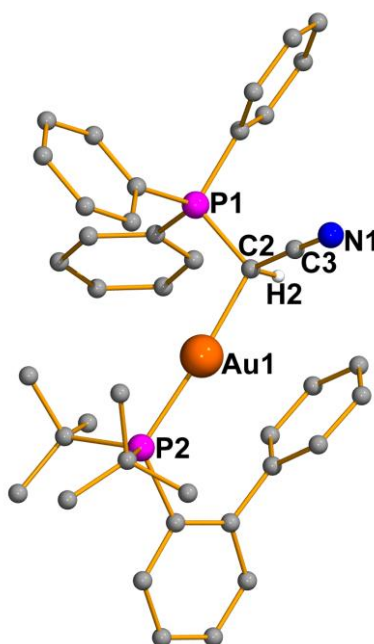


**Figure 2.21.** Molecular structure of **11** determined by single crystal X-ray diffraction. Anions and hydrogen atoms, except the one at C1, are omitted for clarity. Selected bond lengths [Å] and angles [°]: Au(1)-P(2) 2.291(2), Au(1)-C(2) 2.096(8), P(1)-C(2) 1.801(9), C(2)-C(3) 1.45(1), C(3)-N(1) 1.17(1), P(2)-Au(1)-C(2) 175.5(3), C(2)-C(3)-N(1) 179(1).

For the silver and copper phosphine derivatives, **12** and **13**, no coupling between the ylide and the triphenylphosphine ligands is observed. In both cases the  $C_{\alpha}$ -H is observed as a simple doublet since coupling with the ylide phosphorus atom is maintained, and the  $^{31}\text{P}\{^1\text{H}\}$  NMR spectra at room temperature show two singlets. For complex **12** a sharp peak at 25.92 ppm is observed due to the ylide phosphorus atom, whereas the triphenylphosphine phosphorus is observed as a broad singlet at 12.44 ppm (Figure 2.22(a)). Such broad signals are typical for silver-bound phosphine groups due to the weak Ag-P bond. The  $^{31}\text{P}\{^1\text{H}\}$  NMR spectrum at -70 °C is significantly different since at this temperature the phosphorus-silver coupling can

### 2.3. Synthesis of Mononuclear Ylide Complexes

be observed. The signal from the  $\text{PPh}_3$  ligand is observed as two doublets at 11.80 ppm with  $^1J_{^{109}\text{Ag-P}} = 628.2 \text{ Hz}$  and  $^1J_{^{107}\text{Ag-P}} = 544.1 \text{ Hz}$  (Figure 2.22(b)).

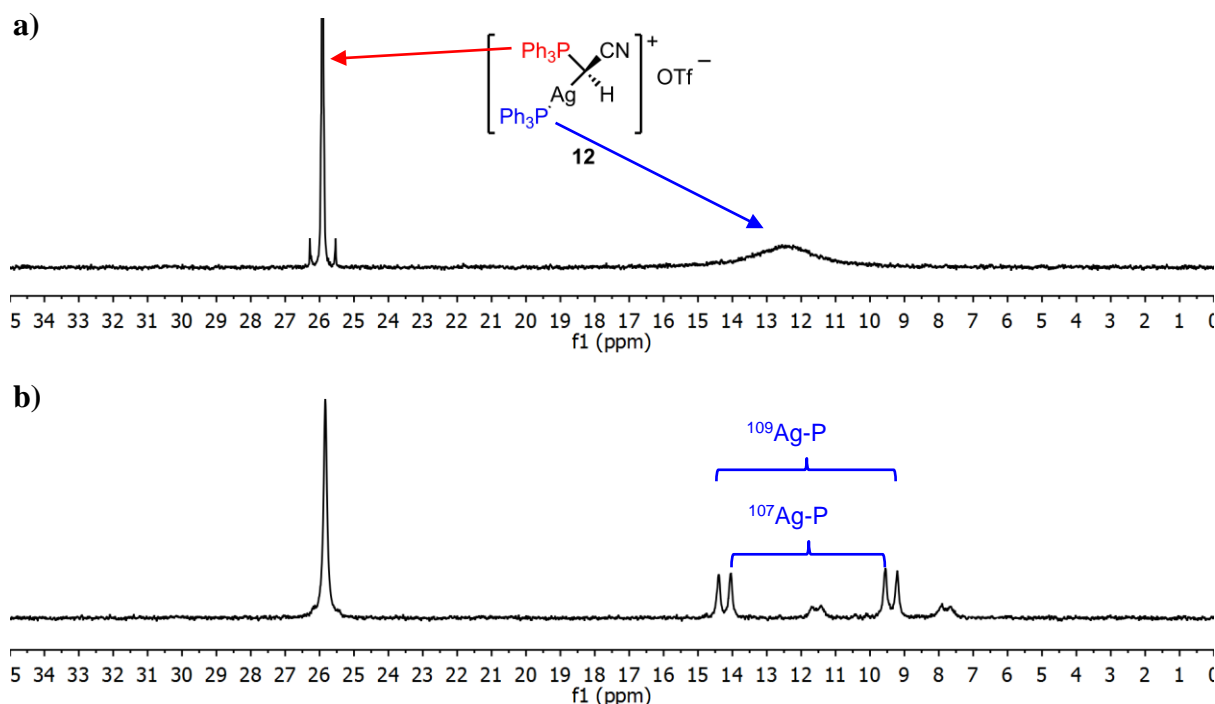


**Figure 2.22.**  $^{31}\text{P}\{^1\text{H}\}$  NMR spectrum of complex **12** in  $\text{CD}_2\text{Cl}_2$  at room temperature (a) and  $-70^\circ\text{C}$  (b).

These silver and copper complexes differ from the gold derivatives since a linear coordination about the metal is no longer favourable and additional stabilisation of the structures by coordination of the  $\text{C}\equiv\text{N}$  can occur. This is evidenced by a significant decrease in the infrared absorption frequency of the  $\text{C}\equiv\text{N}$  bond to  $2188 \text{ cm}^{-1}$  for **12** and  $2153 \text{ cm}^{-1}$  for **13**, values only slightly higher than for the free ylide, **3** ( $2136 \text{ cm}^{-1}$ ), as a result of a loss of electron density from the triple bond.

The molecular structure of complex **12** was determined by single crystal X-ray diffraction (Figure 2.23). Suitable crystals were grown by the slow diffusion of *n*-pentane into a solution of the complex in dichloromethane. This complex has a dimeric structure with a distorted tetrahedral coordination around the silver. In addition to bonding to the ylide carbon atom and the triphenylphosphine group, the silver also forms a bond with the nitrogen of the  $\text{C}\equiv\text{N}$  and a bond with one of the oxygen atoms of the triflate anion. The bond distance  $\text{Ag(1)-O(2)}$

2.7949(19) Å is long for a silver-oxygen bond, indicating the triflate anion is only weakly bound to the silver.

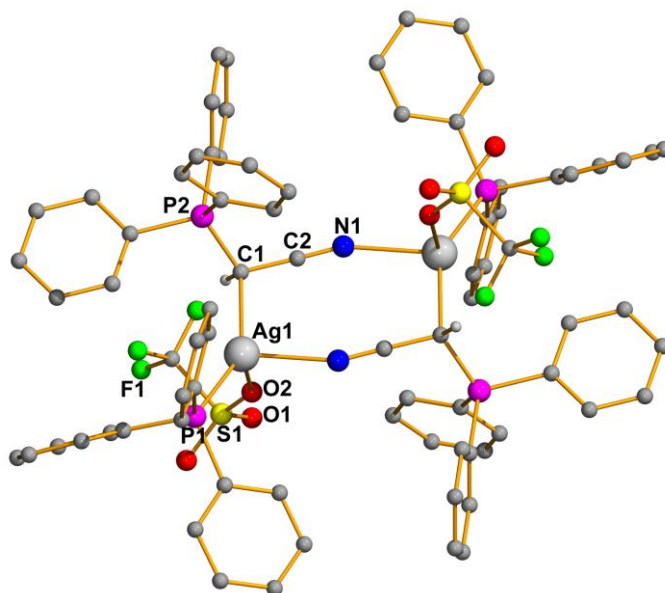
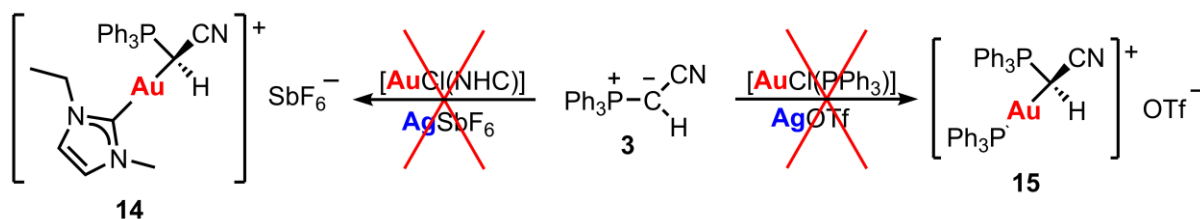


**Figure 2.23.** Molecular structure of **8** determined by single crystal X-ray diffraction. Hydrogen atoms, except the one at C1, are omitted for clarity. Selected bond lengths [Å] and angles [°]: Ag(1)-C(1) 2.286(2), Ag(1)-P(1) 2.4021(8), Ag(1)-N(1) 2.3567(19), Ag(1)-O(2) 2.7949(19), C(1)-C(2) 1.422(3), N(1)-C(2) 1.156(3), P(2)-C(1) 1.760(2), C(1)-Ag(1)-P(1) 147.70(5), C(1)-Ag(1)-N(1) 97.28(7), N(1)-Ag(1)-P(1) 110.99(5), C(1)-Ag(1)-O(2) 79.553(70), P(1)-Ag(1)-O(2) 114.605(48), N(1)-Ag(1)-O(2) 89.952(60).

Although complexes **9** and **10** bearing the bulky IMes or IPr NHC ligands formed cleanly in high yields as highly stable solids, the analogous reaction with a gold precursor bearing a sterically smaller NHC ligand in an attempt to prepare complex **14** (Scheme 2.17) led to a mixture of products. The same effect was observed with phosphine derivatives. Complex **11** bearing the bulky JohnPhos ligand formed in high yield, however reaction of the free ylide with [AuCl(PPh<sub>3</sub>)] in the presence of a silver salt to form complex **15** led to a complex mixture (Scheme 2.17).

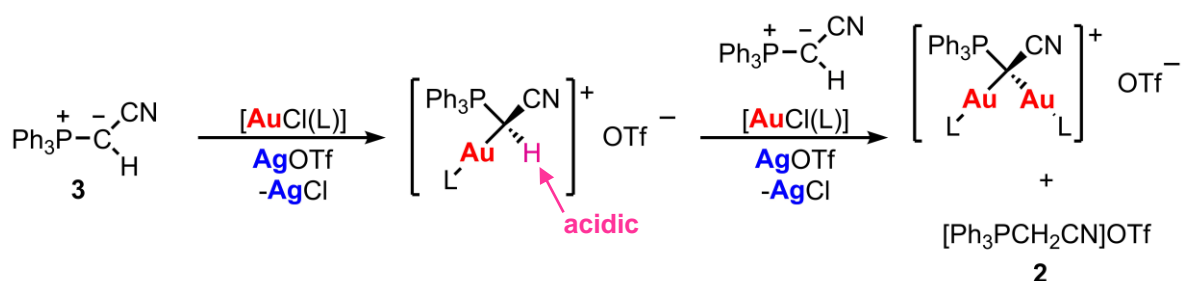


**Scheme 2.17.** Attempted synthesis of cationic ylide gold complexes **14-15** bearing sterically small L groups.



### 2.3. Synthesis of Mononuclear Ylide Complexes

This can be explained because the  $\text{AuL}^+$  fragment is isoelectronic with  $\text{H}^+$ . Coordination of the ylide to  $\text{AuL}^+$  will give complexes in which the acidity of the  $\text{C}_\alpha\text{-H}$  is comparable to, or indeed greater than, the corresponding phosphonium salts. When L is bulky this C-H is protected from further deprotonation and the formation of the mononuclear cationic complexes proceeds cleanly. However, with sterically smaller L, further deprotonation can occur, giving complex mixtures of mononuclear and dinuclear complexes. No external base is present in these reactions, however, the ylide can act both as base and a nucleophile. In the presence of an acidic proton the ylide will act as a base, abstracting the proton to form the phosphonium salt. (Scheme 2.18).



Scheme 2.18. Reaction of cationic complexes (L = small ligand) with further ylide.

Alternative methods for the preparation of complex **15** avoiding the use of the free ylide, **3**, were attempted (Scheme 2.19), however all were unsuccessful:

Reaction of the phosphonium triflate salt, **2**, with  $[\text{AuCl}(\text{PPh}_3)]$  in the presence of caesium carbonate base led to the formation of a mixture of a dinuclear complex, a trinuclear derivative and the free ylide, **3** (Scheme 2.19(i)). Complex **15** was not observed by NMR experiments. It is likely that the high stability of the polynuclear complexes as a result of aurophilic interactions leads preferentially to their formation.

Reaction of the phosphonium triflate salt, **2**, with a stoichiometric amount of  $[\text{Au}(\text{acac})(\text{PPh}_3)]$  led only to formation of the dinuclear complex (Scheme 2.19(ii)). In this reaction, the acac ligand acts as the base, deprotonating the phosphonium salt to form the ylide which will then coordinate to the  $\text{AuPPh}_3$  unit. However, although complex **15** will form as an intermediate in this reaction, the fact that it is more reactive than the initial phosphonium salt means that it

(i)

$$[\text{Ph}_3\text{PCH}_2\text{CN}]\text{OTf} \xrightarrow[\text{Cs}_2\text{CO}_3]{[\text{AuCl}(\text{PPh}_3)]} \text{3} + \left[ \begin{array}{c} \text{Ph}_3\text{P} \text{---} \text{CN} \\ | \quad \diagup \\ \text{Au} \text{---} \text{Au} \\ | \quad \diagdown \\ \text{Ph}_3\text{P} \text{---} \text{PPh}_3 \end{array} \right]^+ \text{OTf}^- \quad \text{26}$$

$$+ \left[ \begin{array}{c} \text{Ph}_3\text{P} \text{---} \text{CN} \\ | \quad \diagup \\ \text{Au} \text{---} \text{Au} \text{---} \text{Au} \\ | \quad \diagdown \quad \diagup \\ \text{NC} \text{---} \text{PPh}_3 \end{array} \right]^+ \text{OTf}^- \quad \text{31}$$

(ii)

$$[\text{Ph}_3\text{PCH}_2\text{CN}]\text{OTf} \xrightarrow{[\text{Au}(\text{acac})(\text{PPh}_3)]} \left[ \begin{array}{c} \text{Ph}_3\text{P} \text{---} \text{CN} \\ | \quad \diagup \\ \text{Au} \text{---} \text{Au} \\ | \quad \diagdown \\ \text{Ph}_3\text{P} \text{---} \text{PPh}_3 \end{array} \right]^+ \text{OTf}^- \quad \text{26} + [\text{Ph}_3\text{PCH}_2\text{CN}]\text{OTf} \quad \text{2}$$

(iii)

$$\begin{array}{c} \text{Ph}_3\text{P} \text{---} \text{CN} \\ | \quad \diagup \\ \text{Au} \text{---} \text{H} \\ | \\ \text{Cl}^- \end{array} \quad \text{6} \xrightarrow[\text{PPh}_3]{\text{AgOTf}} \left[ \begin{array}{c} \text{Ph}_3\text{P} \text{---} \text{CN} \\ | \quad \diagup \\ \text{Au} \text{---} \text{H} \\ | \\ \text{Ph}_3\text{P} \end{array} \right]^+ \text{OTf}^- \quad \text{15} + \left[ \begin{array}{c} \text{Ph}_3\text{P} \text{---} \text{CN} \\ | \quad \diagup \\ \text{Au} \text{---} \text{Au} \\ | \quad \diagdown \\ \text{Ph}_3\text{P} \text{---} \text{PPh}_3 \end{array} \right]^+ \text{OTf}^- \quad \text{26}$$

$$+ [\text{Ph}_3\text{PCH}_2\text{CN}]\text{OTf} \quad \text{2}$$

90

### 2.3. Synthesis of Mononuclear Ylide Complexes

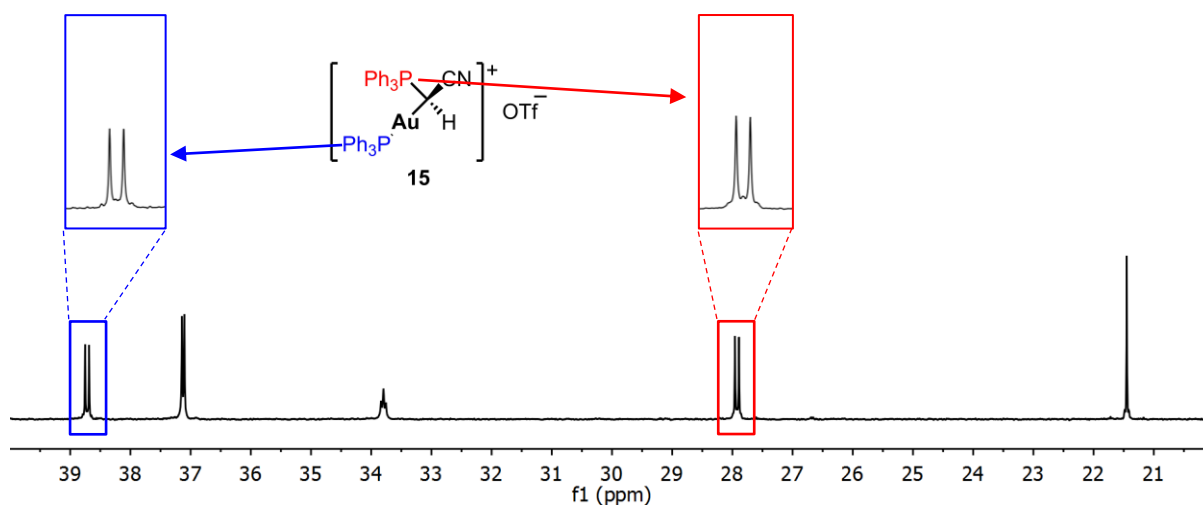
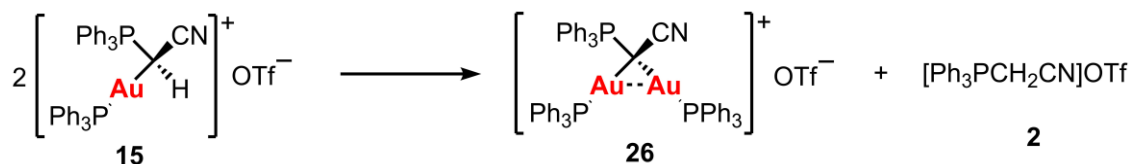
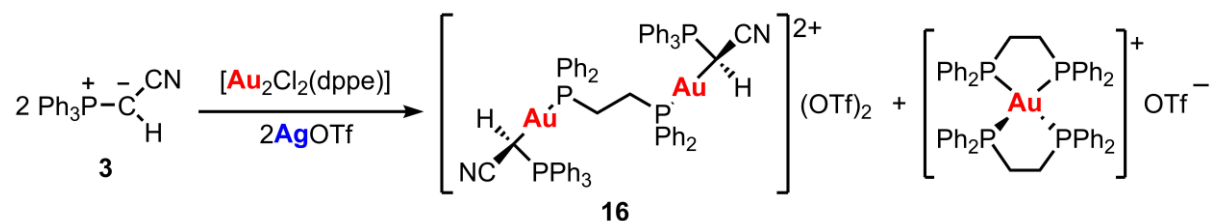


**Figure 2.24.**  $^{31}\text{P}\{^1\text{H}\}$  NMR spectrum for the product mixture from reaction (iii) (Scheme 2.19) in  $\text{CDCl}_3$ .



**Scheme 2.20.** Evolution of complex **15**.

Synthesis of the dicationic dinuclear complex **16** (Scheme 2.21) was also attempted. In this case reaction of two molar equivalents of the free ylide with  $[\text{Au}_2\text{Cl}_2(\text{dppe})]$  and two molar equivalents of  $\text{AgOTf}$  gave the product, however the reaction was not clean and the  $^{31}\text{P}\{^1\text{H}\}$  NMR spectrum shows significant amounts of  $[\text{Au}(\text{dppe})_2]\text{OTf}$  as well as some other minor impurities (Figure 2.25).



**Scheme 2.21.** Synthesis of complex **16**.

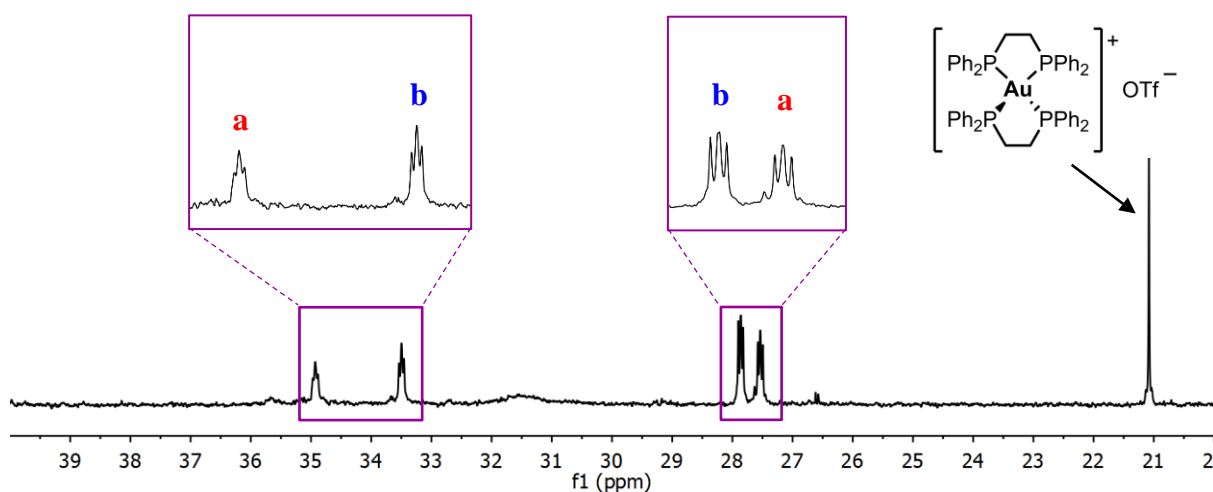


**Figure 2.25.**  $^{31}\text{P}\{^1\text{H}\}$  NMR spectrum for complex **16** with peaks corresponding to each diastereoisomer indicated.

Complex **16** exists as different isomers due to the two asymmetric carbon atoms in the structure. There are two possible diastereoisomers, one of which has two enantiomers, (*R,R*)-**16** and (*S,S*)-**16**, and the other is the *meso* compound (Figure 2.26). The diastereoisomers do not form in equal amounts as can be seen in the  $^{31}\text{P}\{^1\text{H}\}$  NMR spectrum; each diastereoisomer, indicated as **a** and **b** in Figure 2.25 is observed as two multiplets.

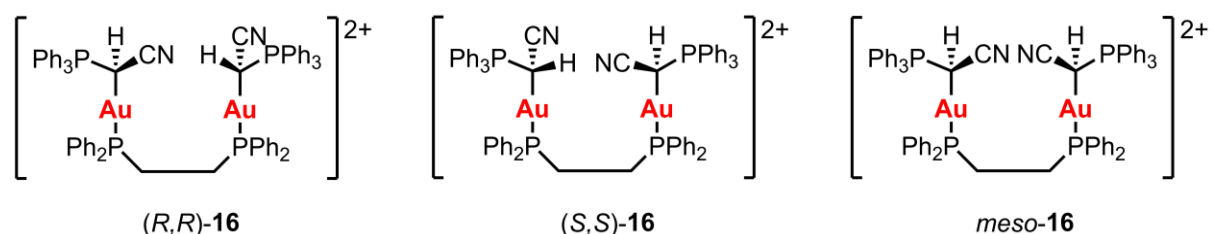


**Figure 2.26.** Isomers of complex **16**.

The molecular structure of the *meso* isomer of complex **16** was determined by single crystal X-ray diffraction analysis (Figure 2.27). In this case crystals were grown by slow diffusion of *n*-pentane into a solution of the mixture of reaction products in dichloromethane. This complex displays an aurophilic interaction between the two gold atoms with a distance of 3.0368(9) Å. The geometry about each gold is distorted significantly from linear coordination of the two ligands with angles C(1)-Au(1)-P(2) 169.4(2)° and C(47)-Au(2)-P(3) 168.6(2)°, likely due to steric hindrance between the phosphine ligand and the triphenylphosphine group of the ylide ligand. The two different gold-carbon bonds are quite different with Au(1)-C(1) 2.125(9) Å and Au(2)-C(47) 2.085(9) Å.

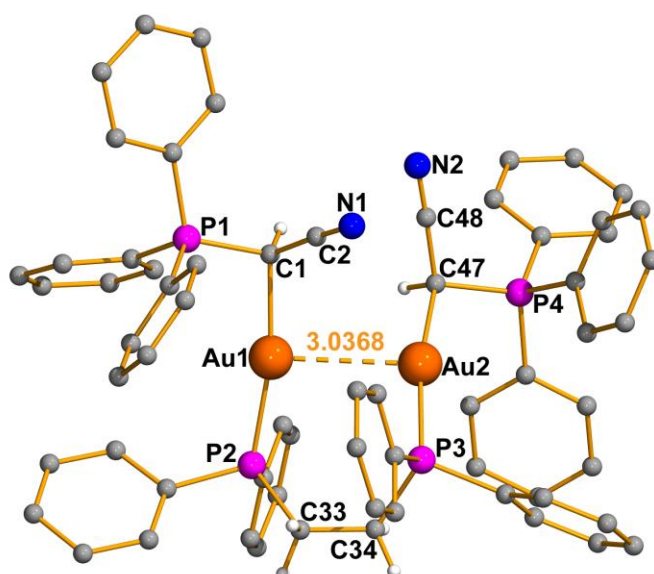
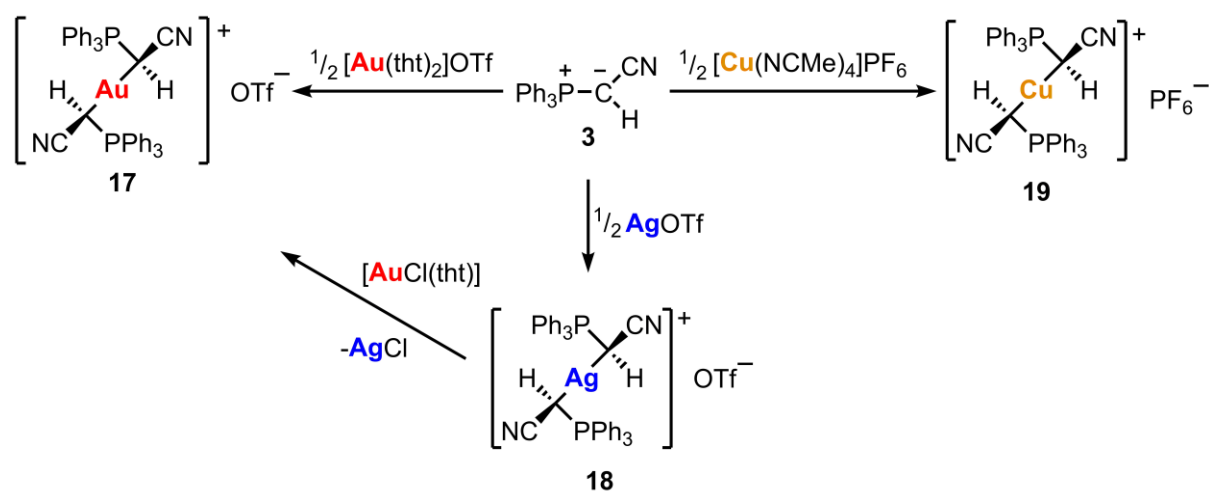


**Figure 2.27.** Molecular structure of **16** determined by single crystal X-ray diffraction. Phenyl hydrogen atoms, anions and solvent molecules are omitted for clarity. Selected bond lengths [Å] and angles [°]: Au(1)-Au(2) 3.0368(9), Au(1)-C(1) 2.125(9), Au(1)-P(2) 2.271(2), Au(2)-C(47) 2.085(9), Au(2)-P(3) 2.267(3), C(1)-C(2) 1.445(11), N(1)-C(2) 1.151(10), P(1)-C(1) 1.778(9), C(47)-C(48) 1.463(12), N(2)-C(48) 1.153(11), P(4)-C(47) 1.802(8), C(1)-Au(1)-P(2) 169.4(2), C(47)-Au(2)-P(3) 168.6(2).

### 2.3.3. Bis-Ylide Complexes

Reaction of the free ylide, **3**, in a 2:1 molar ratio with a gold, silver or copper precursor bearing labile ligands led to the formation of bis-ylide complexes **17-19** (Scheme 2.22). Complex **17** can also be prepared from complex **18** by a transmetallation reaction.



**Scheme 2.22.** Synthesis of bis-ylide complexes **17-19**.

These bis-ylide complexes all have two asymmetric carbon atoms and hence can exist as different diastereoisomers, however the formation of more than one isomer is only observed for the gold derivative, **17**, whereas one isomer of complexes **18** and **19** forms uniquely. Similarly to complex **16**, the fixed 180° geometry about the gold atom and the fact that the groups attached to each carbon atom are equivalent, leads to three possible configurational isomers for complex **17**. Two of these, (*R,R*)-**17** and (*S,S*)-**17**, are enantiomers, and the third non-optically active isomer, *meso*-**17**, is a diastereoisomer of the other two (Figure 2.28).

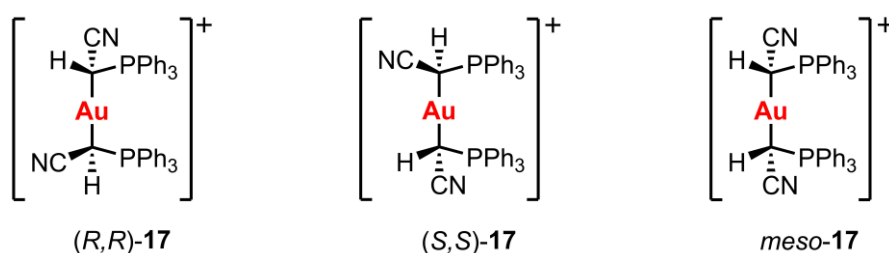


**Figure 2.28.** Isomers of complex **17**.

NMR studies show that both diastereoisomers (the racemic mixture of (*R,R*)-**17** and (*S,S*)-**17** and *meso*-**17**) form in the reaction. In the  $^1\text{H}$  NMR two doublets are observed for the  $\text{C}_{(\alpha)}\text{-H}$  (Figure 2.29(a)). Enantiomers (*R,R*)-**17** and (*S,S*)-**17** are indistinguishable by NMR and only one doublet would be observed for the racemic mixture of these two. The other doublet is due to the presence of the *meso* complex. In the  $^{31}\text{P}\{^1\text{H}\}$  NMR spectrum two signals are observed, one corresponding to the racemic mixture of (*R,R*)-**17** and (*S,S*)-**17** and the other corresponding to the *meso* complex (Figure 2.29(b)). Integration of the signals for the  $\text{C}_{(\alpha)}\text{-H}$  in the  $^1\text{H}$  NMR spectrum shows that the racemic mixture ((*R,R*)-**17** and (*S,S*)-**17**) and the *meso* complex (*meso*-**17**) form in almost equivalent amounts (1 : 1.1), demonstrating the similar thermodynamic stability of these complexes.

### 2.3. Synthesis of Mononuclear Ylide Complexes

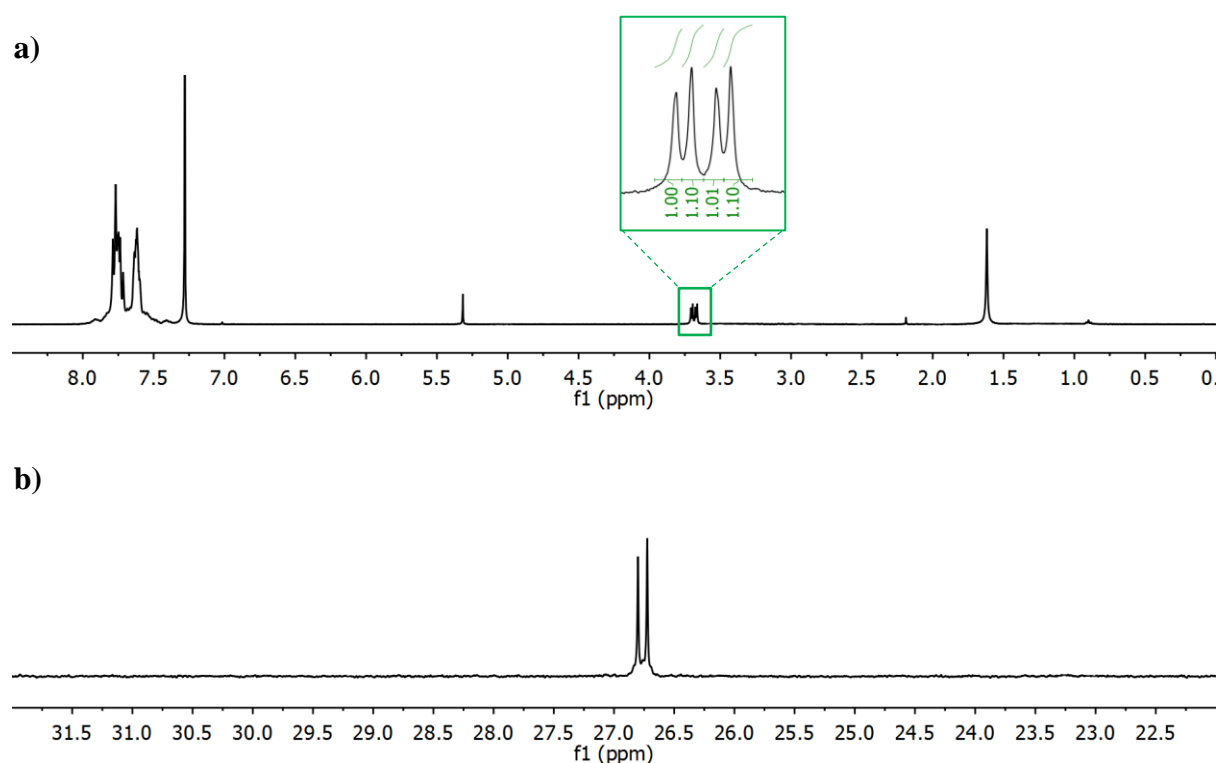


**Figure 2.29.**  $^1\text{H}$  NMR spectrum (a) and  $^{31}\text{P}\{^1\text{H}\}$  NMR spectrum (b) for complex **17** in  $\text{CDCl}_3$ .

Although the analogous silver and copper complexes, **18** and **19**, could theoretically also form as a mixture of diastereoisomers, only one isomer is formed in the reactions for their synthesis. The  $^1\text{H}$  NMR spectrum shows only one doublet for the  $\text{C}_\alpha\text{-H}$  in both cases, and the  $^{31}\text{P}\{^1\text{H}\}$  NMR spectrum shows only a single sharp peak. This difference can be attributed to the different structure of complexes **18** and **19** compared to the gold derivative, **17**. Complex **17** will have a linear coordination about the gold atom and no additional coordination of the  $\text{C}\equiv\text{N}$  to the gold occurs, as shown by the infrared absorption frequency (Table 2.4). Complexes **18** and **19**, however will not adopt a linear geometry and additional stabilisation by coordination of the  $\text{C}\equiv\text{N}$  will be favourable. Again, this is clearly observed by the significantly lower infrared absorption frequency of the  $\text{C}\equiv\text{N}$  in these complexes.

**Table 2.4.** Infrared absorption frequencies for bis-ylide complexes

Complex	$\nu(\text{C}\equiv\text{N})$ ( $\text{cm}^{-1}$ )
<b>17</b>	2210
<b>18</b>	2168
<b>19</b>	2166

The molecular structure of complex **18** was determined by single crystal X-ray diffraction analysis (Figure 2.30). The silver atom has a distorted tetrahedral geometry due to the additional bonding of the C≡N groups, resulting in a polymeric structure. The two silver-carbon bonds are very similar in length (Ag(1)-C(1) 2.394(3) Å and Ag(1)-C(21) 2.333(3) Å). Close examination shows that the favoured diastereoisomer is the mixture of enantiomers. The *meso* complex would not have the required geometry to form such a polymeric structure and hence is less thermodynamically stable and does not form. Based on the IR data, complex **19** is presumed to have an analogous structure.

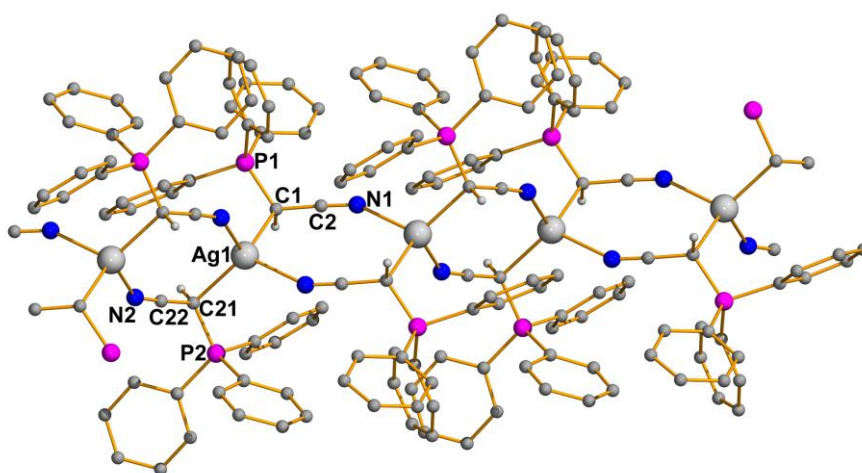


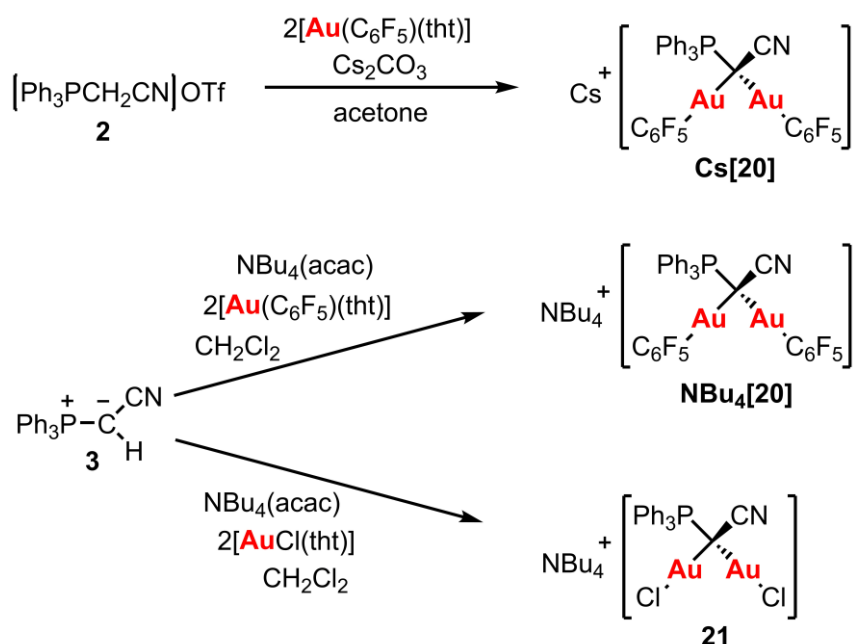
**Figure 2.30.** Molecular structure of **18** determined by single crystal X-ray diffraction. Phenyl hydrogen atoms, anions and solvent molecules are omitted for clarity. Selected bond lengths [Å] and angles [°]: Ag(1)-C(1) 2.394(3), Ag(1)-C(21) 2.333(3), Ag(1)-N(1) 2.341(2), Ag(1)-N(2) 2.337(2), C(1)-C(2) 1.421(4), C(2)-N(1) 1.150(4), P(1)-C(1) 1.736(3), C(21)-C(22) 1.417(4), C(22)-N(2) 1.156(4), P(2)-C(21) 1.751(3), C(21)-Ag(1)-C(1) 110.93(9), N(1)-Ag(1)-C(1) 104.33(9), N(2)-Ag(1)-C(1) 114.05(9), C(21)-Ag(1)-N(1) 118.88(9), C(21)-Ag(1)-N(2) 114.62(9), N(2)-Ag(1)-N(1) 92.68(9).



## 2.4. Synthesis of Polynuclear Yldeide Complexes

### 2.4.1. Anionic Complexes

Reaction of the phosphonium triflate salt, **2**, with two molar equivalents of  $[\text{Au}(\text{C}_6\text{F}_5)(\text{tth})]$  in the presence of excess caesium carbonate led successfully to the formation of anionic dinuclear gold derivative **Cs[20]** with caesium as the cation (Scheme 2.23). In dichloromethane this reaction led to a mixture of **Cs[20]** and the neutral mononuclear complex **5**, however in acetone the reaction was clean and complex **Cs[20]** was obtained as the only product in a yield of 91%. The analogous complex **NBu<sub>4</sub>[20]** with a tetrabutylammonium cation was prepared from the free ylde, **3**, with two molar equivalents of  $[\text{Au}(\text{C}_6\text{F}_5)(\text{tth})]$  using  $\text{NBu}_4(\text{acac})$  as the base and was again obtained in a good yield, 90%. The dichloro complex **21** could also be prepared by this route using  $[\text{AuCl}(\text{tth})]$  in place of  $[\text{Au}(\text{C}_6\text{F}_5)(\text{tth})]$ , and was obtained in an excellent yield of 95%.



**Scheme 2.23.** Synthesis of anionic complexes **20-21**.

The successful deprotonation of the ylde can be confirmed by the lack of the  $\text{C}_\alpha\text{-H}$  signal in the  $^1\text{H}$  NMR spectra of complexes **20-21**, and the presence of the tetrabutylammonium cation in complexes **NBu<sub>4</sub>[20]** and **21** can also clearly be seen by the signals corresponding to the butyl chains (Figure 2.31). Integration of these signals shows the presence of one

tetrabutylammonium group per ylide. The  $^{19}\text{F}$  NMR spectra of complexes **Cs[20]** and **NBu<sub>4</sub>[20]** show clearly the presence of one type of pentafluorophenyl group since the two pentafluorophenyl groups are equivalent in these complexes, and the presence of the Au-Cl bonds in complex **21** is confirmed by a strong absorption at  $316\text{ cm}^{-1}$  in the IR spectrum. The  $\text{C}\equiv\text{N}$  absorption frequencies for **20-21**,  $2160\text{ cm}^{-1}$  and  $2165\text{ cm}^{-1}$ , respectively, are considerably lower than the gold(I) derivatives in which the ylide is mono-coordinate. This can be attributed to the strong electron withdrawing effect of the two Au-X groups at the ylide carbon which leads to a loss of electron density in the  $\text{C}\equiv\text{N}$  bond. The complexes were also successfully observed by high resolution mass spectrometry (ESI-QTOF) with peaks observed at  $m/z = 1028.0199$  corresponding to  $[\text{M}]^-$  for complexes **Cs[20]** and **NBu<sub>4</sub>[20]** and  $m/z = 763.9656$  corresponding to  $[\text{M}]^-$  for complex **17**. The experimentally determined isotopic distribution patterns are in good agreement with the theoretical predictions (Figures 2.32-2.33).

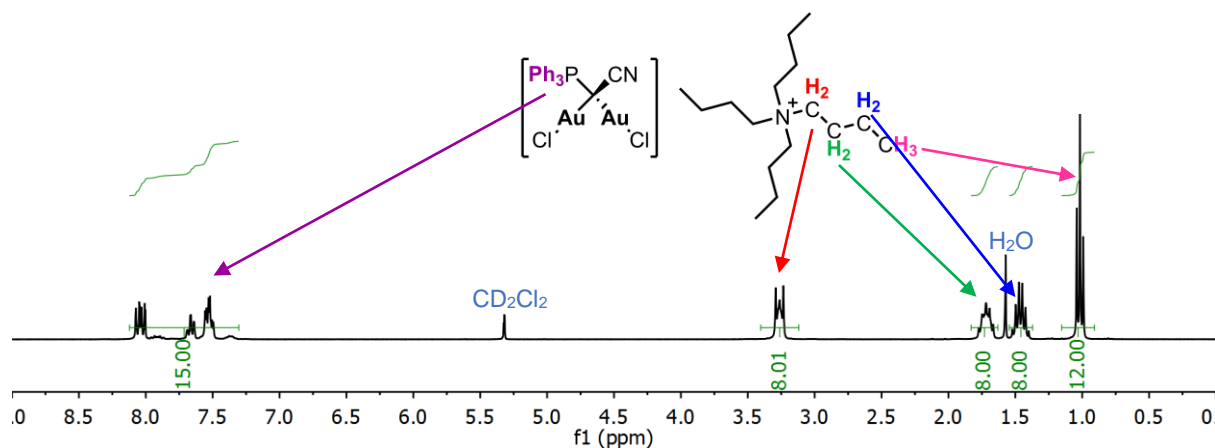


**Figure 2.31.**  $^1\text{H}$  NMR spectrum of complex **21** in  $\text{CD}_2\text{Cl}_2$ .

## 2.4. Synthesis of Polynuclear Ylide Complexes

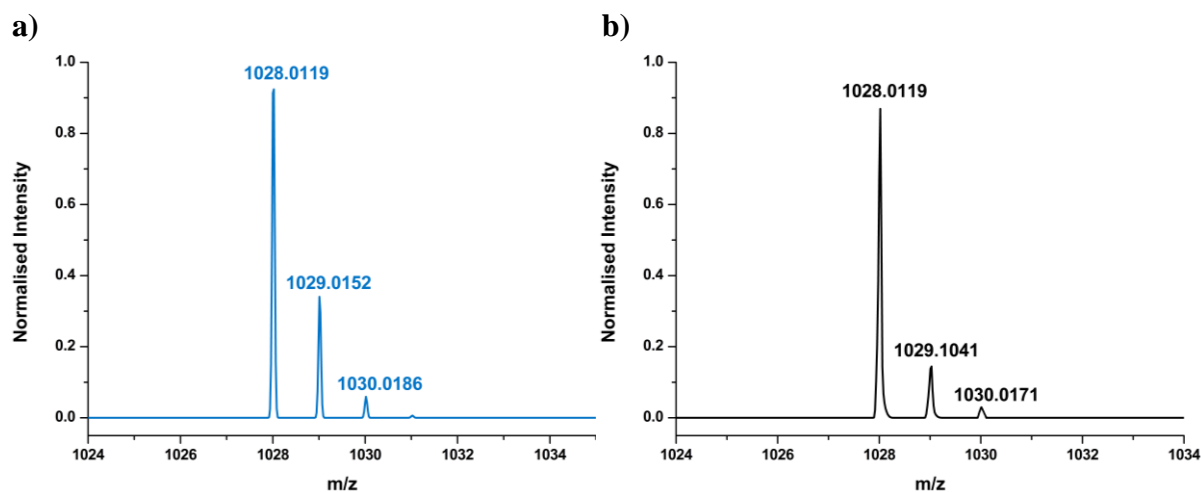


**Figure 2.32.** Calculated (a) and experimentally determined (b) isotopic distribution patterns for  $\text{C}_{32}\text{H}_{15}\text{Au}_2\text{F}_{10}\text{NP} [\text{M}]^-$  for complex **Cs[20]**.

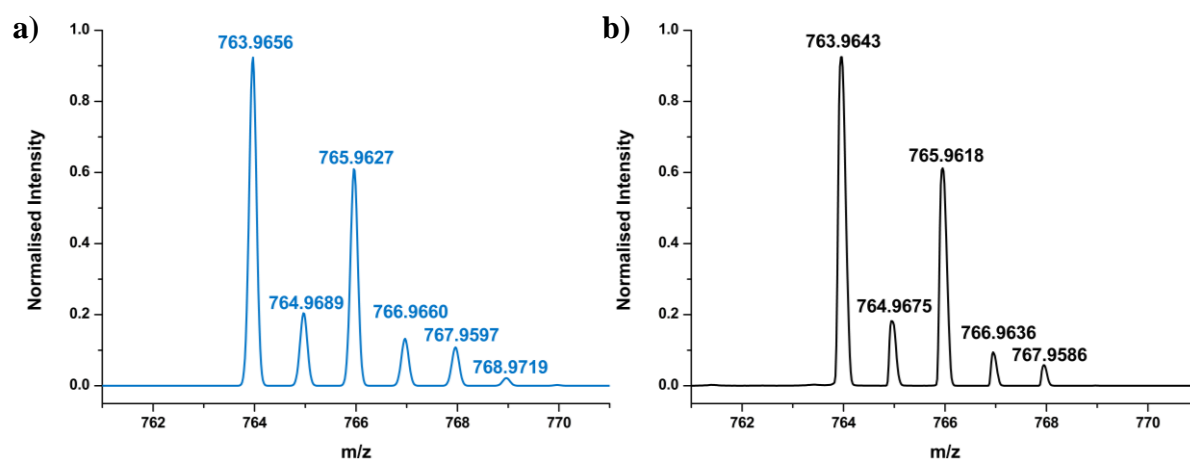
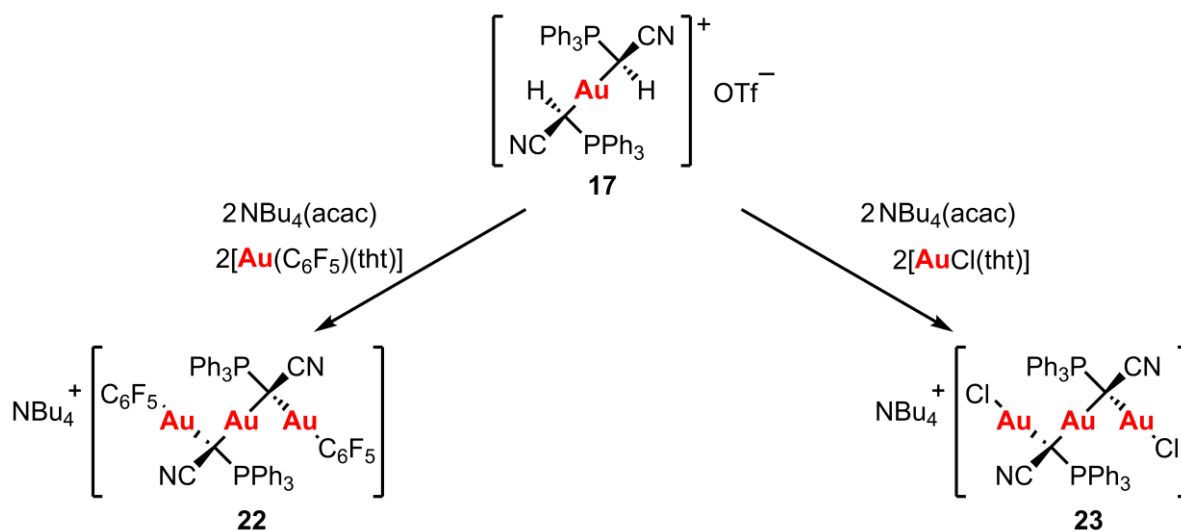


**Figure 2.33.** Calculated (a) and experimentally determined (b) isotopic distribution patterns for  $\text{C}_{20}\text{H}_{15}\text{Au}_2\text{Cl}_2\text{NP} [\text{M}]^-$  for complex **21**.

Anionic trinuclear derivatives of the bis-ylide gold complex **17** could also be prepared in a similar manner by double deprotonation of complex **17** using  $\text{NBu}_4(\text{acac})$  as a base, and subsequent coordination to  $\text{Au}(\text{C}_6\text{F}_5)$  or  $\text{AuCl}$  by displacement of tht from  $[\text{Au}(\text{C}_6\text{F}_5)(\text{tht})]$  or  $[\text{AuCl}(\text{tht})]$  to give complexes **22** and **23**, respectively (Scheme 2.24).



**Scheme 2.24.** Synthesis of anionic complexes **22-23**.

Again, the successful deprotonation could be confirmed by the lack of a  $\text{C}_{(\alpha)}\text{-H}$  signal in the  $^1\text{H}$  NMR spectrum and integration of the tetrabutylammonium and triphenylphosphine signals showed the presence of two ylide units per tetrabutylammonium cation (Figure 2.34). Only one peak at 29.17 ppm is observed in the  $^{31}\text{P}\{^1\text{H}\}$  NMR spectrum of complex **23** showing that only one diastereoisomer has formed from the mixture of diastereoisomers of complex **17**. This is likely to be because one diastereoisomer would have less steric hindrance between the relatively bulky triphenylphosphine groups and hence would be thermodynamically more stable.

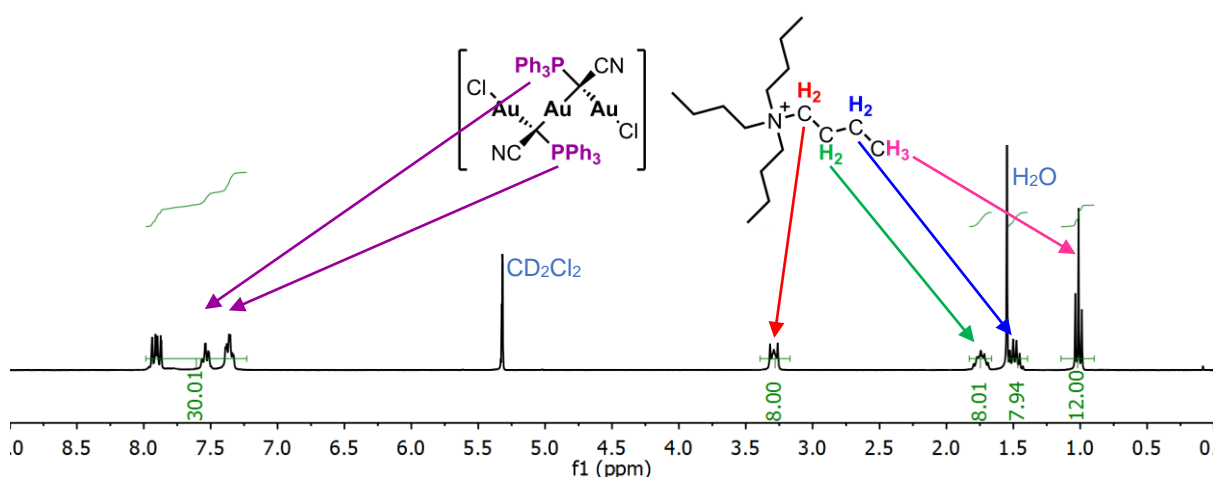


**Figure 2.34.**  $^1\text{H}$  NMR spectrum of complex **23** in  $\text{CD}_2\text{Cl}_2$

## 2.4. Synthesis of Polynuclear Yldiide Complexes

Both complexes were identified by high resolution mass spectrometry (ESI-QTOF) with peaks observed at  $m/z = 1525.0710$  corresponding to  $[\mathbf{M}]^-$  for complex **22**, and  $m/z = 1261.0241$  corresponding to  $[\mathbf{M}]^-$  for complex **23** with isotopic distribution patterns in good agreement with the theoretical prediction (Figures 2.35-2.36).

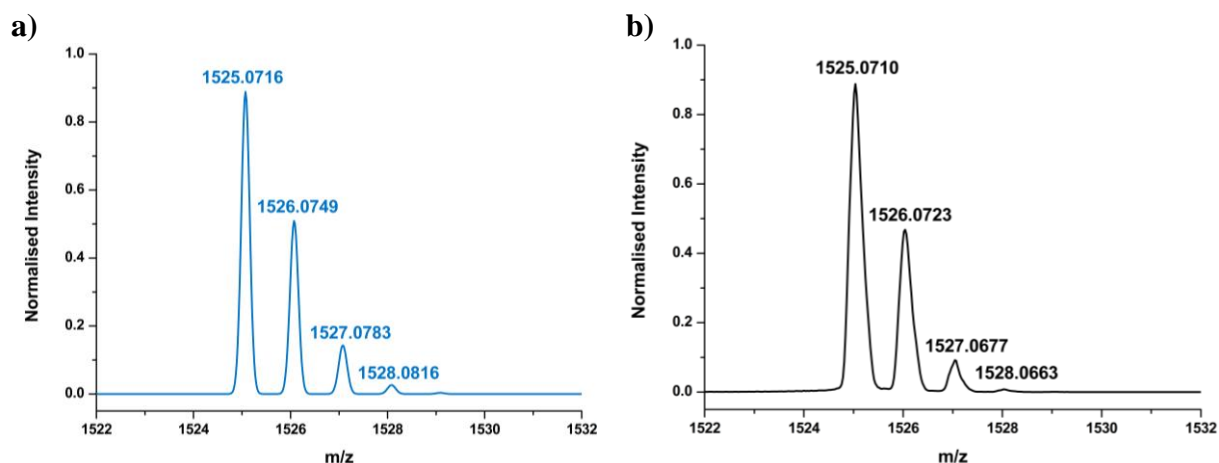


**Figure 2.35.** Calculated (a) and experimentally determined (b) isotopic distribution patterns for  $\text{C}_{52}\text{H}_{30}\text{Au}_3\text{F}_{10}\text{N}_2\text{P}_2$   $[\mathbf{M}]^-$  for complex **22**.

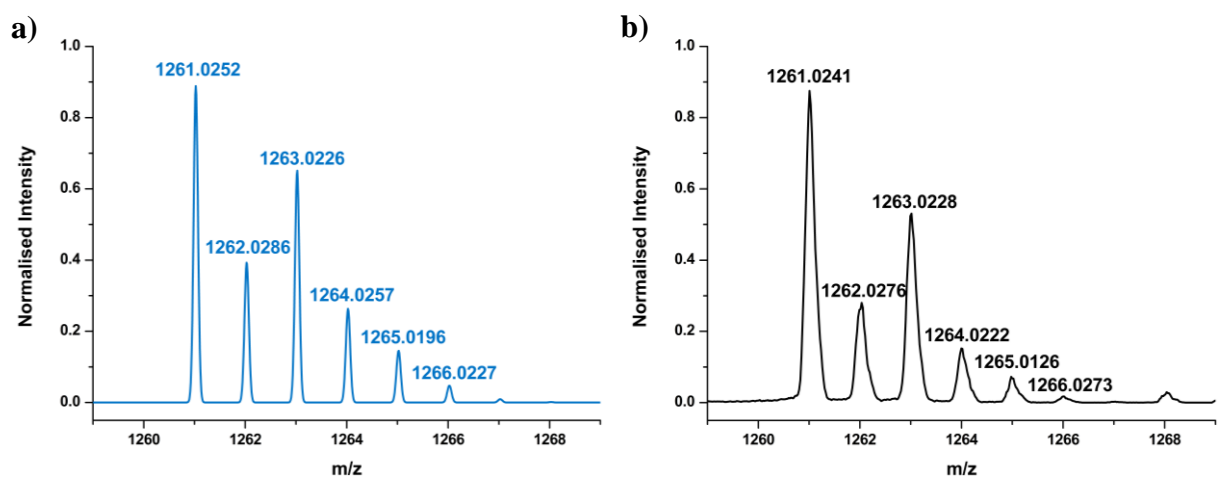
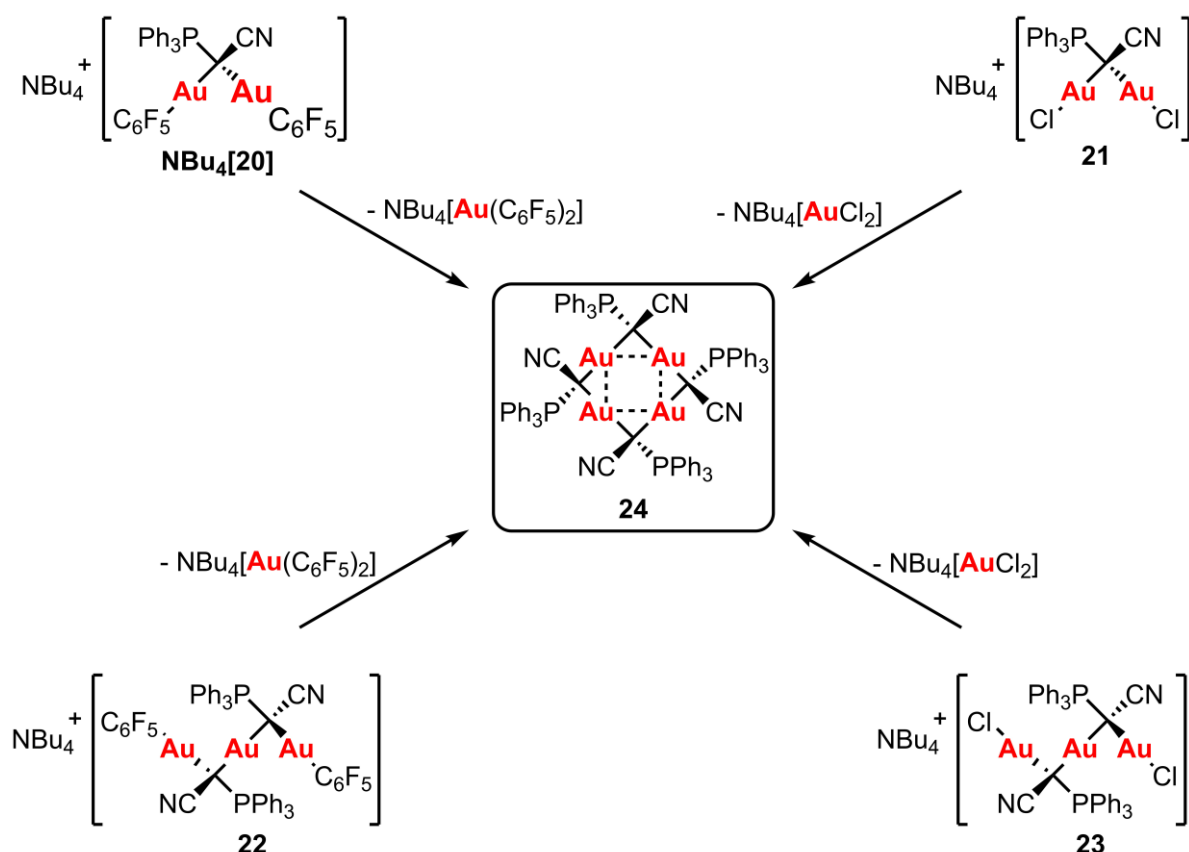


**Figure 2.36.** Calculated (a) and experimentally determined (b) isotopic distribution patterns for  $\text{C}_{46}\text{H}_{30}\text{Au}_3\text{Cl}_2\text{N}_2\text{P}_2$   $[\mathbf{M}]^-$  for complex **23**.

Complexes **20-23** were unstable in solution and over time all gradually formed the more thermodynamically stable tetranuclear complex, **24**, by loss of  $\text{NBu}_4[\text{AuX}_2]$  ( $\text{X} = \text{C}_6\text{F}_5, \text{Cl}$ ) (Scheme 2.25).



**Scheme 2.25.** Formation of tetranuclear complex **24** from complexes **20-23**.

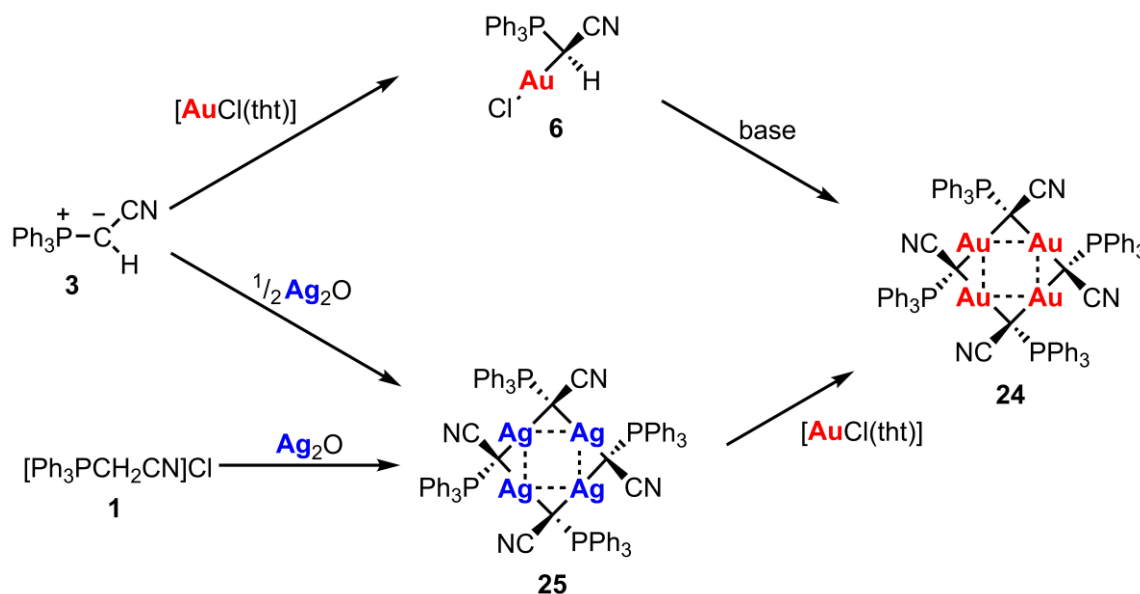
#### 2.4.2. Neutral Complexes

The neutral tetrameric gold complex, **24**, could also be prepared by reaction of complex **6** with a variety of different bases including *n*-BuLi, NBu<sub>4</sub>(acac) and Cs<sub>2</sub>CO<sub>3</sub>, in each case the chloride ligand was removed as the corresponding chloride salt LiCl, NBu<sub>4</sub>Cl or CsCl (Scheme 2.26). The yields in these reactions were only moderate (54-55%).

The analogous silver tetramer, complex **25**, could be prepared from the free ylide, **3**, with 0.5 equivalents of Ag<sub>2</sub>O. The Ag<sub>2</sub>O acts as a base, deprotonating the ylide and allowing coordination to silver, with complex **25** obtained in a yield of 86%. Complex **25** could also be prepared from the commercially available phosphonium chloride salt, **1**, with one equivalent of Ag<sub>2</sub>O. In this case, the precipitation of silver chloride drives the reaction and can readily be removed from the product by filtration of the reaction solution through a pad of celite. The final complex was obtained in a slightly lower yield of 78%. Reaction of complex **25** with [AuCl(tht)] led to the formation of complex **24**, by a transmetallation reaction driven by the precipitation of silver chloride. This method gave complex **24** by a very clean reaction and in

## 2.4. Synthesis of Polynuclear Ylide Complexes

an excellent yield of 92%. Both complexes **24** and **25** were obtained as white solids and were highly stable under ambient conditions.



**Scheme 2.26.** Synthesis of tetranuclear complex **24** and **25**.

The infrared absorption frequencies for the  $\text{C}\equiv\text{N}$  bond for complexes **24** and **25**,  $2154\text{ cm}^{-1}$  and  $2110\text{ cm}^{-1}$ , respectively, are considerably lower than the values for the phosphonium salts or the monocoordinated ylide complexes. This can again be attributed to the presence of two electron withdrawing metal atoms at the ylide carbon atom resulting in a reduction of electron density in the  $\text{C}\equiv\text{N}$  triple bond.

Two different isomers of **24** were characterised by single crystal X-ray diffraction (Figure 2.37). One of the isomers, **24a**, crystallises in a tetragonal crystal system with only one quarter of the molecule observed in the asymmetric unit (Figure 2.37(a)). The other, **24b**, is monoclinic and the entire molecule is observed in the asymmetric unit (Figure 2.37(b)). Isomer **24a** features alternating upwards facing  $\text{CN}$  and  $\text{PPh}_3$  groups. Linear coordination is observed about the gold centres and aurophilic interactions are present with  $\text{Au-Au}$  distances of  $3.0710(5)$  and  $3.0711(5)\text{ \AA}$ . Isomer **24b** has two adjacent upwards facing  $\text{CN}$  groups. The coordination about the gold centres is almost linear in every case and again aurophilic interactions are present between all of the gold atoms.

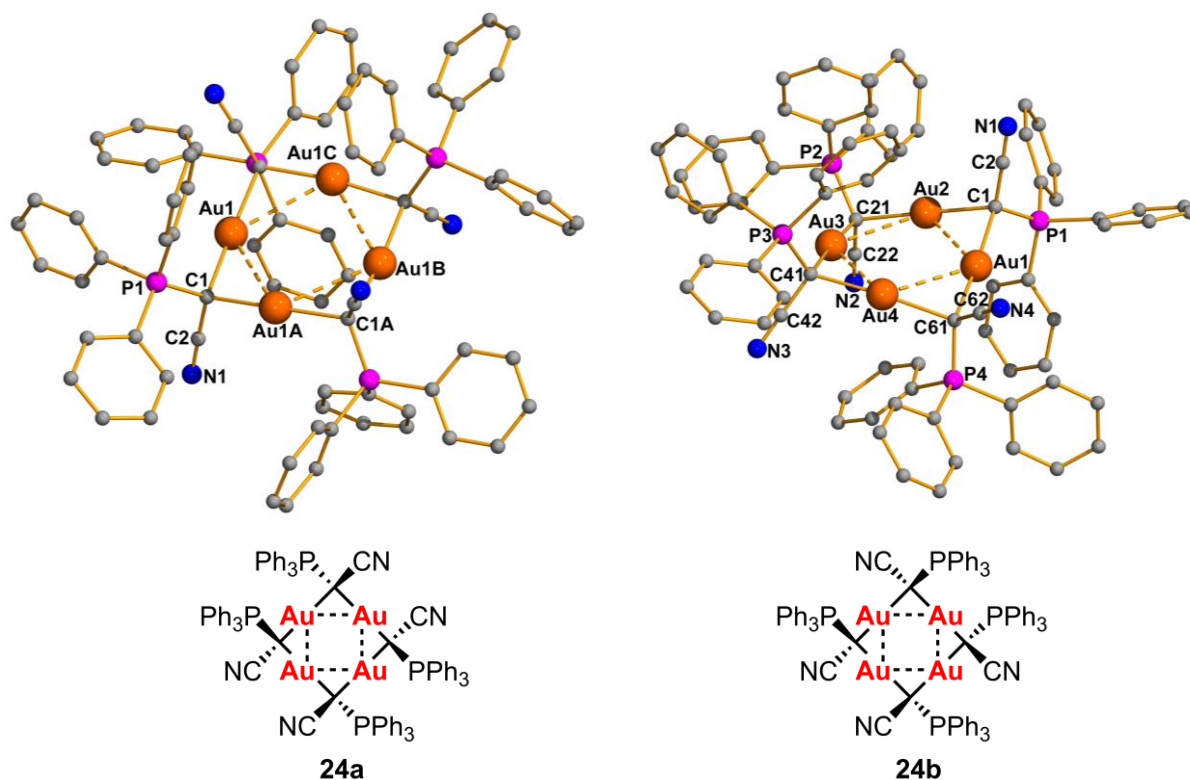


**Figure 2.37.** Molecular structure of isomers **24a** and **24b** determined by single crystal X-ray diffraction. Phenyl hydrogen atoms, anions and solvent molecules are omitted for clarity. Selected bond lengths [Å] and angles [°]  
**24a:** Au(1)-C(1) 2.090(9), Au(1A)-C(1) 2.099(10), P(1)-C(1) 1.765(11), C(1)-C(2) 1.410(16), C(2)-N(1) 1.159(14), Au(1)-Au(1A) 3.0710(5), Au(1)-Au(1C) 3.0711(5), C(1)-Au(1A)-C(1A) 172.5(3), C(1)-C(2)-N(1) 178.1(11); **24b:** Au(1)-C(1) 2.140(10), Au(1)-C(61) 2.129(10), Au(2)-C(1) 2.125(9), Au(2)-C(21) 2.127(11), Au(3)-C(21) 2.115(9), Au(3)-C(41) 2.110(9), Au(4)-C(41) 2.120(10), Au(4)-C(61) 2.136(10), Au(1)-Au(2) 2.9706(8), Au(2)-Au(3) 2.9708(8), Au(3)-Au(4) 3.0362(9), Au(4)-Au(1) 2.9775(8), P(1)-C(1) 1.727(10), C(1)-C(2) 1.427(15), C(2)-N(1) 1.153(15), P(2)-C(21) 1.745(10), C(21)-C(22) 1.433(14), C(22)-N(2) 1.150(14), P(3)-C(41) 1.741(10), C(41)-C(42) 1.432(15), C(42)-N(3) 1.152(15), P(4)-C(61) 1.729(9), C(61)-C(62) 1.427(13), C(62)-N(4) 1.155(14), C(1)-Au(1)-C(61) 174.8(4), C(21)-Au(2)-C(1) 178.0(4), C(41)-Au(3)-C(21) 176.1(4), C(61)-Au(4)-C(41) 171.9(4), C(1)-C(2)-N(1) 178.5(13), C(21)-C(22)-N(2) 178.2(10), C(41)-C(42)-N(3) 179.2(12), C(61)-C(62)-N(4) 179.3(12).

Complex **25** was also characterised by single crystal X-ray diffraction (Figure 2.38). In this case only one isomer was observed which has a tetragonal structure with one quarter of the molecule in the asymmetric unit. Similarly to the gold derivative **24a**, a linear coordination is observed about the silver centres and metallophilic interactions are observed between the silver atoms. No coordination of the nitrile group to silver is observed.



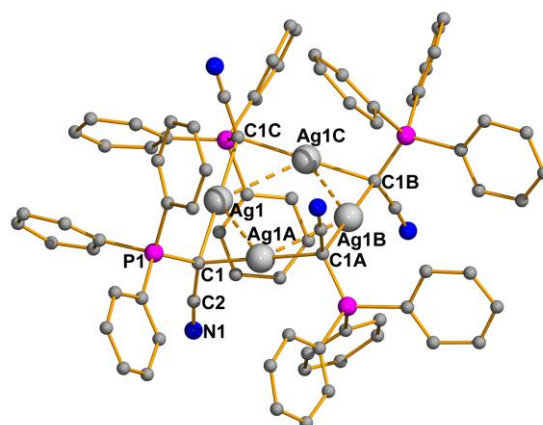
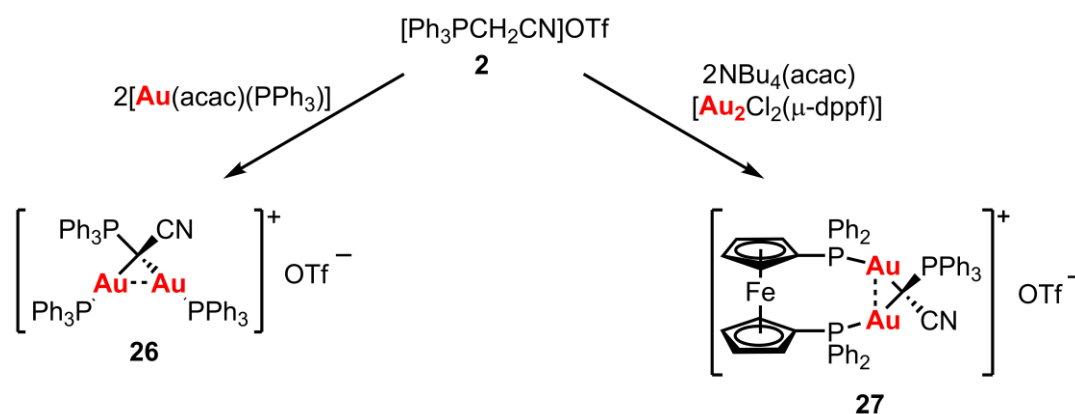


**Figure 2.38.** Molecular structure of **25** determined by single crystal X-ray diffraction. Phenyl hydrogen atoms, anions and solvent molecules are omitted for clarity. Selected bond lengths [Å] and angles [°]: Ag(1)-C(1) 2.147(15), Ag(1A)-C(1) 2.147(15), P(1)-C(1) 1.720(18), C(1)-C(2) 1.43(3), C(2)-N(1) 1.13(2), Ag(1)-Ag(1A) 2.9201(18), Ag(1)-Ag(1C) 2.9202(18), C(1)-Ag(1A)-C(1A) 179.6(7), C(1)-C(2), N(1) 174.4(19).

### 2.4.3. Cationic Complexes

Dinuclear cationic gold phosphine derivatives **26** and **27** with bridging ylde ligands were prepared from the phosphonium triflate salt, **2**, using acac as the base in both cases (Scheme 2.27). In the synthesis of complex **27** the tetrabutylammonium chloride formed in the reaction was readily removed by washing the reaction mixture with water. Both complexes were obtained cleanly and in good yields of 89% and 90%, respectively.



**Scheme 2.27.** Synthesis of cationic gold phosphine complexes **26** and **27**.

The lack of C $_{\alpha}$ -H signal in the  $^1\text{H}$  NMR spectra of both complexes indicates successful deprotonation of the phosphonium salt. For complex **27** phosphorus-phosphorus coupling between the ylide phosphorus atom and the triphenylphosphine ligands can clearly be seen in the  $^{31}\text{P}\{^1\text{H}\}$  NMR spectrum. A doublet at 37.27 ppm corresponding to the triphenylphosphine

ligands and a triplet at 34.27 ppm ( $^3J_{\text{PP}} = 6.3$  Hz) for the ylide phosphorus atom are observed since both AuPPh<sub>3</sub> groups are equivalent (Figure 2.39).

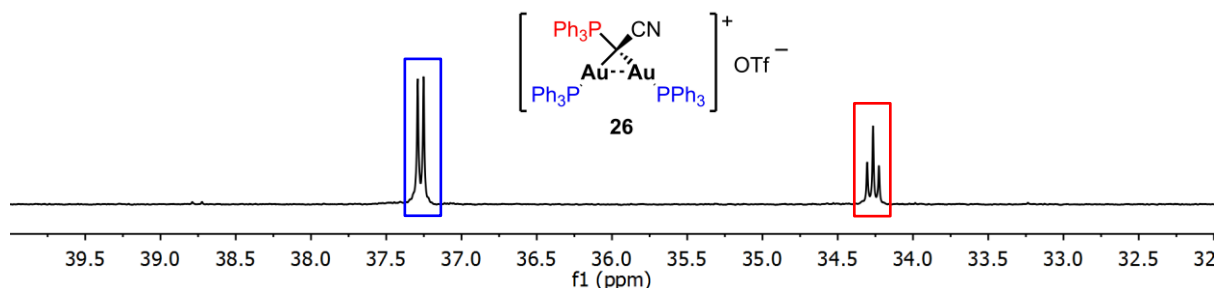


**Figure 2.39.**  $^{31}\text{P}\{^1\text{H}\}$  NMR spectrum for complex **26** in  $\text{CD}_2\text{Cl}_2$ .

For complex **27**, the flexibility of the phosphine at room temperature causes the ferrocene C-H signals to be observed as broad singlets in the  $^1\text{H}$  NMR spectrum (Figure 2.40(a)) whilst in the  $^{31}\text{P}\{^1\text{H}\}$  NMR spectrum, the phosphine is observed as a broad signal and the signal for the ylide phosphorus atom appears as a pseudo-triplet due to coupling with the two phosphorus atoms of the dppf ligand (Figure 2.40(b)).

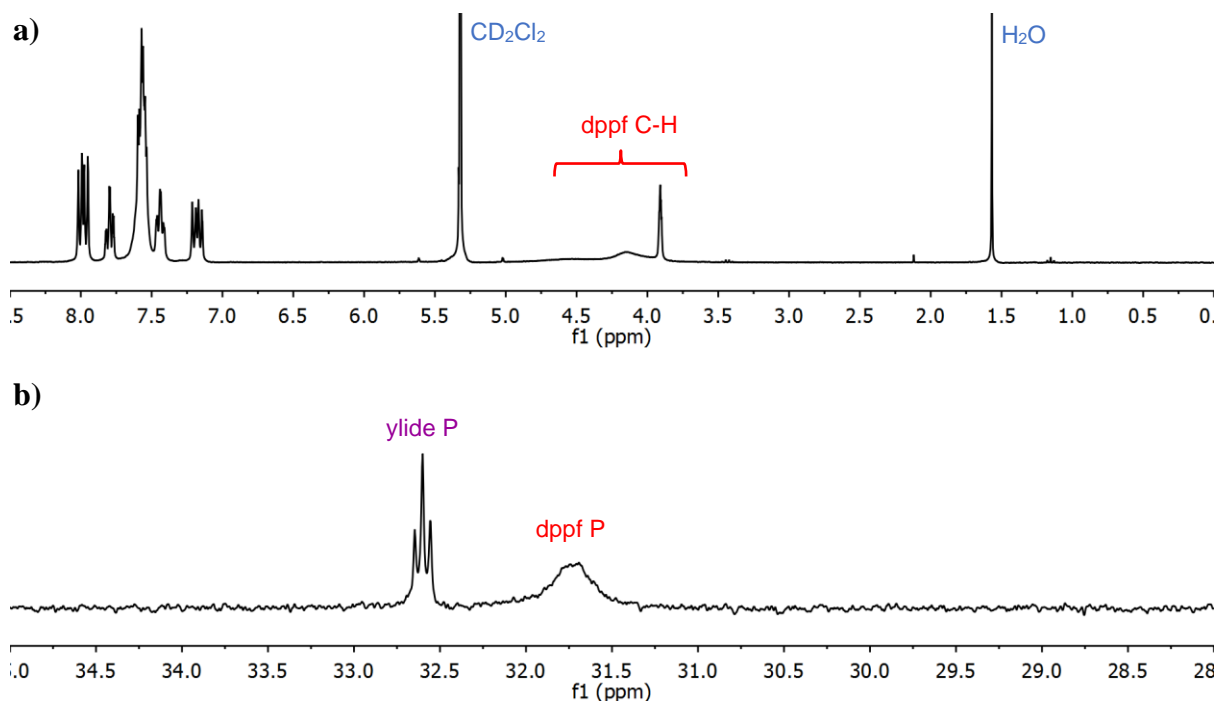


**Figure 2.40.**  $^1\text{H}$  NMR spectrum for complex **27** in  $\text{CD}_2\text{Cl}_2$  at room temperature (a),  $^{31}\text{P}\{^1\text{H}\}$  NMR spectrum for complex **27** in  $\text{CD}_2\text{Cl}_2$  at room temperature (b).

## 2.4. Synthesis of Polynuclear Yldeide Complexes

At -80 °C each of the ferrocene C-H signals can be observed as a separate singlet in the  $^1\text{H}$  NMR spectrum (Figure 2.41(a)) and three multiplets are observed in the  $^{31}\text{P}\{^1\text{H}\}$  NMR spectrum due to the inequivalence of the two phosphorus atoms in the dppf ligand at this temperature (Figure 2.41(b)).

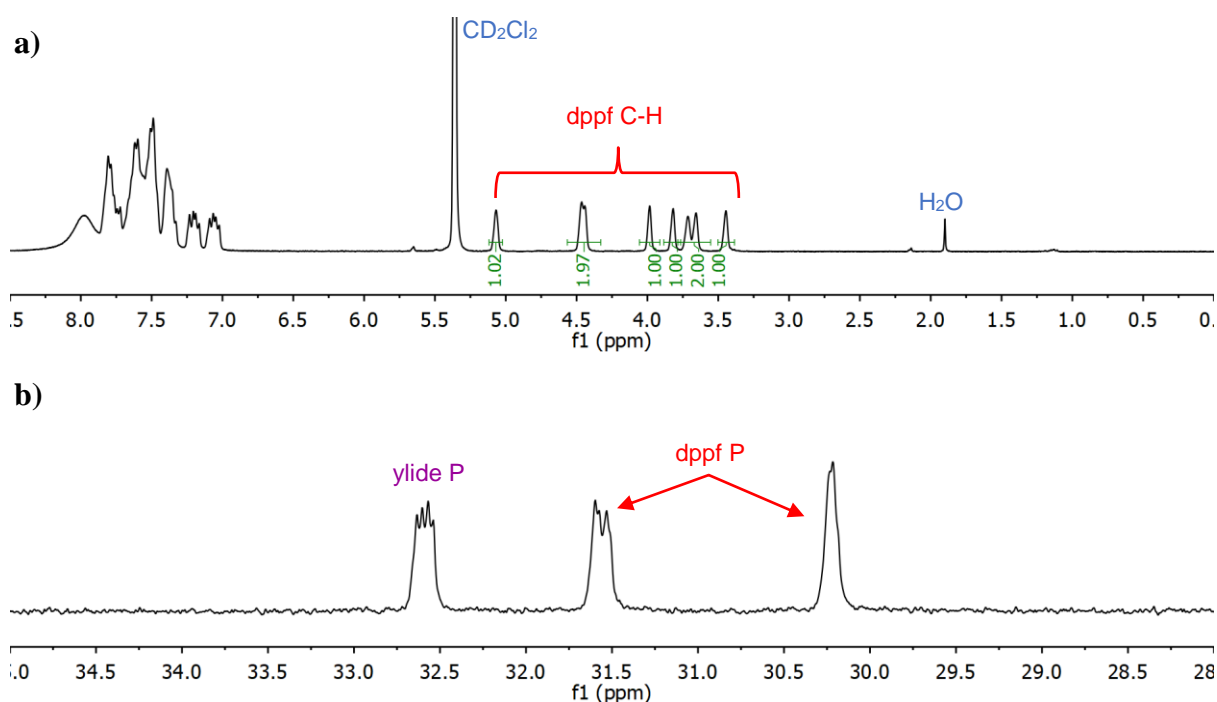


**Figure 2.41.**  $^1\text{H}$  NMR spectrum for complex **27** in  $\text{CD}_2\text{Cl}_2$  at -80 °C (a),  $^{31}\text{P}\{^1\text{H}\}$  NMR spectrum for complex **27** in  $\text{CD}_2\text{Cl}_2$  at -80 °C (b).

The molecular structures of both complexes were determined by single crystal X-ray diffraction (Figure 2.42). For complex **26** both gold atoms have an almost linear coordination. The slight distortion from 180° is due to the sterically bulky triphenylphosphine groups. The Au(2)-C(1)-Au(1) angle of 90.7(3)° is reduced significantly from that typical of a tetrahedron (109.5°) due to the presence of an aurophilic interaction which causes the two gold atoms to be closer in proximity. A gold-gold distance Au(1)-Au(2) of 2.9829(4) Å is observed. For complex **27**, again an almost linear coordination is observed about each gold centre with angles C(1)-Au(1)-P(2) 171.2(5)° and C(1)-Au(2)-P(3) 173.9(5)°. One of the gold carbon bonds is slightly longer than the other: Au(1)-C(1) 2.142(16) Å and Au(2)-C(1) 2.192(18) Å. This is likely due to steric hindrance. An aurophilic interaction is observed between the gold centres with a distance Au(1)-Au(2) 2.8423(13) Å.

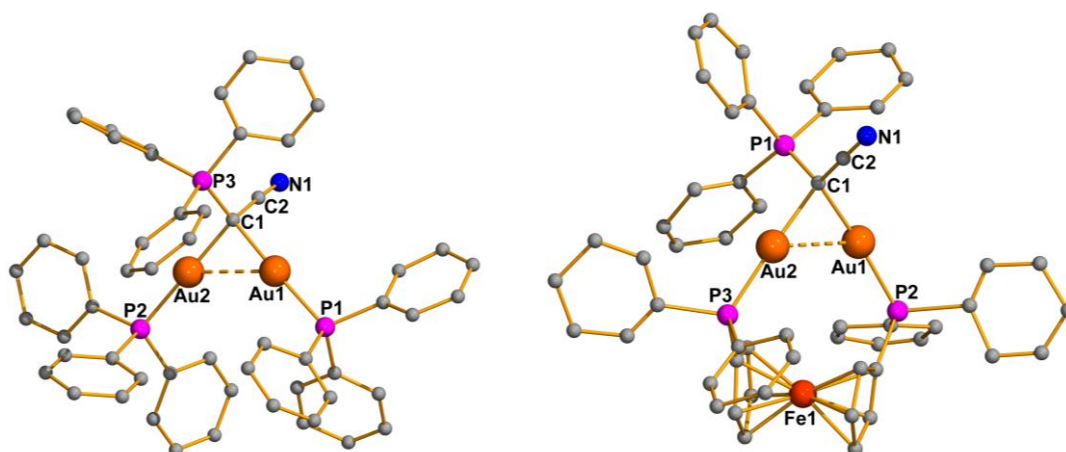
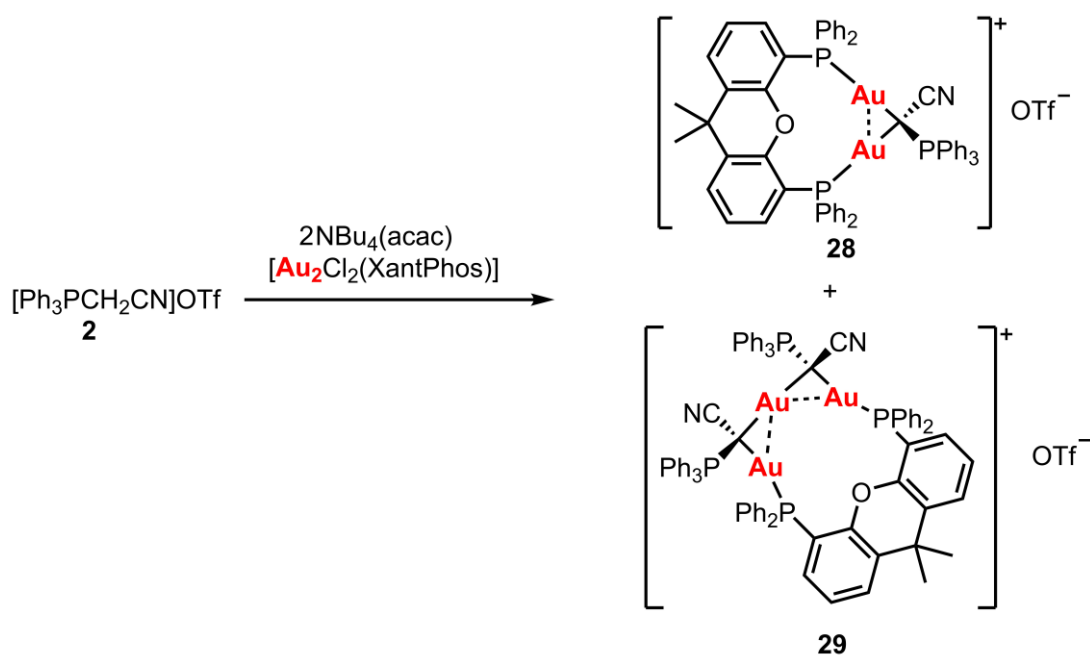


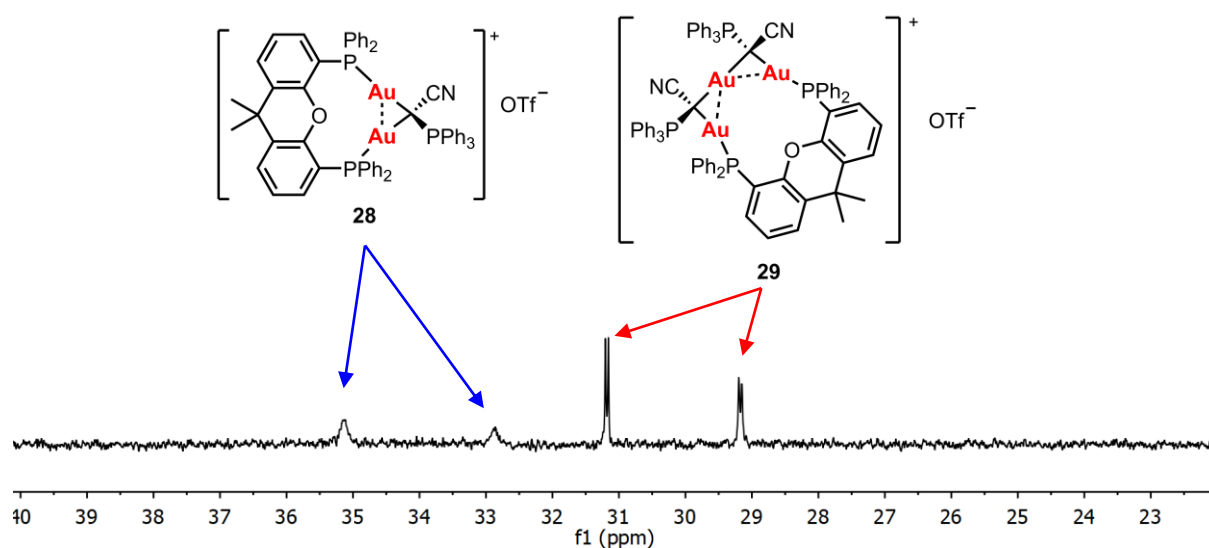
**Figure 2.42.** Molecular structures of **26** and **27** determined by single crystal X-ray diffraction. Phenyl hydrogen atoms, anions and solvent molecules are omitted for clarity. Selected bond lengths [Å] and angles [°] **26**: Au(1)-C(1) 2.096(7), Au(1)-P(1) 2.268(2), Au(1)-Au(2) 2.9829(4), Au(2)-C(1) 2.095(9), Au(2)-P(2) 2.257(2), C(1)-C(2) 1.434(11), C(2)-N(1) 1.149(11), P(3)-C(1) 1.764(8), C(1)-Au(1)-P(1) 173.2(2), C(1)-Au(2)-P(2) 178.6(2), Au(2)-C(1)-Au(1) 90.7(3); **27**: Au(1)-C(1) 2.142(16), Au(1)-P(2) 2.247(6), Au(1)-Au(2) 2.8423(13), Au(2)-C(1) 2.192(18), Au(2)-P(3) 2.237(5), C(1)-C(2) 1.38(3), C(2)-N(1) 1.22(3), C(1)-P(1) 1.732(18), C(1)-Au(1)-P(2) 171.2(5), C(1)-Au(2)-P(3) 173.9(5), Au(2)-C(1)-Au(1) 81.9(6).

Although complex **27** with the flexible diphosphine, dppf, forms readily and in high yield, the analogous reaction with a more rigid diphosphine, XantPhos, led to a mixture of products (Scheme 2.28). These can be seen in the  $^{31}\text{P}\{^1\text{H}\}$  NMR spectrum (Figure 2.43).



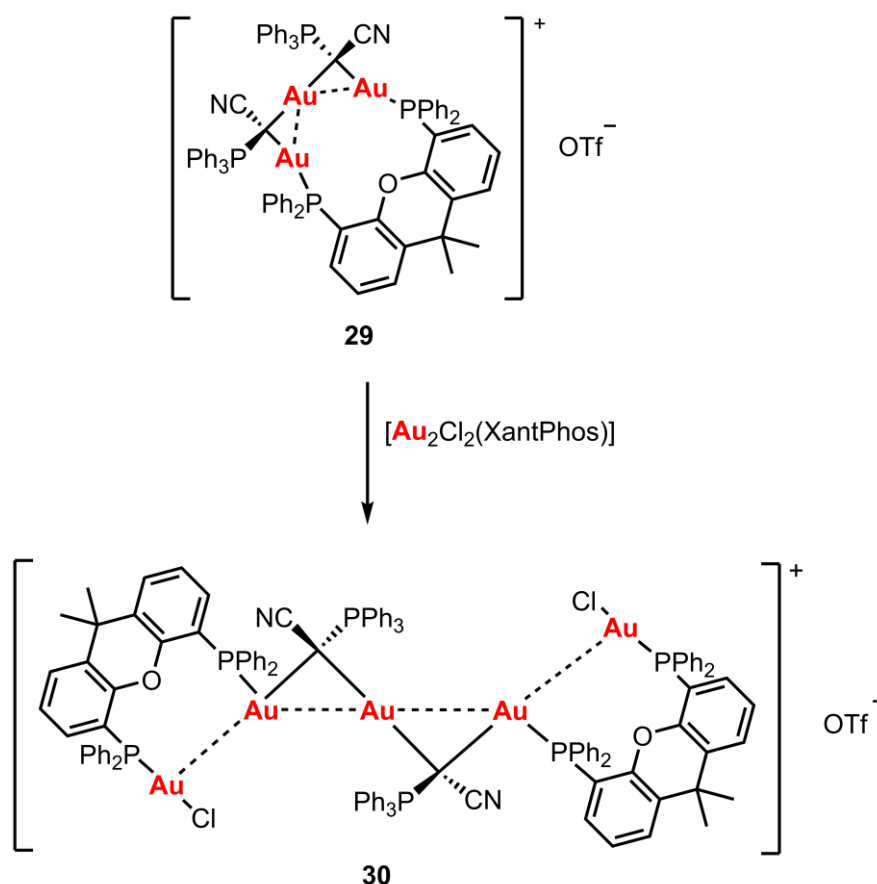
**Scheme 2.28.** Synthesis of XantPhos derivatives **28** and **29**.

## 2.4. Synthesis of Polynuclear Ylride Complexes



**Figure 2.43.**  $^{31}\text{P}\{^1\text{H}\}$  NMR spectrum showing mixture of products **28** and **29**.

It is likely that the geometry and rigidity of the XantPhos ligand means that despite the stoichiometry of the reaction, formation of dinuclear complex **28** with a bridging ylride ligand is less favourable. Attempts to grow crystals from the reaction mixture for X-ray diffraction studies led to the formation of crystals of pentanuclear derivative **30**, the formation of which can be explained by reaction of complex **29** with  $[\text{Au}_2\text{Cl}_2(\text{XantPhos})]$  (Scheme 2.29).

Scheme 2.29. Formation of **30**.

This complex was not detected by NMR of the reaction mixture and formed in too small a quantity to enable NMR or IR analysis, however the molecular structure was determined by single crystal X-ray diffraction (Figure 2.44). This complex has two asymmetric carbon atoms and hence could exist as different diastereoisomers, however only this *meso* isomer crystallised. Auophilic interactions are present linking the five gold atoms in a chain and hence providing stability to this structure with distances Au(1)-Au(2) 2.9197(8) Å and Au(2)-C(1) 2.104(18) Å. The three central gold atoms are in a linear arrangement with the Au(2)-Au(1)-Au(2A) angle of 180°. There is a linear coordination of the two ylide ligands about the central gold atom, however the other two gold atoms have a coordination somewhat distorted from linearity with angles C(1)-Au(2)-P(2) 167.8(5)° and P(3)-Au(3)-Cl(1) 166.71(16)°. This is likely to be due to the steric repulsion between the bulky phosphine groups and the phosphonium of the ylide.

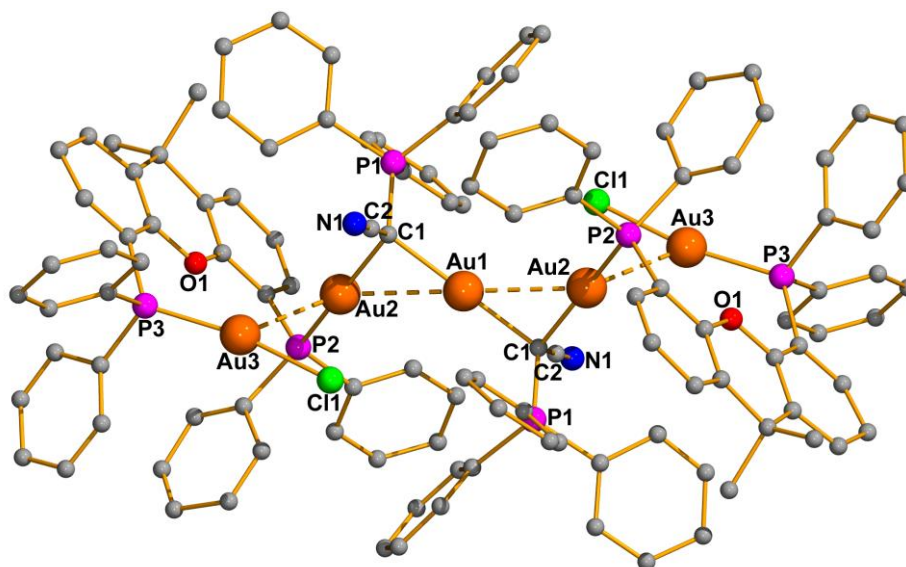
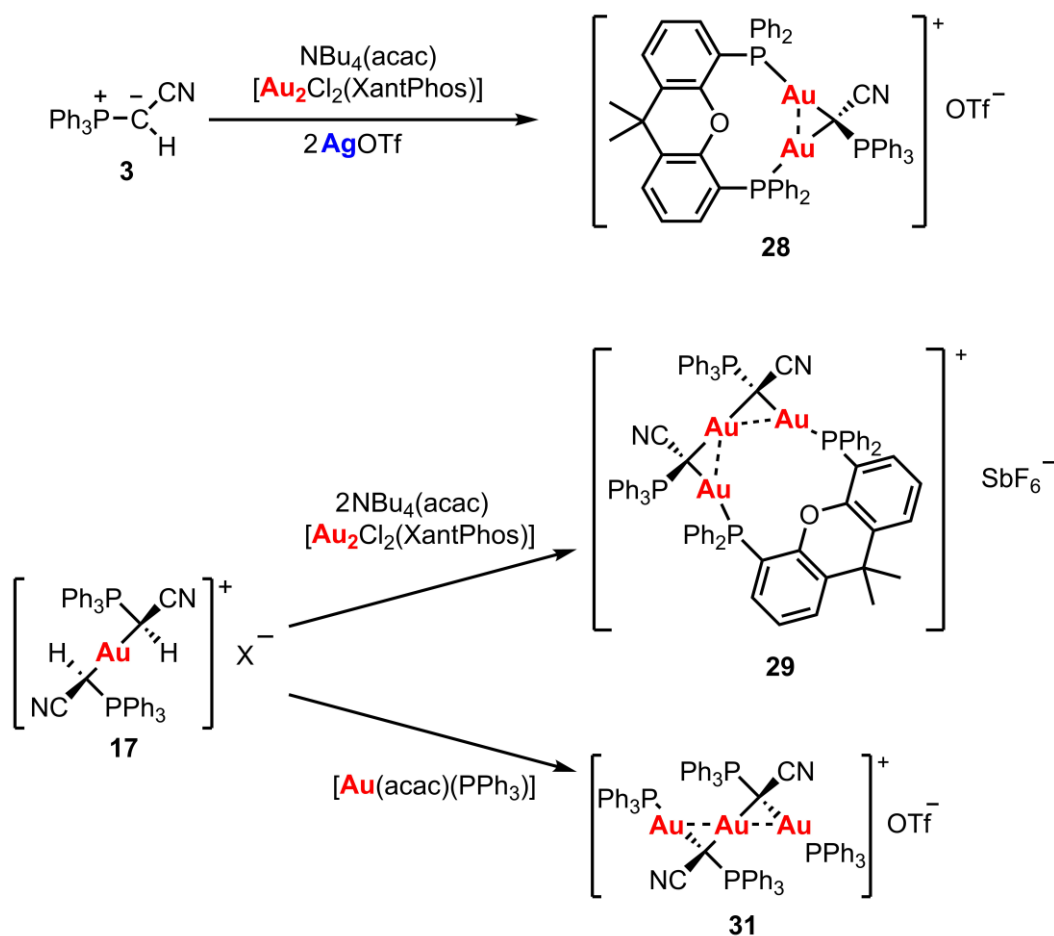


**Figure 2.44.** Molecular structure of **30** determined by single crystal X-ray diffraction. Phenyl hydrogen atoms, anions and solvent molecules are omitted for clarity. Selected bond lengths [Å] and angles [°]: Au(1)-C(1) 2.079(17), Au(1)-Au(2) 2.9197(8), Au(2)-C(1) 2.104(18), Au(2)-P(2) 2.254(5), Au(2)-Au(3) 3.0286(11), Au(3)-P(3) 2.231(6), Au(3)-Cl(1) 2.365(4), P(1)-C(1) 1.774(17), C(1)-C(2) 1.42(2), C(2)-N(1) 1.13(2), C(1)-Au(1)-C(1A) 179.998(1), C(1)-Au(2)-P(2) 167.8(5), P(3)-Au(3)-Cl(1) 166.71(16), Au(2)-Au(1)-Au(2A) 180.0, C(1)-C(2)-N(1) 177(2).

Both complexes **28** and **29** could be prepared cleanly by alternative routes (Scheme 2.30). Reaction of the free ylide with  $[\text{Au}_2\text{Cl}_2(\text{XantPhos})]$  and  $\text{NBu}_4(\text{acac})$  in the presence of silver triflate led to the formation of **28** in a yield of 90%. The acac acts as a base to deprotonate the ylide, and the precipitation of silver chloride will drive the reaction. Complex **29** was prepared from the bis-ylide complex **17** by reaction with two equivalents of  $\text{NBu}_4(\text{acac})$  and one of  $[\text{Au}_2\text{Cl}_2(\text{XantPhos})]$ . In this case, the addition of a silver salt was not required and the tetrabutylammonium chloride which forms in the reaction was readily removed by washing the reaction solution with water, with the final product obtained in a good yield of 74%. A similar triphenylphosphine gold derivative, complex **31** was also prepared from complex **17** by reaction with two equivalents of  $[\text{Au}(\text{acac})\text{PPh}_3]$  and was obtained in a yield of 88%.

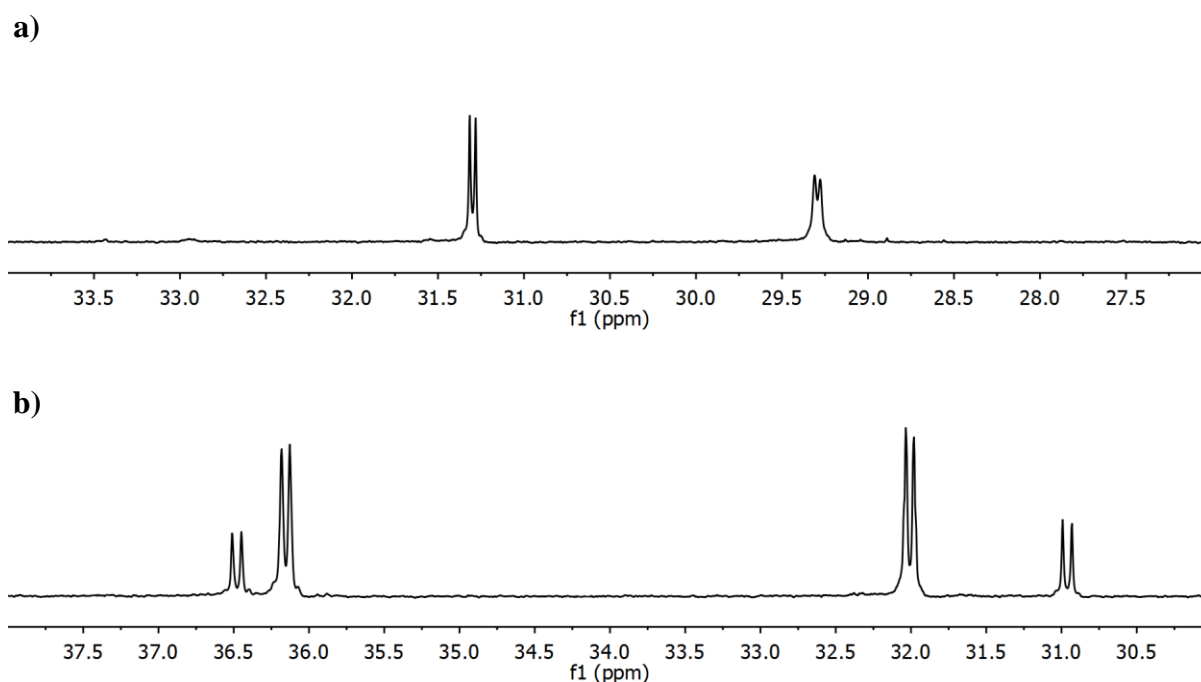


**Scheme 2.30.** Synthesis of complexes **28**, **29** and **31**.

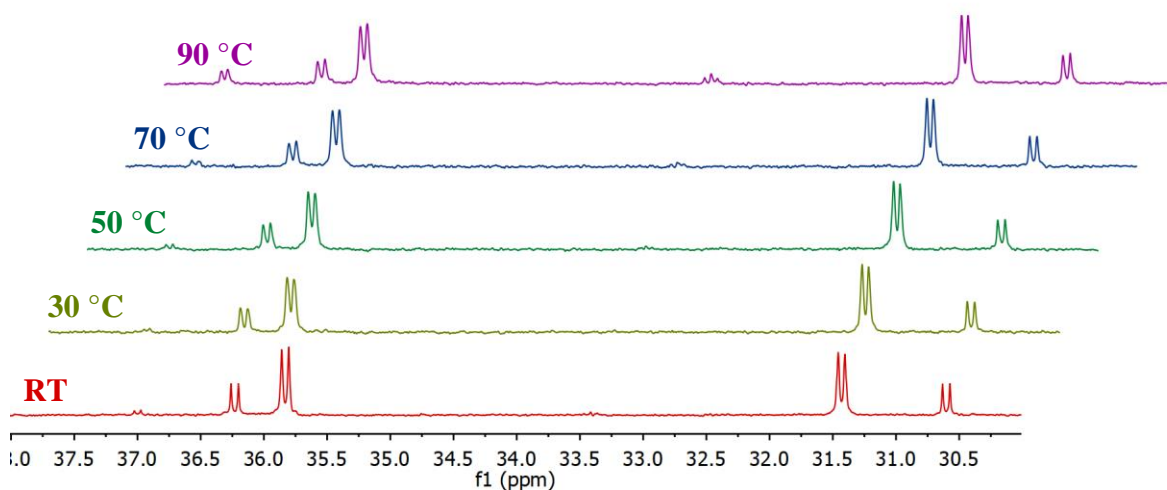
Complexes **29** and **31** both have two asymmetric carbon atoms and hence could exist as a mixture of diastereoisomers. The  $^{31}\text{P}\{^1\text{H}\}$  NMR spectrum of complex **29** shows two doublets at 31.30 ppm and 29.29 ppm with  $^3J_{\text{PP}} = 5.5$  Hz due to the ylide phosphorus atom and the XantPhos phosphorus atom, respectively (Figure 2.45(a)) indicating that only one diastereoisomer formed in this case. In the  $^{31}\text{P}\{^1\text{H}\}$  NMR spectrum of complex **31**, however, four doublets are observed (Figure 2.45(b)) indicating that a mixture of diastereoisomers has formed. As with complex **17** these would be the racemic mixture of (*R,R*)-**31** and (*S,S*)-**31**, and the non-optically active *meso* complex. This was further proven by high temperature NMR studies in DMSO (Figure 2.46). Upon heating, no change in the integral of the peaks was observed, eliminating the possibility of rotamers. At 90 °C the complex started to decompose.



## 2.4. Synthesis of Polynuclear Yldiide Complexes



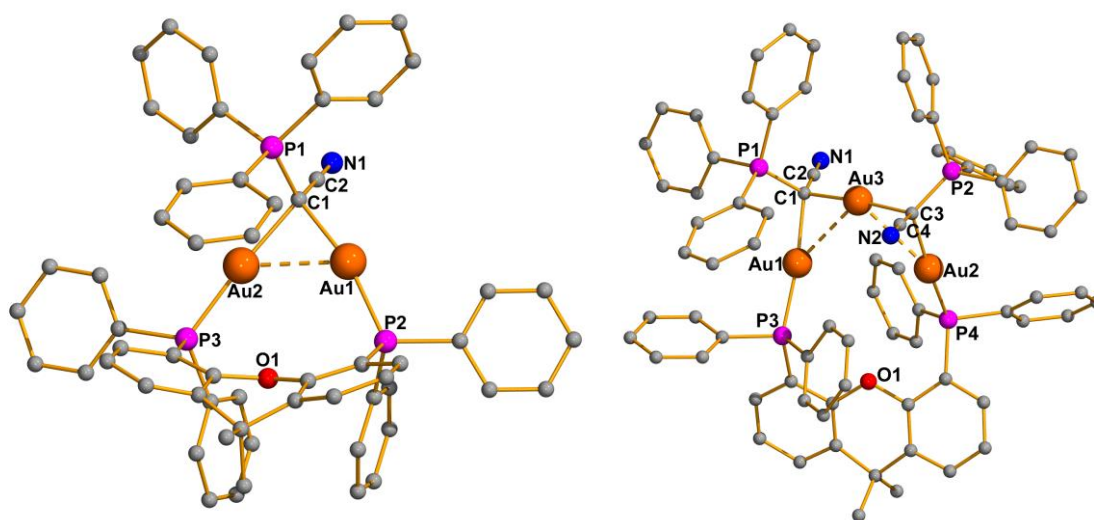
**Figure 2.45.**  $^{31}\text{P}\{^1\text{H}\}$  NMR spectra for complex **29** (a) and **31** (b) in  $\text{CDCl}_3$  at room temperature.



**Figure 2.46.** Variable temperature  $^{31}\text{P}\{^1\text{H}\}$  NMR spectra for complex **29** in  $\text{DMSO}$ .

The molecular structures of the two XantPhos derivatives, **28** and **29** were successfully determined by single crystal X-ray diffraction (Figure 2.47). The structure of complex **28** is very similar to that of the dppf derivative, **27**. The coordination about the gold atoms is slightly distorted from linearity with angles  $\text{C}(1)\text{-Au}(1)\text{-P}(2)$   $165.98(9)^\circ$  and  $\text{C}(1)\text{-Au}(2)\text{-P}(3)$   $171.77(9)$ , due to the rigidity of the XantPhos ligand. A strong aurophilic interaction is observed with a gold-gold distance  $\text{Au}(1)\text{-Au}(2)$   $2.7512(12)$  Å. For the trinuclear

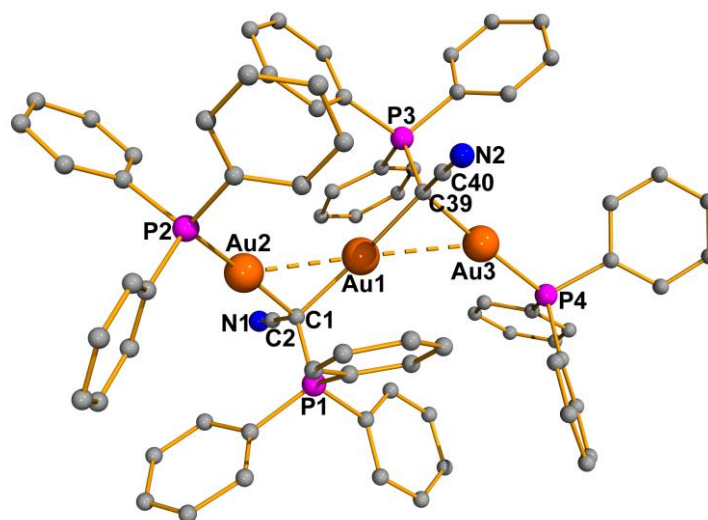
derivative, **29**, aurophilic interactions are observed between the outer gold atoms with the central gold atom with distances Au(1)-Au(3) 2.9395(12) Å and Au(2)-Au(3) 2.9517(10) Å. The coordination about the central gold atom is close to linear with angle C(1)-Au(3)-C(3) 175.5(3)°, however the coordination about the other gold atoms is more distorted with angles C(1)-Au(1)-P(3) 168.2(2)° and C(3)-Au(2)-P(4) 170.2(2)°. Again, this is due to the rigidity of the XantPhos ligand.



**Figure 2.47.** Molecular structures of **28** and **29** determined by single crystal X-ray diffraction. Hydrogen atoms, anions and solvent molecules are omitted for clarity. Selected bond lengths [Å] and angles [°] **28**: Au(1)-C(1) 2.117(3), Au(1)-P(2) 2.2571(11), Au(1)-Au(2) 2.7512(12), Au(2)-C(1) 2.143(3), Au(2)-P(3) 2.2523(11), P(1)-C(1) 1.754(3), C(1)-C(2) 1.424(5), C(2)-N(1) 1.154(5), C(1)-Au(1)-P(2) 165.98(9), C(1)-Au(2)-P(3) 171.77(9), C(1)-C(2)-N(1) 179.5(4), Au(1)-C(1)-Au(2) 80.45(11); **29**: Au(1)-C(1) 2.111(8), Au(1)-P(3) 2.263(2), Au(1)-Au(3) 2.9395(12), Au(2)-C(3) 2.099(7), Au(2)-P(4) 2.261(2), Au(2)-Au(3) 2.9517(10), Au(3)-C(1) 2.099(8), Au(3)-C(3) 2.096(8), P(1)-C(1) 1.769(8), C(1)-C(2) 1.427(12), C(2)-N(1) 1.151(11), P(2)-C(3) 1.752(8), C(3)-C(4) 1.438(11), C(4)-N(2) 1.156(11), C(1)-Au(1)-P(3) 168.2(2), C(3)-Au(2)-P(4) 170.2(2), C(1)-Au(3)-C(3) 175.5(3), C(1)-C(2)-N(1) 178.5(9), C(3)-C(4)-N(2) 176.8(8), Au(1)-C(1)-Au(3) 88.5(3), Au(2)-C(1)-Au(3) 89.4(3).

The molecular structure of the *meso* diastereoisomer of complex **31** was also determined by single crystal X-ray diffraction (Figure 2.48). The large triphenylphosphine groups are directed in opposite directions to minimise repulsions. An almost linear coordination is observed about each of the gold centres with a slight distortion observed for the outer gold atoms (angles C(1)-Au(2)-P(2) 172.2(2)° and C(39)-Au(3)-P(4) 174.5(2)°), due to the steric repulsions of the bulky phosphine groups. Aurophilic interactions are present between the gold atoms with

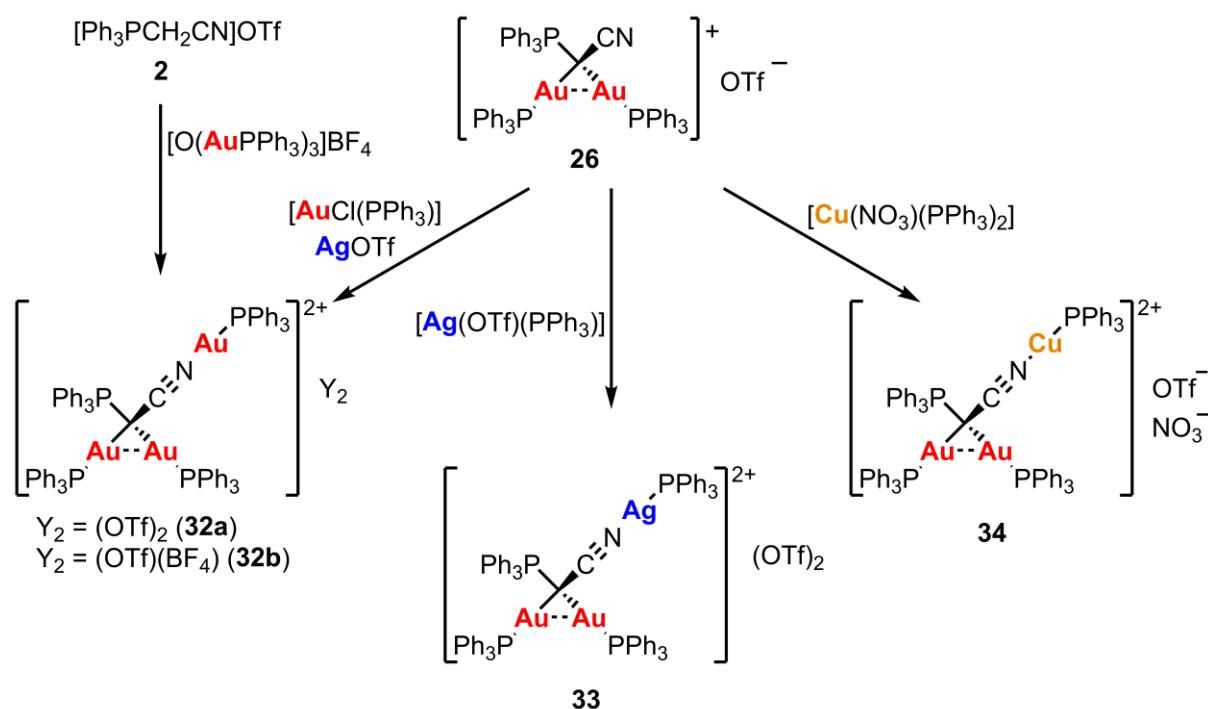
distances Au(1)-Au(2) 2.9723(5) Å and Au(1)-Au(3) 3.0501(5) Å and an angle Au(2)-Au(1)-Au(3) 169.063(13)°.



**Figure 2.48.** Molecular structures **31** determined by single crystal X-ray diffraction. Hydrogen atoms, anions and solvent molecules are omitted for clarity. Selected bond lengths [Å] and angles [°]: Au(1)-C(1) 2.097(7), Au(1)-C(39) 2.110(7), Au(1)-Au(2) 2.9723(5), Au(1)-Au(3) 3.0501(5), Au(2)-C(1) 2.096(7), Au(2)-P(2) 2.265(2), Au(3)-C(39) 2.089(7), Au(3)-P(4) 2.270(2), P(1)-C(1) 1.762(7), C(1)-C(2) 1.476(10), C(2)-N(1) 1.075(10), P(3)-C(39) 1.739(7), C(39)-C(40) 1.449(11), C(40)-N(2) 1.155(10), C(1)-Au(1)-C(39) 177.0(3), C(1)-Au(2)-P(2) 172.2(2), C(39)-Au(3)-P(4) 174.5(2), Au(2)-Au(1)-Au(3) 169.063(13), C(1)-C(2)-N(1) 175.5(7), C(39)-C(40)-N(2) 177.1(8), Au(2)-C(1)-Au(1) 90.3(3), Au(3)-C(39)-Au(1) 93.2(3).

#### 2.4.4. Heterometallic Complexes with N Coordination

Trinuclear complexes **32-34** were prepared from complex **22** by reaction with a gold, silver or copper precursor bearing a triphenylphosphine group and a labile ligand (Scheme 2.31). For the gold derivative, **32a**, the precursor [Au(OTf)(PPh<sub>3</sub>)] was prepared *in situ* by reaction of [AuCl(PPh<sub>3</sub>)] and AgOTf, driven by the precipitation of silver chloride. Complex **32a** was obtained in a yield of 87%. This same complex but with one tetrafluoroborate and one triflate anion be prepared from the phosphonium triflate salt directly by reaction with the oxonium [O(AuPPh<sub>3</sub>)<sub>3</sub>]BF<sub>4</sub> which can deprotonate the phosphonium salt twice and allow the possibility for coordination of the ylide to three AuPPh<sub>3</sub> groups. The yield of complex **32b** by this route was slightly lower, 73%. Complexes **33** and **34** were both obtained in excellent yields of 98% and 99%, respectively.

Scheme 2.31. Synthesis of complexes **32-34**.Table 2.5. Infrared absorption frequencies for complexes **32-34**

Complex	$\nu(\text{C}\equiv\text{N})$ ( $\text{cm}^{-1}$ )
<b>26</b>	2173
<b>32</b>	2171
<b>33</b>	2160
<b>34</b>	2166

The additional coordination through the nitrogen atom results in a reduction in the  $\text{C}\equiv\text{N}$  absorption frequency in the infrared spectrum of complexes **32-34** compared to complex **26**. For the gold derivative, **32**, the difference is only slight since the gold-nitrogen bond is relatively weak. For complexes **33** and **34** the stronger coordination to silver or copper results in a more significant difference.

## 2.4. Synthesis of Polynuclear Yldiide Complexes

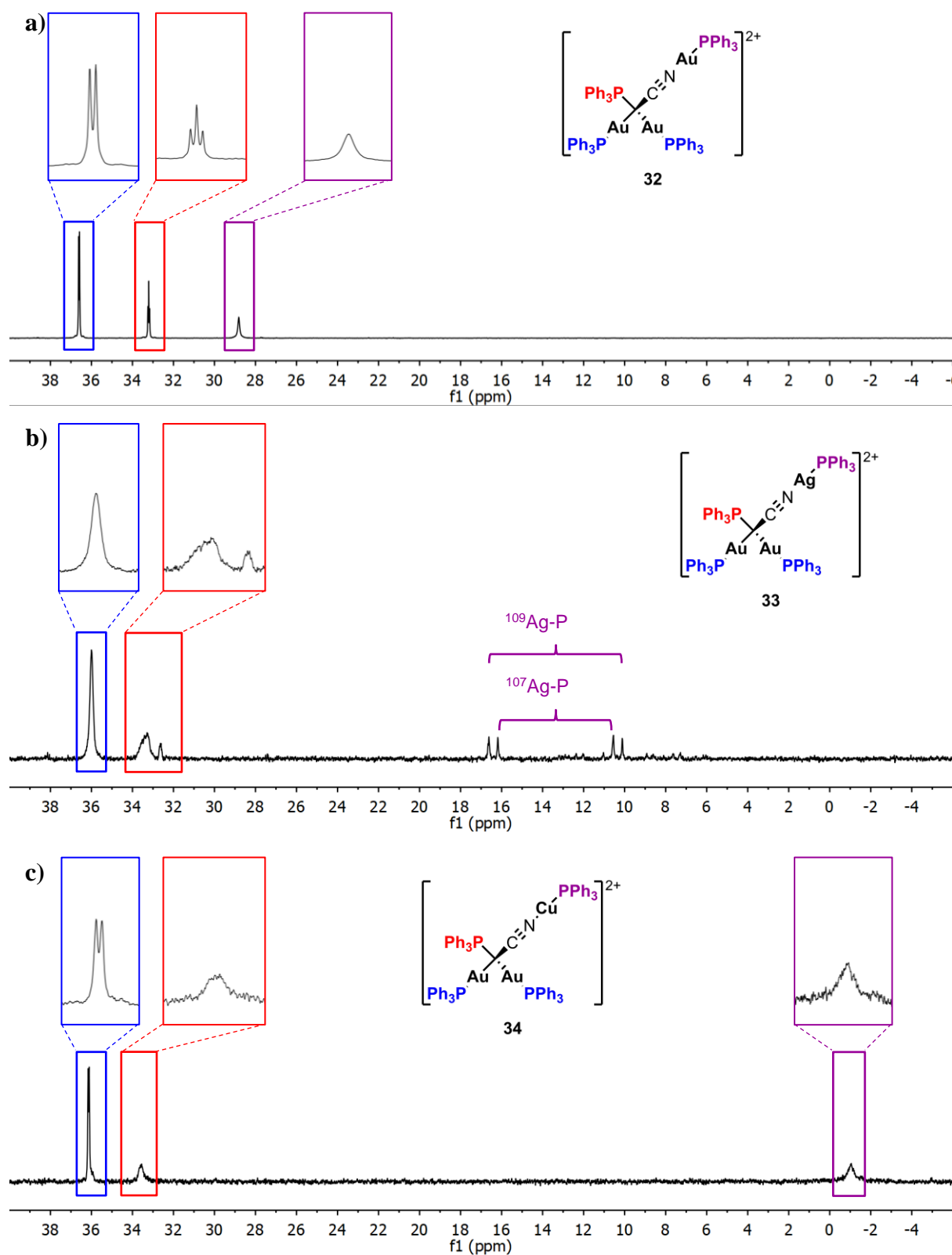


**Figure 2.49.**  $^{31}\text{P}\{^1\text{H}\}$  NMR spectra in  $\text{CDCl}_3$  for complex **32** at room temperature (a), complex **33** at  $-50\text{ }^\circ\text{C}$  (b) and complex **34** at  $-50\text{ }^\circ\text{C}$  (c).

The  $^{31}\text{P}\{^1\text{H}\}$  NMR spectra of complexes **32-34** each show an additional peak compared to complex **26** as a result of the additional triphenylphosphine group, and for all three complexes at room temperature the doublet and triplet peaks observed for complex **26** are still present but appear at different chemical shifts (Figure 2.49). No coupling to the additional triphenylphosphine group is observed. For complex **33** the  $^{31}\text{P}\{^1\text{H}\}$  spectrum at  $-50\text{ }^{\circ}\text{C}$  shows two doublets at 13.37 ppm due to the phosphorus-silver coupling with  $^1J_{109\text{Ag-P}} = 786.5\text{ Hz}$  and  $^1J_{107\text{Ag-P}} = 683.5\text{ Hz}$ . At this temperature, the doublet and triplet peaks for the  $\text{AuPPh}_3$  and ylide phosphorus atom are observed as more complex multiplets.

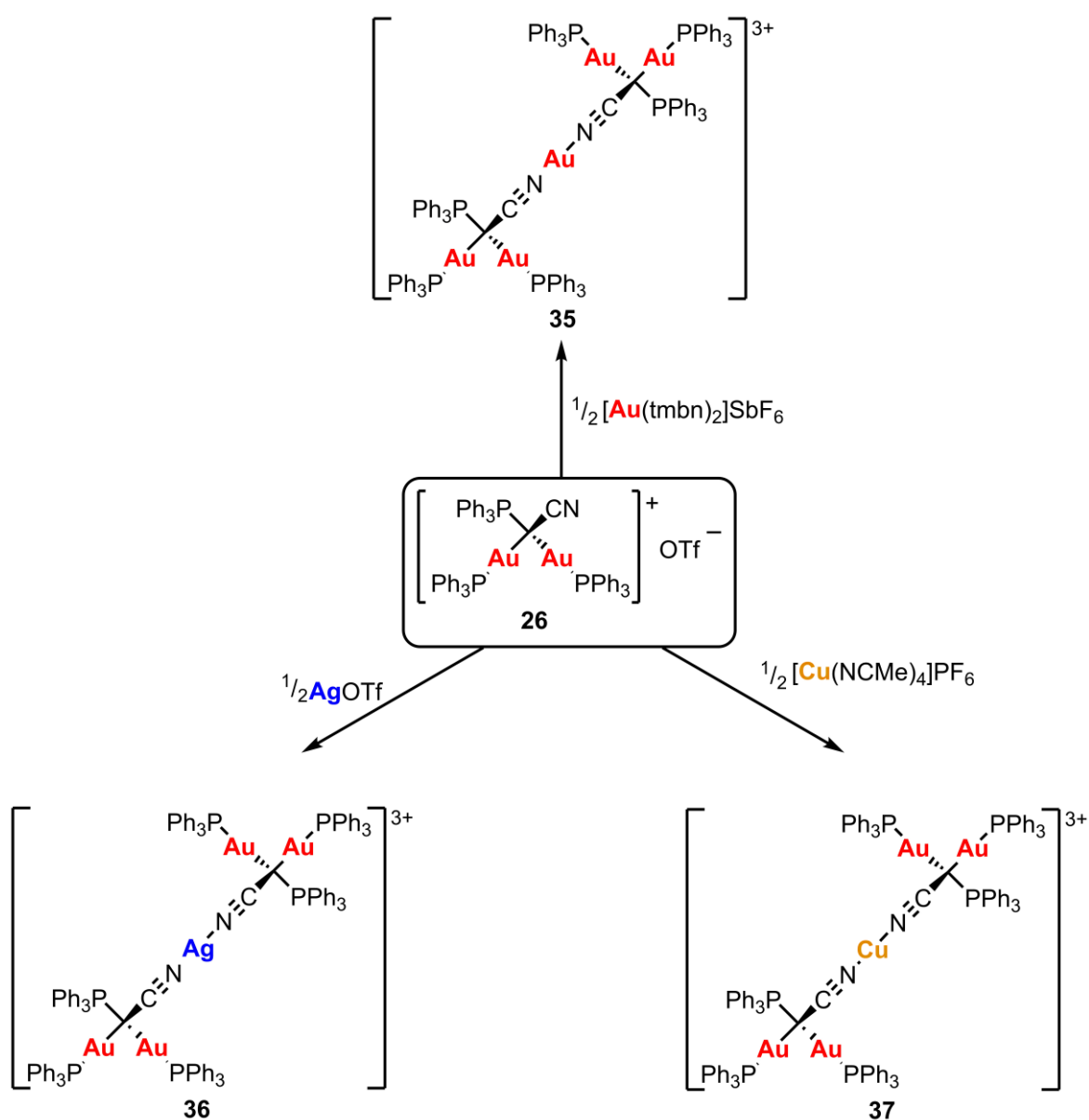
Polynuclear derivatives **35-37** were prepared by reaction of complex **26** with  $[\text{Au}(\text{tmbn})_2]\text{SbF}_6$  (tmbn = 2,4,6-trimethoxybenzonitrile),  $\text{AgOTf}$  or  $[\text{Cu}(\text{NCMe})_4]\text{PF}_6$  (Scheme 2.32). Although complex **35** formed, separation from the trimethoxybenzonitrile was not possible. Complexes **36** and **37**, however were obtained cleanly in yields of 73% and 84%, respectively. Successful reaction was observed by a colour change. The starting complex, **26**, is a white solid however **35** and **37** were pale yellow solids and **36** was a pale orange solid.

Infrared absorption frequencies for the  $\text{C}\equiv\text{N}$  bond indicate successful coordination of the nitrogen atom to the metal centres since they appear at lower values than that of complex **26** as a result of a loss of electron density from the triple bond (Table 2.6).

**Table 2.6.** Infrared absorption frequencies for complexes **35-37**

Complex	$\nu(\text{C}\equiv\text{N})\text{ (cm}^{-1}\text{)}$
<b>35</b>	2172
<b>36</b>	2166
<b>37</b>	2167

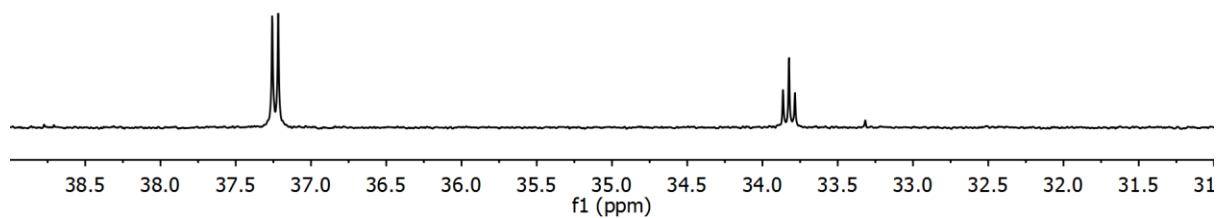
## 2.4. Synthesis of Polynuclear Yldiide Complexes



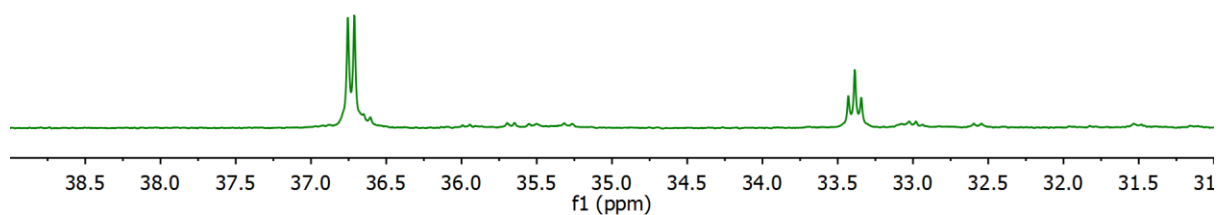
**Scheme 2.32.** Synthesis of complexes 35-37.

The  $^{31}\text{P}\{^1\text{H}\}$  NMR spectra for complexes **35-37** show peaks analogous to those for complex **26**, however they appear at different chemical shifts when measured in the same solvent, another indication of successful coordination of the nitrile group (Figure 2.50).

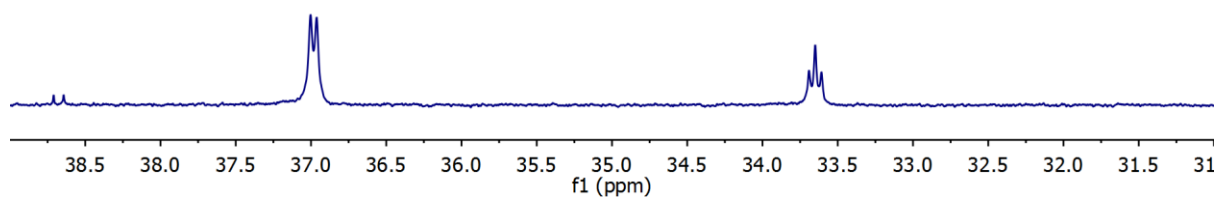
a)



b)



c)



d)

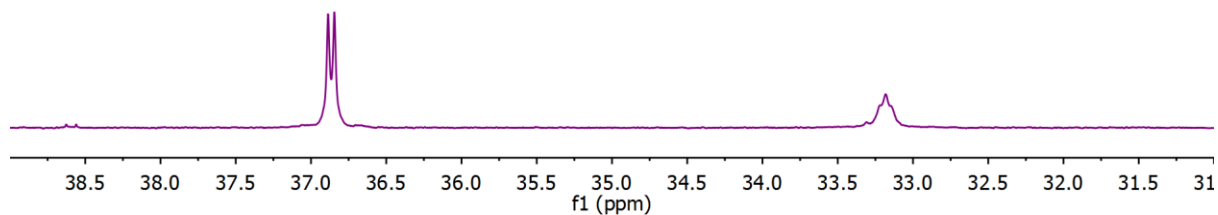


**Figure 2.50.**  $^{31}\text{P}\{^1\text{H}\}$  NMR spectra for complex **26** (a), complex **35** (b), complex **36** (c) and complex **37** (d) in  $\text{CDCl}_3$  at room temperature.



## 2.5. Luminescence

Polynuclear complexes **36** and **37** were luminescent at 77 K. The excitation and emission maxima and emission lifetimes are shown in Table 2.7.

**Table 2.7.** Excitation and emission maxima for complexes **36** and **37**.

Complex	Excitation $\lambda^{\max}$ (nm)	Emission $\lambda^{\max}$ (nm)	$\tau_0$ ( $\mu$ s)
<b>36</b>	296, 339	668, 539	440
<b>37</b>	357	523	1666

Complex **36** has two excitation bands and two emission bands (Figure 2.51). Excitation at 296 nm results in a weak emission at 668 nm (Figure 2.51(a)). Taking into account the low energy emission for this band and the large Stokes shift, the origin of the emission likely to be due to metal interactions and could be a metal-centred or cluster-centred. The other excitation band at 339 nm has a corresponding emission band at 539 nm (Figure 2.51(b)) and can be assigned to a metal to ligand charge transfer (MLCT) from the silver to the nitrile groups. The lifetime of this emission indicates phosphorescence.

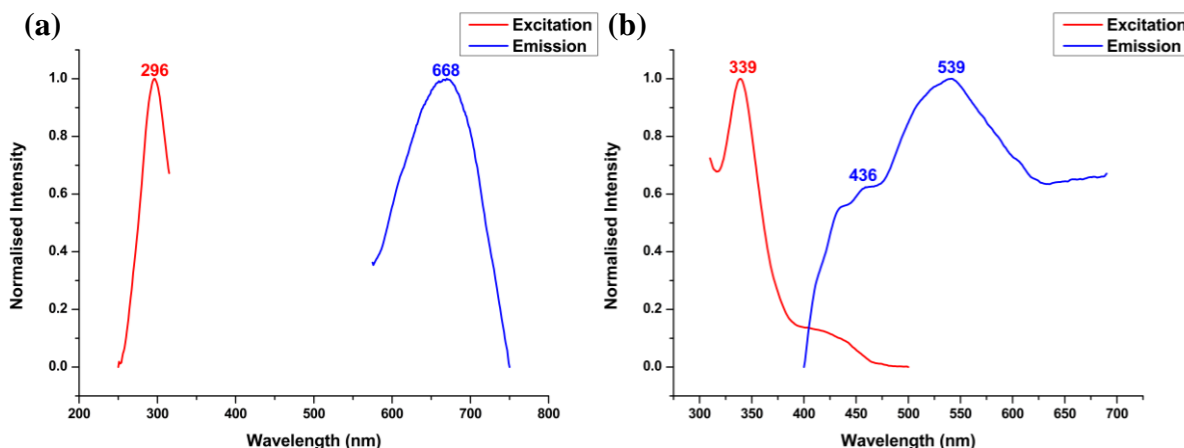


**Figure 2.51.** Excitation and emission spectra for complex **36** at 77 K.

Complex **37** has only one excitation and one emission band (Figure 2.52). Excitation at 357 nm results in an emission at 523 nm. This is assigned to a metal to ligand charge transfer transition from the copper to the nitrile ligands. The long lifetime indicates phosphorescence.

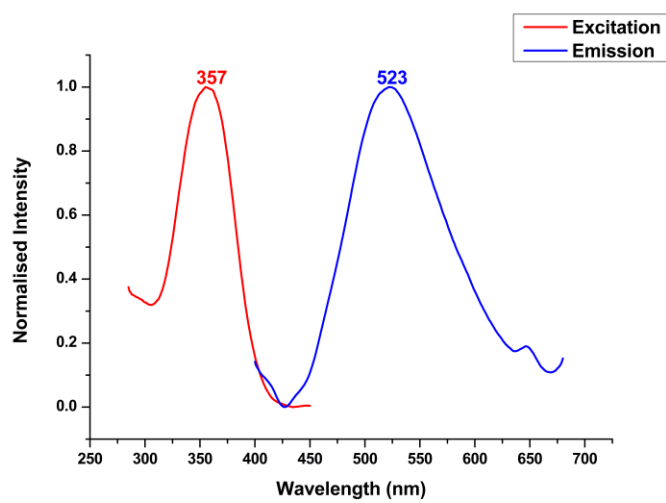
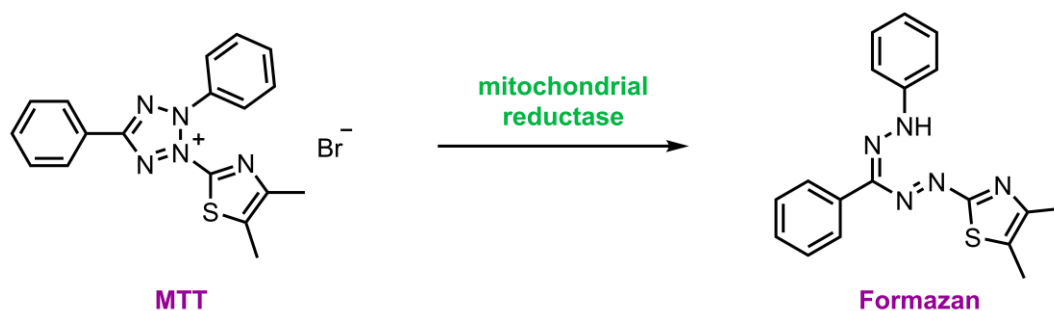


**Figure 2.52.** Excitation and emission spectra for complex **37** at 77 K.

## 2.6. Biological Activity

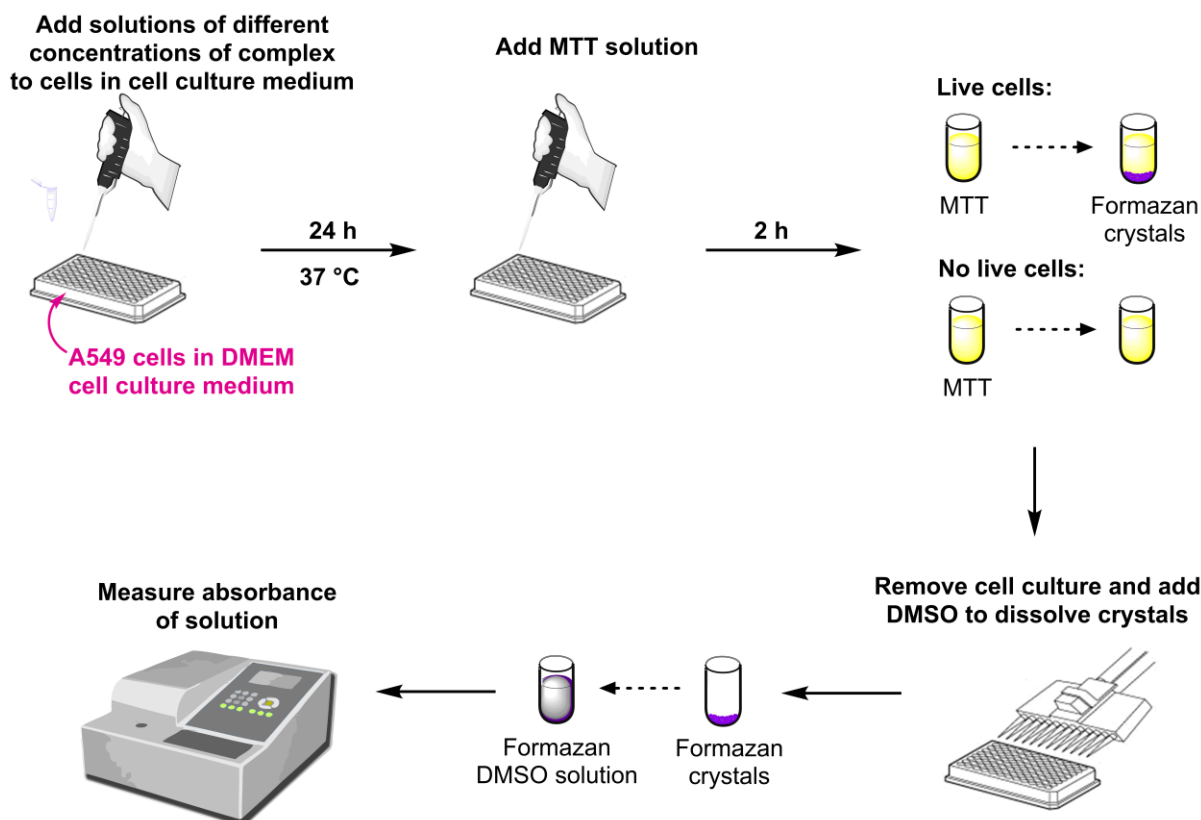
The biological activity of several of the ylide complexes was studied by MTT assay for lung carcinoma cell line A549. This cell line was chosen since it is one which shows cisplatin resistance and hence there is a need to look for alternative treatments.

The MTT (3-(4,5-dimethylthiazol-2-yl)-2,5-diphenyltetrazolium bromide) tetrazolium reduction assay is a well-known method for testing the anti-proliferative activity of compounds, first described by Mosmann in 1983.<sup>173</sup> It is a quantitative colorimetric assay based on the cleavage of the yellow, water-soluble tetrazolium salt, MTT, to form dark blue/purple, water-insoluble formazan crystals (Scheme 2.33).



**Scheme 2.33.** Reduction of MTT to formazan by mitochondrial reductase.

This reaction occurs only in the presence of living cells since it is caused by the mitochondrial reductase enzyme, succinate hydrogenase. The resulting formazan crystals can be solubilised in DMSO and the optical density of the resulting solution measured with a spectrophotometer. The absorbance of the solution is directly proportional to the concentration of formazan, which is directly proportional to the number of metabolically active cells. This technique therefore allows the determination of the number of living cells after a certain incubation time with a complex, and if measurements with various concentrations of complex are taken, a curve of cell viability against concentration may be drawn, allowing determination of the half maximal inhibitory concentration (IC<sub>50</sub>) of the complex. A schematic representation of the technique is shown in Scheme 2.34.

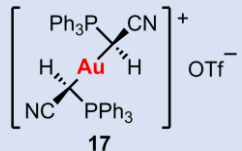
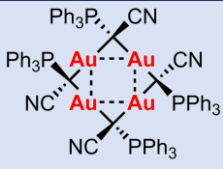
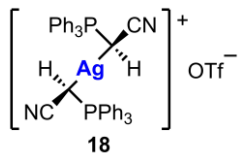
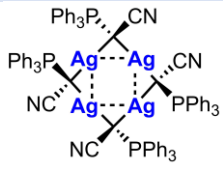
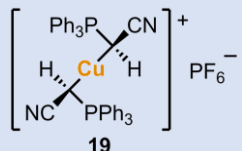


**Scheme 2.34.** Schematic representation MTT assay method.

The calculated  $IC_{50}$  values for the bis-ylide complexes **17-19** and tetramers **24** and **25** after 24 h incubation with A549 cells is shown in Table 2.8. The bis-ylide complexes were chosen as suitable candidates due to their similarity to bis-NHC complexes which are known to show good anticancer activity. Only the silver derivative, **18**, showed activity at the concentrations tested ( $<50 \mu\text{M}$ ) but was not particularly active with an  $IC_{50}$  of  $48.39 \pm 2.66 \mu\text{M}$ . The tetrameric complexes **24** and **25** were also tested. Unfortunately, the gold complex precipitated in the cell culture medium and consequently did not show anticancer activity. The silver derivative, **25**, however, did show a reasonable activity with an  $IC_{50}$  value of  $19.09 \pm 1.25 \mu\text{M}$ .

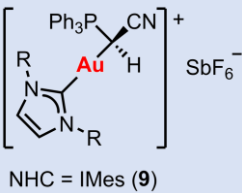
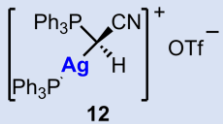
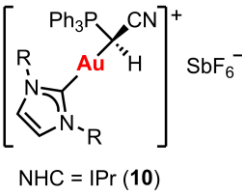
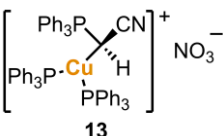
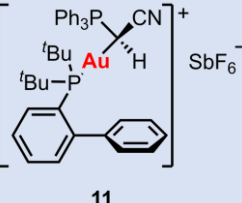
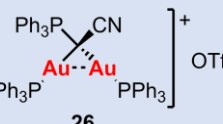
## 2.6. Biological Activity

**Table 2.8.** IC<sub>50</sub> values for Complexes **17-19** and **24-25** after 24 h Incubation with A549 Cells

Complex	IC <sub>50</sub> (μM)	Complex	IC <sub>50</sub> (μM)
 <b>17</b>	>50	 <b>24</b>	>50
 <b>18</b>	48.39 ± 2.66	 <b>25</b>	19.09 ± 1.25
 <b>19</b>	>50		

Since the presence of a phosphine ligand can improve the lipophilicity of a complex and often results in an increased anticancer activity, the activity of triphenylphosphine derivatives **12**, **13** and **26** was tested along with JohnPhos derivative, **11**. The anticancer activity of NHC derivatives **9** and **10** was also tested. The calculated IC<sub>50</sub> values are shown in Table 2.9.

**Table 2.9.** IC<sub>50</sub> values for Complexes **9-13** and **26** after 24 h Incubation with A549 Cells

Complex	IC <sub>50</sub> (μM)	Complex	IC <sub>50</sub> (μM)
 NHC = IMes ( <b>9</b> )	15.43 ± 0.73	 <b>12</b>	4.40 ± 0.73
 NHC = IPr ( <b>10</b> )	10.26 ± 0.90	 <b>13</b>	3.83 ± 0.69
 <b>11</b>	12.18 ± 1.22	 <b>26</b>	5.38 ± 0.76

The mononuclear gold complexes **9-11** all showed good anticancer activities with  $IC_{50}$  values in the range 10-15  $\mu M$ , the best of these being complex **10** bearing the IPr NHC ligand. A significant improvement in activity is observed upon changing from a mononuclear to a dinuclear gold complex, comparing the two gold phosphine derivatives **11** and **26** with  $IC_{50}$  values of 12.18  $\mu M$  and 5.38  $\mu M$ , respectively. This can readily be seen in the graph of cell viability against concentration where complex **26** has a steeper curve indicating greater antiproliferative activity at lower concentrations (Figure 2.53). Since the mononuclear gold triphenylphosphine derivative, **15**, could not be isolated and tested, it cannot be concluded whether this improvement in activity is due to changing the phosphine group from JohnPhos to triphenylphosphine or due to the additional gold atom.

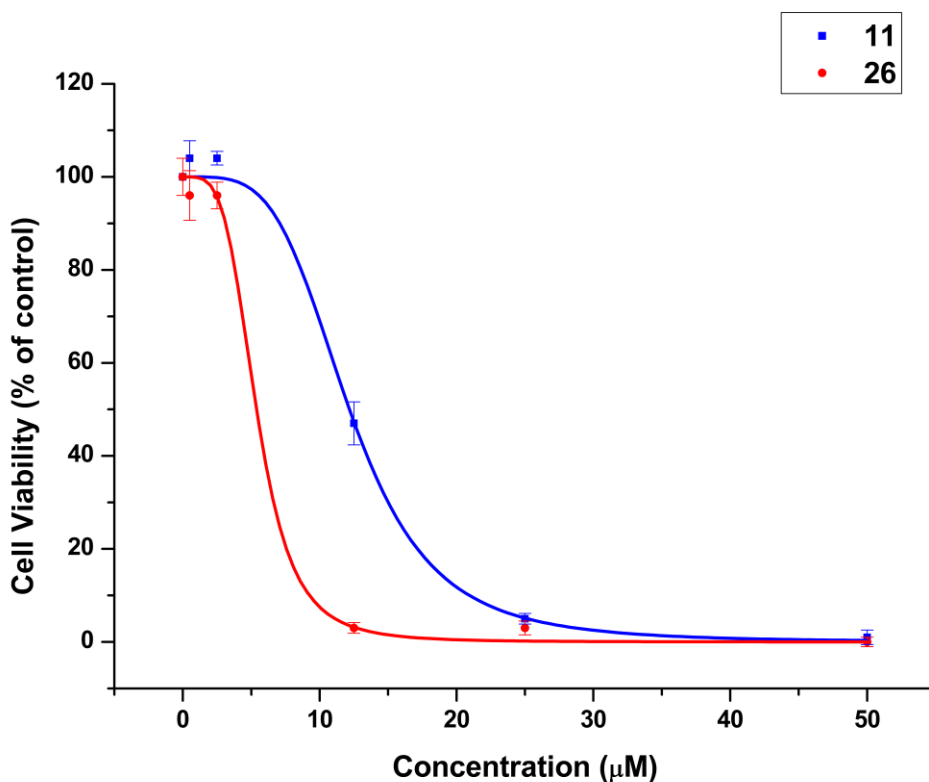


**Figure 2.53.** Graph of cell viability (% of control) against concentration ( $\mu M$ ) for complexes **11** and **26** (Each point is the average of eight measurements, where error bars represent the standard deviation. Curve generated by a sigmoidal non-linear regression 4-parameter logistic analysis).

The silver and copper triphenylphosphine derivatives, **12** and **13** also showed excellent activity in A549 cells with incredibly low  $IC_{50}$  values of 4.40 and 3.83  $\mu M$ , respectively. The graph of

## 2.6. Biological Activity

cell viability against concentration for the three triphenylphosphine complexes **12**, **13** and **26** shows that they all have very similar curves (Figure 2.54). The copper complex, **13**, has the steepest curve and hence the highest activity, however the differences are not significant within error. It should also be noted that in these studies the complexes were incubated with the cancer cells for just 24 h and show  $IC_{50}$  values far superior to cis-platin when measured under the same conditions which has an  $IC_{50}$  value of 114  $\mu M$ .

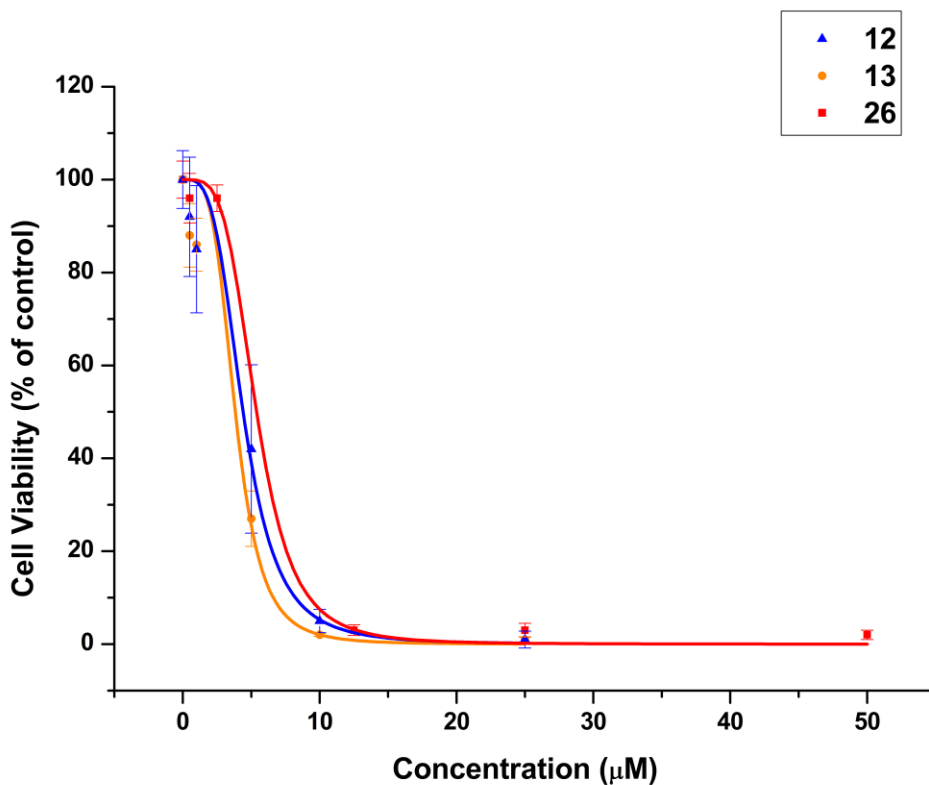


**Figure 2.54.** Graph of cell viability (% of control) against concentration ( $\mu M$ ) for complexes **12**, **13** and **26** (Each point is the average of eight measurements, where error bars represent the standard deviation. Curve generated by a sigmoidal non-linear regression 4-parameter logistic analysis).

## 2.7. Conclusions

The coordination chemistry of the cyano-stabilised ylide, triphenylphosphoniumcyanomethylide with gold has been thoroughly explored. Several mononuclear gold(I) and gold(III) derivatives have been prepared and structurally characterised. The synthesis of cationic mononuclear gold(I) derivatives of triphenylphosphoniumcyanomethylide requires the presence of a bulky ligand such as a IPr or JohnPhos at the gold centre. When a small NHC ligand or PPh<sub>3</sub> was used, further deprotonation of the ylide occurred leading to the formation of dinuclear complexes. Mononuclear silver and copper derivatives were also prepared. In these complexes additional coordination of the C≡N nitrogen atom to the metal is observed, stabilising the structure. This additional C≡N coordination is not observed in any of the gold complexes. This difference in coordination between gold and the other coinage metals influenced the outcome of the synthesis of the bis-ylide complexes. For the bis-ylide gold derivative, two diastereoisomers of the product formed, however with silver and copper the formation of only one diastereoisomer was observed. This is because the stabilising effect of the additional coordination of the nitrogen to the metal centre would only be possible in one of the diastereoisomers. The silver derivative was structurally characterised showing the favoured diastereoisomer to be the racemic mixture of enantiomers rather than the *meso* complex. A polymeric structure was observed in the solid state.

Polynuclear derivatives of the cyano-stabilised phosphonium ylide species were also prepared. The negatively charged complexes were found to be unstable in solution and over time formed the more stable neutral tetranuclear complex. Gold and silver tetranuclear species with bridging ylide ligands could also be synthesised by different routes and two different conformers were structurally characterised. The cationic derivatives were highly stable and many examples with different structural frameworks were prepared and characterised. Additional coordination through the nitrogen of the C≡N was also achieved, resulting in some polynuclear heterometallic derivatives. Two of these were found to be luminescent.

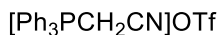


## 2.7. Conclusions

---

The anticancer activity of several of the complexes in A549 cells was tested. The metal triphenylphosphine derivatives were found to be the most active with very low  $IC_{50}$  values. Amongst them the copper and silver complexes were slightly more active than the gold species.

## 2.8. Experimental



2

To a solution of  $[\text{Ph}_3\text{PCH}_2\text{CN}]\text{Cl}$  (0.6756 g, 2.0 mmol) in  $\text{CH}_2\text{Cl}_2$  (10 ml) was added  $\text{AgOTf}$  (0.5139 g, 2.0 mmol) and the mixture stirred for 1 h at room temperature with the exclusion of light.  $\text{AgCl}$  was removed by filtration through celite and the pale yellow filtrate concentrated under reduced pressure to approximately 1 ml. The product was precipitated with *n*-hexane, collected by vacuum filtration and dried to give  $[\text{Ph}_3\text{PCH}_2\text{CN}]\text{OTf}$  as a white solid (0.8632 g, 96 %).

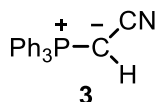
**IR ( $\text{cm}^{-1}$ ):**  $\nu(\text{C}\equiv\text{N})$  2250;  $\nu(\text{OTf})$  1281 ( $\text{SO}_3$ ), 1226 ( $\text{CF}_3$ ), 1151 ( $\text{CF}_3$ ), 1028 ( $\text{SO}_3$ ).

**$^1\text{H}$  NMR (300 MHz,  $\text{CDCl}_3$ )**  $\delta$  8.02 – 7.57 (m, 15H, Ph), 5.05 (d,  $^2J_{\text{HP}} = 15.1$  Hz, 2H,  $\text{CH}_2$ ).

**$^{31}\text{P}\{^1\text{H}\}$  NMR (121 MHz,  $\text{CDCl}_3$ )**  $\delta$  21.53. (s,  $\text{PPh}_3$ ).

**$^{19}\text{F}$  NMR (282 MHz,  $\text{CDCl}_3$ )**  $\delta$  -78.45 (s, OTf).

**$^{13}\text{C}$  APT (75 MHz,  $\text{CDCl}_3$ )**  $\delta$  136.30 (d,  $^4J_{\text{CP}} = 3.2$  Hz, *p*- $\text{PPh}_3$ ), 133.98 (d,  $^3J_{\text{CP}} = 10.8$  Hz, *m*- $\text{PPh}_3$ ), 130.89 (d,  $^2J_{\text{CP}} = 13.4$  Hz, *o*- $\text{PPh}_3$ ), 115.83 (d,  $^1J_{\text{CP}} = 89.0$  Hz, *ipso*- $\text{PPh}_3$ ), 111.54 (d,  $^2J_{\text{CP}} = 9.5$  Hz,  $\text{C}\equiv\text{N}$ ), 15.43 (d,  $^1J_{\text{CP}} = 56.7$  Hz,  $\text{CH}_2$ ).



To a solution of  $[\text{Ph}_3\text{PCH}_2\text{CN}]\text{Cl}$  (0.6756 g, 2.0 mmol) in  $\text{H}_2\text{O}$  (20 ml) was added  $\text{NaOH}$  (25% soln) solution. A white precipitate immediately formed and addition was continued until the reaction mixture was alkaline. The solid was collected by vacuum filtration, dissolved in  $\text{CH}_2\text{Cl}_2$  (10 ml) and dried over  $\text{Na}_2\text{SO}_4$ . The solution was concentrated to approximately 1 ml and  $\text{Et}_2\text{O}$  (10 ml) added to precipitate a white solid which was collected and vacuum dried to give the crude product. NMR showed the presence of  $\text{Ph}_3\text{PO}$ . The crude product was dissolved in toluene, filtered through celite and the solution concentrated under reduced pressure to approximately 1 ml.  $\text{Et}_2\text{O}$  was added to precipitate the pure product as a white solid which was collected and vacuum dried.

**IR ( $\text{cm}^{-1}$ ):**  $\nu(\text{C}\equiv\text{N})$  2136.

**$^1\text{H}$  NMR (400 MHz,  $\text{CD}_2\text{Cl}_2$ )**  $\delta$  7.77 – 7.39 (m, 15H,  $\text{PPh}_3$ ), 1.56 (d,  $^2J_{\text{HP}} = 7.3$  Hz, 1H, CH)

**$^{31}\text{P}\{^1\text{H}\}$  NMR (162 MHz,  $\text{CD}_2\text{Cl}_2$ )**  $\delta$  23.29 ( $\text{PPh}_3$ ).

## 2.8. Experimental

**$^{13}\text{C}$  APT (75 MHz,  $\text{CD}_2\text{Cl}_2$ )**  $\delta$  133.30 (d,  $^3J_{\text{CP}} = 10.0$  Hz, *m*-PPh<sub>3</sub>), 133.13 (d,  $^4J_{\text{CP}} = 2.9$  Hz, *p*-PPh<sub>3</sub>), 129.59 (d,  $^2J_{\text{CP}} = 12.3$  Hz, *o*-PPh<sub>3</sub>), 128.05 (d,  $^1J_{\text{CP}} = 91.6$  Hz, *ipso*-PPh<sub>3</sub>), -2.02 (d,  $^1J_{\text{CP}} = 135.6$  Hz, CH).



4

To a solution of  $[\text{Ph}_3\text{PCH}_2\text{CN}]\text{Cl}$  (0.0676 g, 0.2 mmol) in  $\text{CH}_2\text{Cl}_2$  (10 ml) was added  $[\text{Au}(\text{C}_6\text{F}_5)(\text{tht})]$  (0.0904 g, 0.2 mmol) and the mixture stirred for 30 min at room temperature. The colourless solution was concentrated under reduced pressure to approximately 1 ml and *n*-pentane (10 ml) added to precipitate a white solid which was collected and vacuum dried to give the product (0.1150 g, 81%).

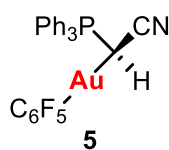
**IR ( $\text{cm}^{-1}$ )**  $\nu(\text{C}\equiv\text{N})$  2255;  $\nu(\text{C}_6\text{F}_5)$  1500, 951, 801;  $\nu(\text{Au}-\text{Cl})$  316.

**$^1\text{H}$  NMR (300 MHz,  $\text{CD}_2\text{Cl}_2$ )**  $\delta$  8.02 – 7.63 (m, 15H, Ph), 5.06 (d,  $^3J_{\text{HP}} = 14.5$  Hz, 2H,  $\text{CH}_2$ ).

**$^{31}\text{P}\{^1\text{H}\}$  NMR (121 MHz,  $\text{CD}_2\text{Cl}_2$ )**  $\delta$  20.76 (s, PPh<sub>3</sub>).

**$^{19}\text{F}$  NMR (282 MHz,  $\text{CD}_2\text{Cl}_2$ )**  $\delta$  -115.89 – -116.13 (m, 2F, *o*- $\text{C}_6\text{F}_5$ ), -162.60 (t,  $^3J_{\text{FF}} = 20.1$  Hz, 1F, *p*- $\text{C}_6\text{F}_5$ ), -163.99 – -164.36 (m, 2F, *m*- $\text{C}_6\text{F}_5$ ).

**$^{13}\text{C}$  APT (75 MHz,  $\text{CD}_2\text{Cl}_2$ )**  $\delta$  137.16 (d,  $^4J_{\text{CP}} = 3.1$  Hz, *p*-PPh<sub>3</sub>), 134.43 (d,  $^3J_{\text{CP}} = 10.9$  Hz, *m*-PPh<sub>3</sub>), 131.50 (d,  $^2J_{\text{CP}} = 13.4$  Hz, *o*-PPh<sub>3</sub>), 115.67 (d,  $^1J_{\text{CP}} = 89.0$  Hz, *ipso*-PPh<sub>3</sub>), 111.36 (d,  $^2J_{\text{CP}} = 9.2$  Hz,  $\text{C}\equiv\text{N}$ ), 17.63 (d,  $^1J_{\text{CP}} = 56.4$  Hz, CH).



To a solution of **3** (0.0301 g, 0.1 mmol) in  $\text{CH}_2\text{Cl}_2$  (5 ml) was added  $[\text{Au}(\text{C}_6\text{F}_5)(\text{tht})]$  (0.0452 g, 0.1 mmol) and the solution stirred for 2 h. The solution was filtered through celite, concentrated under reduced pressure to approximately 1 ml and *n*-pentane added to precipitate a white solid which was collected and vacuum dried to give the product (0.0658 g, 99%).

**HRMS (ESI-QTOF)  $m/z$ :**  $[\text{M}+\text{Na}]^+$  Calcd for  $\text{C}_{26}\text{H}_{16}\text{AuF}_5\text{NNaP}$  688.0498; Found 688.0483.

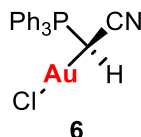
**IR ( $\text{cm}^{-1}$ ):**  $\nu(\text{C}\equiv\text{N})$  2201,  $\nu(\text{C}_6\text{F}_5)$  1499, 953, 797.

**$^1\text{H}$  NMR (300 MHz,  $\text{CD}_2\text{Cl}_2$ )**  $\delta$  8.07 – 7.53 (m, 15H, PPh<sub>3</sub>), 3.33 (d,  $^2J_{\text{HP}} = 12.5$  Hz, 1H, CH).

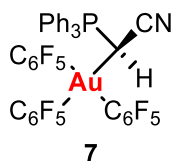
**$^{31}\text{P}\{^1\text{H}\}$  NMR (121 MHz,  $\text{CD}_2\text{Cl}_2$ )**  $\delta$  27.28 (s, PPh<sub>3</sub>).

**$^{19}\text{F}$  NMR (282 MHz,  $\text{CD}_2\text{Cl}_2$ )**  $\delta$  -116.57 – -116.99 (m, 2F, *o*- $\text{C}_6\text{F}_5$ ), -161.40 (t,  $^3J_{\text{FF}} = 20.0$  Hz, 1F, *p*- $\text{C}_6\text{F}_5$ ), -163.64 – -164.18 (m, 2F, *m*- $\text{C}_6\text{F}_5$ ).

**$^{13}\text{C}$  APT (75 MHz,  $\text{CD}_2\text{Cl}_2$ )**  $\delta$  135.04 (d,  $^4J_{\text{CP}} = 3.0$  Hz, *p*- $\text{PPh}_3$ ), 134.15 (d,  $^3J_{\text{CP}} = 9.9$  Hz, *m*- $\text{PPh}_3$ ), 130.42 (d,  $^2J_{\text{CP}} = 12.6$  Hz, *o*- $\text{PPh}_3$ ), 122.91 (d,  $^1J_{\text{CP}} = 88.5$  Hz, *ipso*- $\text{PPh}_3$ ), 119.76 (d,  $^2J_{\text{CP}} = 6.9$  Hz,  $\text{C}\equiv\text{N}$ ), 11.22 (d,  $^1J_{\text{CP}} = 51.6$  Hz, CH).



To a solution of **3** (0.0904 g, 0.3 mmol) in  $\text{CH}_2\text{Cl}_2$  (5 ml) was added  $[\text{AuCl}(\text{tht})]$  (0.0962 g, 0.3 mmol) and the solution stirred for 1 h. The solution was filtered through celite, concentrated under reduced pressure to approximately 1 ml and  $\text{Et}_2\text{O}$  added to precipitate a white solid which was collected and vacuum dried to give the product (0.1330 g, 83%). Spectral data are in agreement with previously reported values.



To a solution of **3** (0.0301 g, 0.1 mmol) in  $\text{CH}_2\text{Cl}_2$  (5 ml) was added  $[\text{Au}(\text{C}_6\text{F}_5)_3(\text{tht})]$  (0.0786 g, 0.1 mmol) and the solution stirred for 2 h. The solution was filtered through celite, concentrated under reduced pressure to approximately 1 ml and *n*-pentane added to precipitate a white solid which was collected and vacuum dried to give the product (0.0959 g, 96%).

**IR ( $\text{cm}^{-1}$ ):**  $\nu(\text{C}\equiv\text{N})$  2227,  $\nu(\text{C}_6\text{F}_5)$  1478, 968, 805, 791.

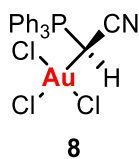
**$^1\text{H}$  NMR (300 MHz,  $\text{CD}_2\text{Cl}_2$ )**  $\delta$  7.79 – 7.35 (m, 15H,  $\text{PPh}_3$ ), 2.36 (d,  $^2J_{\text{HP}} = 4.5$  Hz, 1H, CH).

**$^{31}\text{P}\{^1\text{H}\}$  NMR (121 MHz,  $\text{CD}_2\text{Cl}_2$ )**  $\delta$  24.48 (s,  $\text{PPh}_3$ ).

**$^{19}\text{F}$  NMR (282 MHz,  $\text{CD}_2\text{Cl}_2$ )**  $\delta$  -122.08 – -122.46 (m, 2F, *o*- $\text{C}_6\text{F}_5$ ), -123.05 – -123.54 (m, 4F, *o*- $\text{C}_6\text{F}_5$ ), -158.63 (t,  $^3J_{\text{FF}} = 19.8$  Hz, 1F, *p*- $\text{C}_6\text{F}_5$ ), -158.65 (t,  $^3J_{\text{FF}} = 19.8$  Hz, 2F, *p*- $\text{C}_6\text{F}_5$ ), -162.17 – -162.57 (m, 4F, *m*- $\text{C}_6\text{F}_5$ ), -162.96 – -163.34 (m, 2F, *m*- $\text{C}_6\text{F}_5$ ).

**$^{13}\text{C}$  APT (75 MHz,  $\text{CD}_2\text{Cl}_2$ )**  $\delta$  134.30 (d,  $^4J_{\text{CP}} = 3.0$  Hz, *p*- $\text{PPh}_3$ ), 133.27 (d,  $^3J_{\text{CP}} = 10.5$  Hz, *m*- $\text{PPh}_3$ ), 130.06 (d,  $^2J_{\text{CP}} = 12.8$  Hz, *o*- $\text{PPh}_3$ ), 124.33 (d,  $^1J_{\text{CP}} = 93.5$  Hz, *ipso*- $\text{PPh}_3$ ), 6.60 (d,  $^1J_{\text{CP}} = 130.9$  Hz, CH).

## 2.8. Experimental



Method 1: To a solution of **3** (0.0301 g, 0.1 mmol) in CH<sub>2</sub>Cl<sub>2</sub> (5 ml) was added [AuCl<sub>3</sub>(tht)] (0.0783 g, 0.1 mmol) and the solution stirred for 2 h. The solution was filtered through celite, concentrated under reduced pressure to approximately 1 ml and *n*-pentane added to precipitate a yellow solid which was collected and vacuum dried to give the product (0.0544 g, 90%).

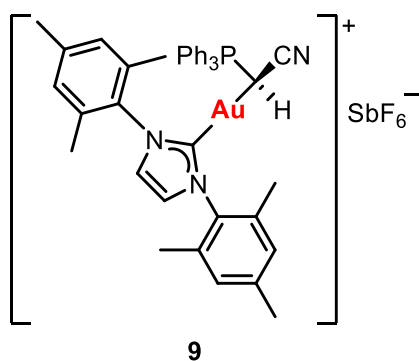
Method 2: To a solution of **2** (0.0534 g, 0.1 mmol) in CH<sub>2</sub>Cl<sub>2</sub> (5 ml) was added an equimolar amount of a standardised Cl<sub>2</sub> solution in CCl<sub>4</sub>. The solution immediately became yellow and was stirred for 1 h at room temperature. The solution was concentrated under reduced pressure to approximately 1 ml and Et<sub>2</sub>O (10 ml) added to precipitate a yellow solid (0.0580 g, 96%)

**IR** (cm<sup>-1</sup>)  $\nu$ (C≡N) 2228,  $\nu$ (Au-Cl) 360, 342, 315.

**<sup>1</sup>H NMR (300 MHz, CD<sub>2</sub>Cl<sub>2</sub>)**  $\delta$  8.25 – 7.38 (m, 15H, PPh<sub>3</sub>), 5.09 (d, <sup>2</sup>*J*<sub>HP</sub> = 13.1 Hz, 1H, CH).

**<sup>31</sup>P{<sup>1</sup>H} NMR (121 MHz, CD<sub>2</sub>Cl<sub>2</sub>)**  $\delta$  24.87 (s, PPh<sub>3</sub>).

**<sup>13</sup>C APT (75 MHz, CD<sub>2</sub>Cl<sub>2</sub>)**  $\delta$  136.43 (d, <sup>4</sup>*J*<sub>CP</sub> = 3.1 Hz, *p*-PPh<sub>3</sub>), 135.23 (d, <sup>3</sup>*J*<sub>CP</sub> = 10.1 Hz, *m*-PPh<sub>3</sub>), 130.85 (d, <sup>2</sup>*J*<sub>CP</sub> = 13.1 Hz, *o*-PPh<sub>3</sub>), 118.33 (d, <sup>1</sup>*J*<sub>CP</sub> = 88.0 Hz, *ipso*-PPh<sub>3</sub>), 114.98 (d, <sup>2</sup>*J*<sub>CP</sub> = 6.6 Hz, C≡N), 16.42 (d, <sup>1</sup>*J*<sub>CP</sub> = 51.6 Hz, CH).



To a solution of **3** (0.0301 g, 0.1 mmol) in CH<sub>2</sub>Cl<sub>2</sub> (5 ml) was added chloro-gold-1,3-bis(2,4,6-trimethylphenyl)imidazol-2-ylidene [AuCl(IMes)] (0.0537 g, 0.1 mmol) and AgSbF<sub>6</sub> (0.0343 g, 0.1 mmol) and the mixture stirred for 1 h with the exclusion of light. The solution was filtered through celite, the filtrate concentrated under reduced pressure to approximately 1 ml and Et<sub>2</sub>O (10 ml) added to precipitate a white solid which was collected and vacuum dried to give the product (0.0861 g, 83%).

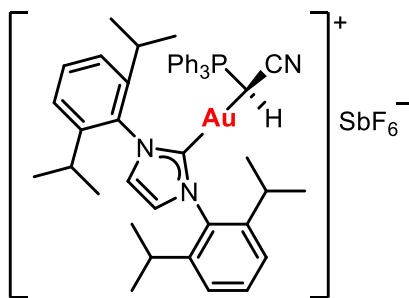
**HRMS (ESI-QTOF) m/z:** [M]<sup>+</sup> Calcd for C<sub>41</sub>H<sub>40</sub>AuN<sub>3</sub>P 802.2620, Found 802.2648.

**IR** ( $\text{cm}^{-1}$ )  $\nu(\text{C}\equiv\text{N})$  2211.

**$^1\text{H}$  NMR (400 MHz,  $\text{CD}_2\text{Cl}_2$ )**  $\delta$  7.86 – 7.74 (m, 3H,  $\text{PPh}_3$ ), 7.61 – 7.50 (m, 6H,  $\text{PPh}_3$ ), 7.48 – 7.34 (m, 6H,  $\text{PPh}_3$ ), 7.17 (s, 2H, CH (imidazole)), 7.05 – 6.95 (m, 4H,  $\text{CH}^{\text{AR}}$ ), 3.05 (d,  $^2J_{\text{HP}} = 13.5$  Hz, 1H, CH), 2.36 (s, 6H,  $\text{CH}_3$ ), 1.97 (s, 6H,  $\text{CH}_3$ ), 1.94 (s, 6H,  $\text{CH}_3$ ).

**$^{31}\text{P}\{^1\text{H}\}$  NMR (162 MHz,  $\text{CD}_2\text{Cl}_2$ )**  $\delta$  28.10 (s,  $\text{PPh}_3$ )

**$^{13}\text{C}$  APT (75 MHz,  $\text{CD}_2\text{Cl}_2$ )**  $\delta$  181.47 (s, C (NHC)), 140.63 (s,  $p\text{-C}^{\text{AR}}$ ), 135.38 (d,  $^4J_{\text{CP}} = 3.0$  Hz,  $p\text{-PPh}_3$ ), 134.81 (s,  $ipso\text{-C}^{\text{AR}}$ ), 135.20 (s,  $o\text{-C}$  (AR)), 133.56 (d,  $^3J_{\text{CP}} = 9.9$  Hz,  $m\text{-PPh}_3$ ), 130.62 (d,  $^2J_{\text{CP}} = 12.7$  Hz,  $o\text{-PPh}_3$ ), 130.00 (s,  $m\text{-CH}$  (AR)), 129.98 (s,  $m\text{-CH}$  (AR)), 123.68 (s, CH (imidazole)), 121.86 (d,  $^1J_{\text{CP}} = 88.6$  Hz,  $ipso\text{-PPh}_3$ ), 118.46 (d,  $^2J_{\text{CP}} = 7.8$  Hz,  $\text{C}\equiv\text{N}$ ), 21.50 (s,  $\text{CH}_3$ ), 18.03 (s  $\text{CH}_3$ ), 18.00 (s,  $\text{CH}_3$ ), 10.68 (d,  $^1J_{\text{CP}} = 51.5$  Hz, CH).



**10**

To a solution of **3** (0.0301 g, 0.1 mmol) in  $\text{CH}_2\text{Cl}_2$  (5 ml) was added chloro-gold-1,3-bis(2,6-diisopropylphenyl)imidazol-2-ylidene [ $\text{AuCl}(\text{IPr})$ ] (0.0621 g, 0.1 mmol) and  $\text{AgSbF}_6$  (0.0343 g, 0.1 mmol) and the mixture stirred for 1 h with the exclusion of light. The solution was filtered through celite, the filtrate concentrated under reduced pressure to approximately 1 ml and  $\text{Et}_2\text{O}$  (10 ml) added to precipitate a white solid which was collected and vacuum dried to give the product (0.1021 g, 91%).

**HRMS (ESI-QTOF) m/z:**  $[\text{M}]^+$  Calcd for  $\text{C}_{47}\text{H}_{52}\text{AuN}_3\text{P}$  886.3559, Found 886.2598.

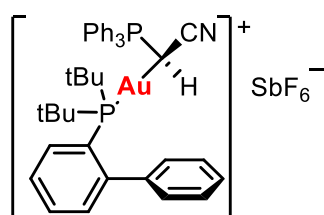
**IR** ( $\text{cm}^{-1}$ )  $\nu(\text{C}\equiv\text{N})$  2214

**$^1\text{H}$  NMR (400 MHz,  $\text{CD}_2\text{Cl}_2$ )**  $\delta$  7.79 – 7.69 (m, 3H,  $\text{CH}^{\text{AR}}$ ), 7.63 (t,  $^3J_{\text{HH}} = 7.8$  Hz, 2H,  $\text{CH}^{\text{AR}}$ ), 7.47 (m, 6H,  $\text{CH}^{\text{AR}} + \text{PPh}_3$ ), 7.39 – 7.30 (m, 10H,  $\text{PPh}_3$ ), 7.27 (s, 2H, CH (imidazole)), 3.04 (d,  $^2J_{\text{HP}} = 14.3$  Hz, 1H, CH), 2.45 (septuplet,  $^3J_{\text{HH}} = 6.9$  Hz, 4H,  $\text{CH}(\text{CH}_3)_2$ ), 1.13 (d,  $^3J_{\text{HH}} = 6.9$  Hz, 6H,  $\text{CH}(\text{CH}_3)_2$ ), 1.07 (d,  $^3J_{\text{HH}} = 6.9$  Hz, 6H,  $\text{CH}(\text{CH}_3)_2$ ).

**$^{31}\text{P}\{^1\text{H}\}$  NMR (162 MHz,  $\text{CD}_2\text{Cl}_2$ )**  $\delta$  28.72 (s,  $\text{PPh}_3$ )

## 2.8. Experimental

**$^{13}\text{C}$  APT (75 MHz,  $\text{CD}_2\text{Cl}_2$ )**  $\delta$  183.11 (s, C (NHC)), 146.30 (s *ipso*-C (AR)), 135.41 (d,  $^4J_{\text{CP}} = 3.1$  Hz, *p*-PPh<sub>3</sub>), 134.10 (s, *o*-C<sup>AR</sup>), 133.47 (d,  $^3J_{\text{CP}} = 9.9$  Hz, *m*-PPh<sub>3</sub>), 131.63 (s, *p*-CH (AR)), 130.71 (d,  $^2J_{\text{CP}} = 12.7$  Hz, *o*-PPh<sub>3</sub>), 124.93 (s, *m*-CH (AR)), 124.77 (s, CH (imidazole)), 121.37 (d,  $^1J_{\text{CP}} = 88.6$  Hz, *ipso*-PPh<sub>3</sub>), 118.06 (d,  $^2J_{\text{CP}} = 6.9$  Hz, C $\equiv$ N), 29.37 (s, CH(CH<sub>3</sub>)<sub>2</sub>), 25.01 (s, CH(CH<sub>3</sub>)<sub>2</sub>), 24.90 (s, CH(CH<sub>3</sub>)<sub>2</sub>), 24.19 (s, CH(CH<sub>3</sub>)<sub>2</sub>), 24.15 (s, CH(CH<sub>3</sub>)<sub>2</sub>), 10.56 (d,  $^1J_{\text{CP}} = 51.7$  Hz, CH).



11

To a solution of **3** (0.0301 g, 0.1 mmol) in  $\text{CH}_2\text{Cl}_2$  (5 ml) was added [AuCl(JohnPhos)] (0.0531 g, 0.1 mmol) and AgSbF<sub>6</sub> (0.0343 g, 0.1 mmol) and the mixture stirred for 1 h with the exclusion of light. The solution was filtered through celite, the filtrate concentrated under reduced pressure to approximately 1 ml and Et<sub>2</sub>O (10 ml) added to precipitate a white solid which was collected and vacuum dried to give the product (0.0950 g, 92%).

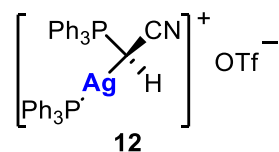
**HRMS (ESI-QTOF) m/z:** [M]<sup>+</sup> Calcd for C<sub>40</sub>H<sub>43</sub>AuNP<sub>2</sub> 796.2531, Found 796.2550.

**IR (cm<sup>-1</sup>)**  $\nu(\text{C}\equiv\text{N})$  2200

**$^1\text{H}$  NMR (300 MHz,  $\text{CD}_2\text{Cl}_2$ )**  $\delta$  7.87 – 7.80 (m, 4H, ), 7.77 – 7.51 (m, 16H), 7.40 – 7.35 (m, 1H, ), 7.29 – 7.25 (m, 2H, ), 7.23 – 7.13 (m, 1H), 2.08 (dd,  $^2J_{\text{HP}} = 12.2$ ,  $^3J_{\text{HP}} = 7.5$  Hz, 1H, CH), 1.35 (d,  $^3J_{\text{HP}} = 15.7$  Hz, 9H, <sup>t</sup>Bu), 0.97 (d,  $^3J_{\text{HP}} = 15.7$  Hz, 9H, <sup>t</sup>Bu).

**$^{31}\text{P}\{^1\text{H}\}$  NMR (121 MHz,  $\text{CD}_2\text{Cl}_2$ )**  $\delta$  64.31 (d,  $^3J_{\text{PP}} = 8.4$  Hz, P (JohnPhos)), 26.94 (d,  $^3J_{\text{PP}} = 8.4$  Hz, P (ylide)).

**$^{13}\text{C}$  APT (75 MHz,  $\text{CD}_2\text{Cl}_2$ )**  $\delta$  149.25 (d,  $^2J_{\text{CP}} = 14.0$  Hz, C (JohnPhos)), 144.98 (d,  $^3J_{\text{CP}} = 6.3$  Hz, C (JohnPhos)), 135.65 (d,  $^4J_{\text{CP}} = 3.0$  Hz, *p*-PPh<sub>3</sub>), 134.66 (d,  $^4J_{\text{CP}} = 2.3$  Hz, CH (JohnPhos)), 133.73 (d,  $^3J_{\text{CP}} = 9.7$  Hz, *m*-PPh<sub>3</sub>), 131.72 (d,  $^4J_{\text{CP}} = 2.4$  Hz, CH (JohnPhos)), 130.73 (d,  $^2J_{\text{CP}} = 12.6$  Hz, *o*-PPh<sub>3</sub>), 130.27 (s, CH (JohnPhos)), 129.73 (s, CH (JohnPhos)), 128.97 (s, CH (JohnPhos)), 128.14 (d,  $^3J_{\text{CP}} = 6.7$  Hz, CH (JohnPhos)), 127.77 (s, CH (JohnPhos)), 126.36 (d,  $^1J_{\text{CP}} = 43.8$  Hz, C (JohnPhos)), 121.80 (d,  $^1J_{\text{CP}} = 88.3$  Hz, *ipso*-PPh<sub>3</sub>), 38.13 (d,  $^1J_{\text{CP}} = 23.2$  Hz, C (<sup>t</sup>Bu)), 37.83 (d,  $^1J_{\text{CP}} = 22.8$  Hz, C (<sup>t</sup>Bu)), 31.31 (d,  $^2J_{\text{CP}} = 6.5$  Hz, CH<sub>3</sub> (<sup>t</sup>Bu)), 30.59 (d,  $^2J_{\text{CP}} = 6.3$  Hz, CH<sub>3</sub> (<sup>t</sup>Bu)), 17.53 (dd,  $^1J_{\text{CP}} = 68.6$ ,  $^2J_{\text{CP}} = 53.7$  Hz, CH).



To a solution of **3** (0.0602 g, 0.2 mmol) in CH<sub>2</sub>Cl<sub>2</sub> (5 ml) was added [Ag(OTf)(PPh<sub>3</sub>)] (0.1038 g, 0.2 mmol) and the mixture stirred for 1 h with the exclusion of light. The solution was filtered through celite, the filtrate concentrated under reduced pressure to approximately 1 ml and Et<sub>2</sub>O (10 ml) added to precipitate a white solid which was collected and vacuum dried to give the product (0.1461 g, 89%).

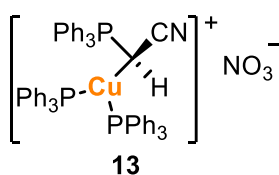
**IR** (cm<sup>-1</sup>) ν(C≡N) 2188

**<sup>1</sup>H NMR (300 MHz, CD<sub>2</sub>Cl<sub>2</sub>)** δ 7.80 – 7.17 (m, 30H, 2 x PPh<sub>3</sub>), 2.86 (d, <sup>2</sup>J<sub>HP</sub> = 4.3 Hz, 1H, CH).

**<sup>31</sup>P{<sup>1</sup>H} NMR (121 MHz, CD<sub>2</sub>Cl<sub>2</sub>, 298 K)** δ 25.92 (s, PPh<sub>3</sub> (ylide)), 12.48 (s, br, Ag-PPh<sub>3</sub>).

**<sup>31</sup>P{<sup>1</sup>H} NMR (121 MHz, CD<sub>2</sub>Cl<sub>2</sub>, 203 K)** δ 25.83 (s, PPh<sub>3</sub> (ylide)), 11.81 (dd, <sup>1</sup>J<sub>109Ag-P</sub> = 628.2 Hz, <sup>1</sup>J<sub>107Ag-P</sub> 544.1 Hz).

**<sup>13</sup>C APT (75 MHz, CD<sub>2</sub>Cl<sub>2</sub>)** δ 134.56 (d, <sup>4</sup>J<sub>CP</sub> = 2.9 Hz, *p*-PPh<sub>3</sub> (ylide)), 134.26 (d, <sup>2</sup>J<sub>CP</sub> = 15.9 Hz, *o*-PPh<sub>3</sub>), 133.39 (d, <sup>3</sup>J<sub>CP</sub> = 9.9 Hz, *m*-PPh<sub>3</sub> (ylide)), 131.65 (s, *p*-PPh<sub>3</sub>, 130.34 (d, <sup>2</sup>J<sub>CP</sub> = 12.5 Hz, *o*-PPh<sub>3</sub> (ylide)), 129.77 (d, <sup>3</sup>J<sub>CP</sub> = 10.2 Hz, *m*-PPh<sub>3</sub>), 124.50 (d, <sup>1</sup>J<sub>CP</sub> = 90.6 Hz, *ipso*-PPh<sub>3</sub> (ylide)), 1.17 (d, <sup>1</sup>J<sub>CP</sub> = 83.2 Hz, CH).



To a solution of **3** (0.0602 g, 0.1 mmol) in CH<sub>2</sub>Cl<sub>2</sub> (5 ml) was added [Cu(NO<sub>3</sub>)(PPh<sub>3</sub>)<sub>2</sub>] (0.1303 g, 0.1 mmol) and the mixture stirred for 1 h. The solution was filtered through celite, the filtrate concentrated under reduced pressure to approximately 1 ml and Et<sub>2</sub>O (10 ml) added to precipitate a white solid which was collected and vacuum dried to give the product (0.1585 g, 83%).

**IR** (cm<sup>-1</sup>) ν(C≡N) 2153.

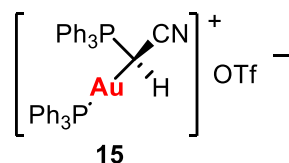
**<sup>1</sup>H NMR (300 MHz, CD<sub>2</sub>Cl<sub>2</sub>)** δ 7.69 – 7.11 (m, 45H, 3 x PPh<sub>3</sub>), 1.78 (d, <sup>2</sup>J<sub>HP</sub> = 5.9 Hz, 1H, CH).



## 2.8. Experimental

**$^{31}\text{P}\{^1\text{H}\}$  NMR (121 MHz,  $\text{CD}_2\text{Cl}_2$ )**  $\delta$  23.12 (s,  $\text{PPh}_3$  (ylide)), -1.36 (s, br,  $\text{PPh}_3$ ).

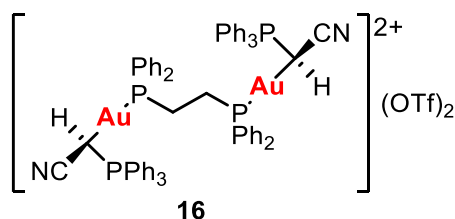
**$^{13}\text{C}$  APT (75 MHz,  $\text{CD}_2\text{Cl}_2$ )**  $\delta$  134.15 (d,  $^2J_{\text{CP}} = 14.8$  Hz, *o*- $\text{PPh}_3$ ), 133.59 (d,  $^4J_{\text{CP}} = 3.0$  Hz, *p*- $\text{PPh}_3$  (ylide)), 133.24 (d,  $^3J_{\text{CP}} = 10.3$  Hz, *m*- $\text{PPh}_3$  (ylide)), 132.67 (d,  $^1J_{\text{CP}} = 31.8$  Hz, *ipso*- $\text{PPh}_3$ ), 130.71 (s, *p*- $\text{PPh}_3$ ), 129.81 (d,  $^2J_{\text{CP}} = 12.5$  Hz, *o*- $\text{PPh}_3$  (ylide)), 129.31 (d,  $^3J_{\text{CP}} = 9.3$  Hz, *m*- $\text{PPh}_3$ ), 126.66 (d,  $^1J_{\text{CP}} = 92.5$  Hz, *ipso*- $\text{PPh}_3$  (ylide)), 1.21 (s, CH).



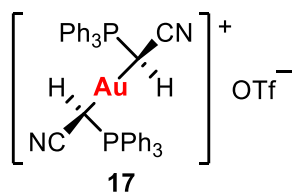
To a solution of complex **6** (0.0534g, 0.1 mmol) in  $\text{CH}_2\text{Cl}_2$  (5 ml) was added  $\text{AgOTf}$  (0.0257 g, 0.1 mmol) and  $\text{PPh}_3$  (0.0262 g, 0.1 mmol) and the mixture stirred for 3 h with the exclusion of light. The solution was filtered through celite, the filtrate concentrated under reduced pressure to approximately 1 ml and *n*-pentane added to precipitate a white solid. A mixture of **15**, **2** and **26** was obtained. The peaks corresponding to **15** in the NMR spectra could be identified.

**$^1\text{H}$  NMR (400 MHz,  $\text{CDCl}_3$ )**  $\delta$  7.86 – 7.13 (m, 2 x  $\text{PPh}_3$ ), 4.32 (dd,  $^2J_{\text{HP}} = 13.0$  Hz,  $^3J_{\text{HP}} = 8.6$  Hz, 1H, CH).

**$^{31}\text{P}\{^1\text{H}\}$  NMR (162 MHz,  $\text{CDCl}_3$ )**  $\delta$  38.72 (d,  $^3J_{\text{PP}} = 10.6$  Hz,  $\text{PPh}_3$ ), 27.92 (d,  $^3J_{\text{PP}} = 10.6$  Hz,  $\text{PPh}_3$  (ylide)).



$[\text{Au}_2\text{Cl}_2(\text{dppe})]$  (0.0432 g, 0.05 mmol),  $\text{AgOTf}$  (0.0257 g, 0.1 mmol) and **3** (0.0301 g, 0.1 mmol) were dissolved in  $\text{CH}_2\text{Cl}_2$  (5 ml) and the mixture stirred for 4 h with the exclusion of light. The solution was filtered through celite, the filtrate concentrated under reduced pressure to approximately 1 ml and  $\text{Et}_2\text{O}$  (10 ml) added to precipitate a white solid which was collected and vacuum dried. A mixture of diastereoisomers of **16** and  $[\text{Au}(\text{dppe})_2](\text{OTf})$  was obtained.



Method 1: To a solution of [AuCl(tht)] (0.0321 g, 0.1 mmol) in CH<sub>2</sub>Cl<sub>2</sub> (5 ml) was added [Ag(OTf)(ttht)] (0.0345 g, 0.1 mmol) and the mixture stirred for 1 h with the exclusion of light. Precipitated silver chloride was removed by filtration through celite and to the filtrate was added a solution of **3** (0.0602 g, 0.2 mmol) in CH<sub>2</sub>Cl<sub>2</sub> (5 ml) and the mixture stirred for 1 h. The solution was concentrated under reduced pressure to approximately 1 ml and Et<sub>2</sub>O (10 ml) added to precipitate a white solid which was collected and vacuum dried to give the product (0.0718 g, 76%).

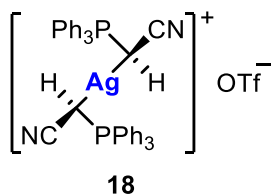
Method 2: To a solution of **18** (0.0430 g, 0.05 mmol) in CH<sub>2</sub>Cl<sub>2</sub> (3 ml) was added [AuCl(tht)] (0.0161 g, 0.05 mmol) and the mixture stirred for 15 min with the exclusion of light. The solution was filtered through celite, the filtrate concentrated under reduced pressure to approximately 1 ml and Et<sub>2</sub>O added to precipitate a white solid which was collected and vacuum dried to give the product (0.0443 g, 93%)

**IR** (cm<sup>-1</sup>) ν(C≡N) 2210

**<sup>1</sup>H NMR** (400 MHz, CD<sub>2</sub>Cl<sub>2</sub>) δ 8.66 – 6.85 (m, 30H, PPh<sub>3</sub>), 3.38 (d, <sup>2</sup>J<sub>HP</sub> = 12.8 Hz, 1H, CH), 3.37 (d, <sup>2</sup>J<sub>HP</sub> = 12.8 Hz, 1H, CH (diastereoisomer)).

**<sup>31</sup>P{<sup>1</sup>H} NMR** (162 MHz, CD<sub>2</sub>Cl<sub>2</sub>) δ 26.69 (s, PPh<sub>3</sub>), 26.64 (s, PPh<sub>3</sub> (diastereoisomer)).

**<sup>13</sup>C APT** (75 MHz, CD<sub>2</sub>Cl<sub>2</sub>) δ 135.51 (d, <sup>4</sup>J<sub>CP</sub> = 2.8 Hz, *p*-PPh<sub>3</sub>), 133.77 (d, <sup>3</sup>J<sub>CP</sub> = 10.0 Hz, *m*-PPh<sub>3</sub>), 130.77 (d, <sup>2</sup>J<sub>CP</sub> = 12.8 Hz, *o*-PPh<sub>3</sub>), 121.76 (d, <sup>1</sup>J<sub>CP</sub> = 88.6 Hz, *ipso*-PPh<sub>3</sub>), 118.46 (d, <sup>2</sup>J<sub>CP</sub> = 9.2 Hz, C≡N), 9.94 (d, <sup>1</sup>J<sub>CP</sub> = 52.1 Hz, CH).



**3** (0.0602 g, 0.2mmol) and AgOTf (0.0257 g, 0.1 mmol) were mixed in CH<sub>2</sub>Cl<sub>2</sub> (5 ml) and the mixture stirred for 3 h with the exclusion of light. The solution was concentrated under reduced pressure to approximately 1 ml and Et<sub>2</sub>O (10 ml) added to precipitate a white solid which was collected and vacuum dried to give the product (0.0768 g, 89%).

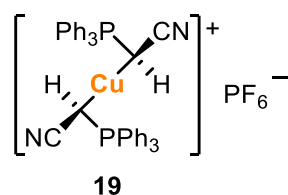
## 2.8. Experimental

**IR** (cm<sup>-1</sup>)  $\nu(\text{C}\equiv\text{N})$  2168

**<sup>1</sup>H NMR** (400 MHz, CD<sub>2</sub>Cl<sub>2</sub>)  $\delta$  8.12 – 7.28 (m, 30H, PPh<sub>3</sub>), 2.76 (d, <sup>2</sup>*J*<sub>HP</sub> = 8.7 Hz, 1H, CH).

**<sup>31</sup>P{<sup>1</sup>H} NMR** (162 MHz, CD<sub>2</sub>Cl<sub>2</sub>)  $\delta$  26.58 (s, PPh<sub>3</sub>).

**<sup>13</sup>C APT** (75 MHz, CD<sub>2</sub>Cl<sub>2</sub>)  $\delta$  135.17 (d, <sup>4</sup>*J*<sub>CP</sub> = 3.1 Hz, *p*-PPh<sub>3</sub>), 133.35 (d, <sup>3</sup>*J*<sub>CP</sub> = 9.8 Hz, *m*-PPh<sub>3</sub>), 130.72 (d, <sup>2</sup>*J* = 12.6 Hz, *o*-PPh<sub>3</sub>), 123.25 (d, <sup>1</sup>*J*<sub>CP</sub> = 89.7 Hz, *ipso*-PPh<sub>3</sub>), 0.82 (d, <sup>1</sup>*J*<sub>CP</sub> = 66.6 Hz, CH).



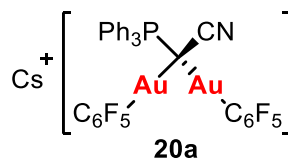
**3** (0.0602 g, 0.2 mmol) and [Cu(NCMe)<sub>4</sub>]PF<sub>6</sub> (0.0373 g, 0.1 mmol) were mixed in CH<sub>2</sub>Cl<sub>2</sub> (5 ml) and the mixture stirred for 3 h. The solution was filtered through celite, the filtrate concentrated under reduced pressure to approximately 1 ml and Et<sub>2</sub>O (10 ml) added to precipitate a white solid which was collected and vacuum dried to give the product (0.0600 g, 74%).

**IR** (cm<sup>-1</sup>)  $\nu(\text{C}\equiv\text{N})$  2166

**<sup>1</sup>H NMR** (300 MHz, CD<sub>2</sub>Cl<sub>2</sub>)  $\delta$  7.97 – 6.89 (m, 30H, PPh<sub>3</sub>), 2.10 (d, <sup>2</sup>*J*<sub>HP</sub> = 4.0 Hz, 2H, CH).

**<sup>31</sup>P{<sup>1</sup>H} NMR** (121 MHz, CD<sub>2</sub>Cl<sub>2</sub>)  $\delta$  24.43 (s, PPh<sub>3</sub>).

**<sup>13</sup>C NMR** (75 MHz, CD<sub>2</sub>Cl<sub>2</sub>)  $\delta$  134.16 (d, <sup>4</sup>*J*<sub>CP</sub> = 3.0 Hz, *p*-PPh<sub>3</sub>), 133.37 (d, <sup>3</sup>*J*<sub>CP</sub> = 10.4 Hz, *m*-PPh<sub>3</sub>), 130.07 (d, <sup>2</sup>*J*<sub>CP</sub> = 12.6 Hz, *o*-PPh<sub>3</sub>), 125.38 (d, <sup>1</sup>*J*<sub>CP</sub> = 93.1 Hz, *ipso*-PPh<sub>3</sub>), 1.83 (d, <sup>1</sup>*J*<sub>CP</sub> = 130.9 Hz, CH).



To a solution of **2** (0.0451 g, 0.1 mmol) in acetone (5 ml) was added [Au(C<sub>6</sub>F<sub>5</sub>)(tbt)] (0.0904 g, 0.2 mmol) and Cs<sub>2</sub>CO<sub>3</sub> (excess) and the mixture stirred for 3 h. The mixture was filtered through celite, the filtrate concentrated under reduced pressure to approximately 1 ml and *n*-hexane added to precipitate a white solid which was collected and vacuum dried to give the product (0.1056 g, 91%).

**HRMS (ESI-QTOF) m/z:** [M]<sup>+</sup> Calcd for C<sub>32</sub>H<sub>15</sub>Au<sub>2</sub>F<sub>10</sub>NP 1028.0199, Found 1028.0199

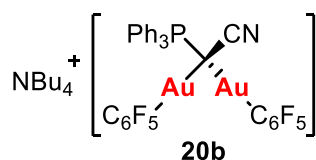
**IR** ( $\text{cm}^{-1}$ )  $\nu(\text{C}\equiv\text{N})$  2165,  $\nu(\text{C}_6\text{F}_5)$  1503, 951, 794.

**$^1\text{H}$  NMR (400 MHz, Acetone)**  $\delta$  8.28 – 8.18 (m, 6H,  $\text{PPh}_3$ ), 7.73 – 7.63 (m, 3H,  $\text{PPh}_3$ ), 7.59 – 7.54 (m, 6H,  $\text{PPh}_3$ ).

**$^{31}\text{P}\{^1\text{H}\}$  NMR (162 MHz, Acetone)**  $\delta$  32.37 (s,  $\text{PPh}_3$ ).

**$^{19}\text{F}$  NMR (376 MHz, Acetone)**  $\delta$  -116.81 – -117.03 (m, 4F, *o*- $\text{C}_6\text{F}_5$ ), -166.23 (t,  $^3J_{\text{FF}} = 19.8$  Hz, 2F, *p*- $\text{C}_6\text{F}_5$ ), -166.42 – -166.84 (m, 4F, *m*- $\text{C}_6\text{F}_5$ ).

**$^{13}\text{C}$  APT (101 MHz, Acetone)**  $\delta$  134.75 (d,  $^3J_{\text{CP}} = 8.9$  Hz, *m*- $\text{PPh}_3$ ), 133.22 (d,  $^4J_{\text{CP}} = 2.8$  Hz, *p*- $\text{PPh}_3$ ), 130.46 (d,  $^1J_{\text{CP}} = 86.8$  Hz, *ipso*- $\text{PPh}_3$ ), 129.49 (d,  $^2J_{\text{CP}} = 11.6$  Hz, *o*- $\text{PPh}_3$ ), 127.65 (s,  $\text{C}\equiv\text{N}$ ).



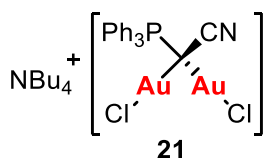
To a solution of **3** (0.0301 g, 0.1 mmol) and  $[\text{Au}(\text{C}_6\text{F}_5)(\text{tht})]$  (0.0904 g, 0.2 mmol) in  $\text{CH}_2\text{Cl}_2$  (5 ml) was added  $\text{NBu}_4(\text{acac})$  (0.0342 g, 0.1 mmol) and the mixture stirred for 3 h. The solution was filtered through celite, the filtrate concentrated under reduced pressure to approximately 1 ml and *n*-hexane added to precipitate a white solid which was collected and vacuum dried to give the product (0.1243 g, 98%).

**HRMS (ESI-QTOF) m/z:**  $[\text{M}]^+$  Calcd for  $\text{C}_{32}\text{H}_{15}\text{Au}_2\text{F}_{10}\text{NP}$  1028.0199, Found 1028.0199

**$^1\text{H}$  NMR (400 MHz,  $\text{CD}_2\text{Cl}_2$ )**  $\delta$  8.45 – 7.30 (m, 15H,  $\text{PPh}_3$ ), 3.17 – 3.04 (m, 8H,  $\text{CH}_2$ ), 1.67 – 1.49 (m, 8H,  $\text{CH}_2$ ), 1.39 (h,  $^3J_{\text{HH}} = 7.4$  Hz, 8H,  $\text{CH}_2$ ), 0.96 (t,  $^3J_{\text{HH}} = 7.3$  Hz, 12H,  $\text{CH}_3$ ).

**$^{31}\text{P}\{^1\text{H}\}$  NMR (162 MHz,  $\text{CD}_2\text{Cl}_2$ )**  $\delta$  32.08 (s,  $\text{PPh}_3$ ).

**$^{19}\text{F}$  NMR (376 MHz,  $\text{CD}_2\text{Cl}_2$ )**  $\delta$  -115.46 – -115.70 (m, 4F, *o*- $\text{C}_6\text{F}_5$ ), -162.92 (t,  $^3J_{\text{FF}} = 20.1$  Hz, 2F, *p*- $\text{C}_6\text{F}_5$ ), -163.91 – -164.12 (m, 4F, *m*- $\text{C}_6\text{F}_5$ ).



To a solution of **3** (0.0301 g, 0.1 mmol) and  $[\text{AuCl}(\text{tht})]$  (0.0641 g, 0.2 mmol) in  $\text{CH}_2\text{Cl}_2$  (5 ml) was added  $\text{NBu}_4(\text{acac})$  (0.0342 g, 0.1 mmol) and the mixture stirred for 3 h. The solution was filtered through celite, the filtrate concentrated under reduced pressure to approximately 1 ml

## 2.8. Experimental

and Et<sub>2</sub>O added to precipitate a white solid which was collected and vacuum dried to give the product (0.0961 g, 95%)

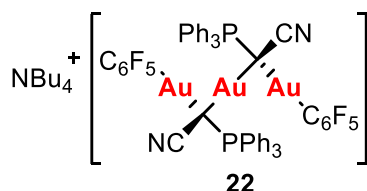
**HRMS (ESI-QTOF) m/z:** [M]<sup>+</sup> Calcd for C<sub>20</sub>H<sub>15</sub>Au<sub>2</sub>Cl<sub>2</sub>NP 763.9656, Found 763.9643.

**IR (cm<sup>-1</sup>)** ν(C≡N) 2160.

**<sup>1</sup>H NMR (300 MHz, CD<sub>2</sub>Cl<sub>2</sub>)** δ 8.25 – 7.28 (m, 15H, PPh<sub>3</sub>), 3.39 – 3.07 (m, 8H, CH<sub>2</sub>), 1.85 – 1.63 (m, 8H, CH<sub>2</sub>), 1.46 (h, <sup>3</sup>J<sub>HH</sub> = 7.3 Hz, 8H, CH<sub>2</sub>), 1.02 (t, <sup>3</sup>J<sub>HH</sub> = 7.3 Hz, 12H, CH<sub>3</sub>).

**<sup>31</sup>P{<sup>1</sup>H} NMR (121 MHz, CD<sub>2</sub>Cl<sub>2</sub>)** δ 28.95 (s, PPh<sub>3</sub>).

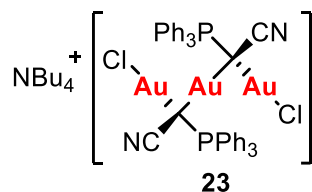
**<sup>13</sup>C APT (75 MHz, CD<sub>2</sub>Cl<sub>2</sub>)** δ 134.37 (d, <sup>3</sup>J<sub>CP</sub> = 9.0 Hz, *m*-PPh<sub>3</sub>), 133.38 (d, <sup>4</sup>J<sub>CP</sub> = 2.8 Hz, *p*-PPh<sub>3</sub>), 129.48 (d, <sup>2</sup>J<sub>CP</sub> = 11.9 Hz, *o*-PPh<sub>3</sub>), 128.21 (d, <sup>1</sup>J<sub>CP</sub> = 87.2 Hz, *ipso*-PPh<sub>3</sub>), 125.94 (s, C≡N), 59.72 (s, CH<sub>2</sub>), 24.64 (s, CH<sub>2</sub>), 20.42 (s, CH<sub>2</sub>) 14.08 (s, CH<sub>3</sub>).



To a solution of **17** (0.0660 g, 0.07 mmol) in CH<sub>2</sub>Cl<sub>2</sub> (5 ml) was added [Au(C<sub>6</sub>F<sub>5</sub>)(tht)] (0.0474 g, 0.14 mmol) and NBu<sub>4</sub>(acac) (0.0628 g, 0.14 mmol) and the mixture stirred for 2 h. The solution was filtered through celite, the filtrate concentrated under reduced pressure to approximately 1 ml and *n*-hexane added to precipitate a white solid which was collected and vacuum dried to give the product (0.0936 g, 38%).

**HRMS (ESI-QTOF) m/z:** [M]<sup>+</sup> Calcd for C<sub>52</sub>H<sub>30</sub>Au<sub>3</sub>F<sub>10</sub>N<sub>2</sub>P<sub>2</sub> 1526.0716, Found 1525.0710.

**IR (cm<sup>-1</sup>)** ν(C≡N) 2153.



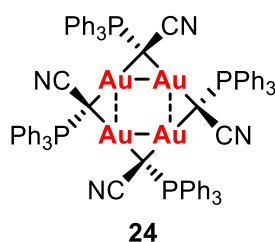
To a solution of **17** (0.2071 g, 0.2 mmol) in THF (5 ml) was added [AuCl(tht)] (0.1282 g, 0.4 mmol) and NBu<sub>4</sub>(acac) (0.3206 g, 0.4 mmol) and the mixture stirred for 2 h. The solution was cooled to 0 °C and a white precipitate formed which was collected by filtration, washed with Et<sub>2</sub>O and vacuum dried to give the product (0.0761 g, 13%).

**HRMS (ESI-QTOF) m/z:** [M]<sup>+</sup> Calcd for C<sub>46</sub>H<sub>30</sub>Au<sub>3</sub>Cl<sub>2</sub>N<sub>2</sub>P<sub>2</sub> 1261.0252, Found 1261.0241.

**IR** ( $\text{cm}^{-1}$ )  $\nu(\text{C}\equiv\text{N})$  2154

**$^1\text{H}$  NMR** (300 MHz,  $\text{CD}_2\text{Cl}_2$ )  $\delta$  7.98 – 7.26 (m, 30H, Ph), 3.38 – 3.21 (m, 8H,  $\text{CH}_2$ ), 1.80–1.69 (m, 8H,  $\text{CH}_2$ ), 1.54 – 1.39 (m, 8H,  $\text{CH}_2$ ), 1.01 (t,  $^3J_{\text{HH}} = 7.3$  Hz, 12H,  $\text{CH}_3$ ).

**$^{31}\text{P}\{^1\text{H}\}$  NMR** (121 MHz,  $\text{CD}_2\text{Cl}_2$ )  $\delta$  29.17 (s,  $\text{PPh}_3$ ).



To a solution of **25** (0.2041 g, 0.125 mmol) in  $\text{CH}_2\text{Cl}_2$  (10 ml) was added  $[\text{AuCl}(\text{tht})]$  (0.1603 g, 0.5 mmol) and the mixture stirred for 2 h with the exclusion of light. The solution was filtered through celite to give a yellow filtrate. The filtrate was concentrated under reduced pressure to approximately 1 ml and  $\text{Et}_2\text{O}$  (10 ml) added to precipitate a pale-yellow solid which was collected and vacuum dried to give the product (0.2284 g, 92%).

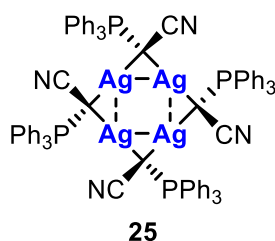
**MS** (ESI+)  $m/z$ : 1988.8  $[\text{M}]^+$ , 1791.3  $[\text{M}-\text{Au}]^+$ , 1293.9  $[\text{M}-\{\text{Au}_2 \text{C}(\text{PPh}_3)(\text{C}\equiv\text{N})\}]^+$

**IR** ( $\text{cm}^{-1}$ )  $\nu(\text{C}\equiv\text{N})$  2154

**$^1\text{H}$  NMR** (300 MHz,  $\text{CD}_2\text{Cl}_2$ )  $\delta$  7.81 – 7.42 (m, Ph).

**$^{31}\text{P}\{^1\text{H}\}$  NMR** (121 MHz,  $\text{CD}_2\text{Cl}_2$ )  $\delta$  28.92 (s,  $\text{PPh}_3$ )

**$^{13}\text{C}$  APT** (75 MHz,  $\text{CD}_2\text{Cl}_2$ )  $\delta$  134.13 (d,  $^3J_{\text{CP}} = 9.0$  Hz, *m*- $\text{PPh}_3$ ), 132.76 (s, *p*- $\text{PPh}_3$ ), 129.37 (d,  $^2J_{\text{HP}} = 12.4$  Hz, *o*- $\text{PPh}_3$ ), 129.04 (d,  $^1J_{\text{CP}} = 85.9$  Hz, *ipso*- $\text{PPh}_3$ ), 127.03 (s,  $\text{C}\equiv\text{N}$ ).



Method 1: To a solution of **3** (0.3013 g, 1.0 mmol) in  $\text{CH}_2\text{Cl}_2$  (10 ml) was added  $\text{Ag}_2\text{O}$  (0.1159 g, 0.5 mmol) and the mixture stirred for 12 h with the exclusion of light. The resulting pale-yellow solution was filtered through celite and the filtrate concentrated under reduced pressure to approximately 1 ml.  $\text{Et}_2\text{O}$  (10 ml) was added to precipitate a white solid which was collected and vacuum dried to give the product (0.3506 g, 86%).

## 2.8. Experimental

Method 2: To a solution of **1** (0.3378 g, 1.0 mmol) in CH<sub>2</sub>Cl<sub>2</sub> (10 ml) was added Ag<sub>2</sub>O (0.2317 g, 1.0 mmol) and the mixture stirred for 12 h with the exclusion of light. The solution was filtered through celite and the resulting pale-yellow filtrate concentrated under reduced pressure to approximately 1 ml. Et<sub>2</sub>O (10 ml) was added to precipitate a white solid which was collected and vacuum dried to give the product (0.3179 g, 78%).

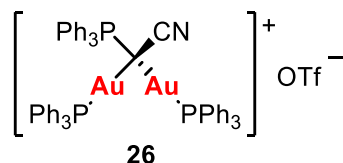
**MS (MALDI) m/z:** 1740 [M+Ag]<sup>+</sup>, 1331 [M-{AgC(PPh<sub>3</sub>)(C≡N)}+Ag]<sup>+</sup>, 816 [M-2{AgC(PPh<sub>3</sub>)(C≡N)}]<sup>+</sup>, 408 [M-3{AgC(PPh<sub>3</sub>)(C≡N)}]<sup>+</sup>.

**IR (cm<sup>-1</sup>)** ν(C≡N) 2109

**<sup>1</sup>H NMR (300 MHz, CD<sub>2</sub>Cl<sub>2</sub>)** δ 8.33 – 6.82 (m, PPh<sub>3</sub>).

**<sup>31</sup>P{<sup>1</sup>H} NMR (121 MHz, CD<sub>2</sub>Cl<sub>2</sub>)** δ 29.52 (m, PPh<sub>3</sub>).

**<sup>13</sup>C NMR (75 MHz, CD<sub>2</sub>Cl<sub>2</sub>)** δ 133.29 (d, <sup>3</sup>J<sub>CP</sub> = 8.9 Hz, *m*-PPh<sub>3</sub>), 132.72 (d, <sup>4</sup>J<sub>CP</sub> = 2.7 Hz, *p*-PPh<sub>3</sub>), 130.81 (d, <sup>1</sup>J<sub>CP</sub> = 87.3 Hz, *ipso*-PPh<sub>3</sub>), 129.62 (d, <sup>2</sup>J<sub>HP</sub> = 11.7 Hz, *o*-PPh<sub>3</sub>).



To a solution of **2** (0.2257 g, 0.5 mmol) in CH<sub>2</sub>Cl<sub>2</sub> (10 ml) was added [Au(acac)(PPh<sub>3</sub>)] (0.5594 g, 1.0 mmol) and the mixture stirred for 4 h. The solution was filtered through celite, the filtrate concentrated under reduced pressure to approximately 1 ml and Et<sub>2</sub>O (10 ml) added to precipitate a white solid which was collected and vacuum dried to give the product (0.6093 g, 89%).

**HRMS (ESI-QTOF) m/z:** [M]<sup>+</sup> Calcd for C<sub>56</sub>H<sub>45</sub>Au<sub>2</sub>NP<sub>3</sub> 1218.2090, Found 1218.2033.

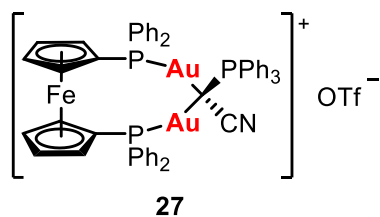
**IR (cm<sup>-1</sup>)** ν(C≡N) 2168, ν(OTf) 1271 (SO<sub>3</sub>), 1222 (CF<sub>3</sub>), 1156 (CF<sub>3</sub>), 1029 (SO<sub>3</sub>).

**<sup>1</sup>H NMR (400 MHz, CDCl<sub>3</sub>)** δ 8.23 – 6.51 (m, PPh<sub>3</sub>).

**<sup>31</sup>P{<sup>1</sup>H} NMR (162 MHz, CDCl<sub>3</sub>)** δ 37.21 (d, <sup>3</sup>J<sub>PP</sub> = 6.5 Hz, Au-PPh<sub>3</sub>), 33.82 (t, <sup>3</sup>J<sub>PP</sub> = 6.5 Hz, C-PPh<sub>3</sub>).

**<sup>19</sup>F NMR (376 MHz, CDCl<sub>3</sub>)** δ -77.97 (OTf).

**<sup>13</sup>C APT (101 MHz, CDCl<sub>3</sub>)** δ 169.94 (s, C-C≡N), 133.97 (s, *p*-Ph<sub>3</sub>P-C), 133.68 (d, <sup>3</sup>J<sub>CP</sub> = 14.0 Hz, *m*-Ph<sub>3</sub>P-Au), 133.10 (d, <sup>3</sup>J<sub>CP</sub> = 9.5 Hz, *m*-Ph<sub>3</sub>P-C), 132.23 (s, *p*-Ph<sub>3</sub>P-Au), 129.66 (d, <sup>2</sup>J<sub>CP</sub> = 12.2 Hz, *o*-Ph<sub>3</sub>P-C), 129.48 (d, <sup>2</sup>J<sub>CP</sub> = 11.8 Hz, *o*-Ph<sub>3</sub>P-Au), 128.29 (d, <sup>1</sup>J<sub>CP</sub> = 57.8 Hz, *ipso*-Ph<sub>3</sub>P-Au), 126.58 (d, <sup>1</sup>J<sub>CP</sub> = 88.6 Hz, *ipso*-Ph<sub>3</sub>P-C), 124.28 (s, C≡N).



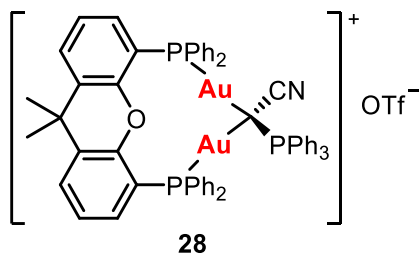
To a solution of **2** (0.451 g, 0.1 mmol) in  $\text{CH}_2\text{Cl}_2$  (5 ml) was added  $[\text{Au}_2\text{Cl}_2(\text{dppf})]$  (0.1019 g, 0.1 mmol) and  $\text{NBu}_4(\text{acac})$  (0.0683 g, 0.2 mmol) and the mixture stirred for 4 hours. The bright orange solution was concentrated under reduced pressure to approximately 1 ml and  $\text{Et}_2\text{O}$  (10 ml) was added to precipitate a bright orange solid which was collected and vacuum dried to give the product (0.1285 g, 90%).

**HRMS (ESI-QTOF) m/z:**  $[\text{M}]^+$  Calcd for  $\text{C}_{54}\text{H}_{43}\text{Au}_2\text{FeNP}_3$  1248.1285, Found 1248.1223.

**IR** ( $\text{cm}^{-1}$ )  $\nu(\text{C}\equiv\text{N})$  2173

**$^1\text{H}$  NMR (300 MHz,  $\text{CD}_2\text{Cl}_2$ )**  $\delta$  8.21 – 7.88 (m, 6H, Ph), 7.83 – 7.77 (m, 3H, Ph), 7.66 – 7.50 (m, 17H, Ph), 7.47 – 7.41 (m, 5H, Ph), 7.37 – 7.00 (m, 4H, Ph), 5.05 – 3.60 (m, 10H, Cp).

**$^{31}\text{P}\{^1\text{H}\}$  NMR (121 MHz,  $\text{CD}_2\text{Cl}_2$ )**  $\delta$  33.12 (t,  $^3J_{\text{PP}} = 5.4$  Hz,  $\text{PPh}_3$ ), 31.67 (m, dppf).



To a solution of **3** (0.0301 g, 0.1 mmol) in  $\text{CH}_2\text{Cl}_2$  (5 ml) was added  $[\text{Au}_2\text{Cl}_2(\text{XantPhos})]$  (0.1043 g, 0.1 mmol),  $\text{AgOTf}$  (0.0514 g, 0.2 mmol) and  $\text{NBu}_4(\text{acac})$  (0.0342 g, 0.1 mmol) and the mixture stirred for 2 h. The solution was filtered through celite, the filtrate concentrated under reduced pressure to approximately 1 ml and  $\text{Et}_2\text{O}$  (10 ml) added to precipitate a white solid which was collected and vacuum dried to give the product (0.1280 g, 90%).

**HRMS (ESI-QTOF) m/z:**  $[\text{M}]^+$  Calcd for  $\text{C}_{59}\text{H}_{47}\text{Au}_2\text{NOP}_3$  1272.2196, Found 1272.2193.

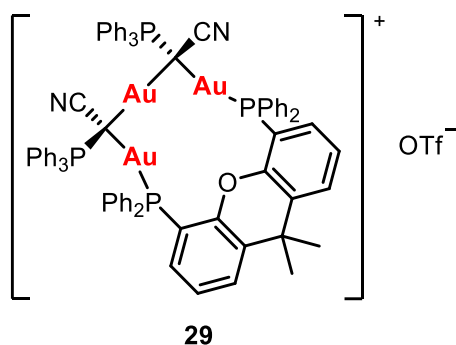
**IR** ( $\text{cm}^{-1}$ )  $\nu(\text{C}\equiv\text{N})$  2175.

**$^1\text{H}$  NMR (300 MHz,  $\text{CD}_2\text{Cl}_2$ )**  $\delta$  8.05 – 7.89 (m, 6H, XantPhos), 7.82 – 7.69 (m, 2H, XantPhos), 7.66 – 7.03 (m, 27H, Ph), 6.97 – 6.91 (m, 4H, XantPhos), 6.53 – 6.45 (m, 2H, XantPhos), 1.90 (s, 3H, Me), 1.53 (s, 3H, Me).

**$^{31}\text{P}\{^1\text{H}\}$  NMR (121 MHz,  $\text{CD}_2\text{Cl}_2$ )**  $\delta$  35.14 (s, XantPhos), 32.85 (s,  $\text{PPh}_3$ ).



## 2.8. Experimental

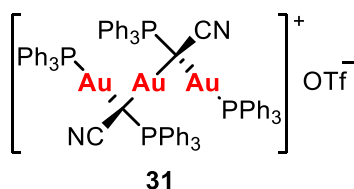


To a solution of **17** (0.1035 g, 0.1 mmol) in  $\text{CH}_2\text{Cl}_2$  (5 ml) was added  $[\text{Au}_2\text{Cl}_2(\text{XantPhos})]$  (0.1043 g, 0.1 mmol) and  $\text{NBu}_4(\text{acac})$  (0.0683 g, 0.2 mmol) and the mixture stirred for 1 h. The solution was filtered through celite, the filtrate concentrated under reduced pressure to approximately 1 ml and  $\text{Et}_2\text{O}$  added to precipitate a white solid which was collected and vacuum dried to give the product (0.1439 g, 74%).

**IR** ( $\text{cm}^{-1}$ )  $\nu(\text{C}\equiv\text{N})$  2160.

**$^1\text{H}$  NMR** (300 MHz,  $\text{CD}_2\text{Cl}_2$ )  $\delta$  8.20 – 6.25 (m, 56H, XantPhos + Ph), 1.70 (s, 3H, Me), 1.27 (s, 3H, Me).

**$^{31}\text{P}\{^1\text{H}\}$  NMR** (121 MHz,  $\text{CD}_2\text{Cl}_2$ )  $\delta$  31.18 (d,  $^3J_{\text{PP}} = 5.5$  Hz,  $\text{PPh}_3$ ), 29.18 (d,  $^3J_{\text{PP}} = 5.4$  Hz, XantPhos).



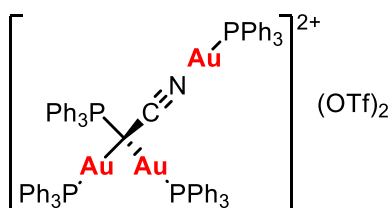
To a solution of **17** (0.1035 g, 0.1 mmol) in  $\text{CH}_2\text{Cl}_2$  (5 ml) was added  $[\text{Au}(\text{acac})(\text{PPh}_3)]$  (0.1118 g, 0.2 mmol) and the mixture stirred for 4 h. The solution was filtered through celite, the filtrate concentrated under reduced pressure to approximately 1 ml and  $\text{Et}_2\text{O}$  added to precipitate a white solid which was collected and vacuum dried to give the product (0.1641 g, 88%).

**MS** (ESI+)  $m/z$ : 1715.1  $[\text{M}]^+$ .

**IR** ( $\text{cm}^{-1}$ )  $\nu(\text{C}\equiv\text{N})$  2161

**$^1\text{H}$  NMR** (400 MHz,  $\text{CDCl}_3$ )  $\delta$  8.15 – 6.80 (m, Ph).

**$^{31}\text{P}\{^1\text{H}\}$  NMR** (162 MHz,  $\text{CDCl}_3$ )  $\delta$  36.37 (d,  $^3J_{\text{PP}} = 7.5$  Hz), 36.20 (d,  $^3J_{\text{PP}} = 6.8$  Hz), 32.24 (d,  $^3J_{\text{PP}} = 6.5$  Hz), 30.89 (d,  $^3J_{\text{PP}} = 7.4$  Hz).

**32**

Method 1: To a solution of [AuCl(PPh<sub>3</sub>)] (0.0495 g, 0.1 mmol) in CH<sub>2</sub>Cl<sub>2</sub> (5 ml) was added AgOTf (0.0257 g, 0.1 mmol) and the mixture stirred for 1 h with the exclusion of light. **26** (0.1368 g, 0.1 mmol) was added and the mixture stirred for a further 2 h. The solution was filtered through celite, the filtrate concentrated under reduced pressure to approximately 1 ml and Et<sub>2</sub>O added to precipitate a white solid which was collected and vacuum dried to give the product (0.1719 g, 87%).

Method 2: To a solution of **2** (0.0451 g, 0.1 mmol) in CH<sub>2</sub>Cl<sub>2</sub> (20 ml) was added [O{Au(PPh<sub>3</sub>)}<sub>3</sub>]BF<sub>4</sub> (0.1481 g, 0.1 mmol) and the mixture stirred for 4 h at room temperature. The solution was concentrated under reduced pressure to approximately 2 ml and Et<sub>2</sub>O added to precipitate a white solid which was collected and vacuum dried to give the product (0.1402 g, 73 %).

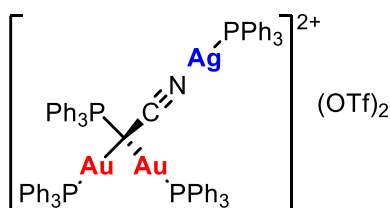
**IR (cm<sup>-1</sup>)** ν(C≡N) 2171

**<sup>1</sup>H NMR (400 MHz, CDCl<sub>3</sub>)** δ 7.95 – 7.05 (m, Ph).

**<sup>31</sup>P{<sup>1</sup>H} NMR (162 MHz, CDCl<sub>3</sub>)** δ 36.51 (d, <sup>3</sup>J<sub>PP</sub> = 7.3 Hz, Au-PPh<sub>3</sub>), 33.26 (t, <sup>3</sup>J<sub>PP</sub> = 7.3 Hz, C-PPh<sub>3</sub>), 29.08 (s, N-Au-PPh<sub>3</sub>).

**<sup>19</sup>F NMR (376 MHz, CDCl<sub>3</sub>)** δ -77.83 (s, OTf), -153.30 (s, BF<sub>4</sub>).

**<sup>13</sup>C APT (101MHz, CDCl<sub>3</sub>)** δ 134.70 (d, <sup>4</sup>J<sub>CP</sub> = 2.7, *p*-Ph<sub>3</sub>P-C), 134.09 (d, <sup>3</sup>J<sub>CP</sub> = 13.6, *m*-Ph<sub>3</sub>P-C), 133.73 (d, <sup>3</sup>J<sub>CP</sub> = 6.9, *m*-Ph<sub>3</sub>P-Au), 133.16 (d, <sup>3</sup>J<sub>CP</sub> = 9.9, *m*-Ph<sub>3</sub>P-N), 132.58 (d, <sup>4</sup>J<sub>CP</sub> = 2.5, *p*-Ph<sub>3</sub>P-N), 132.44 (s, *p*-Ph<sub>3</sub>P-Au), 130.16 (d, <sup>2</sup>J<sub>CP</sub> = 12.5, *o*-Ph<sub>3</sub>P-N), 129.64 (d, <sup>2</sup>J<sub>CP</sub> = 12.1, *o*-Ph<sub>3</sub>P-Au), 129.57 (d, <sup>2</sup>J<sub>CP</sub> = 12.4, *o*-Ph<sub>3</sub>P-C), 127.83 (d, <sup>1</sup>J<sub>CP</sub> = 59.0, *ipso*-Ph<sub>3</sub>PAu-N), 126.94, (d, <sup>1</sup>J<sub>CP</sub> = 66.3, *ipso*-Ph<sub>3</sub>PAu-C), 125.06 (d, <sup>1</sup>J<sub>CP</sub> = 89.4, *ipso*-Ph<sub>3</sub>P-C).

**33**

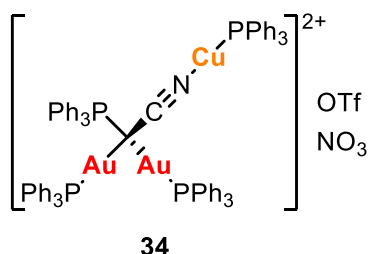
## 2.8. Experimental

To a solution of **26** (0.0684 g, 0.05 mmol) in CH<sub>2</sub>Cl<sub>2</sub> (5 ml) was added [Ag(OTf)(PPh<sub>3</sub>)] (0.0260 g, 0.05 mmol) and the mixture stirred for 1 h. The solution was filtered through celite, the filtrate concentrated under reduced pressure to approximately 1 ml and Et<sub>2</sub>O added to precipitate a white solid which was collected and vacuum dried to give the product (0.0925 g, 98%).

**IR** (cm<sup>-1</sup>)  $\nu(\text{C}\equiv\text{N})$  2160

**<sup>1</sup>H NMR** (300 MHz, CDCl<sub>3</sub>)  $\delta$  8.61 – 6.67 (m, Ph).

**<sup>31</sup>P{<sup>1</sup>H} NMR** (121 MHz, CDCl<sub>3</sub>)  $\delta$  36.93 (d, <sup>3</sup>J<sub>PP</sub> = 6.6 Hz, Au-PPh<sub>3</sub>), 33.62 (t, <sup>3</sup>J<sub>PP</sub> = 6.7 Hz, C-PPh<sub>3</sub>), 11.51 (s, Ag-PPh<sub>3</sub>).

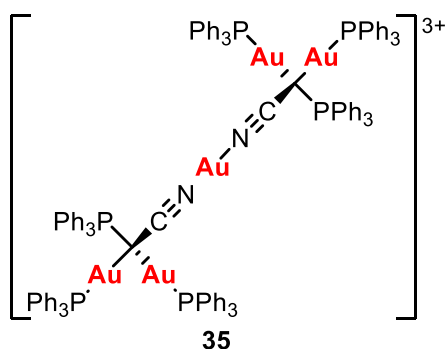


To a solution of **26** (0.0684 g, 0.05 mmol) in CH<sub>2</sub>Cl<sub>2</sub> (5 ml) was added [Cu(NO<sub>3</sub>)(PPh<sub>3</sub>)<sub>2</sub>] (0.0325 g, 0.05 mmol) and the mixture stirred for 1 h. The solution was filtered through celite, the filtrate concentrated under reduced pressure to approximately 1 ml and *n*-hexane added to precipitate a white solid which was collected and vacuum dried to give the product (0.0825 g, 99%).

**IR** (cm<sup>-1</sup>)  $\nu(\text{C}\equiv\text{N})$  2166

**<sup>1</sup>H NMR** (300 MHz, CDCl<sub>3</sub>)  $\delta$  8.15 – 6.90 (m, Ph).

**<sup>31</sup>P{<sup>1</sup>H} NMR** (121 MHz, CDCl<sub>3</sub>)  $\delta$  37.08 (d, <sup>3</sup>J<sub>PP</sub> = 6.4 Hz, Au-PPh<sub>3</sub>), 33.66 (t, <sup>3</sup>J<sub>PP</sub> = 6.4 Hz, C-PPh<sub>3</sub>), -0.35 (s, Cu-PPh<sub>3</sub>).

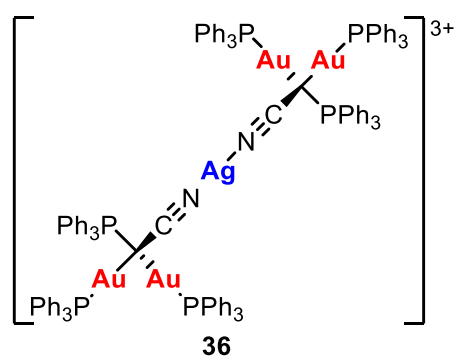


To a solution of **26** (0.0684 g, 0.05 mmol) in  $\text{CH}_2\text{Cl}_2$  (10 ml) was added  $[\text{Au}(\text{tmbn})_2]\text{SbF}_6$  (0.0205 g, 0.025 mmol) and the mixture stirred for 2 h. The solution was filtered through celite, the resulting yellow filtrate concentrated under reduced pressure to approximately 1 ml and  $\text{Et}_2\text{O}$  added to precipitate a pale yellow solid which was collected and vacuum dried. A mixture of the product and tmbn was obtained

**IR** ( $\text{cm}^{-1}$ )  $\nu(\text{C}\equiv\text{N})$  2172

**$^1\text{H}$  NMR (300 MHz,  $\text{CDCl}_3$ )**  $\delta$  8.15 – 6.85 (m, Ph).

**$^{31}\text{P}\{^1\text{H}\}$  NMR (121 MHz,  $\text{CDCl}_3$ )**  $\delta$  36.48 (d,  $^3J_{\text{PP}} = 7.2$  Hz, Au- $\text{PPh}_3$ ), 33.16 (t,  $^3J_{\text{PP}} = 7.2$  Hz, C- $\text{PPh}_3$ ).



To a solution of **26** (0.8207 g, 0.6 mmol) in acetone (20 ml) was added  $\text{AgOTf}$  (0.0771 g, 0.3 mmol) and the mixture stirred for 3 h at room temperature with the exclusion of light. The mixture was filtered through celite and the resulting pale yellow solution concentrated to dryness under reduced pressure to give **36** as a pale orange solid (0.6594 g, 73 %).

**IR** ( $\text{cm}^{-1}$ )  $\nu(\text{C}\equiv\text{N})$  2166

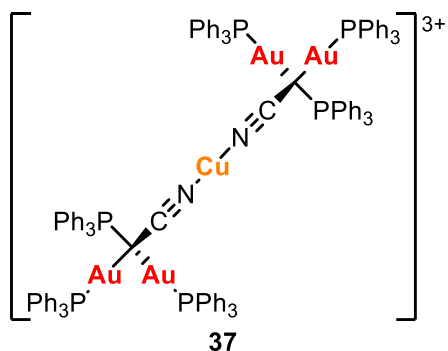
**$^1\text{H}$  NMR (300 MHz, Acetone)**  $\delta$  7.32 – 8.09 (m, Ph).

**$^{31}\text{P}\{^1\text{H}\}$  NMR (121 MHz, Acetone)**  $\delta$  37.39 (d,  $^3J_{\text{PP}} = 6.1$ , Au $\text{PPh}_3$ ), 33.83 (t,  $^3J_{\text{PP}} = 6.1$ ,  $\text{PPh}_3$ ).

**$^{19}\text{F}$  NMR (376 MHz, Acetone)**  $\delta$  -77.70 (s, OTf).

**$^{13}\text{C}$  APT (101 MHz,  $\text{CDCl}_3$ )** 134.15 (s, *p*- $\text{Ph}_3\text{P-C}$ ), 133.64 (d,  $^3J_{\text{CP}} = 14.2$  Hz, *m*- $\text{Ph}_3\text{P-Au}$ ), 133.06 (d,  $^3J_{\text{CP}} = 9.6$  Hz, *m*- $\text{Ph}_3\text{P-C}$ ), 132.22 (s, *p*- $\text{Ph}_3\text{P-Au}$ ), 129.77 (d,  $^2J_{\text{CP}} = 12.3$  Hz, *o*- $\text{Ph}_3\text{P-C}$ ), 129.47 (d,  $^2J_{\text{CP}} = 12.1$  Hz, *o*- $\text{Ph}_3\text{P-Au}$ ), 128.10 (d,  $^1J_{\text{CP}} = 58.2$  Hz, *ipso*- $\text{Ph}_3\text{P-Au}$ ), 126.02 (d,  $^1J_{\text{CP}} = 88.9$  Hz, *ipso*- $\text{Ph}_3\text{P-C}$ ), 125.05 (s,  $\text{C}\equiv\text{N}$ ).

## 2.8. Experimental



To a solution of **26** (0.2734 g, 0.2 mmol) in acetonitrile (20 ml) was added  $[\text{Cu}(\text{NCMe})_4]\text{BF}_4$  (0.0315 g, 0.1 mmol) and the mixture stirred for 3 h at room temperature. The mixture was filtered through celite and the resulting yellow solution concentrated to dryness under reduced pressure to give **33** as a pale yellow solid (0.2415 g, 84 %).

**IR** ( $\text{cm}^{-1}$ )  $\nu(\text{C}\equiv\text{N})$  2167

**$^1\text{H}$  NMR** (400 MHz,  $\text{CDCl}_3$ )  $\delta$  7.11 – 7.80 (m, Ph).

**$^{31}\text{P}\{^1\text{H}\}$  NMR** (162 MHz,  $\text{CDCl}_3$ )  $\delta$  36.84 (d,  $^3J_{\text{PP}} = 6.8$ ,  $\text{AuPPh}_3$ ), 33.22 (t,  $^3J_{\text{PP}} = 6.8$ ,  $\text{PPh}_3$ ).

**$^{19}\text{F}$  NMR** (376 MHz,  $\text{CDCl}_3$ )  $\delta$  -77.76 (s, OTf), -153.82 (s,  $\text{BF}_4$ ).



# Chapter 3 – Allenyl Gold Complexes

## 3.1. Introduction

Allenes are well known within organic chemistry. They are valuable building blocks for the synthesis of more complex molecular targets and can participate in a variety of different types of reaction including nucleophilic and electrophilic additions<sup>174</sup>, cycloadditions<sup>175</sup>, cyclisations as well as various palladium-<sup>176</sup> and gold-catalysed reactions<sup>177</sup>. Their potential application in natural product synthesis<sup>178</sup>, pharmaceutical chemistry<sup>179</sup> and materials science has resulted in the recent development of new synthetic methodologies. The allene moiety has now been found in over 150 natural products and their intrinsic axial chirality means allenes are of great utility in organic chemistry due to their unique structure and reactivity. In the past few decades there has been a huge increase in interest in allene chemistry and many research groups have now focussed their attention on the synthesis and application of these highly versatile compounds, which for many years were considered only chemical curiosities.

In organometallic chemistry, allenes are somewhat less common.  $\pi$ -Bound metal allene complexes have been reported as catalytic intermediates and many examples of isolable complexes in which the allene is  $\pi$ -bound to the metal have been reported and structurally characterised.<sup>180</sup>  $\sigma$ -Bound  $\eta^1$ -allenyl transition metal complexes, however, are considerably rarer and only known for a few transition metals. Challenging syntheses along with little known application have resulted in a lack of interest in such complexes until recently. Their chemical potential as well as the useful bonding information they can provide has only started to be realised in the last two decades and the diverse chemistry and versatility of these cumulated ligands is now gaining more interest.<sup>181</sup> They do, however, still remain somewhat elusive species in organometallic chemistry.

### 3.1.1. Allenes – Structure and Axial Chirality

The symmetry and isomerism of allenes has fascinated chemists for many years. The allene unit is comprised of three carbon atoms with two adjacent C=C double bonds and a C-C-C bond angle of 180°. The central carbon atom is therefore sp hybridised while the terminal C

atoms are  $sp^2$  hybridised. The two adjacent  $\pi$ -orbitals formed as a result of the overlap of the p-orbitals are orthogonal and consequently the substituents at the terminal carbon atoms are also orthogonal, resulting in axial chirality when different substituents are present at the terminal carbon atoms. (Figure 3.1).

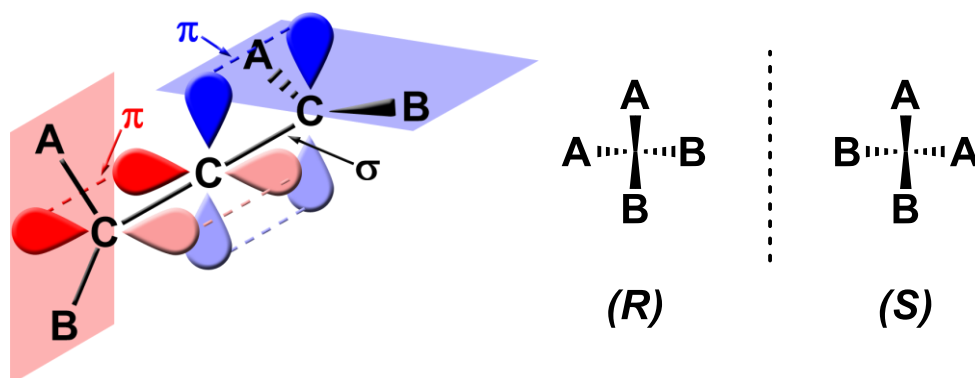


**Figure 3.1.** Allene orbitals and enantiomers where  $A > B$ .

### 3.1.2. History

The correct structure of allenes and higher cumulenes as well as their axial chirality was predicted by Van't Hoff in 1875<sup>182</sup> only very shortly after the tetrahedral geometry of carbon was first suggested and at a time when some of the most significant developments in organic chemistry were made. Van't Hoff used tetrahedrons to model the bonding in organic molecules, considering the carbon atom to be at the centre of each tetrahedron. Allenes were therefore comprised of three tetrahedrons (Figure 3.2).

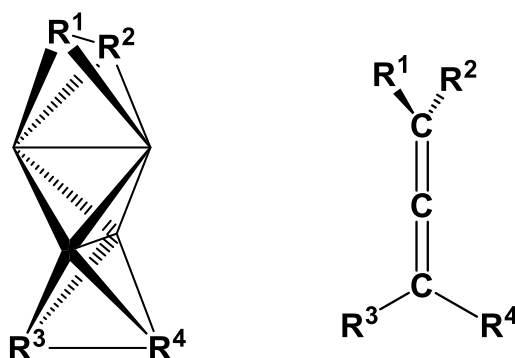


**Figure 3.2.** Van't Hoff's tetrahedron model for an allene.

Although several experimental investigations were made in the following years, many chemists doubted the existence of such allene bond systems, considering them to be highly unstable. The



### 3.1. Introduction

first documented synthesis of an allene was the synthesis of “glutinic acid” reported in 1887 by Burton and Pechmann,<sup>183</sup> however their aim was actually to disprove the existence of such compounds and the lack of analytical tools at the time meant that it was almost impossible to distinguish between allenes and alkynes. Burton and Pechmann initially proposed an alkyne structure for “glutinic acid” and it was not until the introduction of IR spectroscopy and the discovery of the characteristic allene C=C=C vibration at around 1950 cm<sup>-1</sup> that allenes could readily be identified. The revised structure for “glutinic acid” was published by Jones and co-workers in 1954 (Figure 3.3).<sup>184</sup>

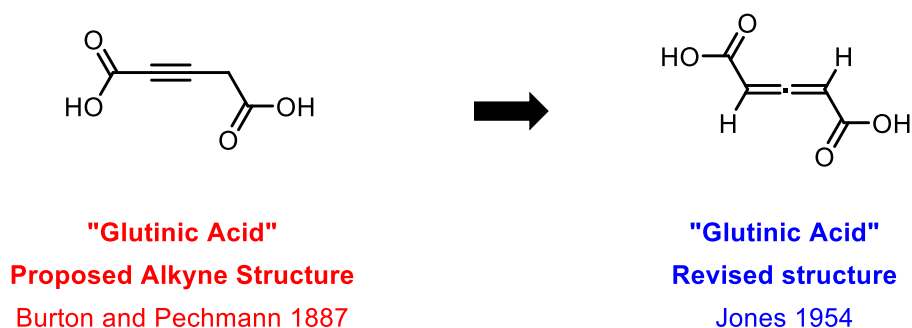


**Figure 3.3.** “Glutinic acid” proposed alkyne and revised allene structure.

Many problems with the incorrect characterisation of allenic natural products were encountered at the beginning of the twentieth century (Figure 3.4). In 1906 Semmler proposed an allene structure for carlina oxide, a furan derivative extracted from the roots of *Carlina acualis*,<sup>185</sup> however this was later revised with the help of Raman spectroscopy and is actually the isomeric alkyne (Figure 3.4(a)).<sup>186</sup> Another case is pyrethrolone which was reported by Staudinger and Ruzicka to have an allene structure.<sup>187</sup> This incorrect assignment was based on the cleavage of the natural product by ozonolysis but later spectroscopic investigations revealed the correct structure to be a conjugated diene (Figure 3.4(b)).<sup>188</sup> Similarly, for many well-known natural products which do have an allene structure, the correct determination of the allene was made long after their original isolation, for example the carotinoid peridinin which was first isolated in 1890<sup>189</sup> but not correctly characterised until 1971,<sup>190</sup> some 81 years later! The huge number of naturally occurring allenes shows that they represent an important structural class of compounds and can no longer be considered mere curiosities.

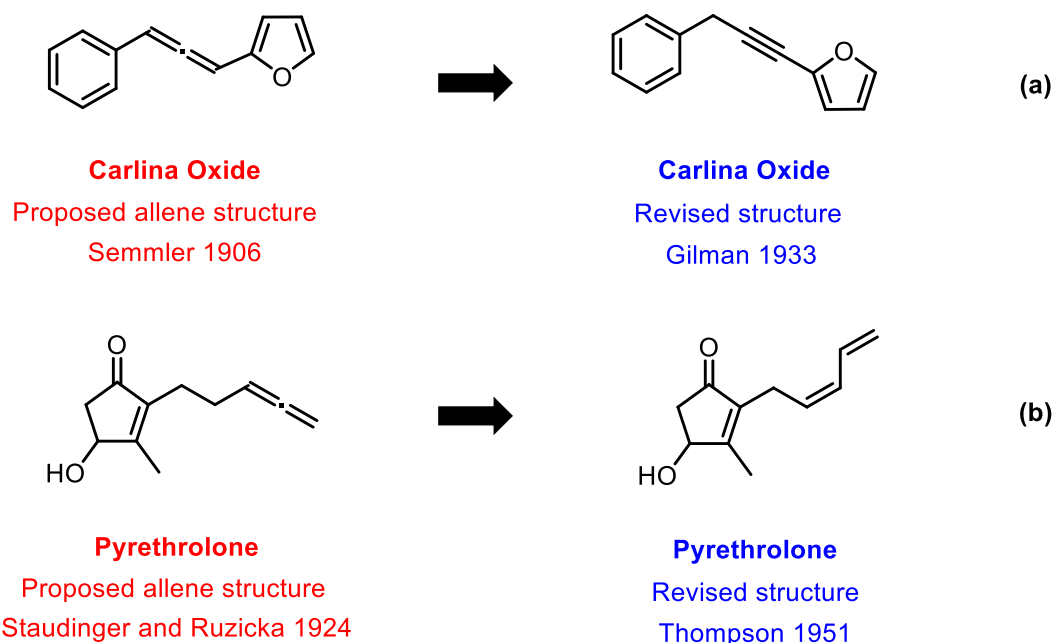
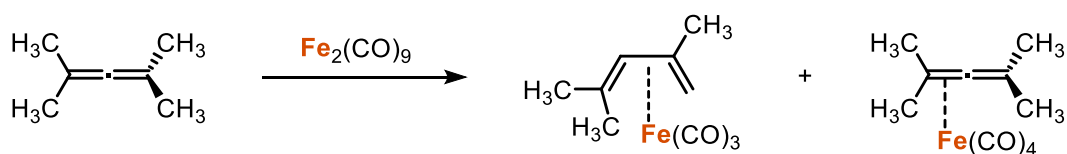


**Figure 3.4.** Incorrectly assigned allene natural products and the corrected structures.

The first  $\pi$ -bound metal-allene complex was reported in 1967 by Pettit with the preparation of a tetramethylallene iron complex by reaction of tetramethylallene with  $\text{Fe}_2(\text{CO})_9$ . The authors reported the formation of two different complexes in the reaction, one being 2,4-dimethyl-1,3-pentadiene iron tricarbonyl and the other the iron-allene complex (Scheme 3.1). The complexes were characterised by NMR spectroscopy and it was suggested that in solution at room temperature the  $\text{Fe}(\text{CO})_4$  unit of the allene complex is rapidly moving between the two allene double bonds.<sup>191</sup>



**Scheme 3.1.** Synthesis of first  $\pi$ -bound metal-allene complex.

Many examples of  $\pi$ -bound metal-allene complexes have subsequently been isolated and structurally characterised by single crystal X-ray diffraction. One of the earliest examples is the bis(triphenylphosphino)palladium  $\pi$ -allene complex reported by Okamoto and co-workers in 1974 (Figure 3.5).<sup>192</sup> The structure clearly shows that one of the allene  $\pi$ -bonds coordinates to palladium resulting in the allene being significantly distorted from linearity with the

C(1)-C(8)-C(15) bond angle of  $148.3(8)^\circ$ . The C(1)-C(8) bond is lengthened slightly to  $1.401(11)$  Å compared to free allene ( $1.31$  Å) due to a loss of electron density to palladium. The uncoordinated C-C allene bond, C(8)-C(15), has a bond distance typical for that of an allene at  $1.304(12)$  Å.

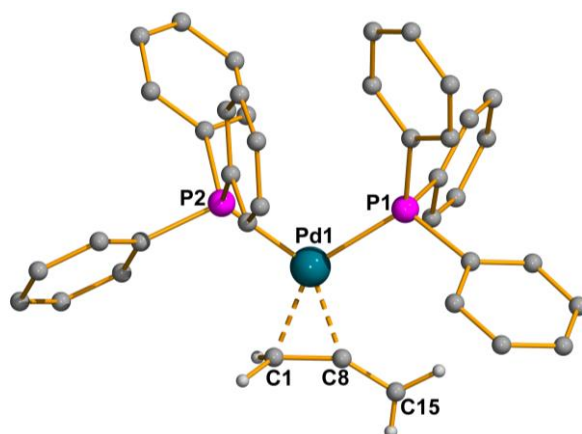
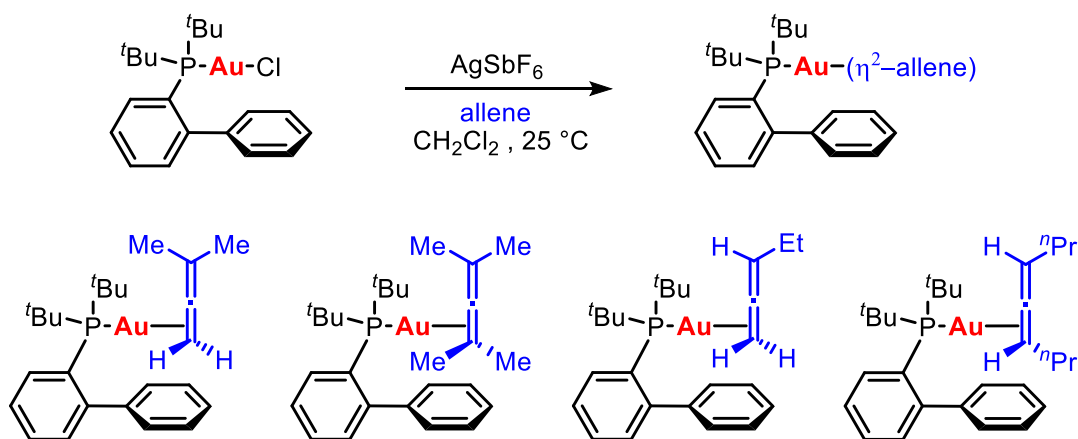


**Figure 3.5.** Molecular structure of  $\text{Pd}(\eta^2\text{-CH}_2\text{=C=CH}_2)(\text{PPh}_3)_2$  determined by single crystal X-ray diffraction. Triphenylphosphine hydrogen atoms are omitted for clarity. Selected bond lengths [Å] and angles [ $^\circ$ ]: Pd(1)-C(1)  $2.118(9)$ , Pd(1)-C(2)  $2.067(8)$ , Pd(1)-P(1)  $2.314(2)$ , Pd(1)-P(2)  $2.324(2)$ , C(1)-C(8)  $1.401(11)$ , C(8)-C(15)  $1.304(12)$ , C(1)-C(8)-C(15)  $148.3(8)$ .

Gold(I)  $\pi$ -allene complexes were reported in 2010 by the group of Widenhoefer<sup>193</sup> and were prepared by a procedure previously used for the synthesis of gold(I)  $\pi$ -alkene,  $\pi$ -diene and  $\pi$ -alkyne complexes (see Chapter 1). Chloride abstraction from  $[\text{AuCl}(\text{JohnPhos})]$  with  $\text{AgSbF}_6$  and subsequent addition of allene allowed the isolation of a series of gold(I)  $\pi$ -allene complexes (Scheme 3.2).<sup>112</sup>



**Scheme 3.2.** Synthesis of gold(I)  $\pi$ -allene complexes.

Three examples were successfully characterised by single crystal X-ray diffraction (Figure 3.6). In each case the gold is coordinated to the less hindered double bond of the allene. The C-C bond distances for the double bond bound to gold are slightly longer than the uncoordinated allene bond.

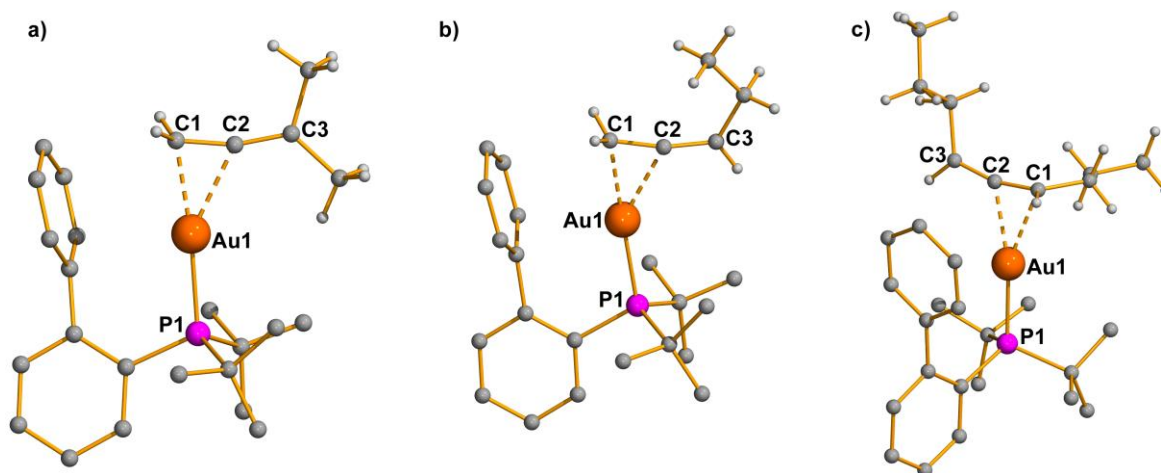
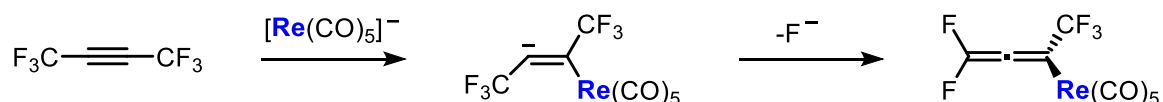


**Figure 3.6.** Molecular structures of  $[\text{Au}(\eta^2\text{-CH}_2\text{=C=CMe}_2)(\text{JohnPhos})]^+$  (a),  $[\text{Au}(\eta^2\text{-CH}_2\text{=C=CHEt})(\text{JohnPhos})]^+$  (b) and  $[\text{Au}(\eta^2\text{-CH}^i\text{Pr=C=CH}^i\text{Pr})(\text{JohnPhos})]^+$  (c) determined by single crystal X-ray diffraction. JohnPhos hydrogen atoms are omitted for clarity. Selected bond lengths [ $\text{\AA}$ ] and angles [ $^\circ$ ] **a**: Au(1)-C(1) 2.191(5), Au(1)-C(2) 2.306(5), Au(1)-P(1) 2.309(1), C(1)-C(2) 1.340(7), C(2)-C(3) 1.311(7), C(1)-C(2)-C(3) 165.0(5). **b**: Au(1)-C(1) 2.208(4), Au(1)-C(2) 2.238(4), Au(1)-P(1) 2.298(1), C(1)-C(2) 1.348(6), C(2)-C(3) 1.310(6), C1-C2-C3=166.4(4). **c**: Au(1)-C(1) 2.269(2), Au(1)-C(2) 2.219(2), Au(1)-P(1) 2.2953(6), C(1)-C(2) 1.329(4), C(2)-C(3) 1.314(4), C(1)-C(2)-C(3) 164.2(3).

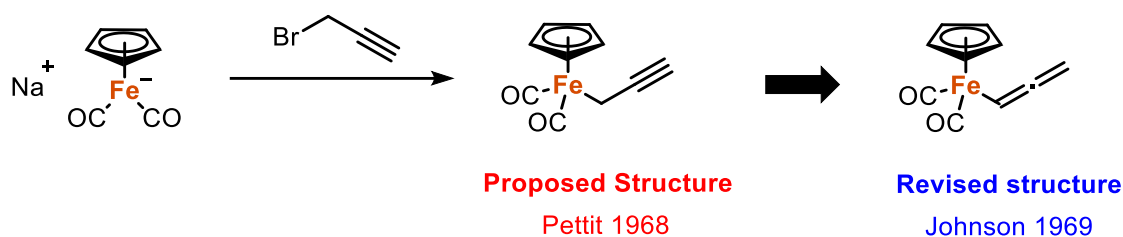
The first  $\sigma\text{-}\eta^1$ -allenyl transition metal complex was the rhenium complex reported by the group of Stone in 1966.<sup>194</sup> This was prepared by reaction of hexafluorobut-2-yne with  $[\text{Re}(\text{CO})_5]^-$  and was believed to proceed via addition of the rhenium anion to the acetylene followed by elimination of fluoride (Scheme 3.3).<sup>195</sup> The allene structure of the product was established by  $^1\text{H}$  and  $^{19}\text{F}$  NMR spectrometry and IR spectroscopy.



**Scheme 3.3.** Synthesis of the first  $\sigma\text{-}\eta^1$ -allenyl transition metal complex.

In 1968 Jolly and Pettit reported the synthesis of a propargyl iron complex by reaction of  $\text{Na}[\text{Fe}(\text{CO})_2\text{Cp}]$  with propargyl bromide (Scheme 3.4).<sup>196</sup> One year later it was pointed out by

Johnson that the large coupling constant reported for the protons of the propargyl ligand (6.5 Hz) could only be derived from an allene  $\pi$ -interaction and the complex was indeed an allenyl iron complex. The C=C=C stretching frequency in the IR spectrum was obscured by the C=O signal making the characterisation difficult. In the same paper Johnson reported the synthesis of an allenyl cobalt complex by reaction of bis(dimethylglyoximate)pyridine cobalt(I) anion with propargyl bromide.<sup>197</sup>



**Scheme 3.4.** Synthesis of  $\sigma$ - $\eta^1$ -allenyl iron complex.

The first allenyl metal complex to be characterised by single crystal X-ray diffraction was the tris(trifluoromethyl)allenyl manganese derivative reported in 1978 (Figure 3.7). The allenyl structure of the ligand can clearly be seen by the C=C bond distances of C(5)-C(6) 1.2907(2) Å and C(6)-C(7) 1.2530(2) Å. The C(5)-C(6)-C(7) bond angle is only slightly distorted from linearity at 176.723(10)°.

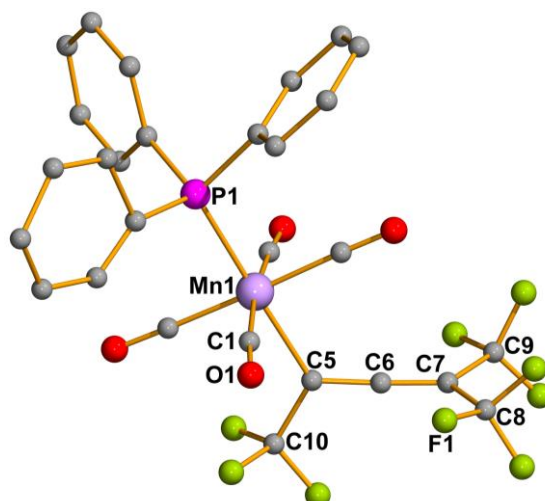
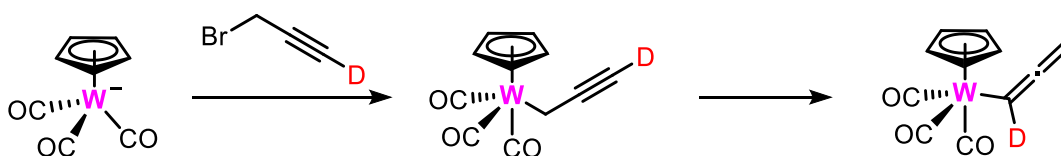


**Figure 3.7.** Molecular structures of  $[\text{Mn}(\eta^1\text{-C}(\text{CF}_3)=\text{C}=\text{C}(\text{CF}_3)_2)(\text{CO})_4(\text{PPh}_3)]$  determined by single crystal X-ray diffraction. Hydrogen atoms are omitted for clarity. Selected bond lengths [Å] and angles [°]: Mn(1)-P(1) 2.3192(4), Mn(1)-C(5) 2.1102(4), C(5)-C(6) 1.2907(2), C(6)-C(7) 1.2530(2), C(5)-C(6)-C(7) 176.723(10).

Allenyl complexes of several transition metals have now been successfully isolated and structurally characterised by single crystal X-ray diffraction, including: tungsten,<sup>198-200</sup> ruthenium,<sup>201-211</sup> osmium,<sup>202,212,213</sup> iridium,<sup>214</sup> platinum,<sup>215,216</sup> chromium,<sup>217,218</sup> rhodium,<sup>219-221</sup> zirconium,<sup>222-226</sup> hafnium<sup>227-229</sup> and palladium.<sup>230-233</sup> However, although allenyl complexes of the coinage metals have been suggested as intermediates in various reactions, no examples have previously been isolated or characterised.

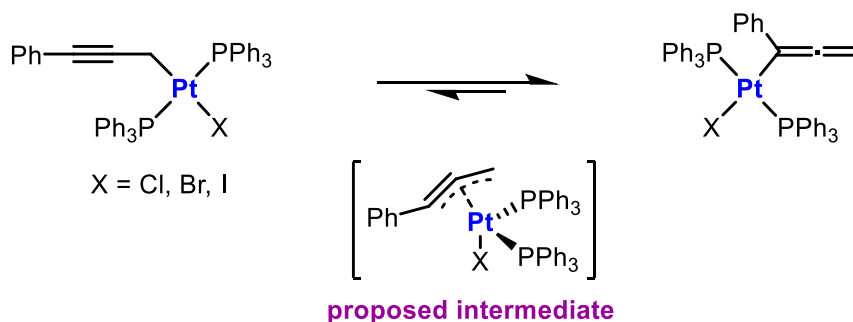
### 3.1.3. Tautomerism in Allenyl Metal Complexes

One important aspect of  $\eta^1$ -allenyl metal complexes which has attracted attention is their tautomeric behaviour with  $\eta^1$ -propargyl complexes. Such allene-propargyl tautomerism processes are very common in organic chemistry and can be reversible,<sup>234,235</sup> however the analogous rearrangements in transition metal complexes are quite rare.<sup>236</sup> The first evidence of propargyl-allenyl tautomerism in a complex was found with complexes of tungsten. Addition of propargyl bromide to  $[\text{W}(\text{CO})_3\text{Cp}]^-$  initially gave the  $\eta^1$ -propargyl complex, however, on heating the  $\eta^1$ -allenyl complex was produced. When the deuterium labelled  $\text{BrCH}_2\text{C}\equiv\text{CD}$  was used,  $[\text{W}(\text{CO})_3\text{Cp}(\text{CH}_2\text{C}\equiv\text{CD})]$  formed which then gave  $[\text{W}(\text{CO})_3\text{Cp}(\text{CD}=\text{C}=\text{CH}_2)]$  exclusively (Scheme 3.5), ruling out a 1,3-hydrogen shift mechanism. The tautomerism was also found to be an intramolecular process since addition of  $[\text{W}(\text{CO})_3\text{Cp}]^-$  had no effect on the rate. A 1,3-metal migration was suggested.<sup>237-239</sup>



**Scheme 3.5.** Synthesis and isomerisation of propargyl tungsten complex.

The first reversible example of such a tautomerism process in metal complexes was reported in 1995 for complexes of platinum. The complex  $[\text{Pt}(\eta^1\text{-CH}_2\text{C}\equiv\text{CPh})\text{Cl}(\text{PPh}_3)_2]$  underwent slow tautomerisation upon heating to yield an equilibrium mixture of the  $\eta^1$ -allenyl and  $\eta^1$ -propargyl species. The pure  $\eta^1$ -allenyl tautomer gave the same equilibrium mixture upon dissolution, showing that the tautomerisation is reversible (Scheme 3.6). A 5-coordinate intermediate was suggested.<sup>240-242</sup>



**Scheme 3.6.** Reversible propargyl-allenyl tautomerisation of  $[\text{Pt}(\eta^1\text{-CH}_2\text{C}\equiv\text{CPh})\text{X}(\text{PPh}_3)_2]$  and proposed 5-coordinate intermediate.

### 3.1.4. Triphenylpropargyl Phosphonium Bromide

Triphenylpropargyl phosphonium bromide (Figure 3.8. (a)) is a functionalised phosphonium salt which can readily isomerise into the allenyl (Figure 3.8. (b)) or  $\alpha$ -alkynyl (Figure 3.8 (c)) phosphonium salts and therefore has the potential for some very interesting chemistry.

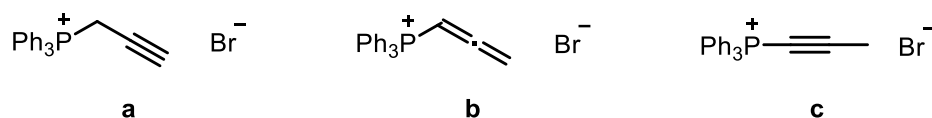
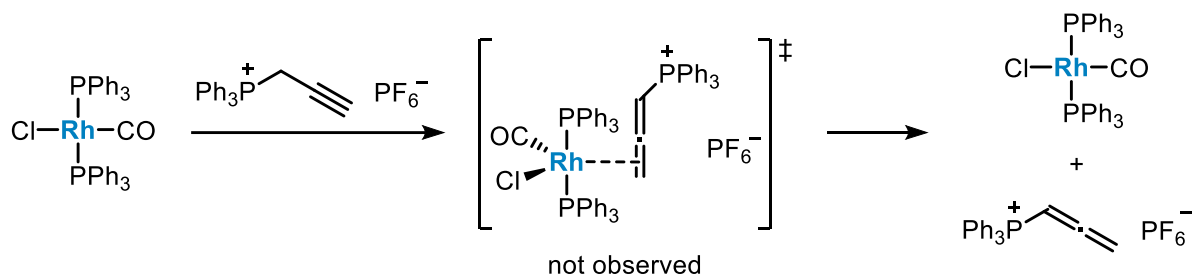


**Figure 3.8.** Isomeric structures of propargyl (a), allenyl (b) and  $\alpha$ -alkynyl (c) phosphonium bromide salts.

In 1977 Schweizer reported that treatment of the propargyl phosphonium salt with potassium *tert*-butoxide gives the allenyl isomer, whereas heating in phenol leads to the  $\alpha$ -alkynyl species.<sup>118</sup> Bagdasaryan and co-workers, however, found a solvent dependence for the propargylic rearrangement with a mixture of the  $\alpha$ -alkynyl and allenyl isomers found in solution in chloroform and a mixture of the propargyl and  $\alpha$ -alkynyl isomers in solution in acetonitrile.<sup>119</sup> More recently Hill and co-workers reported a rhodium catalysed version of this rearrangement in which addition of  $[\text{RhCl}(\text{CO})(\text{PPh}_3)_2]$  to the propargyl phosphonium salt resulted in the formation of the allenyl isomer, with the reaction proceeding via an  $\eta^2$ -allenyl phosphonium complex (Scheme 3.7).<sup>243</sup>



**Scheme 3.7.** Rhodium catalysed formation of allenylphosphonium salt.

Computational studies of the relative energies of the different isomeric forms of this phosphonium salt found that the propargyl isomer is the least favourable in the gas phase, tetrahydrofuran solution and chloroform solution. In THF the allenyl isomer is slightly lower in energy than the alkynyl isomer, however, in chloroform the alkynyl isomer is favoured (Figure 3.9).<sup>244</sup> It is therefore not surprising that such propargylic rearrangements occur.

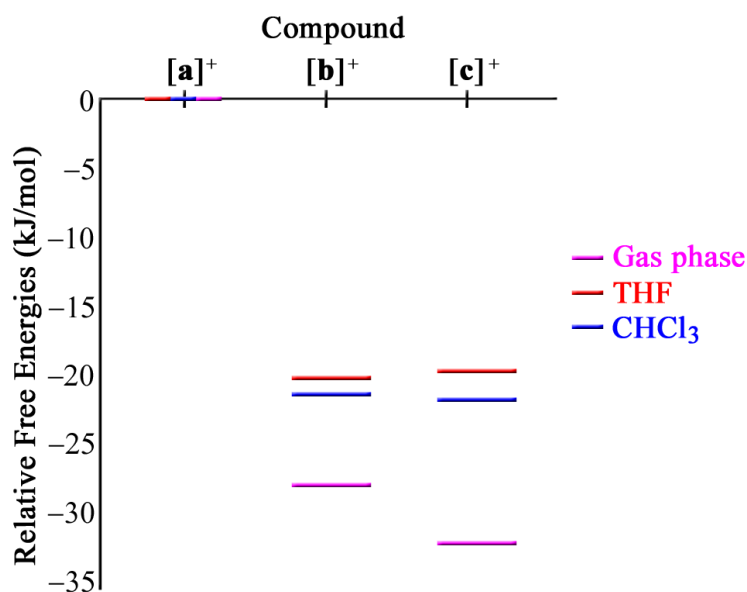


**Figure 3.9.** Relative energies ( $\Delta G$ , kJ/mol) of the isomeric cations  $\mathbf{a}^+$  -  $\mathbf{c}^+$ .

Triphenylpropargylphosphonium bromide has successfully been used to prepare  $\eta^2$ -allenyl complexes of ruthenium, platinum, rhodium and iridium. A vinyl ruthenium complex was also reported by reaction of  $[\text{RuClH}(\text{CO})(\text{PPh}_3)_3]$  with triphenylpropargyl phosphonium bromide and  $\text{NH}_4\text{PF}_6$  as a result of addition of ruthenium hydride across the alkyne bond.<sup>245</sup>

As with all phosphonium salts bearing protons at the  $\alpha$ -carbon, triphenylpropargylphosphonium bromide is the precursor to a phosphonium ylide which,



similarly to the phosphonium salt, has several isomers. There therefore exists the possibility for a variety of different ylide metal complexes (Figure 3.10).

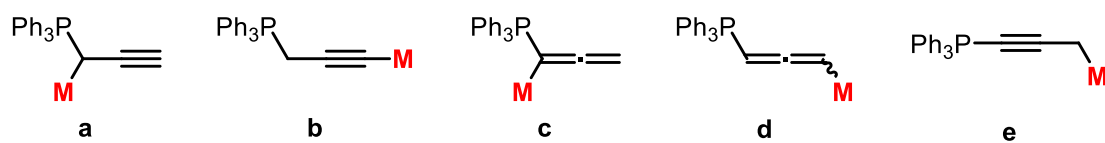


**Figure 3.10.** Possible structures for ylide metal complexes derived from triphenylpropargylphosphonium bromide.

The propargyl isomer could be deprotonated and subsequently coordinate to a metal atom at the  $\alpha$ -carbon to give isomer **a** or the  $\gamma$ -carbon to give a linear coordination of the metal to the alkyne group, isomer **b**. Similarly, the allenyl isomer could be deprotonated at either the  $\alpha$ - or  $\gamma$ -carbon and coordinate a metal atom to give isomers **c** or **d**, respectively. The  $\alpha$ -alkynyl isomer has only one potential site for deprotonation, the  $\gamma$ -carbon, which after coordination to a metal atom would give isomer **e**. No examples of any such  $\sigma$ -coordination complexes of this ylide have previously been reported. Since triphenylpropargyl phosphonium bromide will readily isomerise to the allenyl isomer it is a promising candidate for the potential formation of allenyl metal complexes.

## 3.2. Propargyl Phosphonium Salts

### 3.2.1. Triphenylpropargylphosphonium bromide isomerism in solution

The solvent dependence of the isomeric form of triphenylpropargylphosphonium bromide in solution over time was studied by NMR spectroscopy. The results are shown in Table 3.1.

**Table 3.1.** Percentage of isomers **a**, **b** and **c** of triphenylpropargylphosphonium bromide present after 1 h, 10 h and 24 h in solution in various solvents

Solvent	1 h a : b : c	10 h a : b : c	24 h a : b : c
Acetone- <i>d</i> <sub>6</sub>	100 : 0 : 0	0 : 100 : 0	0 : 84 : 16
Acetonitrile- <i>d</i> <sub>3</sub>	100 : 0 : 0	100 : 0 : 0	100 : 0 : 0
Chloroform- <i>d</i>	100 : 0 : 0	29 : 71 : 0	0 : 98 : 2
Dichloromethane- <i>d</i> <sub>2</sub>	100 : 0 : 0	16 : 84 : 0	0 : 97 : 3
DMSO- <i>d</i> <sub>6</sub>	100 : 0 : 0	100 : 0 : 0	89 : 11 : 0
Methanol- <i>d</i> <sub>4</sub>	100 : 0 : 0	Addition product formed	

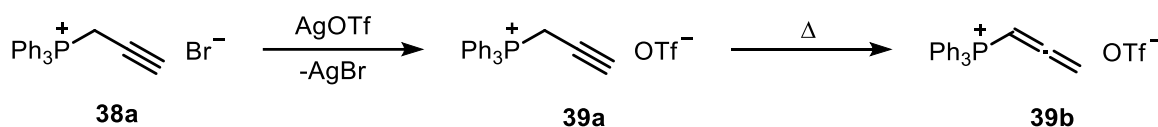
In all solvents after 1 h only the propargyl isomer **a** (Figure 3.8) was observed. After 10 h in solution significant amounts of the allenyl isomer **b** were observed in chloroform and dichloromethane solutions and in acetone complete conversion to the allenyl isomer had occurred. In DMSO and acetonitrile, however, no isomerism was observed after 10 h. After 24 h in solution in acetone, chloroform and dichloromethane no propargyl isomer remained. In acetone 16% of the  $\alpha$ -alkynyl isomer **c** was observed, whereas in chloroform and dichloromethane only trace amounts were present. This shows the solvent can have a huge effect on the tautomer present in solution and consequently on the reactivity.

### 3.2.2. Triphenylpropargylphosphonium triflate

The reaction of triphenylpropargylphosphonium bromide with silver triflate was carried out in order to change the coordinating bromide anion for the far less coordinating triflate anion.

### 3.2. Propargyl Phosphonium Salts

Reaction of triphenylpropargylphosphonium bromide, **38a**, with a stoichiometric amount of silver triflate in dichloromethane gave triphenylpropargylphosphonium triflate, **39a**, in a yield of 93%. Heating a dichloromethane solution of the salt to 40 °C for 10 min resulted in complete conversion into the allene isomer, **39b** (Scheme 3.8).



**Scheme 3.8.** Synthesis of propargyl and allenyl phosphonium triflate salts.

The infrared absorption frequencies for the bromide salt **38a** and the triflate salts **39a** and **39b** are shown in Table 3.2. The strong absorption band at 1909 cm<sup>-1</sup> present only in salt **39b** clearly shows the presence of the allene isomer.

**Table 3.2.** Infrared absorption frequencies

Phosphonium Salt	$\nu$ (cm <sup>-1</sup> )
<b>38a</b>	3148 C≡CH, 2111 C≡C
<b>39a</b>	3261 C≡CH
<b>39b</b>	3055 C=CH <sub>2</sub> , 1909 C=C=C

The isomers **39a** and **39b** could readily be identified by <sup>1</sup>H NMR spectroscopy (Figure 3.11). In the <sup>1</sup>H NMR spectrum of isomer **39a** the propargyl C-H appears as a doublet of triplets at 2.30 ppm with coupling constants of <sup>4</sup>J<sub>HP</sub> = 6.8 Hz and <sup>4</sup>J<sub>HH</sub> = 2.5 Hz. This shift is characteristic for a shielded proton next to a C≡C triple bond. In the allenyl isomer, **39b**, however, the C-H appears at a much higher chemical shift, 6.96 ppm. The C-H proton will be deshielded as a result of being next to a C=C double bond and in close proximity to the positively charged phosphorus atom of the triphenylphosphine group. Again, the signal is observed as a doublet of triplets but with higher coupling constants compared to the propargyl isomer, <sup>4</sup>J<sub>HP</sub> = 7.8 Hz and <sup>4</sup>J<sub>HH</sub> 6.6 Hz. The enhanced HH coupling is a result of the allenyl π-bonds.

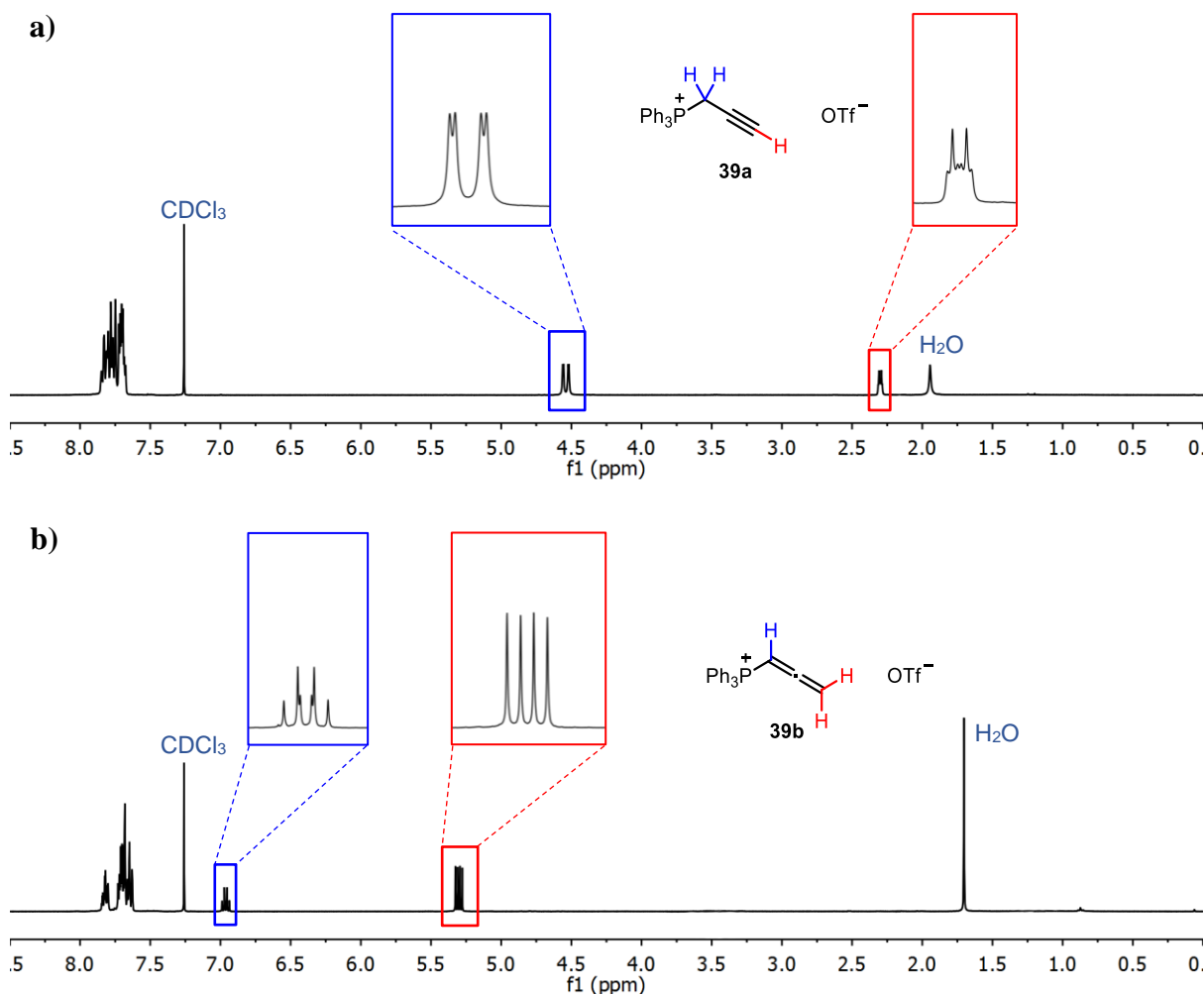


**Figure 3.11.**  $^1\text{H}$  NMR spectra of **39a** (a) and **39b** (b) in  $\text{CDCl}_3$  at room temperature.

The molecular structures of both salts **39a** and **39b** were obtained by single crystal X-ray diffraction (Figure 3.12). Suitable crystals were grown by slow diffusion of *n*-hexane into a solution of the complex in dichloromethane. For salt **39a** the bond length  $\text{C}(2)\text{--}\text{C}(3)$  1.176(8) Å is typical of that for a  $\text{C}\equiv\text{C}$  triple bond, *cf.* 1.20 Å in ethyne,<sup>246</sup> highlighting the presence of the alkyne isomer. The  $\text{C}(1)\text{--}\text{C}(2)\text{--}\text{C}(3)$  bond angle is very close to linear at  $177.5(6)^\circ$ . For complex **39b** the bond distances  $\text{C}(7)\text{--}\text{C}(8)$  and  $\text{C}(8)\text{--}\text{C}(9)$  are 1.257(4) and 1.250(4) Å, respectively. These distances are characteristic for  $\text{C}\text{--}\text{C}$  double bonds. The bond angle  $\text{C}(7)\text{--}\text{C}(8)\text{--}\text{C}(9)$  is almost linear at  $178.1(3)^\circ$  as would be expected for an allene.

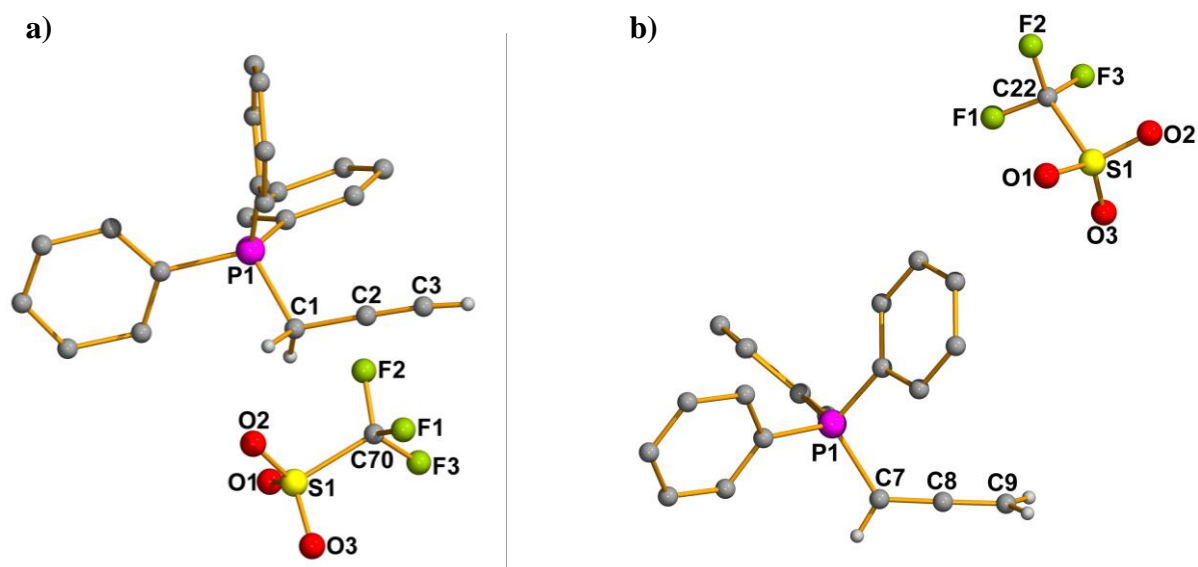
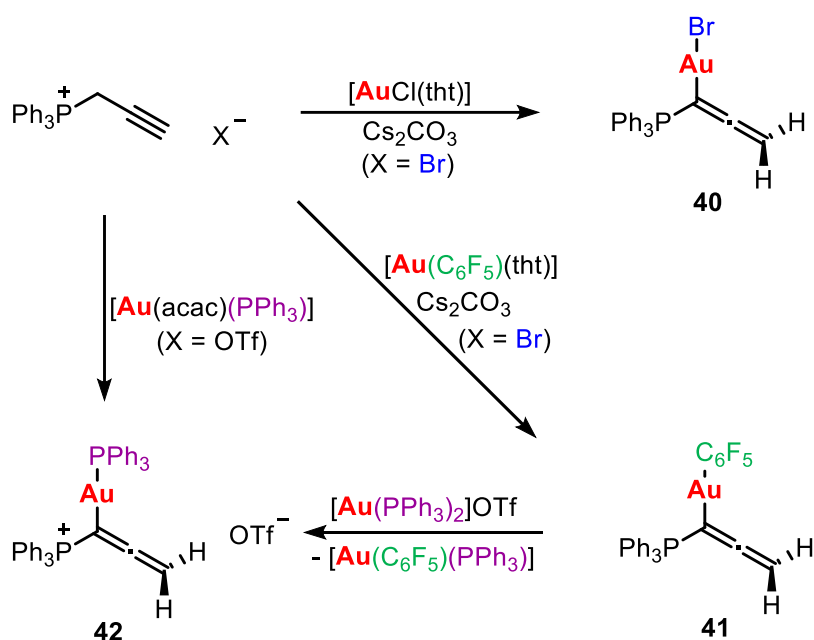


**Figure 3.12.** Molecular structures of **39a** (a) and **39b** (b) determined by single crystal X-ray diffraction. Selected bond lengths [ $\text{\AA}$ ] and angles [ $^\circ$ ] **39a**: P(1)-C(1) 1.819(6), C(1)-C(2) 1.459(8), C(2)-C(3) 1.176(8), C(1)-C(2)-C(3) 177.5(6). **39b**: P(1)-C(7) 1.769(3), C(7)-C(8) 1.257(4), C(8)-C(9) 1.250(4), C(9)-C(8)-C(7) 178.1(3).

### 3.3. Allenyl Gold Complexes from Triphenylpropargylphosphonium Salts

#### 3.3.1. Synthesis of Allenyl Gold Complexes

Reaction of triphenylpropargylphosphonium bromide with  $[\text{AuX}(\text{tht})]$  ( $\text{X} = \text{Cl}, \text{C}_6\text{F}_5$ ) in dichloromethane in the presence of caesium carbonate led to the formation of the unprecedented allenyl gold complexes **40** and **41** in good yields of 63% and 85%, respectively (Scheme 3.9). Reaction of the phosphonium triflate salt with  $[\text{Au}(\text{acac})(\text{PPh}_3)]$  gave the allenyl gold phosphine complex **42**, however the yield was only moderate, 50%. A more effective synthetic route was the reaction of complex **41** with  $[\text{Au}(\text{PPh}_3)_2]\text{OTf}$  which gave complex **42** in a yield of 60%. The driving force in this reaction is the formation of the stable  $[\text{Au}(\text{C}_6\text{F}_5)(\text{PPh}_3)]$  which can readily be separated due to its high solubility in organic solvents.



Scheme 3.9. Synthesis of complexes **40-42**.

The IR spectra of complexes **40-42** clearly show the presence of the allene by the characteristic  $\text{C}=\text{C}=\text{C}$  absorption at around  $1900\text{ cm}^{-1}$  (Table 3.3).

**Table 3.3.** Infrared absorption frequencies

Complex	$\nu(\text{C}=\text{CH}_2)$ ( $\text{cm}^{-1}$ )	$\nu(\text{C}=\text{C}=\text{C})$ ( $\text{cm}^{-1}$ )
<b>40</b>	3068	1906
<b>41</b>	3055	1901
<b>42</b>	3054	1911

In the  $^1\text{H}$  NMR spectra of complexes **40** and **41** the allene  $\text{CH}_2$  protons are observed as a doublet with coupling constant  $^4J_{\text{HP}} = 16.0$  Hz due to coupling with the  $\text{PPh}_3$  group. Despite the presence of the second phosphorus atom in complex **42**, the  $\text{CH}_2$  protons are still observed as a doublet with  $^4J_{\text{HP}} = 15.6$  Hz due to coupling only with the ylide  $\text{PPh}_3$ . The  $^{13}\text{C}$  APT spectra show the characteristic signals for the allene carbon atoms with signals at 83.8, 216.5 and 65.6 ppm for complex **40**. Not all of the quaternary carbon signals are observed in the  $^{13}\text{C}$  APT spectra of complexes **41** and **42**, with resonances at 215.9 and 64.0 ppm for complex **41** and 66.5 ppm for complex **42**.

The molecular structures of complexes **40-42** were determined by single crystal X-ray diffraction (Figure 3.13). The expected linear coordination about the gold centres can clearly be seen with angles of  $179.66(10)^\circ$  (**40**),  $175.24(9)^\circ$  (**41**),  $177.7(3)^\circ$  (**42**), the slight distortion is due to the steric hindrance between the bulky triphenylphosphine group of the allenyl unit and the other ligand at gold. The Au-C distances are within values found for Au-C  $\sigma$ -bonds. The similarity of the bond lengths C(1)-C(2) and C(2)-C(3), 1.296(5) and 1.304(5) Å for **40**, 1.304(4) and 1.300(4) Å for **41** and 1.293(16) and 1.290(19) Å for **42**, highlights the presence of the allenyl isomer. These are also comparable to the carbon-carbon bond length in ethene, 1.34 Å.

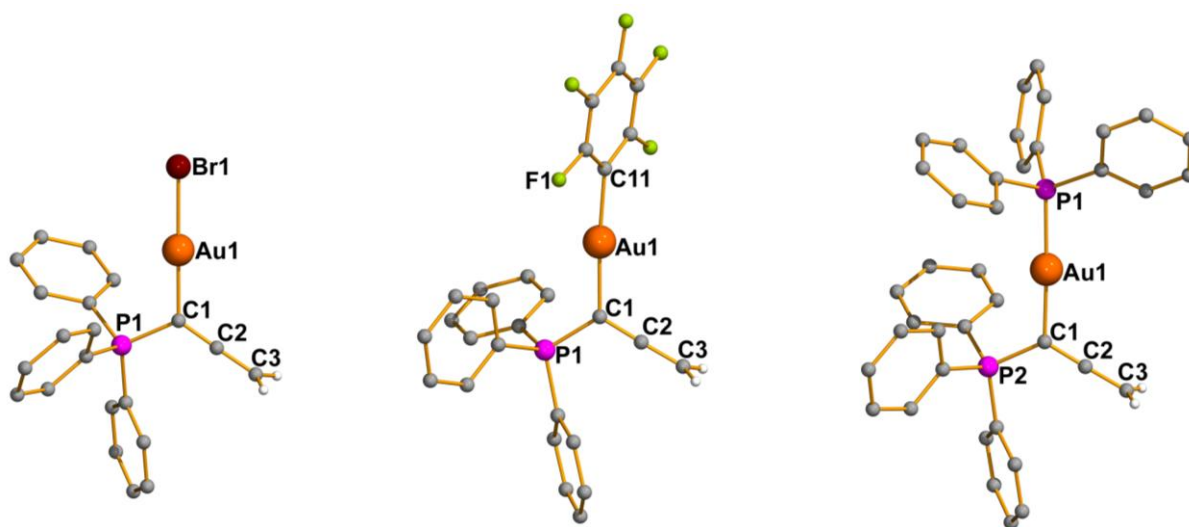
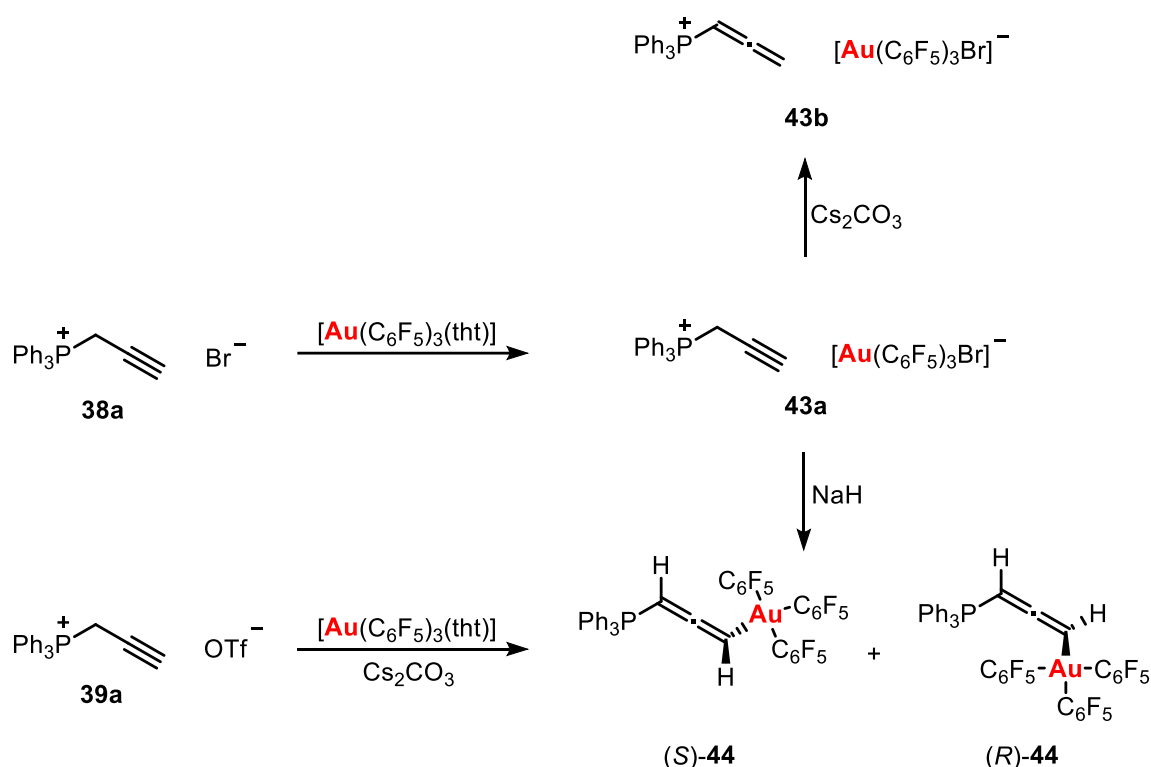


**Figure 3.13.** Molecular structures of **40-42** determined by single crystal X-ray diffraction. Phenyl hydrogen atoms, anions and solvent molecules are omitted for clarity. Selected bond lengths [Å] and angles [°] **40**: Au(1)-C(1) 2.032(4), Au(1)-Br(1) 2.3980(4), C(1)-P(1) 1.769(3), C(1)-C(2) 1.296(5), C(2)-C(3) 1.304(5), C(1)-Au(1)-Br(1) 179.66(10), C(1)-C(2)-C(3) 178.6(4). **41**: Au(1)-C(1) 2.055(2), Au(1)-C(11) 2.036(2), C(1)-P(1) 1.770(2), C(1)-C(2) 1.304(4), C(2)-C(3) 1.300(4), C(11)-Au(1)-C(1) 175.24(9), C(3)-C(2)-C(1) 178.4(3). **42**: Au(1)-C(1) 2.063(11), Au(1)-P(1) 2.265(3), C(1)-P(2) 1.758(11), C(1)-C(2) 1.293(16), C(2)-C(3) 1.290(19), C(1)-Au(1)-P(1) 177.7(3), C(3)-C(2)-C(1) 178.6(14).

With the aim of obtaining allenyl gold(III) complexes which are unknown in the literature, the reaction of triphenylpropargylphosphonium bromide with the gold(III) derivative  $[\text{Au}(\text{C}_6\text{F}_5)_3(\text{tht})]$  was carried out in dichloromethane (Scheme 3.10). This reaction resulted in the formation of phosphonium aurate salt **43a** in which the alkyne triple bond is maintained. Attempts to coordinate the  $\text{Au}(\text{C}_6\text{F}_5)_3$  unit by a reaction with excess caesium carbonate, a method analogous to that for the preparation of allenyl gold(I) complexes, led only to isomerisation to the allene isomer salt **43b**. Reaction of **43a** with the stronger base, sodium hydride, resulted in deprotonation, isomerisation to the allenyl isomer and coordination of the  $\text{Au}(\text{C}_6\text{F}_5)_3$  unit to the  $\gamma$ -carbon atom to give chiral allenyl gold(III) complex **44** in a yield of 65%. Complex **44** could also be prepared by the synthetically simpler route in which triphenylpropargylphosphonium triflate is reacted with  $[\text{Au}(\text{C}_6\text{F}_5)_3(\text{tht})]$  in the presence of excess caesium carbonate. In this case an intermediate phosphonium aurate salt analogous to **53** is not produced since the triflate ion is too weakly coordinating to bind to the gold centre.



### 3.3. Allenyl Gold Complexes from Triphenylpropargylphosphonium Salts



**Scheme 3.10.** Synthesis of allenyl gold(III) derivatives.

The <sup>1</sup>H NMR spectrum of complex **44** confirms the coordination of the gold(III) centre to the γ-carbon atom as the protons of the outer allenyl carbon atoms each appear as a doublet of doublets coupling themselves and also to the phosphorus atom, with <sup>4</sup>J<sub>HP</sub> = 12.8 Hz, <sup>4</sup>J<sub>HH</sub> = 6.0 Hz (Au-CH) and <sup>2</sup>J<sub>HP</sub> = 14.0 Hz, <sup>4</sup>J<sub>HH</sub> = 6.0 Hz (CH(PPh<sub>3</sub>)). In the <sup>13</sup>C APT spectrum the allenic carbon atoms (Ph<sub>3</sub>P)HC=C=CH(AuR<sub>3</sub>) appear at 86.4, 205.6 and 65.6, respectively, downshielded compared with those of the gold(I) species. An absorption at 1907 cm<sup>-1</sup> is observed in the IR spectrum due to the C=C=C fragment.

The formation of complex **44** by deprotonation of the γ-carbon atom is unusual since the proton at the α-carbon of the phosphonium salt would be more acidic as a negative charge here would be stabilised by the positively charged phosphorus of the triphenylphosphine group. It is likely that the triphenylphosphine and tris-pentafluorophenyl gold(III) groups are too sterically bulky to be in close proximity resulting in regioselectivity in the coordination to the γ-carbon.

The molecular structure of **44** was unambiguously determined by single crystal X-ray diffraction methods (Figure 3.14). Complex **44** is an axially chiral allenyl derivative which

crystallises in the space group  $P2_1/c$  with both the (*S*) and (*R*) enantiomers in the asymmetric unit. The bond distances C(1)-C(2) of 1.276(7) Å and C(2)-C(3) of 1.322(9) Å for the (*S*) enantiomer and C(67)-C(68) of 1.276(9) Å and 1.322(9) Å for the (*R*) enantiomer are typical of those for carbon-carbon double bonds. The Au-C bond distances to the carbon atoms of the pentafluorophenyl moieties and to the carbon atom of the allenyl ligand are very similar. A square planar coordination is observed about the gold(III) centres.

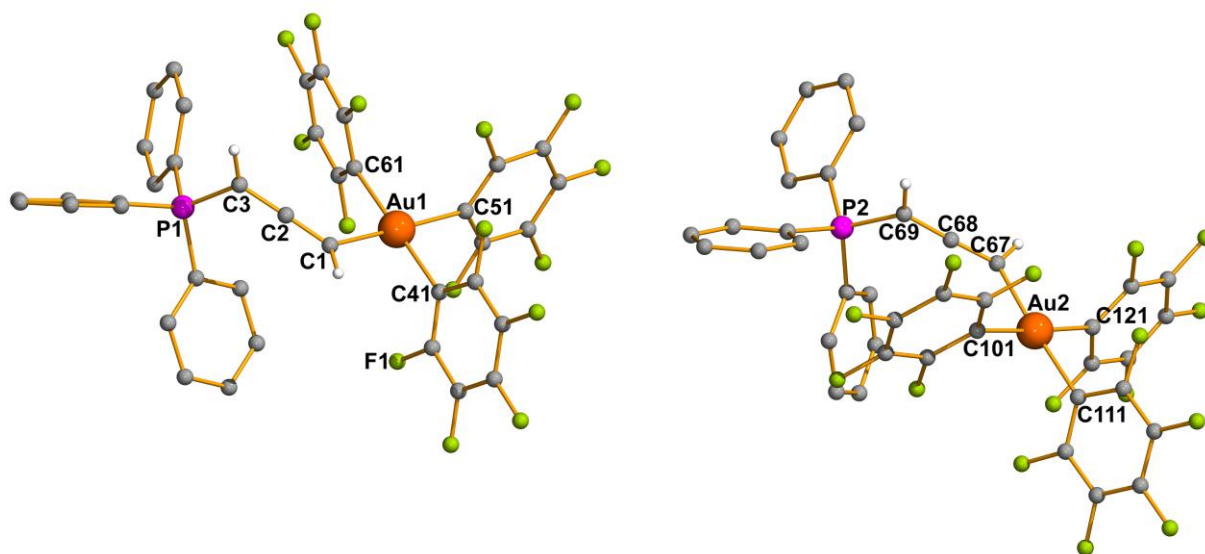


**Figure 3.14.** Molecular structures of both enantiomers of complex **44** determined by single crystal X-ray diffraction. Phenyl hydrogen atoms and solvent molecules are omitted for clarity. Selected bond lengths [Å] and angles [°]: Au(1)-C(1) 2.076(7), Au(1)-C(41) 2.056(6), Au(1)-C(51) 2.070(6), Au(1)-C(61) 2.063(6), C(1)-C(2) 1.276(9), C(2)-C(3) 1.322(9), C(3)-P(1) 1.769(6), Au(2)-C(67) 2.055(7), Au(2)-C(101) 2.063(6), Au(2)-C(111) 2.064(6), Au(2)-C(121) 2.062(6), C(67)-C(68) 1.276(9), C(68)-C(69) 1.322(9), C(69)-P(2) 1.757(7), C(51)-Au(1)-C(1) 176.7(2), C(41)-Au(1)-C(61) 177.9(2), C(1)-C(2)-C(3) 176.3(7), C(67)-Au(2)-C(111) 175.7(3), C(121)-Au(2)-C(101) 177.4(2), C(67)-C(68)-C(69) 177.8(7).

The stability of the allenyl gold complexes at different temperatures was determined by variable temperature NMR experiments (Figure 3.15-16). No dynamic NMR effects were observed at low or high temperature indicating a high thermal stability for the complexes. This is likely to be due to the electron-withdrawing phosphonium group.

### 3.3. Allenyl Gold Complexes from Triphenylpropargylphosphonium Salts

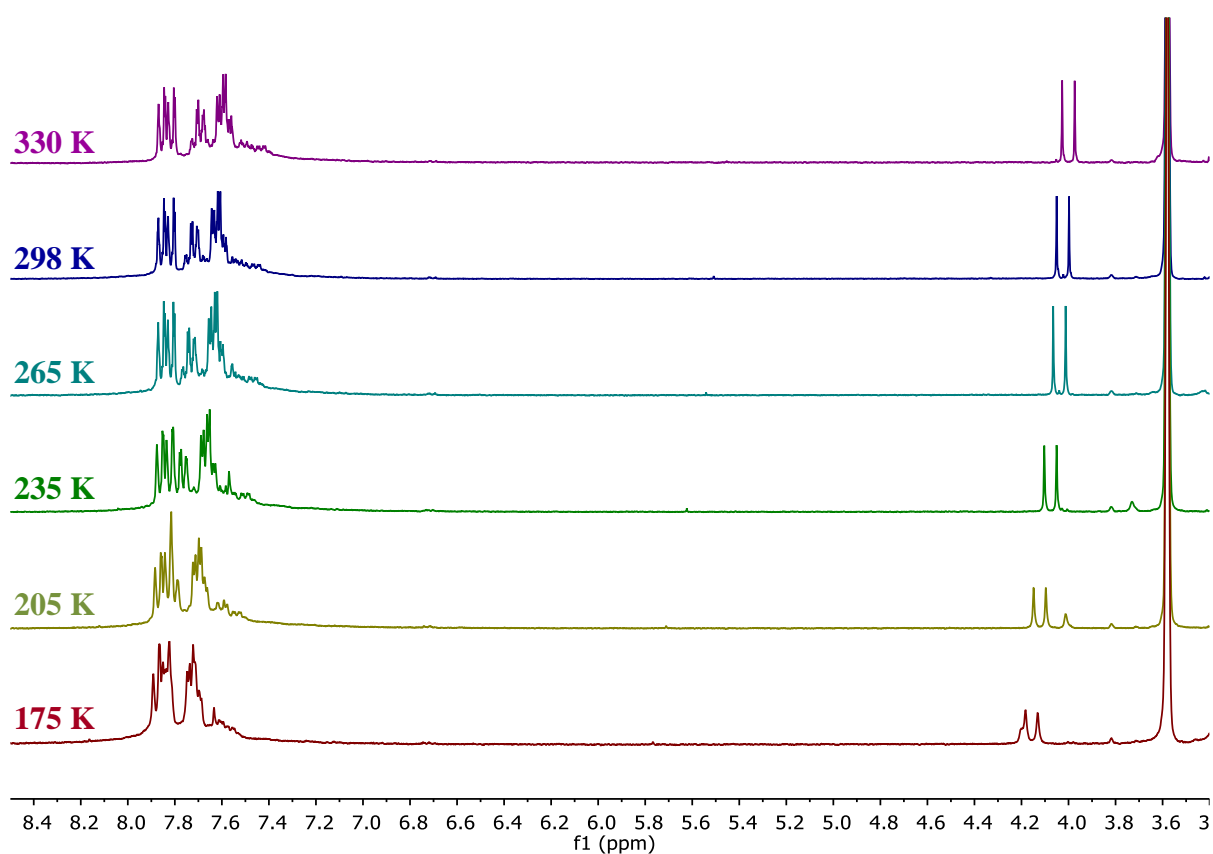


Figure 3.15.  $^1\text{H}$  NMR spectra for complex **40** in THF at different temperatures.

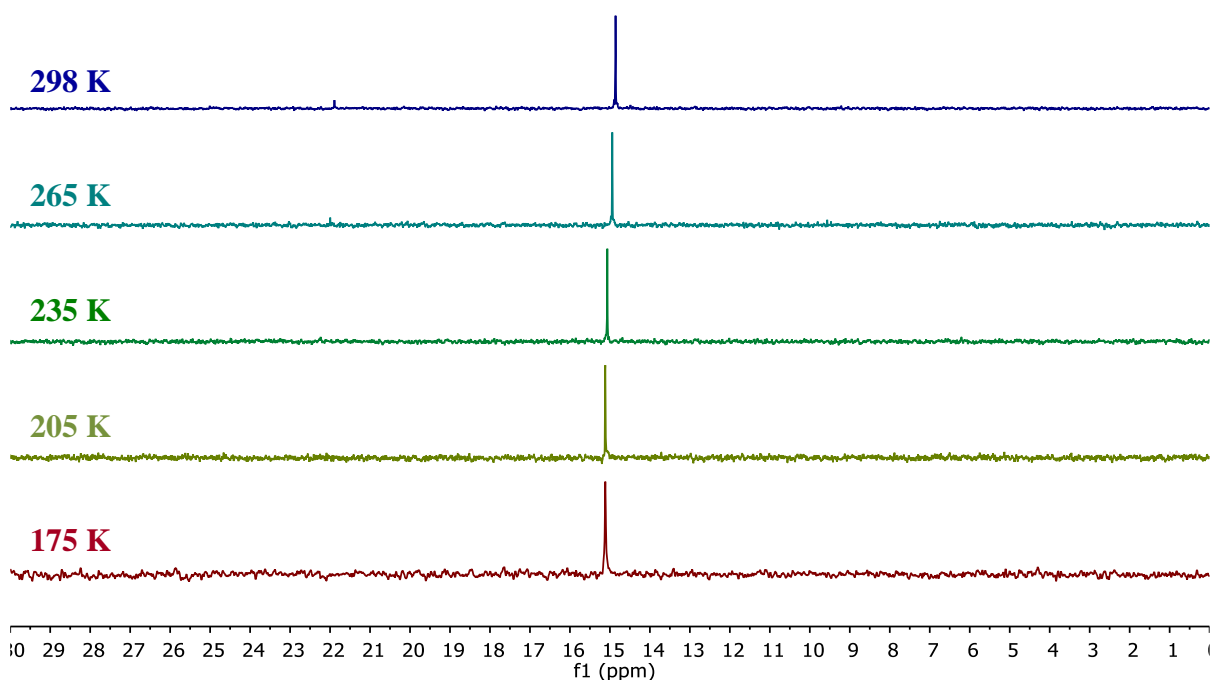
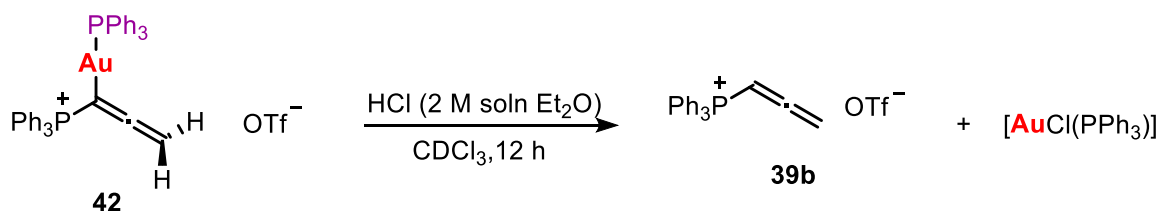
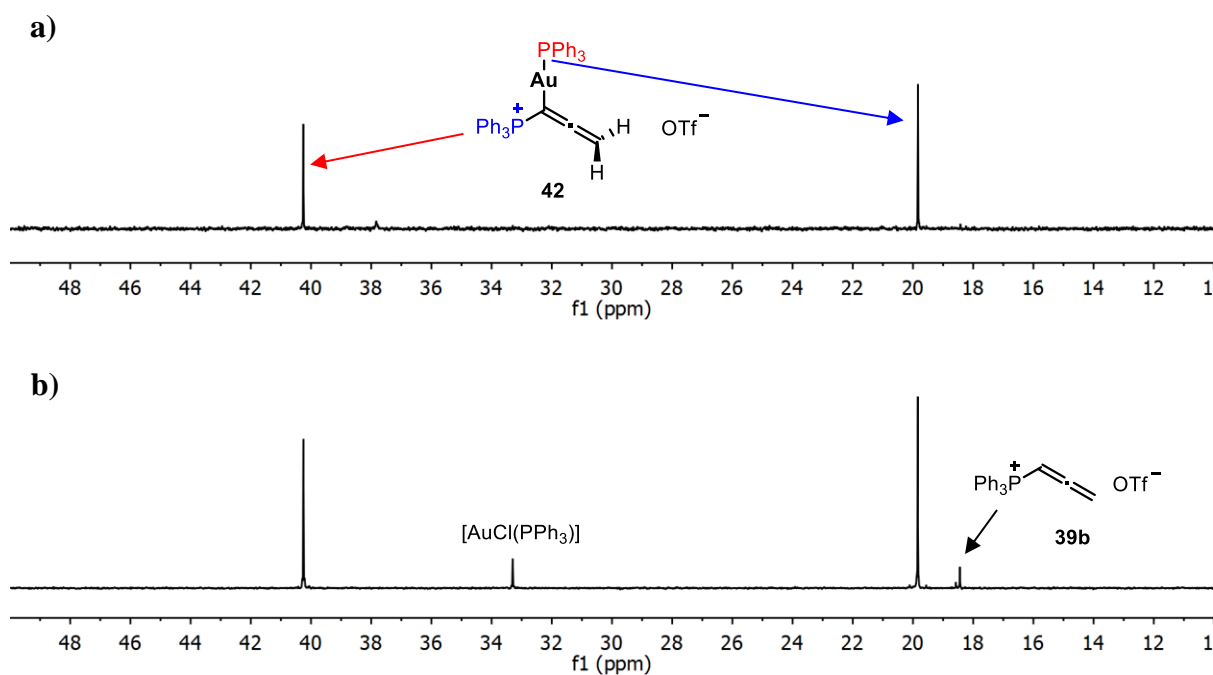


Figure 3.16.  $^{31}\text{P}\{^1\text{H}\}$  NMR spectra for complex **40** in THF at different temperatures.

A protodeauration experiment was carried out with complex **36** by addition of a stoichiometric amount of a solution of HCl in diethyl ether to a solution of the complex in deuterated chloroform at room temperature (Scheme 3.11). NMR experiments showed the formation of  $[\text{AuCl}(\text{PPh}_3)]$  and the phosphonium salt after 12 hours (Figure 3.17). This process could be relevant in a catalytic cycle as the key step for the release of a catalyst.



**Scheme 3.11.** Protodeauration of complex **42**.

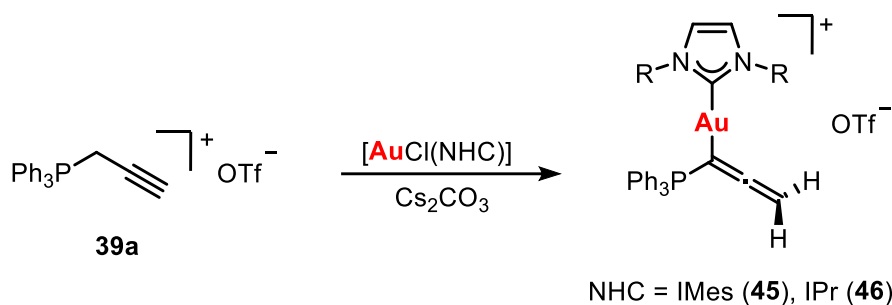


**Figure 3.17.**  $^{31}\text{P}\{^1\text{H}\}$  NMR spectra for complex **42** (a) and complex **42** 12 h after addition of HCl (b).

### 3.3.2. Influence of Steric and Electronic Properties

In order to determine if the regioselectivity found in the allenyl gold complexes was due to steric effects or the oxidation state of gold, additional gold(I) complexes were prepared in which the gold bears a sterically bulky NHC ligand (Scheme 3.12).

### 3.3. Allenyl Gold Complexes from Triphenylpropargylphosphonium Salts



**Scheme 3.12.** Synthesis of allenyl gold(I) NHC complexes.

Reaction of the phosphonium triflate salt with  $[\text{AuCl}(\text{NHC})]$  (NHC = IMes, IPr) in the presence of  $\text{Cs}_2\text{CO}_3$  gave allenyl gold(I) complexes **45** and **46**. Despite the huge steric bulk of the NHC ligand, coordination at the  $\alpha$ -carbon of the allenyl ligand still occurs.

**Table 3.4.** Selected Infrared Absorption Frequencies for Complexes **45** and **46**

Complex	$\nu(\text{C}=\text{CH}_2)$ ( $\text{cm}^{-1}$ )	$\nu(\text{C}=\text{C}=\text{C})$ ( $\text{cm}^{-1}$ )
<b>45</b>	3062	1910
<b>46</b>	-	1908

Selected IR absorption frequencies for complexes **45** and **46** are shown in Table 3.4. For both complexes a characteristic allene  $\text{C}=\text{C}=\text{C}$  absorption at around  $1900\text{ cm}^{-1}$  is observed. In the  $^1\text{H}$  NMR spectra the allenyl  $\text{CH}_2$  protons are observed as a doublet at 4.08 ppm with  $^4J_{\text{HP}} = 16.1\text{ Hz}$  for **45** and at 3.99 ppm with  $^4J_{\text{HP}} = 15.8\text{ Hz}$  for **39**. Not all of the allenyl carbons are observed in the  $^{13}\text{C}$  APT spectra with signals at 216.7 and 65.0 ppm for complex **45** and a signal at 64.6 ppm for complex **46**.

The molecular structures of **45** and **46** were determined by single crystal X-ray diffraction analysis (Figure 3.18). In both cases a linear coordination is observed about gold with angles  $177.66(13)^\circ$  (**45**) and  $177.66(9)^\circ$  (**46**), the slight distortion due to the steric bulk of the NHC ligands and the triphenylphosphine group. In both cases the allenyl C-C bond distances are similar with distances of 1.305(5) and 1.297(5) Å for **45** and 1.309(3) and 1.298(4) Å for **46**, comparable to the C-C bond distances in ethene. The  $\text{C}=\text{C}=\text{C}$  bond angles are almost linear at  $178.3(4)^\circ$  for **45** and  $179.1(3)^\circ$  for **46**.

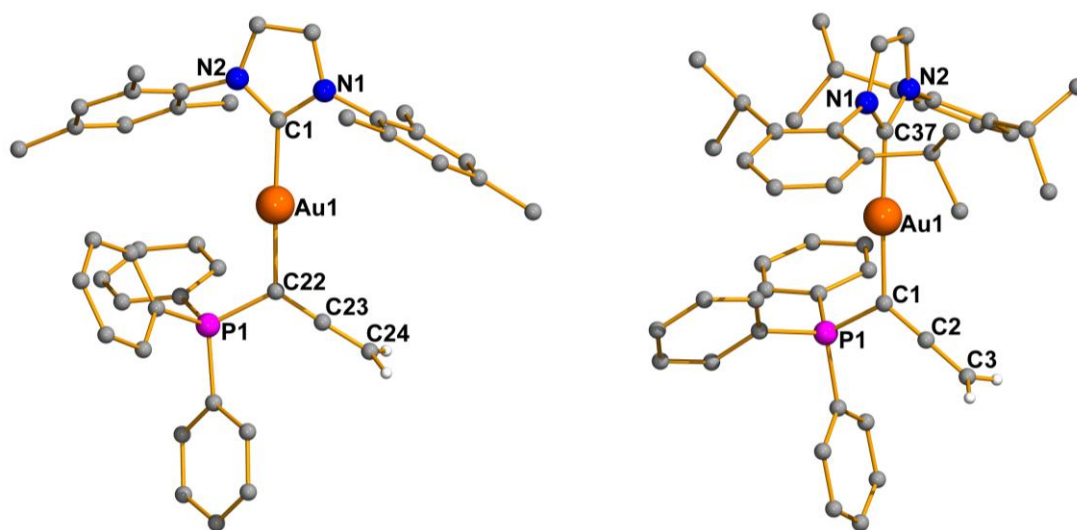
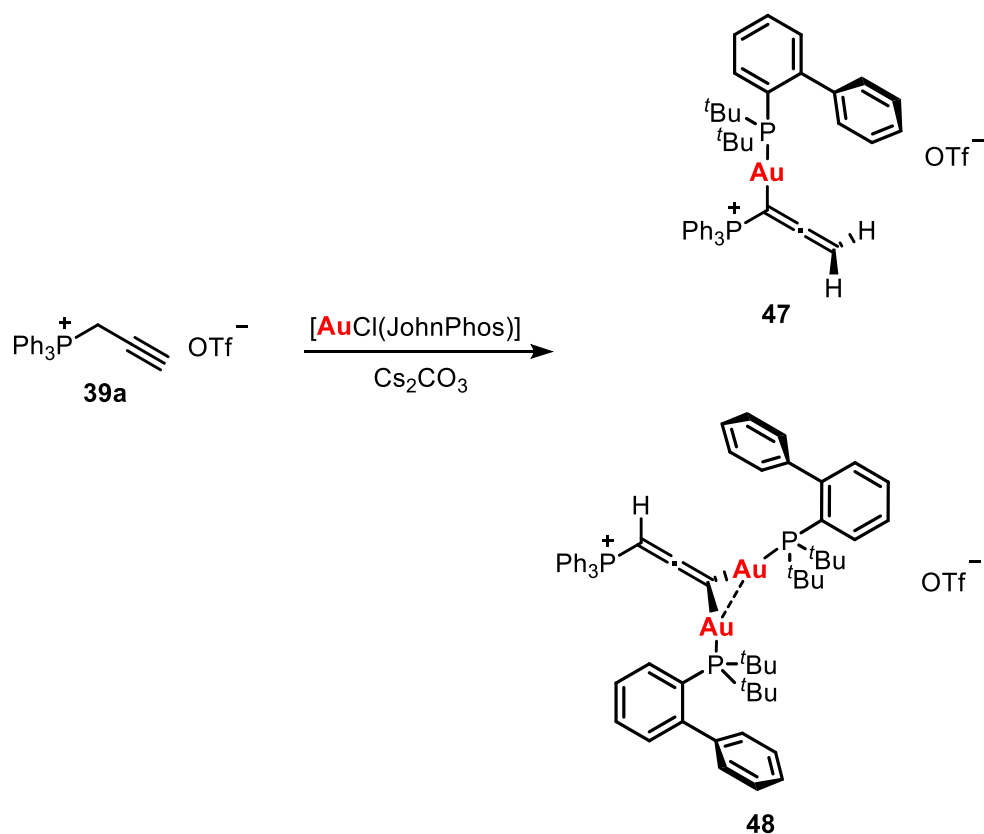


**Figure 3.18.** Molecular structures of complexes **45** and **46** determined by single crystal X-ray diffraction. Phenyl hydrogen atoms, anions and solvent molecules are omitted for clarity. Selected bond lengths [Å] and angles [°]  
**45:** Au(1)-C(1) 2.015(4), Au(1)-C(22) 2.048(4), P(1)-C(22) 1.776(3), C(22)-C(23) 1.305(5), C(23)-C(24) 1.297(5), C(1)-Au(1)-C(22) 177.66(13), C(24)-C(23)-C(22) 178.3(4). **46:** Au(1)-C(37) 2.017(2), Au(1)-C(1) 2.051(2), C(1)-P(1) 1.775(2), C(1)-C(2) 1.309(3), C(2)-C(3) 1.298(4), C(37)-Au(1)-C(1) 177.66(9), C(3)-C(2)-C(1) 179.1(3).

When a bulky phosphine gold(I) precursor was used, a different reactivity was observed. Reaction of the phosphonium triflate salt, **39a**, with [AuCl(JohnPhos)] in the presence of caesium carbonate gave two products, **47** and **48** (Scheme 3.13).

The expected allenyl gold(I) complex, **47**, in which the gold is bound to the  $\alpha$ -carbon of the allenyl ligand is observed by NMR spectroscopy by the presence of a doublet of doublets at 4.29 ppm in the  $^1\text{H}$  NMR spectrum with  $^4J_{\text{HP}} = 16.1$  Hz and  $^5J_{\text{HP}} = 3.8$  Hz due to the allenyl  $\text{CH}_2$  coupling with the triphenylphosphine and the JohnPhos phosphorus atoms. The  $^{31}\text{P}\{^1\text{H}\}$  NMR spectrum shows two doublets at 63.84 ppm (JohnPhos) and 18.84 ppm ( $\text{PPh}_3$ ) with  $^3J_{\text{PP}} = 2.0$  Hz. However, an additional doublet at 62.65 ppm and triplet at 18.95 ppm with  $^4J_{\text{PP}} = 6.5$  Hz are also observed in the  $^{31}\text{P}\{^1\text{H}\}$  NMR spectrum due to the presence of complex **48** in which two gold phosphine units are bound to the  $\gamma$ -carbon atom of the allenyl ligand (Figure 3.19). It is likely that this complex forms due to the favourable  $\text{Au}\cdots\text{Au}$  interactions.

### 3.3. Allenyl Gold Complexes from Triphenylpropargylphosphonium Salts



**Scheme 3.13.** Synthesis of complexes **47** and **48**.

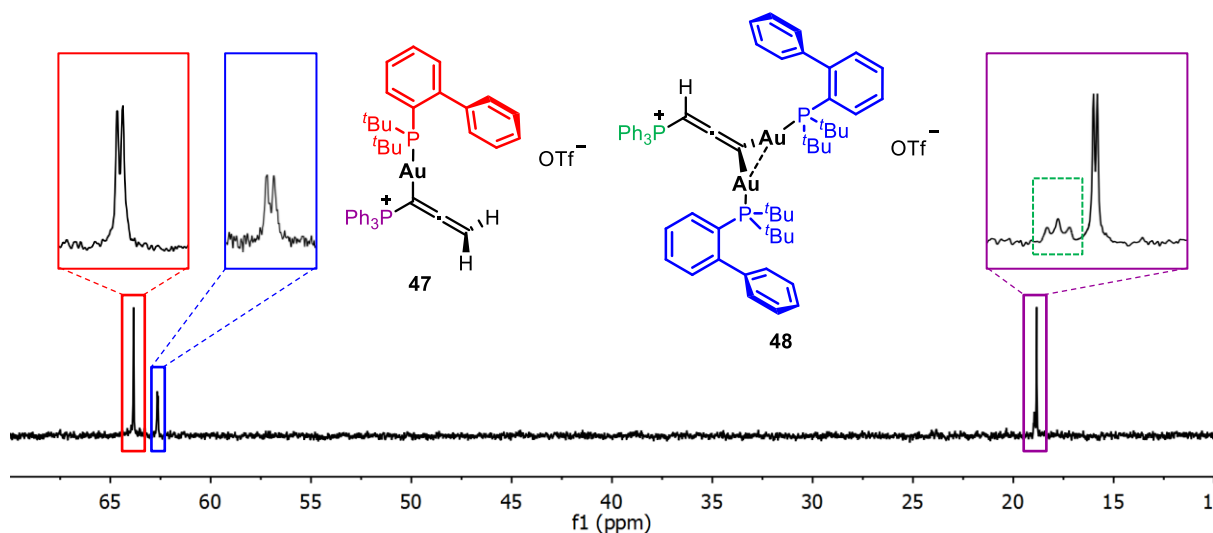


**Figure 3.19.**  $^{31}\text{P}\{^1\text{H}\}$  NMR spectrum of reaction mixture from the formation of complexes **47** and **48** in  $\text{CD}_2\text{Cl}_2$ .

The molecular structure of the dinuclear complex, **48**, was determined by single crystal X-ray diffraction (Figure 3.20). The coordination about each gold atom is slightly distorted from linearity due to the presence of the bulky phosphine groups, with angles C(1)-Au(1)-P(2)  $174.22(10)^\circ$  and C(1)-Au(2)-P(3)  $173.95(10)^\circ$ . One of the allene bonds is slightly shorter than

the other with distances C(1)-C(2) 1.251(5) Å and C(2)-C(3) 1.364(5) Å, however both are still comparable to the typical distance for a carbon-carbon double bond. The C=C=C angle is practically linear at 178.7(4)°.

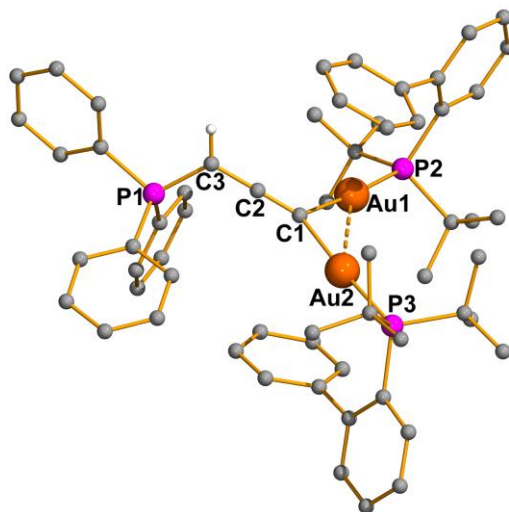
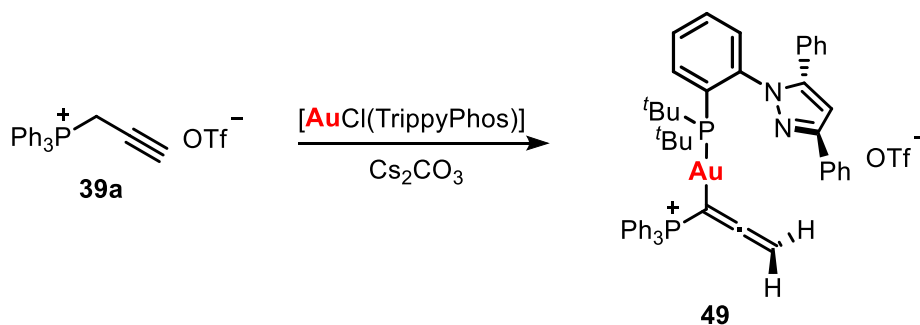


**Figure 3.20.** Molecular structures of complex **48** determined by single crystal X-ray diffraction. Phenyl hydrogen atoms and solvent molecules are omitted for clarity. Selected bond lengths [Å] and angles [°]: Au(1)-C(1) 2.052(3), Au(1)-P(2) 2.2780(9), Au(1)-Au(2) 3.1487(2), Au(2)-C(1) 2.038(4), Au(2)-P(3) 2.2891(9), C(1)-C(2) 1.251(5), C(2)-C(3) 1.364(5), C(3)-P(1) 1.721(4), C(1)-Au(1)-P(2) 174.22(10), C(1)-Au(2)-P(3) 173.95(10), C(1)-C(2)-C(3) 178.7(4).

When the even more sterically demanding phosphine, 1-[2-[bis(tert-butyl)phosphino]phenyl]-3,5-diphenyl-1H-pyrazole (TrippyPhos), is used, only one product, **49**, is formed in which one gold phosphine unit is bound to the  $\alpha$ -carbon of the allenyl ligand (Scheme 3.14). In this case the steric bulk of the phosphine is so great that the formation of a dinuclear species would not be possible. Despite the hindrance of the  $\text{PPh}_3$  group coordination at the  $\alpha$ -carbon is still preferable.



**Scheme 3.14.** Synthesis of complex **49**.



### 3.3. Allenyl Gold Complexes from Triphenylpropargylphosphonium Salts

The allenyl CH<sub>2</sub> protons of complex **41** are observed in the <sup>1</sup>H NMR spectrum as a doublet of doublets at 4.23 ppm (<sup>4</sup>J<sub>HP</sub> = 16.0 Hz, <sup>5</sup>J<sub>HP</sub> = 4.1 Hz) due to coupling with both the ylide and the TrippyPhos phosphorus atoms (Figure 3.21(a)). The <sup>31</sup>P{<sup>1</sup>H} NMR spectrum presents two doublets at 60.76 ppm and 19.39 ppm (<sup>3</sup>J<sub>PP</sub> = 1.6 Hz) due to the TrippyPhos and ylide phosphorus atoms, respectively (Figure 3.21(b)).

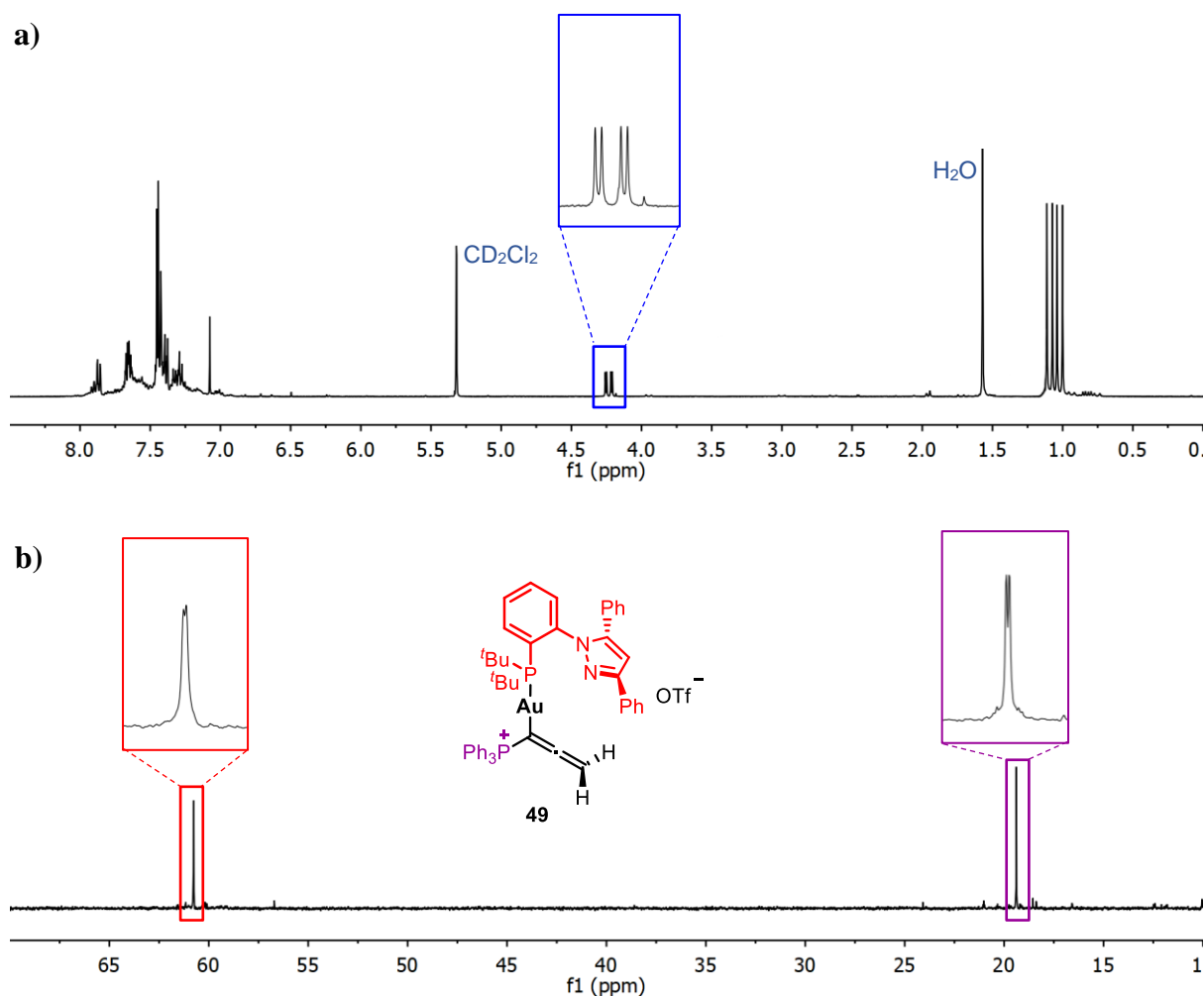
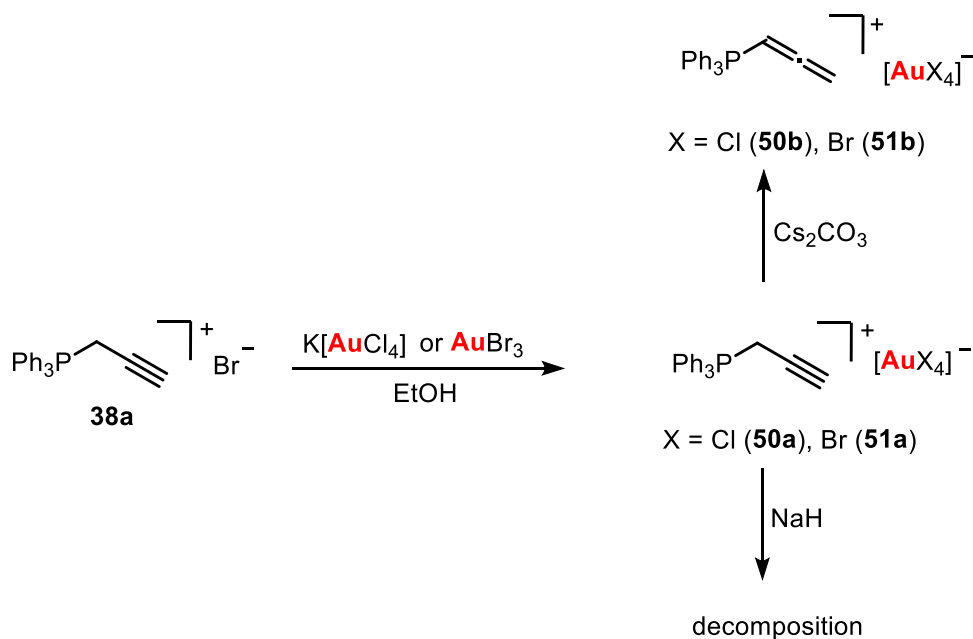


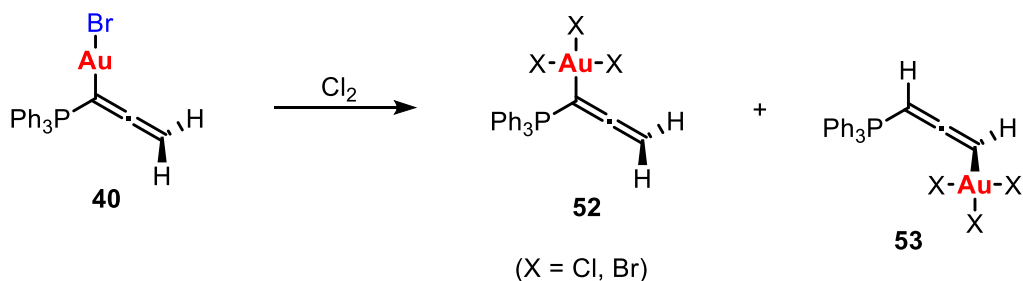
**Figure 3.21.** <sup>1</sup>H NMR spectrum (a) and <sup>31</sup>P{<sup>1</sup>H} NMR spectrum (b) of complex **49** in CD<sub>2</sub>Cl<sub>2</sub> at room temperature.

In an attempt to prepare a further gold(III) derivative, phosphonium aurate salts **50a** and **51a** were prepared (Scheme 3.15). Reaction with caesium carbonate led only to isomerisation to the allene in both cases to give salts **50b** and **51b** and no coordination of the allenyl group to gold was observed. Use of a stronger base led to decomposition.



**Scheme 3.15.** Synthesis of salts **50a-b** and **51a-b**.

The oxidation of complex **40** with  $\text{Cl}_2$  to give a gold(III) derivative was attempted (Scheme 3.16).



**Scheme 3.16.** Oxidation of complex **40**.

A mixture of products was obtained due to the mixture of halide ligands. In the  $^{31}\text{P}\{^1\text{H}\}$  NMR spectrum two groups of signals are clearly observed (Figure 3.22). The signals at around 21 ppm are assigned to complex **52** with coordination to gold through the  $\alpha$ -carbon atom of the allenyl ligand. Different derivatives are possible with different mixtures of Br and Cl. The signals at around 7 ppm indicate a different coordination and are proposed to be a result of the formation of complex **53** with coordination through the  $\gamma$ -carbon of the allenyl ligand to gold. Again, different derivatives are possible due to the mixture of Cl and Br.

### 3.3. Allenyl Gold Complexes from Triphenylpropargylphosphonium Salts

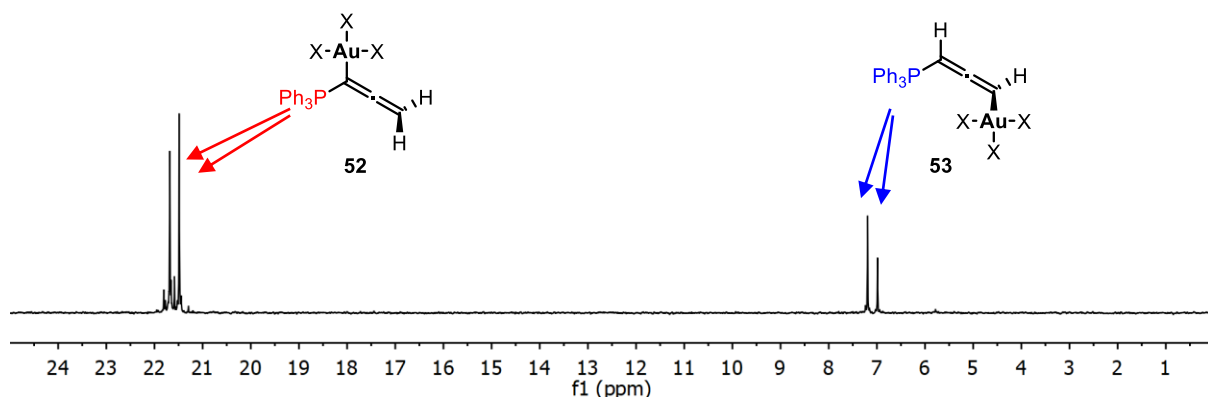


**Figure 3.22.**  $^{31}\text{P}\{^1\text{H}\}$  NMR spectrum from the reaction mixture from the oxidation of **40**.

Crystals were obtained from the reaction mixture and measured by single crystal X-ray diffraction. The molecular structure of a derivative of complex **52** was found in which two bromide ligands and one chloride ligand are bound to gold (Figure 3.23). A square-planar coordination is observed about the gold(III) centre. The carbon-carbon bond distance in the allenyl ligand are clearly double bonds with distances C(1)-C(2) 1.276(15) Å and C(2)-C(3) 1.328(16) Å. The C=C=C bond angle is almost linear, C(1)-C(2)-C(3) 179.1(12)°.

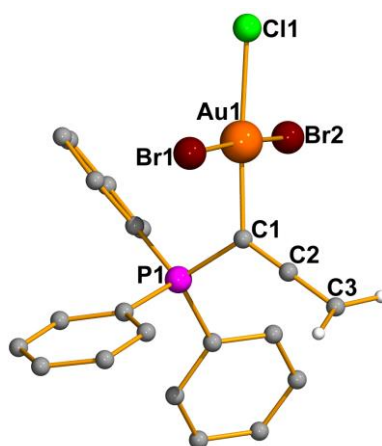
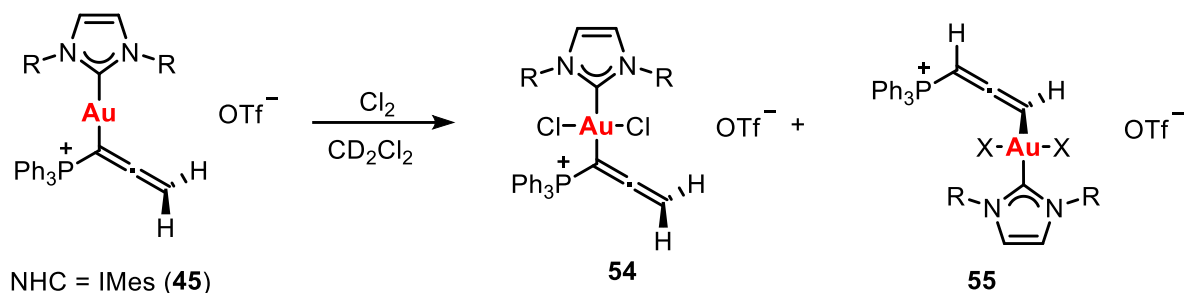


**Figure 3.23.** Molecular structures of complex **52** determined by single crystal X-ray diffraction. Phenyl hydrogen atoms and solvent molecules are omitted for clarity. Selected bond lengths [Å] and angles [°]: Au(1)-Br(1) 2.3709(14), Au(1)-Br(2) 2.3752(15), Au(1)-Cl(1) 2.391(2), Au(1)-C(1) 2.034(10), P(1)-C(1) 1.801(10), C(1)-C(2) 1.276(15), C(2)-C(3) 1.328(16), Br(1)-Au(1)-Br(2) 175.24(5), C(1)-Au(1)-Cl(1) 175.4(3), C(1)-C(2)-C(3) 179.1(12).

The oxidation of complex **45** with  $\text{Cl}_2$  was also attempted (Scheme 3.17). In this case only two signals were observed in the  $^{31}\text{P}\{^1\text{H}\}$  NMR spectrum, assigned to the products **54** and **55** (Figure 3.24(b)). Three doublets are observed in the  $^1\text{H}$  NMR spectrum, these are assigned to the  $\text{CH}_2$  group of the allenyl ligand in complex **54**, and the two separate protons of the allenyl ligand in complex **55** (Figure 3.24(a)).



Scheme 3.17. Oxidation of complex **45**.

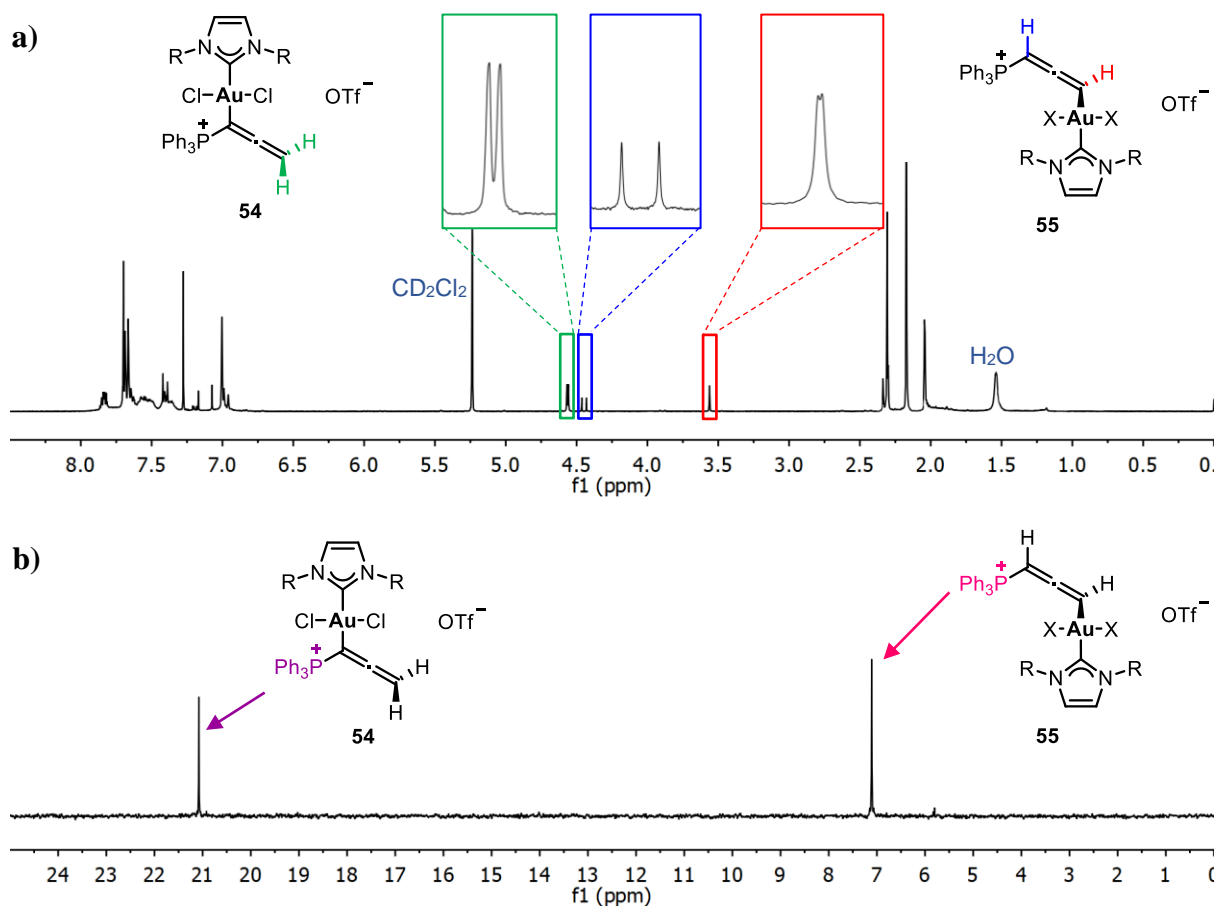
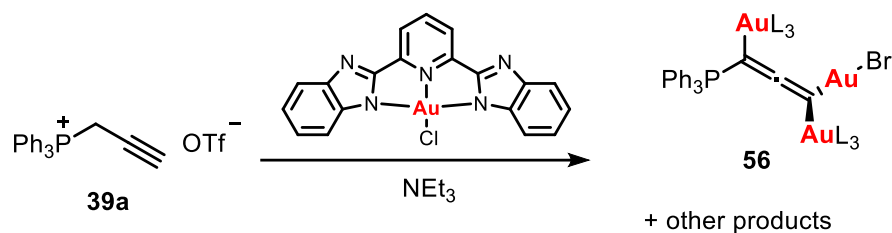


Figure 3.24.  $^1\text{H}$  NMR spectrum (a) and  $^{31}\text{P}\{^1\text{H}\}$  NMR spectrum (b) for the reaction mixture from the oxidation of complex **45** in  $\text{CD}_2\text{Cl}_2$ .

### 3.3. Allenyl Gold Complexes from Triphenylpropargylphosphonium Salts

To prepare a more stable gold(III) derivative, a gold(III) precursor bearing a tridentate 2,6-bis(benzimidazol-2'-yl)pyridine ligand was used. Reaction of this precursor with triphenylpropargylphosphonium triflate in the presence of triethylamine led to a mixture of products (Scheme 3.18). One of these crystallised from the mixture and was characterised by single crystal X-ray diffraction as complex **56**.



**Scheme 3.18.** Synthesis of complex **56**.

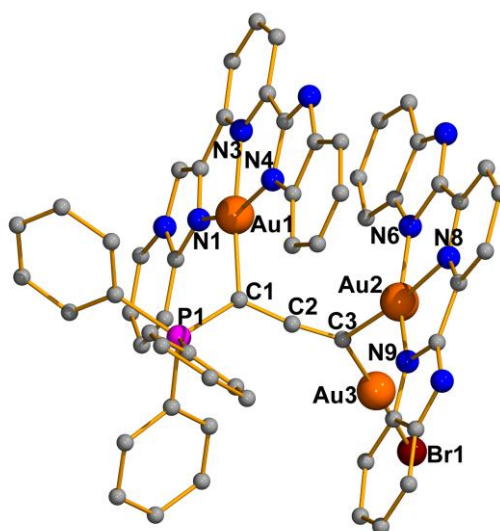
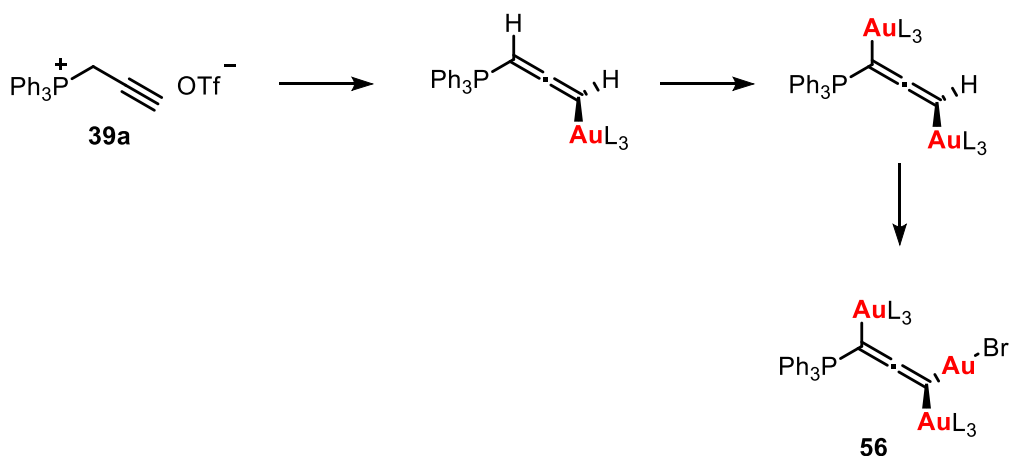


**Figure 3.25.** Molecular structures of complex **56** determined by single crystal X-ray diffraction. Phenyl hydrogen atoms and solvent molecules are omitted for clarity. Selected bond lengths [Å] and angles [°]: Au(1)-C(1) 2.065(10), Au(1)-N(1) 2.026(9), Au(1)-N(3) 2.038(9), Au(1)-N(4) 2.017(8), Au(2)-C(3) 2.055(11), Au(2)-N(6) 2.016(10), Au(2)-N(8) 2.053(9), Au(2)-N(9) 1.988(10), Au(3)-C(3) 2.016(11), Au(3)-Br(1) 2.3853(16), P(1)-C(1) 1.774(11), C(1)-C(2) 1.338(15), C(2)-C(3) 1.219(15), C(1)-Au(1)-N(3) 172.9(4), N(1)-Au(1)-N(4) 158.8(4), C(3)-Au(2)-N(8) 173.2(4), N(6)-Au(2)-N(9) 159.4(4), C(3)-Au(3)-Br(1) 177.5(4), C(1)-C(2)-C(3) 172.2(10).

The molecular structure of complex **56** is shown in Figure 3.25. A distorted square planar coordination is observed about the gold(III) centres, Au(1) and Au(2), and a linear coordination about the gold(I) centre with angle C(3)-Au(3)-Br(1) 177.5(4)°. One of the allene bonds is longer than the other with distances C(1)-C(2) 1.338(15) Å and C(2)-C(3) 1.219(15) Å. The

C=C=C bond is also slightly distorted from linearity with an angle C(1)-C(2)-C(3) of  $172.2(10)^\circ$ . This is due to the steric repulsion between the bulky ligands.

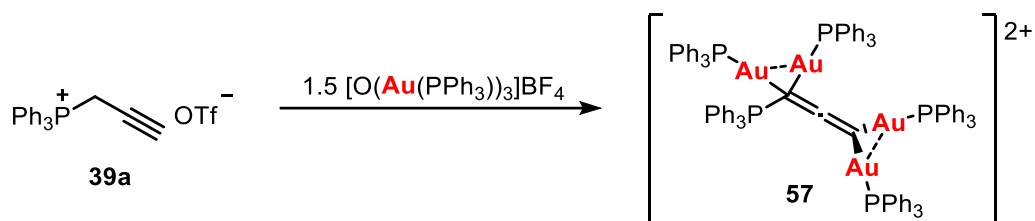
In complex **56** the allenyl ligand is fully aurated. Two gold(III) units are bound, one at the  $\alpha$ -carbon and one at the  $\gamma$ -carbon atom. An additional gold(I) is also bound at the  $\gamma$ -carbon atom. The formation of this complex can be proposed to proceed via initial formation of the mononuclear allenyl gold(III) complex with coordination at the  $\gamma$ -carbon of the allenyl ligand. In the presence of excess base further deprotonation will occur however due to the bulkiness of the gold(III) precursor, coordination of a second unit at the  $\gamma$ -carbon is unfavourable and hence coordination at the  $\alpha$ -carbon occurs. Additional base finally results in further deprotonation at the  $\gamma$ -carbon. It is likely that the reduction to gold(I) occurs in the work-up as a result of washing with water and due to the smaller size of the Au-Br, this can successfully coordinate to the  $\gamma$ -carbon (Scheme 3.19).



**Scheme 3.19.** Formation of complex **56**.

To fully aurate the allenyl ligand with gold(I), reaction of triphenylpropargylphosphonium triflate with 1.5 equivalents of  $[\text{O}(\text{Au}(\text{PPh}_3))_3]\text{BF}_4$  was carried out (Scheme 3.20). The tetranuclear derivative, **57**, formed and was successfully characterised by single crystal X-ray diffraction.

### 3.3. Allenyl Gold Complexes from Triphenylpropargylphosphonium Salts



**Scheme 3.20.** Synthesis of complex **57**.

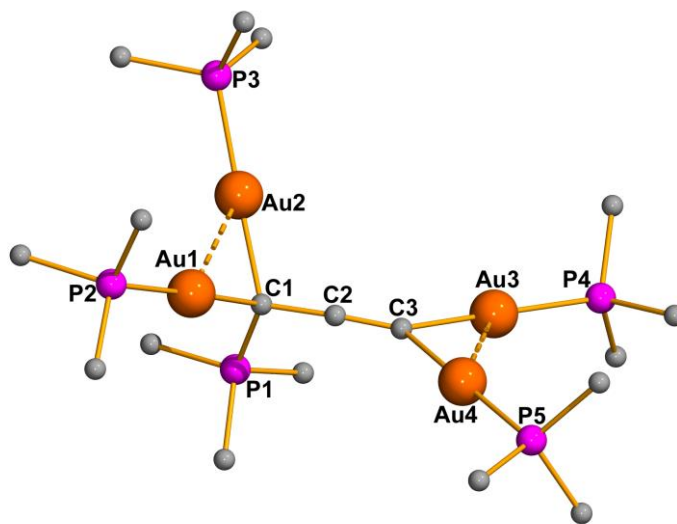
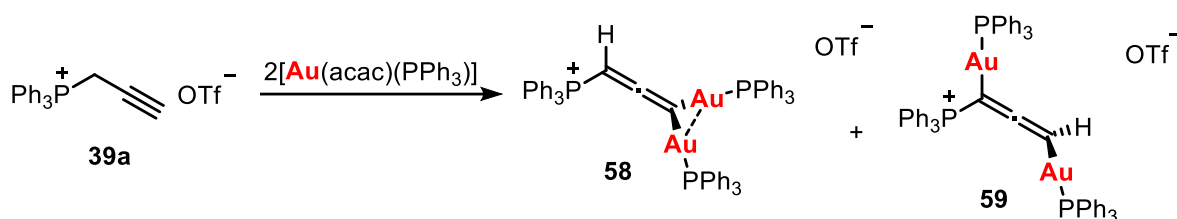


**Figure 3.26.** Molecular structures of complex **57** determined by single crystal X-ray diffraction (Phenyl rings, anions and solvent molecules are omitted for clarity.). Selected bond lengths [Å] and angles [°]: Au(1)-C(1) 2.122(14), Au(1)-P(2) 2.280(5), Au(1)-Au(2) 2.8994(10), Au(2)-C(1) 2.099(14), Au(2)-P(3) 2.267(4), Au(3)-C(3) 2.068(13), Au(3)-P(4) 2.273(4), Au(3)-Au(4) 2.9176(9), Au(4)-C(3) 2.070(14), Au(4)-P(5) 2.261(4), P(1)-C(1) 1.756(14), C(1)-C(2) 1.398(19), C(2)-C(3) 1.251(19), C(1)-Au(1)-P(2) 177.1(4), C(1)-Au(2)-P(3) 177.2(4), C(3)-Au(3)-P(4) 175.5(4), C(3)-Au(4)-P(5) 178.4(4), C(1)-C(2)-C(3) 174.1(15).

The molecular structure of complex **57** is shown in Figure 3.26. The coordination about each of the gold centres is linear and aurophilic interactions are observed with distances Au(1)-Au(2) 2.8994(10) Å and Au(3)-Au(4) 2.9176(9) Å. The C=C=C bond angle is slightly distorted from linearity with an angle C(1)-C(2)-C(3) 174.1(15)°. One of the allenyl carbon-carbon bonds is considerably shorter than the other with distances C(1)-C(2) 1.398(19) Å and C(2)-C(3) 1.251(19) Å.

To observe whether two gold(I) atoms would preferentially bind to the  $\gamma$ -carbon atom of the allenyl ligand with an aurophilic interaction, or bind one at each carbon atom, the reaction of **39a** with two equivalents of [Au(acac)(PPh<sub>3</sub>)] was carried out (Scheme 3.21). Initial NMR

studies after 10 min reaction time showed the presence of mononuclear complex **42** and unreacted starting material. However, after 10 h reaction time complex **42** was no longer observed. Two new doublets are observed in the  $^1\text{H}$  NMR spectrum and are assigned to complexes **58** and **59** (Figure 3.27(a)).  $^{31}\text{P}\{^1\text{H}\}$  NMR studies show the presence of significant amounts of triphenylphosphine oxide. The other signals can be assigned to complexes **58** and **59** (Figure 3.27(b)).



Scheme 3.21. Synthesis of complexes **58** and **59**.

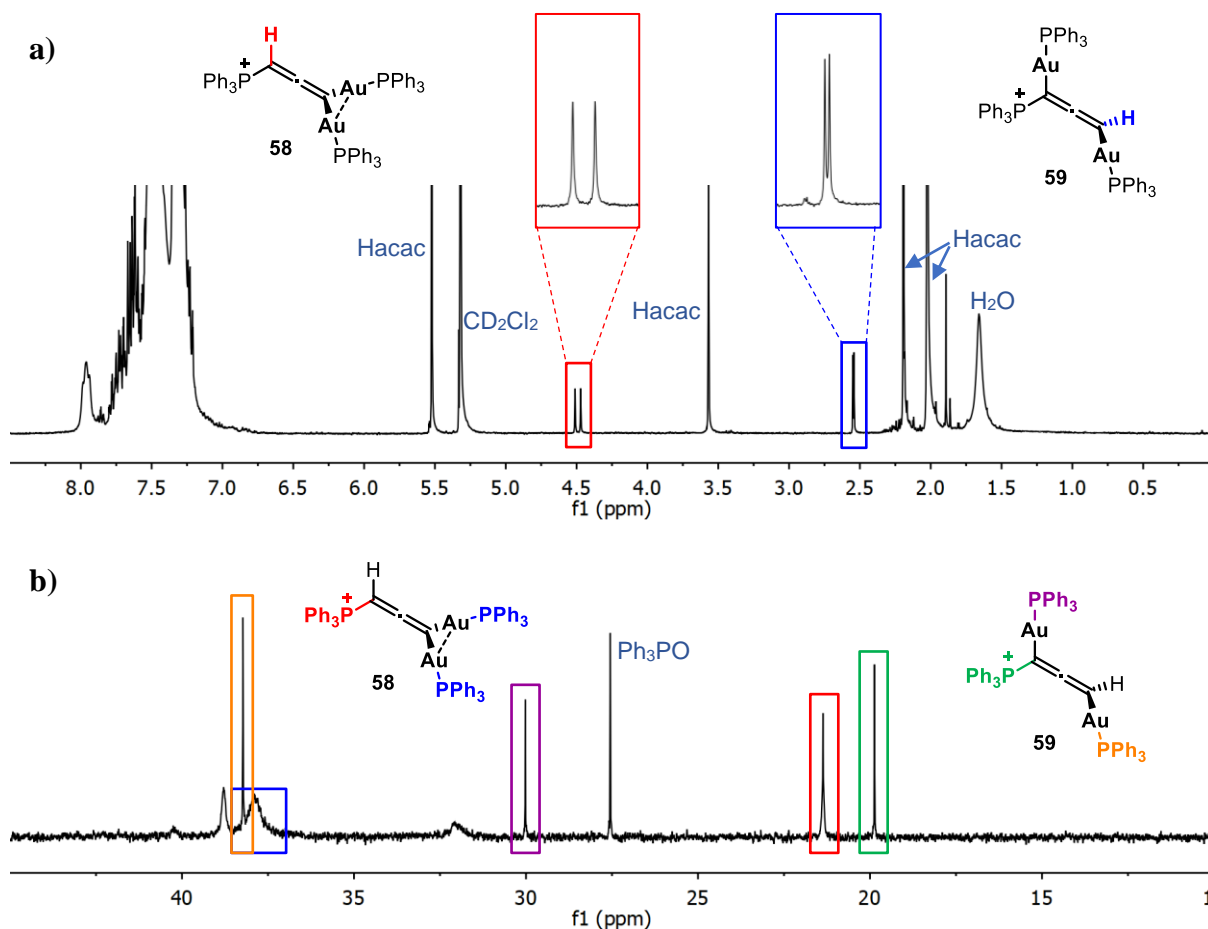
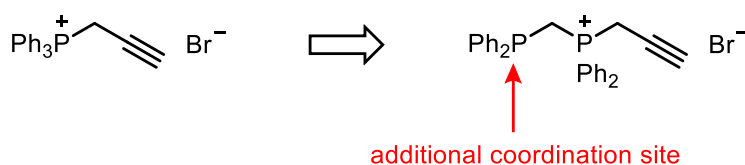


Figure 3.27.  $^1\text{H}$  NMR spectrum (a) and  $^{31}\text{P}\{^1\text{H}\}$  NMR spectrum of complexes **58** and **59** in  $\text{CD}_2\text{Cl}_2$  at room temperature.



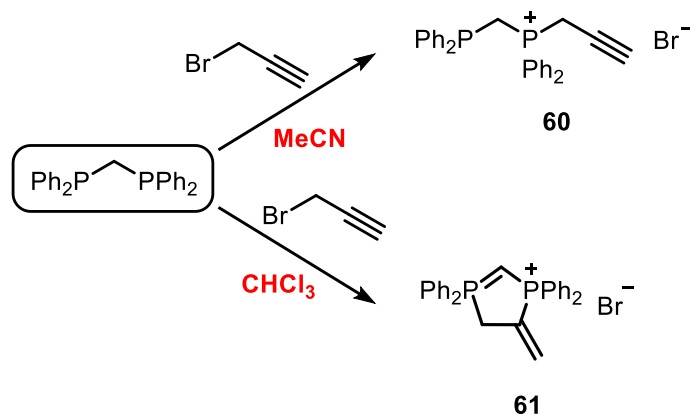
### 3.4. Propargyl Functionalised 1,1-Bis(diphenylphosphino)methane Derivatives

Following the success with the triphenylpropargylphosphonium salts, attempts were made to prepare an analogous propargyl functionalised phosphonium salt from a diphosphine, hence providing an additional coordination site.



**Figure 3.28.** Diphosphine derived propargyl phosphonium salt.

Reaction of 1,1-bis(diphenylphosphino)methane with propargyl bromide in acetonitrile did give the expected phosphonium salt, **60**, however the same reaction in chloroform led to the formation of an unusual cyclic diphosphole **61** (Scheme 3.22).



**Scheme 3.22.** Synthesis of salts **60** and **61**.

Both salts could readily be identified by NMR spectroscopy. The  $^1\text{H}$  NMR spectrum of salt **60** shows a doublet of triplets at 2.11 ppm ( $^4J_{\text{HP}} = 6.9$  Hz and  $^4J_{\text{HH}} = 2.7$  Hz) for the propargyl CH, a doublet of doublets at 4.73 ppm ( $^2J_{\text{HP}} = 15.5$  Hz and  $^4J_{\text{HH}} = 2.8$  Hz) for the propargyl CH<sub>2</sub> and a further doublet of doublets at 4.47 ppm ( $^2J_{\text{HP}} = 14.8$  Hz and  $^2J_{\text{HP}} = 1.5$  Hz) for the dppm CH<sub>2</sub> (Figure 3.29(a)). Two doublets are observed in the  $^{31}\text{P}\{^1\text{H}\}$  NMR spectrum at 25.94 ppm

for the phosphonium P and at -25.94 ppm for the phosphine P with  $^2J_{\text{PP}} = 59.1$  Hz (Figure 3.29(b)).

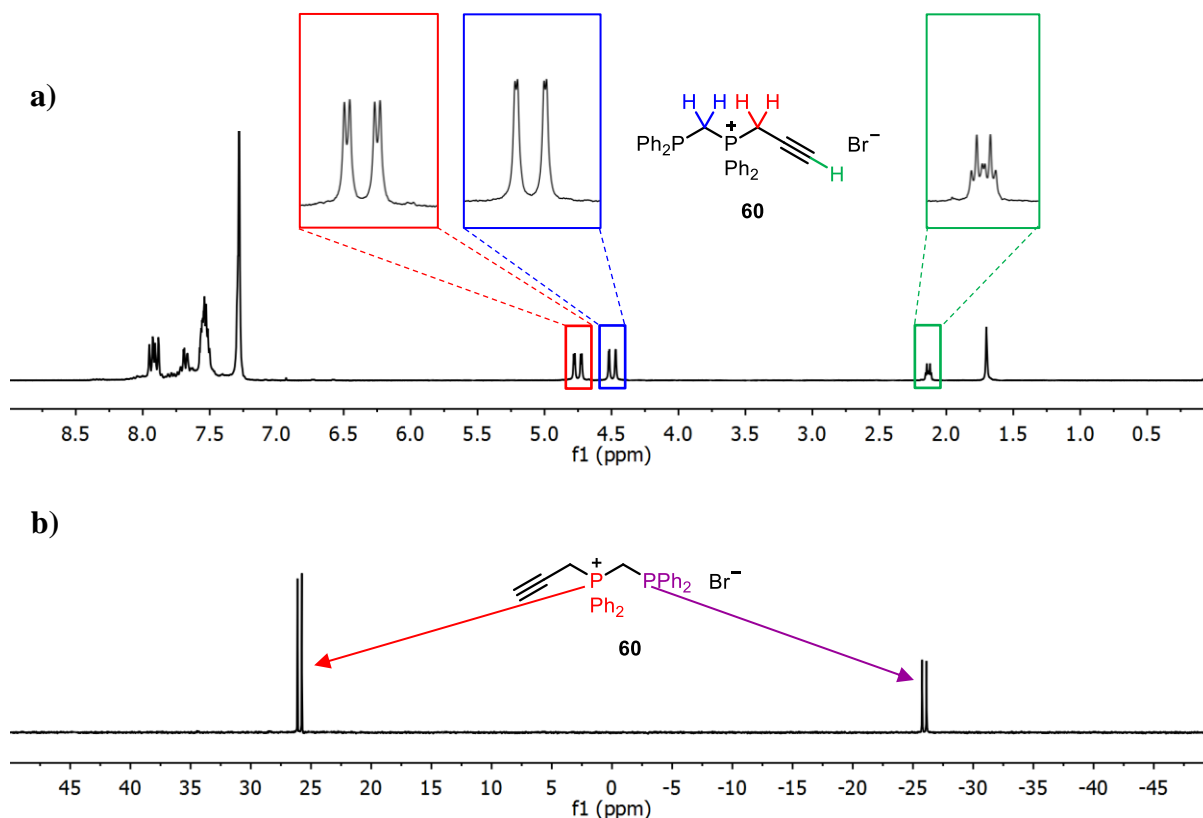


**Figure 3.29.**  $^1\text{H}$  NMR spectrum (a) and  $^{31}\text{P}\{^1\text{H}\}$  NMR spectrum (b) for salt **60** in  $\text{CDCl}_3$ .

For salt **61** four non-aromatic proton signals are observed in the  $^1\text{H}$  NMR spectrum (Figure 3.30(a)). The proton at C(1) is observed as a triplet of doublets at 2.01 ppm ( $^2J_{\text{HP}} = 6.4$  Hz,  $^5J_{\text{HH}} = 1.1$  Hz) due to coupling with the phosphorus atoms and the *trans* proton at C(4). The protons at C(2) are observed as a doublet of doublets at 4.31 ppm due to coupling with the nearest phosphorus atom and the *trans* proton at C(4). The protons at C(4) are each observed as a doublet due to coupling with the nearest phosphorus atom. The *trans* proton appears at 7.03 ppm with  $^3J_{\text{HP}} = 36.2$  Hz whereas the *cis* proton appears at 5.86 ppm with a smaller coupling constant of  $^3J_{\text{HP}} = 17.3$  Hz. The  $^{31}\text{P}\{^1\text{H}\}$  NMR spectrum is a second order spectrum for an AB spin system (Figure 3.30(b)). The calculated chemical shifts are 32.28 and 31.64 ppm with  $^2J_{\text{PP}} = 61.9$  Hz.

### 3.4. Propargyl Functionalised 1,1-Bis(diphenylphosphino)methane Derivatives

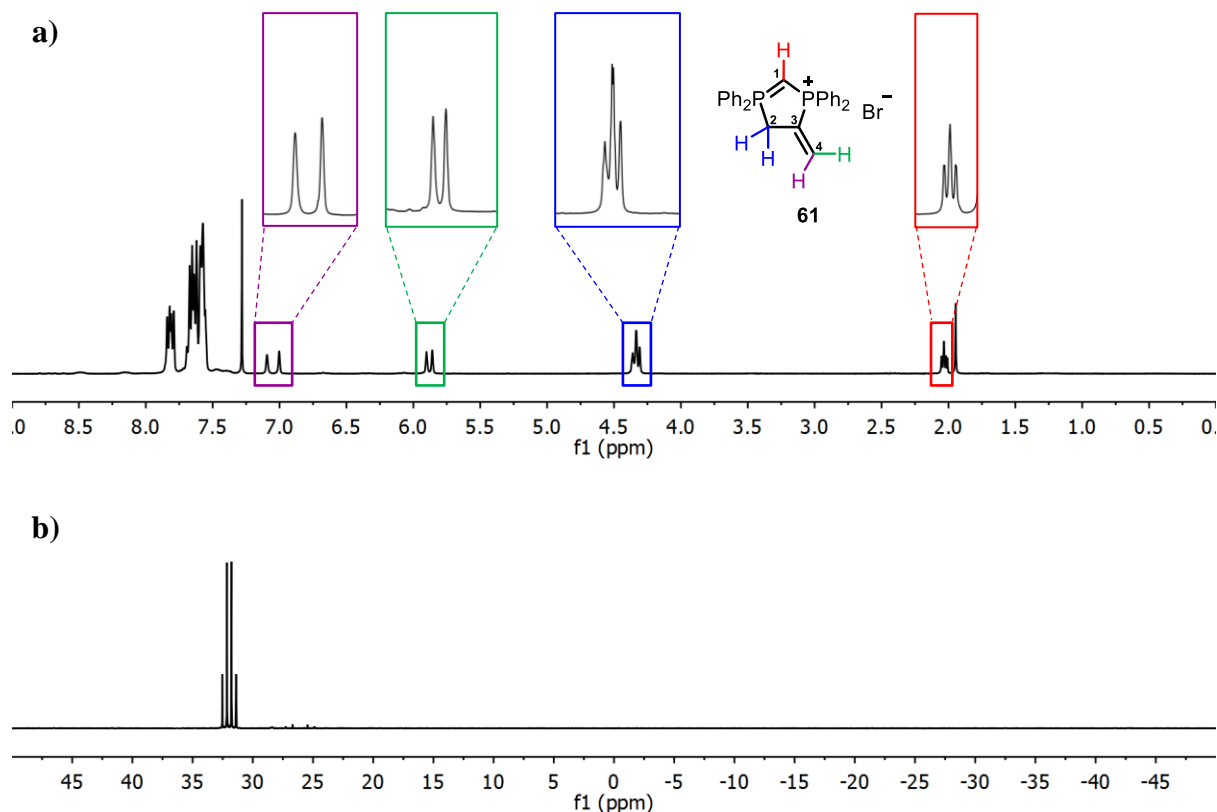


**Figure 3.30.**  $^1\text{H}$  NMR spectrum (a) and  $^{31}\text{P}\{^1\text{H}\}$  NMR spectrum (b) for salt **61** in  $\text{CDCl}_3$ .

The stability of propargylphosphonium salt **60** in solution was studied by NMR spectroscopy. In acetonitrile no isomerisation was observed after 24 h, however in solution in chloroform considerable amounts of salt **61** were observed after 24 h (Figure 3.31). The mechanism for the formation of salt **61** was suggested to proceed via first isomerisation of the propargyl unit into the allene and subsequent cyclisation to give **61** (Scheme 3.23).

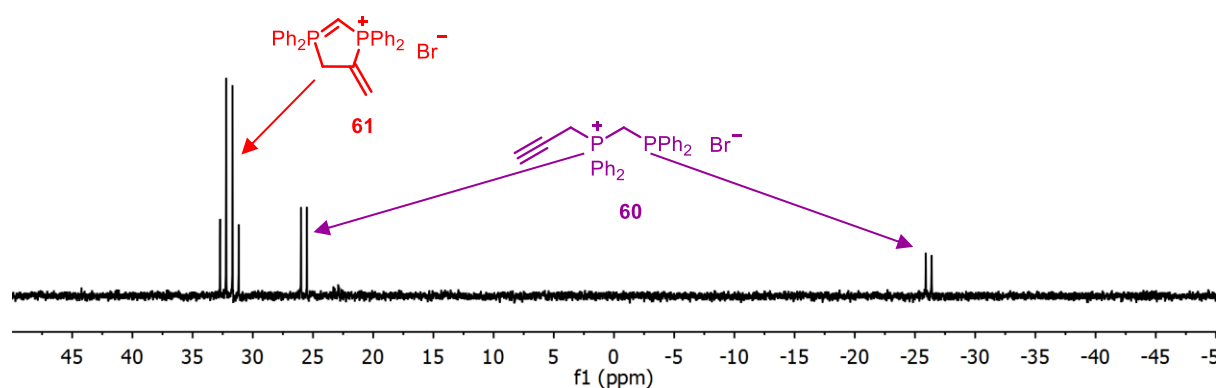
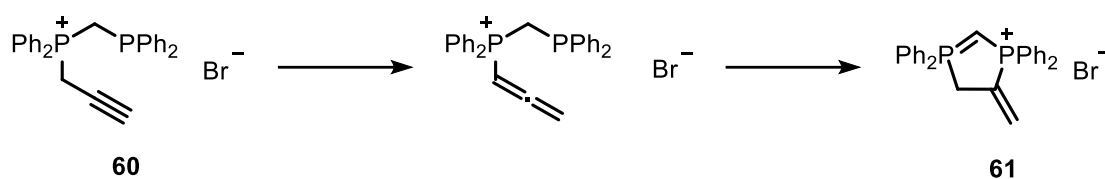
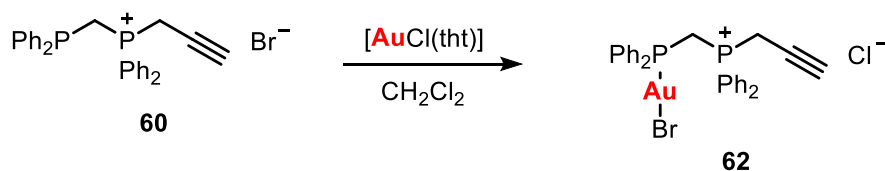


**Figure 3.31.**  $^{31}\text{P}\{^1\text{H}\}$  NMR spectrum of salt **60** after 24 h in  $\text{CDCl}_3$ .



**Scheme 3.23.** Suggested formation of salt **61**.

Reaction of salt **60** with  $[\text{AuCl}(\text{tht})]$  in dichloromethane led to the formation of complex **62** (Scheme 3.24). Coordination of the phosphine to gold could be confirmed by a change in chemical shift in the  $^{31}\text{P}\{^1\text{H}\}$  NMR spectrum of the phosphine P signal from -25.94 to 19.71 ppm. The phosphonium P signal at 23.90 ppm remains at a very similar chemical shift to that of salt **60** (Figure 3.32). No tautomerisation of the propargyl unit is observed.



**Scheme 3.24.** Synthesis of complex **62**.

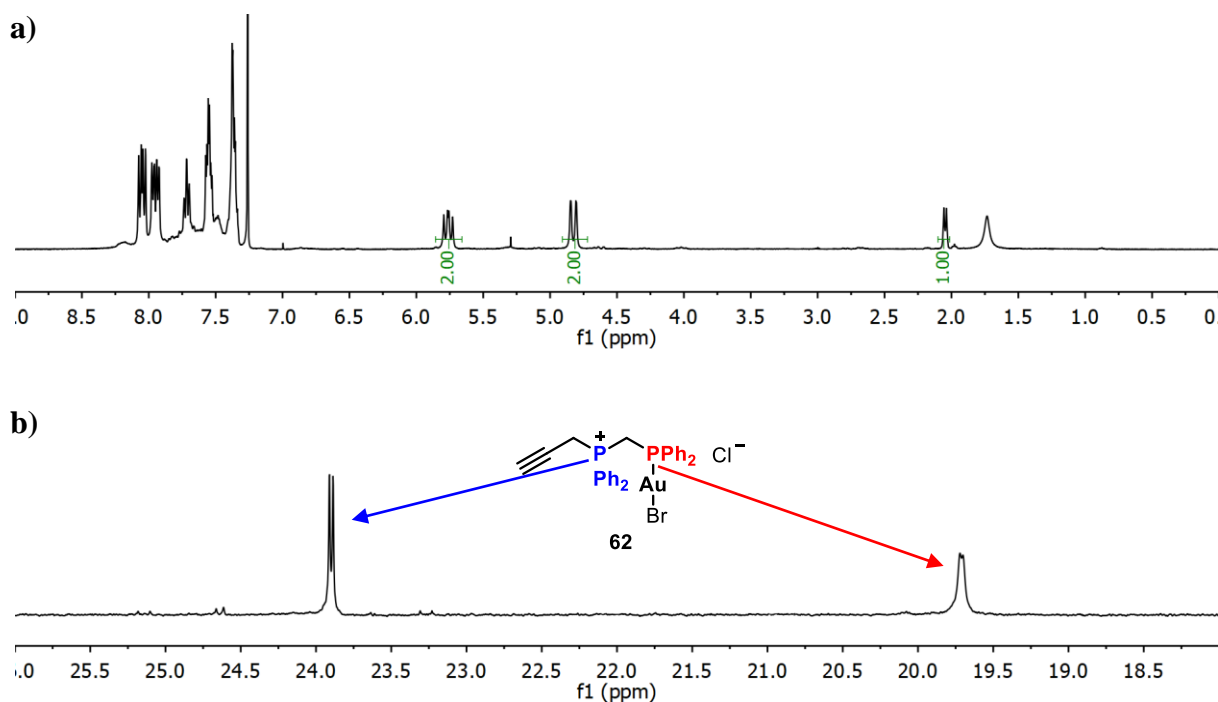
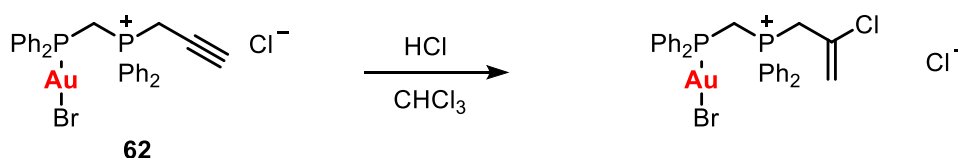


**Figure 3.32.**  $^1\text{H}$  NMR spectrum (a) and  $^{31}\text{P}\{^1\text{H}\}$  NMR spectrum (b) for complex **62**.

### 3.4. Propargyl Functionalised 1,1-Bis(diphenylphosphino)methane Derivatives

Crystals of complex **62** were grown in chloroform and measured by single crystal X-ray diffraction. The molecular structure determined was actually that of complex **62** following the addition of HCl to the alkyne triple bond (Scheme 3.25). This reaction is likely to have occurred upon crystallisation due to significant amounts of HCl in the chloroform used to grow the crystals.



**Scheme 3.25.** Addition of HCl to complex **62**.

The molecular structure is shown in Figure 3.33. The coordination of the phosphine to the gold can clearly be seen.

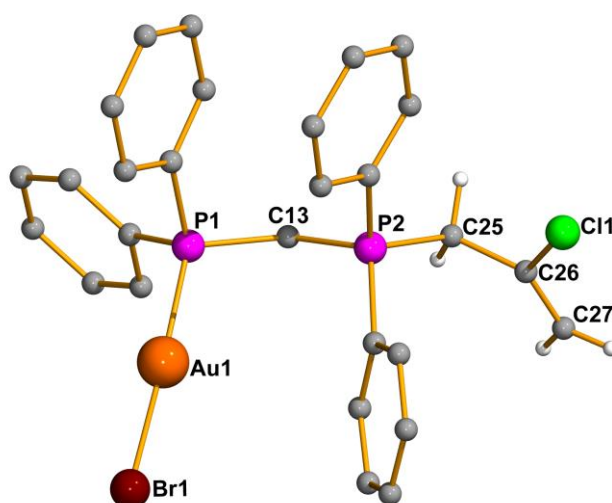
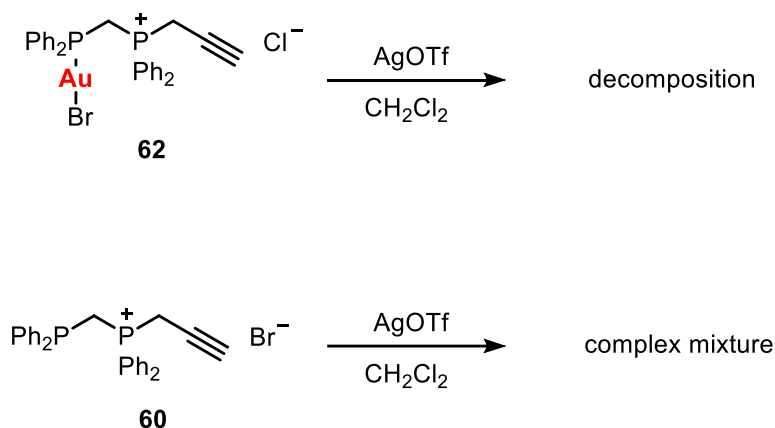


**Figure 3.33.** Molecular structure of the complex formed upon addition of HCl to **62** determined by single crystal X-ray diffraction. Phenyl hydrogen atoms, anions and solvent molecules are omitted for clarity. Selected bond lengths [Å] and angles [°]: Au(1)-P(1) 2.2331(19), Au(1)-Br(1) 2.3858(12), P(1)-C(13) 1.836(7), P(2)-C(13) 1.801(7), P(2)-C(25) 1.818(8), C(25)-C(26) 1.490(10), C(26)-Cl(1) 1.727(8), C(26)-C(27) 1.333(12), P(1)-Au(1)-Br(1) 174.93(6).

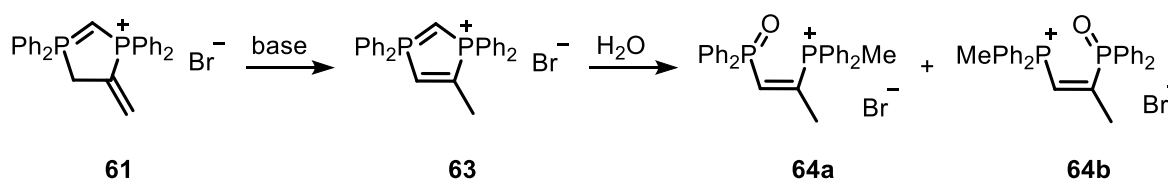
In order to prepare further derivatives from complex **62**, attempts were made to change the chloride anion for a less coordinating triflate anion. Reaction of complex **62** with a stoichiometric amount of silver triflate led to rapid decomposition. An alternative route

involving changing the anion before the coordination to gold, i.e. by reaction of salt **60** with silver triflate led to a mixture of products, likely due to coordination of the silver to the free phosphine group (Scheme 3.26).



**Scheme 3.26.** Attempts to exchange the halide anion for triflate.

Attempts were also made to prepare coordination complexes from salt **61**, however these proved unsuccessful (Scheme 3.27). **61** slowly isomerises to **63** in solution. This reaction also occurs more rapidly in the presence of a base. The formation of **63** could readily be identified by NMR spectroscopy due to the loss of the vinylic CH signals and the presence of a new CH<sub>3</sub> signal. The <sup>31</sup>P{<sup>1</sup>H} NMR spectrum shows two doublets. Salt **63** was found to be unstable towards hydrolysis, readily forming the hydrolysis products **64a** and **64b** which could be identified by mass spectrometry.

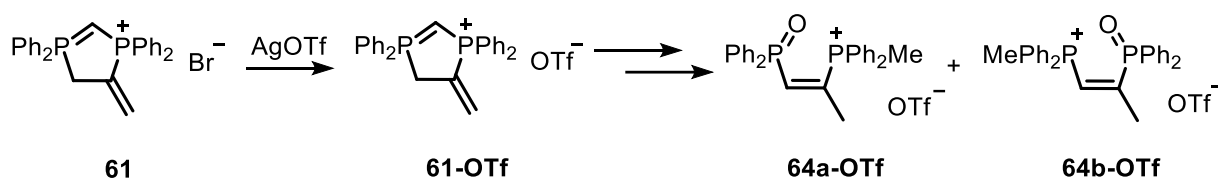


**Scheme 3.27.** Reactions of salt **61**.

Reaction of salt **61** with silver triflate did successfully give the salt **61-OTf** following the precipitation of silver bromide (Scheme 3.28). Attempts to grow crystals of this salt were made but the crystals obtained were actually of the triflate derivative of complex **64a**. This is because over time in solution salt **61-OTf** isomerises to the methyl derivative **63-OTf** and this then

### 3.4. Propargyl Functionalised 1,1-Bis(diphenylphosphino)methane Derivatives

undergoes hydrolysis. The molecular structure determined by single crystal X-ray diffraction is shown in Figure 3.34.



**Scheme 3.28.** Reactions of salt **61**.

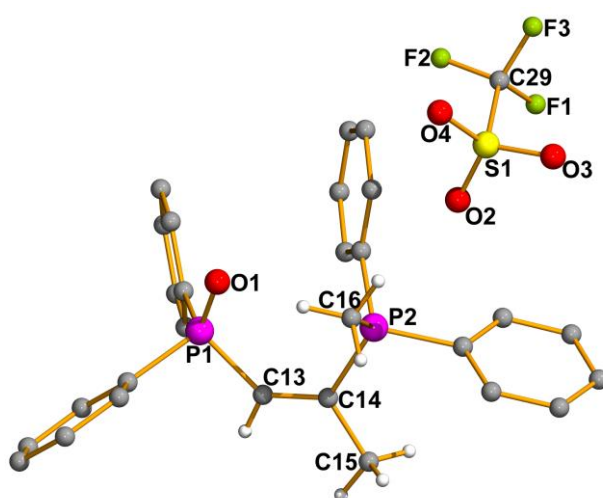
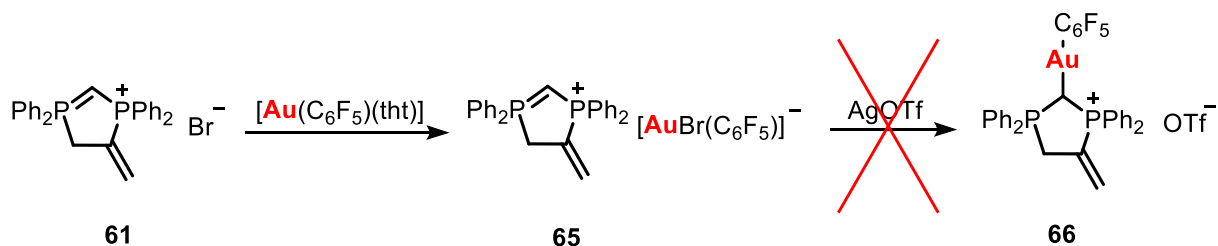


**Figure 3.34.** Molecular structure of **64a-OTf** determined by single crystal X-ray diffraction. Phenyl hydrogen atoms are omitted for clarity. Selected bond lengths [Å] and angles [°]: P(1)-O(1) 1.4860(13), P(1)-C(13) 1.8019(18), C(13)-C(14) 1.335(2), C(14)-C(15) 1.511(2), C(14)-P(2) 1.8264(17), P(2)-C(16) 1.7820(19).

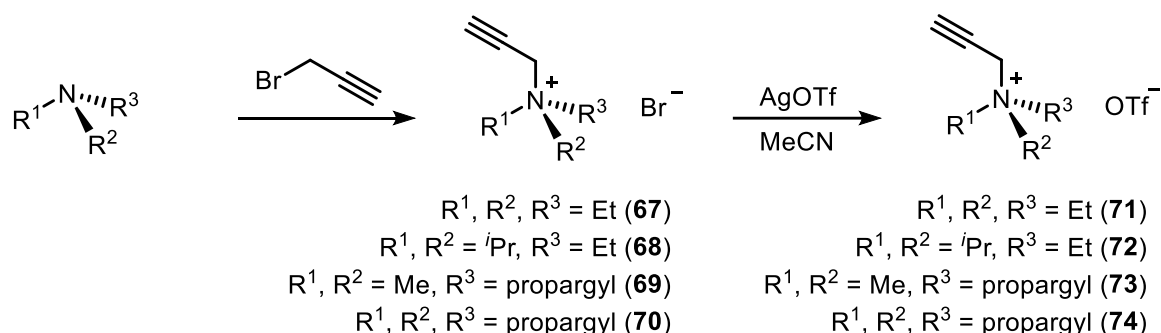
Reaction of salt **61** with  $[\text{Au}(\text{C}_6\text{F}_5)(\text{tht})]$  gave the aurate salt **65**. This could readily be identified by NMR studies with the diphosphole unit observed in the  $^1\text{H}$  and  $^{31}\text{P}\{^1\text{H}\}$  NMR spectra. The  $^{19}\text{F}$  NMR spectrum clearly shows the presence of the  $\text{C}_6\text{F}_5$  ligand. Attempts to coordinate gold to the ylide-type carbon of diphosphole unit by abstraction of the bromide ligand with silver triflate to form complex **66**, gave a mixture of products.



**Scheme 3.29.** Synthesis of **65** and attempted synthesis of **66**.

### 3.5. Propargyl Functionalised Ammonium Salt Derivatives

To compare the difference in reactivity between propargyl functionalised phosphonium salts and ammonium salts, a series of propargyl functionalised ammonium salts were prepared by reaction of amines with propargyl bromide. In all cases the ammonium salts formed cleanly as highly insoluble solids, soluble only in DMSO and acetonitrile. The more soluble triflate salts were prepared by reaction of the ammonium bromide salts with silver triflate in acetonitrile (Scheme 3.30).

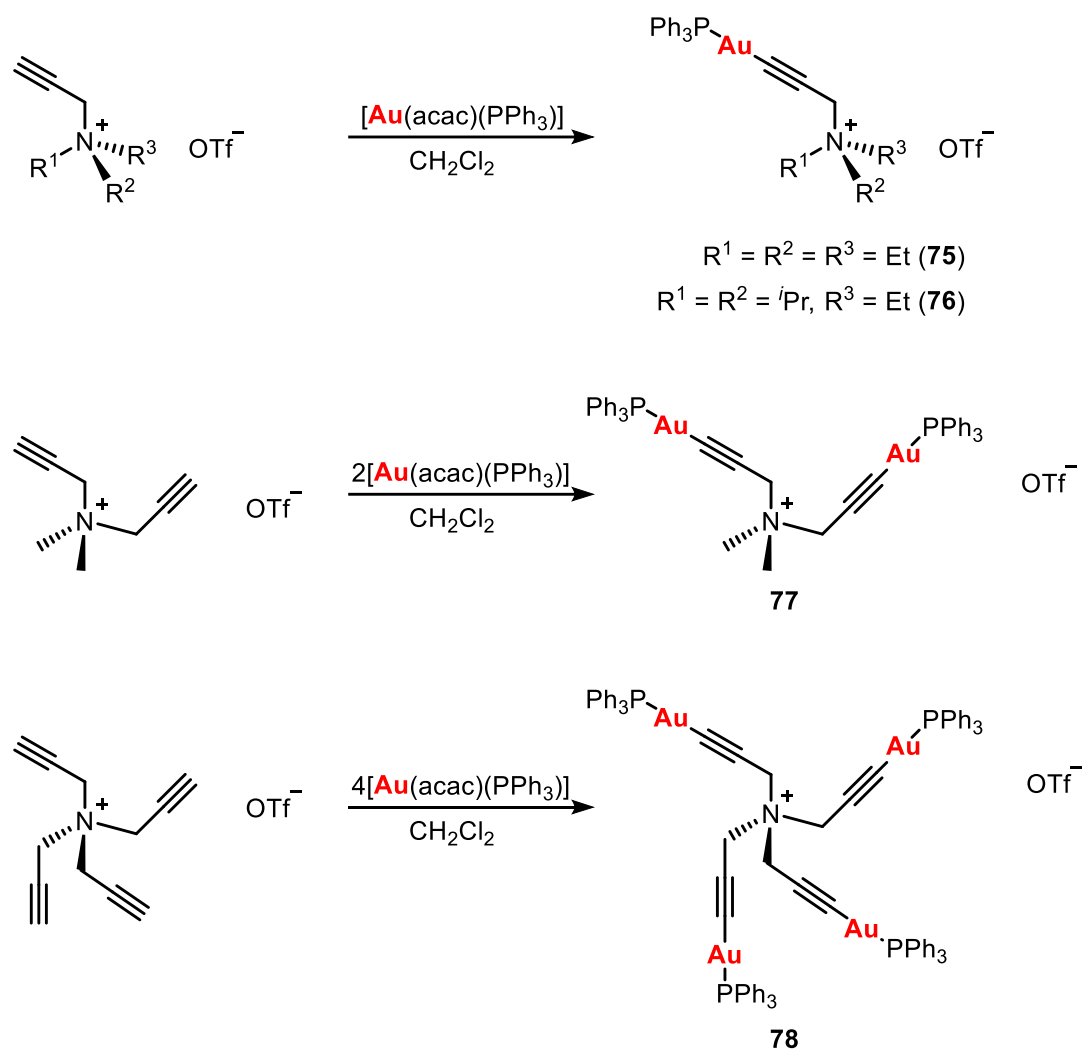


**Scheme 3.30.** Synthesis of salts **67-74**.

Reaction of the ammonium salts, **71-74** with [Au(acac)(PPh<sub>3</sub>)] in dichloromethane gave complexes **75-78** in good yields 68-90% (Scheme 3.31). The loss of the propargyl CH signal in the <sup>1</sup>H NMR spectra confirms coordination of the gold at the terminal C of the propargyl unit. Only one signal at around 40 ppm is observed in the <sup>31</sup>P{<sup>1</sup>H} NMR spectrum in each case.



### 3.5. Propargyl Functionalised Ammonium Salt Derivatives



**Scheme 3.31.** Synthesis of complexes **75-78**.

**Table 3.5.** Selected  $^1\text{H}$  NMR and  $^{31}\text{P}\{^1\text{H}\}$  NMR Peaks for Complexes **75-78** in  $\text{CH}_2\text{Cl}_2$ .

Complex	$^1\text{H}$ NMR $\text{C}_\alpha\text{-H}$ (ppm)	$^{31}\text{P}\{^1\text{H}\}$ NMR (ppm)
<b>75</b>	3.99	41.17
<b>76</b>	4.10	41.22
<b>77</b>	4.27	41.23
<b>78</b>	4.45	41.25

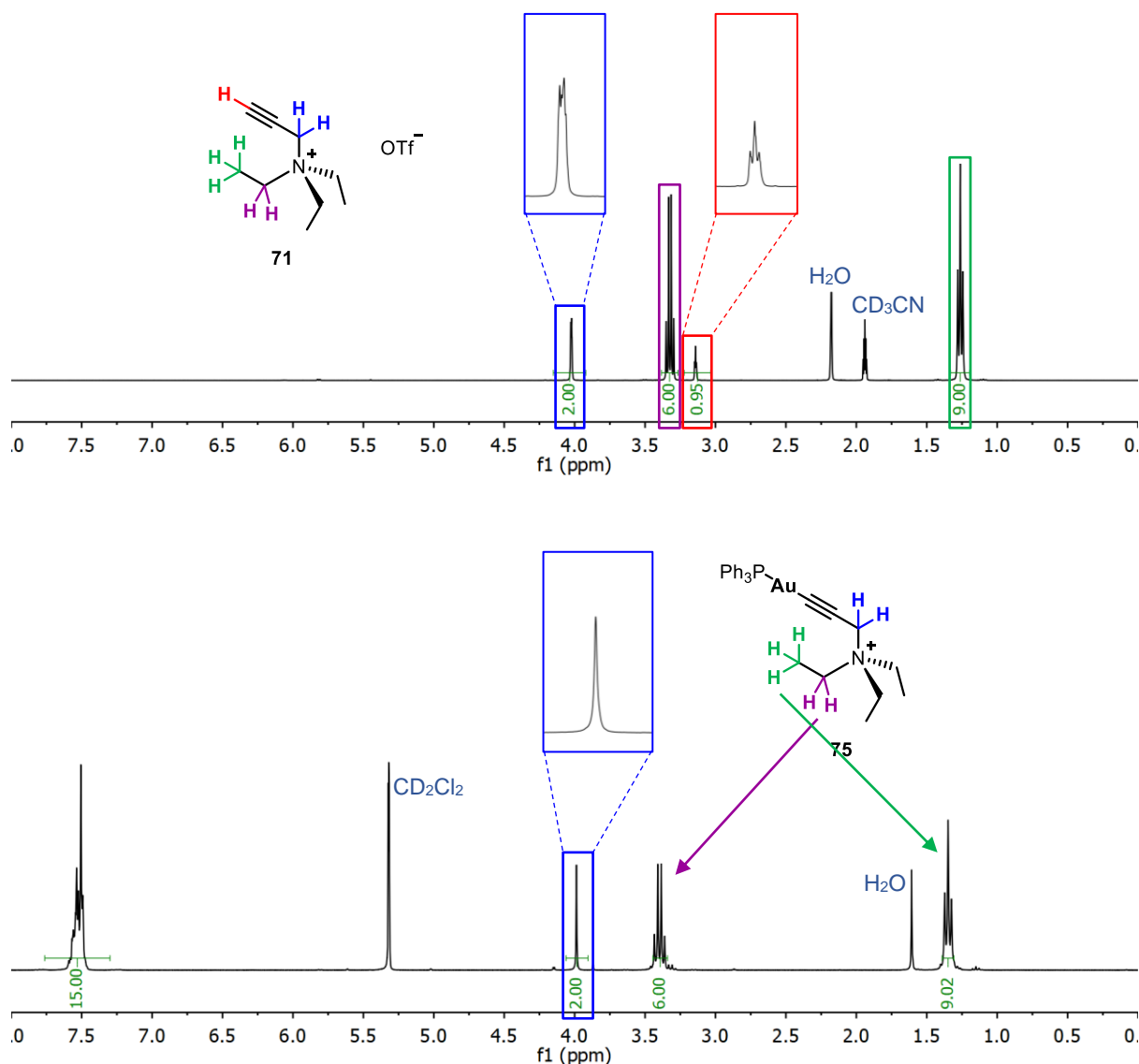


**Figure 3.35.**  $^1\text{H}$  NMR spectrum of **71** in  $\text{CD}_3\text{CN}$  (a) and **75** in  $\text{CD}_2\text{Cl}_2$  (b) at room temperature.

**Table 3.6.** Selected Infrared Absorption Frequencies for Complexes **75-78**.

Complex	$\nu(\text{C}\equiv\text{C})$ ( $\text{cm}^{-1}$ )
<b>75</b>	2146
<b>76</b>	2144
<b>77</b>	2142
<b>78</b>	2141

Complexes **75-78** display an absorption band in the IR spectrum at around  $2140\text{ cm}^{-1}$  corresponding to the  $\text{C}\equiv\text{C}$  stretch. No allene band is observed indicating that no tautomerisation to the allene occurred in any case. This is not surprising since in order to tautomerise

deprotonation at the propargyl CH<sub>2</sub> would have to occur, forming a nitrogen ylide. Nitrogen ylides are far less stable than their phosphorus analogues since a  $\pi$ -bond cannot form between the ammonium nitrogen atom and the carbon, and stabilisation occurs only through electrostatic interactions.

Complex **78** was characterised by single crystal X-ray diffraction (Figure 3.36).

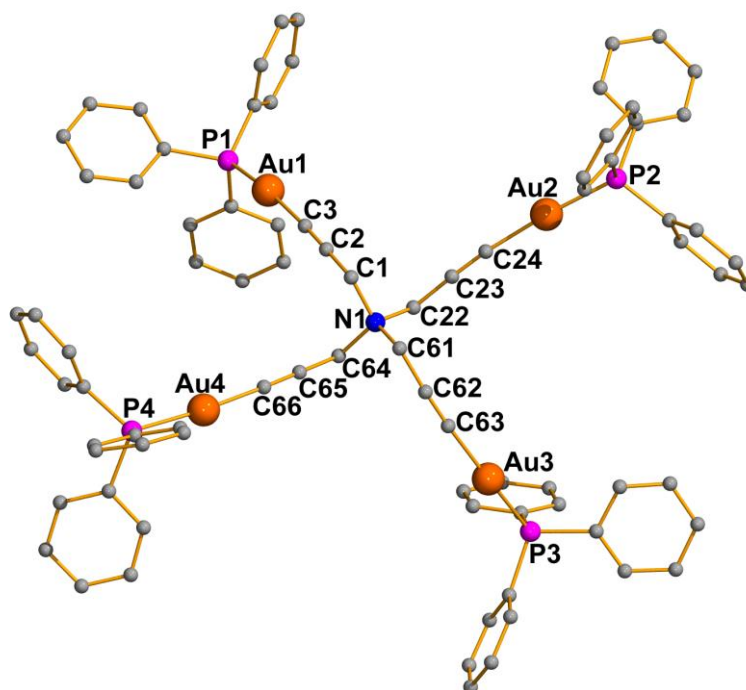


**Figure 3.36.** Molecular structure of **78** determined by single crystal X-ray diffraction. Phenyl hydrogen atoms, anions and solvent molecules are omitted for clarity. Selected bond lengths [Å] and angles [°]: Au(1)-C(3) 1.990(16), Au(1)-P(1) 2.275(4), Au(2)-C(24) 2.000(17), Au(2)-P(2) 2.264(4), Au(3)-P(3) 2.271(4), Au(3)-C(63) 2.02(2), Au(4)-C(66) 1.977(17), Au(4)-P(4) 2.274(4), N(1)-C(1) 1.501(18), N(1)-C(22) 1.505(18), N(1)-C(61) 1.521(18), N(1)-C(64) 1.520(18), C(1)-C(2) 1.46(2), C(2)-C(3) 1.22(2), C(22)-C(23) 1.43(2), C(23)-C(24) 1.20(2), C(61)-C(62) 1.45(2), C(62)-C(63) 1.18(2), C(64)-C(65) 1.45(2), C(65)-C(66) 1.22(2), C(3)-Au(1)-P(1) 170.7(5), C(24)-Au(2)-P(2) 173.6(4), C(63)-Au(3)-P(3) 169.8(4), C(66)-Au(4)-P(4) 176.0(5), C(1)-C(2)-C(3) 179.4(16), C(22)-C(23)-C(24) 175.8(16), C(61)-C(62)-C(63) 176.3(16), C(64)-C(65)-C(66) 173.7(15).

A distorted linear coordination is observed about each gold atom with angles C(3)-Au(1)-P(1) 170.7(5)°, C(24)-Au(2)-P(2) 173.6(4)°, C(63)-Au(3)-P(3) 169.8(4)° and C(66)-Au(4)-P(4) 176.0(5)°. This distortion is likely to be due to steric hindrance between the bulky triphenylphosphine ligands. The propargyl units are maintained as evidenced by the carbon-

carbon bond lengths C(1)-C(2) 1.46(2) Å and C(2)-C(3) 1.22(2) Å, typical values for a single and triple bond, respectively. The C-C≡C bond angles are practically linear in each case.

The molecules of **78** are linked by intermolecular aurophilic interactions creating a polymeric structure (Figure 3.37) with distances Au(1)-Au(4A) 3.5056(11) Å and Au(2)-Au(3) 3.1888(9) Å.

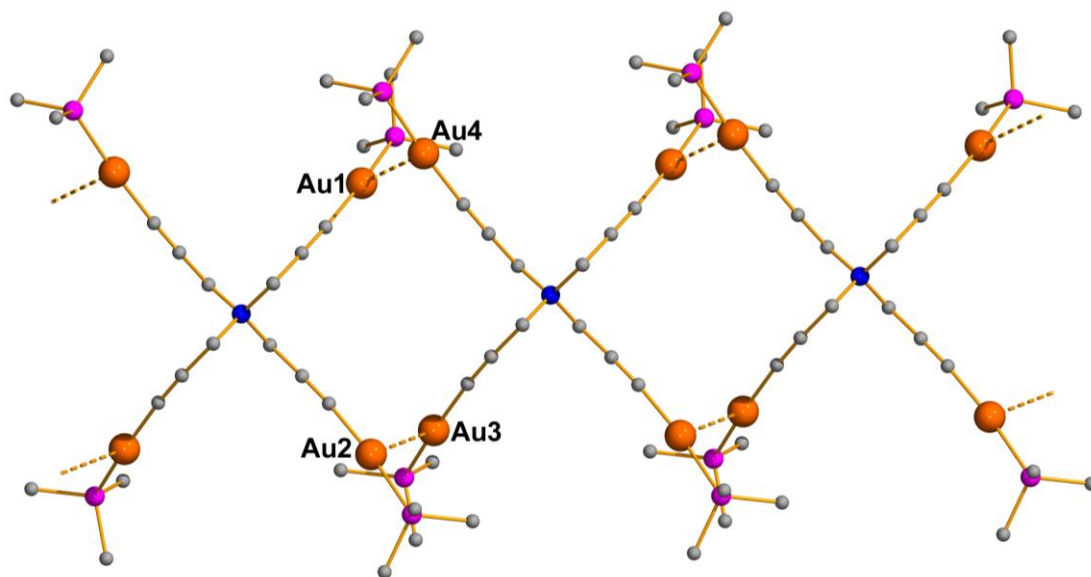
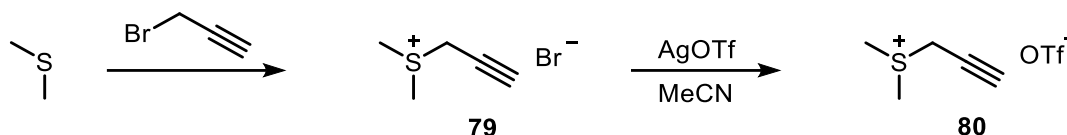


**Figure 3.37.** Intramolecular aurophilic interactions in the structure of **78**.

### 3.6. Propargyl Functionalised Sulfonium Salt Derivatives

A propargyl functionalised sulfonium salt was prepared by reaction of dimethylsulfide with propargyl bromide. The sulfonium bromide salt **79** was highly insoluble and was therefore reacted with silver triflate in acetonitrile to give the sulfonium triflate salt **80** (Scheme 3.32).



**Scheme 3.32.** Synthesis of salt **79** and **80**.

As with the phosphonium salt **38**, the solvent dependence of the isomeric form of **80** in solution was studied by NMR spectroscopy. In all solvents after 24 h only the propargyl tautomer was observed with no formation of the allene derivative. Refluxing the salt in acetonitrile for 1 week, however, did lead to some conversion to the allene tautomer (Figure 3.38).

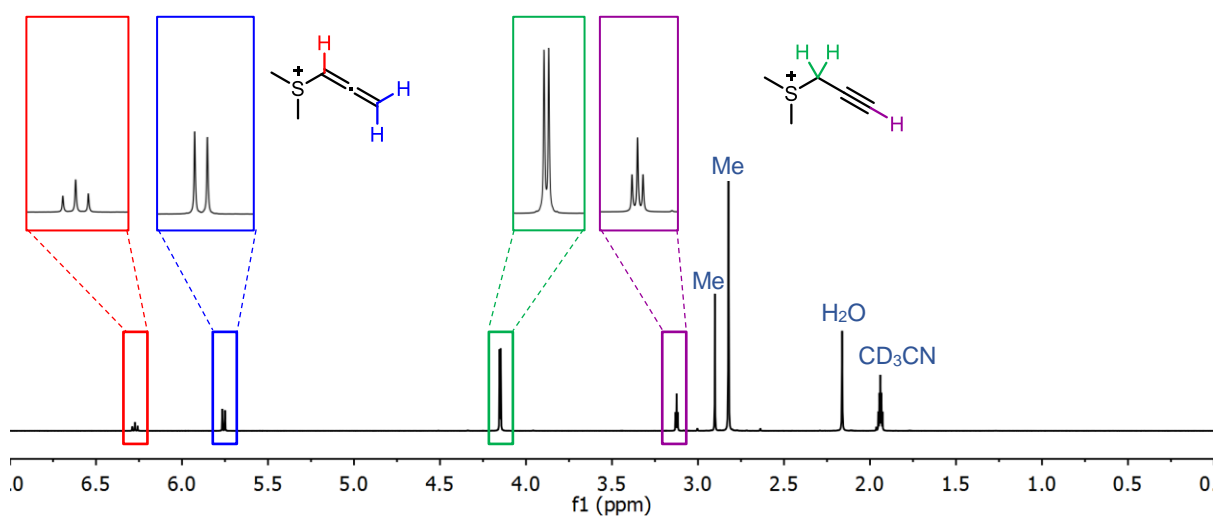
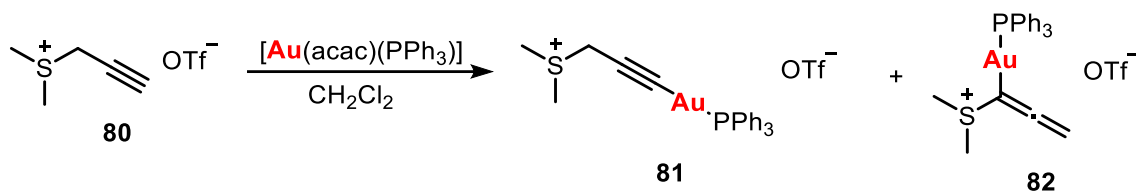


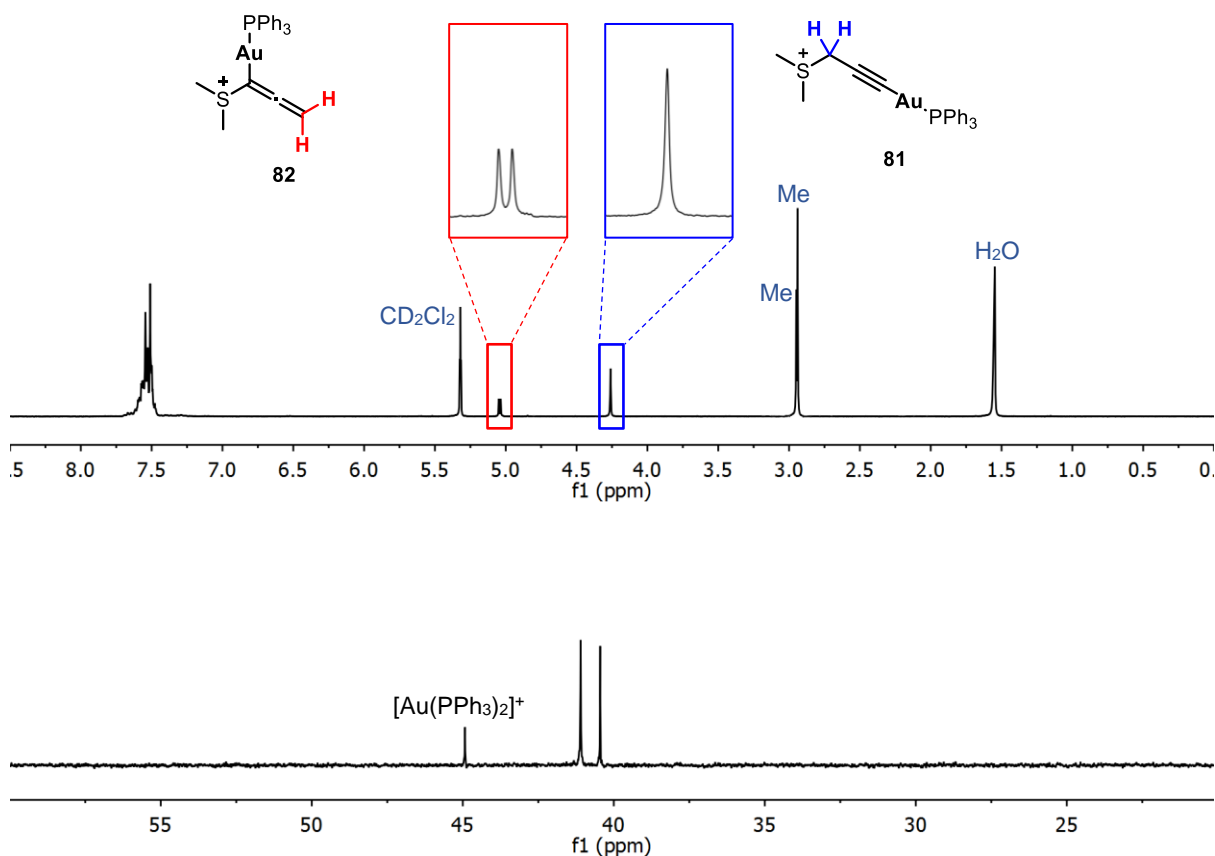
**Figure 3.38.** <sup>1</sup>H NMR spectrum of salt **80** after 1 week at reflux in CD<sub>3</sub>CN.

Reaction of salt **80** with [Au(acac)(PPh<sub>3</sub>)] in dichloromethane led to the formation of a mixture of complexes **81** and **82** (Scheme 3.33).



**Scheme 3.33.** Synthesis of complexes **81** and **82**.

The propargyl  $\text{CH}_2$  in complex **81** appears as a singlet at 4.26 ppm in the  $^1\text{H}$  NMR spectrum. The allenyl  $\text{CH}_2$  in complex **82** appears as a doublet at 5.04 ppm ( $^5J_{\text{HP}} = 4.0$  Hz) due to coupling with the triphenylphosphine group. A singlet for each complex is observed in the  $^{31}\text{P}\{^1\text{H}\}$  NMR spectrum of the mixture. A small peak at 44.93 ppm is also observed due to the formation of small amounts of  $[\text{Au}(\text{PPh}_3)_2]^+$ .

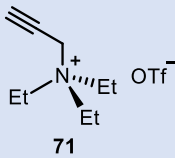
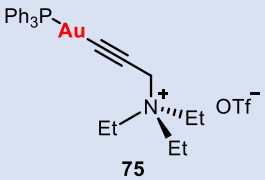
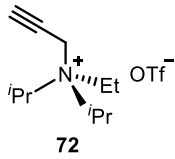
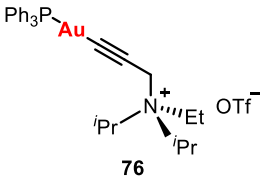
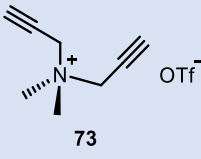
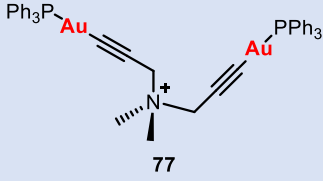
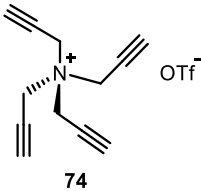
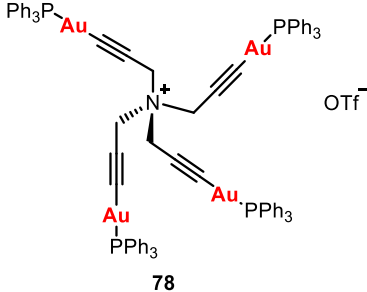


**Figure 3.39.**  $^1\text{H}$  NMR spectrum (a) and  $^{31}\text{P}\{^1\text{H}\}$  NMR spectrum (b) of complexes **81** and **82** in  $\text{CD}_2\text{Cl}_2$ .

### 3.7. Biological Activity

Since propargyl gold phosphine complexes are known to exhibit anticancer activity, the activity of the propargyl ammonium salt derivatives, **75-78** was studied in cancer cell line A549. The activity of the corresponding ammonium salts **71-74** was also tested. The MTT assay was used as described in Chapter 2. The calculated  $IC_{50}$  values are shown in Table 3.7.

**Table 3.7.**  $IC_{50}$  values for Salts **71-74** and Complexes **75-78** after 24 h Incubation with A549 Cells

Complex	$IC_{50}$ ( $\mu$ M)	Complex	$IC_{50}$ ( $\mu$ M)
 71	>50	 75	$14.85 \pm 1.96$
 72	>50	 76	$15.38 \pm 1.28$
 73	>50	 77	$5.24 \pm 0.64$
 74	>50	 78	>50

None of the ammonium salts showed any anticancer activity towards A549 cells. Complexes **75** and **76** bearing one -AuPPh<sub>3</sub> unit showed very similar activities with  $IC_{50}$  values of 14.85  $\mu$ M and 15.38  $\mu$ M, respectively. Complex **77** with an additional -AuPPh<sub>3</sub> unit showed a

significantly improved anticancer activity with an incredibly low  $IC_{50}$  value of  $5.24 \mu M$ . The graph of cell viability (% of control) against concentration for complexes **75-77** clearly shows an improvement in activity at low concentrations (Figure 3.40). Complex **78** bearing four  $AuPPh_3$  units was expected to show a high anticancer activity, however this complex had limited solubility in the cell culture medium and precipitated during the experiment and hence did not show anticancer activity.

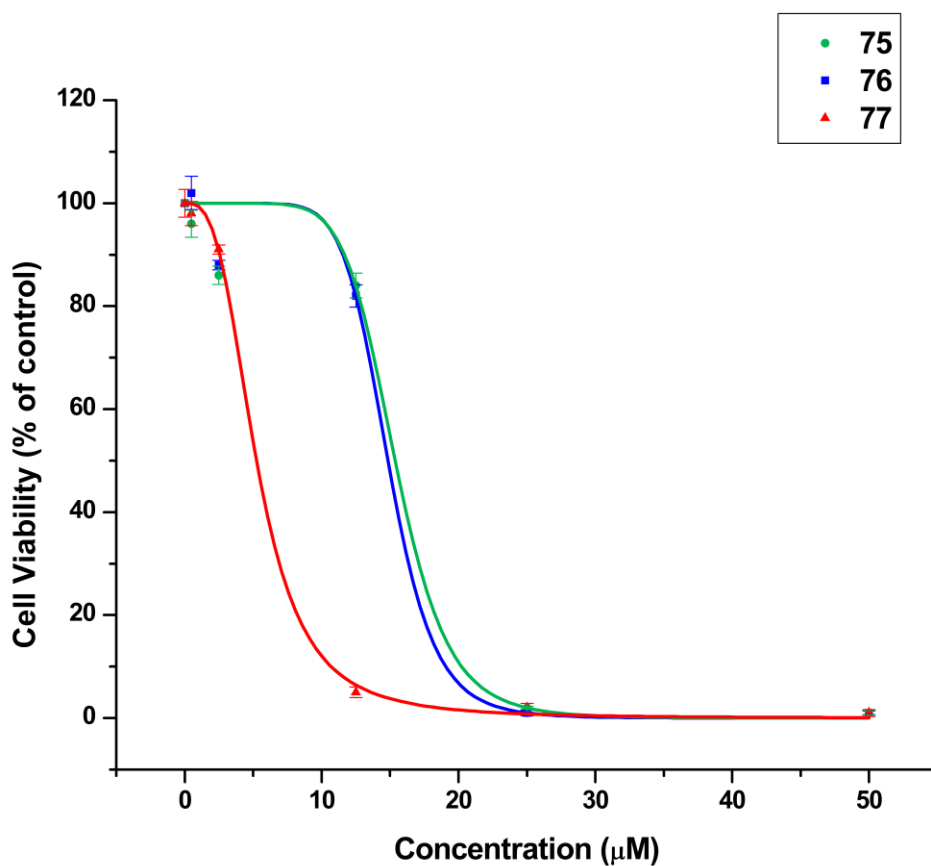


**Figure 3.40.** Graph of cell viability (% of control) against concentration ( $\mu M$ ) for complexes **75-77** (Each point is the average of eight measurements, where error bars represent the standard deviation. Curve generated by a sigmoidal non-linear regression 4-parameter logistic analysis).



## 3.8. Conclusions

In this chapter the coordination chemistry of propargyl functionalised phosphonium, ammonium and sulfonium salts with gold has been explored.

The tautomeric behaviour of triphenylpropargylphosphonium bromide in solution in different solvents has been studied. The results show that in all solvents except acetonitrile tautomerisation to the allenyl isomer occurs at room temperature. Heating a solution of the phosphonium salt increased the rate of this process with full tautomerisation to the allenyl form observed after 10 min at 40 °C.

Triphenylpropargylphosphonium bromide has successfully been used to prepare the first examples of allenyl gold complexes, with the structures unambiguously determined by single crystal X-ray diffraction. Stability experiments found the complexes to be highly stable in solution. An interesting regioselectivity was observed between gold(I) and gold(III), with gold(I) binding preferentially to the  $\alpha$ -carbon of the allenyl ligand, despite the presence of sterically bulky ligands. Gold(III), however, was found to bind to the  $\gamma$ -carbon of the allenyl ligand. When two gold(I) atoms were present, coordination at the  $\gamma$ -carbon was preferable due to the possibility of the formation of a stabilising *aurophilic* interaction.

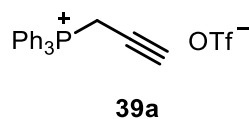
A propargyl functionalised derivative of dppm has also been prepared. In all solvents other than acetonitrile a cyclisation was observed forming a cyclic diphosphole species. This was presumed to proceed via the allenyl intermediate and hence did not occur in acetonitrile where the propargyl-allenyl tautomerism is disfavoured. Attempts were made to prepare coordination complexes of both the cyclic and open derivatives, however this was complicated due to the instability of the ligand towards hydrolysis in solution.

Several propargyl functionalised ammonium salts were prepared. No tautomerisation to the allenyl forms was observed in solution. Gold(I) triphenylphosphine derivatives were prepared with coordination to gold through the terminal alkyne carbon of the propargyl unit in each case.

A propargyl functionalised sulfonium salt was prepared. No tautomerisation to the allenyl form was observed in solution in any solvent at room temperature over time, however after reflux for 1 week a small amount of the allenyl tautomer was observed. Reaction of the propargyl sulfonium salt with  $[\text{Au}(\text{acac})(\text{PPh}_3)]$  led to a mixture of the propargyl and allenyl products which could readily be identified by NMR spectroscopy.

The biological activity of the propargyl ammonium derivatives was studied. The ammonium salts were found to show no anticancer activity, however, the gold derivatives showed an excellent activity against A549 cells. The presence of more than one gold triphenylphosphine unit increased the activity. However, the tetranuclear derivative lacked solubility in the cell culture medium and hence showed no antiproliferative activity.

### 3.9. Experimental



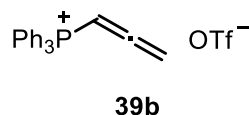
To a solution of  $[\text{Ph}_3\text{PCH}_2\text{C}\equiv\text{CH}]\text{Br}$  (0.0763 g, 0.2 mmol) in  $\text{CH}_2\text{Cl}_2$  (20 ml) was added  $\text{AgOTf}$  (0.0514 g, 0.2 mmol) and the mixture stirred for 2 h at room temperature with the exclusion of light. The mixture was filtered through celite and the resulting colourless solution concentrated under reduced pressure to approximately 2 ml. The product was precipitated with *n*-hexane, collected by vacuum filtration and dried to give **39a** as a white solid (0.0836 g, 93 %).

**IR** ( $\text{cm}^{-1}$ )  $\nu(\text{C}\equiv\text{C}-\text{H})$  3261,  $\nu(\text{OTf})$  1282 ( $\text{SO}_3$ ), 1246 ( $\text{CF}_3$ ), 1159 ( $\text{CF}_3$ ), 1029 ( $\text{SO}_3$ ).

**$^1\text{H}$  NMR (400 MHz,  $\text{CDCl}_3$ )**  $\delta$  2.24 (dt,  $^4J_{\text{HP}} = 6.8$  Hz and  $^4J_{\text{HH}} = 2.8$  Hz, 1H, CH), 4.48 (dd,  $^2J_{\text{HP}} = 15.2$  Hz and  $^4J_{\text{HH}} = 2.8$  Hz, 2H,  $\text{CH}_2$ ), 7.61 – 7.79 (m, 15H, Ph).

**$^{31}\text{P}\{^1\text{H}\}$  NMR (162 MHz,  $\text{CDCl}_3$ )**  $\delta$  21.97 (s,  $\text{PPh}_3$ ).

**$^{19}\text{F}$  NMR (376 MHz,  $\text{CDCl}_3$ )**  $\delta$  -78.24 (s, OTf).



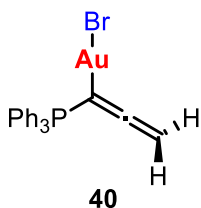
A solution of **39a** (0.0100 g) in  $\text{CDCl}_3$  was heated to 40 °C for 10 min. NMR studies indicated full conversion to the product. Removal of solvent gave the product as a pale orange solid.

**IR** ( $\text{cm}^{-1}$ )  $\nu(\text{C}=\text{CH}_2)$  3055,  $\nu(\text{C}=\text{C}=\text{C})$  1909,  $\nu(\text{OTf})$  1262 ( $\text{SO}_3$ ), 1222 ( $\text{CF}_3$ ), 1145 ( $\text{CF}_3$ ), 1029 ( $\text{SO}_3$ ).

**$^1\text{H}$  NMR (400 MHz,  $\text{CDCl}_3$ )**  $\delta$  5.24 (dd,  $^2J_{\text{HP}} = 12.8$  Hz and  $^4J_{\text{HH}} = 6.4$  Hz, 2H,  $\text{CH}_2$ ), 6.90 (dt,  $^4J_{\text{HP}} = 8.0$  Hz and  $^4J_{\text{HH}} = 6.4$  Hz, 1H, CH), 7.57 – 7.79 (m, 15H, Ph).

**$^{31}\text{P}\{^1\text{H}\}$  NMR (162 MHz,  $\text{CDCl}_3$ )**  $\delta$  18.62 (s,  $\text{PPh}_3$ ).

**$^{19}\text{F}$  NMR (376 MHz,  $\text{CDCl}_3$ )**  $\delta$  -78.20 (s, OTf).



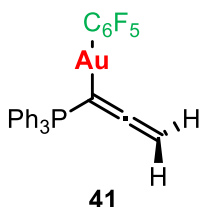
To a solution of **38a** (0.0763 g, 0.2 mmol) in  $\text{CH}_2\text{Cl}_2$  (20 ml) was added  $[\text{AuCl}(\text{tht})]$  (0.0321 g, 0.1 mmol) and the mixture stirred for 4 h at room temperature with excess  $\text{Cs}_2\text{CO}_3$ . The mixture was filtered through celite and the resulting orange solution concentrated under reduced pressure to approximately 2 ml. The product was precipitated with ethanol, collected by vacuum filtration and dried to give **9** as an orange solid (0.0364 g, 63 %).

**IR** ( $\text{cm}^{-1}$ )  $\nu(\text{C}=\underline{\text{CH}_2})$  3068,  $\nu(\text{C}=\text{C}=\text{C})$  1906.

**$^1\text{H}$  NMR** (400 MHz,  $\text{CDCl}_3$ )  $\delta$  7.54 – 7.76 (m, 15 H, Ph), 4.09 (d,  $^4J_{\text{HP}} = 16.0$  Hz, 2 H,  $\text{CH}_2$ ).

**$^{31}\text{P}\{^1\text{H}\}$  NMR** (162 MHz,  $\text{CDCl}_3$ )  $\delta$  17.30 (s,  $\text{PPh}_3$ ).

**$^{13}\text{C}$  APT** (76 MHz,  $\text{CDCl}_3$ )  $\delta$  216.54 (s,  $\text{C}=\underline{\text{C}}=\text{C}$ ), 133.95 (d,  $^3J_{\text{CP}} = 9.0$  Hz, *m*- $\text{Ph}_3\text{P}$ ), 133.72, (d,  $^4J_{\text{CP}} = 2.9$  Hz, *p*- $\text{Ph}_3\text{P}$ ), 129.30 (d,  $^2J_{\text{CP}} = 12.4$  Hz, *o*- $\text{Ph}_3\text{P}$ ), 122.44 (d,  $^1J_{\text{CP}} = 89.1$  Hz, *ipso*- $\text{Ph}_3\text{P}$ ), 83.88 (d,  $^1J_{\text{CP}} = 50.2$  Hz,  $\underline{\text{C}}(\text{PPh}_3)$ ), 65.63 (d,  $^3J_{\text{CP}} = 20.9$  Hz,  $\text{CH}_2$ ).



To a solution of  $[\text{Ph}_3\text{PCH}_2\text{C}\equiv\text{CH}]\text{Br}$  (0.0381 g, 0.1 mmol) in  $\text{CH}_2\text{Cl}_2$  (20 ml) was added  $[\text{Au}(\text{C}_6\text{F}_5)(\text{tht})]$  (0.0452 g, 0.1 mmol) and the mixture stirred for 3 h at room temperature with excess  $\text{Cs}_2\text{CO}_3$ . The mixture was filtered through celite and the resulting pale yellow solution concentrated under reduced pressure to approximately 2 ml. The product was precipitated with ethanol, collected by vacuum filtration and dried to give **41** as a pale yellow solid (0.0566 g, 85 %).

**IR** ( $\text{cm}^{-1}$ )  $\nu(\text{C}=\underline{\text{CH}_2})$  3055,  $\nu(\text{C}=\text{C}=\text{C})$  1901,  $\nu(\text{C}_6\text{F}_5)$  1500, 953, 794.

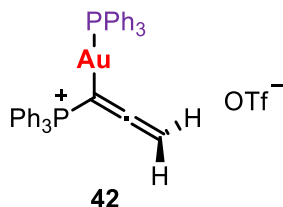
**$^1\text{H}$  NMR** (400 MHz,  $\text{CDCl}_3$ )  $\delta$  4.12 (d,  $^4J_{\text{HP}} = 16.0$ , 2 H,  $\text{CH}_2$ ), 7.39 – 7.83 (m, 15 H, Ph).

**$^{31}\text{P}\{^1\text{H}\}$  NMR** (162 MHz,  $\text{CDCl}_3$ )  $\delta$  19.22 (s,  $\text{PPh}_3$ ).

**$^{19}\text{F}$  NMR** (376 MHz,  $\text{CDCl}_3$ )  $\delta$  -115.77 – -115.92 (m, 2 F, *o*- $\text{C}_6\text{F}_5$ ), -161.14 (t,  $^3J_{\text{FF}} = 20.3$ , 1 F, *p*- $\text{C}_6\text{F}_5$ ), -163.28 – -163.43 (m, 2 F, *m*- $\text{C}_6\text{F}_5$ ).

### 3.9. Experimental

**$^{13}\text{C}$  APT (76 MHz,  $\text{CDCl}_3$ )**  $\delta$  215.98 (s,  $\text{C}=\text{C}=\text{C}$ ), 134.22 (d,  $^3J_{\text{CP}} = 9.0$  Hz, *m*- $\text{Ph}_3\text{P}$ ), 133.71 (d,  $^4J_{\text{CP}} = 2.9$  Hz, *p*- $\text{Ph}_3\text{P}$ ), 129.40 (d,  $^2J_{\text{CP}} = 12.3$  Hz, *o*- $\text{Ph}_3\text{P}$ ), 123.32 (d,  $^1J_{\text{CP}} = 88.5$  Hz, *i*- $\text{Ph}_3\text{P}$ ), 64.00 (d,  $^3J_{\text{CP}} = 22.2$  Hz,  $\text{CH}_2$ ).



Method 1:  $[\text{Ph}_3\text{PCH}_2\text{C}\equiv\text{CH}]\text{Br}$  (0.0450 g, 0.1 mmol) and  $[\text{Au}(\text{acac})(\text{PPh}_3)]$  (0.0559 g, 0.1 mmol) were stirred in  $\text{CH}_2\text{Cl}_2$  (20 ml) for 1 h at room temperature. The mixture was filtered through celite and the resulting yellow solution concentrated under reduced pressure to 2 ml. The product was precipitated with *n*-hexane, collected by vacuum filtration and dried to give **42** as an orange solid (0.0526 g, 58 %).

Method 2: **41** (0.0664 g, 0.1 mmol) and  $[\text{Au}(\text{PPh}_3)_2]\text{OTf}$  (0.0870 g, 0.1 mmol) were stirred in  $\text{CH}_2\text{Cl}_2$  (20 ml) for 30 min at room temperature. The mixture was filtered through celite and the resulting colourless solution concentrated under reduced pressure to approximately 2 ml. The product was precipitated with diethyl ether, collected by vacuum filtration and dried to give **42** as a white solid (0.0452 g, 50 %).

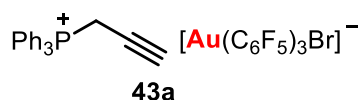
**IR** ( $\text{cm}^{-1}$ )  $\nu(\text{C}=\underline{\text{CH}_2})$  3054,  $\nu(\text{C}=\text{C}=\text{C})$  1911, (OTf) 1266 ( $\text{SO}_3$ ), 1225 ( $\text{CF}_3$ ), 1159 ( $\text{CF}_3$ ), 1030 ( $\text{SO}_3$ ).

**$^1\text{H}$  NMR (400 MHz,  $\text{CDCl}_3$ )**  $\delta$  4.50 (d,  $^4J_{\text{HP}} = 15.6$  Hz, 2 H,  $\text{CH}_2$ ), 7.44 – 7.80 (m, 30 H, Ph).

**$^{31}\text{P}\{^1\text{H}\}$  NMR (162 MHz,  $\text{CDCl}_3$ )**  $\delta$  19.85 (s,  $\underline{\text{PPh}_3}$ ), 40.24 (s,  $\text{Au}\underline{\text{PPh}_3}$ ).

**$^{19}\text{F}$  NMR (376 MHz,  $\text{CDCl}_3$ )**  $\delta$  -77.98 (s, OTf).

**$^{13}\text{C}$  APT (76 MHz,  $\text{CDCl}_3$ )**  $\delta$  134.64 (d,  $^4J_{\text{CP}} = 2.9$  Hz, *p*- $\text{PPh}_3$ ), 134.04 (d,  $^2J_{\text{CP}} = 13.6$  Hz, *o*- $\text{PPh}_3$ ), 133.91 (d,  $^3J_{\text{CP}} = 9.1$  Hz, *m*- $\text{PPh}_3$ ), 132.36 (d,  $^4J_{\text{CP}} = 2.5$  Hz, *p*- $\text{PPh}_3$ ), 130.00 (d,  $^2J_{\text{CP}} = 12.4$  Hz, *o*- $\text{Ph}_3\text{P}$ ), 129.67 (d,  $^3J_{\text{CP}} = 11.5$  Hz, *m*- $\text{Ph}_3\text{P}$ ), 128.61 (d,  $^1J_{\text{CP}} = 57.1$  Hz, *ipso*- $\text{Ph}_3\text{P}$ ), 122.04 (d,  $^1J_{\text{CP}} = 90.6$  Hz, *i*- $\text{Ph}_3\text{P}$ ), 66.52 (d,  $^3J_{\text{CP}} = 21.1$  Hz,  $\text{CH}_2$ ).



$[\text{Ph}_3\text{PCH}_2\text{C}\equiv\text{CH}]\text{Br}$  (0.1372 g, 0.36 mmol) and  $[\text{Au}(\text{C}_6\text{F}_5)_3(\text{tht})]$  (0.2839 g, 0.36 mmol) were stirred in  $\text{CH}_2\text{Cl}_2$  (20 ml) overnight at room temperature. The colourless solution was

concentrated under reduced pressure to 2 ml. The product was precipitated with *n*-hexane, collected by vacuum filtration and dried to give **43a** as a white solid (0.3782 g, 97 %).

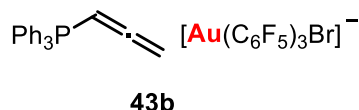
**IR** (cm<sup>-1</sup>)  $\nu(\text{C}\equiv\text{C-H})$  3305,  $\nu(\text{C}\equiv\text{C})$  2214,  $\nu(\text{C}_6\text{F}_5)$  1505, 963, 793.

**<sup>1</sup>H NMR (400 MHz, CDCl<sub>3</sub>)**  $\delta$  7.67 – 7.92 (m, 15 H, Ph), 4.18 (dd, <sup>2</sup>*J*<sub>HP</sub> = 14.8 Hz, <sup>4</sup>*J*<sub>HH</sub> = 2.4 Hz, 2 H, CH<sub>2</sub>), 2.37 (dt, <sup>4</sup>*J*<sub>HP</sub> = 6.8, <sup>4</sup>*J*<sub>HH</sub> = 2.4, 1 H, CH).

**<sup>31</sup>P{<sup>1</sup>H} NMR (162 MHz, CDCl<sub>3</sub>)**  $\delta$  21.26 (s, PPh<sub>3</sub>).

**<sup>19</sup>F NMR (376 MHz, CDCl<sub>3</sub>)**  $\delta$  -120.93 – -121.04 (m, 4 F, *o*-C<sub>6</sub>F<sub>5</sub>), -121.78 – -121.88 (m, 2 F, *o*-C<sub>6</sub>F<sub>5</sub>), -158.82 (t, <sup>3</sup>*J*<sub>FF</sub> = 18.8, 1 F, *p*-C<sub>6</sub>F<sub>5</sub>), -159.91 (t, <sup>3</sup>*J*<sub>FF</sub> = 18.8, 2 F, *p*-C<sub>6</sub>F<sub>5</sub>), -162.31 – -162.44 (m, 2 F, *m*-C<sub>6</sub>F<sub>5</sub>), -162.69 – -162.84 (m, 4 F, *m*-C<sub>6</sub>F<sub>5</sub>).

**<sup>13</sup>C APT (101 MHz, CDCl<sub>3</sub>)**  $\delta$  136.33 (d, <sup>4</sup>*J*<sub>CP</sub> = 2.9 Hz, *p*-PPh<sub>3</sub>), 133.62 (d, <sup>3</sup>*J*<sub>CP</sub> = 10.1 Hz, *m*-PPh<sub>3</sub>), 130.93 (d, <sup>2</sup>*J*<sub>CP</sub> = 13.0 Hz, *o*-PPh<sub>3</sub>), 116.52 (d, <sup>1</sup>*J*<sub>CP</sub> = 88.0 Hz, *i*-Ph), 77.77 (d, <sup>3</sup>*J*<sub>CP</sub> = 9.6 Hz, CH), 70.21 (d, <sup>2</sup>*J*<sub>CP</sub> = 12.1 Hz,  $\text{C}\equiv\text{CH}$ ), 17.84 (d, <sup>1</sup>*J*<sub>CP</sub> = 58.4 Hz, CH<sub>2</sub>).



**43a** (0.1079 g, 0.1 mmol) was stirred in CH<sub>2</sub>Cl<sub>2</sub> (20 ml) for 2 h at room temperature with excess Cs<sub>2</sub>CO<sub>3</sub>. The mixture was filtered through celite and the resulting yellow solution concentrated under reduced pressure to 2 ml. The product was precipitated with *n*-hexane, collected by vacuum filtration and dried to give **43b** as a pale orange solid (0.0486 g, 45 %).

**IR** (cm<sup>-1</sup>)  $\nu(\text{C}=\text{CH}_2)$  3063,  $\nu(\text{C}=\text{C}=\text{C})$  1914,  $\nu(\text{C}_6\text{F}_5)$  1504, 963, 793.

**<sup>1</sup>H NMR (400 MHz, CDCl<sub>3</sub>)**  $\delta$  7.52 – 7.89 (m, 15 H, Ph), 6.45 (dt, <sup>2</sup>*J*<sub>HP</sub> = 8.4 Hz, <sup>4</sup>*J*<sub>HH</sub> = 6.8 Hz, 1 H, CH), 5.36 (dd, <sup>4</sup>*J*<sub>HP</sub> = 12.8 Hz, <sup>4</sup>*J*<sub>HH</sub> = 6.8 Hz, 2 H, CH<sub>2</sub>).

**<sup>31</sup>P{<sup>1</sup>H} NMR (162 MHz, CDCl<sub>3</sub>)**  $\delta$  18.29 (s, PPh<sub>3</sub>).

**<sup>19</sup>F NMR (376 MHz, CDCl<sub>3</sub>)**  $\delta$  -120.80 – -120.89 (m, 4 F, *o*-C<sub>6</sub>F<sub>5</sub>), -121.71 – -121.84 (m, 2 F, *o*-C<sub>6</sub>F<sub>5</sub>), -158.98 (t, <sup>3</sup>*J*<sub>FF</sub> = 20.1 Hz, 1 F, *p*-C<sub>6</sub>F<sub>5</sub>), -160.14 (t, <sup>3</sup>*J*<sub>FF</sub> = 19.7 Hz, 2 F, *p*-C<sub>6</sub>F<sub>5</sub>), -162.42 – -162.56 (m, 2 F, *m*-C<sub>6</sub>F<sub>5</sub>), -162.87 – -163.03 (m, 4 F, *m*-C<sub>6</sub>F<sub>5</sub>).

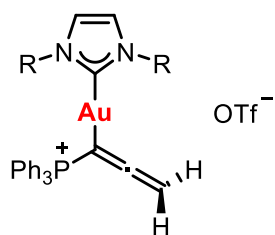


Method 2: [Ph<sub>3</sub>PCH=C=CH<sub>2</sub>]<sup>+</sup>OTf<sup>-</sup> (0.0901 g, 0.2 mmol) and [Au(C<sub>6</sub>F<sub>5</sub>)<sub>3</sub>(tht)] (0.1573 g, 0.2 mmol) were stirred in CH<sub>2</sub>Cl<sub>2</sub> (20 ml) for 30 min at room temperature with excess Cs<sub>2</sub>CO<sub>3</sub>. The mixture was filtered through celite and the resulting orange/brown solution concentrated under reduced pressure to 2 ml. The product was precipitated with *n*-hexane, collected by vacuum filtration and dried to give **44** as an orange solid (0.1013 g, 51 %).

**<sup>1</sup>H NMR (400 MHz, CDCl<sub>3</sub>)** δ 7.42 – 7.89 (m, 15 H, Ph), 5.84 (dd, <sup>4</sup>J<sub>HP</sub> = 12.8 Hz, <sup>4</sup>J<sub>HH</sub> = 6.0 Hz, 1 H, Au-CH), 4.88 (dd, <sup>2</sup>J<sub>HP</sub> = 14.0 Hz, <sup>4</sup>J<sub>HH</sub> = 6.0 Hz, 1 H, CH(PPh<sub>3</sub>)).

**<sup>19</sup>F NMR (376 MHz, CDCl<sub>3</sub>)** δ -121.41 – -121.75 (m, *o*-C<sub>6</sub>F<sub>5</sub>), -154.39 (t, <sup>3</sup>J<sub>FF</sub> = 20.0 Hz, *p*-C<sub>6</sub>F<sub>5</sub>), -155.74 (t, <sup>3</sup>J<sub>FF</sub> = 20.3 Hz, *p*-C<sub>6</sub>F<sub>5</sub>), -159.14 – -159.35 (m, *m*-C<sub>6</sub>F<sub>5</sub>), -160.36 – -160.47 (m, *m*-C<sub>6</sub>F<sub>5</sub>).

**<sup>13</sup>C APT (75 MHz, CDCl<sub>3</sub>)** δ 205.63 (s, C=C=C), 147.41 – 146.96 (m, C<sub>6</sub>F<sub>5</sub>), 144.39 – 143.88 (m, C<sub>6</sub>F<sub>5</sub>), 140.24 – 139.86 (m, C<sub>6</sub>F<sub>5</sub>), 139.21 – 138.68 (m, C<sub>6</sub>F<sub>5</sub>), 136.98 – 136.61 (m, C<sub>6</sub>F<sub>5</sub>), 135.64 – 135.34 (m, C<sub>6</sub>F<sub>5</sub>), 134.92 (d, <sup>4</sup>J<sub>CP</sub> = 2.9 Hz, *p*-PPh<sub>3</sub>), 133.44 (d, <sup>3</sup>J<sub>CP</sub> = 10.2 Hz, *m*-PPh<sub>3</sub>), 130.15 (d, <sup>2</sup>J<sub>CP</sub> = 12.9 Hz, *o*-PPh<sub>3</sub>) 119.97 (d, <sup>1</sup>J<sub>CP</sub> = 91.3 Hz, *i*-PPh<sub>3</sub>), 86.41 (d, <sup>3</sup>J<sub>CP</sub> = 15.1 Hz, Au-CH), 60.45 (d, <sup>1</sup>J<sub>CP</sub> = 104.3 Hz, CH(PPh<sub>3</sub>)).

NHC = IMes (**45**)

To a solution of **39a** (0.0450 g, 0.1 mmol) was added [AuCl(IMes)] (0.0538 g, 0.1 mmol) and excess Cs<sub>2</sub>CO<sub>3</sub> and the mixture stirred for 4 h at room temperature. The solution was filtered through celite and the yellow filtrate concentrated under reduced pressure to approximately 1 ml. Et<sub>2</sub>O (10 ml) was added to precipitate the product which was collected by filtration and vacuum dried to give **45** as an orange solid (0.0491 g, 52%).

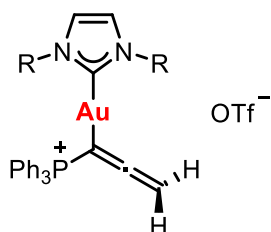
**HRMS (ESI-QTOF) m/z:** [M]<sup>+</sup> Calcd for C<sub>42</sub>H<sub>41</sub>AuN<sub>2</sub>P 801.2667, Found 801.2693.

IR (cm<sup>-1</sup>) ν(C=C=C) 1911.

**<sup>1</sup>H NMR (300 MHz, CDCl<sub>3</sub>)** δ 7.93 – 6.67 (m, 21H, PPh<sub>3</sub>, Mesityl-H, Imidazole C-H), 4.08 (d, <sup>4</sup>J<sub>HP</sub> = 16.0 Hz, 2H, CH<sub>2</sub>), 2.32 (s, 6H, Me), 1.96 (s, 12H, Me).

**<sup>31</sup>P{<sup>1</sup>H} NMR (121 MHz, CDCl<sub>3</sub>)** δ 19.22.

**<sup>13</sup>C APT (75 MHz, CDCl<sub>3</sub>)** δ 216.69 (d, <sup>2</sup>J<sub>CP</sub> = 4.0 Hz, C=C=C), 184.51 (s, N-C-N IMes), 139.70 (s, C4 Mes), 134.69 (s, C2/C6 Mes), 134.61 (s, C1 Mes), 134.05 (d, <sup>4</sup>J<sub>CP</sub> = 3.0 Hz, *p*-PPh<sub>3</sub>), 133.64 (d, <sup>2</sup>J<sub>CP</sub> = 9.1 Hz, *o*-PPh<sub>3</sub>), 129.54 (d, <sup>3</sup>J<sub>CP</sub> = 8.5 Hz, *m*-PPh<sub>3</sub>), 129.43 (s, CH Mes), 123.06 (s, CH imidazole), 122.28 (d, <sup>1</sup>J<sub>CP</sub> = 89.0 Hz, *i*-PPh<sub>3</sub>), 65.01 (d, <sup>3</sup>J<sub>CP</sub> = 21.4 Hz, C=C=CH<sub>2</sub>), 21.32 (s, Me), 17.78 (s, Me).

NHC = IPr (**46**)

To a solution of **39a** (0.0310 g, 0.069 mmol) was added [AuCl(IPr)] (0.0430 g, 0.069 mmol) and excess Cs<sub>2</sub>CO<sub>3</sub> and the mixture stirred for 4 h at room temperature. The solution was filtered through celite and the yellow filtrate concentrated under reduced pressure to



### 3.9. Experimental

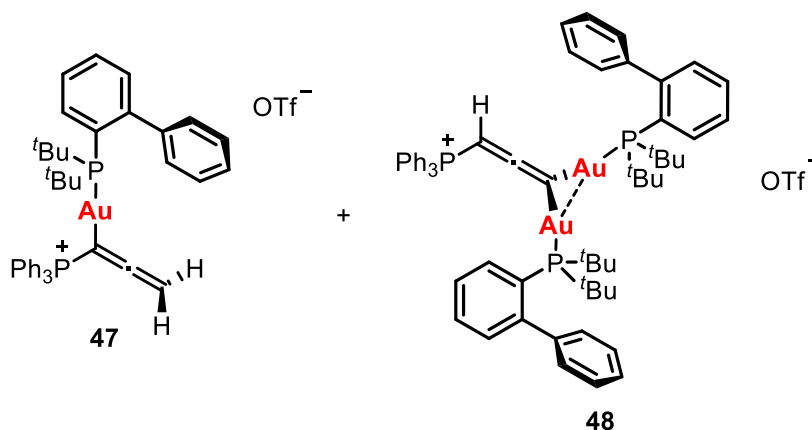
approximately 1 ml. Et<sub>2</sub>O (10 ml) was added to precipitate the product which was collected by filtration and vacuum dried to give **46** as an orange solid (0.0363 g, 51%).

**HRMS (ESI-QTOF) m/z:** [M]<sup>+</sup> Calcd for C<sub>48</sub>H<sub>53</sub>AuN<sub>2</sub>P 885.3606; Found 885.3607.

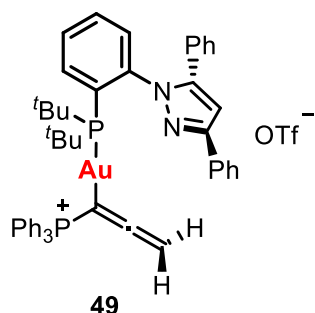
**<sup>1</sup>H NMR (300 MHz, CD<sub>2</sub>Cl<sub>2</sub>)** δ 7.82 – 6.81 (m, 23H, IPr + CH imidazole + PPh<sub>3</sub>), 4.01 (d, <sup>4</sup>J<sub>HP</sub> = 15.8 Hz, 2H, CH<sub>2</sub>), 2.50 (hept, <sup>3</sup>J<sub>HH</sub> = 6.8 Hz, 4H, CH <sup>i</sup>Pr), 1.20 (d, <sup>3</sup>J<sub>HH</sub> = 6.8 Hz, 12H, CH<sub>3</sub> <sup>i</sup>Pr), 1.10 (d, <sup>3</sup>J<sub>HH</sub> = 6.8 Hz, 12H, CH<sub>3</sub> <sup>i</sup>Pr).

**<sup>31</sup>P{<sup>1</sup>H} NMR (121 MHz, CD<sub>2</sub>Cl<sub>2</sub>)** δ 19.82 (s, PPh<sub>3</sub>).

**<sup>13</sup>C APT (75 MHz, CD<sub>2</sub>Cl<sub>2</sub>)** δ 146.38 (s, C2/C6 IPr), 134.36 (d, <sup>4</sup>J<sub>CP</sub> = 3.0 Hz, *p*-PPh<sub>3</sub>), 134.02 (d, <sup>3</sup>J<sub>CP</sub> = 9.0 Hz, *m*-PPh<sub>3</sub>), 131.32 (s, C3/C5 IPr), 129.92 (d, <sup>2</sup>J<sub>CP</sub> = 12.4 Hz, *o*-PPh<sub>3</sub>), 124.74 (s, CH imidazole), 122.43 (d, <sup>1</sup>J<sub>CP</sub> = 89.2 Hz, *i*-PPh<sub>3</sub>), 64.60 (d, <sup>3</sup>J<sub>CP</sub> = 21.0 Hz, C=C=CH<sub>2</sub>), 29.33 (s, CH <sup>i</sup>Pr), 24.77 (s, CH<sub>3</sub> <sup>i</sup>Pr), 24.17 (s, CH<sub>3</sub> <sup>i</sup>Pr).



To a solution of **39a** (0.0451 g, 0.1 mmol) was added [AuCl(JohnPhos)] (0.0531 g, 0.1 mmol) and excess Cs<sub>2</sub>CO<sub>3</sub> and the mixture stirred for 4 h at room temperature. The solution was filtered through celite and the filtrate concentrated under reduced pressure to approximately 1 ml. Et<sub>2</sub>O (10 ml) was added to precipitate the product which was collected by filtration and vacuum dried to give a mixture of **47** and **48**.

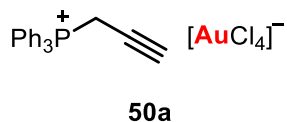


To a solution of **39a** (0.0451 g, 0.1 mmol) was added [AuCl(TrippyPhos)] (0.0673 g, 0.1 mmol) and excess Cs<sub>2</sub>CO<sub>3</sub> and the mixture stirred for 4 h at room temperature. The solution was filtered through celite and the filtrate concentrated under reduced pressure to approximately 1 ml. Et<sub>2</sub>O (10 ml) was added to precipitate the product which was collected by filtration and vacuum dried to give a mixture of **49** as an orange solid.

**HRMS (ESI-QTOF) m/z:** [M]<sup>+</sup> Calcd for C<sub>50</sub>H<sub>50</sub>AuN<sub>2</sub>P<sub>2</sub> 937.3109; Found 937.3085.

**<sup>1</sup>H NMR (400 MHz, CD<sub>2</sub>Cl<sub>2</sub>)** δ 7.99 – 6.95 (m, 30H, TrippyPhos + PPh<sub>3</sub>), 4.23 (dd, <sup>4</sup>J<sub>HP</sub> = 16.0 Hz, <sup>5</sup>J<sub>HP</sub> = 4.1 Hz, 2H, CH<sub>2</sub>), 1.09 (d, <sup>3</sup>J<sub>HP</sub> = 15.7 Hz, 9H, CH<sub>3</sub> <sup>t</sup>Bu), 1.02 (d, <sup>3</sup>J<sub>HP</sub> = 15.7 Hz, 9H, CH<sub>3</sub> <sup>t</sup>Bu).

**<sup>31</sup>P{<sup>1</sup>H} NMR (162 MHz, CD<sub>2</sub>Cl<sub>2</sub>)** δ 60.76 (d, <sup>3</sup>J<sub>PP</sub> = 1.7 Hz, TrippyPhos), 19.39 (d, <sup>3</sup>J<sub>PP</sub> = 1.7 Hz, PPh<sub>3</sub>).



To a solution of **38a** (0.1906 g, 0.5 mmol) in EtOH (10 ml) was added KAuCl<sub>4</sub> (0.1889 g, 0.5 mmol). A bright orange solid precipitated which was collected and vacuum dried to give the product (0.2610 g, 82%).

**<sup>1</sup>H NMR (300 MHz, CDCl<sub>3</sub>)** δ 8.06 – 7.58 (m, 15H, PPh<sub>3</sub>), 4.35 (dd, <sup>2</sup>J<sub>HP</sub> = 15.0 Hz, CH<sub>2</sub>, <sup>4</sup>J<sub>HH</sub> = 2.8 Hz, 2H), 2.39 (dt, <sup>4</sup>J<sub>HP</sub> = 6.7 Hz, <sup>4</sup>J<sub>HH</sub> 2.8 Hz, 1H, CH).

**<sup>31</sup>P{<sup>1</sup>H} NMR (121 MHz, CDCl<sub>3</sub>)** δ 21.33 (s, PPh<sub>3</sub>).

**<sup>13</sup>C APT (75 MHz, CDCl<sub>3</sub>)** δ 136.28 (d, <sup>4</sup>J<sub>CP</sub> = 3.1 Hz, *p*-PPh<sub>3</sub>), 133.88 (d, <sup>3</sup>J<sub>CP</sub> = 10.1 Hz, *m*-PPh<sub>3</sub>), 130.98 (d, <sup>2</sup>J<sub>CP</sub> = 13.0 Hz, *o*-PPh<sub>3</sub>), 116.67 (d, <sup>1</sup>J<sub>CP</sub> = 87.9 Hz, *i*-PPh<sub>3</sub>), 77.87 (d, <sup>3</sup>J<sub>CP</sub> = 9.6 Hz, CH<sub>2</sub>), 18.21 (d, <sup>1</sup>J<sub>CP</sub> = 58.0 Hz, CH).

### 3.9. Experimental

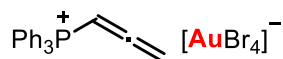


**51a**

To a solution of **38a** (0.0763 g, 0.2 mmol) in EtOH (10 ml) was added AuBr<sub>3</sub> (0.0873 g, 0.2 mmol). A bright orange solid precipitate which was collected and vacuum dried to give the product (0.0874 g, 53%).

**<sup>1</sup>H NMR (400 MHz, CDCl<sub>3</sub>)** δ 8.21 – 7.54 (m, 15H, PPh<sub>3</sub>), 4.42 (dd, <sup>2</sup>J<sub>HP</sub> = 15.0 Hz, <sup>4</sup>J<sub>HH</sub> = 2.8 Hz, 2H, CH<sub>2</sub>), 2.39 (dt, <sup>4</sup>J<sub>HP</sub> = 6.6 Hz, <sup>4</sup>J<sub>HH</sub> = 2.8 Hz, 1H, CH).

**<sup>31</sup>P{<sup>1</sup>H} NMR (162 MHz, CDCl<sub>3</sub>)** δ 21.42.

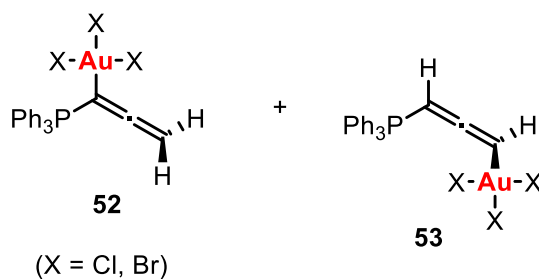


**51b**

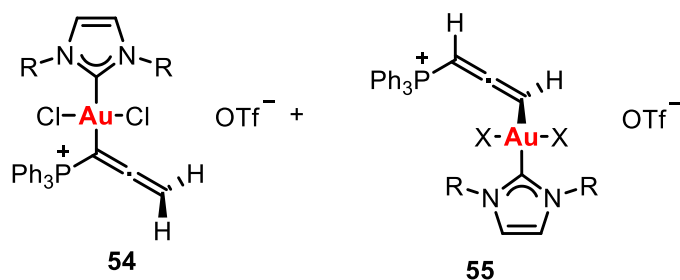
To a solution of **51a** (10 mg) in CD<sub>2</sub>Cl<sub>2</sub> (1 ml) was added Cs<sub>2</sub>CO<sub>3</sub> and the solution stirred for 1 h. The solution was filtered through celite and NMR spectrum of the filtrate was recorded.

**<sup>1</sup>H NMR (400 MHz, CD<sub>2</sub>Cl<sub>2</sub>)** δ 8.25 – 7.44 (m, 15H, PPh<sub>3</sub>), 6.50 (dt, <sup>2</sup>J<sub>HP</sub> = 8.2 Hz, <sup>4</sup>J<sub>HH</sub> = 6.6 Hz, 1H, CH), 5.40 (dd, <sup>4</sup>J<sub>HP</sub> = 12.7 Hz, <sup>4</sup>J<sub>HH</sub> 6.6 Hz, 2H, CH<sub>2</sub>).

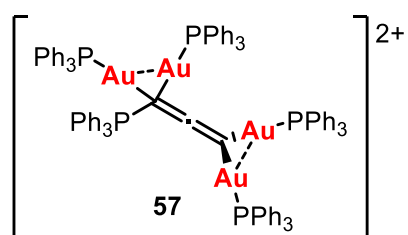
**<sup>31</sup>P{<sup>1</sup>H} NMR (162 MHz, CD<sub>2</sub>Cl<sub>2</sub>)** δ 18.20 (s, PPh<sub>3</sub>)



To a solution of **40** (0.0057 g, 0.01 mmol) in CD<sub>2</sub>Cl<sub>2</sub> (1 ml) was added Cl<sub>2</sub> (0.5M soln in CCl<sub>4</sub>, 20 μl) and the solution stirred for 1 h. NMR spectra of the solution were recorded.



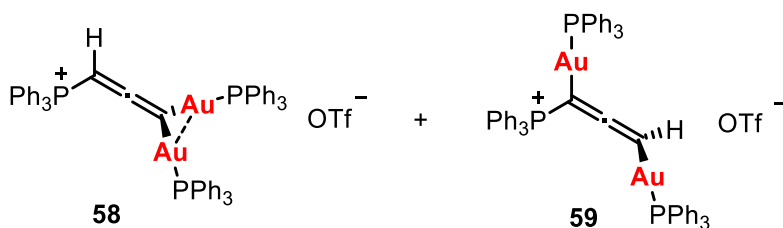
To a solution of **46** (0.0056 g) in  $\text{CD}_2\text{Cl}_2$  (1 ml) was added  $\text{Cl}_2$  (0.5 M soln in  $\text{CCl}_4$ , 11.8  $\mu\text{l}$ ) and the solution stirred for 1 h. NMR spectra of the solution were recorded.



To a solution of **39a** (0.0451 g, 0.1 mmol) in  $\text{CH}_2\text{Cl}_2$  (10 ml) was added  $[\text{O}(\text{AuPPh}_3)_3]\text{BF}_4$  (0.2222 g, 0.15 mmol) and the solution stirred for 2 h. The solution was filtered through celite, the filtrate concentrated under reduced pressure to approximately 1 ml and  $\text{Et}_2\text{O}$  added to precipitate a white solid which was collected and vacuum dried to give the product (0.1296 g, 55%).

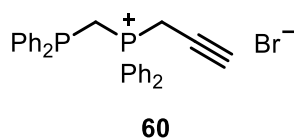
$^1\text{H}$  NMR (400 MHz,  $\text{CDCl}_3$ )  $\delta$  7.98 – 7.23 (m,  $\text{PPh}_3$ ).

$^{31}\text{P}\{^1\text{H}\}$  NMR (162 MHz,  $\text{CDCl}_3$ )  $\delta$  37.86 (s,  $\text{C}=\text{C}=\text{C}(\text{AuPPh}_3)_2$ ), 32.10 (s,  $\text{Ph}_3\text{PAu}-\text{C}(\text{PPh}_3)=\text{C}=\text{C}$ ), 18.52 (s,  $\text{Ph}_3\text{PC}$ ).



To a solution of **39a** (0.0045 g, 0.01 mmol) in  $\text{CD}_2\text{Cl}_2$  (1 ml) was added  $[\text{Au}(\text{acac})(\text{PPh}_3)]$  (0.0112 g, 0.02 mmol) and the solution stirred for 10 h. NMR spectra of the solution were recorded.

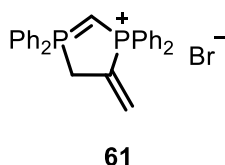
### 3.9. Experimental



To a solution of dppm (1.92 g, 5.0 mmol) in acetonitrile (20 ml) was added propargyl bromide (1.08 ml, 80% soln in toluene, 10 mmol) and the solution stirred for 2 days at room temperature. The solution was concentrated to dryness under reduced pressure and the crude solid recrystallised  $\text{CH}_2\text{Cl}_2/\text{Et}_2\text{O}$  to give a pale orange solid which was vacuum dried to give the product (1.9379 g, 77%).

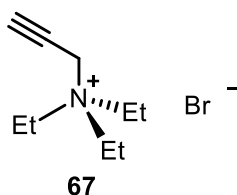
**$^1\text{H}$  NMR (300 MHz,  $\text{CD}_2\text{Cl}_2$ )**  $\delta$  7.96 – 7.19 (m, 20H, Ph), 4.76 (dd,  $^2J_{\text{HP}} = 15.6$  Hz,  $^4J_{\text{HH}} = 2.8$  Hz, 2H,  $\text{CH}_2\text{C}\equiv\text{CH}$ ), 4.43 (dd,  $^2J_{\text{HP}} = 14.8$  Hz,  $^2J_{\text{HP}} = 1.4$  Hz, 2H,  $\text{CH}_2$ ), 2.24 (dt,  $^4J_{\text{HP}} = 6.9$  Hz,  $^4J_{\text{HH}} = 2.8$  Hz, 1H,  $\text{C}\equiv\text{CH}$ ).

**$^{31}\text{P}\{^1\text{H}\}$  NMR (121 MHz,  $\text{CD}_2\text{Cl}_2$ )**  $\delta$  25.57 (d,  $^2J_{\text{PP}} = 59.6$  Hz,  $\text{PPh}_2\text{CH}_2\text{C}\equiv\text{CH}$ ), -26.58 (d,  $^2J_{\text{PP}} = 59.7$  Hz,  $\text{PPh}_2$ ).



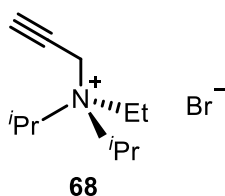
To a solution of dppm (5.77 g, 15.0 mmol) in  $\text{CHCl}_3$  (30 ml) was added propargyl bromide (1.62 ml, 80% soln toluene, 15 mmol) and the solution stirred for 4 days at room temperature. The solution was concentrated under reduced pressure to approximately 1 ml and  $\text{Et}_2\text{O}$  (10 ml) was added to precipitate a beige solid which was collected and vacuum dried to give the product (5.29 g, 70%).

**$^1\text{H}$  NMR (400 MHz,  $\text{CDCl}_3$ )**  $\delta$  7.91 – 7.41 (m, 20H, Ph), 7.03 (d,  $^3J_{\text{HP}} = 36.3$  Hz, 1H,  $\text{C}=\text{CH}_2$  (*trans*)), 5.86 (d,  $^3J_{\text{HP}} = 17.7$  Hz, 1H,  $\text{C}=\text{CH}_2$  (*cis*)), 4.31 (dd,  $^2J_{\text{CP}} = 11.4$  Hz,  $^2J_{\text{CP}} = 9.7$  Hz, 3H), 2.01 (ddd,  $^2J_{\text{HP}} = 7.6$  Hz,  $^2J_{\text{HP}} = 6.2$  Hz,  $^5J_{\text{HH}} 1.3$  Hz, 1H).



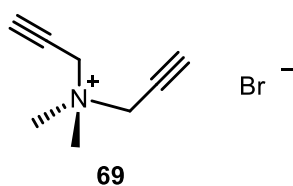
Triethylamine (1.39 ml, 10.0 mmol) and propargyl bromide (1.08 ml, 10 mmol) were mixed. A white solid formed which was collected, washed with Et<sub>2</sub>O and vacuum dried to give the product (2.1795 g, 99%).

**<sup>1</sup>H NMR (400 MHz, DMSO)** δ 4.36 (d, <sup>4</sup>J<sub>HH</sub> = 2.6 Hz, 2H, CH<sub>2</sub>C≡CH), 4.04 (t, <sup>4</sup>J<sub>HH</sub> = 2.5 Hz, 1H, C≡CH), 3.34 (q, <sup>3</sup>J<sub>HH</sub> = 7.2 Hz, 6H, CH<sub>2</sub>), 1.22 (t, <sup>3</sup>J<sub>HH</sub> = 7.2 Hz, 9H, CH<sub>3</sub>).



N,N-Diisopropylethylamine (1.74 ml, 10 mmol) and propargyl bromide (1.08 ml, 10 mmol) were mixed. A white solid formed which was collected, washed with Et<sub>2</sub>O and vacuum dried to give the product (0.8802 g, 35%).

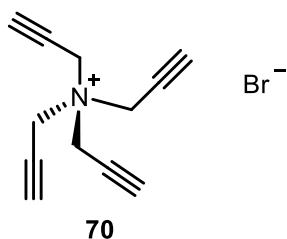
**<sup>1</sup>H NMR (400 MHz, DMSO)** δ 4.41 (d, <sup>4</sup>J<sub>HH</sub> = 2.6 Hz, 2H, CH<sub>2</sub>C≡CH), 4.06 (hept, <sup>3</sup>J<sub>HH</sub> = 6.6 Hz, 2H, CH <sup>i</sup>Pr), 4.01 (t, <sup>4</sup>J<sub>HH</sub> = 2.6 Hz, 1H, C≡CH), 3.44 (q, <sup>3</sup>J<sub>HH</sub> = 7.2 Hz, 2H, CH<sub>2</sub> Et), 1.42 (t, <sup>3</sup>J<sub>HH</sub> = 6.5 Hz, 12H, CH<sub>3</sub> <sup>i</sup>Pr), 1.30 (t, <sup>3</sup>J<sub>HH</sub> = 7.2 Hz, 3H, CH<sub>3</sub> Et).



3-Dimethylamino-1-propyne (1.08 ml, 10 mmol) and propargyl bromide (1.08 ml, 10 mmol) were mixed. A white solid formed which was collected, washed with Et<sub>2</sub>O and vacuum dried to give the product (2.0008 g, 99%).

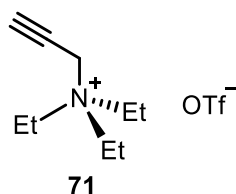
**<sup>1</sup>H NMR (400 MHz, DMSO)** δ 4.50 (d, <sup>4</sup>J<sub>HH</sub> = 2.5 Hz, 2H, CH<sub>2</sub>), 4.13 (t, <sup>4</sup>J<sub>HH</sub> = 2.5 Hz, 1H, CH), 3.18 (s, 3H, Me).

### 3.9. Experimental



Tripropargylamine (1.42 ml, 10 mmol) and propargyl bromide (1.08 ml, 10 mmol) were mixed. After 3 h a white solid formed which was collected, washed with Et<sub>2</sub>O and vacuum dried to give the product (0.5920 g, 22%).

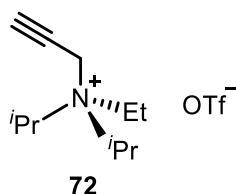
**<sup>1</sup>H NMR (400 MHz, DMSO)** δ 4.53 (d, <sup>4</sup>J<sub>HH</sub> = 2.6 Hz, 2H, CH<sub>2</sub>), 4.21 (t, <sup>4</sup>J<sub>HH</sub> = 2.6 Hz, 1H, CH).



To a solution of **67** (0.2202 g, 1.0 mmol) in acetonitrile (10 ml) was added AgOTf (0.2569 g, 1.0 mmol) and the solution stirred for 30 min. The solution was filtered through celite, the filtrate concentrated under reduced pressure to approximately 1 ml and Et<sub>2</sub>O (10 ml) added to precipitate a white solid which was collected and vacuum dried to give the product (0.2555 g, 88%).

**<sup>1</sup>H NMR (400 MHz, CD<sub>3</sub>CN)** δ 4.02 (d, <sup>4</sup>J<sub>HH</sub> = 2.6 Hz, 1H, CH<sub>2</sub>), 3.32 (q, <sup>3</sup>J<sub>HH</sub> = 7.3 Hz, 6H, CH<sub>2</sub> Et), 3.14 (t, <sup>4</sup>J<sub>HH</sub> = 2.6 Hz, 1H, CH), 1.26 (t, <sup>3</sup>J<sub>HH</sub> = 7.3 Hz, 9H, CH<sub>3</sub> Et).

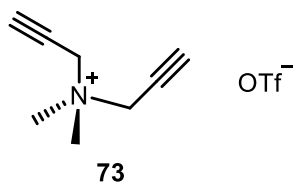
**<sup>19</sup>F NMR (376 MHz, CD<sub>3</sub>CN)** δ -79.30 (OTf)



To a solution of **68** (0.2482 g, 1.0 mmol) in acetonitrile (10 ml) was added AgOTf (0.2569 g, 1.0 mmol) and the solution stirred for 30 min. The solution was filtered through celite, the filtrate concentrated under reduced pressure to approximately 1 ml and Et<sub>2</sub>O (10 ml) added to precipitate a white solid which was collected and vacuum dried to give the product (0.2793 g, 88%).

**$^1\text{H}$  NMR (400 MHz,  $\text{CD}_3\text{CN}$ )**  $\delta$  4.10 – 4.09 (m, 2H,  $\text{CH}_2\text{C}\equiv\text{CH}$ ), 4.05 (hept,  $^3J_{\text{HH}} = 6.7$  Hz, 2H,  $\text{CH}^i\text{Pr}$ ), 3.43 (q,  $^3J_{\text{HH}} = 7.3$  Hz, 2H,  $\text{CH}_2$  Et), 3.14 (t,  $^4J_{\text{HH}} = 2.6$  Hz, 1H,  $\text{C}\equiv\text{CH}$ ), 1.48 (d,  $^3J_{\text{HH}} = 6.7$  Hz, 6H,  $\text{CH}_3^i\text{Pr}$ ), 1.45 (d,  $^3J_{\text{HH}} = 6.7$  Hz, 6H,  $\text{CH}_3^i\text{Pr}$ ), 1.35 (t,  $^3J_{\text{HH}} = 7.3$  Hz, 3H,  $\text{CH}_3$  Et).

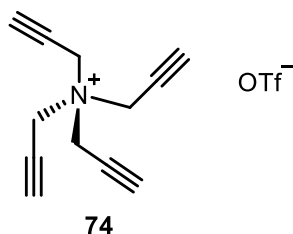
**$^{19}\text{F}$  NMR (376 MHz,  $\text{CD}_3\text{CN}$ )**  $\delta$  -79.30 (OTf).



To a solution of **69** (0.2021 g, 1.0 mmol) in acetonitrile (10 ml) was added AgOTf (0.2569 g, 1.0 mmol) and the solution stirred for 30 min. The solution was filtered through celite, the filtrate concentrated under reduced pressure to approximately 1 ml and  $\text{Et}_2\text{O}$  (10 ml) added to precipitate a white solid which was collected and vacuum dried to give the product (0.2297 g, 85%).

**$^1\text{H}$  NMR (400 MHz,  $\text{CD}_3\text{CN}$ )**  $\delta$  4.24 (d,  $^4J_{\text{HH}} = 2.5$  Hz, 2H,  $\text{CH}_2$ ), 3.26 (t,  $^4J_{\text{HH}} = 2.5$  Hz, 1H,  $\text{CH}$ ), 3.17 (s, 3H, Me).

**$^{19}\text{F}$  NMR (376 MHz,  $\text{CD}_3\text{CN}$ )**  $\delta$  -79.32 (OTf)



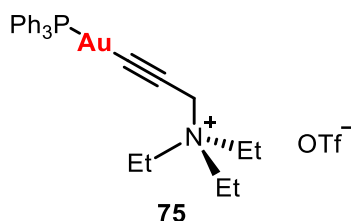
To a solution of **70** (0.2501 g, 1.0 mmol) in acetonitrile (10 ml) was added AgOTf (0.2569 g, 1.0 mmol) and the solution stirred for 30 min. The solution was filtered through celite, the filtrate concentrated under reduced pressure to approximately 1 ml and  $\text{Et}_2\text{O}$  (10 ml) added to precipitate a white solid which was collected and vacuum dried to give the product (0.2986 g, 94%).

**$^1\text{H}$  NMR (400 MHz,  $\text{CD}_3\text{CN}$ )**  $\delta$  4.41 (d,  $^4J_{\text{HH}} = 2.6$  Hz, 2H,  $\text{CH}_2$ ), 3.32 (t,  $^4J_{\text{HH}} = 2.6$  Hz, 1H,  $\text{CH}$ ).

**$^{19}\text{F}$  NMR (376 MHz,  $\text{CD}_3\text{CN}$ )**  $\delta$  -79.32 (OTf).



### 3.9. Experimental



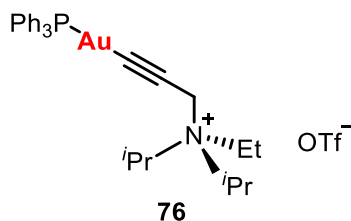
**71** (0.0289 g, 0.1 mmol) and [Au(acac)(PPh<sub>3</sub>)] (0.0559 g, 0.1 mmol) were mixed in CH<sub>2</sub>Cl<sub>2</sub> (5 ml) and the solution stirred for 1 h. The solution was filtered through celite, the filtrate concentrated under reduced pressure to approximately 1 ml and Et<sub>2</sub>O (10 ml) added to precipitate a white solid which was collected and vacuum dried to give the product (0.0535 g, 72%).

**HRMS (ESI-QTOF) m/z:** [M]<sup>+</sup> Calcd for C<sub>27</sub>H<sub>32</sub>AuNP 598.1932; Found 598.1945.

**<sup>1</sup>H NMR (300 MHz, CD<sub>2</sub>Cl<sub>2</sub>)** δ 7.78 – 7.18 (m, 15H, PPh<sub>3</sub>), 3.99 (s, 2H, CH<sub>2</sub>C≡C), 3.40 (q, <sup>3</sup>J<sub>HH</sub> = 7.3 Hz, 6H, CH<sub>2</sub> Et), 1.35 (t, <sup>3</sup>J<sub>HH</sub> = 7.3 Hz, 9H, CH<sub>3</sub> Et).

**<sup>31</sup>P{<sup>1</sup>H} NMR (121 MHz, CD<sub>2</sub>Cl<sub>2</sub>)** δ 41.17 (s, PPh<sub>3</sub>)

**<sup>13</sup>C APT (75 MHz, CD<sub>2</sub>Cl<sub>2</sub>)** δ 134.76 (d, <sup>2</sup>J<sub>CP</sub> = 13.7 Hz, *o*-PPh<sub>3</sub>), 132.42 (d, <sup>4</sup>J<sub>CP</sub> = 2.3 Hz, *p*-PPh<sub>3</sub>), 129.87 (d, <sup>3</sup>J<sub>CP</sub> = 11.3 Hz, *m*-PPh<sub>3</sub>), 129.82 (d, <sup>1</sup>J<sub>CP</sub> = 56.3 Hz, *i*-PPh<sub>3</sub>), 53.20 (CH<sub>2</sub> Et), 50.35 (s, CH<sub>2</sub>C≡C), 8.20 (s, CH<sub>3</sub> Et).



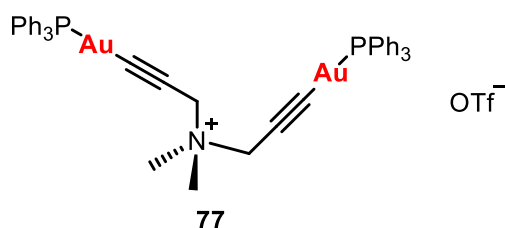
**72** (0.0317 g, 0.1 mmol) and [Au(acac)(PPh<sub>3</sub>)] (0.0559 g, 0.1 mmol) were mixed in CH<sub>2</sub>Cl<sub>2</sub> (5 ml) and the solution stirred for 1 h. The solution was filtered through celite, the filtrate concentrated under reduced pressure to approximately 1 ml and Et<sub>2</sub>O (10 ml) added to precipitate a white solid which was collected and vacuum dried to give the product (0.0621 g, 80%).

**HRMS (ESI-QTOF) m/z:** [M]<sup>+</sup> Calcd for C<sub>29</sub>H<sub>36</sub>AuNP 636.2245; Found 626.2277.

**<sup>1</sup>H NMR (300 MHz, CD<sub>2</sub>Cl<sub>2</sub>)** δ 7.86 – 7.14 (m, 15H, PPh<sub>3</sub>), 4.19 – 4.11 (m, 2H, CH *i*Pr), 4.10 (s, 2H, CH<sub>2</sub>C≡C), 3.48 (q, *J* = 7.3 Hz, 2H, CH<sub>2</sub> Et), 1.60 (d, <sup>3</sup>J<sub>HH</sub> = 6.8 Hz, 6H, *i*Pr), 1.56 (d, <sup>3</sup>J<sub>HH</sub> = 6.8 Hz, 6H, CH<sub>3</sub> *i*Pr), 1.44 (t, <sup>3</sup>J<sub>HH</sub> = 7.3 Hz, 3H, CH<sub>3</sub>).

**<sup>31</sup>P{<sup>1</sup>H} NMR (121 MHz, CD<sub>2</sub>Cl<sub>2</sub>)** δ 41.22 (s, PPh<sub>3</sub>)

**$^{13}\text{C}$  APT (75 MHz,  $\text{CD}_2\text{Cl}_2$ )**  $\delta$  134.76 (d,  $^2J_{\text{CP}} = 13.5$  Hz, *o*-PPh<sub>3</sub>), 132.42 (s, *p*-PPh<sub>3</sub>), 129.87 (d,  $^3J_{\text{CP}} = 11.4$  Hz, *m*-PPh<sub>3</sub>), 63.62 (s, CH <sup>*i*</sup>Pr), 52.94 (s, CH<sub>2</sub> Et), 49.56 (s, CH<sub>2</sub>C $\equiv$ C), 19.21 (CH<sub>3</sub> <sup>*i*</sup>Pr), 19.03 (CH<sub>3</sub> <sup>*i*</sup>Pr), 10.78 (CH<sub>3</sub> Et).



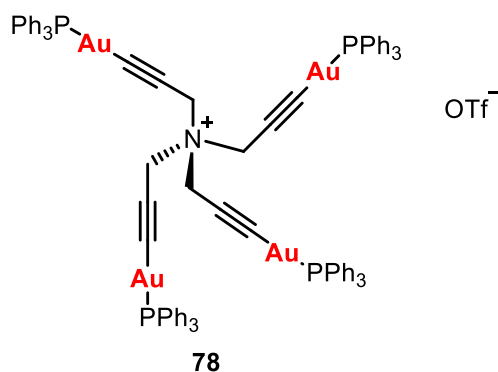
**73** (0.0271 g, 0.1 mmol) and [Au(acac)(PPh<sub>3</sub>)] (0.1119 g, 0.2 mmol) were mixed in CH<sub>2</sub>Cl<sub>2</sub> (5 ml) and the solution stirred for 1 h. The solution was filtered through celite, the filtrate concentrated under reduced pressure to approximately 1 ml and Et<sub>2</sub>O (10 ml) added to precipitate a white solid which was collected and vacuum dried to give the product (0.0707 g, 68%).

**HRMS (ESI-QTOF) m/z:** [M]<sup>+</sup> Calcd for C<sub>44</sub>H<sub>40</sub>Au<sub>2</sub>NP<sub>2</sub> 1038.1962; Found 1038.1999.

**$^1\text{H}$  NMR (300 MHz,  $\text{CD}_2\text{Cl}_2$ )**  $\delta$  7.58 – 7.47 (m, 15H, PPh<sub>3</sub>), 4.27 (s, 2H, CH<sub>2</sub>), 3.24 (s, 3H, Me).

**$^{31}\text{P}\{^1\text{H}\}$  NMR (121 MHz,  $\text{CD}_2\text{Cl}_2$ )**  $\delta$  41.23 (s, PPh<sub>3</sub>).

**$^{13}\text{C}$  APT (75 MHz,  $\text{CD}_2\text{Cl}_2$ )**  $\delta$  134.80 (d,  $^2J_{\text{CP}} = 13.6$  Hz, *o*-PPh<sub>3</sub>), 132.39 (s, *p*-PPh<sub>3</sub>), 129.86 (d,  $^3J_{\text{CP}} = 11.2$  Hz, *m*-PPh<sub>3</sub>), 56.10 (s, CH<sub>2</sub>), 49.86 (s, Me).



**74** (0.0160 g, 0.05 mmol) and [Au(acac)(PPh<sub>3</sub>)] (0.1119 g, 0.2 mmol) were mixed in CH<sub>2</sub>Cl<sub>2</sub> (5 ml) and the solution stirred for 1 h. The solution was filtered through celite, the filtrate concentrated under reduced pressure to approximately 1 ml and Et<sub>2</sub>O (10 ml) added to

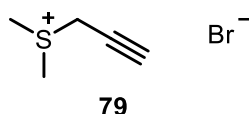
### 3.9. Experimental

precipitate a white solid which was collected and vacuum dried to give the product (0.0970 g, 90%).

**$^1\text{H}$  NMR (300 MHz,  $\text{CD}_2\text{Cl}_2$ )**  $\delta$  7.55 – 7.50 (m, 15H,  $\text{PPh}_3$ ), 4.45 (s, 2H,  $\text{CH}_2$ ).

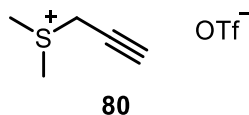
**$^{31}\text{P}\{^1\text{H}\}$  NMR (121 MHz,  $\text{CD}_2\text{Cl}_2$ )**  $\delta$  41.25 (s,  $\text{PPh}_3$ ).

**$^{13}\text{C}$  APT (75 MHz,  $\text{CD}_2\text{Cl}_2$ )**  $\delta$  138.13 (d,  $^2J_{\text{CP}} = 141.6$  Hz,  $\text{C}\equiv\text{C-Au}$ ), 134.80 (d,  $^2J_{\text{CP}} = 13.9$  Hz, *o*- $\text{PPh}_3$ ), 132.38 (d,  $^4J_{\text{CP}} = 2.5$  Hz, *p*- $\text{PPh}_3$ ), 129.87 (d,  $^1J_{\text{CP}} = 56.9$  Hz, *i*- $\text{PPh}_3$ ), 129.86 (d,  $^3J_{\text{CP}} = 11.4$  Hz, *m*- $\text{PPh}_3$ ), 88.63 (d,  $^3J_{\text{CP}} = 27.0$  Hz,  $\text{CH}_2\text{C}\equiv\text{C}$ ), 49.69 (s,  $\text{CH}_2$ ).



Dimethyl sulfide (0.73 ml, 10 mmol) and propargyl bromide (1.08 ml, 10 mmol) were mixed. A solid formed which was washed with  $\text{Et}_2\text{O}$  and vacuum dried to give the product (0.4686 g, 26%).

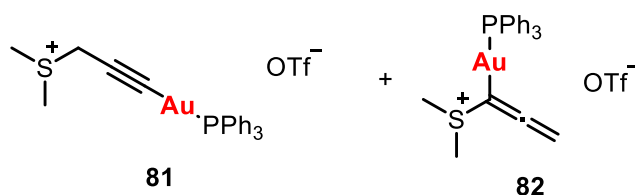
**$^1\text{H}$  NMR (400 MHz,  $\text{CD}_3\text{CN}$ )**  $\delta$  4.54 (d,  $^4J_{\text{HH}} = 2.6$  Hz, 2H,  $\text{CH}_2$ ), 3.13 (t,  $^4J_{\text{HH}} = 2.6$  Hz, 1H,  $\text{CH}$ ), 2.96 (s, 6H, Me).



To a solution of **79** (0.1811 g, 1.0 mmol) in acetonitrile (10 ml) was added  $\text{AgOTf}$  (0.2569 g, 1.0 mmol) and the mixture stirred for 30 min. The solution was filtered through celite, the filtrate concentrated under reduced pressure to approximately 1 ml and  $\text{Et}_2\text{O}$  (10 ml) added to precipitate a white solid which was collected and vacuum dried to give the product (0.2275 g, 91%).

**$^1\text{H}$  NMR (400 MHz,  $\text{CD}_2\text{Cl}_2$ )**  $\delta$  4.35 (d,  $^4J_{\text{HH}} = 2.6$  Hz, 2H,  $\text{CH}_2$ ), 2.97 (s, 6H, Me), 2.86 (t,  $^4J_{\text{HH}} = 2.6$  Hz, 1H,  $\text{CH}$ ).

**$^{19}\text{F}$  NMR (376 MHz,  $\text{CD}_2\text{Cl}_2$ )**  $\delta$  -78.97 ( $\text{OTf}$ ).



**80** (0.0250 g, 0.1 mmol) and [Au(acac)(PPh<sub>3</sub>)] (0.0559 g, 0.1 mmol) were mixed in CH<sub>2</sub>Cl<sub>2</sub> (5 ml) and the solution stirred for 1 h. The solution was filtered through celite, the filtrate concentrated under reduced pressure to approximately 1 ml and Et<sub>2</sub>O (10 ml) added to precipitate a white solid which was collected and vacuum dried to give the a mixture of **81** and **82** (0.0420 g, 59%).

<sup>1</sup>H NMR (300 MHz, CD<sub>2</sub>Cl<sub>2</sub>) δ 7.60 – 7.48 (m, PPh<sub>3</sub>), 5.04 (d, <sup>5</sup>J<sub>HP</sub> = 4.0 Hz, CH<sub>2</sub> **82**), 4.26 (s, CH<sub>2</sub> **81**), 2.95 (s, Me, **82**), 2.94 (s, Me, **81**).

<sup>31</sup>P{<sup>1</sup>H} NMR (121 MHz, CD<sub>2</sub>Cl<sub>2</sub>) δ 41.10 (s, PPh<sub>3</sub>), 40.45 (s, PPh<sub>3</sub>).

# Chapter 4 – NHC Gold Complexes

## 4.1. Introduction

*N*-Heterocyclic carbenes (NHCs) have made a huge impact on organometallic chemistry in recent years. They make attractive ligands due to their strong  $\sigma$ -donor capacity and the fact that a broad variety of substituents can be introduced at the nitrogen atoms, allowing both the steric and electronic properties to be fine-tuned. NHC gold complexes have received considerable attention due to their numerous and varied applications.

### 4.1.1. Basic Concepts

NHCs are defined as heterocyclic species containing a carbene carbon atom and at least one nitrogen atom in the ring structure.<sup>247</sup> Classical NHCs feature a five-membered heterocycle and are derived from imidazolium, dihydroimidazolium, benzimidazolium or triazolium salts. Examples in which the carbene centre is stabilised by one nitrogen and one alternative heteroatom such as sulfur or oxygen are also known and prepared from thiazolium or oxazolium salts (Figure 4.1).

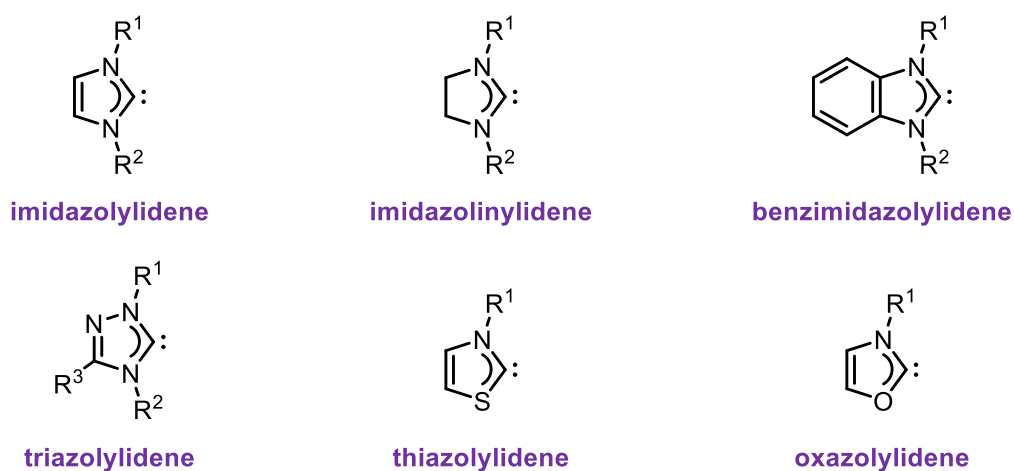


**Figure 4.1.** Classical NHCs.

NHCs have some unusual electronic properties which can explain their remarkable stability compared to typical free carbenes. They exhibit a singlet ground state electron configuration

where the HOMO is best described as a formally  $sp^2$ -hybridised lone pair and the LUMO an occupied p orbital at the carbon atom. The nitrogen atoms provide stabilisation through their  $\sigma$ -electron withdrawing and  $\pi$ -electron donating properties, lowering the energy of the occupied  $\sigma$ -orbital and donating electron density into the empty p orbital (Figure 4.2). The cyclic structure of NHCs also favours the singlet state by forcing the carbene carbon into a bent  $sp^2$ -like arrangement.

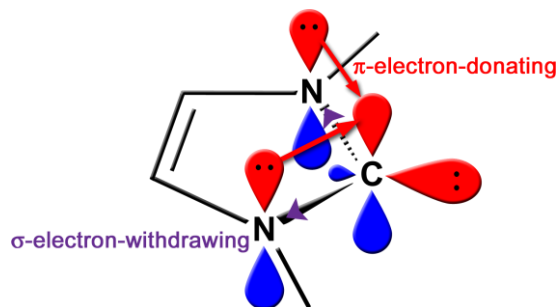


**Figure 4.2.** NHC orbitals.

The C-N bonds in NHCs have partial double bond character as evidenced by the bond distances found in the molecular structures determined by single crystal X-ray diffraction (Figure 4.3). The C-N bond in the NHC 1,3-bis(1-adamantyl)imidazol-2-ylidene was found to have a distance of 1.37 Å (Figure 4.3 (a)), compared to 1.33 Å for the parent imidazolium salt<sup>248</sup> (Figure 4.3 (b)) and 1.49 Å for the saturated derivative<sup>249</sup> (Figure 4.3 (c)).

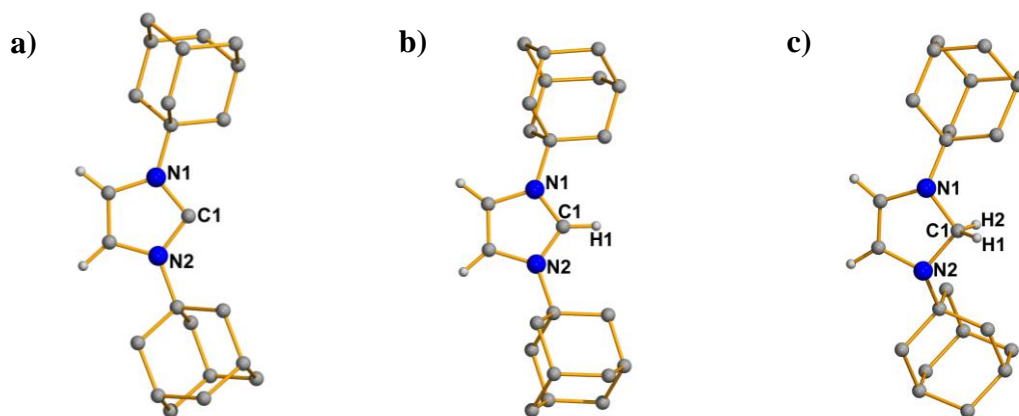


**Figure 4.3.** Molecular structures of 1,3-bis(1-adamantyl)imidazol-2-ylidene (a), 1,3-bis(1-adamantyl)imidazolium tetraphenylborate (b) and 1,3-bis(1-adamantyl)-2,3-dihydro-1*H*-imidazole (c) determined by single crystal X-ray diffraction. Adamantyl hydrogen atoms are omitted for clarity. Selected bond lengths [Å] and angles [°]: a: C(1)-N(1) 1.367(2), C(1)-N(2) 1.373(2), N(1)-C(1)-N(2) 102.2(2). b: C(1)-N(1) 1.328(4), C(1)-N(2) 1.331(3), N(1)-C(1)-N(2) 109.7(3). c: C(1)-N(1) 1.4851(47), C(1)-N(2) 1.4875(45), N(1)-C(1)-N(2) 104.3(3).

While most conventional carbenes are electrophilic, the lone pair in the plane of the ring results in NHCs being highly nucleophilic. They are incredibly strong  $\sigma$ -donors and will readily bind to a wide range of metallic and non-metallic species, however they exhibit only very weak  $\pi$ -accepting properties. The coordination chemistry of NHCs is therefore more comparable to that of P, N or O donating ligands than to Schrock or Fischer carbenes and they were initially considered mimics of phosphines as ligands in organometallic complexes.<sup>250</sup> In general, however, NHCs are more electron-donating than phosphines, resulting in metal-ligand bonds that are more thermally and chemically inert towards cleavage. Some exceptions do arise due to steric constraints. For example, a study of the relative bond dissociation energies for NHC ruthenium(II) complexes found a linear decrease in metal-ligand bond strength with increasing bulkiness of the NHC, however, for all but the bulkiest adamantyl NHC, the metal-ligand bond dissociation energies for the NHC complexes were greater than that of the analogous complex with the most Lewis basic phosphine tested,  $\text{PCy}_3$  (Figure 4.4).<sup>251</sup> The high stability of NHC complexes has led NHCs to become ever more popular ligands in organometallic chemistry.

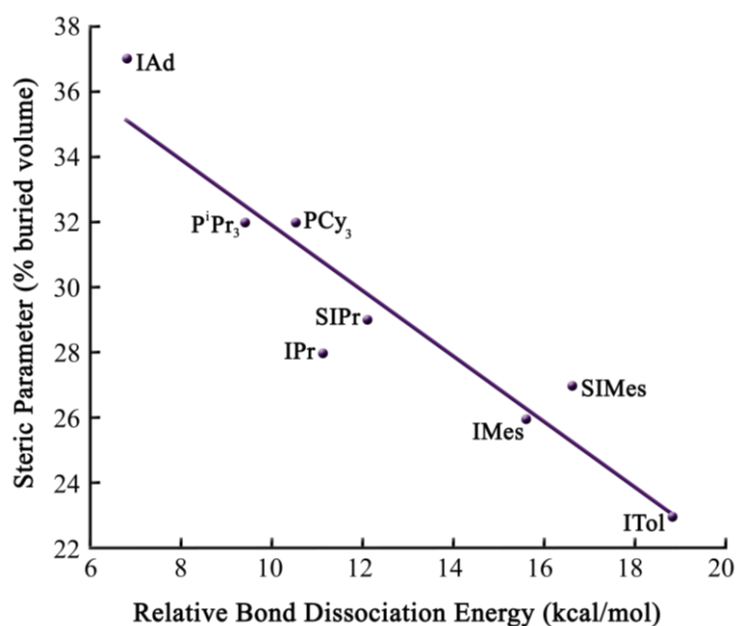
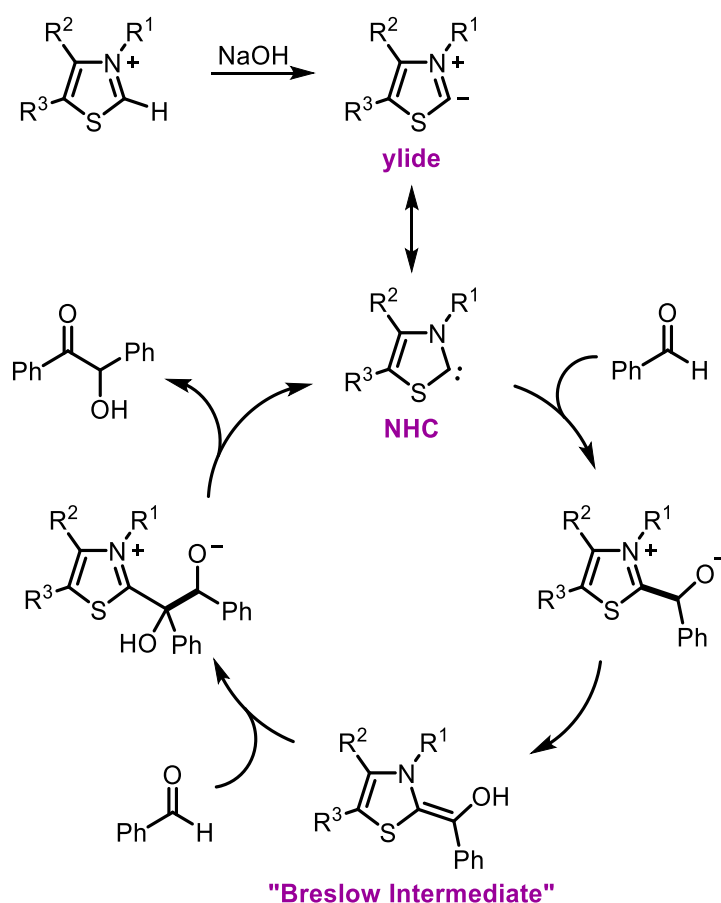


**Figure 4.4.** Relative bond dissociation energy (kcal/mol) vs steric parameter (% buried volume) for complexes  $[\text{RuClCp}^*(\text{L})]$  (IAd = 1,3-bis(adamantyl)imidazol-2-ylidene, IPr = 1,3-bis(2,6-diisopropylphenyl)imidazol-2-ylidene, SIPr = 1,3-bis(2,6-diisopropylphenyl)imidazolin-2-ylidene, IMes = 1,3-bis(2,4,6-trimethylphenyl)imidazol-2-ylidene, SIMes = 1,3-bis(2,4,6-trimethylphenyl)imidazolin-2-ylidene, ITol = 1,3-bis(4-methylphenyl)imidazol-2-ylidene).

### 4.1.2. History

The existence of NHCs was first suggested by Ronald Breslow in 1958 when he proposed that benzoin-type condensations catalysed by vitamin B<sub>1</sub> dependant enzymes proceed via the formation of a catalytically active NHC by deprotonation of an azolium salt (Scheme 4.1).<sup>252</sup> The NHC subsequently reacts with an aldehyde to form a so-called “Breslow Intermediate”. The first isolation of such a species was not achieved until 2012.<sup>253</sup>

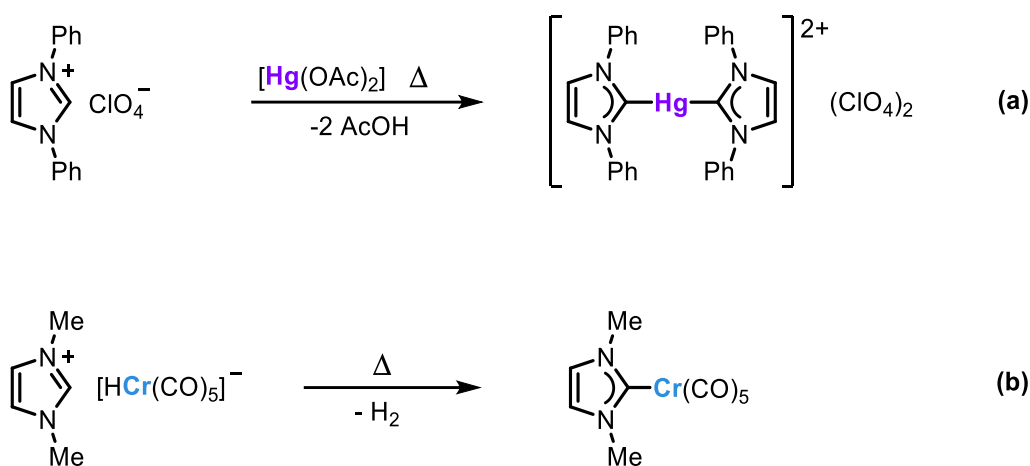


**Scheme 4.1.** Breslow’s proposal for the mechanism of the benzoin condensation.

In the years following Breslow’s proposal it was suggested that NHCs exist only as highly reactive intermediates and are not isolable due to their tendency to dimerise.<sup>254</sup> In 1968, however, a breakthrough was made with the first successful isolation of NHC coordination complexes, achieved separately by Wanzlick and Öfele. Wanzlick prepared a bis-NHC mercury(II) complex by reaction of an imidazolium salt with [Hg(OAc)<sub>2</sub>] (Scheme 4.2(a)).<sup>255</sup> The structure was confirmed by <sup>1</sup>H NMR spectroscopy. In the same year Öfele isolated the first NHC chromium(0) complex (Scheme 4.2(b)), although he was actually trying to prepare

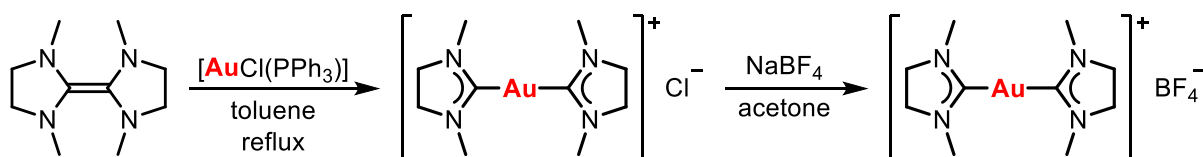


dihydro-complexes by heating heterocyclic salts of chromium.<sup>256</sup> Again, the structure of the NHC product was confirmed by <sup>1</sup>H NMR spectroscopy.



**Scheme 4.2.** Synthesis of the first NHC transition metal complexes by Wanzlick and Öfele.

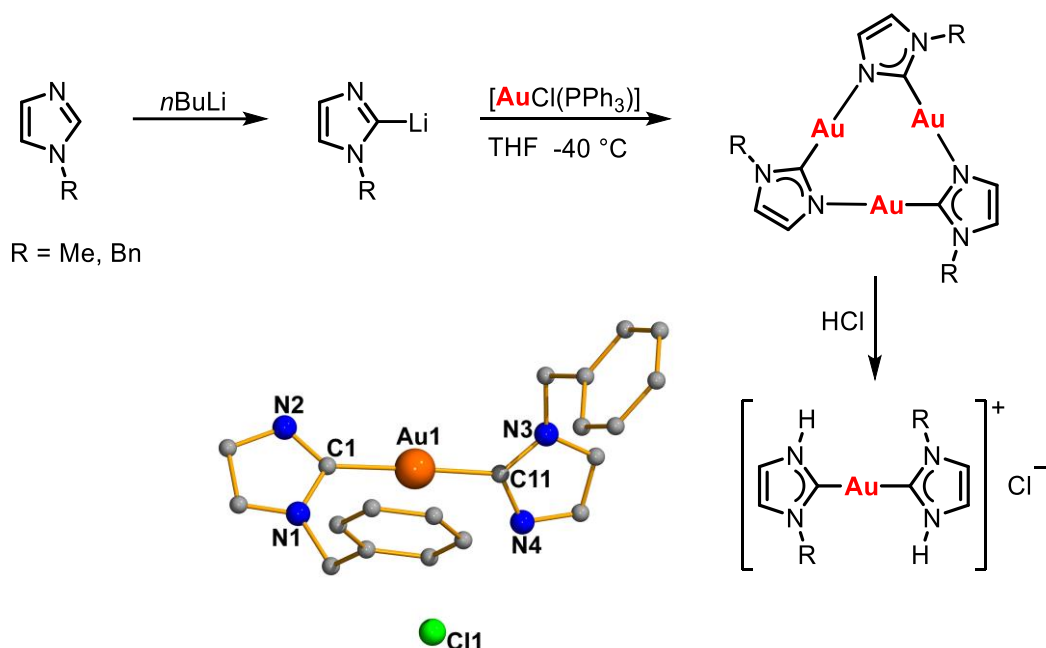
The first NHC gold(I) complex was reported by Lappert and co-workers in 1974, prepared by cleavage of an enetetramine. Heating a toluene solution of tetramethylenetetramine with [AuCl(PPh<sub>3</sub>)] led to precipitation of the bis-NHC gold(I) chloride complex, and subsequent anion metathesis with sodium tetrafluoroborate afforded the more thermally stable bis-NHC gold(I) tetrafluoroborate complex (Scheme 4.3). The complexes were characterised by elemental analysis and <sup>1</sup>H NMR spectroscopy.<sup>257</sup> Although of historical importance, this methodology for the preparation of NHC complexes by the cleavage of enetetramines has very limited scope in terms of ligand diversity and has therefore been little used for the preparation of further NHC gold complexes.<sup>258</sup>



**Scheme 4.3.** Synthesis of the first NHC gold(I) complex

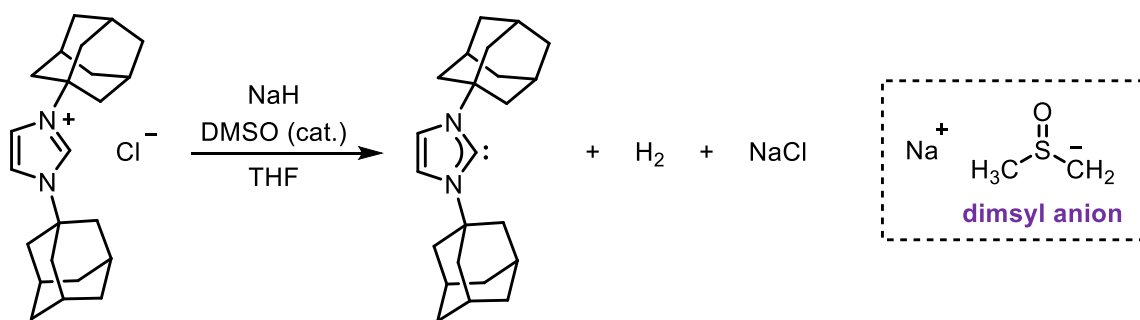
In 1989 Burini and co-workers reported the synthesis of bis-NHC gold(I) complexes by reaction of N-methyl or benzyl imidazole with *n*-butyllithium, followed by addition of [AuCl(PPh<sub>3</sub>)] and HCl (Scheme 4.4). The initial product was proposed to be an unusual cyclic NHC trimer complex based on mass spectrometry data, although the authors did not rule out

the possibility that larger oligomeric structures could form. Treatment with hydrochloric acid led to the formation of the bis-NHC gold(I) complex which was successfully characterised by single crystal X-ray diffraction.<sup>72</sup>



**Scheme 4.4.** Synthesis of a bis-NHC gold(I) complex by Burini. Molecular structure determined by single crystal X-ray diffraction. Hydrogen atoms are omitted for clarity. Selected bond lengths [Å] and angles [°]: Au(1)-C(1) 2.01(1), Au(1)-C(11) 2.02(1), C(1)-N(1) 1.42(1), C(1)-N(2) 1.28(2), C(11)-N(3) 1.34(1), C(11)-N(4) 1.37(1), C(1)-Au(1)-C(11) 175.18(41).

One of the key moments in the history of NHC chemistry came in 1991 with the successful isolation of a free NHC by Arduengo and co-workers. The carbene was prepared by reaction of 1,3-bis(1-adamantyl)imidazolium chloride with sodium hydride in THF with catalytic amounts of DMSO (Scheme 4.5).<sup>248</sup> DMSO reacts with the sodium hydride to form the dimsyl anion which, according to Arduengo, is a better base for imidazolium salts than the sodium hydride itself. The side products formed in the reaction, hydrogen gas and sodium chloride, are readily removable and concentration of the THF filtrate allowed isolation of the product as colourless crystals. The NHC was found to be indefinitely stable under inert atmosphere and also had a high thermal stability, melting without decomposition at 240 °C.



**Scheme 4.5.** Preparation of the first stable free NHC, 1,3-bis(1-adamantyl)imidazol-2-ylidene.

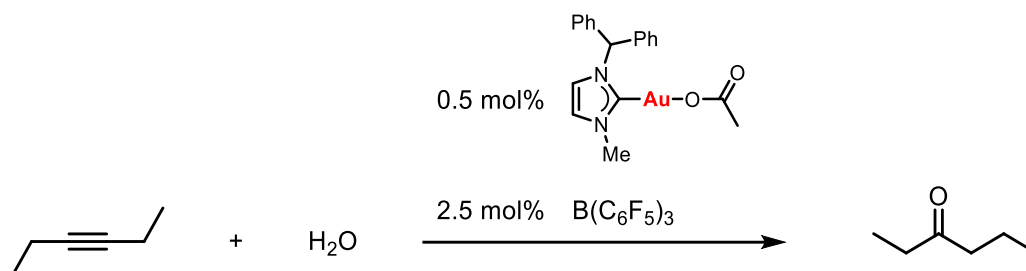
Arduengo's work showed how readily accessible NHCs were and his report led to a renewed interest in NHC chemistry. The relatively simple syntheses and the high stability of their corresponding metal complexes have made NHCs attractive ligands in organometallic chemistry. Various synthetic methods for NHC complexes are known, however most commonly deprotonation of an azolium salt is used, either with an external base or a metal complex bearing a basic ligand.<sup>247</sup> The coordination chemistry of NHCs is now a well-developed field and NHC complexes have been described for all transition metals<sup>259</sup> as well as many main group<sup>260</sup> and f-block metals.<sup>261</sup> In recent years there has been a growing interest in NHC gold complexes due to their numerous applications in catalysis, medicine and luminescence.

### 4.1.3. Applications of NHC Gold Complexes

#### 4.1.3.1. Homogeneous Gold Catalysis

NHC gold(I) complexes are considered powerful tools in organic synthesis due to their use in homogeneous gold catalysis. The strong  $\sigma$ -donor ability of the NHC ligands results in these complexes being more electron rich than many other homogeneous gold catalysts and hence they have a unique catalytic activity.

The first reported use of an NHC gold complex in a catalytic reaction was in 2003 with the gold catalysed hydration of 3-hexyne described by Herrmann and co-workers (Scheme 4.6), showing that NHC gold(I) complexes were able to catalyse the addition of water to non-activated alkynes.<sup>262</sup>



**Scheme 4.6.** Gold catalysed hydration of 3-hexyne with NHC gold(I) catalyst.

Since then, NHC gold complexes have successfully been employed in a wide variety of organic transformations including enyne cycloisomerisations,<sup>263</sup> alkyne hydrations,<sup>262</sup> propargylic ester rearrangement,<sup>264</sup> alkene activation,<sup>265</sup> alkane C-H bond activation<sup>266</sup> and cross-coupling reactions.<sup>267</sup> However, the importance of NHC gold complexes in catalysis comes not only from their high selectivity in directed organic synthetic strategies but also their ability to stabilise reactive intermediates in catalytic reactions. Recently several otherwise highly unstable intermediates have been isolated as a result of the stabilisation imparted by the NHC ligand, including vinyl gold derivatives,<sup>79,80,268</sup> gold(I) hydrides<sup>75</sup> and gold(I) and gold(III) intermediates in gold-only photoredox catalysis,<sup>269</sup> thus providing chemists with a better understanding of the key steps in reaction mechanisms.

#### 4.1.3.2. Biological Applications

NHC gold complexes have also been found to have important biological applications. The strong gold-carbon bond in NHC gold(I) complexes causes them to be inert towards biologically important thiol groups, making them relatively stable *in vivo*, and hence they have potential medical applications.<sup>270</sup>

In 2004 the first report of the antimicrobial activity of NHC gold complexes was published by Çetinkaya and co-workers. A series of bis-NHC gold complexes were found to be effective against a variety of Gram-positive and Gram-negative bacteria (Figure 4.5). Variation of the substituent at the nitrogen atom was found to cause a significant difference in the antimicrobial activity. The complex bearing a *p*-methoxybenzyl group was active against all strains investigated with the exception of *E. Coli*. The complex bearing a *p*-dimethylaminobenzyl group, however, only showed activity against *E. Coli* and was the only complex active against this Gram-negative strain.<sup>271</sup>

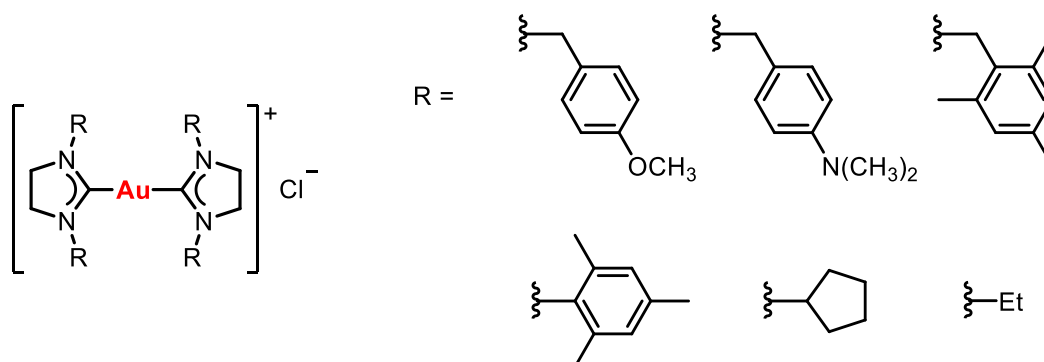


**Figure 4.5.** Cationic bis-NHC gold(I) complexes with antimicrobial activity.

A similar effect was noted by Özdemir in a study of the antibacterial and antifungal properties of a series of chloro NHC gold(I) complexes (Figure 4.6). Complexes bearing methoxy substituents were found to inhibit the growth of Gram-positive bacteria while having no effect on Gram-negative bacteria or fungi. However, the incorporation of a pentamethylbenzyl substituent at the nitrogen atom of the NHC resulted in no antimicrobial activity but good inhibition of fungi was observed.<sup>272</sup>

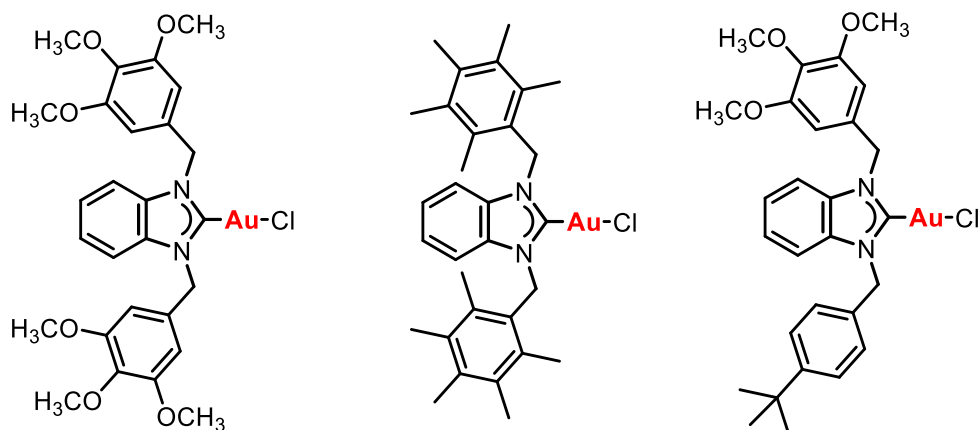


**Figure 4.6.** Chloro NHC gold(I) complexes with antimicrobial and antifungal activity.

Significant contributions to the study of the anticancer activity of NHC gold(I) complexes have been made by the group of Berners-Price.<sup>273</sup> A series of neutral chloro- and 2',3',4',6'-tetra-O-acetyl- $\beta$ -D-glucopyranosyl-1-thiolato-NHC gold(I) complexes were reported (Figure 4.7) in which variation of the alkyl substituents at the NHC ligand allowed modulation of the lipophilic properties of the resultant complexes.<sup>274</sup> The complexes were found to target the mitochondria, an important feature since carcinoma cells have an elevated mitochondrial membrane potential

compared to normal human epithelial cells<sup>275</sup> and exploitation of this phenomenon could allow delivery of the complex to the cancer cells selectively. The same group went on to report a series of homoleptic bis-NHC gold(I) complexes with potent anti-cancer activity which could selectively induce apoptosis in cancer cells, leaving normal cells unaffected.<sup>120,276</sup>

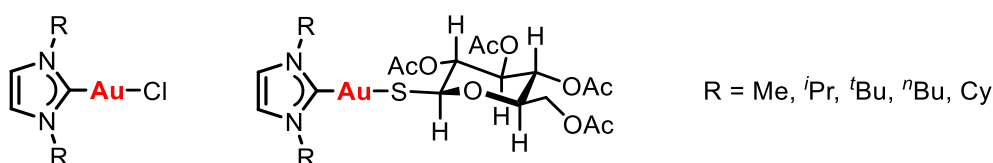


**Figure 4.7.** NHC gold(I) complexes with antitumoural activity.

Ott and co-workers reported how the antiproliferative effects of NHC gold complexes were greater for cationic complexes compared to the neutral complexes. The introduction of a positive charge was found to increase cellular uptake and generally improve the cytotoxic properties.<sup>277</sup>

The importance of the metal on the mechanism of the anticancer activity of NHC complexes has also been studied. Mao and co-workers reported a study of the antiproliferative activities of two cationic bis-NHC gold(I) complexes and their silver analogues (Figure 4.8). The complexes were tested in five different cell lines with the bis-NHC gold(I) complexes showing greater antiproliferative activity and selectivity than the corresponding silver complexes. The similarity in structure of the complexes confirms that the metal plays a role in the mode of action of the complexes.<sup>278</sup>

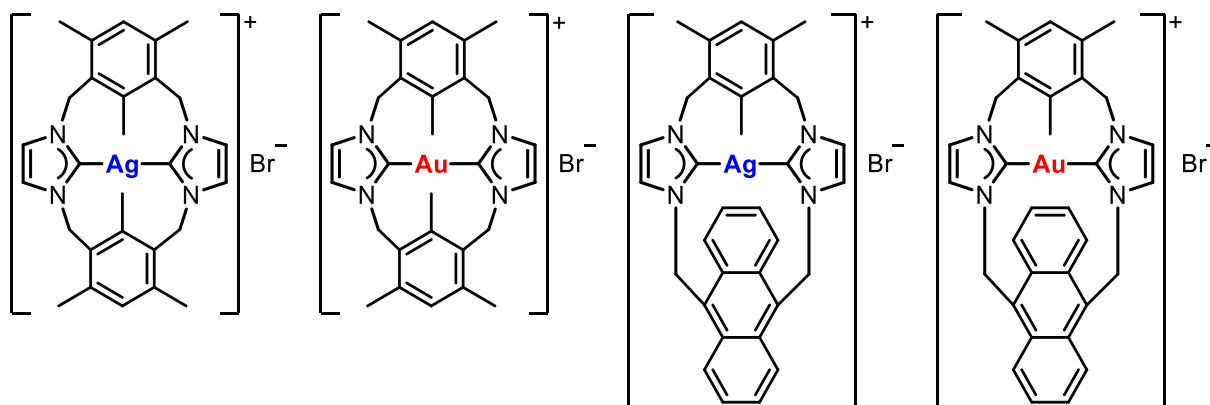


**Figure 4.8.** Bis-NHC silver(I) and gold(I) complexes reported by Mao and co-workers.

#### 4.1. Introduction

Although many studies of the biological activity of NHC gold(I) complexes have been carried out, gold(III) has been far less explored. Generally NHC gold(III) complexes are unstable in biological environments since gold(III) is readily reduced to gold(I) or gold(0) by cellular thiol-containing compounds.<sup>279-281</sup> Che and co-workers were able to overcome this problem by use of a strongly chelating scaffold to stabilise the gold(III) complex. The 2,6-diphenylpyridine NHC gold(III) derivative (Figure 4.9), the synthesis of which was reported by the group of Yam,<sup>282</sup> was found to show antiproliferative effects against a series of human cancer cell lines.<sup>283</sup>

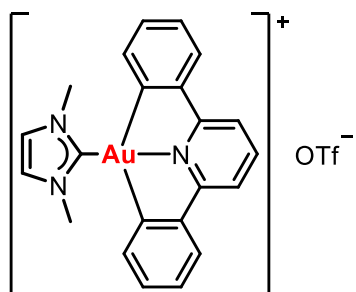
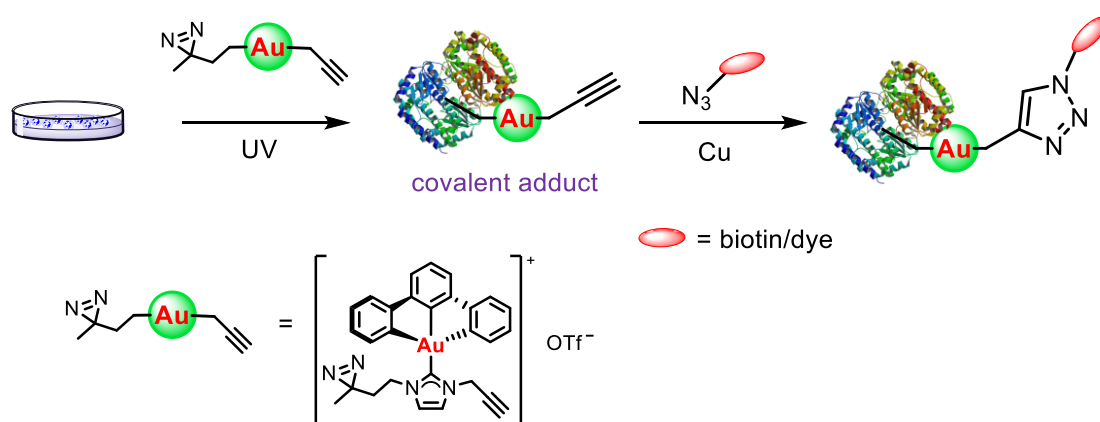


**Figure 4.9.** NHC gold(III) complex with anticancer activity.

More recently modifications to the NHC have been made to incorporate a photoaffinity unit and a clickable alkyne moiety. This allowed the target intracellular proteins to be identified since the complex can covalently bind to the protein through the photoaffinity unit and then a copper catalysed click reaction can be carried out to attach a dye molecule to allow detection (Scheme 4.7).<sup>284</sup>



**Scheme 4.7.** Procedure for the identification of cellular targets of the NHC gold(III) complex.

## 4.1.3.3. Luminescence

Luminescent NHC gold complexes were first reported in 1999 by Lin and co-workers. A series of gold(I) complexes bearing a benzimidazol-2-ylidene ligand were found to exhibit long-lived luminescence at room temperature, both in the solid state and in acetonitrile solutions (Figure 4.10). Multiple emissions were observed for different substituents at the NHC nitrogen atoms and with different ligands at the gold.<sup>285</sup>

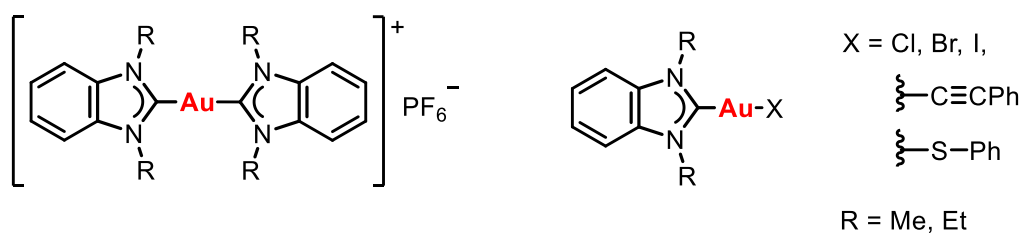


**Figure 4.10.** First examples of luminescent NHC gold(I) complexes.

More recently, Casini and coworkers reported fluorescent NHC gold(I) complexes functionalised with a fluorescent anthracenyl ligand (Figure 4.11(a)). These were found to have low-energy excitation and emission bands at suitable wavelengths for use in cellular distribution studies using fluorescence confocal microscopy whilst also exhibiting cytotoxicity.<sup>286</sup>

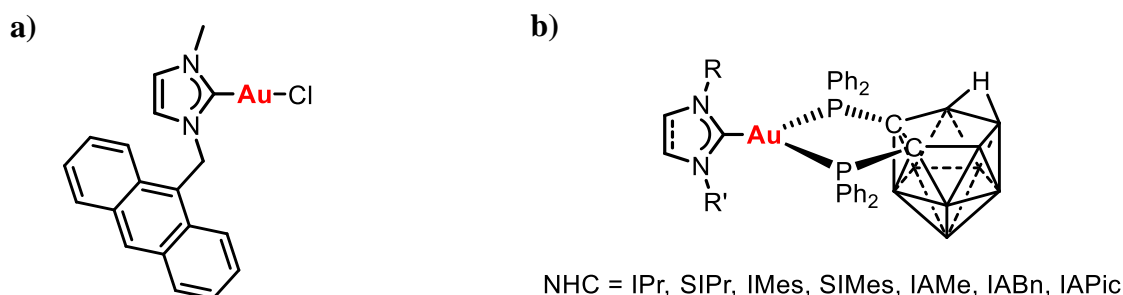


**Figure 4.11.** Luminescent NHC gold(I) complexes. (IPr = 1,3-bis(2,6-diisopropylphenyl)imidazol-2-ylidene, SIPr = 1,3-bis(2,6-diisopropylphenyl)imidazolin-2-ylidene, IMes = 1,3-bis(2,4,6-trimethylphenyl)-imidazol-2-ylidene, SIMes = 1,3-bis(2,4,6-trimethylphenyl)-imidazolin-2-ylidene, IAME = 1-acridinyl-3-methylimidazol-2-ylidene, IABn = 1-acridinyl-3-benzylimidazol-2-ylidene, IAPic = 1-acridinyl-3-(2-picolyl)imidazole-2-ylidene.

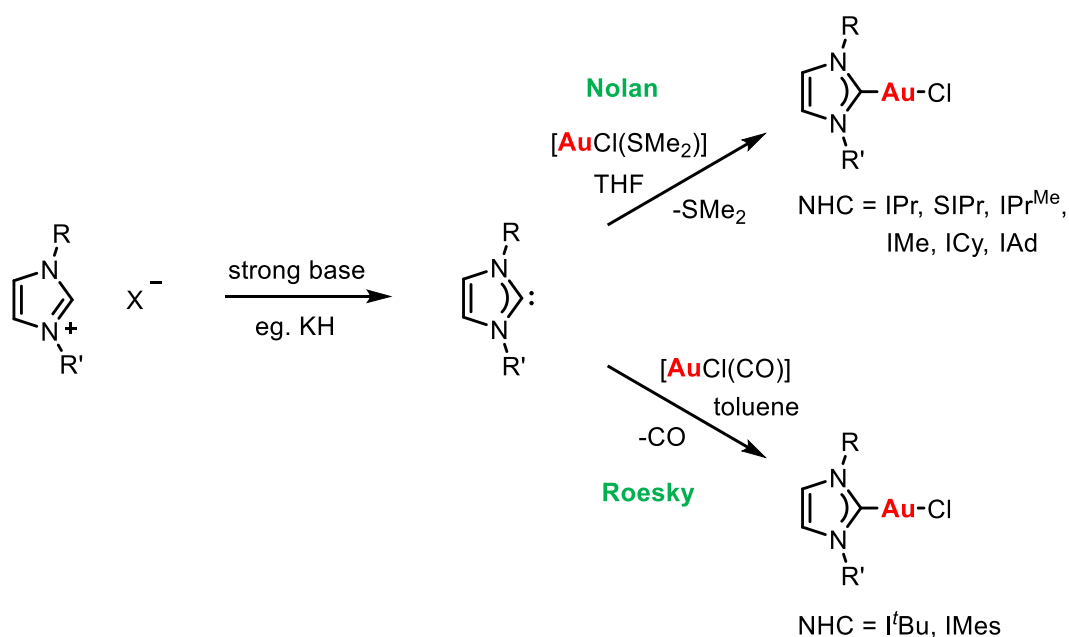
NHC ligands have also been found to stabilise three coordinate gold complexes incorporating a *nido*-carborane diphosphine (Figure 4.11(b)). The resultant complexes were brightly luminescent with incredibly high quantum yields, giving them the potential for future practical



applications such as in OLEDs. The emission of the NHC gold complexes could be changed by simple alterations to the structure of the NHC ligand and hence ligand design could potentially allow the luminescent properties to be fine-tuned for specific applications.<sup>287</sup>

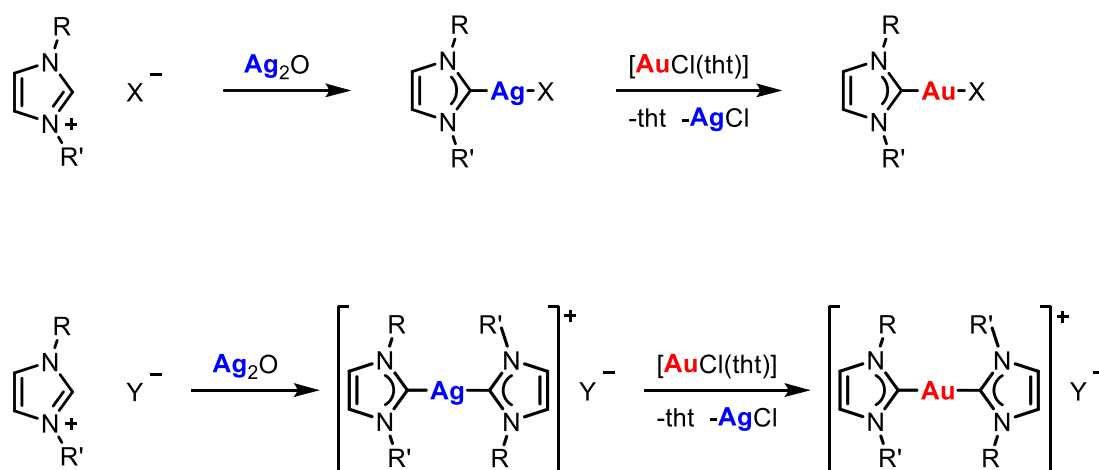
#### 4.1.4. Synthetic Methods for the Preparation of NHC Gold Complexes

The standard methods for the preparation of NHC gold complexes have several disadvantages. Reaction of a free NHC with a gold(I) source was reported almost simultaneously by the groups of Roesky and Nolan in 2005 (Scheme 4.8). It was noted that reaction with AuCl led to poor yields and gave complex mixtures of mono- and bis-carbene species as well as metallic gold.<sup>288</sup> Ligand displacement from a gold(I) precursor bearing a labile ligand was more successful. Nolan carried out the reaction of the free NHC with [AuCl(SMe<sub>2</sub>)] in THF to form the [AuCl(NHC)] complexes in moderate yields. The method was not general, however, and a mixture of products was obtained with the NHC IMes.<sup>288</sup> Roesky described the formation of two [AuCl(NHC)] complexes by reaction of the free NHC with [AuCl(CO)] obtaining the complexes in yields of 67 and 83%.<sup>289</sup> This methodology requires glovebox techniques and anhydrous solvents due to the instability of the free NHC. Often disproportionation and decomposition processes compete, leading to poor yields.



**Scheme 4.8.** Synthesis of [AuCl(NHC)] complexes via free NHCs.

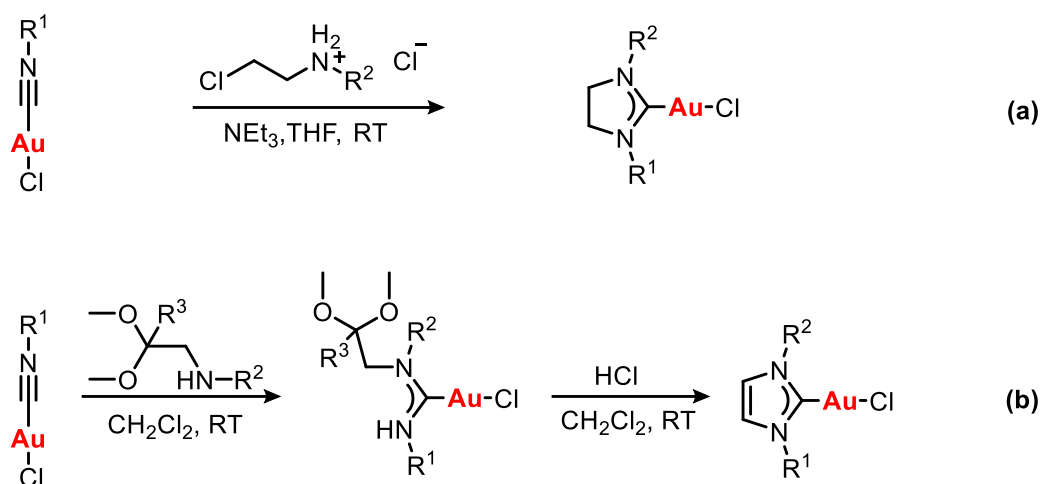
The most popular method for the preparation of NHC gold(I) complexes is the *in situ* preparation of the NHC silver or copper complex and subsequent transmetalation with gold, which is far more versatile, generally does not require the exclusion of air or moisture and results in high yields (Scheme 4.9). This method was first introduced in 1998 by Lin where the synthesis of both mono- and bis-NHC gold(I) complexes was achieved depending on whether a halide or non-coordinating anion was present in the starting imidazolium salt.<sup>290</sup> Later an analogous method was reported in which silver(I) oxide was substituted for copper(I) oxide to give an NHC copper(I) complex which could then undergo transmetalation with gold.<sup>291</sup>



**Scheme 4.9.** General synthesis of NHC gold(I) complexes via transmetalation (X = halide, Y = non-coordinating anion).

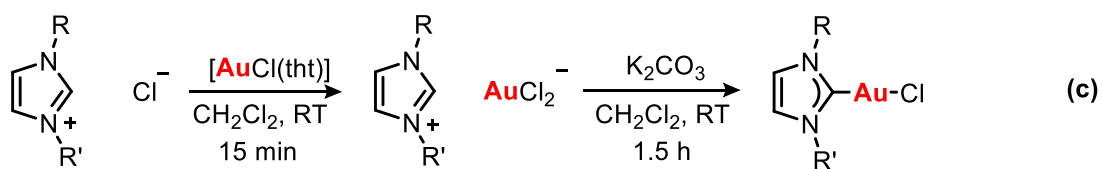
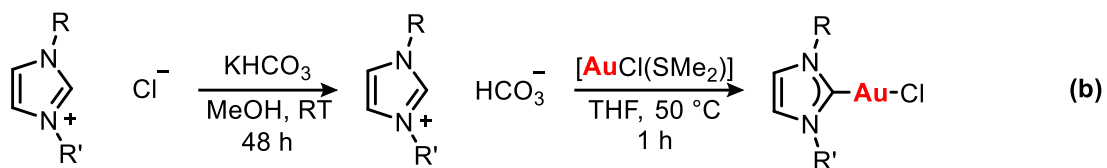
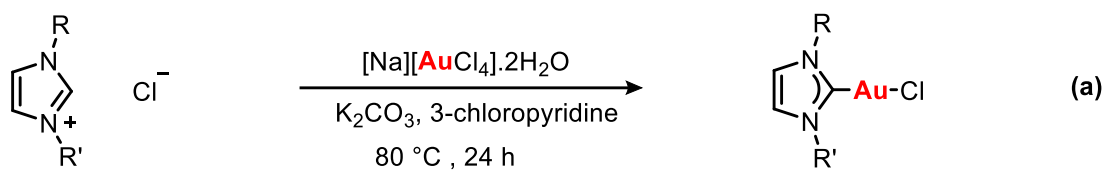
Although successful and high yielding, this method results in a full equivalent of silver or copper to be consumed in the reaction, making this process costly, and the final products may be contaminated with unwanted silver or copper species which is particularly undesirable in the preparation of catalysts or catalyst precursors.

More recently, several alternative methods have been reported. Hashmi and co-workers described a modular template synthesis of unsymmetrical NHC gold, palladium and platinum complexes starting from metal salts, isonitriles and amines with tethered acetal or etal moieties, or with  $\beta$ -chloroammonium salts in the presence of a base (Scheme 4.10).<sup>292-295</sup> However, reaction times were long and in many cases only moderate yields of the final products were obtained.



**Scheme 4.10.** Modular template synthesis for unsymmetrical NHC gold(I) complexes.

Alternative methods starting from imidazolium salts have also been described. In 2012, Zhu and co-workers demonstrated the successful preparation of a series of  $[AuCl(NHC)]$  by heating the tetrachloroaurate salts,  $[Na][AuCl_4] \cdot 2H_2O$  or  $[K][AuCl_4] \cdot 2H_2O$  with imidazolium salts,  $NHC \cdot HCl$ , in 3-chloropyridine for 24 h in the presence of potassium carbonate (Scheme 4.11(a)).<sup>296</sup> Although several complexes were prepared in good yields, this method was not suitable for the synthesis of bulky NHC gold complexes. Taton, Vignolle and co-workers reported the synthesis of bulky NHC gold complexes by heating imidazolium hydrogen carbonates in the presence of  $[AuCl(SMe_2)]$  in good yields (Scheme 4.11(b)).<sup>297</sup> In 2013, a method reported both by our group and the group of Nolan showed that  $[AuX(NHC)]$  complexes could be prepared in excellent yields by reaction of a gold source such as  $[AuCl(tht)]$  or  $[AuCl(SMe_2)]$  and the imidazolium salt in the presence of a weak base, without the need for inert atmosphere or dry solvents (Scheme 4.11(c)).<sup>298,299</sup> This method, however, is limited to NHCs with bulky groups at the nitrogen atoms and decomposition to metallic gold is observed when sterically smaller NHCs are employed.



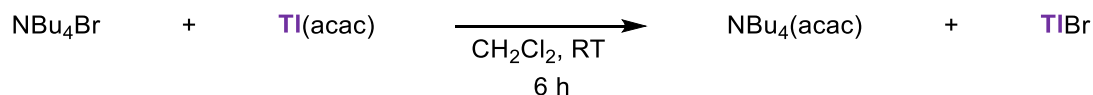
**Scheme 4.11.** Improved methods for the synthesis of NHC gold(I) complexes.

## 4.2. Synthesis of NHC Gold Complexes using Tetrabutylammonium Acetylacetonate

Tetrabutylammonium acetylacetonate,  $\text{NBu}_4(\text{acac})$ , is a reagent which has previously been used in gold chemistry for the synthesis of a variety of gold(I) complexes in which the acac ligand is bound to gold.<sup>300</sup> However, this reagent also has the potential to deprotonate an imidazolium chloride salt to form an NHC with concurrent formation of  $\text{NBu}_4\text{Cl}$ . In the presence of a gold(I) precursor possessing a labile ligand this would lead to formation of the NHC-gold complex.

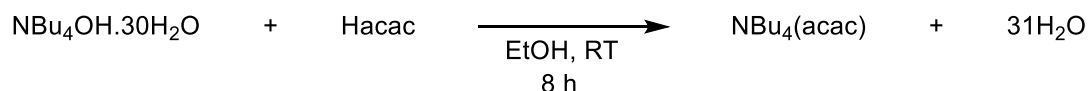
### 4.2.1. Synthesis of Tetrabutylammonium Acetylacetonate

Until now, the main method for the preparation of  $\text{NBu}_4(\text{acac})$  has been the reaction of tetrabutylammonium chloride or bromide with thallium acetylacetonate (Scheme 4.12).<sup>301</sup> Although effective and high yielding, this method requires use of an expensive and toxic thallium compound and is therefore not desirable.



**Scheme 4.12.** Synthesis of tetrabutylammonium acetylacetonate with thallium acetylacetonate.

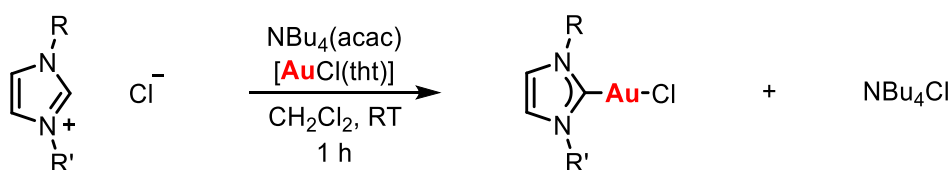
$\text{NBu}_4(\text{acac})$  can readily be prepared by a more economical and sustainable thallium-free method. The reaction of tetrabutylammonium hydroxide hydrate with acetylacetone in ethanol at room temperature leads to the formation of  $\text{NBu}_4(\text{acac})$  in a very high yield, 95% (Scheme 4.13). Excess water is removed by drying a dichloromethane solution of the product over sodium sulfate, and recrystallisation with diethyl ether gives the pure product as a white crystalline solid.  $\text{NBu}_4(\text{acac})$  is air stable and may readily be handled under ambient conditions.



**Scheme 4.13.** Thallium-free synthesis of tetrabutylammonium acetylacetonate.

### 4.2.2. Synthesis of NHC Gold Complexes using Tetrabutylammonium Acetylacetonate

The one-pot reaction of an imidazolium chloride salt with  $[\text{AuCl}(\text{tht})]$  and  $\text{NBu}_4(\text{acac})$  led to the formation of  $[\text{AuCl}(\text{NHC})]$  complexes in 1 h (Scheme 4.14). Reactions were carried out at room temperature under air and anhydrous solvents were not required. Filtration of the reaction solution through a pad of silica led to removal of the  $\text{NBu}_4\text{Cl}$  formed as a side product, and subsequent precipitation from dichloromethane solution by addition of diethyl ether allowed the NHC gold complexes to be obtained cleanly.

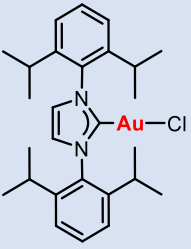
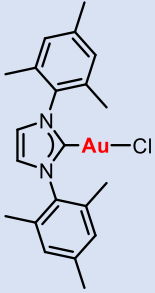
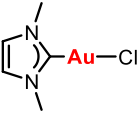
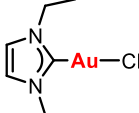
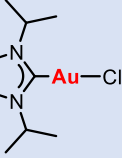
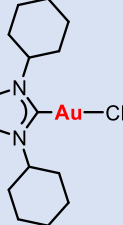
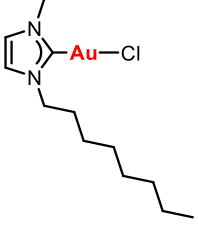
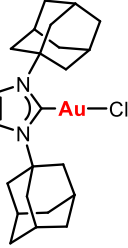


**Scheme 4.14.** Synthesis of  $[\text{AuCl}(\text{NHC})]$ .

The method was tested with a range of commercially available imidazolium chloride salts and found to be successful in both those with bulky groups at the nitrogen atoms as well as the more challenging, sterically smaller imidazolium salts (Table 4.1). In all cases the yields were high, although for complexes **87**, **88** and **90** slightly lower yields are observed due to some decomposition of the product on the silica. NMR studies show full conversion of the starting materials to products therefore it is likely that on a larger scale almost quantitative yields would be obtained.

## 4.2. Synthesis of NHC Gold Complexes using Tetrabutylammonium Acetylacetonate

**Table 4.1.** Scope of the new procedure for the synthesis of [AuCl(NHC)] complexes.

Complex	Yield (%)	Complex	Yield (%)
<p>83</p> 	95	<p>84</p> 	98
<p>85</p> 	94	<p>86</p> 	96
<p>87</p> 	64	<p>88</p> 	67
<p>89</p> 	87	<p>90</p> 	60

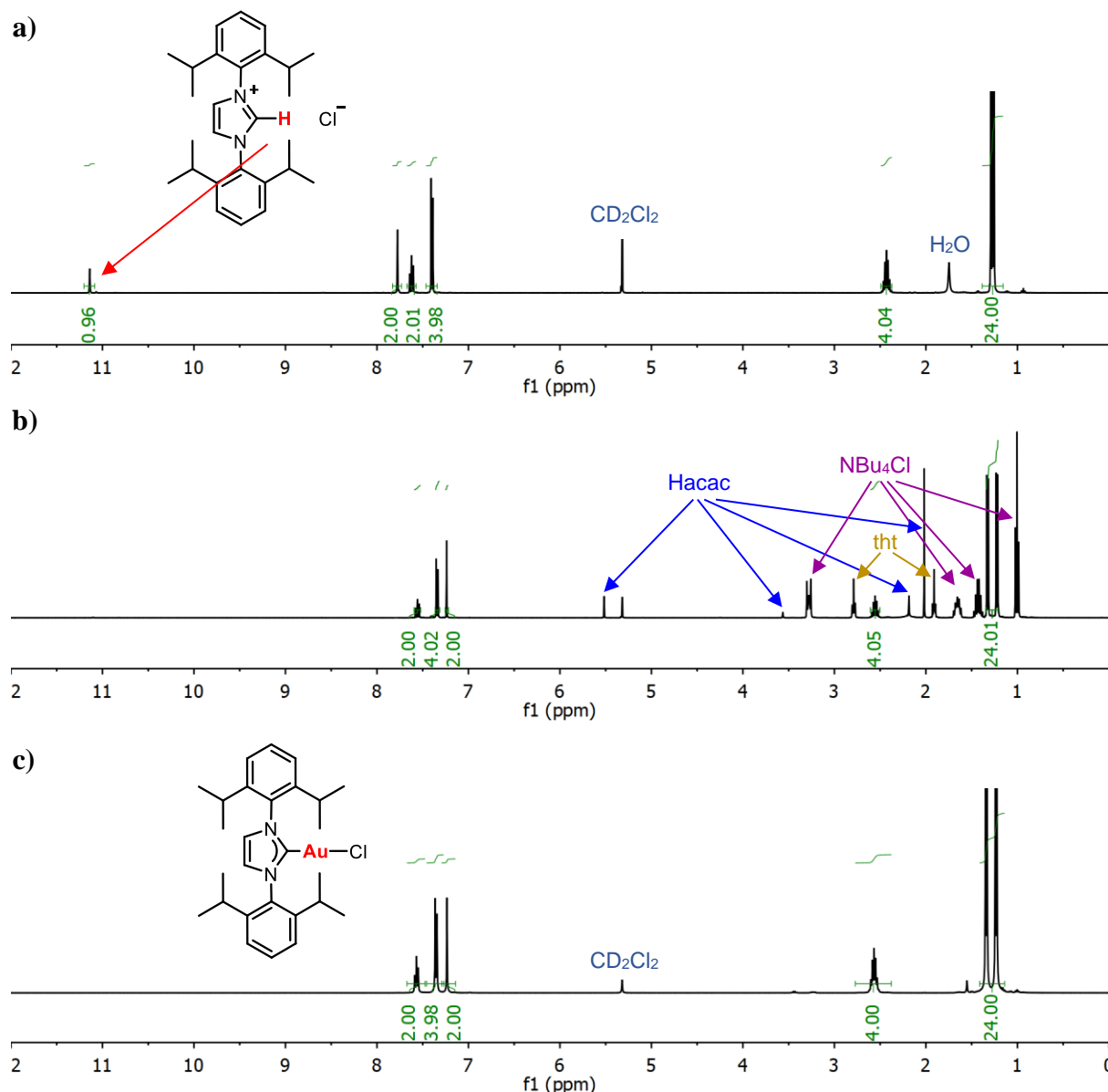


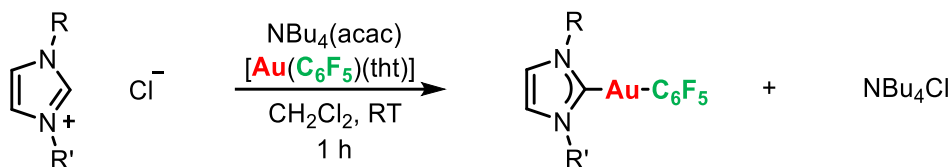
**Figure 4.12.**  $^1\text{H}$  NMR spectrum of starting imidazolium salt (a), reaction mixture after 10 min (b) and isolated product (c).

The  $^1\text{H}$  NMR spectrum of the reaction mixture for the IPr derivative taken after 10 min reaction time shows the presence of the  $[\text{AuCl}(\text{NHC})]$  complex along with the side products tht, Hacac and  $\text{NBu}_4\text{Cl}$  (Figure 4.12(b)) which are readily removed in the work-up. Four signals are observed for Hacac due to the keto and enol forms. No imidazolium salt is present and no other products are formed.



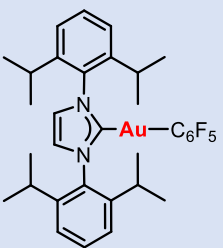
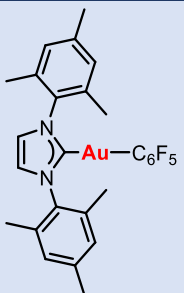
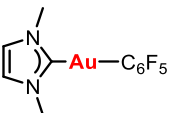
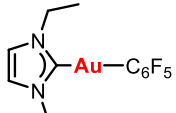
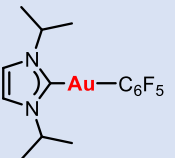
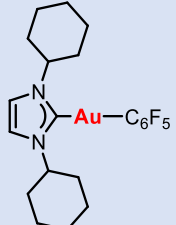
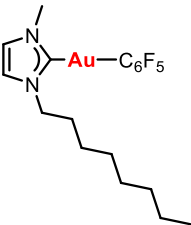
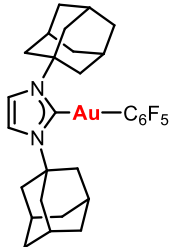
#### 4.2. Synthesis of NHC Gold Complexes using Tetrabutylammonium Acetylacetonate

When  $[\text{Au}(\text{C}_6\text{F}_5)(\text{tht})]$ , rather than  $[\text{AuCl}(\text{tht})]$ , is used as the gold(I) precursor, the  $[\text{Au}(\text{C}_6\text{F}_5)(\text{NHC})]$  complexes are obtained with good to excellent yields (Scheme 4.15). Again, a simple filtration through silica and subsequent precipitation from dichloromethane allows the complexes to be obtained cleanly and the method is successful for both the bulky and smaller NHCs (Table 4.2).



**Scheme 4.15.** Synthesis of  $[\text{Au}(\text{C}_6\text{F}_5)(\text{NHC})]$

**Table 4.2.** Scope of the new procedure for the synthesis of  $[\text{Au}(\text{C}_6\text{F}_5)(\text{NHC})]$  complexes.

Complex	Yield (%)	Complex	Yield (%)
<b>91</b> 	73	<b>92</b> 	80
<b>93</b> 	86	<b>94</b> 	56
<b>95</b> 	61	<b>96</b> 	91
<b>97</b> 	76	<b>98</b> 	52

The molecular structures of complexes **92**, **93**, **95** and **98** were determined by single crystal X-ray diffraction (Figure 4.13). All four complexes have the expected linear geometry around the gold centre with angles ranging from  $173.66(12)^\circ$  for complex **95** to  $177.30(12)^\circ$  for complex **92**. The shortest Au-C distances for the NHC carbon are  $2.013(3)$  Å for **98**,  $2.017(3)$  Å for **95** and  $2.018(5)$  Å for **93**, which correspond to the alkyl substituted NHC ligands, and the longest was  $2.035(2)$  Å for complex **92** with an aryl substituent. These distances are longer than those

found in  $[\text{AuCl}(\text{NHC})]$  complexes,<sup>274</sup> probably because of the higher *trans* influence of the pentafluorophenyl group compared to the chloride ligand.

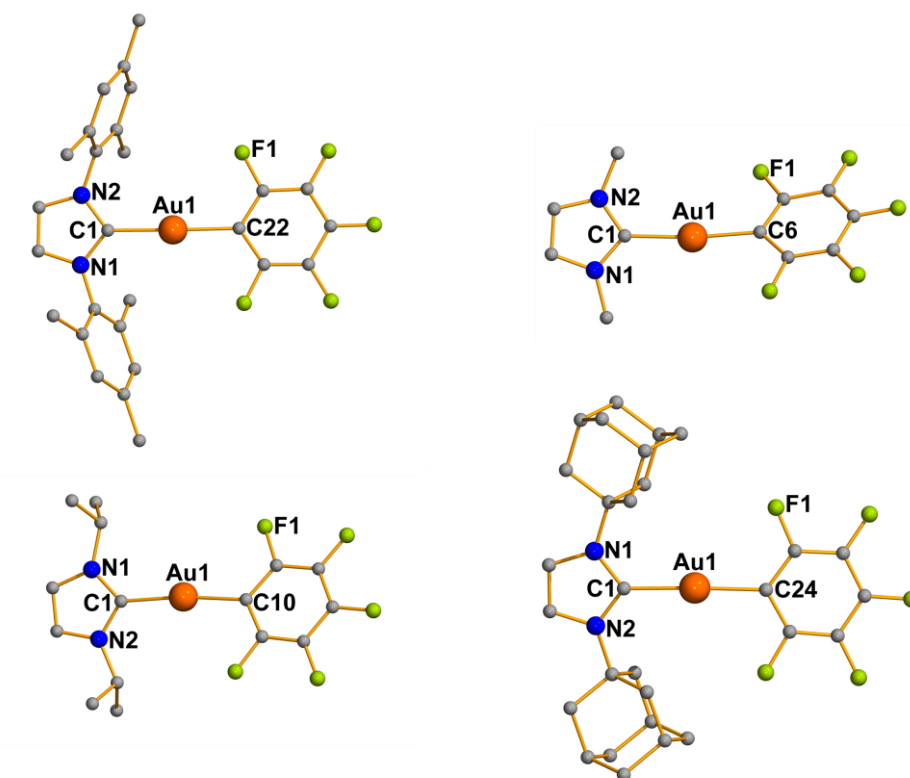


**Figure 4.13.** Molecular structures of complexes **92**, **93**, **95** and **98**. Hydrogen atoms are omitted for clarity. Selected bond lengths [ $\text{\AA}$ ] and angles [ $^\circ$ ] **92**: Au(1)-C(1) 2.013(3), Au(1)-C(22) 2.041(3), N(1)-C(1) 1.358(4), N(2)-C(1) 1.352(4), C(1)-Au(1)-C(22) 177.30(12). **93**: Au(1)-C(1) 2.018(5), Au(1)-C(6) 2.024(6), N(1)-C(1) 1.354(7), N(2)-C(1) 1.337(6), C(1)-Au(1)-C(6) 174.21(17). **95**: Au(1)-C(1) 2.017(3), Au(1)-C(10) 2.040(3), N(1)-C(1) 1.359(4), N(2)-C(1) 1.357(4), C(1)-Au(1)-C(10) 173.66(12). **98**: Au(1)-C(1) 2.035(2), Au(1)-C(24) 2.041(2), N(1)-C(1) 1.361(3), N(2)-C(1) 1.366(3), C(1)-Au(1)-C(24) 177.22(9).

The smaller NHC ligand in complex **93** allows the presence of intramolecular contacts. The molecules are associated in trimers through weak  $\text{Au}\cdots\text{Au}$  interactions of 3.648  $\text{\AA}$ . There are also several  $\text{F}\cdots\text{H}$  contacts between the molecules in the range 2.550–2.820  $\text{\AA}$ . The pentafluorophenyl and imidazolium rings are located in parallel fashion with  $\pi$ -stacking interactions between one of the carbons of the imidazolium moiety and two carbons of the pentafluorophenyl ring (Figure 4.14).

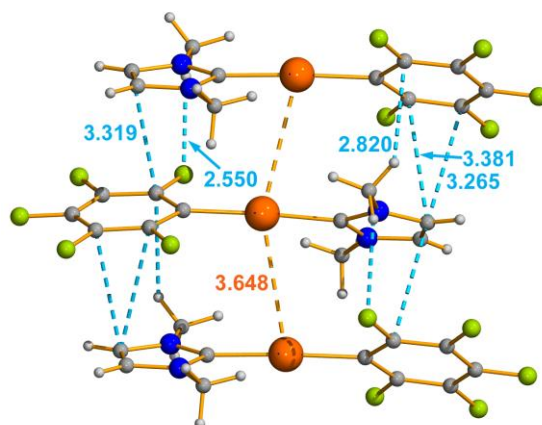
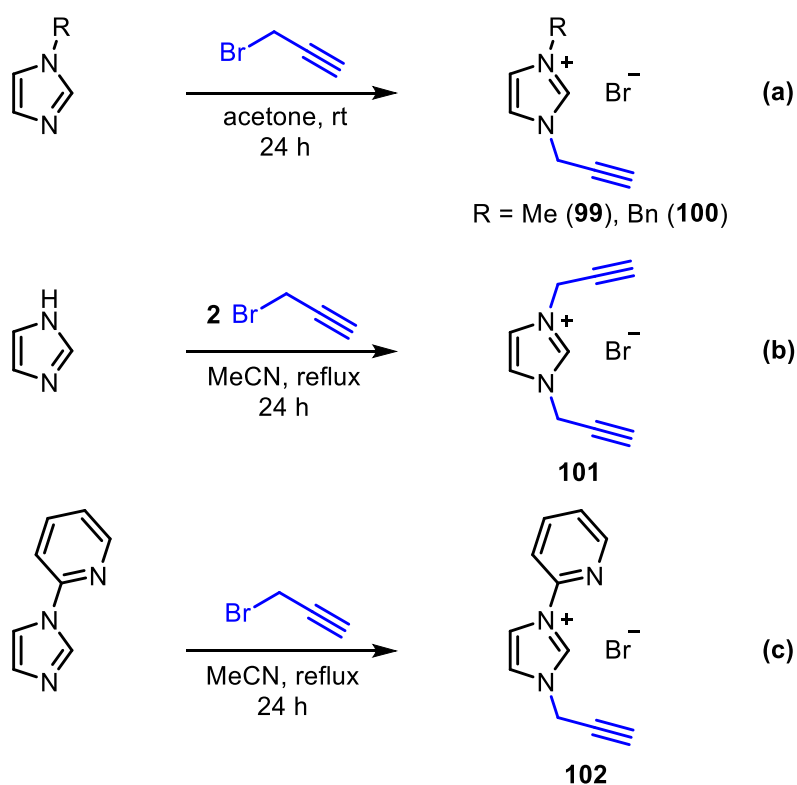


**Figure 4.14.** Association of molecules of **93** in trimers through weak intramolecular  $\text{Au} \cdots \text{Au}$  contacts and secondary bonds [Å].

### 4.3. Synthesis of Propargyl Functionalised Imidazolium Salts

With the aim of subsequently preparing propargyl functionalised NHC gold complexes using the new  $\text{NBu}_4(\text{acac})$  method, a series of propargyl functionalised imidazolium salts (**99-102**) were prepared (Scheme 4.16).

The methyl and benzyl derivatives, **99** and **100**, were prepared by reaction of 1-methyl- or 1-benzylimidazole with propargyl bromide in acetone at room temperature, similar to a previously reported procedure.<sup>302</sup> 1,3-dipropargylimidazolium bromide, **101**, was prepared by heating an acetonitrile solution of imidazole to reflux with an excess of propargyl bromide, a modification to another previously reported procedure.<sup>303-305</sup> The pyridyl derivative, **102**, described for the first time, was prepared similarly by reaction of 1-(2-pyridyl)imidazole with propargyl bromide at reflux in acetonitrile. All of the imidazolium salts, apart from the methyl derivative, were white solids at room temperature and were insoluble in all common organic solvents but soluble in water and alcohols. The methyl derivative was a pale yellow ionic liquid, immiscible with organic solvents but miscible with water and alcohols.



**Scheme 4.16.** Synthesis of propargyl functionalised imidazolium salts **99-102**.

Formation of the imidazolium salts could readily be confirmed by the presence of a signal at a high chemical shift ( $\sim 10$  ppm) in the  $^1\text{H}$  NMR spectrum, corresponding to the proton at the N-C2-N carbon atom. Additionally, a doublet and triplet are observed, corresponding to the  $\text{CH}_2$  and  $\text{CH}$  of the propargyl group, respectively (Figure 4.15).

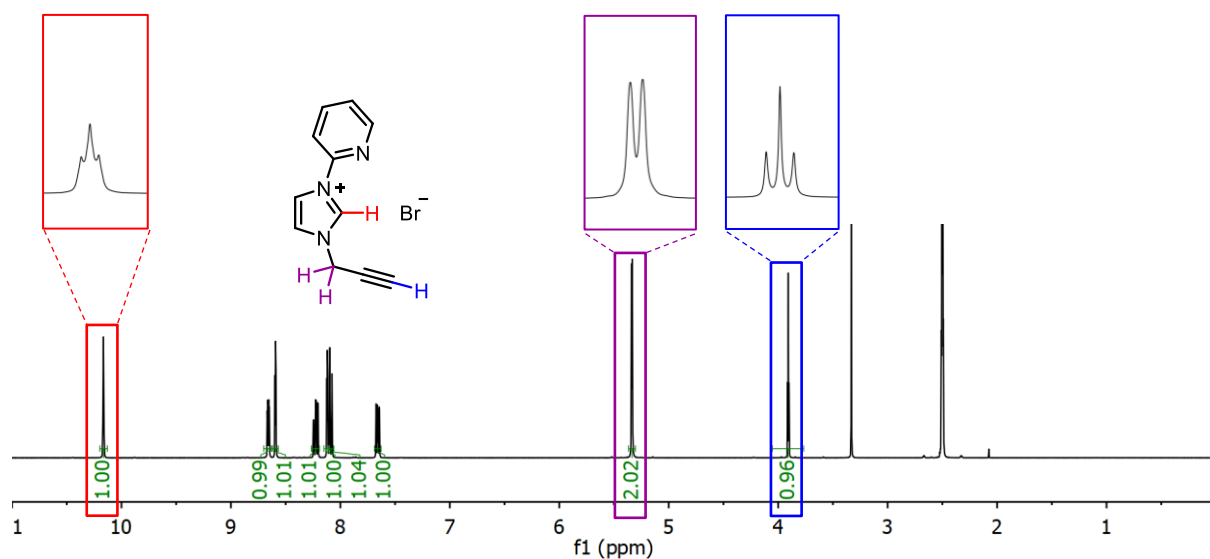
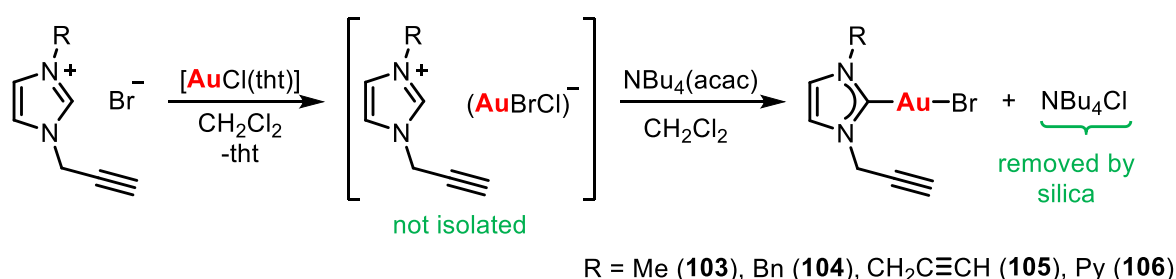


**Figure 4.15.**  $^1\text{H}$  NMR spectrum of imidazolium salt **102** in DMSO.

## 4.4. Synthesis of Propargyl Functionalised NHC Gold Complexes

### 4.4.1. Synthesis of Bromo Derivatives

Addition of a stoichiometric amount of  $[\text{AuCl}(\text{tht})]$  to imidazolium bromide salts **99-102** in dichloromethane led to solutions of the  $[\text{imidazolium}][\text{AuBrCl}]$  salts. Subsequent addition of the  $\text{NBu}_4(\text{acac})$  gave the  $[\text{AuBr}(\text{NHC})]$  complexes **103-106** with reaction times of just 1 h, similarly to with the commercial imidazolium chloride salts (Scheme 4.17). The complexes could be separated from the  $\text{NBu}_4\text{Cl}$  formed in the reaction by filtration through silica and were obtained in good yields (73-82%).



**Scheme 4.17.** Synthesis of  $[\text{AuBr}(\text{NHC})]$  complexes **103-106**.

The successful formation of the NHC could be confirmed by the disappearance of the imidazolium C2-H signal in the  $^1\text{H}$  NMR spectrum. In the  $^{13}\text{C}$  APT spectra the carbene carbon signal appears at a much higher chemical shift ( $\sim 170$  ppm) compared to the starting imidazolium salts (Figure 4.16).

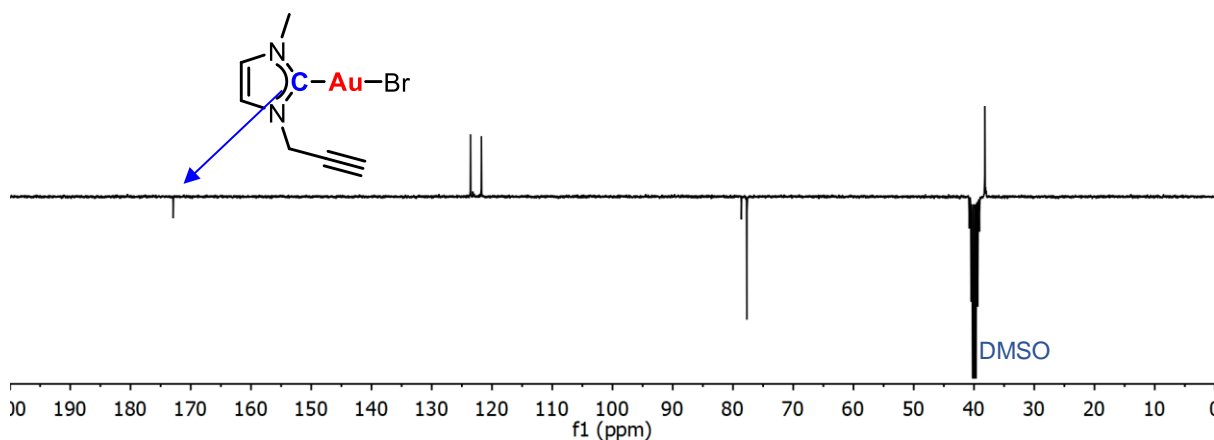


**Figure 4.16.**  $^{13}\text{C}$  NMR spectrum of complex **103** in **DMSO**.

The molecular structures of complexes **103-106** were determined by single crystal X-ray diffraction. Suitable crystals were obtained by the slow diffusion of pentane into solutions of the complexes in dichloromethane. In all of the complexes the carbon-carbon triple bond of the propargyl unit is maintained and no interaction with the gold centre is observed.

Complex **103** with the smallest substituent on the NHC, a methyl group, has a structure in which intermolecular aurophilic interactions are present, with Au...Au distances of 3.324(1) Å (Figure 4.17). The propargyl substituent is orientated perpendicular to the coplanar Br-Au-NHC unit. The Au-C bond distance is 1.985(5) Å, which is the shortest described for an NHC-Au-Br complex and indicates a strong bond, as expected for strong  $\sigma$ -donor NHCs. The Au-Br distance of 2.4038(15) Å is longer than that reported by Meyer and co-workers with an aryl substituted carbene (2.3904(4) Å).<sup>306</sup> The C-C distances within the propargyl unit are C(5)-C(6) 1.472(6) Å and C(6)-C(7) 1.183(7) Å, which correspond to single and triple bonds, respectively. The gold centre is in a linear geometry with a C(1)-Au(1)-Br(1) angle of 174.35(12)°.

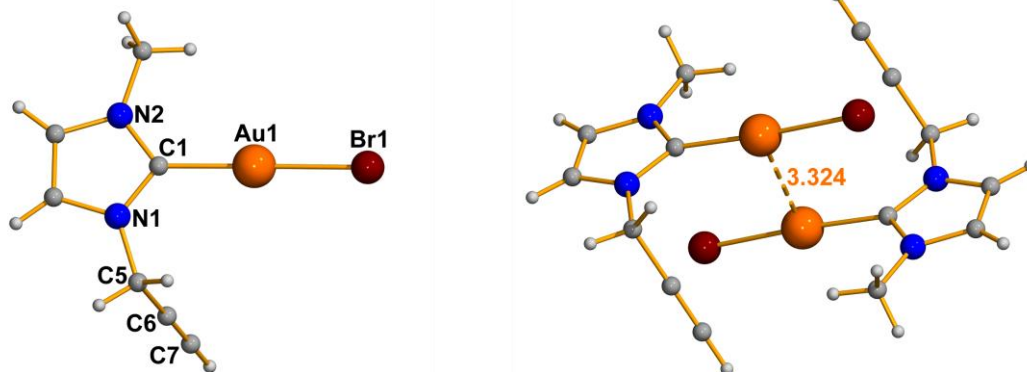


**Figure 4.17.** Molecular structure of complex **103**. Selected bond lengths [Å] and angles [°]: Au(1)-C(1) 1.985(5), Au(1)-Br(1) 2.4038(15), N(1)-C(1) 1.353(6), N(2)-C(1) 1.342(6), C(5)-C(6) 1.472(6), C(6)-C(7) 1.183(7), C(1)-Au(1)-Br(1) 174.35(12).

The structures of complexes **104-106** (Figure 4.18) show patterns similar to those found in **103** with the exception of the aurophilic interactions. The increase in steric demand of the substituents on the nitrogen atom of the imidazole ring causes the disappearance of this intermolecular contact. As expected when changing to substituents with a weaker donor



#### 4.4. Synthesis of Propargyl Functionalised NHC Gold Complexes

capacity the Au-C<sub>carbene</sub> bond distances are slightly longer in these complexes following the order Me < CH<sub>2</sub>C≡CH < CH<sub>2</sub>Ph ≈ Py, although values for Py and CH<sub>2</sub>Ph are similar within the errors and the differences may not be significant. Additionally, a concurrent decrease in the Au-Br distance is observed with increasing Au-C<sub>carbene</sub> bond distance.

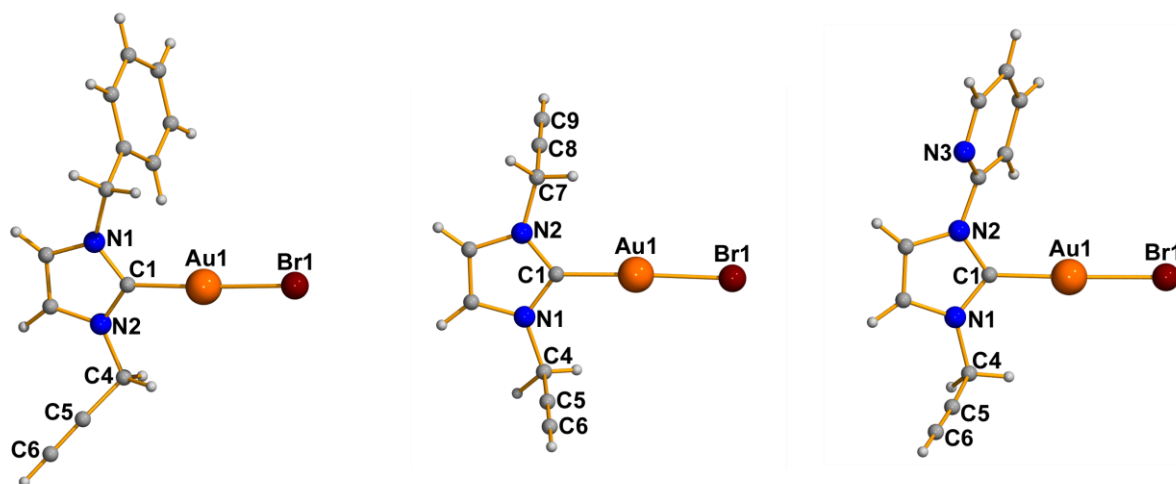
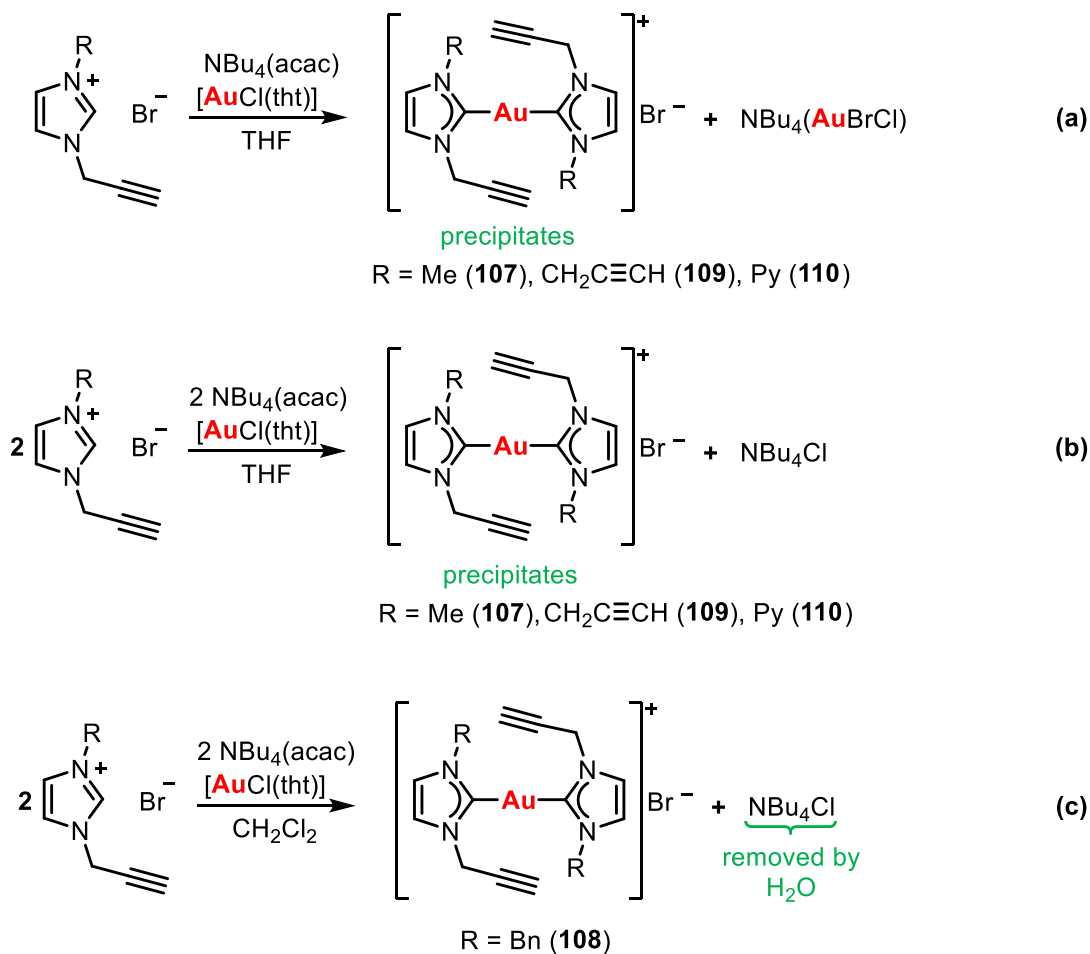


**Figure 4.18.** Molecular structures of complexes **104–106**. Selected bond lengths [Å] and angles [°] **104**: Au(1)–C(1) 2.004(5), Au(1)–Br(1) 2.3927(7), N(1)–C(1) 1.341(6), N(2)–C(1) 1.327(6), C(4)–C(5) 1.453(7), C(5)–C(6) 1.179(7), C(1)–Au(1)–Br(1) 177.78(12); **105**: Au(1)–C(1) 1.994(4), Au(1)–Br(1) 2.4057(4), N(1)–C(1) 1.337(5), N(2)–C(1) 1.346(5), C(5)–C(6) 1.176(7), C(8)–C(9) 1.172(6), C(1)–Au(1)–Br(1) 177.23(12); **106**: Au(1)–C(1) 1.988(10), Au(1)–Br(1) 2.3967(10), N(1)–C(1) 1.347(12), N(2)–C(1) 1.354(11), C(4)–C(5) 1.478(13), C(5)–C(6) 1.191(15), C(8)–C(9) 1.172(6), C(1)–Au(1)–Br(1) 174.6(2).

#### 4.4.2. Synthesis of Bis-NHC Complexes

When the reaction of the imidazolium bromide salts, [AuCl(tht)] and NBu<sub>4</sub>(acac) was carried out in THF, rather than dichloromethane, a white precipitate was observed in all cases except for with the benzyl derivative **100** (Scheme 4.18). This was identified as the bis-carbene species [Au(NHC)<sub>2</sub>Br], and its formation is likely favoured in this case because of its insolubility in THF. Complexes **107**, **108** and **110** could be formed in excellent yields (82–95%) by reaction of 2 equivalents of the imidazolium salt with 1 equivalent of [AuCl(tht)] and 2 equivalents of NBu<sub>4</sub>(acac) in THF with precipitation of the product (Scheme 4.18(b)). Due to its solubility in THF, bis-carbene species **109** was prepared by reaction in dichloromethane followed by washing water to remove NBu<sub>4</sub>Cl, however, **109** also exhibits some water solubility and hence was only isolated in moderate yield (63%).

As with the bromo derivatives, the successful formation of the NHC could be confirmed by the disappearance of the imidazolium C2-H signal in the  $^1\text{H}$  NMR spectrum and the high chemical shift of the C2 carbon signal in the  $^{13}\text{C}$  APT spectrum. For these bis-carbene species the carbene carbon signal was observed at a higher chemical shift than for the bromo derivatives (180-185 ppm), due to the greater *trans* influence of the NHC.



**Scheme 4.18.** Formation of  $[\text{Au}(\text{NHC})_2]\text{Br}$  complexes.

The molecular structures of **109** and **110** were obtained by single crystal X-Ray diffraction. Complex **109** presents an almost ideal linear geometry with a C(1)-Au(1)-C(10) angle of  $178.6(5)^\circ$  (Figure 4.19). The Au-C bond lengths are 2.011(13) Å and 2.015(12) Å, which as expected, are longer than in the  $[\text{AuBr}(\text{NHC})]$  complexes. The molecules are associated in dimers with some secondary  $\pi$ - $\pi$  stacking contacts, resulting in a long  $\text{Au}\cdots\text{Au}$  interaction of 3.797 Å between the gold centres. The distance between the centroids of the imidazolyl rings is 3.848 Å, although there are shorter contacts between the carbene carbon and the nitrogen

#### 4.4. Synthesis of Propargyl Functionalised NHC Gold Complexes

atom of the other molecule. Additionally, a weak Au-C interaction of 3.243 Å is observed with the alkyne carbon. The bromide anions form hydrogen bonds in an octahedral fashion with the protons of the propargyl units, most of which are above the sum of the van der Waals radii, the shortest value being 2.487 Å.

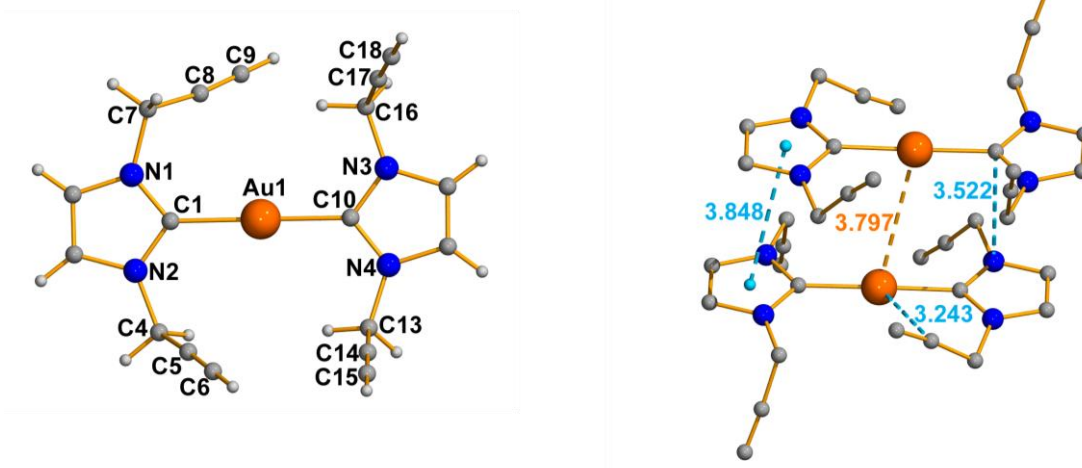


**Figure 4.19.** Molecular structure of complex **109**, and associated dimers through different secondary interactions. Selected bond lengths [Å] and angles [°]: Au(1)-C(10) 2.011(13), Au(1)-C(1) 2.015(12), N(1)-C(1) 1.342(15), N(2)-C(1) 1.353(15), N(3)-C(10) 1.368(16), N(4)-C(10) 1.351(17), C(4)-C(5) 1.469(18), C(5)-C(6) 1.185(19), C(7)-C(8) 1.457(17), C(8)-C(9) 1.182(19), C(13)-C(14) 1.489(18), C(14)-C(15) 1.18(2), C(16)-C(17) 1.466(19); C(10)-Au(1)-C(1) 178.6(5).

The structure of complex **110** is shown in Figure 4.20. The molecule lies in a two-fold axis and therefore only half corresponds to the asymmetric unit. The Au-C distance of 2.21(8) Å is slightly longer than that found in complex **109**, as expected for a weaker  $\sigma$ -donor carbene. The bromide makes a weak hydrogen bonds of 2.522 and 2.594 Å with the alkyne protons, giving rise to a supramolecular structure with formation of squares (Figure 4.21).

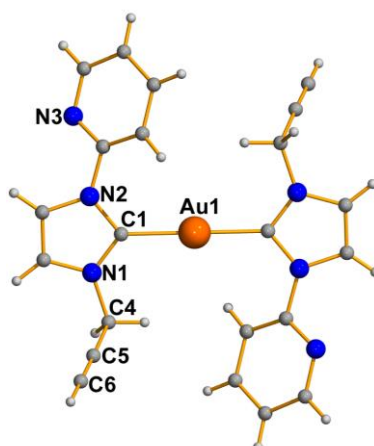


**Figure 4.20.** Molecular structure of complex **110**. Selected bond lengths (Å) and angles (°): Au(1)-C(1) 2.021(8), C(5)-C(6) 1.176(14), C(5)-C(4) 1.463(15); C(1)#1-Au(1)-C(1) 179.997(1). Symmetry transformations used to generate equivalent atoms: (#1)  $-x + \frac{1}{2}, -y + \frac{1}{2}, -z$ .

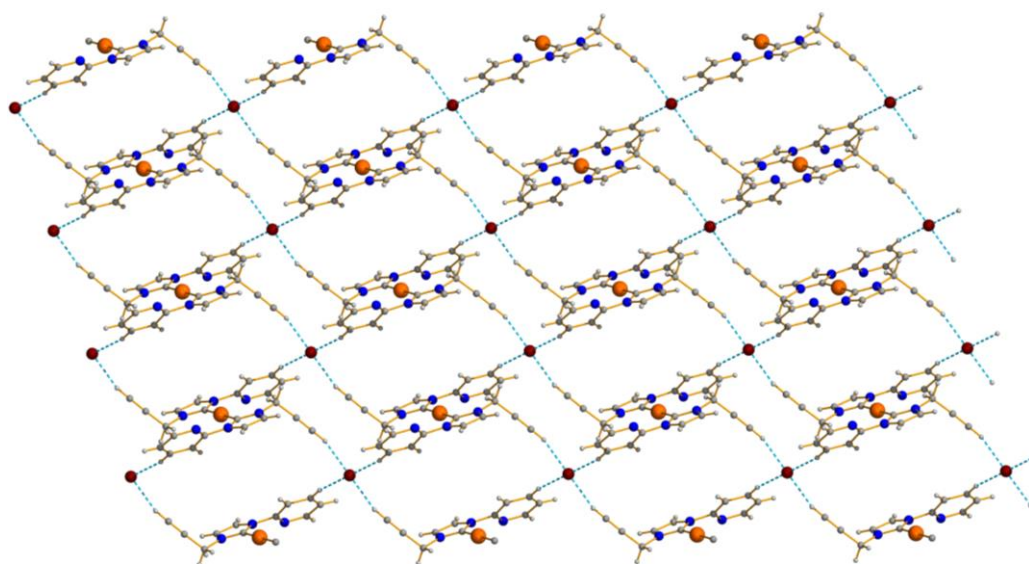
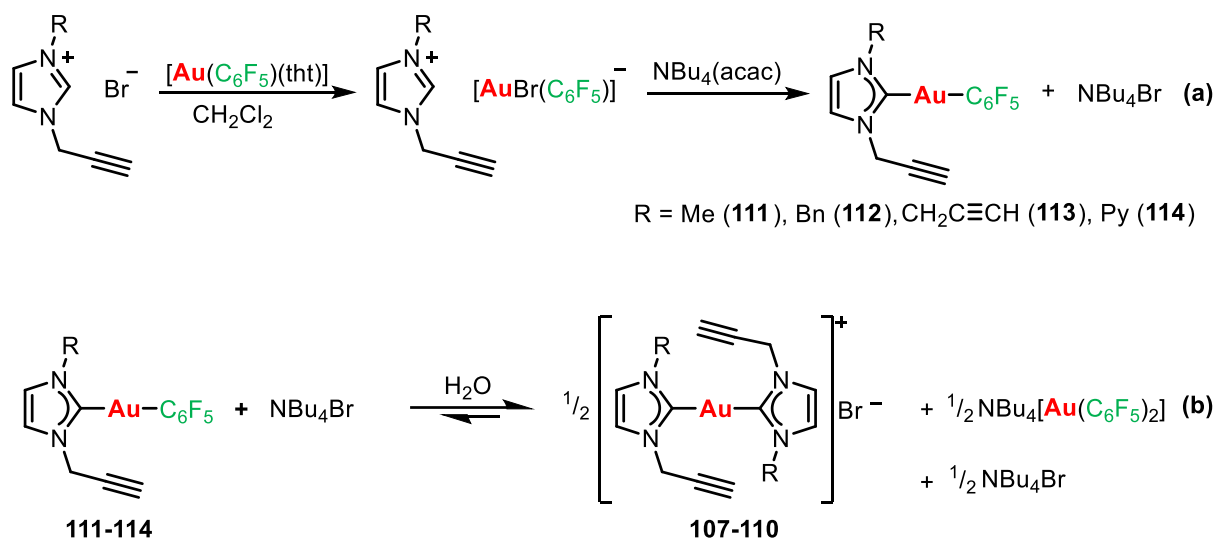


**Figure 4.21.** Formation of a supramolecular structure by Br...H interactions in complex **110**.

#### 4.4.3. Synthesis of Pentafluorophenyl Derivatives

Reaction of the imidazolium salts **99-102** with  $[\text{Au}(\text{C}_6\text{F}_5)(\text{tht})]$  gave the  $[\text{imidazolium}][\text{AuBr}(\text{C}_6\text{F}_5)]$  salts and subsequent addition of  $\text{NBu}_4(\text{acac})$  led to the formation of the  $[\text{Au}(\text{C}_6\text{F}_5)(\text{NHC})]$  complexes **111-114** (Scheme 4.19(a)).

#### 4.4. Synthesis of Propargyl Functionalised NHC Gold Complexes



**Scheme 4.19.** Formation of complexes **29-32** and their equilibrium in water.

Initial NMR studies of the reaction showed the formation of small amounts of  $\text{NBu}_4[\text{Au}(\text{C}_6\text{F}_5)_2]$  (Figure 4.22(a)), and washing the reaction mixture with water led to an increase in the ratio of this product compared to the desired  $[\text{Au}(\text{C}_6\text{F}_5)(\text{NHC})]$  (Figure 4.22(b)). This can be explained by the equilibrium shown in Scheme 4.19(b). Since the bis-carbene species are soluble in water, washing the reaction mixture with water would result in removal of this product, forcing the equilibrium to produce more with concurrent formation of  $\text{NBu}_4[\text{Au}(\text{C}_6\text{F}_5)_2]$ .

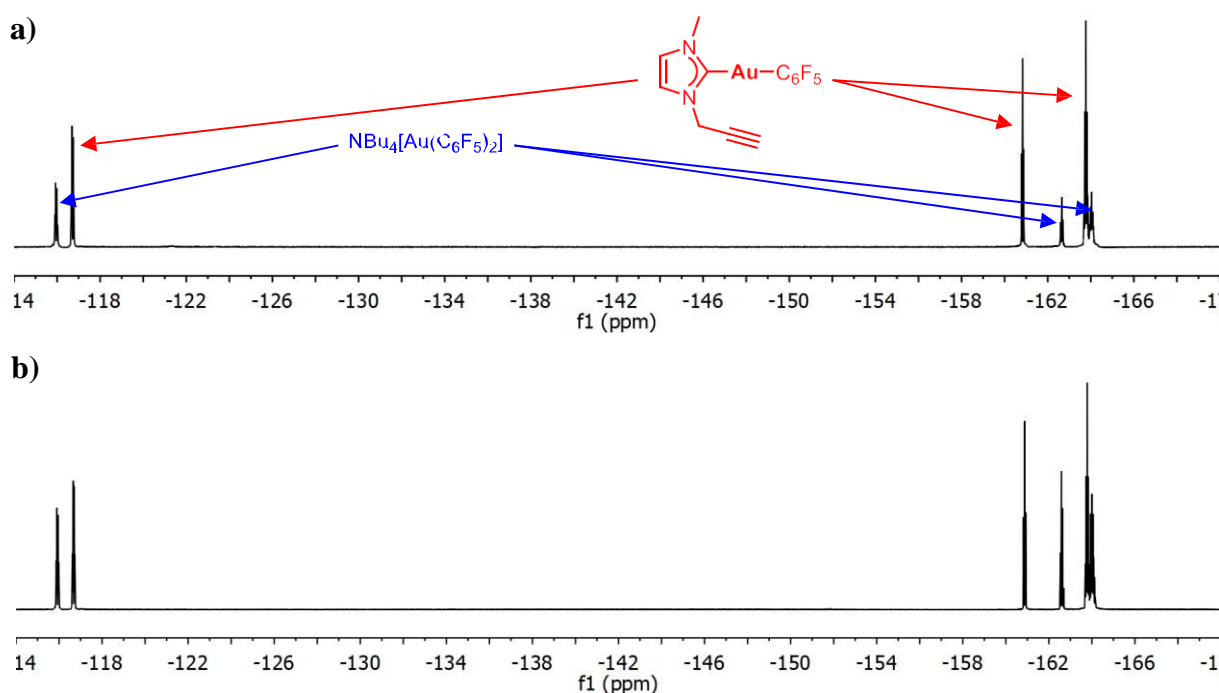


**Figure 4.22.**  $^{19}\text{F}$  NMR of initial reaction mixture (a) and after washing with water (b).

Before washing with water, the equilibrium lies far towards the side of the desired product  $[\text{Au}(\text{C}_6\text{F}_5)(\text{NHC})]$ . These complexes could therefore be obtained cleanly and in high yields by using an alternative purification method. Simply filtering the reaction mixture through silica led to removal of  $\text{NBu}_4\text{Br}$  and any of the by-products formed as a result of the equilibrium of the products, thus leaving the desired complexes **111-114** in good yields (76-87%)

The molecular structure of **113** was obtained by single crystal X-ray diffraction (Figure 4.23). The gold centre is linearly coordinated with a  $\text{C}(1)\text{-Au}(1)\text{-C}(10)$  angle of  $175.79(19)^\circ$ , to two different carbon donor ligands. The  $\text{C}_{\text{carbene}}\text{-Au}$  distance is  $2.022(5)$  Å while the  $\text{C}_{\text{pentafluorophenyl}}\text{-Au}$  distance is  $2.048(5)$  Å. The molecules of **113** are associated in dimers with a weak intermolecular  $\text{Au}\cdots\text{Au}$  interaction of  $3.3506(8)$  Å, together with some slipped  $\pi$ - $\pi$  stacking interactions between the imidazolyl and the pentafluorophenyl rings, the shortest contacts are  $3.388$  Å and  $3.420$  Å.

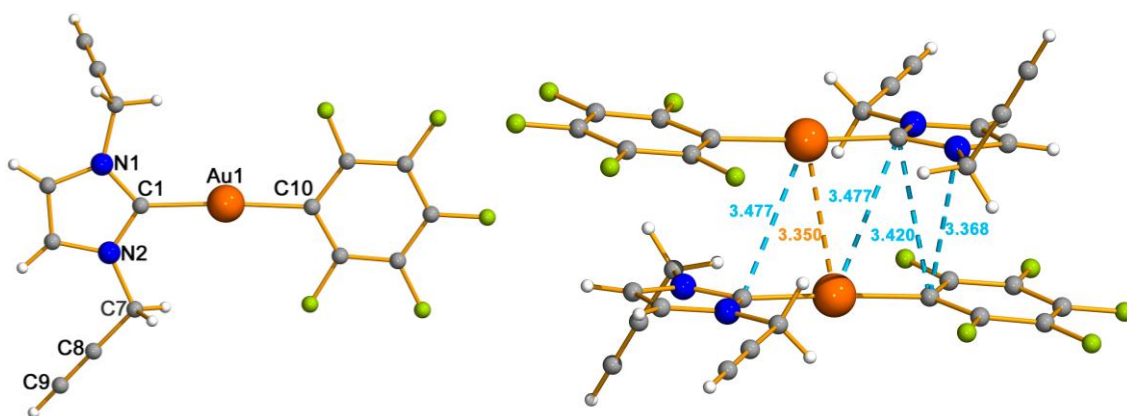
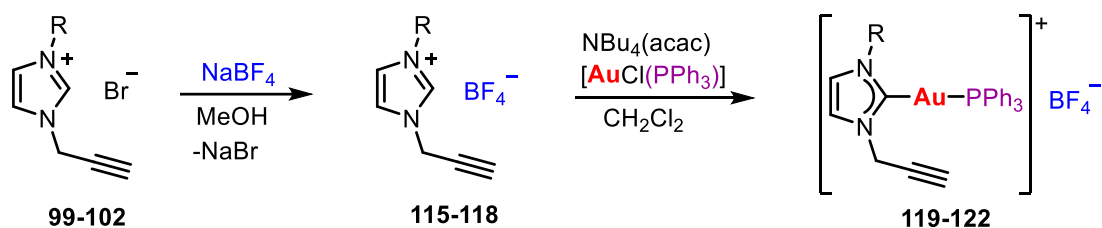


**Figure 4.23.** Molecular structure of complex **113**. Selected bond lengths (Å) and angles ( $^\circ$ ):  $\text{Au}(1)\text{-C}(1)$   $2.022(5)$ ,  $\text{Au}(1)\text{-C}(10)$   $2.048(5)$ ,  $\text{Au}(1)\text{-Au}(1)\#1$   $3.3506(8)$ ,  $\text{N}(1)\text{-C}(1)$   $1.353(7)$ ,  $\text{C}(4)\text{-C}(5)$   $1.462(7)$ ,  $\text{C}(5)\text{-C}(6)$   $1.181(8)$ ,  $\text{C}(7)\text{-C}(8)$   $1.455(8)$ ,  $\text{C}(8)\text{-C}(9)$   $1.184(8)$ ;  $\text{C}(1)\text{-Au}(1)\text{-C}(10)$   $175.79(19)$ .

#### 4.4.4. Synthesis of NHC Gold Phosphine Derivatives

The synthesis of triphenylphosphine derivatives  $[\text{Au}(\text{NHC})(\text{PPh}_3)]^+$  from the imidazolium salts **99-102** was attempted. Since the desired complexes are cationic, the anion of the imidazolium salts was changed for a non-coordinating tetrafluoroborate anion by a metathesis reaction with sodium tetrafluoroborate in methanol, followed by recrystallisation in dichloromethane. The resulting imidazolium tetrafluoroborate salts, **115-118**, were then reacted with  $[\text{AuCl}(\text{PPh}_3)]$  and  $\text{NBu}_4(\text{acac})$  in dichloromethane (Scheme 4.20).

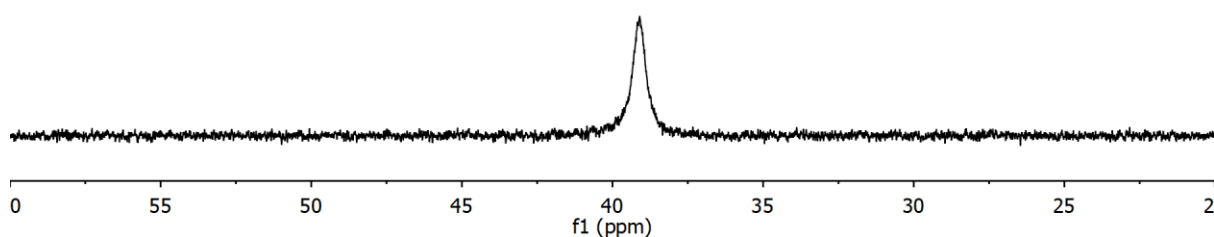
#### 4.4. Synthesis of Propargyl Functionalised NHC Gold Complexes



**Scheme 4.20.** Attempted synthesis of  $[\text{Au}(\text{NHC})(\text{PPh}_3)]\text{BF}_4$

Reaction of the imidazolium tetrafluoroborate salts, **115-118**, with  $[\text{AuCl}(\text{PPh}_3)]$  and  $\text{NBu}_4(\text{acac})$  followed by washing with water to remove  $\text{NBu}_4\text{Cl}$ , gave a white solid in each case.  $^{31}\text{P}\{^1\text{H}\}$  NMR studies in  $\text{CD}_2\text{Cl}_2$  at room temperature showed a broad peak at around 39 ppm (Figure 4.24(a)) and lowering the temperature to  $-80^\circ\text{C}$  allowed observation of three different phosphorus containing products, believed to be the desired  $[\text{Au}(\text{NHC})(\text{PPh}_3)]^+$ ,  $[\text{Au}(\text{PPh}_3)_2]^+$  and a tricoordinate species (Figure 4.24(b)).

a)



b)

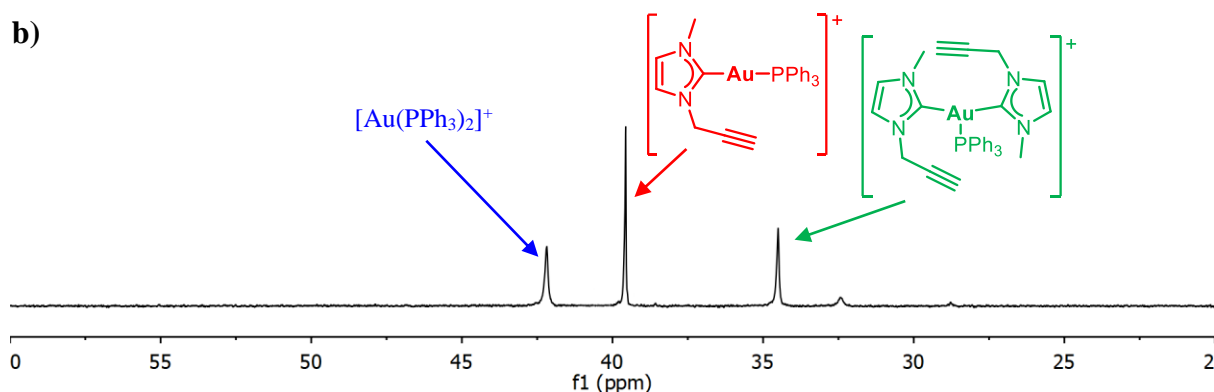
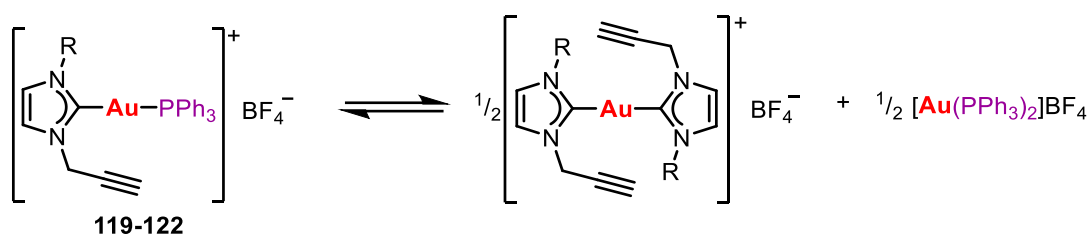


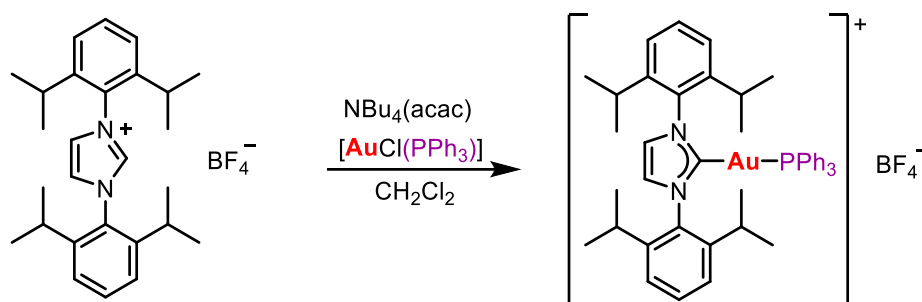
**Figure 4.24.**  $^{31}\text{P}\{^1\text{H}\}$  NMR spectrum of the reaction of **115** with  $[\text{AuCl}(\text{PPh}_3)]$  and  $\text{NBu}_4(\text{acac})$  in  $\text{CD}_2\text{Cl}_2$  at room temperature (a) and  $-80^\circ\text{C}$  (b).

This indicates the presence of an equilibrium in solution at room temperature (Scheme 4.21).



**Scheme 4.21.** Proposed equilibrium of  $[\text{Au}(\text{NHC})(\text{PPh}_3)]\text{BF}_4$  present in solution.

It should be noted, however, that the same equilibrium was not observed when the analogous reaction was carried out with the commercially available 1,3-bis(2,6-diisopropylphenyl)imidazolium tetrafluoroborate salt. Reaction with  $\text{NBu}_4(\text{acac})$  and  $[\text{AuCl}(\text{PPh}_3)]$  gave  $[\text{Au}(\text{IPr})(\text{PPh}_3)]$  as the unique product (Scheme 4.22), observed as a sharp peak at 40.04 ppm in the  $^{31}\text{P}\{^1\text{H}\}$  NMR spectrum at room temperature (Figure 4.25). This product has previously been reported and structurally characterised by the group of Nolan, although it was prepared by an alternative method.<sup>307</sup>



**Scheme 4.22.** Reaction of 1,3-bis(2,6-diisopropylphenyl)imidazolium tetrafluoroborate with  $[\text{AuCl}(\text{PPh}_3)]$  and  $\text{NBu}_4(\text{acac})$ .

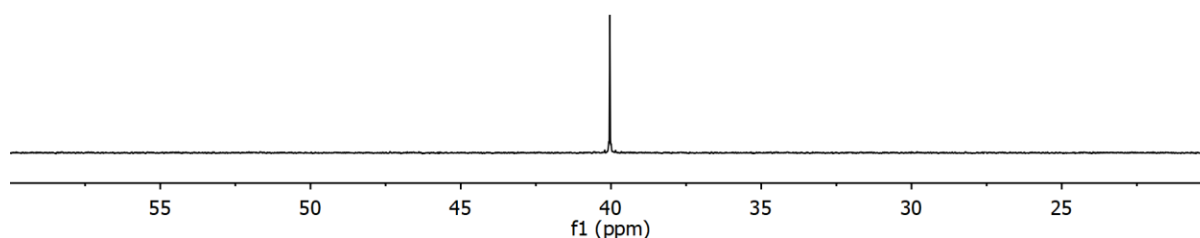
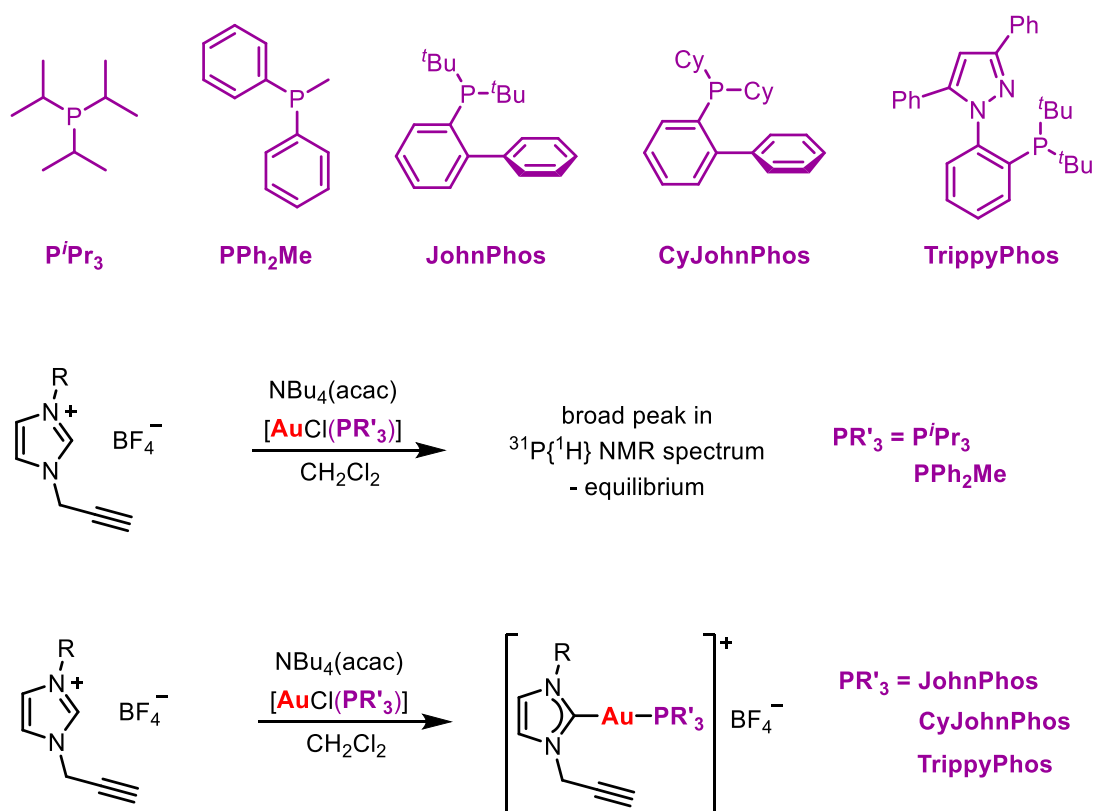


**Figure 4.25.**  $^{31}\text{P}\{^1\text{H}\}$  NMR spectrum of  $[\text{Au}(\text{IPr})(\text{PPh}_3)]\text{BF}_4$  prepared by  $\text{NBu}_4(\text{acac})$  method, in  $\text{CD}_2\text{Cl}_2$  at room temperature.



#### 4.4. Synthesis of Propargyl Functionalised NHC Gold Complexes

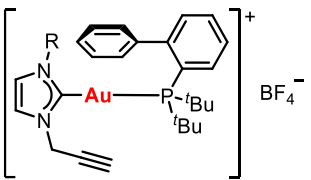
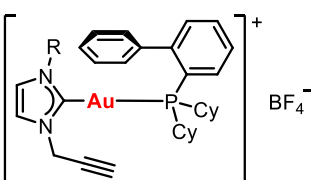
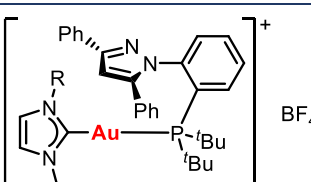
To determine if the equilibrium was due to steric or electronic effects, the method was tested with a series of different gold(I) phosphine precursors of different steric and electronic requirements (Scheme 4.23). With the more  $\sigma$ -donating but sterically smaller phosphines,  $P^iPr_3$  and  $PPh_2Me$  the same effect was observed and broad peaks were observed in the  $^{31}P\{^1H\}$  NMR spectra of the reactions corresponding to the presence of equilibria in solution at room temperature. However, increasing the steric bulk of the phosphine did allow a clean reaction to occur to give a unique product. With JohnPhos, CyJohnPhos and TrippyPhos only one sharp peak was observed in the  $^{31}P\{^1H\}$  NMR spectrum corresponding to the desired  $[Au(NHC)(PR_3)]BF_4$  product.



**Scheme 4.23.** Synthesis of  $[Au(NHC)(PR_3)]BF_4$

The isolated  $[Au(NHC)(PR_3)]BF_4$  complexes are shown in Table 4.3. In all cases the  $NBu_4Cl$  formed in the reaction was removed by washing with water and a dichloromethane solution of the product was dried over sodium sulfate to remove excess water. All products were obtained in moderate-good yields as air stable white solids.

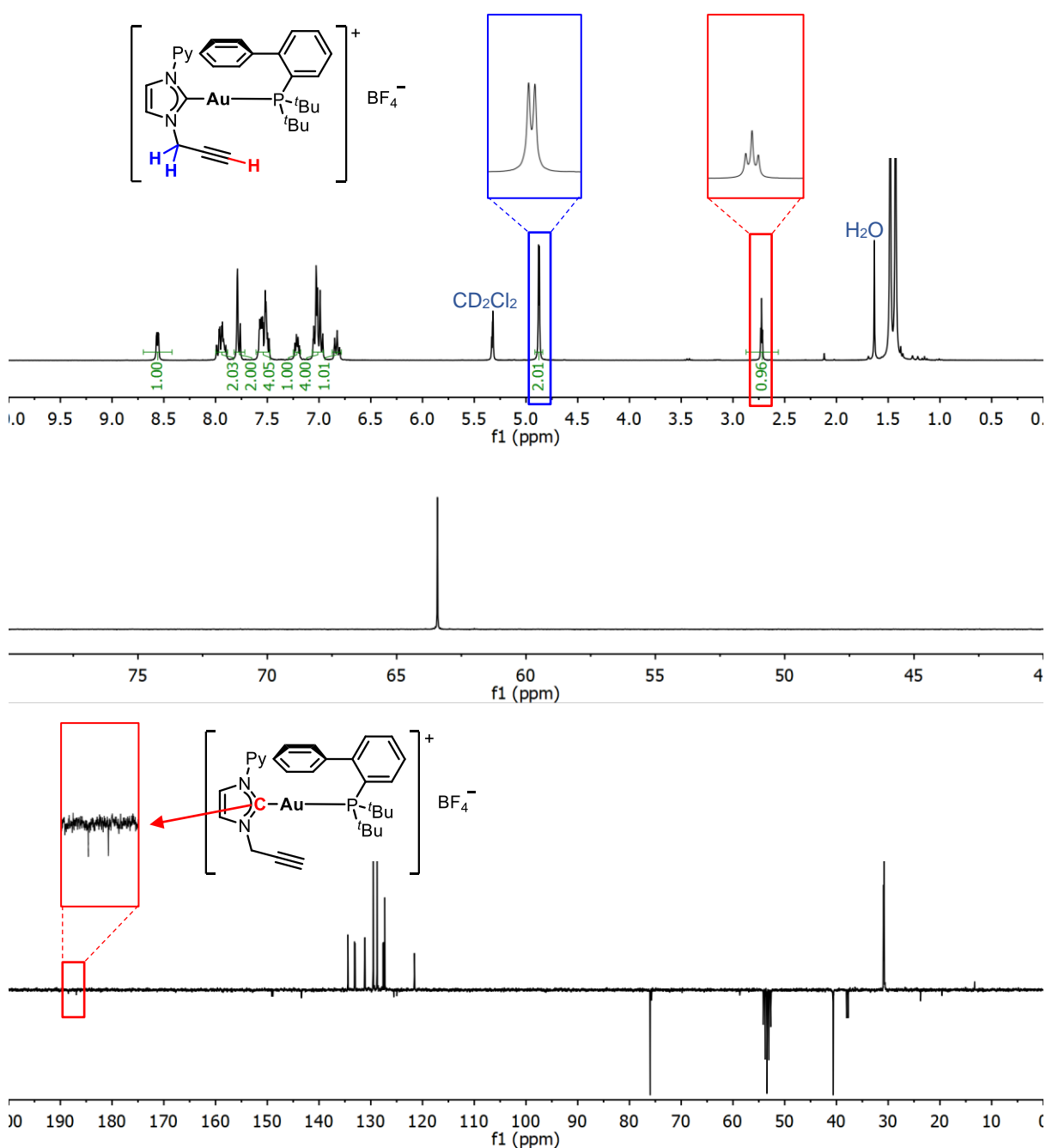
**Table 4.3.** NHC Gold Phosphine Derivatives

Complex	R	$^{31}\text{P}\{^1\text{H}\}$ NMR (ppm)	Yield (%)
			
<b>123</b>	Me	63.66	69
<b>124</b>	Bn	63.78	76
<b>125</b>	$\text{CH}_2\text{C}\equiv\text{CH}$	63.58	63
<b>126</b>	Py	63.42	65
			
<b>127</b>	Me	43.75	70
<b>128</b>	Bn	43.97	54
<b>129</b>	$\text{CH}_2\text{C}\equiv\text{CH}$	43.62	77
<b>130</b>	Py	43.16	71
			
<b>131</b>	Me	60.09	67
<b>132</b>	Bn	60.06	75
<b>133</b>	$\text{CH}_2\text{C}\equiv\text{CH}$	59.97	74
<b>134</b>	Py	59.58	66

Complexes **123-134** were characterised by NMR spectroscopy. Successful formation of the NHC is observed by the disappearance of the imidazolium C2-H signal in the  $^1\text{H}$  NMR spectrum. As with the previous complexes, the propargyl unit of the NHC ligand is observed as a doublet and a triplet (Figure 4.26(a)). A single sharp peak is observed in the  $^{31}\text{P}\{^1\text{H}\}$  NMR spectrum in each case (Figure 4.26(b)). This signal appears at a higher chemical shift than that of the corresponding  $[\text{AuCl}(\text{PR}'_3)]$  complex due to the greater *trans* influence of the NHC

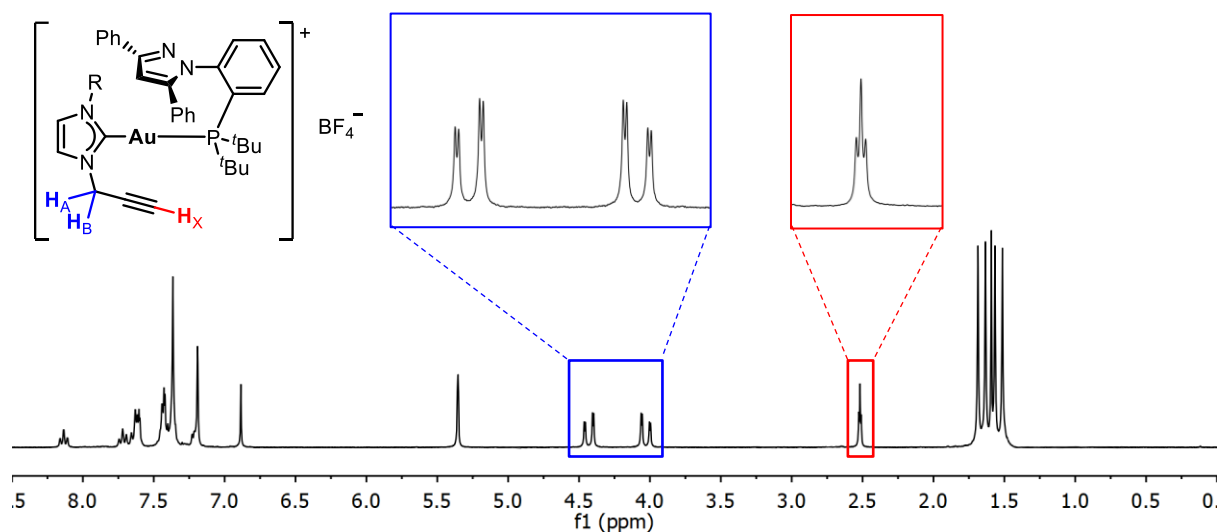
#### 4.4. Synthesis of Propargyl Functionalised NHC Gold Complexes

compared to the chloride ligand. In the  $^{13}\text{C}$  APT spectra the carbene C2 signal appears as a doublet at around 190 ppm (Figure 4.26(c)). This chemical shift is typical for an NHC carbon signal and the doublet is due to coupling with the phosphine ligand, further evidence that both ligands are bound to the gold centre.



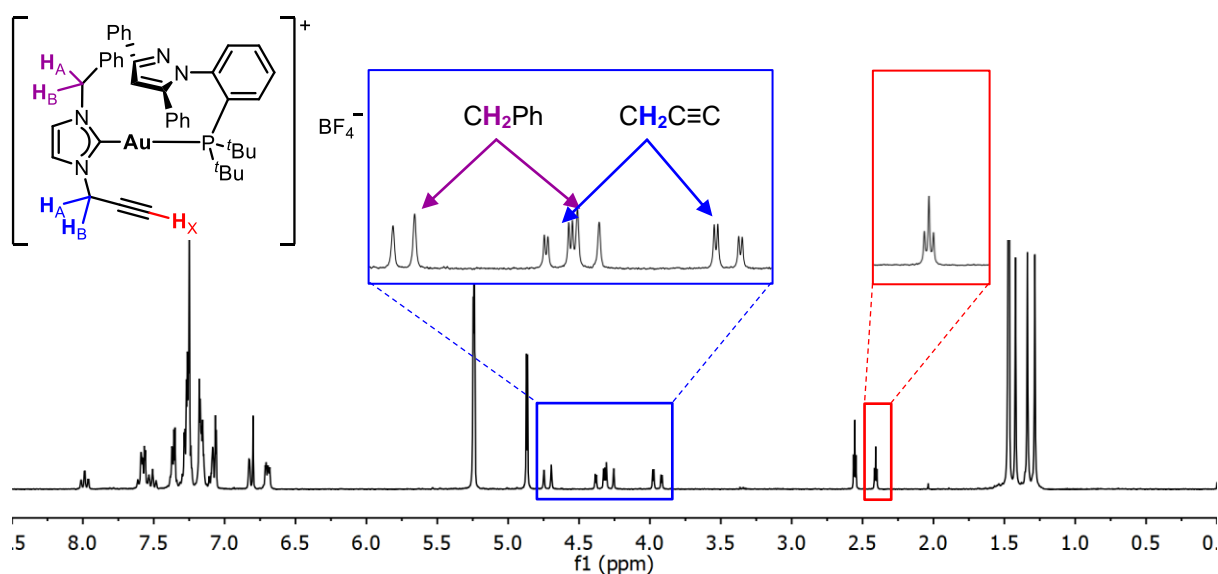
**Figure 4.26.**  $^1\text{H}$  NMR spectrum (a)  $^{31}\text{P}\{^1\text{H}\}$  NMR spectrum (b) and  $^{13}\text{C}$  APT spectrum (c) of complex **126** in  $\text{CD}_2\text{Cl}_2$  at room temperature.

For complexes **131-134**, bearing the very bulky TrippyPhos ligand, an ABX spin pattern is observed for the protons of the propargyl unit in the  $^1\text{H}$  NMR spectrum (Figure 4.27).



**Figure 4.27.**  $^1\text{H}$  NMR spectrum for complex **133** in  $\text{CD}_2\text{Cl}_2$  at room temperature.

For complex **132**, the  $\text{CH}_2$  of the benzyl group is also observed as an AB spin pattern in the  $^1\text{H}$  NMR spectrum (Figure 4.28). In this case the product was obtained as a mixture of **132** and the bis-NHC species, **108**. This could be due to increased steric hindrance between the bulky phosphine and the benzyl group, compared to the smaller NHCs.

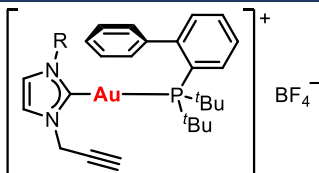
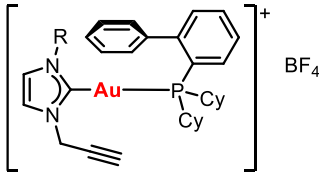
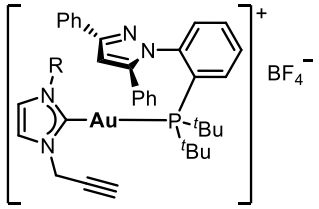


**Figure 4.28.**  $^1\text{H}$  NMR spectrum of complex **132** in  $\text{CD}_2\text{Cl}_2$  at room temperature.

#### 4.4. Synthesis of Propargyl Functionalised NHC Gold Complexes

Complexes **123-134** were characterised by high resolution mass spectrometry. In all cases the molecular ion pair  $[M]^+$  was observed (Table 4.4).

**Table 4.4.** HRMS (ESI-TOF) Calculated and Found  $m/z$  Values

Complex	Peak	$m/z$ Calculated	$m/z$ Found
	$[M]^+$	615.2198	615.2213
	$[M]^+$	691.2511	691.2520
	$[M]^+$	639.2179	639.2198
	$[M]^+$	678.2307	678.2306
	$[M]^+$	678.2307	678.2306
	$[M]^+$	667.2511	667.2546
	$[M]^+$	743.2824	743.2858
	$[M]^+$	691.2511	691.2487
	$[M]^+$	730.2620	730.2599
	$[M]^+$	730.2620	730.2599
	$[M]^+$	757.2729	757.2658
	$[M]^+$	833.3042	833.3049
	$[M]^+$	781.2729	781.2739
	$[M]^+$	820.2838	820.2802
	$[M]^+$	820.2838	820.2802

The JohnPhos derivatives **124-126** were characterised by single crystal X-ray diffraction. The molecular structures are shown in Figure 4.29. In all cases a distorted linear coordination about the gold atom can be observed with angles  $175.76(17)^\circ$  for **124**,  $176.2(2)^\circ$  for **125** and  $173.40(13)^\circ$  for **126**. The distortion is a result of the bulky JohnPhos ligand. In all cases the

propargyl unit is maintained and typical bond distances for carbon-carbon single and triple bonds are observed. The biphenyl group of the JohnPhos is orientated over the gold centre in each case and no interaction of the gold centre with the alkyne of the propargyl side arm is observed in any of the complexes.

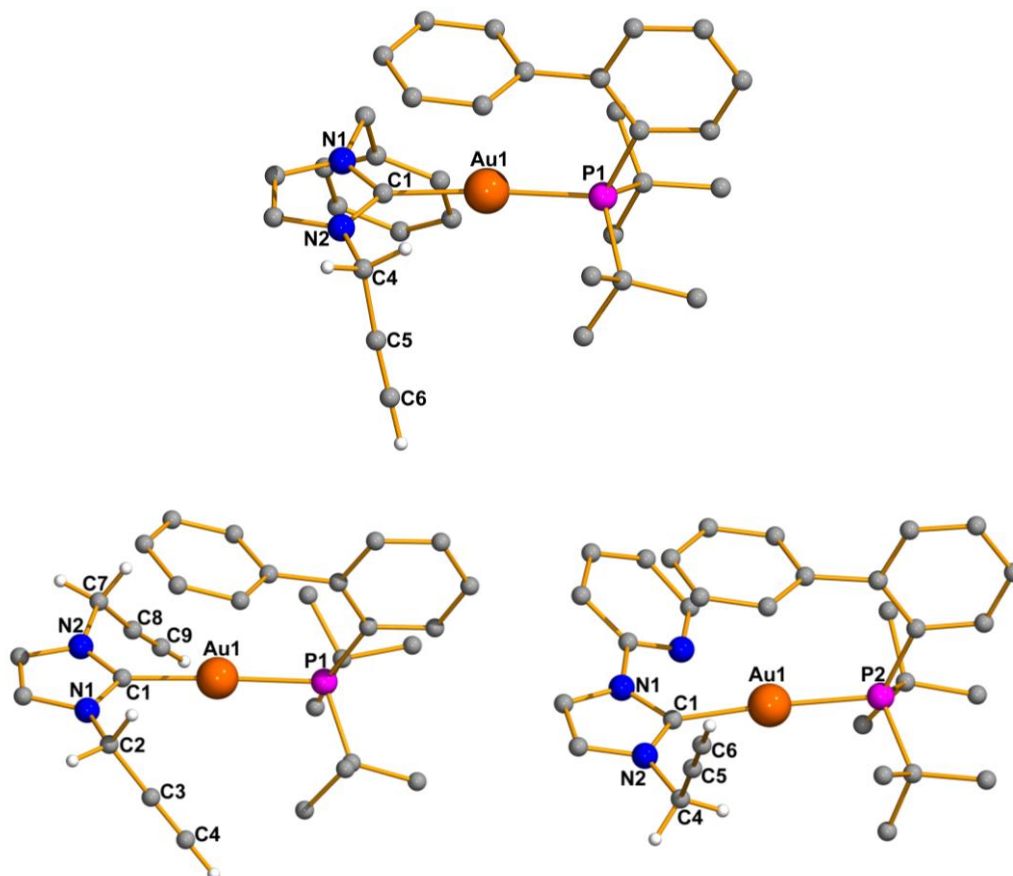


**Figure 4.29.** Molecular structures of complex **124-126**. Selected bond lengths (Å) and angles (°) **124**: Au(1)-P(1) 2.2966(15), Au(1)-C(1) 2.039(6), N(1)-C(1) 1.348(7), N(2)-C(1) 1.343(8), C(4)-C(5) 1.468(9), C(5)-C(6) 1.174(11), C(1)-Au(1)-P(1) 175.76(17), C(4)-C(5)-C(6) 175.9(7); **125**: Au(1)-P(1) 2.2991(16), Au(1)-C(1) 2.031(7), N(1)-C(1) 1.371(10), N(2)-C(1) 1.345(9), C(2)-C(3) 1.465(12), C(3)-C(4) 1.174(13), C(7)-C(8) 1.469(12), C(8)-C(9) 1.167(12), C(1)-Au(1)-P(1) 176.2(2), C(2)-C(3)-C(4) 175.0(9), C(7)-C(8)-C(9) 174.0(8); **126**: Au(1)-P(1) 2.2953(14), Au(1)-C(1) 2.036(4), N(1)-C(1) 1.368(6), N(2)-C(1) 1.334(6), C(4)-C(5) 1.467(7), C(5)-C(6) 1.166(7), C(1)-Au(1)-P(2) 173.40(13), C(4)-C(5)-C(6) 179.2(6).

The CyJohnPhos derivatives, **127-130**, were also characterised by single crystal X-ray diffraction. The molecular structures are shown in Figure 4.30. Again, a distorted linear coordination about the gold centre is observed in each case. The biphenyl ligand lies over the

#### 4.4. Synthesis of Propargyl Functionalised NHC Gold Complexes

gold centre and the propargyl side arms are maintained. No interaction of the gold centre with the alkyne of the propargyl unit is observed. The Au-C<sub>carbene</sub> bond distances are very similar to those for the JohnPhos, indicating a very similar  $\sigma$ -donor capacity between JohnPhos and CyJohnPhos.

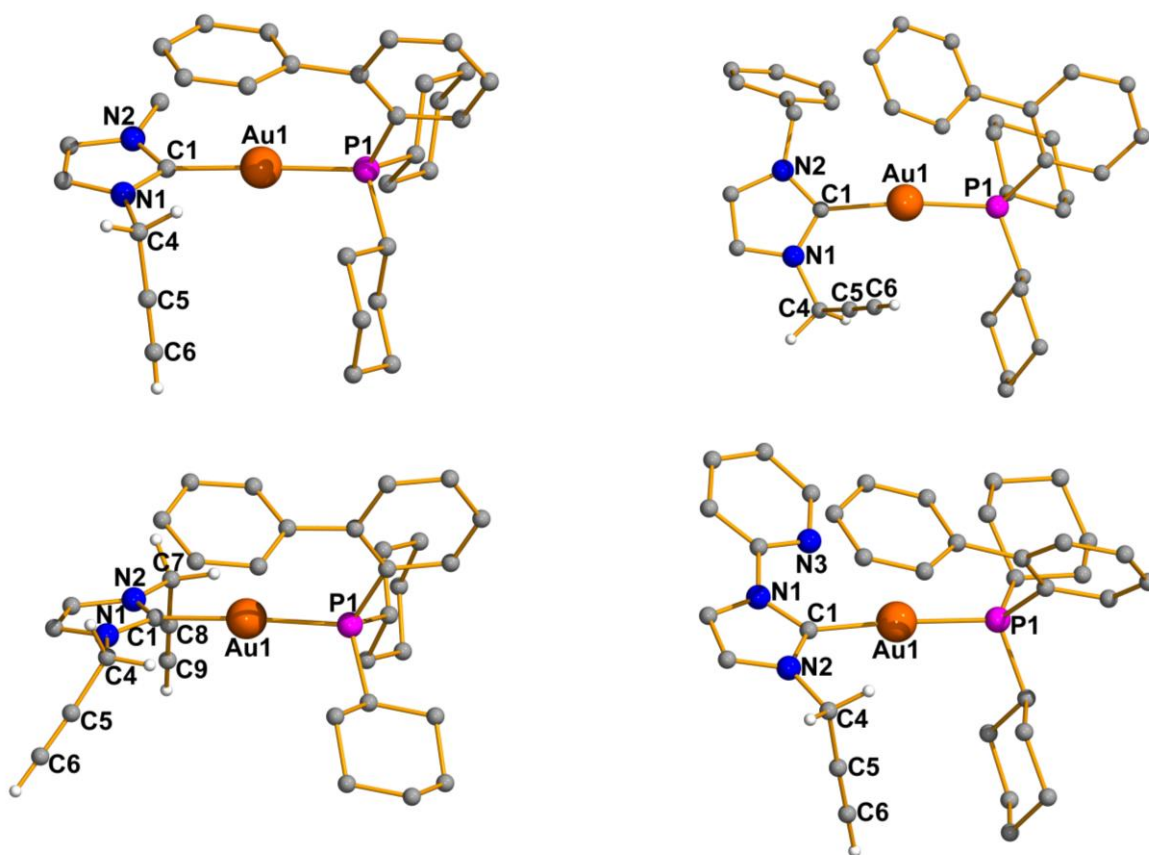
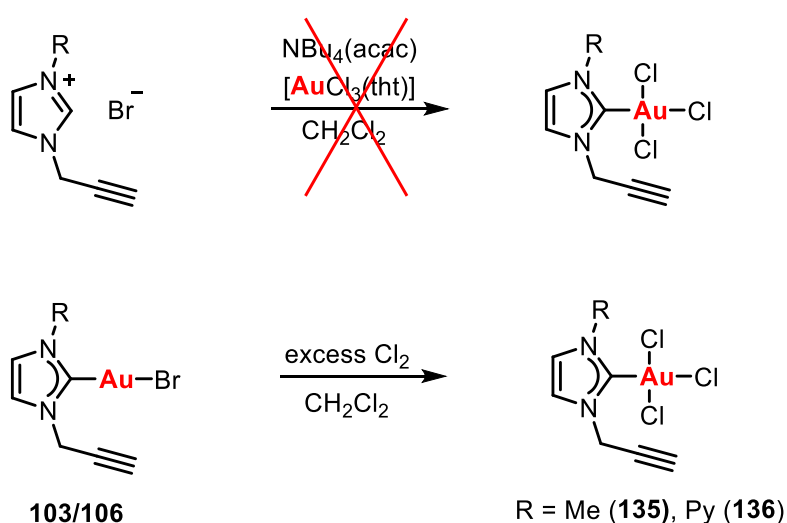


**Figure 4.30.** Molecular structures of complex **127-130**. Selected bond lengths (Å) and angles (°) **127**: Au(1)-C(1) 2.032(3), Au(1)-P(1) 2.2817(7), N(1)-C(1) 1.358(3), N(2)-C(1) 1.342(3), C(4)-C(5) 1.468(4), C(5)-C(6) 1.174(4), C(1)-Au(1)-P(1) 176.89(8), C(6)-C(5)-C(4) 179.3(3); **128**: Au(1)-C(1) 2.064(7), Au(1)-P(1) 2.287(2), N(1)-C(1) 1.330(10), N(2)-C(1) 1.331(10), C(4)-C(5) 1.452(14), C(5)-C(6) 1.184(15), C(1)-Au(1)-P(1) 170.6(2), C(6)-C(5)-C(4) 177.9(11); **129**: Au(1)-C(1) 2.032(5), Au(1)-P(1) 2.2774(13), N(1)-C(1) 1.345(6), N(2)-C(1) 1.346(6), C(4)-C(5) 1.456(9), C(5)-C(6) 1.159(9), C(7)-C(8) 1.457(8), C(8)-C(9) 1.175(9), C(1)-Au(1)-P(1) 176.37(14), C(6)-C(5)-C(4) 178.4(7), C(9)-C(8)-C(7) 178.9(6); **130**: Au(1)-C(1) 2.033(3), Au(1)-P(1) 2.2692(8), N(1)-C(1) 1.359(3), N(2)-C(1) 1.344(3), C(4)-C(5) 1.441(4), C(5)-C(6) 1.188(5), C(1)-Au(1)-P(1) 173.03(8), C(6)-C(5)-C(4) 178.3(4).

## 4.4.5. Gold(III) Derivatives

Attempts to form gold(III) derivatives from the imidazolium salts directly by addition of  $\text{NBu}_4(\text{acac})$  and  $\text{AuCl}_3(\text{tht})$  were unsuccessful and reduction to gold(I) was observed. However, the gold(III) derivatives could readily be prepared by oxidation of the NHC gold(I) complexes with  $\text{Cl}_2$ . Addition of an excess of  $\text{Cl}_2$  solution in  $\text{CCl}_4$  to a solution of the NHC gold bromide complexes, **103** and **106**, led to the formation of the gold(III) derivatives  $[\text{AuCl}_3(\text{NHC})]$ , **135** and **136** (Scheme 4.24).



**Scheme 4.24.** Synthesis of NHC gold(III) complexes **135-136**.

Complexes **135** and **136** were characterised by single crystal X-ray diffraction. Suitable crystals were grown by slow diffusion of pentane into a solution of the complex in dichloromethane. The molecular structures are shown in Figure 4.31. The presence of three chloride ligands at the gold centre can readily be observed and square planar coordination is observed about the gold centre in both cases. The propargyl unit shows typical distances for a carbon-carbon single and triple bond and the  $\text{C-C}\equiv\text{C}$  bond angles are practically linear.



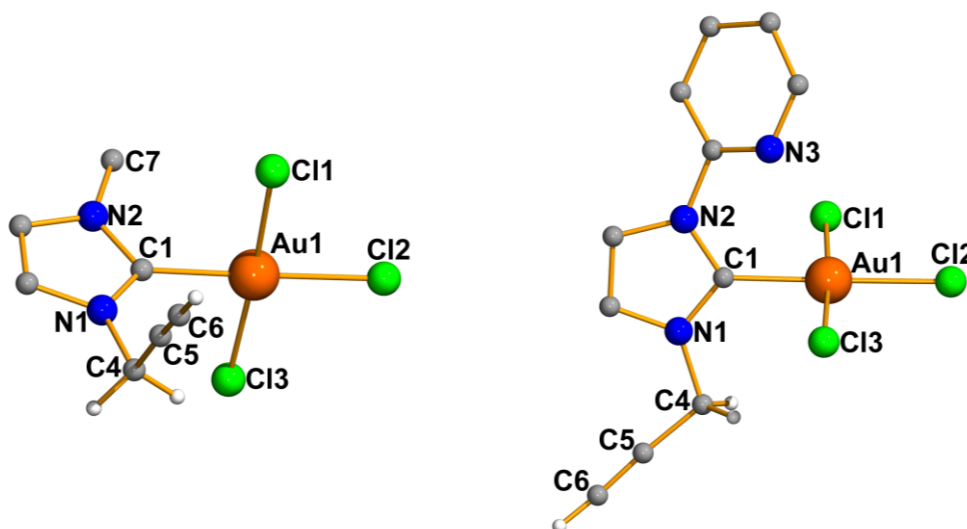
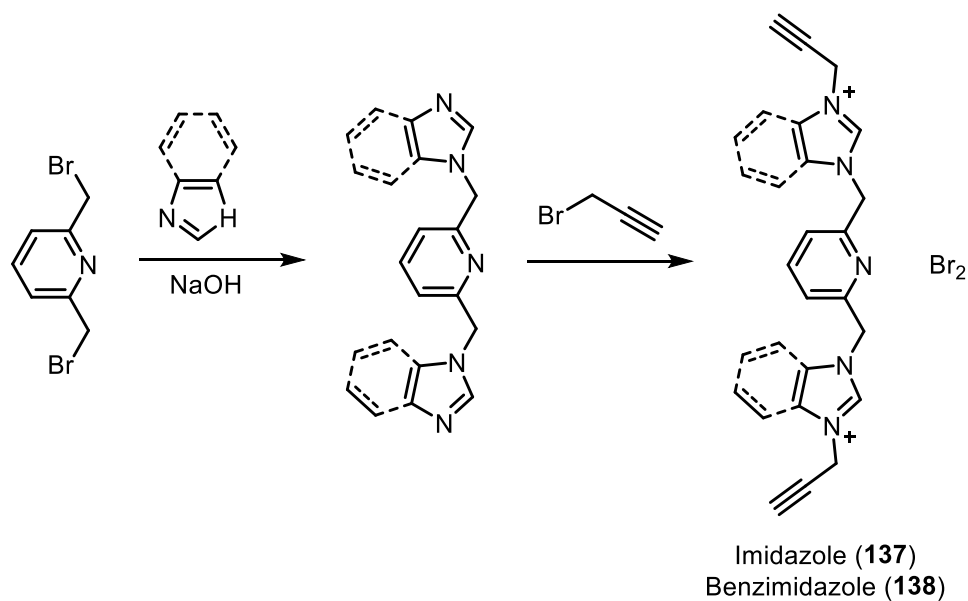


**Figure 4.31.** Molecular structures of complex **135** and **136**. Selected bond lengths (Å) and angles (°) **135**: Au(1)-C(1) 2.008(19), Au(1)-Cl(2) 2.324(5), Au(1)-Cl(3) 2.346(4), Au(1)-Cl(1) 2.352(4), N(1)-C(1) 1.30(3), N(2)-C(1) 1.37(3), C(4)-C(5) 1.43(4), C(5)-C(6) 1.11(4), C(1)-Au(1)-Cl(2) 179.0(5), Cl(3)-Au(1)-Cl(1) 176.92(14), C(6)-C(5)-C(4) 174(3); **136**: Au(1)-C(1) 1.993(3), Au(1)-Cl(3) 2.2802(9), Au(1)-Cl(1) 2.2827(9), Au(1)-Cl(2) 2.3166(9), N(1)-C(1) 1.338(5), N(2)-C(1) 1.343(4), C(4)-C(5) 1.458(5), C(5)-C(6) 1.181(6), Cl(3)-Au(1)-Cl(1) 176.30(3), C(1)-Au(1)-Cl(2) 179.20(10), C(6)-C(5)-C(4) 176.4(4).

#### 4.4.6. Di-NHC Complexes

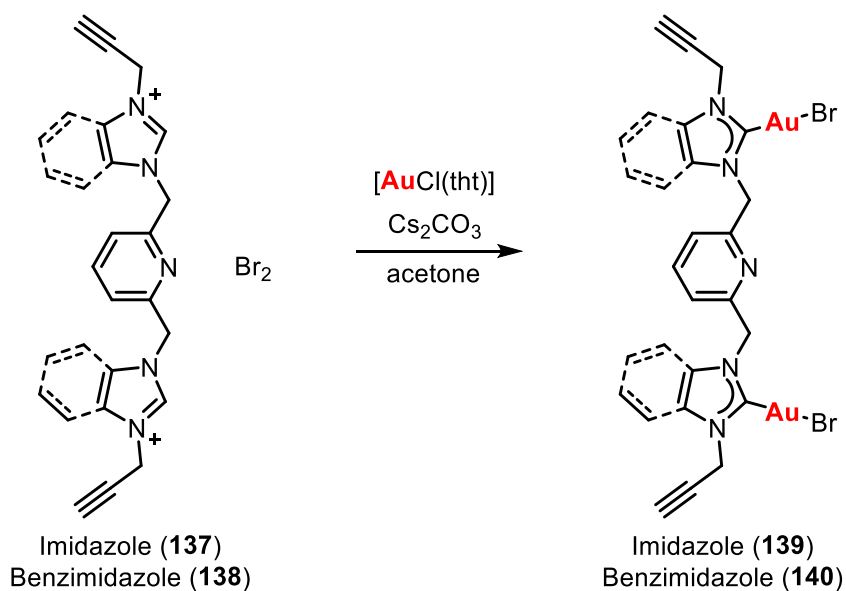
Since polynuclear gold complexes are of interest due to their potential luminescence and enhanced biological activity, attempts were made to prepare propargyl-functionalised NHC derivatives bearing more than one NHC which could hence coordinate more than one gold centre.

Two imidazolium salts bridged by a dimethylpyridine unit were prepared by reaction of 2,6-bis(bromomethyl)pyridine with imidazole or benzimidazole in the presence of NaOH, and subsequent alkylation with propargyl bromide to give **137** and **138** (Scheme 4.25).



**Scheme 4.25.** Synthesis of di-imidazolium salts **137** and **138**.

The di-NHC gold bromide derivatives, **139** and **140**, were prepared by reaction of the imidazolium salts with  $[\text{AuCl}(\text{tht})]$  in acetone with excess  $\text{Cs}_2\text{CO}_3$  (Scheme 4.26). The poor solubility of the products led to low yields in these reactions.



**Scheme 4.26.** Synthesis of di-NHC gold bromide complexes **139-140**.

#### 4.4. Synthesis of Propargyl Functionalised NHC Gold Complexes

Successful formation of the NHC could be confirmed by the disappearance of the imidazolium C-H signal in the  $^1\text{H}$  NMR spectrum. The propargyl side arms are maintained in both cases and observed as a doublet and triplet in the  $^1\text{H}$  NMR spectrum (Figure 4.32).

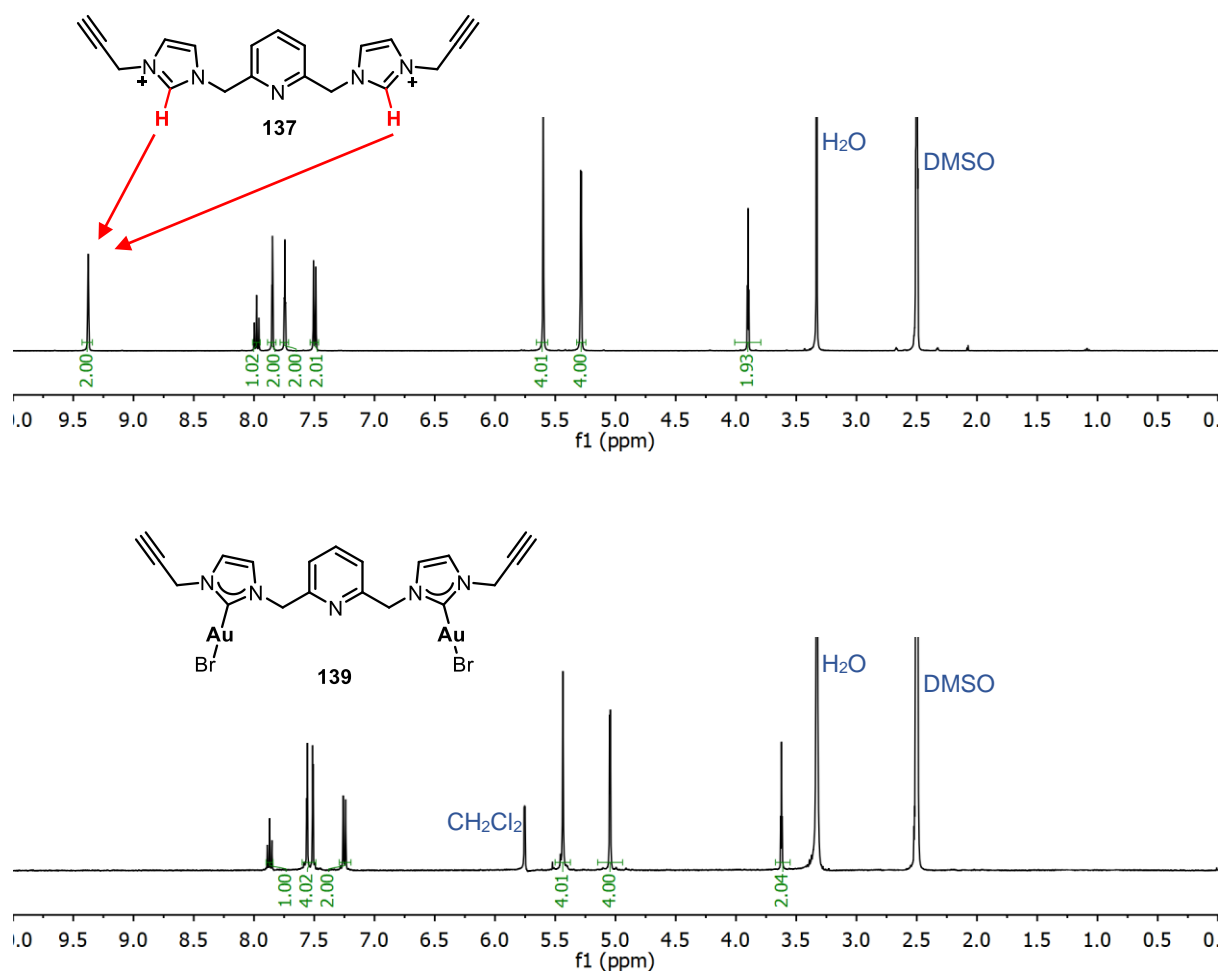


**Figure 4.32.**  $^1\text{H}$  NMR spectrum for salt **139** (a) and complex **141** (b) in DMSO at room temperature.

Complex **139** was characterised by single crystal X-ray diffraction. The molecular structure is shown in Figure 4.33. The two NHC-Au-Br units are angled in opposite directions, bringing the gold centres in close proximity, however the Au-Au distance, 4.414 Å, is too long to be considered an aurophilic interaction. A linear coordination is observed about each gold(I) centre with angles C(1)-Au(1)-Br(1) 177.2(6)° and C(14)-Au(2)-Br(2) 177.9(5)°. The propargyl units can readily be observed by the carbon-carbon bond lengths which show typical distances for a single and triple bond.

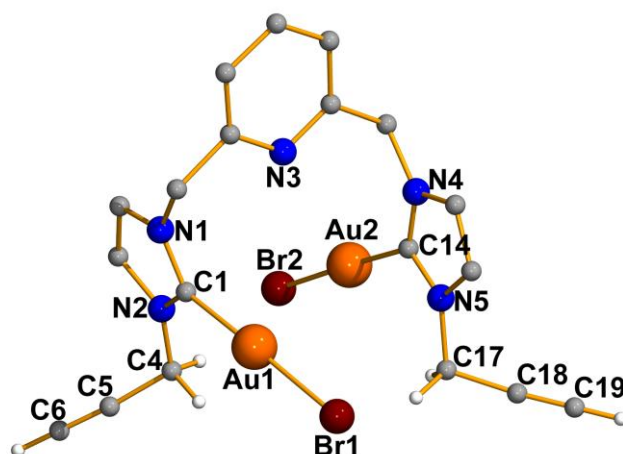
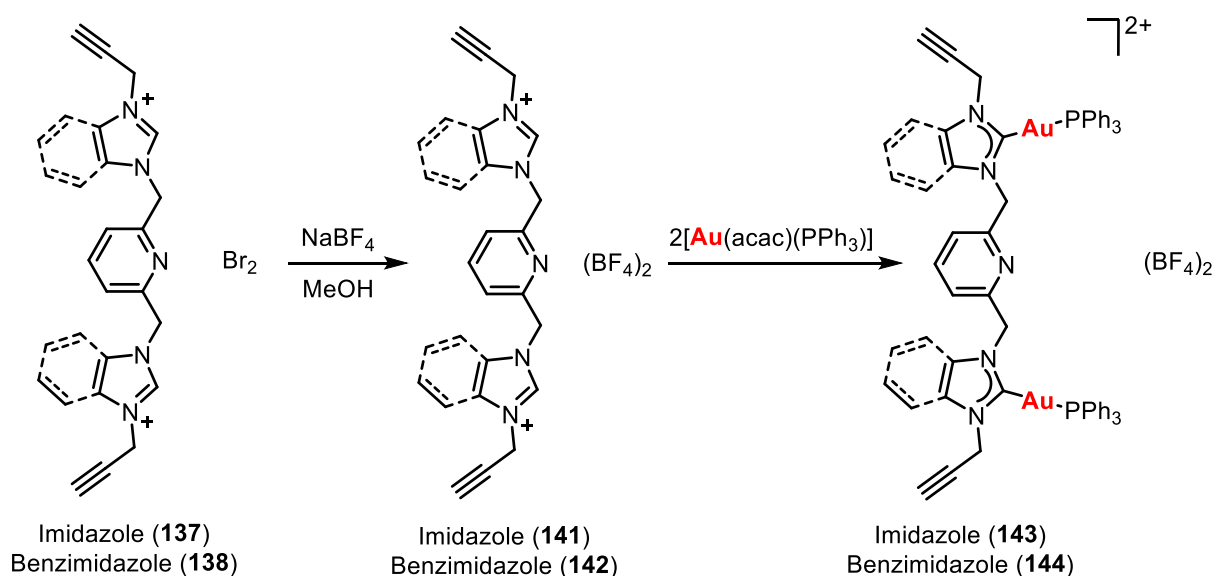


**Figure 4.33.** Molecular structures of complex **139**. Selected bond lengths (Å) and angles (°): Au(1)-C(1) 2.005(17), Au(1)-Br(1) 2.400(2), Au(2)-C(14) 2.023(17), Au(2)-Br(2) 2.393(2), N(1)-C(1) 1.34(2), N(2)-C(1) 1.32(2), N(4)-C(14) 1.31(2), N(5)-C(14) 1.32(2), C(4)-C(5) 1.46(3), C(5)-C(6) 1.14(3), C(17)-C(18) 1.46(2), C(18)-C(19) 1.17(2), C(1)-Au(1)-Br(1) 177.2(6), C(14)-Au(2)-Br(2) 177.9(5), C(6)-C(5)-C(4) 175(2), C(19)-C(18)-C(17) 173(2).

Attempts were also made to prepare NHC gold phosphine derivatives from imidazolium salts **137** and **139**. Initially the  $\text{BF}_4$  salts, **141** and **142**, were prepared by reaction with  $\text{NaBF}_4$  in methanol. Addition of two equivalents of  $[\text{Au}(\text{acac})(\text{PPh}_3)]$  led to the formation of the  $[\text{Au}_2(\text{NHC})_2(\text{PPh}_3)_2](\text{BF}_4)_2$  complexes, **143** and **144** (Scheme 4.27), which similarly to the mononuclear  $[\text{Au}(\text{NHC})(\text{PPh}_3)]\text{BF}_4$  complexes presented equilibria in solution with broad  $^{31}\text{P}\{^1\text{H}\}$  NMR spectra observed at room temperature (Figure 4.34).



**Scheme 4.27.** Synthesis of complexes **143-144**.

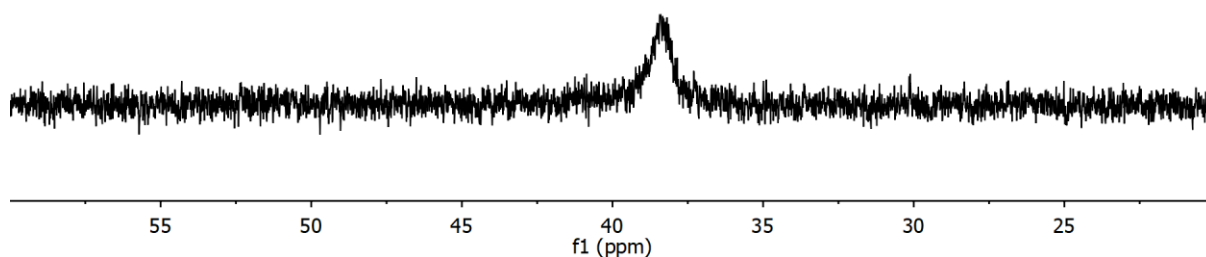


**Figure 4.34.**  $^{31}\text{P}\{^1\text{H}\}$  NMR spectrum of complex **144** in **DMSO** at room temperature.

Crystals of complex **144** were grown and measured by single crystal X-ray diffraction, showing that in the solid state the  $[\text{Au}_2(\text{NHC})_2(\text{PPh}_3)_2](\text{BF}_4)_2$  complex does exist (Figure 4.35). Similarly to complex **139**, the gold triphenylphosphine units are angled in opposite directions. This minimises the steric repulsions between the bulky triphenylphosphine groups. A linear coordination is observed about each gold centre. No tautomerisation of the propargyl side arms is observed.

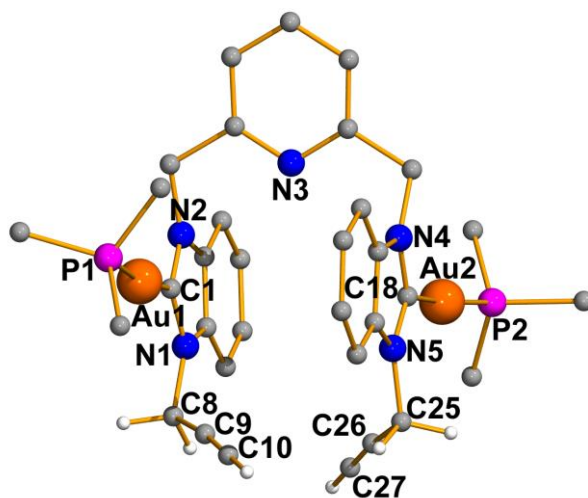
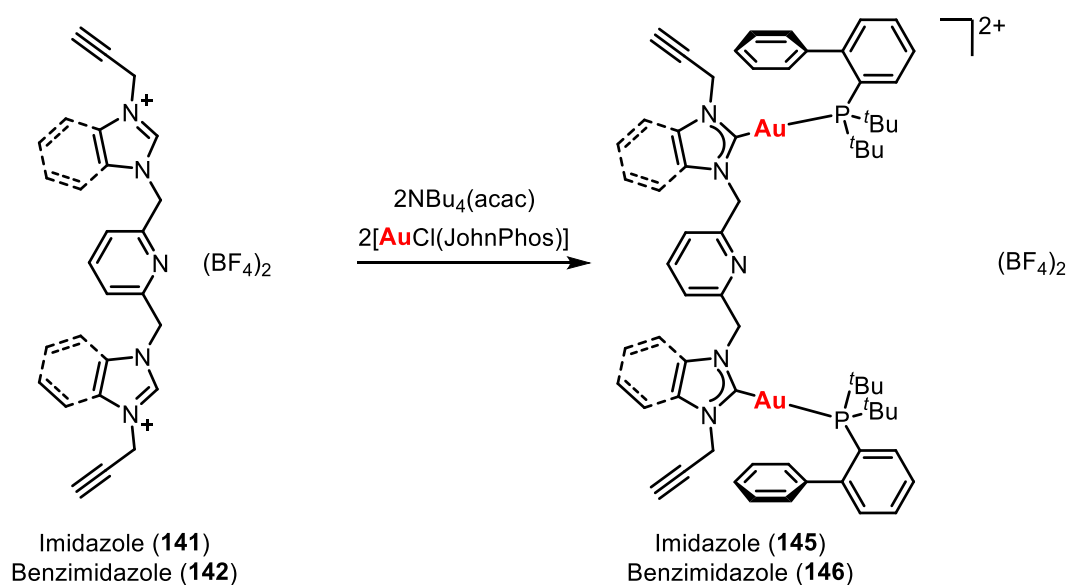


**Figure 4.35.** Molecular structures of complex **144** ( $\text{PPh}_3$  phenyl rings are omitted for clarity). Selected bond lengths ( $\text{\AA}$ ) and angles ( $^\circ$ ): Au(1)-C(1) 2.045(7), Au(1)-P(1) 2.280(2), Au(2)-C(18) 2.043(8), Au(2)-P(2) 2.274(2), N(1)-C(1) 1.349(9), N(2)-C(1) 1.327(10), N(4)-C(18) 1.333(10), N(5)-C(18) 1.343(10), C(8)-C(9) 1.438(11), C(9)-C(10) 1.183(11), C(25)-C(26) 1.482(11), C(26)-C(27) 1.179(11), C(1)-Au(1)-P(1) 172.0(2), C(18)-Au(2)-P(2) 173.3(2), C(10)-C(9)-C(8) 173.2(9), C(27)-C(26)-C(25) 172.8(10).

When the bulky JohnPhos phosphine was used the equilibrium in solution was not observed. Complexes **145** and **146** were prepared by reaction of imidazolium salts **141** and **142** with two

equivalents of  $[\text{AuCl}(\text{JohnPhos})]$  and two equivalents of  $\text{NBu}_4(\text{acac})$ . Successful formation of the di-NHC is observed by the loss of the imidazolium C-H signal in the  $^1\text{H}$  NMR spectrum. The propargyl  $\text{CH}_2$  and  $\text{CH}$  protons are still observed as a singlet and triplet (Figure 4.36(a)). A single sharp peak is observed in the  $^{31}\text{P}\{^1\text{H}\}$  spectrum (Figure 4.36(b)).



**Scheme 4.28** Synthesis of complexes **145** and **146**.

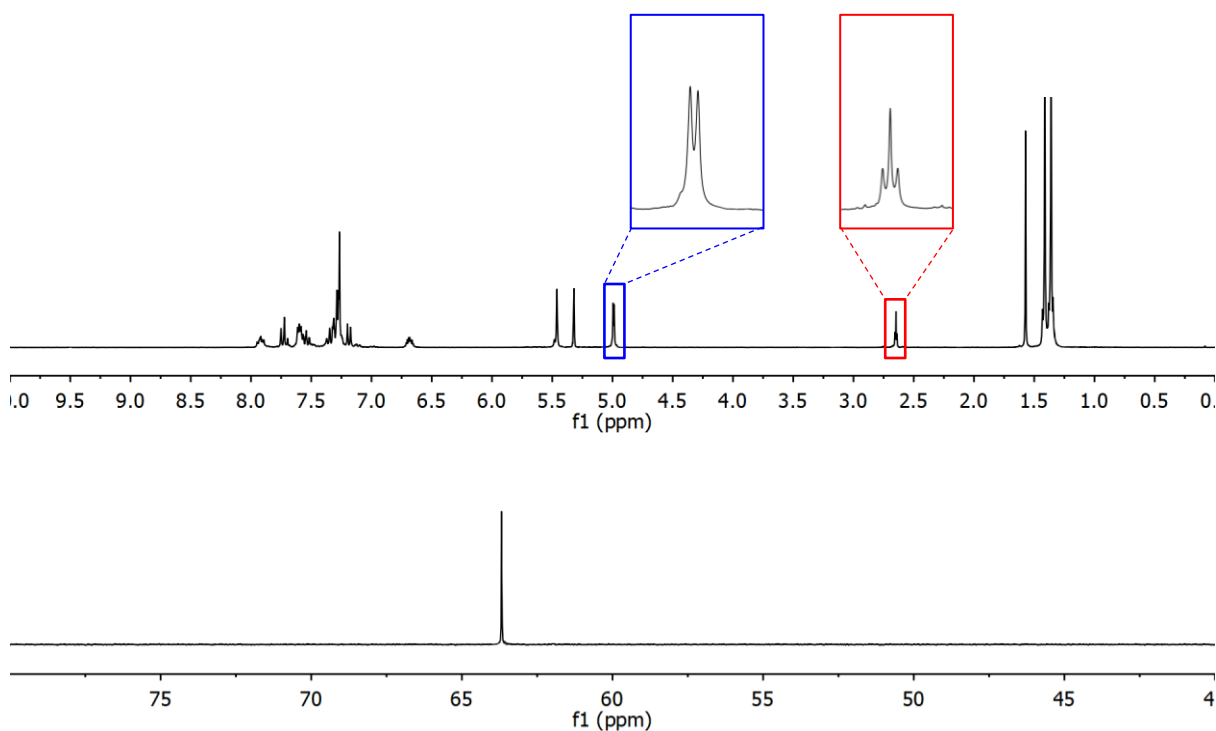
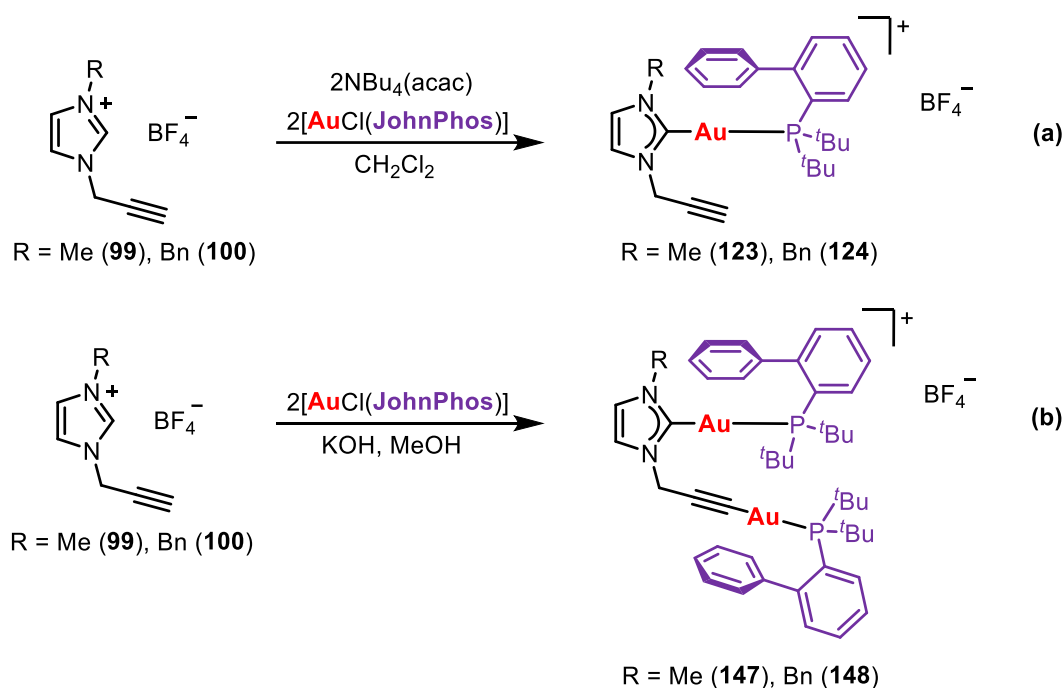


**Figure 4.36.**  $^1\text{H}$  NMR spectrum (a) and  $^{31}\text{P}\{^1\text{H}\}$  NMR spectrum (b) of **145** in  $\text{CD}_2\text{Cl}_2$  at room temperature.

## 4.5. Functionalisation of the Propargyl Unit

### 4.5.1. Dinuclear NHC Gold JohnPhos Derivatives

Attempts were made to coordinate an additional -AuJohnPhos unit to the propargyl side arm of complexes **123** and **124**. Reaction of imidazolium salt **99** with 2 equivalents of [AuCl(JohnPhos)] and 2 equivalents of NBu<sub>4</sub>(acac) led only to the formation of mononuclear complex **123** and unreacted starting material even after 24 h reaction time, suggesting NBu<sub>4</sub>(acac) is not a strong enough base to deprotonate the propargyl CH (Scheme 4.29(a)). When the reaction is carried out in methanol using potassium hydroxide as the base, the desired dinuclear complexes form (Scheme 4.29(b)).



**Scheme 4.29.** Synthesis of complexes **147** and **148**.

<sup>1</sup>H NMR spectroscopy confirms the deprotonation of the alkyne C-H. The propargyl CH<sub>2</sub> is observed as a doublet at 4.67 ppm (<sup>4</sup>J<sub>HP</sub> = 1.6 Hz) due to weak coupling with the JohnPhos phosphorus atom (Figure 4.37(a)). Two peaks are observed in the <sup>31</sup>P{<sup>1</sup>H} NMR spectrum at similar chemical shifts since the two phosphorus atoms are in similar chemical environments, both bound to a gold atom bearing a carbon ligand (Figure 4.37(b)).

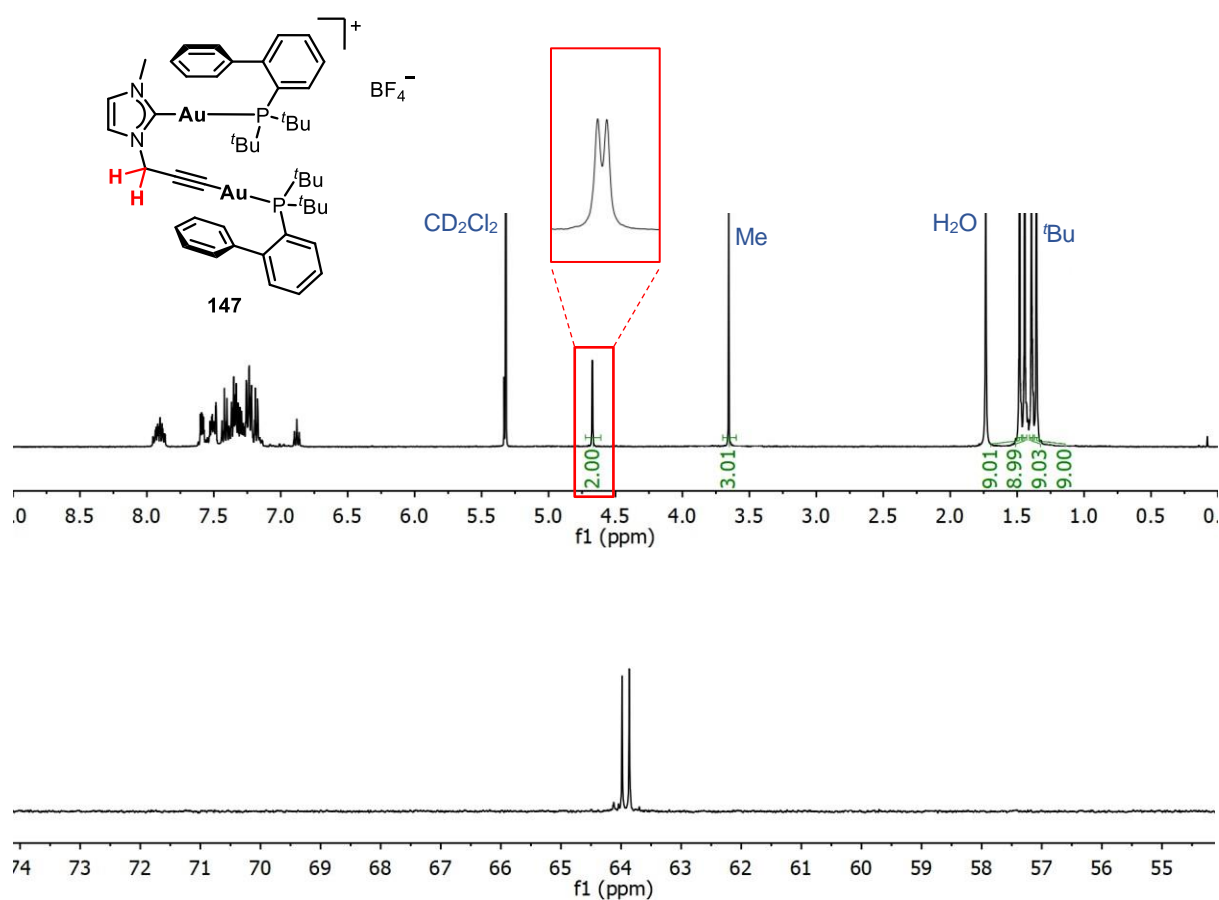


**Figure 4.37.**  $^1\text{H}$  NMR spectrum (a) and  $^{31}\text{P}\{^1\text{H}\}$  NMR spectrum (b) of complex **147** in  $\text{CD}_2\text{Cl}_2$  at room temperature.

The identity of the products is also confirmed by HRMS(ESI-QTOF) with the molecular ion peaks  $[\text{M}]^+$  observed as the most intense peaks (Table 4.5).

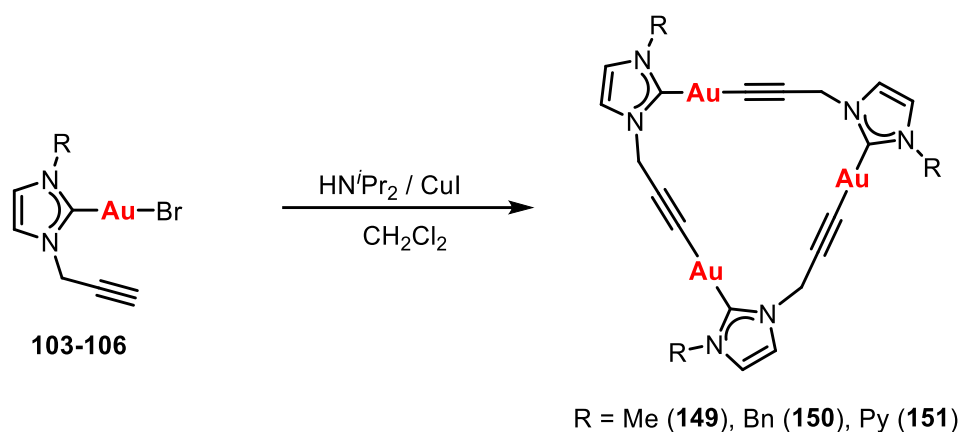
**Table 4.5.** HRMS (ESI-TOF) Calculated and Found  $m/z$  Values

Complex	Peak	$m/z$ Calculated	$m/z$ Found
<b>147</b>	$[\text{M}]^+$	1109.3636	1109.3650
<b>148</b>	$[\text{M}]^+$	1185.3949	1185.3899



## 4.5.2. Formation of Trimers

Reaction of the bromo NHC gold complexes **103**, **104** and **106** with  $\text{HN}^i\text{Pr}_2$  in the presence of CuI as a catalyst led to the elimination of both the alkyne proton and the bromide ligand bound to gold to afford the sparingly soluble trimeric complexes **149-151** (Scheme 4.30).



**Scheme 4.30.** Synthesis of trimers **149-151**.

The elimination of the alkyne proton was confirmed by  $^1\text{H}$  NMR spectroscopy (Figure 4.38). The propargyl  $\text{CH}_2$ , which in the starting complexes, **103-106**, was observed as a doublet, is now observed as a singlet and the triplet corresponding to the alkyne CH is no longer present.

The trimeric nature of the products was confirmed by HRMS(ESI-QTOF) with spectra showing the molecular ion peaks  $[\text{M}+\text{Na}]^+$  as the most intense peaks (Table 4.6).

**Table 4.6.** HRMS (ESI-TOF) Calculated and Found  $m/z$  Values

Complex	Peak	$m/z$ Calculated	$m/z$ Found
<b>149</b>	$[\text{M}+3\text{MeOH}+\text{Na}]^+$	1067.1503	1067.1523
<b>150</b>	$[\text{M}+\text{Na}]^+$	1199.1655	1199.1721
<b>151</b>	$[\text{M}+\text{Na}]^+$	1160.1043	1160.1031

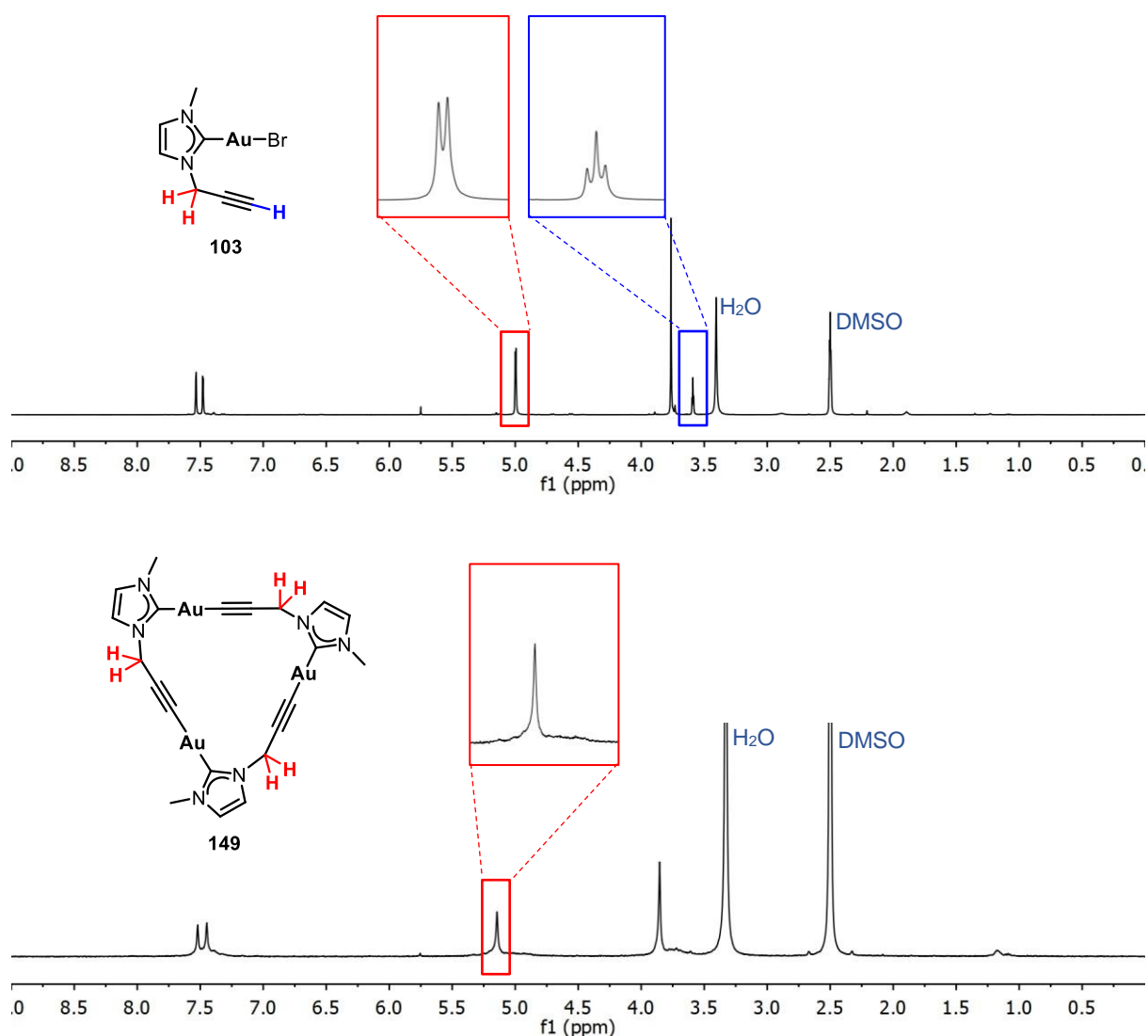


**Figure 4.38.**  $^1\text{H}$  NMR spectrum of starting complex **103** (a) and trimer product **149** (b) in **DMSO** at room temperature.

The IR spectra of complexes **149-151** lack the  $\text{C}\equiv\text{C-H}$  vibration present in the starting complexes at around  $3260\text{ cm}^{-1}$  (Figure 4.39), while the  $-\text{C}\equiv\text{C}-$  vibration mode at around  $2160\text{ cm}^{-1}$  is maintained (Figure 4.40).

#### 4.5. Functionalisation of the Propargyl Unit

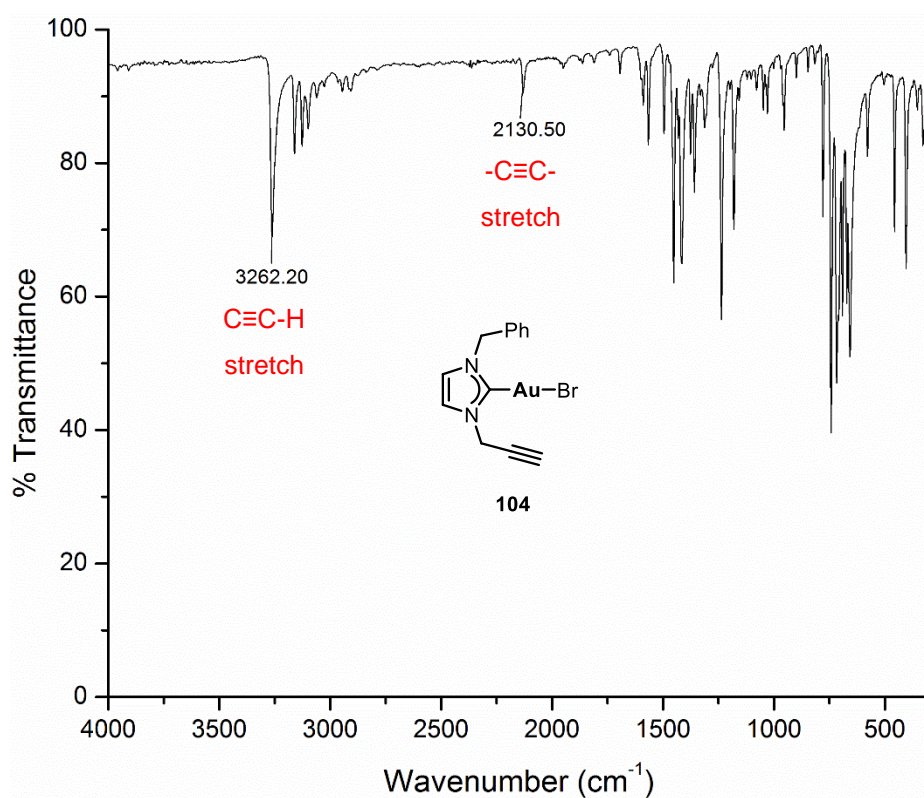


Figure 4.39. IR Spectrum of complex **104**.

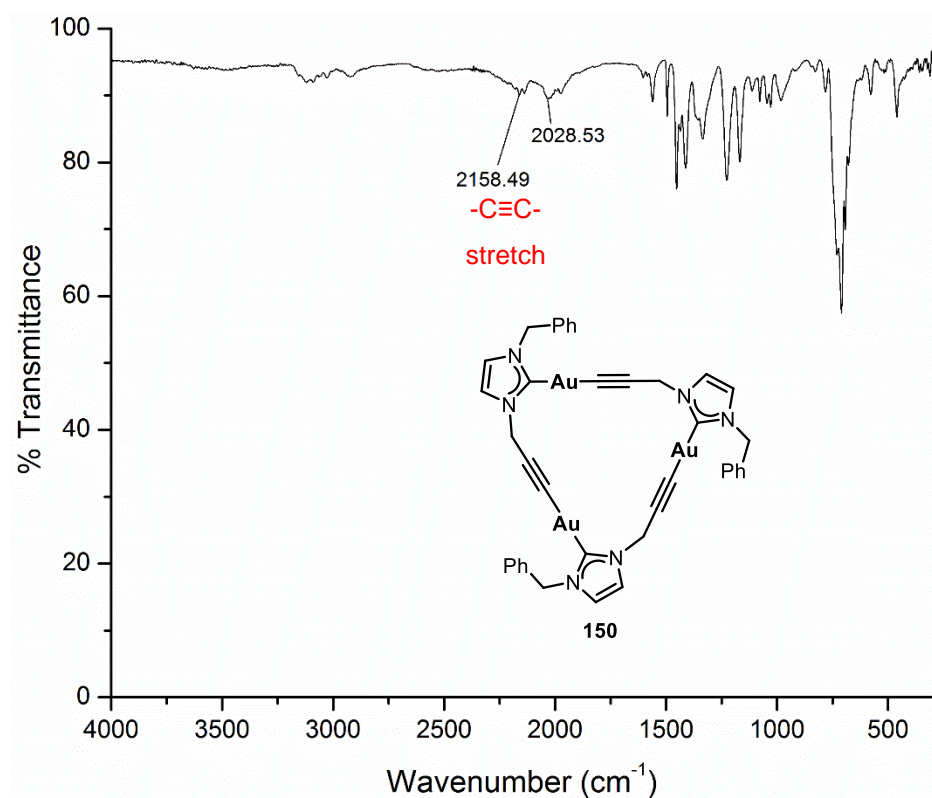
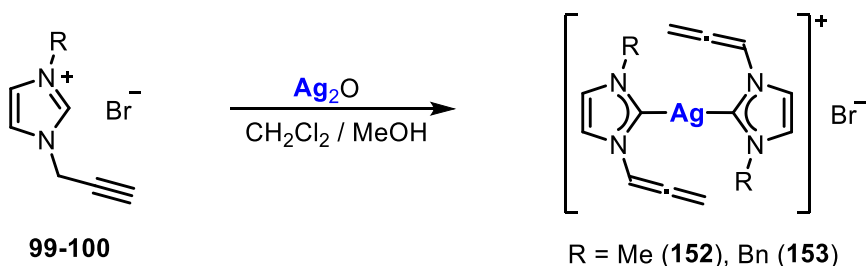


Figure 4.40. IR Spectrum of complex **150**.

## 4.5.3. Propargyl-Allenyl Tautomerism

Reaction of the imidazolium salts **99** and **100** with  $\text{Ag}_2\text{O}$  gave the bis-NHC silver bromide derivatives **152** and **153** in which the propargyl side arm has tautomerised to the allenyl form (Scheme 4.31).



**Scheme 4.31.** Synthesis of bis-NHC silver complexes **152** and **153**.

The allenyl unit is readily observed in the  $^1\text{H}$  NMR spectrum by the presence of a triplet at a high chemical shift (7.35 ppm for **152** and 7.56 ppm for **153**) corresponding to the CH and a doublet at around 5.6 ppm (5.68 ppm for **152** and 5.57 ppm for **153** with coupling constant  $^4J_{\text{HH}} = 6.4$  Hz in both cases) corresponding to the  $\text{CH}_2$  (Figure 4.41).

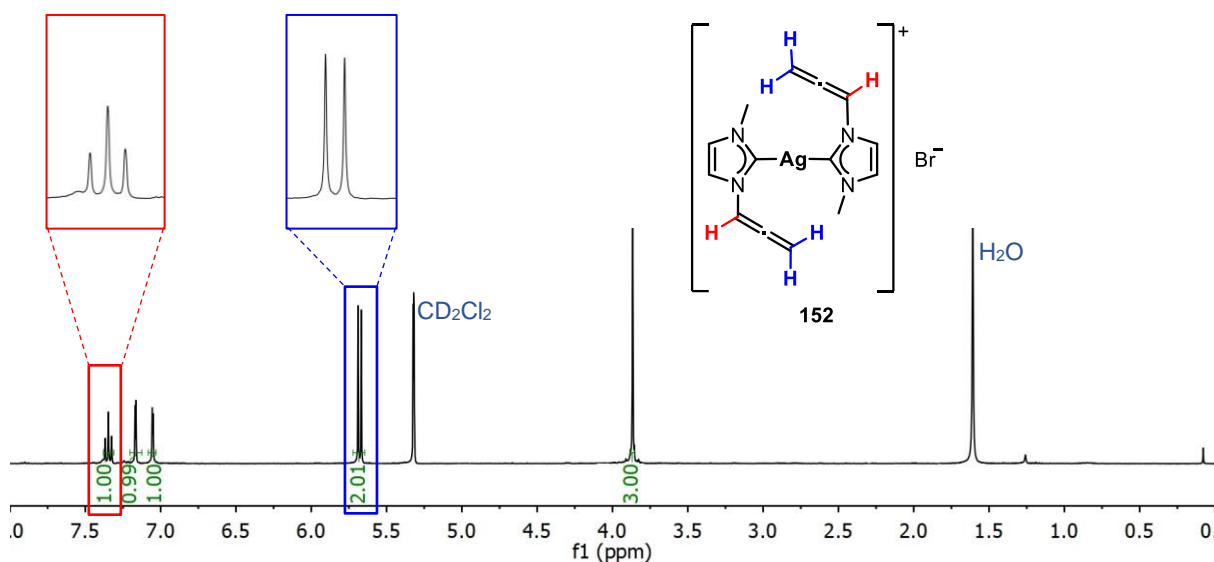


**Figure 4.41.**  $^1\text{H}$  NMR spectrum of complex **152** in  $\text{CD}_2\text{Cl}_2$  at room temperature.

The molecular structure of complex **153** was determined by single crystal X-ray diffraction (Figure 4.42).

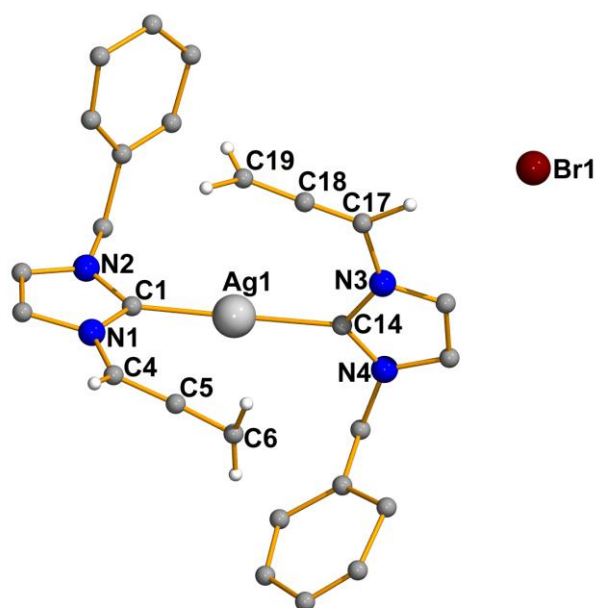
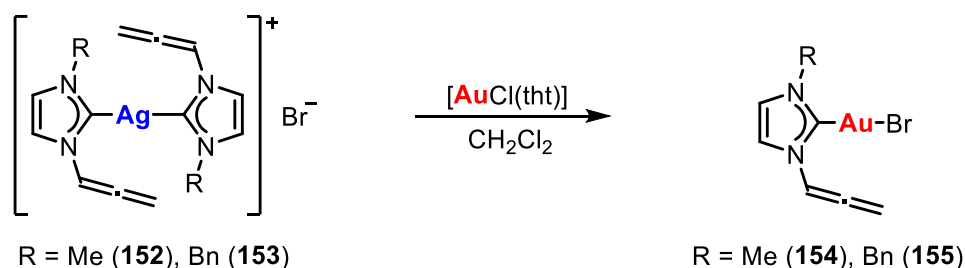


**Figure 4.42.** Molecular structure of complex **153**. Selected bond lengths (Å) and angles (°): Ag(1)-C(1) 2.062(10), Ag(1)-C(14) 2.156(9), C(4)-C(5) 1.362(13), C(5)-C(6) 1.303(16), C(17)-C(18) 1.226(13), C(18)-C(19) 1.308(17), C(1)-Ag(1)-C(14) 168.24(10), C(6)-C(5)-C(4) 175.6(12), C(17)-C(18)-C(19) 178.2(14).

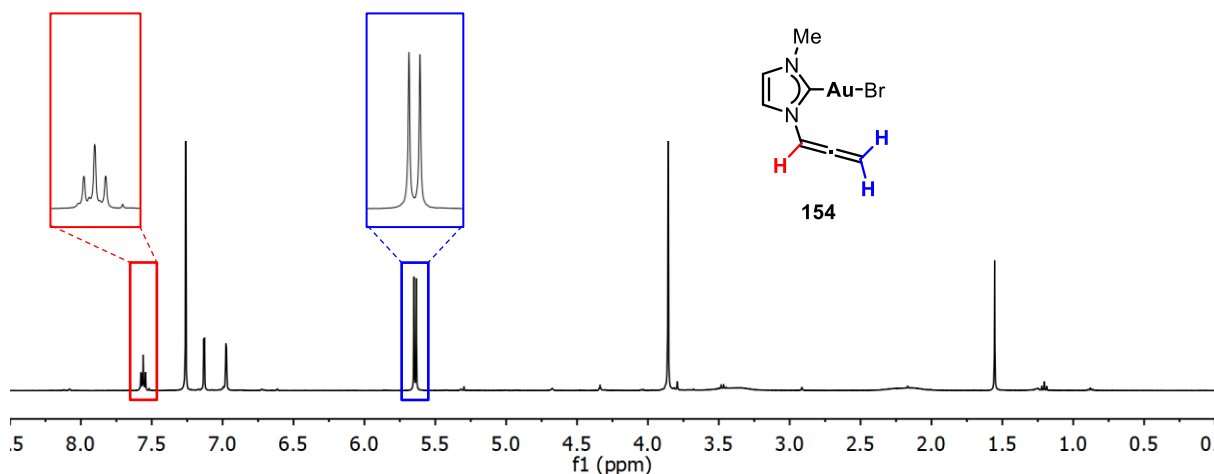
A distorted linear coordination is observed about the silver with C(1)-Ag(1)-C(14) angle of 168.24(10)°. The allenyl nature of the side arm can be seen by the similarity of the carbon bond distances C(4)-C(5) 1.362(13) Å and C(5)-C(6) 1.303(16) Å indicating two carbon-carbon double bonds.

Reaction of complexes **152** and **153** with two equivalents of [AuCl(tht)] led to the formation of the allenyl functionalised NHC gold complexes **154** and **155** in excellent yields (99%) (Scheme 4.32).



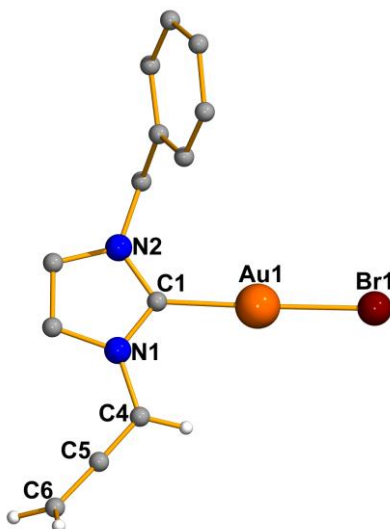
**Scheme 4.32.** Synthesis of complexes **154-155**.

As with complexes **152-153**, the allenyl side arm can clearly be seen in the  $^1\text{H}$  NMR spectra by the presence of a triplet at around 7.5 ppm due to the CH and a doublet at around 5.6 ppm due to the  $\text{CH}_2$  (Figure 4.43).



**Figure 4.43.**  $^1\text{H}$  NMR spectrum of complex **154** in  $\text{CDCl}_3$  at room temperature.

The molecular structure of complex **155** was determined by single crystal X-ray diffraction (Figure 4.44). The presence of the bromide anion can clearly be seen and a linear coordination about the gold centre is observed. The similarity of the C-C bond distances  $\text{C}(4)\text{-C}(5)$  1.284(19) Å and  $\text{C}(5)\text{-C}(6)$  1.352(18) Å highlights the presence of the allenyl unit. The  $\text{C}=\text{C}=\text{C}$  angle is practically linear.

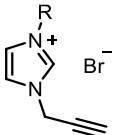
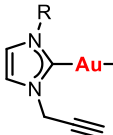
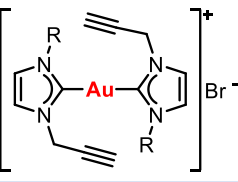
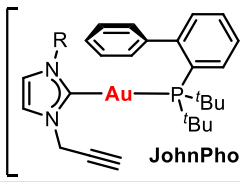
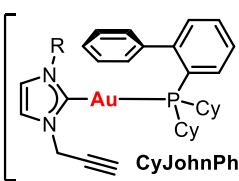
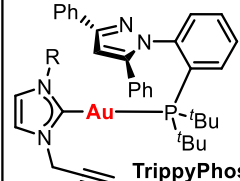


**Figure 4.44.** Molecular structure of complex **155**. Selected bond lengths (Å) and angles ( $^\circ$ ):  $\text{Au}(1)\text{-C}(1)$  2.019(12),  $\text{Au}(1)\text{-Br}(1)$  2.339(2),  $\text{N}(1)\text{-C}(1)$  1.321(17),  $\text{N}(2)\text{-C}(1)$  1.322(17),  $\text{C}(4)\text{-C}(5)$  1.284(19),  $\text{C}(5)\text{-C}(6)$  1.352(18),  $\text{C}(1)\text{-Au}(1)\text{-Br}(1)$  178.3(3),  $\text{C}(4)\text{-C}(5)\text{-C}(6)$  177.8(15).

## 4.6. Biological Activity

The biological activity of the imidazolium salts **99-102**, bromo NHC gold(I) bromide derivatives **103-106**, bis-NHC gold(I) complexes **107-110** and phosphine derivatives **123-134** was studied by MTT assay for lung carcinoma cell line A549. A technique analogous to that described in Chapter 2 was used. The calculated IC<sub>50</sub> values for the imidazolium salts and NHC complexes after 24 h incubation with A549 cells are shown in Table 4.7.

**Table 4.7.** IC<sub>50</sub> Values for Imidazolium Salts and NHC Gold Complexes after 24 h Incubation with A549 Cells

Complex	IC <sub>50</sub> (μM)	Complex	IC <sub>50</sub> (μM)
			
<b>99</b>	>100	<b>103</b>	39.44 ± 10.48
<b>100</b>	>100	<b>104</b>	2.93 ± 1.73
<b>101</b>	>100	<b>105</b>	>100
<b>102</b>	>100	<b>106</b>	79.11 ± 11.32
			
<b>107</b>	32.00 ± 8.33	<b>123</b>	4.69 ± 0.18
<b>108</b>	1.50 ± 0.30	<b>124</b>	5.01 ± 0.67
<b>109</b>	27.80 ± 2.10	<b>125</b>	4.74 ± 0.47
<b>110</b>	23.84 ± 3.51	<b>126</b>	5.96 ± 0.86
			
<b>127</b>	4.78 ± 0.13	<b>131</b>	8.59 ± 0.93
<b>128</b>	1.84 ± 0.46	<b>132</b>	4.09 ± 1.09
<b>129</b>	5.64 ± 0.18	<b>133</b>	5.67 ± 0.29
<b>130</b>	4.86 ± 0.44	<b>134</b>	5.90 ± 0.58

As expected, the imidazolium salts did not show anti-proliferative activity, with  $IC_{50}$  values  $>100\text{ }\mu\text{M}$  in all cases. The NHC gold complexes, however, were active.

The  $[\text{Au}(\text{NHC})\text{Br}]$  complexes, **103-106** showed only moderate activity, probably due to their instability in the cell culture medium. The bis-propargyl derivative, **105**, decomposed and hence showed no antiproliferative activity. The benzyl derivative, **104**, was the most stable of these complexes and showed excellent activity with an  $IC_{50}$  value of  $2.93 \pm 1.73\text{ }\mu\text{M}$ .

All of the cationic NHC gold complexes all showed good stability in the cell culture medium. The  $[\text{Au}(\text{NHC})_2]\text{Br}$  complexes showed moderate antiproliferative activity, apart from the benzyl derivative, **108**, which again showed excellent activity with a very low  $IC_{50}$  value of  $1.50 \pm 0.30\text{ }\mu\text{M}$ . This is very promising since this complex is also water soluble and hence could be used to develop new anticancer treatments.

The NHC gold phosphine derivatives showed excellent antiproliferative activity with  $IC_{50} < 10\text{ }\mu\text{M}$  in all cases. No significant differences were observed upon changing the phosphine, probably due to the similar steric and electronic properties of the phosphines used. Changing the substituent on the nitrogen of the NHC also had little effect on the antiproliferative activity of the complex, although in all of the complexes tested the benzyl derivatives were generally the most active, probably due to their greater solubility.

A graph of cell viability (% of control) against concentration of complex for the derivatives of the methyl NHC is shown in Figure 4.45. The higher activity of the  $[\text{Au}(\text{NHC})(\text{Phosphine})]^+$  derivatives can clearly be seen by the steeper slopes of the corresponding curves.



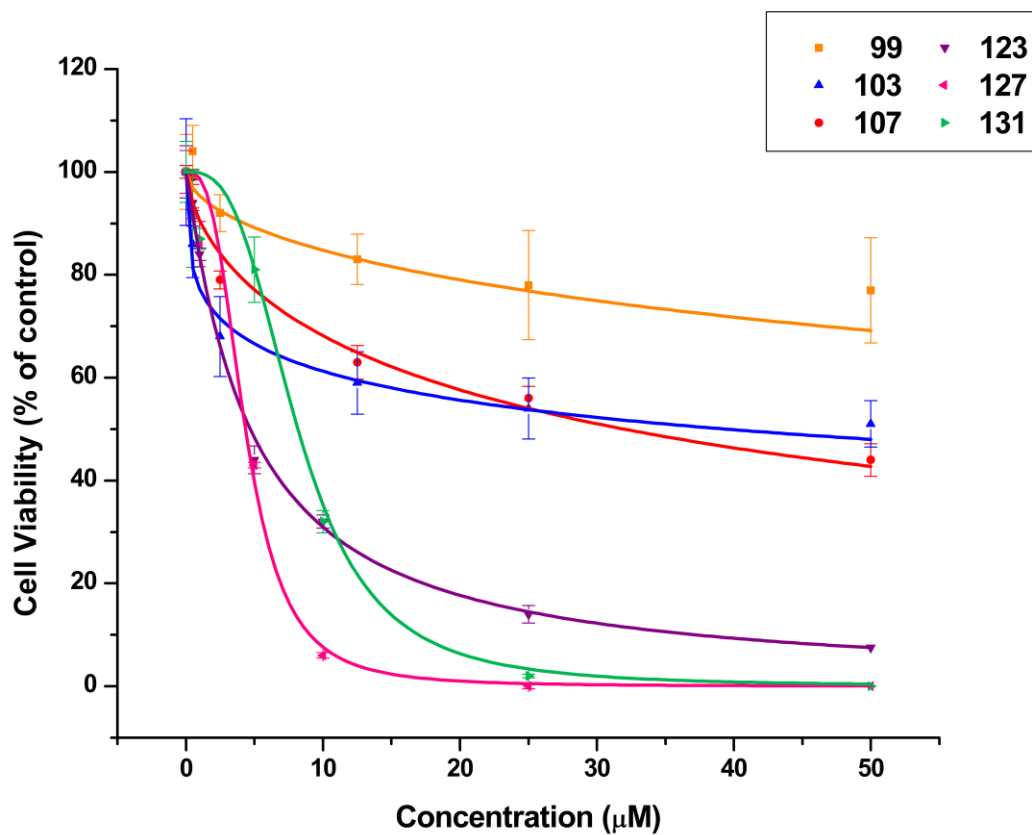


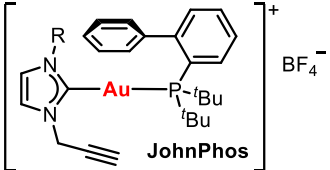
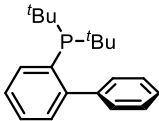
**Figure 4.45.** Cell viability (% of control) vs Concentration ( $\mu\text{M}$ ) for complexes of the methyl functionalised NHC (Each point is the average of eight measurements, where error bars represent the standard deviation. Curve generated by a sigmoidal non-linear regression 4-parameter logistic analysis).

## 4.7. Luminescence

The NHC gold phosphine derivatives, **123-134**, all exhibited luminescence in the solid state both at room temperature and at 77 K.

The excitation and emission maxima for the JohnPhos derivatives, **123-126**, and free JohnPhos are shown in Table 4.8.

**Table 4.8.** Excitation and Emission Maxima for Complexes **123-126** and JohnPhos

Complex	Temperature (K)	Excitation $\lambda_{\max}$ (nm)	Emission $\lambda_{\max}$ (nm)	$\tau_0$ ( $\mu$ s)
				
<b>123</b>	298	286	546	107.1
	77	290, 332	552, 444	2282.3
<b>124</b>	298	296	501	204.7
	77	290, 323	502, 442	2091.2
<b>125</b>	298	277	551	83.0
	77	287	547	1740.6
<b>126</b>	298	303	548	
	77	297, 364	542, 457	1592.8
				
<b>JohnPhos</b> (free ligand)	298	371	527	

The non-coordinated JohnPhos ligand does exhibit luminescence at room temperature with an excitation at 371  $\text{cm}^{-1}$  and emission at 527  $\text{cm}^{-1}$  (Figure 4.46). This is due to intraligand  $\pi$ - $\pi^*$  transitions within the biphenyl group.

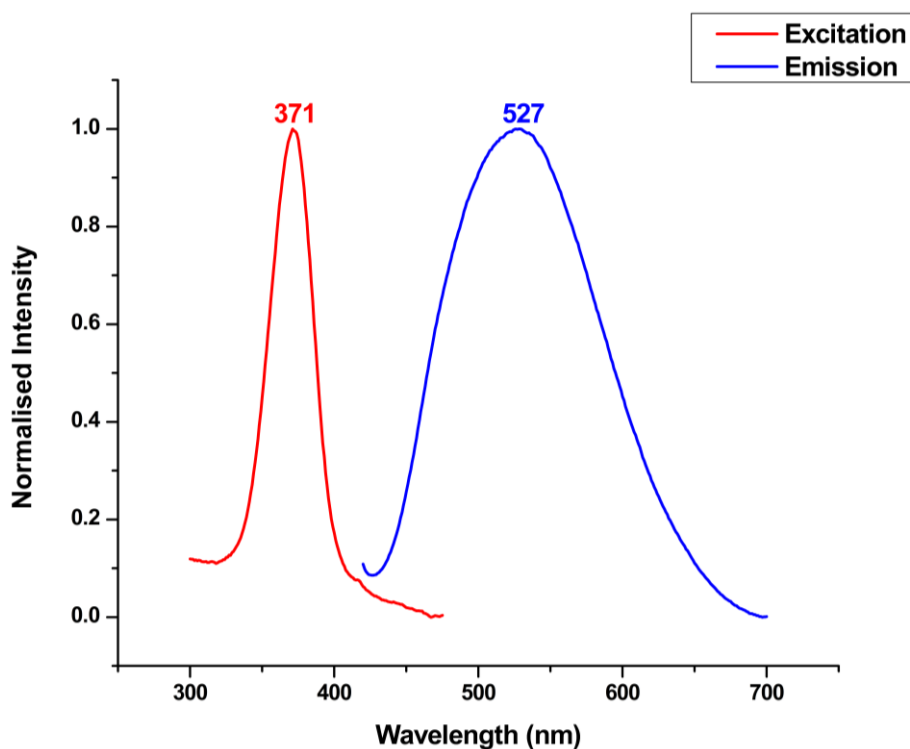


**Figure 4.46.** Excitation and emission maxima for JohnPhos at room temperature.

The emission due to the intraligand transition in the phosphine is not observed in complexes **123-126** at room temperature. One excitation band and one emission band are observed in each case but there is a much larger Stokes shift compared to the bands for the free ligand and the wavelength of the emission varies upon changing the NHC ligand (Figure 4.47). The long lifetimes indicate that this is a phosphorescent emission and it can therefore be assigned to a ligand to metal to ligand charge transfer (LMLCT).

At 77 K an additional, less intense excitation band and emission band are observed. This band is due to intraligand transitions within the JohnPhos and the wavelength of emission is modified with respect to the free ligand due to coordination to the metal (Figure 4.48)

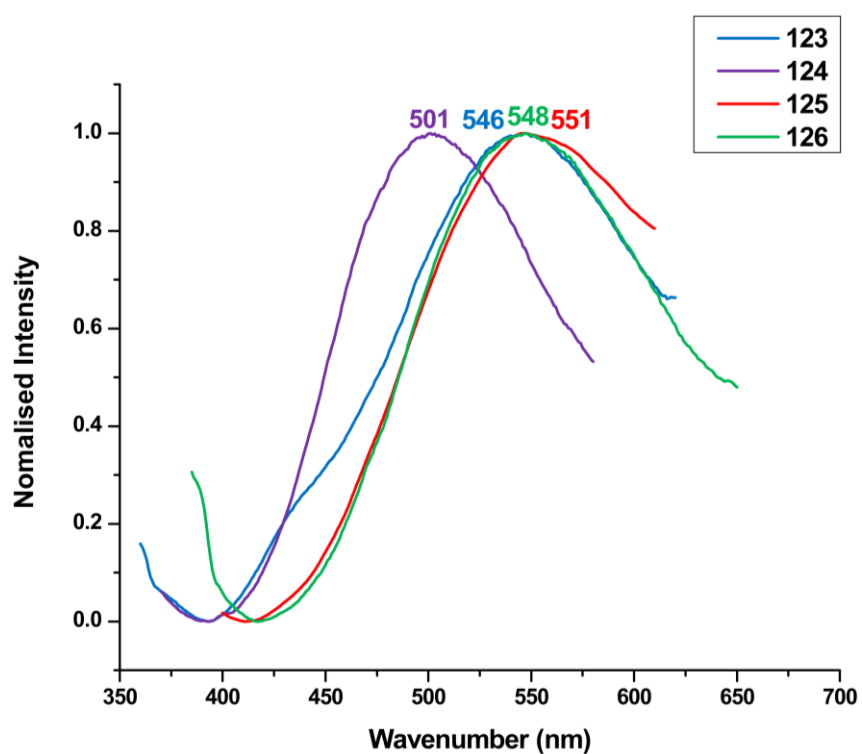


Figure 4.47. Emission bands for complexes **123-126** at room temperature.

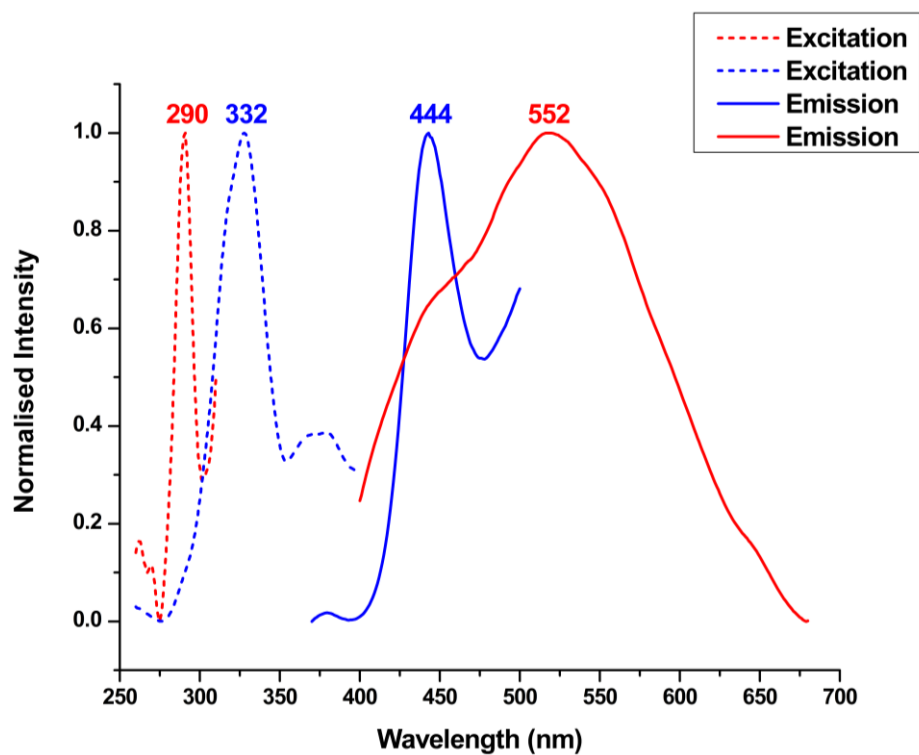
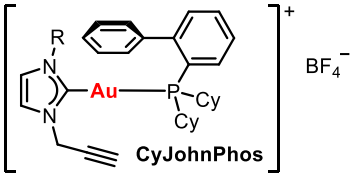
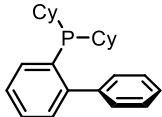


Figure 4.48. Excitation and emission bands for complex **123** at 77 K.

## 4.7. Luminescence

The excitation and emission maxima for the CyJohnPhos derivatives, **127-130**, and free CyJohnPhos are shown in Table 4.9.

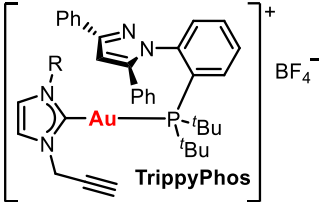
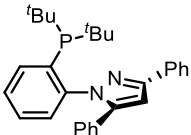
**Table 4.9.** Excitation and Emission Maxima for Complexes **127-130** and CyJohnPhos

Complex	Temperature (K)	Excitation $\lambda_{\max}$ (nm)	Emission $\lambda_{\max}$ (nm)	$\tau_0$ ( $\mu$ s)
				
<b>127</b>	298	281, 344	472, 373	293.7
	77	283, 346	492, 466	4606.4
<b>128</b>	298	318, 358	480	152.8
	77	310, 345	465	2081.9
<b>129</b>	298	297	497	211.3
	77	291	496	3597.2
<b>130</b>	298	303, 388	549, 455	443.2
	77	289, 392	528, 480	2399.0
				
<b>CyJohnPhos</b> (free ligand)	298	362	492	

Similarly to Johnphos, CyJohnPhos is luminescent at room temperature with an excitation band at 362  $\text{cm}^{-1}$  and an emission band at 492  $\text{cm}^{-1}$  as a result of intraligand  $\pi$ - $\pi^*$  transitions within the biphenyl group. Complexes **127**, **128** and **130** exhibit two excitation and two emission bands at room temperature and at 77 K. The high energy excitation band and corresponding emission are assigned to a ligand to metal to ligand charge transfer (LMLCT) due to the large Stokes shift and the long lifetimes which indicate phosphorescence. The other band is an intraligand charge transfer in the CyJohnPhos ligand, modified due to coordination to the gold centre. In complex **129** this intraligand charge transfer band is not observed at room temperature or at 77 K.

The excitation and emission maxima for the CyJohnPhos derivatives, **131-134**, and free TrippyPhos are shown in Table 4.10.

**Table 4.10.** Excitation and Emission Maxima for Complexes **131-134** and TrippyPhos

Complex	Temperature (K)	Excitation $\lambda_{\text{max}}$ (nm)	Emission $\lambda_{\text{max}}$ (nm)	$\tau_0$ ( $\mu\text{s}$ )
				
<b>131</b>	298	385	465	303.2
	77	315, 392	522, 460	8371.3
<b>132</b>	298	381	468	195.0
	77	310, 365	535, 459	9091.8
<b>133</b>	298	386	464	190.7
	77	307, 377	489, 456	4887.8
<b>134</b>	298	388	468	103.7
	77	308	494, 465	4808.7
				
<b>TrippyPhos</b> (free ligand)	298	391	526	

The TrippyPhos ligand is intensely luminescent at room temperature with an excitation band at 391  $\text{nm}$  and an emission band at 526  $\text{nm}$  as a result of intraligand  $\pi-\pi^*$  transitions. Complexes **131-134** have one excitation and one emission band at room temperature. The emission band does not change upon changing the NHC ligand, however the lifetimes suggest that this is a phosphorescent emission and therefore cannot be assigned to an intraligand transition. This band is assigned to a ligand to metal charge transfer (LMCT) from the phosphine ligand to the gold. At 77 K an additional excitation and emission band are observed with a larger Stokes shift. This band is assigned to ligand to metal to ligand charge transfer (LMLCT) similar to complexes **123-130**.

## 4.8. Conclusions

A new thallium-free synthesis for tetrabutylammonium acetylacetonate starting from relatively cheap precursors has been described. This reagent has been shown to be effective in the formation of NHCs from their corresponding imidazolium salts with reactions carried out at room temperature, in air and with reaction times of just 1 hour. The method was tested with several commercially available imidazolium salts and was shown to be incredibly versatile, allowing NHC gold complexes to be prepared both with very bulky NHCs as well as smaller NHCs bearing a simple alkyl chains at the nitrogen atoms. The synthesis of pentafluorophenyl gold derivatives from the imidazolium salts was also possible and several examples were characterised by single crystal X-ray diffraction.

Propargyl functionalised imidazolium salts were prepared by the alkylation of imidazoles with propargyl bromide. Bromo-, pentafluorophenyl- and bis-NHC gold complexes derived from these imidazolium salts were prepared using the tetrabutylammonium acetylacetonate method and structurally characterised. In all cases the propargyl side arms were maintained. Cationic gold phosphine derivatives could also be prepared; however, a bulky phosphine was required for a clean reaction. With smaller phosphines an equilibrium was observed in solution, although it is possible that the  $[\text{Au}(\text{NHC})(\text{PR}_3)]^+$  complexes do exist in the solid state. The NHC complexes bearing the bulky phosphines were characterised by single crystal X-ray diffraction.

Attempts to prepare NHC gold(III) derivatives from  $[\text{AuCl}_3(\text{tbt})]$  were unsuccessful and resulted in the reduction to gold(I). However, the  $[\text{AuCl}_3(\text{NHC})]$  derivatives were accessible by the oxidation of the  $[\text{AuBr}(\text{NHC})]$  complexes with  $\text{Cl}_2$  and two examples were characterised by single crystal X-ray diffraction. Three chloride ligands were coordinated to the gold(III) centre and no mixture of chloride and bromide was observed. This is due to the large excess of chlorine used in the oxidation reaction.

Dinuclear NHC gold complexes derived from a di-imidazolium salt were prepared and characterised. In all cases the propargyl side arm was maintained. As with the mononuclear NHC gold complexes, the triphenylphosphine derivatives were found to exist in equilibrium in

solution. One example was characterised by single crystal X-ray diffraction, showing that these complexes can exist in the solid state.

Studies into the possible functionalisation of the propargyl side arm were also carried out. Tetrabutylammonium acetylacetonate was found to be too weak a base to deprotonate the alkyne CH, however, the use of potassium hydroxide was successful and allowed dinuclear gold JohnPhos derivatives to be prepared. Reaction of the NHC gold bromo complexes with diisopropylamine resulted in the formation of highly insoluble trimeric species. All were characterised by high resolution mass spectrometry and one example was sufficiently soluble to be characterised by NMR spectroscopy. Infrared spectra of the complexes suggest that the triple bond is maintained.

The use of silver oxide to prepare NHC complexes from the imidazolium salts successfully gave the bis-NHC silver derivatives, however in this case a tautomerism of the propargyl unit occurred. The presence of the allenyl unit could be observed in the  $^1\text{H}$  NMR spectrum as well as in the molecular structure determined by single crystal X-ray diffraction. Transmetallation with  $[\text{AuCl}(\text{tht})]$  allowed the allenyl functionalised NHC gold complexes to be accessed. One example was successfully characterised by single crystal X-ray diffraction. The allenyl unit could readily be seen by the similarity of the carbon-carbon bond lengths in the molecular structure.

The antiproliferative activity of the complexes against lung cancer cell line A549 was tested by MTT assay. The imidazolium salts showed no activity. Some of the  $[\text{AuBr}(\text{NHC})]$  complexes were unstable in the cell culture medium used for the study and hence showed poor activities, however, the cationic complexes were all highly stable and showed antiproliferative activity. The phosphine derivatives were the most active with very low  $\text{IC}_{50}$  values.

The NHC gold phosphine derivatives were also found to be luminescent in the solid state, both at room temperature and at 77 K. In all cases emission bands assigned to ligand to metal to ligand charge transfer transitions were observed. For the JohnPhos and CyJohnPhos derivatives, emission bands assigned to intraligand  $\pi\pi^*$  transitions were also observed.

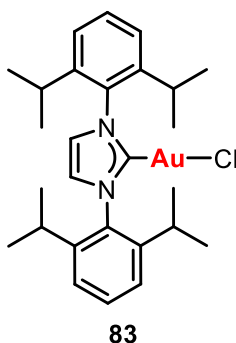


## 4.9. Experimental

### NBu<sub>4</sub>(acac)

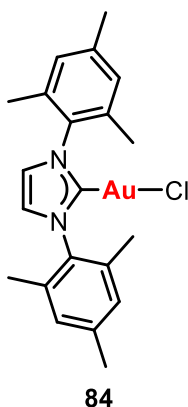
To a solution of tetrabutylammonium hydroxide 30-hydrate (1.600 g, 2.0 mmol) in ethanol (10 ml) was added acetylacetone (0.2 ml, 2 mmol) and the solution stirred for 8 h. Solvent was removed *in vacuo* to leave a pale yellow residue which was dissolved in CH<sub>2</sub>Cl<sub>2</sub> (10 ml) and dried over Na<sub>2</sub>SO<sub>4</sub>. The solution was concentrated to minimum volume and diethyl ether (10 ml) was added to precipitate an off-white solid which was collected and vacuum dried to give the product (0.649 g, 95%).

Spectral data are in agreement with values previously reported in the literature.



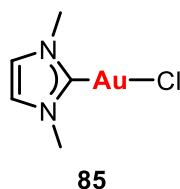
1,3-Bis(2,6-diisopropylphenyl)imidazolium chloride (0.0850 g, 0.2 mmol) and [AuCl(tht)] (0.0641 g, 0.2 mmol) were mixed in CH<sub>2</sub>Cl<sub>2</sub> (10 ml) until a colourless solution formed (5 min). NBu<sub>4</sub>(acac) (0.0683 g, 0.2 mmol) was added and the mixture stirred for 1 h. The solution was filtered through a plug of silica and the colourless filtrate evaporated to minimum volume. Pentane was added to precipitate a white solid which was collected and vacuum dried to give the product (0.1182 g, 95%).

Spectral data are in agreement with values previously reported in the literature.



1,3-Bis(2,4,6-trimethylphenyl)imidazolium chloride (0.1023 g, 0.3 mmol) and [AuCl(tht)] (0.0962 g, 0.3 mmol) were mixed in CH<sub>2</sub>Cl<sub>2</sub> (10 ml) until a colourless solution formed (5 min). NBu<sub>4</sub>(acac) (0.1025 g, 0.3 mmol) was added and the mixture stirred for 1 h. The solution was filtered through a plug of silica and the colourless filtrate evaporated to minimum volume. Pentane was added to precipitate a white solid which was collected and vacuum dried to give the product (0.1582 g, 98%).

Spectral data are in agreement with values previously reported in the literature.

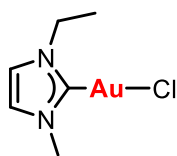


1,3-dimethylimidazolium chloride (0.0397 g, 0.3 mmol) and [AuCl(tht)] (0.0962 g, 0.3 mmol) were mixed in CH<sub>2</sub>Cl<sub>2</sub> (10 ml) until a colourless solution formed (5 min). NBu<sub>4</sub>(acac) (0.1025 g, 0.3 mmol) was added and the mixture stirred for 1 h. The solution was filtered through a plug of silica and the colourless filtrate evaporated to minimum volume. Pentane was added to precipitate a white solid which was collected and vacuum dried to give the product (0.1582 g, 98%).

Spectral data are in agreement with values previously reported in the literature.

#### 4.9. Experimental

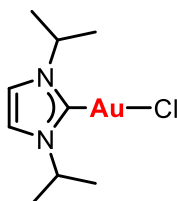
---



**86**

1-ethyl-3-methylimidazolium chloride (0.0440 g, 0.3 mmol) and [AuCl(tht)] (0.0962 g, 0.3 mmol) were mixed in CH<sub>2</sub>Cl<sub>2</sub> (10 ml) until a colourless solution formed (5 min). NBu<sub>4</sub>(acac) (0.1025 g, 0.3 mmol) was added and the mixture stirred for 1 h. The solution was filtered through a plug of silica and the colourless filtrate evaporated to minimum volume. Pentane was added to precipitate a white solid which was collected and vacuum dried to give the product (0.0987 g, 96%).

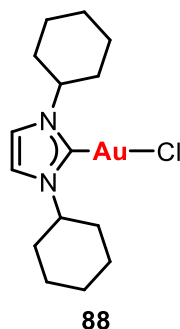
Spectral data are in agreement with values previously reported in the literature.



**87**

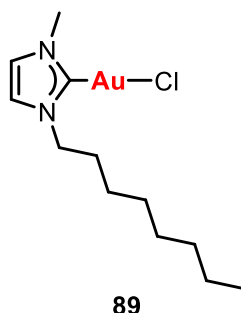
1,3-diisopropyl imidazolium chloride (0.0377 g, 0.2 mmol) and [AuCl(tht)] (0.0641 g, 0.2 mmol) were mixed in CH<sub>2</sub>Cl<sub>2</sub> (10 ml) until a colourless solution formed (5 min). NBu<sub>4</sub>(acac) (0.0683 g, 0.2 mmol) was added and the mixture stirred for 1 h. The solution was filtered through a plug of silica and the colourless filtrate evaporated to minimum volume. Pentane was added to precipitate a white solid which was collected and vacuum dried to give the product (0.0649 g, 64%).

Spectral data are in agreement with values previously reported in the literature.



1,3-dicyclohexyl imidazolium chloride (0.0806 g, 0.3 mmol) and [AuCl(tht)] (0.0962 g, 0.3 mmol) were mixed in CH<sub>2</sub>Cl<sub>2</sub> (10 ml) until a colourless solution formed (5 min). NBu<sub>4</sub>(acac) (0.1025 g, 0.3 mmol) was added and the mixture stirred for 1 h. The solution was filtered through a plug of silica and the colourless filtrate evaporated to minimum volume. Pentane was added to precipitate a white solid which was collected and vacuum dried to give the product (0.0931 g, 67%).

Spectral data are in agreement with values previously reported in the literature.



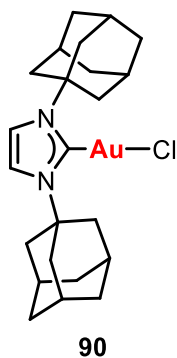
1-octyl-3-methylimidazolium chloride (0.0692 g, 0.3 mmol) and [AuCl(tht)] (0.0962 g, 0.3 mmol) were mixed in CH<sub>2</sub>Cl<sub>2</sub> (10 ml) until a colourless solution formed (5 min). NBu<sub>4</sub>(acac) (0.1025 g, 0.3 mmol) was added and the mixture stirred for 1 h. The solution was filtered through a plug of silica and the colourless filtrate evaporated to minimum volume. Pentane was added to precipitate a white solid which was collected and vacuum dried to give the product (0.1112 g, 87%).

**<sup>1</sup>H NMR (400 MHz, CDCl<sub>3</sub>)** δ 6.93 (d, *J* = 1.9 Hz, 1H, CH imidazole), 6.92 (d, *J* = 1.9 Hz, 1H, CH imidazole), 4.13 (t, *J* = 7.3 Hz, 2H, CH<sub>2</sub>CH<sub>2</sub>(CH<sub>2</sub>)<sub>5</sub>CH<sub>3</sub>), 3.82 (s, 3H, Me), 1.88 – 1.74 (m, 2H, CH<sub>2</sub>CH<sub>2</sub>(CH<sub>2</sub>)<sub>5</sub>CH<sub>3</sub>), 1.27 (m, 10H, CH<sub>2</sub>CH<sub>2</sub>(CH<sub>2</sub>)<sub>5</sub>CH<sub>3</sub>), 0.86 (t, *J* = 6.9 Hz, 3H, CH<sub>2</sub>CH<sub>2</sub>(CH<sub>2</sub>)<sub>5</sub>CH<sub>3</sub>).

**<sup>13</sup>C NMR (101 MHz, CDCl<sub>3</sub>)** δ 170.88 (s, N-C-N), 121.81 (s, CH imidazole), 120.56 (s, CH imidazole), 51.53 (s, CH<sub>2</sub>CH<sub>2</sub>(CH<sub>2</sub>)<sub>5</sub>CH<sub>3</sub>), 38.37 (s, Me), 31.78 (s, CH<sub>2</sub>CH<sub>2</sub>(CH<sub>2</sub>)<sub>5</sub>CH<sub>3</sub>), 31.18

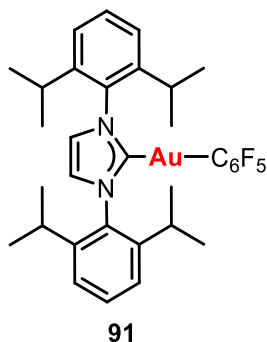
#### 4.9. Experimental

(s, CH<sub>2</sub>CH<sub>2</sub>(CH<sub>2</sub>)<sub>5</sub>CH<sub>3</sub>), 29.15 (s, CH<sub>2</sub>CH<sub>2</sub>(CH<sub>2</sub>)<sub>5</sub>CH<sub>3</sub>), 26.48 (s, CH<sub>2</sub>CH<sub>2</sub>(CH<sub>2</sub>)<sub>5</sub>CH<sub>3</sub>), 22.67 (s, CH<sub>2</sub>CH<sub>2</sub>(CH<sub>2</sub>)<sub>5</sub>CH<sub>3</sub>), 14.15 (s, CH<sub>2</sub>CH<sub>2</sub>(CH<sub>2</sub>)<sub>5</sub>CH<sub>3</sub>).



1,3-bis(1-adamantyl)imidazolium chloride (0.1119 g, 0.3 mmol) and [AuCl(tht)] (0.0962 g, 0.3 mmol) were mixed in CH<sub>2</sub>Cl<sub>2</sub> (10 ml) until a colourless solution formed (5 min). NBu<sub>4</sub>(acac) (0.1025 g, 0.3 mmol) was added and the mixture stirred for 1 h. The solution was filtered through a plug of silica and the colourless filtrate evaporated to minimum volume. Pentane was added to precipitate a white solid which was collected and vacuum dried to give the product (0.1027 g, 60%).

Spectral data are in agreement with values previously reported in the literature

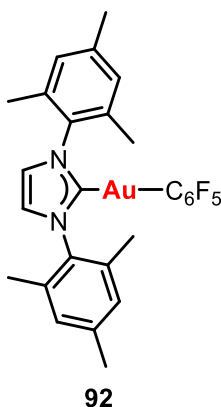


1,3-Bis(2,6-diisopropylphenyl)imidazolium chloride (0.0850 g, 0.2 mmol) and [Au(C<sub>6</sub>F<sub>5</sub>)(tht)] (0.0904 g, 0.2 mmol) were mixed in CH<sub>2</sub>Cl<sub>2</sub> (10 ml) until a colourless solution formed (5 min). The solution was concentrated to dryness under reduced pressure to give a white solid which was washed several times with hexane. The solid was dissolved in CH<sub>2</sub>Cl<sub>2</sub> (10 ml), NBu<sub>4</sub>(acac) (0.0683 g, 0.2 mmol) was added and the mixture stirred for 1 h. The solution was filtered through a plug of silica and the colourless filtrate evaporated to minimum volume. Pentane was added to precipitate a white solid which was collected and vacuum dried to give the product (0.1098 g, 73%).

**$^1\text{H}$  NMR (300 MHz,  $\text{CDCl}_3$ )**  $\delta$  7.49 (t,  $J = 7.8$  Hz, 2H,  $p\text{-C}_6\text{H}_3$ ), 7.29 (d,  $J = 7.8$  Hz, 4H,  $m\text{-C}_6\text{H}_3$ ), 7.20 (s, 2H,  $\underline{\text{CH}}$  imidazole), 2.62 (sept,  $J = 6.9$  Hz, 4H,  $\underline{\text{CH}}\text{Me}_2$ ), 1.36 (d,  $J = 6.9$  Hz, 6H,  $\text{CHMe}_2$ ), 1.24 (d,  $J = 6.9$  Hz, 6H,  $\text{CHMe}_2$ ).

**$^{19}\text{F}$  NMR (376 MHz,  $\text{CDCl}_3$ )**  $\delta$  -115.28 – -116.84 (m,  $o\text{-C}_6\text{F}_5$ ), -161.20 (t,  $J = 20.0$  Hz,  $p\text{-C}_6\text{F}_5$ ), -162.46 – -165.76 (m,  $m\text{-C}_6\text{F}_5$ ).

**$^{13}\text{C}$  NMR (75 MHz,  $\text{CDCl}_3$ )**  $\delta$  192.15 (s, N- $\underline{\text{C}}$ -N, (observed by HMBC)), 145.93 (s,  $i\text{-C}_6\text{H}_3$ ), 134.25 (s,  $o\text{-C}_6\text{H}_3$ ), 130.61 (s,  $p\text{-C}_6\text{H}_3$ ), 124.16 (s,  $m\text{-C}_6\text{H}_3$ ), 123.14 (s,  $\underline{\text{CH}}$  imidazole), 29.02 (s,  $\underline{\text{CH}}\text{Me}_2$ ), 24.48 (s, Me), 24.17 (s, Me).



1,3-Bis(2,4,6-trimethylphenyl)imidazolium chloride (0.1023 g, 0.3 mmol) and  $[\text{Au}(\text{C}_6\text{F}_5)(\text{tbt})]$  (0.1357 g, 0.3 mmol) were mixed in  $\text{CH}_2\text{Cl}_2$  (10 ml) until a colourless solution formed (5 min). The solution was concentrated to dryness under reduced pressure to give a white solid which was washed several times with hexane. The solid was dissolved in  $\text{CH}_2\text{Cl}_2$  (10 ml),  $\text{NBu}_4(\text{acac})$  (0.1025 g, 0.3 mmol) was added and the mixture stirred for 1 h. The solution was filtered through a plug of silica and the colourless filtrate evaporated to minimum volume. Pentane was added to precipitate a white solid which was collected and vacuum dried to give the product (0.1604 g, 80%).

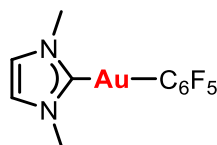
**$^1\text{H}$  NMR (300 MHz,  $\text{CDCl}_3$ )**  $\delta$  7.12 (s, 2H,  $\underline{\text{CH}}$  imidazole), 7.02 (s, 4H,  $\text{C}_6\text{H}_2$ ), 2.35 (s, 6H,  $p\text{-Me}$ ), 2.17 (s, 12H,  $o\text{-Me}$ ).

**$^{19}\text{F}$  NMR (376 MHz,  $\text{CDCl}_3$ )**  $\delta$  -115.94 – -116.11 (m,  $o\text{-C}_6\text{F}_5$ ), -160.84 (t,  $J = 20.0$  Hz,  $p\text{-C}_6\text{F}_5$ ), -163.56 – -163.83 (m,  $m\text{-C}_6\text{F}_5$ ).

**$^{13}\text{C}$  NMR (75 MHz,  $\text{CDCl}_3$ )**  $\delta$  190.50 (s, N- $\underline{\text{C}}$ -N, (observed by HMBC)) 139.63 (s,  $\underline{\text{CH}}$  aromatic), 134.97 (s,  $\underline{\text{CH}}$  aromatic), 134.88 (s,  $\underline{\text{CH}}$  aromatic), 129.44 (s,  $\underline{\text{CH}}$  aromatic), 122.30 (s,  $\underline{\text{CH}}$  imidazole), 21.31 (s,  $\underline{\text{CH}}_3$ ), 18.00 (s,  $\underline{\text{CH}}_3$ ).

#### 4.9. Experimental

---



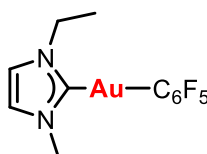
93

1,3-dimethylimidazolium chloride (0.0397 g, 0.3 mmol) and  $[\text{Au}(\text{C}_6\text{F}_5)(\text{tht})]$  (0.1357 g, 0.3 mmol) were mixed in  $\text{CH}_2\text{Cl}_2$  (10 ml) until a colourless solution formed (5 min). The solution was concentrated to dryness under reduced pressure to give a white solid which was washed several times with hexane. The solid was dissolved in  $\text{CH}_2\text{Cl}_2$  (10 ml),  $\text{NBu}_4(\text{acac})$  (0.1025 g, 0.3 mmol) was added and the mixture stirred for 1 h. The solution was filtered through a plug of silica and the colourless filtrate evaporated to minimum volume. Pentane was added to precipitate a white solid which was collected and vacuum dried to give the product (0.1184 g, 86%).

**$^1\text{H}$  NMR (300 MHz,  $\text{CDCl}_3$ )**  $\delta$  6.92 (s, 2H,  $\underline{\text{CH}}$  imidazole), 3.90 (s, 6H, Me).

**$^{19}\text{F}$  NMR (282 MHz,  $\text{CDCl}_3$ )**  $\delta$  -115.96 – -117.07 (m, *o*- $\text{C}_6\text{F}_5$ ), -159.98 (t,  $J$  = 20.0 Hz, *p*- $\text{C}_6\text{F}_5$ ), -162.13 – -164.49 (m, *m*- $\text{C}_6\text{F}_5$ ).

**$^{13}\text{C}$  NMR (75 MHz,  $\text{CDCl}_3$ )**  $\delta$  188.59 (s,  $\text{N}-\underline{\text{C}}-\text{N}$ , (observed by HMBC)), 121.86 (s,  $\underline{\text{CH}}$  imidazole), 37.91 (s, Me).



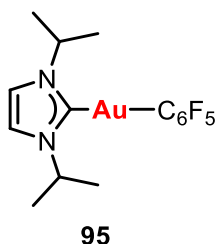
94

1-ethyl-3-methylimidazolium chloride (0.0440 g, 0.3 mmol) and  $[\text{Au}(\text{C}_6\text{F}_5)(\text{tht})]$  (0.1357 g, 0.3 mmol) were mixed in  $\text{CH}_2\text{Cl}_2$  (10 ml) until a colourless solution formed (5 min). The solution was concentrated to dryness under reduced pressure to give a white solid which was washed several times with hexane. The solid was dissolved in  $\text{CH}_2\text{Cl}_2$  (10 ml),  $\text{NBu}_4(\text{acac})$  (0.1025 g, 0.3 mmol) was added and the mixture stirred for 1 h. The solution was filtered through a plug of silica and the colourless filtrate evaporated to minimum volume. Pentane was added to precipitate a white solid which was collected and vacuum dried to give the product (0.0797 g, 56%).

**$^1\text{H}$  NMR (300 MHz,  $\text{CDCl}_3$ )**  $\delta$  6.96 (d,  $J = 1.9$  Hz, 1H,  $\text{CH}$  imidazole), 6.92 (d,  $J = 1.9$  Hz, 1H,  $\text{CH}$  imidazole), 4.28 (q,  $J = 7.3$  Hz, 2H,  $\text{CH}_2$ ), 3.91 (s, 3H, Me), 1.53 (t,  $J = 7.3$  Hz, 3H,  $\text{CH}_2\text{CH}_3$ ).

**$^{19}\text{F}$  NMR (282 MHz,  $\text{CDCl}_3$ )**  $\delta$  -115.07 – -117.62 (m,  $o\text{-C}_6\text{F}_5$ ), -159.97 (t,  $J = 19.9$  Hz,  $p\text{-C}_6\text{F}_5$ ), -161.74 – -165.12 (m,  $m\text{-C}_6\text{F}_5$ ).

**$^{13}\text{C}$  NMR (75 MHz,  $\text{CDCl}_3$ )**  $\delta$  187.85 (s,  $\text{N}-\text{C}-\text{N}$ , (observed by HMBC)), 121.77 (s,  $\text{CH}$  imidazole), 120.09 (s,  $\text{CH}$  imidazole), 46.24 (s,  $\text{CH}_2$ ), 38.05 (s, Me), 16.83 (s,  $\text{CH}_3$ ).



1,3-diisopropyl imidazolium chloride (0.0566 g, 0.3 mmol) and  $[\text{Au}(\text{C}_6\text{F}_5)(\text{tht})]$  (0.1357 g, 0.3 mmol) were mixed in  $\text{CH}_2\text{Cl}_2$  (10 ml) until a colourless solution formed (5 min). The solution was concentrated to dryness under reduced pressure to give a white solid which was washed several times with hexane. The solid was dissolved in  $\text{CH}_2\text{Cl}_2$  (10 ml),  $\text{NBu}_4(\text{acac})$  (0.1025 g, 0.3 mmol) was added and the mixture stirred for 1 h. The solution was filtered through a plug of silica and the colourless filtrate evaporated to minimum volume. Pentane was added to precipitate a white solid which was collected and vacuum dried to give the product (0.0940 g, 61%).

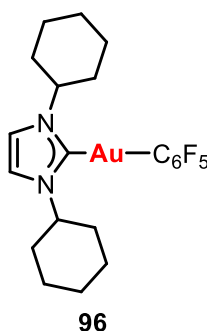
**$^1\text{H}$  NMR (300 MHz,  $\text{CDCl}_3$ )**  $\delta$  6.99 (s, 2H,  $\text{CH}$  imidazole), 5.06 (hept,  $J = 6.8$  Hz, 2H,  $\text{CHMe}_2$ ), 1.54 (d,  $J = 6.8$  Hz, 12H,  $\text{CHMe}_2$ ).

**$^{19}\text{F}$  NMR (282 MHz,  $\text{CDCl}_3$ )**  $\delta$  -115.88 – -116.74 (m,  $o\text{-C}_6\text{F}_5$ ), -160.10 (t,  $J = 19.9$  Hz,  $p\text{-C}_6\text{F}_5$ ), -162.78 – -163.64 (m,  $m\text{-C}_6\text{F}_5$ ).

**$^{13}\text{C}$  NMR (75 MHz,  $\text{CDCl}_3$ )**  $\delta$  185.72 (s,  $\text{N}-\text{C}-\text{N}$ , (observed by HMBC)), 116.88 (s,  $\text{CH}$  imidazole), 53.47 (s,  $\text{CHMe}_2$ ), 23.72 (s, Me).



#### 4.9. Experimental

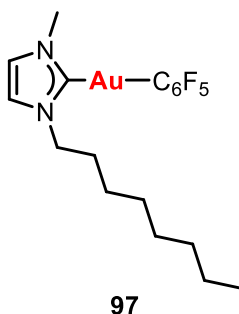


1,3-dicyclohexyl imidazolium chloride (0.0537 g, 0.2 mmol) and  $[\text{Au}(\text{C}_6\text{F}_5)(\text{tht})]$  (0.0904 g, 0.2 mmol) were mixed in  $\text{CH}_2\text{Cl}_2$  (10 ml) until a colourless solution formed (5 min). The solution was concentrated to dryness under reduced pressure to give a white solid which was washed several times with hexane. The solid was dissolved in  $\text{CH}_2\text{Cl}_2$  (10 ml),  $\text{NBu}_4(\text{acac})$  (0.0683 g, 0.2 mmol) was added and the mixture stirred for 1 h. The solution was filtered through a plug of silica and the colourless filtrate evaporated to minimum volume. Pentane was added to precipitate a white solid which was collected and vacuum dried to give the product (0.1083 g, 91%).

**$^1\text{H}$  NMR (300 MHz,  $\text{CDCl}_3$ )**  $\delta$  6.95 (s, 2H,  $\text{CH}$  imidazole), 4.58 (tt,  $J = 12.2, 3.6$  Hz, 2H,  $\text{CH}$  (Cy)), 2.27 – 2.11 (m, 4H, Cy), 1.98 – 1.85 (m, 4H, Cy), 1.74 (ddd,  $J = 24.4, 12.2, 3.6$  Hz, 6H, Cy), 1.60 – 1.39 (m, 4H, Cy), 1.24 (qt,  $J = 12.2, 3.6$  Hz, 2H, Cy).

**$^{19}\text{F}$  NMR (282 MHz,  $\text{CDCl}_3$ )**  $\delta$  -115.08 – -117.34 (m, *o*- $\text{C}_6\text{F}_5$ ), -160.20 (t,  $J = 20.0$  Hz, *p*- $\text{C}_6\text{F}_5$ ), -162.06 – -166.57 (m, *m*- $\text{C}_6\text{F}_5$ ).

**$^{13}\text{C}$  NMR (75 MHz,  $\text{CDCl}_3$ )**  $\delta$  185.99 (s, N-C-N, (observed by HMBC)), 117.26 (s,  $\text{CH}$  imidazole), 61.21 (s,  $\text{CH}$  (Cy)), 34.54 (s, Cy), 25.69 (s, Cy), 25.32 (s, Cy).



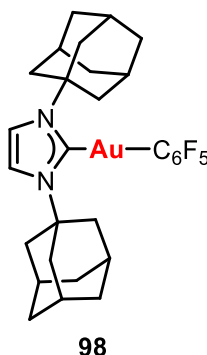
1-octyl-3-methylimidazolium chloride (0.0462 g, 0.2 mmol) and  $[\text{Au}(\text{C}_6\text{F}_5)(\text{tht})]$  (0.0904 g, 0.2 mmol) were mixed in  $\text{CH}_2\text{Cl}_2$  (10 ml) until a colourless solution formed (5 min). The solution was concentrated to dryness under reduced pressure to give a white solid which was washed several times with hexane. The solid was dissolved in  $\text{CH}_2\text{Cl}_2$  (10 ml),  $\text{NBu}_4(\text{acac})$  (0.0683 g,

0.2 mmol) was added and the mixture stirred for 1 h. The solution was filtered through a plug of silica and the colourless filtrate evaporated to minimum volume. Pentane was added to precipitate a white solid which was collected and vacuum dried to give the product (0.0854 g, 76%).

**$^1\text{H}$  NMR (300 MHz,  $\text{CDCl}_3$ )**  $\delta$  6.94 (d,  $J = 1.9$  Hz, 1H,  $\text{CH}$  imidazole), 6.91 (d,  $J = 1.8$  Hz, 1H,  $\text{CH}$  imidazole), 4.21 (t,  $J = 7.2$  Hz, 2H,  $\text{CH}_2\text{CH}_2(\text{CH}_2)_5\text{CH}_3$ ), 3.91 (s, 3H, Me), 1.98 – 1.79 (m, 2H,  $\text{CH}_2\text{CH}_2(\text{CH}_2)_5\text{CH}_3$ ), 1.38 – 1.21 (m, 10H,  $\text{CH}_2\text{CH}_2(\text{CH}_2)_5\text{CH}_3$ ), 0.86 (t,  $J = 6.8$  Hz, 3H,  $\text{CH}_2\text{CH}_2(\text{CH}_2)_5\text{CH}_3$ ).

**$^{19}\text{F}$  NMR (282 MHz,  $\text{CDCl}_3$ )**  $\delta$  -114.78 – -118.16 (m, *o*- $\text{C}_6\text{F}_5$ ), -160.08 (t,  $J = 19.9$  Hz, *p*- $\text{C}_6\text{F}_5$ ), -162.36 – -164.72 (m, *m*- $\text{C}_6\text{F}_5$ ).

**$^{13}\text{C}$  NMR (75 MHz,  $\text{CDCl}_3$ )**  $\delta$  188.17 (s, N-C-N, (observed by HMBC)), 121.63 (s,  $\text{CH}$  imidazole), 120.63 (s,  $\text{CH}$  imidazole), 51.26 (s,  $\text{CH}_2\text{CH}_2(\text{CH}_2)_5\text{CH}_3$ ), 38.04 (s, Me), 31.86 (s,  $\text{CH}_2\text{CH}_2(\text{CH}_2)_5\text{CH}_3$ ), 31.45 (s,  $\text{CH}_2\text{CH}_2(\text{CH}_2)_5\text{CH}_3$ ), 29.22 (s,  $\text{CH}_2\text{CH}_2(\text{CH}_2)_5\text{CH}_3$ ), 29.14 (s,  $\text{CH}_2\text{CH}_2(\text{CH}_2)_5\text{CH}_3$ ), 26.52 (s,  $\text{CH}_2\text{CH}_2(\text{CH}_2)_5\text{CH}_3$ ), 22.74 (s,  $\text{CH}_2\text{CH}_2(\text{CH}_2)_5\text{CH}_3$ ), 14.19 (s,  $\text{CH}_2\text{CH}_2(\text{CH}_2)_5\text{CH}_3$ ).



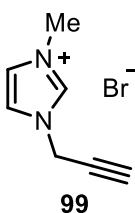
1,3-bis(1-adamantyl)imidazolium chloride (0.0746 g, 0.2 mmol) and  $[\text{Au}(\text{C}_6\text{F}_5)(\text{tht})]$  (0.0904 g, 0.2 mmol) were mixed in  $\text{CH}_2\text{Cl}_2$  (10 ml) until a colourless solution formed (5 min). The solution was concentrated to dryness under reduced pressure to give a white solid which was washed several times with hexane. The solid was dissolved in  $\text{CH}_2\text{Cl}_2$  (10 ml),  $\text{NBu}_4(\text{acac})$  (0.0683 g, 0.2 mmol) was added and the mixture stirred for 1 h. The solution was filtered through a plug of silica and the colourless filtrate evaporated to minimum volume. Pentane was added to precipitate a white solid which was collected and vacuum dried to give the product (0.0728 g, 52%).

## 4.9. Experimental

**$^1\text{H}$  NMR (300 MHz,  $\text{CDCl}_3$ )**  $\delta$  7.11 (s, 2H,  $\text{CH}$  imidazole), 2.61 (m, 12H,  $\text{CH}_2$  adamantyl), 2.29 (s, 6H,  $\text{CH}$  adamantyl), 1.80 (m, 12H,  $\text{CH}_2$  adamantyl).

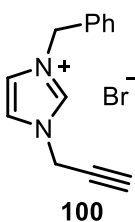
**$^{19}\text{F}$  NMR (282 MHz,  $\text{CDCl}_3$ )**  $\delta$  -114.12 – -115.46 (m, *o*- $\text{C}_6\text{F}_5$ ), -160.46 (t,  $J$  = 20.0 Hz, *p*- $\text{C}_6\text{F}_5$ ), -162.64 – -164.07 (m, *m*- $\text{C}_6\text{F}_5$ ).

**$^{13}\text{C}$  NMR (75 MHz,  $\text{CDCl}_3$ )**  $\delta$  185.48 (s, N- $\text{C}$ -N, (observed by HMBC)), 115.52 (s,  $\text{CH}$  imidazole), 59.37 (s, N- $\text{C}$  adamantyl), 44.58 (s,  $\text{CH}_2$  adamantyl), 35.94 (s,  $\text{CH}_2$  adamantyl), 30.20 (s,  $\text{CH}$  adamantyl).



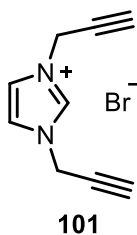
Propargyl bromide (2.99 g, 20.09 mmol, 80 wt% solution in toluene) was added drop wise to *N*-methylimidazole (1.5 g, 18.27 mmol) under nitrogen atmosphere at room temperature and stirred until a significant increase in the viscosity occurred. The solution was subsequently diluted with 25 ml of acetone and stirred overnight. The obtained white solid was collected by filtration, washed three times with 25 ml acetone and dried under vacuum to give the product (2.44 g, 66%).

Spectral data are in agreement with values previously reported in the literature.<sup>302</sup>



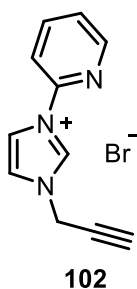
Propargyl bromide (6.05 g, 40.66 mmol, 80 wt% solution in toluene) was added drop wise to a solution of *N*-benzylimidazole (5 g, 40.26 mmol) and acetone (10 ml) under nitrogen atmosphere and stirred at room temperature for 24 h. The solvent was decanted, the raw product was washed with ethyl acetate (100 ml) and acetone (100 ml) and dried under vacuum to give a white solid (7.54 g, 86%).

Spectral data are in agreement with values previously reported in the literature.<sup>302</sup>



To a solution of imidazole (0.2723 g, 4.0 mmol) in acetonitrile (30 ml) was added propargylbromide (0.86 ml, 8.0 mmol, 80% wt solution in toluene) and the mixture heated to reflux for 24h. After cooling to room temperature, solvent was removed *in vacuo* to leave an oily solid which was recrystallized acetonitrile/Et<sub>2</sub>O, washed with further Et<sub>2</sub>O and vacuum dried to give the product as a beige solid (0.2851 g, 32%).

Spectral data are in agreement with values previously reported in the literature.<sup>303-305</sup>

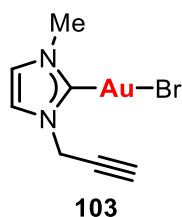


To a solution of 1-pyridylimidazole (0.7259 g, 5.0 mmol) in acetonitrile (50 ml) was added propargylbromide (1.1 ml, 10.0 mmol, 80% wt solution in toluene) and the mixture heated to reflux for 24h. A pale yellow precipitate formed which was collected by vacuum filtration, washed with Et<sub>2</sub>O and vacuum dried to give the product (0.9504 g, 72%).

**<sup>1</sup>H NMR (300 MHz, DMSO)**  $\delta$  10.20 (s, 1H, N-CH-N, imidazole), 8.65 (dd, <sup>3</sup>*J*<sub>HH</sub> = 4.8, <sup>4</sup>*J*<sub>HH</sub> = 1.0 Hz, 1H, Py), 8.60 (m, 1H, CH), 8.27 – 8.18 (m, 1H, Py), 8.16 – 8.05 (m, 2H, Py and CH), 7.72 – 7.60 (m, 1H, Py), 5.35 (d, <sup>4</sup>*J*<sub>HH</sub> = 2.6 Hz, 2H, CH<sub>2</sub>), 3.92 (t, <sup>4</sup>*J*<sub>HH</sub> = 2.6 Hz, 1H, C≡CH).

**<sup>13</sup>C APT (75 MHz, DMSO)**  $\delta$  149.25 (s, CH (Py)), 146.29 (s, *ipso*-Py), 140.63 (s, CH (Py)), 135.13 (s, N-C-N), 125.39 (s, CH (Py)), 123.38 (s, CH), 119.74 (s, CH), 114.49 (s, CH (Py)), 79.30 (s, C≡CH), 75.85 (s, C≡CH), 39.24 (s, CH<sub>2</sub>-C≡CH).

## 4.9. Experimental

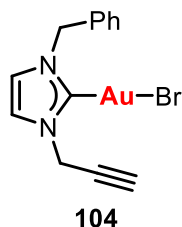


1-Methyl-3-(2-propyn-1-yl)-1*H*-imidazol-3-ium bromide (0.0402 g, 0.2 mmol) and [AuCl(tht)] (0.0641 g, 0.2 mmol) were mixed in CH<sub>2</sub>Cl<sub>2</sub> (10 ml) until a colourless solution formed (5 min). NBu<sub>4</sub>(acac) (0.0683 g, 0.2 mmol) was added and the mixture stirred for 1 h. The solution was filtered through a plug of silica and the colourless filtrate evaporated to minimum volume. Pentane was added to precipitate a white solid which was collected and vacuum dried to give the product (0.0646 g, 82%).

**IR (cm<sup>-1</sup>)**  $\nu(\text{C}\equiv\text{C}-\text{H})$  3240,  $\nu(\text{C}\equiv\text{C})$  2125.

**<sup>1</sup>H NMR (400 MHz, DMSO)**  $\delta$  7.53 (d,  $^3J_{\text{HH}} = 1.9$  Hz, 1H, CH), 7.48 (d,  $^3J_{\text{HH}} = 1.9$  Hz, 1H, CH), 5.00 (d,  $^4J_{\text{HH}} = 2.5$  Hz, 2H, CH<sub>2</sub>), 3.76 (s, 3H, CH<sub>3</sub>), 3.59 (t,  $^4J_{\text{HH}} = 2.5$  Hz, 1H, C $\equiv$ CH).

**<sup>13</sup>C APT (75 MHz, DMSO)**  $\delta$  172.52 (s, N-C-N), 123.16 (s, CH), 121.35 (s, CH), 78.21 (s, C $\equiv$ CH), 77.30 (s, C $\equiv$ CH), 39.88 (s, CH<sub>2</sub>) 37.79 (s, CH<sub>3</sub>).

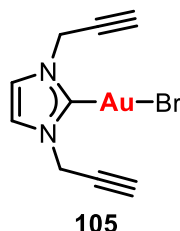


1-Benzyl-3-(2-propyn-1-yl)-1*H*-imidazol-3-ium bromide (0.0554 g, 0.2 mmol) and [AuCl(tht)] (0.0641 g, 0.2 mmol) were mixed in CH<sub>2</sub>Cl<sub>2</sub> (10 ml) until a colourless solution formed (5 min). NBu<sub>4</sub>(acac) (0.0683 g, 0.2 mmol) was added and the mixture stirred for 1 h. The solution was filtered through a plug of silica and the colourless filtrate evaporated to minimum volume. Pentane was added to precipitate a white solid which was collected and vacuum dried to give the product (0.0696 g, 74%).

**IR (cm<sup>-1</sup>)**  $\nu(\text{C}\equiv\text{C}-\text{H})$  3262,  $\nu(\text{C}\equiv\text{C})$  2131.

**<sup>1</sup>H NMR (300 MHz, DMSO)**  $\delta$  7.60 (d,  $^3J_{\text{HH}} = 2.0$  Hz, 1H, CH), 7.57 (d,  $^3J_{\text{HH}} = 2.0$  Hz, 1H, CH), 7.42 – 7.27 (m, 5H, Ph), 5.36 (s, 2H, CH<sub>2</sub>-Ph), 5.03 (d,  $^4J_{\text{HH}} = 2.5$  Hz, 2H, CH<sub>2</sub>-C $\equiv$ CH), 3.60 (t,  $^4J_{\text{HH}} = 2.5$  Hz, 1H, C $\equiv$ CH).

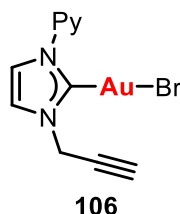
**$^{13}\text{C}$  APT (75 MHz, DMSO)**  $\delta$  172.55 (s, N-C-N), 136.44 (s, *ipso-Ph*), 128.78 (s, *m-Ph*), 128.18 (s, *p-Ph*), 127.65 (s, *o-Ph*), 122.10 (s, CH), 121.87 (s, CH), 78.02 (s, C $\equiv$ CH), 77.39 (s, C $\equiv$ CH), 53.85 (s, CH<sub>2</sub>-Ph), 40.03 (s, CH<sub>2</sub>-C $\equiv$ CH).



1,3-bis(2-propyn-1-yl)-1*H*-imidazol-3-ium bromide (0.0450 g, 0.2 mmol) and [AuCl(tht)] (0.0641 g, 0.2 mmol) were mixed in CH<sub>2</sub>Cl<sub>2</sub> (10 ml) until a colourless solution formed (5 min). NBu<sub>4</sub>(acac) (0.0683 g, 0.2 mmol) was added and the mixture stirred for 1 h. The solution was filtered through a plug of silica and the colourless filtrate evaporated to minimum volume. Pentane was added to precipitate a white solid which was collected and vacuum dried to give the product (0.0616 g, 73%).

**$^1\text{H}$  NMR (300 MHz, CD<sub>2</sub>Cl<sub>2</sub>)**  $\delta$  7.29 (s, 2H, CH), 5.04 (d,  $^4J_{\text{HH}} = 2.6$  Hz, 4H, CH<sub>2</sub>), 2.63 (t,  $^4J_{\text{HH}} = 2.6$  Hz, 1H, C $\equiv$ CH).

**$^{13}\text{C}$  APT (75 MHz, CD<sub>2</sub>Cl<sub>2</sub>)**  $\delta$  175.44 (s, N-C-N), 121.09 (s, CH), 76.22 (s, C $\equiv$ CH), 41.48 (s, CH<sub>2</sub>-C $\equiv$ CH).



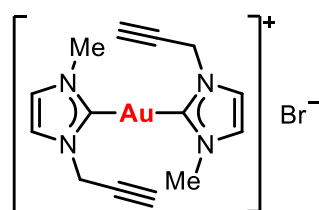
1-Pyridyl-3-(2-propyn-1-yl)-1*H*-imidazol-3-ium bromide (0.0528 g, 0.2 mmol) and [AuCl(tht)] (0.0641 g, 0.2 mmol) were mixed in CH<sub>2</sub>Cl<sub>2</sub> (10 ml) until a colourless solution formed (5 min). NBu<sub>4</sub>(acac) (0.0683 g, 0.2 mmol) was added and the mixture stirred for 1 h. The solution was filtered through a plug of silica and the colourless filtrate evaporated to minimum volume. Pentane was added to precipitate a white solid which was collected and vacuum dried to give the product (0.0718 g, 78%).

**IR (cm<sup>-1</sup>)**  $\nu(\text{C}\equiv\text{C}-\text{H})$  3260,  $\nu(\text{C}\equiv\text{C})$  2160.

## 4.9. Experimental

**$^1\text{H}$  NMR (300 MHz, DMSO)**  $\delta$  8.63 (m, 1H, Py), 8.20 (dd,  $^3J_{\text{HH}} = 7.1$ ,  $^4J_{\text{HH}} = 1.0$  Hz, 1H, Py), 8.17 – 8.09 (m, 1H, Py), 8.03 (d,  $^3J_{\text{HH}} = 2.1$  Hz, 1H, CH), 7.82 (d,  $^3J_{\text{HH}} = 2.1$  Hz, 1H, CH), 7.61 (m, 1H, Py), 5.17 (d,  $^4J_{\text{HH}} = 2.5$  Hz, 2H,  $\text{CH}_2$ ), 3.69 (t,  $^4J_{\text{HH}} = 2.5$  Hz, 1H,  $\text{C}\equiv\text{CH}$ ).

**$^{13}\text{C}$  APT (75 MHz, DMSO)**  $\delta$  171.96 (s, N-C-N), 150.28 (s, *ipso*-Py), 149.17 (s, CH (Py)), 139.61 (s, CH (Py)), 124.75 (s, CH (Py)), 122.43 (s, CH), 121.50 (s, CH), 118.07 (s, CH (Py)), 77.87 (s,  $\text{C}\equiv\text{CH}$ ), 77.80 (s,  $\text{C}\equiv\text{CH}$ ), 40.91 (s,  $\text{CH}_2\text{-C}\equiv\text{CH}$ ).



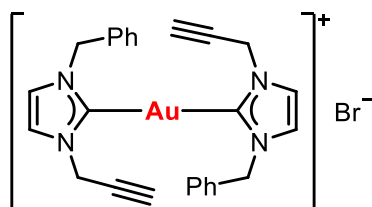
107

1-Methyl-3-(2-propyn-1-yl)-1*H*-imidazol-3-ium bromide (0.0804 g, 0.4 mmol) and  $[\text{AuCl}(\text{tht})]$  (0.0641 g, 0.2 mmol) were mixed in THF (10 ml) until a colourless solution formed (5 min).  $\text{NBu}_4(\text{acac})$  (0.1366 g, 0.4 mmol) was added and the mixture stirred. After approximately 30 min a white precipitate formed. The mixture was left stirring for 12 h and then the precipitate collected by vacuum filtration and dried to give the product (0.0848 g, 82%).

**HRMS (ESI/QTOF)  $m/z$ :**  $[\text{M}]^+$  Calcd for  $\text{C}_{14}\text{H}_{16}\text{AuN}_4$  437.1035; Found 437.1049.

**$^1\text{H}$  NMR (300 MHz, DMSO)**  $\delta$  7.60 (d,  $^3J_{\text{HH}} = 1.8$  Hz, 1H, CH imidazole), 7.55 (d,  $^3J_{\text{HH}} = 1.8$  Hz, 1H, CH imidazole), 5.13 (d,  $^4J_{\text{HH}} = 2.5$  Hz, 2H,  $\text{CH}_2$ ), 3.90 (s, 3H, Me), 3.65 (t,  $^4J_{\text{HH}} = 2.5$  Hz, 1H,  $\text{C}\equiv\text{CH}$ ).

**$^{13}\text{C}$  APT (75 MHz, DMSO)**  $\delta$  183.28 (s, N-C-N), 123.51 (s, CH), 122.05 (s, CH), 78.60 (s,  $\text{C}\equiv\text{CH}$ ), 77.45 (s,  $\text{C}\equiv\text{CH}$ ), 39.69 (s,  $\text{CH}_2\text{-C}\equiv\text{CH}$ ), 37.75 (s,  $\text{CH}_3$ ).



108

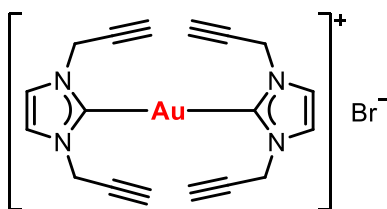
1-Benzyl-3-(2-propyn-1-yl)-1*H*-imidazol-3-ium bromide (0.1109 g, 0.4 mmol) and  $[\text{AuCl}(\text{tht})]$  (0.0641 g, 0.2 mmol) were mixed in  $\text{CH}_2\text{Cl}_2$  (10 ml) until a colourless solution

formed (5 min).  $\text{NBu}_4(\text{acac})$  (0.1366 g, 0.4 mmol) was added and the mixture stirred for 1 h. The solution was washed with  $\text{H}_2\text{O}$  (3 x 25 ml) and dried over  $\text{Na}_2\text{SO}_4$ . The solution was evaporated to minimum volume under reduced pressure and pentane added to precipitate a white solid which was collected and vacuum dried to give the product (0.0803 g, 63%).

**HRMS (ESI/QTOF)  $m/z$ :**  $[\text{M}]^+$  Calcd for  $\text{C}_{26}\text{H}_{24}\text{AuN}_4$  589.1661; Found 589.1634.

**$^1\text{H}$  NMR (300 MHz, DMSO)**  $\delta$  7.70 (s, 1H, CH), 7.66 (s, 1H, CH), 7.34 (m, 5H, Ph), 5.44 (s, 2H,  $\text{CH}_2\text{-Ph}$ ), 5.13 (d,  $^4J_{\text{HH}} = 1.9$  Hz, 2H,  $\text{CH}_2\text{-C}\equiv\text{CH}$ ), 3.64 (s, 1H,  $\text{C}\equiv\text{CH}$ ).

**$^{13}\text{C}$  APT (75 MHz, DMSO)**  $\delta$  182.89 (s, N-C-N), 136.68 (s, *ipso-Ph*), 128.79 (s, *m-Ph*), 128.15 (s, *p-Ph*), 127.63 (s, *o-Ph*), 122.75 (s, CH), 122.49 (s, CH), 78.36 (s,  $\text{C}\equiv\text{CH}$ ), 77.54 (s,  $\text{C}\equiv\text{CH}$ ), 53.82 (s,  $\text{CH}_2\text{-Ph}$ ), 39.96 (s,  $\text{CH}_2\text{-C}\equiv\text{CH}$ ).



109

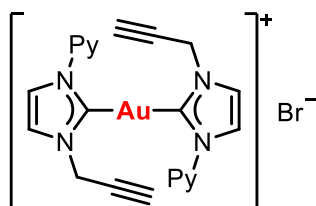
1,3-bis(2-propyn-1-yl)-1*H*-imidazol-3-ium bromide (0.0900 g, 0.4 mmol) and  $[\text{AuCl}(\text{tht})]$  (0.0641 g, 0.2 mmol) were mixed in THF (10 ml) until a colourless solution formed (5 min).  $\text{NBu}_4(\text{acac})$  (0.1366 g, 0.4 mmol) was added and the mixture stirred. After approximately 30 min a white precipitate formed. The mixture was left stirring for 12 h and then the precipitate collected by vacuum filtration and dried to give the product (0.1074 g, 95%).

**HRMS (ESI/QTOF)  $m/z$ :**  $[\text{M}]^+$  Calcd for  $\text{C}_{18}\text{H}_{16}\text{AuN}_4$  485.1035; Found 485.1044.

**$^1\text{H}$  NMR (300 MHz, DMSO)**  $\delta$  7.68 (s, 1H, CH), 5.20 (d,  $^4J_{\text{HH}} = 2.5$  Hz, 2H,  $\text{CH}_2$ ), 3.66 (t,  $^4J_{\text{HH}} = 2.5$  Hz, 1H,  $\text{C}\equiv\text{CH}$ ).

**$^{13}\text{C}$  APT (75 MHz, DMSO)**  $\delta$  183.12 (s, N-C-N), 122.32 (s, CH), 78.27 (s,  $\text{C}\equiv\text{CH}$ ), 77.64 (s,  $\text{C}\equiv\text{CH}$ ), 40.13 (s,  $\text{CH}_2\text{-C}\equiv\text{CH}$ ).



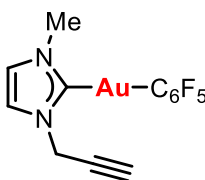
**110**

1-Pyridyl-3-(2-propyn-1-yl)-1*H*-imidazol-3-ium bromide (0.1056 g, 0.4 mmol) and [AuCl(tht)] (0.0641 g, 0.2 mmol) were mixed in THF (10 ml) until a colourless solution formed (5 min). NBu<sub>4</sub>(acac) (0.1366 g, 0.4 mmol) was added and the mixture stirred. After approximately 30 min a white precipitate formed. The mixture was left stirring for 12 h and then the precipitate collected by vacuum filtration and dried to give the product (0.1159 g, 90%).

**HRMS (ESI/QTOF) m/z:** [M]<sup>+</sup> Calcd for C<sub>22</sub>H<sub>18</sub>AuN<sub>6</sub> 563.1253; Found 563.1247.

**<sup>1</sup>H NMR (300 MHz, DMSO)** δ 8.54 (m, 1H, Py), 8.15 (d, <sup>3</sup>J<sub>HH</sub> = 2.0 Hz, 1H, CH), 8.13 (d, <sup>3</sup>J<sub>HH</sub> = 5.3 Hz, 1H, Py), 8.01 (m, 1H, Py), 7.91 (d, <sup>3</sup>J<sub>HH</sub> = 2.0 Hz, 1H, CH), 7.59 (m, 1H, Py), 5.27 (d, <sup>4</sup>J<sub>HH</sub> = 2.4 Hz, 2H, CH<sub>2</sub>), 3.69 (t, <sup>4</sup>J<sub>HH</sub> = 2.4 Hz, 1H, C≡CH).

**<sup>13</sup>C APT (75 MHz, DMSO)** δ 181.34 (s, N-C-N), 150.01 (s, *ipso*-Py), 148.95 (s, CH (Py)), 139.67 (s, CH (Py)), 124.65 (s, CH (Py)), 123.10 (s, CH), 121.71 (s, CH), 117.53 (s, CH (Py)), 77.96 (s, C≡CH), 77.83 (s, C≡CH), 40.87 (s, CH<sub>2</sub>-C≡CH).

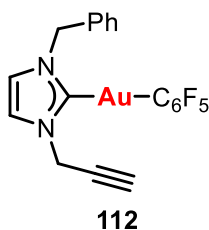
**111**

1-Methyl-3-(2-propyn-1-yl)-1*H*-imidazol-3-ium bromide (0.0804 g, 0.4 mmol) and [Au(C<sub>6</sub>F<sub>5</sub>(tht))] (0.1809 g, 0.4 mmol) were mixed in CH<sub>2</sub>Cl<sub>2</sub> (10 ml) until a colourless solution formed (5 min). NBu<sub>4</sub>(acac) (0.1366 g, 0.4 mmol) was added and the mixture stirred for 1 h. The solution was filtered through a plug of silica and the colourless filtrate evaporated to minimum volume. Pentane was added to precipitate a white solid which was collected and vacuum dried to give the product (0.1466 g, 76%).

**<sup>1</sup>H NMR (300 MHz, CD<sub>2</sub>Cl<sub>2</sub>)** δ 7.23 (d, <sup>3</sup>J<sub>HH</sub> = 1.9 Hz, 1H, CH), 7.02 (d, <sup>3</sup>J<sub>HH</sub> = 1.9 Hz, 1H, CH), 5.09 (d, <sup>4</sup>J<sub>HH</sub> = 2.6 Hz, 2H, CH<sub>2</sub>), 3.90 (s, 3H, CH<sub>3</sub>), 2.61 (t, <sup>4</sup>J<sub>HH</sub> = 2.6 Hz, 1H, C≡CH).

**$^{19}\text{F}$  NMR (377 MHz,  $\text{CD}_2\text{Cl}_2$ )**  $\delta$  -116.54 – -116.86 (m, 2F, *o*- $\text{C}_6\text{F}_5$ ), -160.80 (t,  $^3J_{\text{FF}} = 19.8$  Hz, 1F, *p*- $\text{C}_6\text{F}_5$ ), -163.61 – -163.89 (m, 2F, *m*- $\text{C}_6\text{F}_5$ ).

**$^{13}\text{C}$  APT (75 MHz,  $\text{CD}_2\text{Cl}_2$ )**  $\delta$  188.06 (s, N-C-N), 122.90 (s, CH), 120.73 (s, CH), 76.90 (s,  $\text{C}\equiv\text{CH}$ ), 75.73 (s,  $\text{C}\equiv\text{CH}$ ), 40.90 (s,  $\text{CH}_2\text{-C}\equiv\text{CH}$ ), 38.51 (s,  $\text{CH}_3$ ).

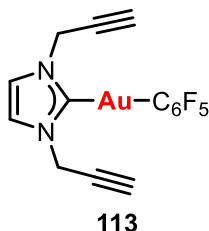


1-Benzyl-3-(2-propyn-1-yl)-1*H*-imidazol-3-ium bromide (0.1109 g, 0.4 mmol) and  $[\text{Au}(\text{C}_6\text{F}_5(\text{tht}))]$  (0.1809 g, 0.4 mmol) were mixed in  $\text{CH}_2\text{Cl}_2$  (10 ml) until a colourless solution formed (5 min).  $\text{NBu}_4(\text{acac})$  (0.1366 g, 0.4 mmol) was added and the mixture stirred for 1 h. The solution was filtered through a plug of silica and the colourless filtrate evaporated to minimum volume. Pentane was added to precipitate a white solid which was collected and vacuum dried to give the product (0.1758 g, 78%).

**$^1\text{H}$  NMR (300 MHz,  $\text{CD}_2\text{Cl}_2$ )**  $\delta$  7.49 – 7.32 (m, 5H, Ph), 7.25 (d,  $^3J_{\text{HH}} = 1.9$  Hz, 1H, CH), 7.03 (d,  $^3J_{\text{HH}} = 1.9$  Hz, 1H, CH), 5.43 (s, 2H,  $\text{CH}_2\text{-Ph}$ ), 5.11 (d,  $^4J_{\text{HH}} = 2.6$  Hz, 1H,  $\text{CH}_2\text{-C}\equiv\text{CH}$ ), 2.61 (t,  $^3J_{\text{HH}} = 2.6$  Hz, 1H,  $\text{C}\equiv\text{CH}$ ).

**$^{19}\text{F}$  NMR (282 MHz,  $\text{CD}_2\text{Cl}_2$ )**  $\delta$  -115.78 – -117.58 (m, 2F, *o*- $\text{C}_6\text{F}_5$ ), -160.81 (t,  $^3J_{\text{FF}} = 19.8$  Hz, 1F, *p*- $\text{C}_6\text{F}_5$ ), -163.16 – -165.55 (m, 2F, *m*- $\text{C}_6\text{F}_5$ ).

**$^{13}\text{C}$  APT (75 MHz,  $\text{CD}_2\text{Cl}_2$ )**  $\delta$  187.70 (s, N-C-N), 136.19 (s, *ipso*-Ph), 129.56 (s, *m*-Ph), 129.21 (s, *p*-Ph), 128.75 (s, *o*-Ph), 121.64 (s, CH), 121.16 (s, CH), 76.76 (s,  $\text{C}\equiv\text{CH}$ ), 75.89 (s,  $\text{C}\equiv\text{CH}$ ), 55.63 (s,  $\text{CH}_2\text{-Ph}$ ), 41.09 (s,  $\text{CH}_2\text{-C}\equiv\text{CH}$ ).



1,3-bis(2-propyn-1-yl)-1*H*-imidazol-3-ium bromide (0.0900 g, 0.4 mmol) and  $[\text{Au}(\text{C}_6\text{F}_5(\text{tht}))]$  (0.1809 g, 0.4 mmol) were mixed in  $\text{CH}_2\text{Cl}_2$  (10 ml) until a colourless solution formed (5 min).  $\text{NBu}_4(\text{acac})$  (0.1366 g, 0.4 mmol) was added and the mixture stirred for 1 h. The solution was

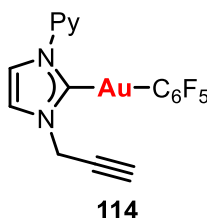
## 4.9. Experimental

filtered through a plug of silica and the colourless filtrate evaporated to minimum volume. Pentane was added to precipitate a white solid which was collected and vacuum dried to give the product (0.1768 g, 87%).

**$^1\text{H}$  NMR (300 MHz,  $\text{CD}_2\text{Cl}_2$ )**  $\delta$  7.29 (s, 2H, CH), 5.10 (d,  $^4J_{\text{HH}} = 2.6$  Hz, 2H,  $\text{CH}_2$ ), 2.63 (t,  $^4J_{\text{HH}} = 2.6$  Hz, 1H,  $\text{C}\equiv\text{CH}$ ).

**$^{19}\text{F}$  NMR (376 MHz,  $\text{CD}_2\text{Cl}_2$ )**  $\delta$  -116.09 – -116.87 (m, 2F, *o*- $\text{C}_6\text{F}_5$ ), -160.34 (t,  $^3J_{\text{FF}} = 19.8$  Hz, 1F, *p*- $\text{C}_6\text{F}_5$ ), -163.26 – -163.61 (m, 2F, *m*- $\text{C}_6\text{F}_5$ ).

**$^{13}\text{C}$  APT (75 MHz,  $\text{CD}_2\text{Cl}_2$ )**  $\delta$  187.87 (s, N-C-N), 121.18 (s, CH), 76.55 (s,  $\text{C}\equiv\text{CH}$ ), 76.03 (s,  $\text{C}\equiv\text{CH}$ ), 41.19 (s,  $\text{CH}_2\text{-C}\equiv\text{CH}$ ).

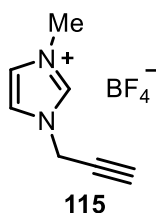


1-Pyridyl-3-(2-propyn-1-yl)-1*H*-imidazol-3-ium bromide (0.1056 g, 0.4 mmol) and  $[\text{Au}(\text{C}_6\text{F}_5)(\text{tht})]$  (0.1809 g, 0.4 mmol) were mixed in  $\text{CH}_2\text{Cl}_2$  (10 ml) until a colourless solution formed (5 min).  $\text{NBu}_4(\text{acac})$  (0.1366 g, 0.4 mmol) was added and the mixture stirred for 1 h. The solution was filtered through a plug of silica and the colourless filtrate evaporated to minimum volume. Pentane was added to precipitate a white solid which was collected and vacuum dried to give the product (0.1911 g, 87%).

**$^1\text{H}$  NMR (300 MHz,  $\text{CD}_2\text{Cl}_2$ )**  $\delta$  8.77 (d,  $^3J_{\text{HH}} = 8.2$  Hz, 1H, Py), 8.62 – 8.41 (m, 1H, Py), 8.01 – 7.85 (m, 2H, Py and CH), 7.51 – 7.19 (m, 2H, Py and CH), 5.28 (d,  $^4J_{\text{HH}} = 2.6$  Hz, 2H,  $\text{CH}_2$ ), 2.68 (t,  $^4J_{\text{HH}} = 2.6$  Hz, 1H,  $\text{C}\equiv\text{CH}$ ).

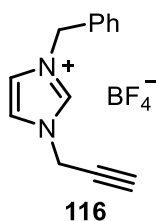
**$^{19}\text{F}$  NMR (376 MHz,  $\text{CD}_2\text{Cl}_2$ )**  $\delta$  -116.43 – -116.65 (m, 2F, *o*- $\text{C}_6\text{F}_5$ ), -160.56 (t,  $^3J_{\text{FF}} = 19.8$  Hz, 1F, *p*- $\text{C}_6\text{F}_5$ ), -163.56 – -163.82 (m, 2F, *m*- $\text{C}_6\text{F}_5$ ).

**$^{13}\text{C}$  APT (75 MHz,  $\text{CD}_2\text{Cl}_2$ )**  $\delta$  186.66 (s, N-C-N), 149.29 (s, CH (Py)), 139.37 (s, CH (Py)), 124.52 (s, CH (Py)), 121.22 (s, CH), 121.08 (s, CH), 120.13 (s, *ipso*-Py), 117.69 (s, CH (Py)), 76.19 (s,  $\text{C}\equiv\text{CH}$ ), 75.23 (s,  $\text{C}\equiv\text{CH}$ ), 42.00 (s,  $\text{CH}_2\text{-C}\equiv\text{CH}$ ).

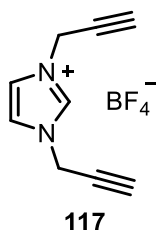


1-Methyl-3-(2-propyn-1-yl)-1*H*-imidazol-3-ium bromide (0.2011, 1.0 mmol) and sodium tetrafluoroborate (0.1098 g, 1.0 mmol) were stirred in acetone (10 ml) for 24 h. A white precipitate formed which was removed by filtering the reaction mixture through celite. The filtrate was concentrated to dryness under reduced pressure to give the product.

Spectral data are in agreement with values previously reported in the literature.<sup>308</sup>



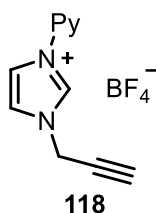
1-Benzyl-3-(2-propyn-1-yl)-1*H*-imidazol-3-ium bromide (0.5543 g, 2.0 mmol) and NaBF<sub>4</sub> (0.2196 g, 2.0 mmol) were dissolved in MeOH (10 ml) and the mixture stirred for 3 h. Solvent was removed under reduced pressure and the solid residue stirred in acetonitrile (20 ml) for 24 h. The solution was filtered through celite, the filtrate concentrated under reduced pressure to approximately 1 ml and Et<sub>2</sub>O added to precipitate a white solid which was collected and vacuum dried to give the product (0.5624 g, 99%).



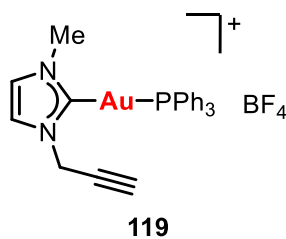
1,3-bis(2-propyn-1-yl)-1*H*-imidazol-3-ium bromide (0.2251 g, 1.0 mmol) and NaBF<sub>4</sub> (0.1098 g, 2.0 mmol) were dissolved in MeOH (10 ml) and the mixture stirred for 3 h. Solvent was removed under reduced pressure and the solid residue stirred in acetonitrile (20 ml) for 24 h. The solution was filtered through celite, the filtrate concentrated under reduced pressure to approximately 1 ml and Et<sub>2</sub>O added to precipitate a white solid which was collected and vacuum dried to give the product (0.2227 g, 96%).

#### 4.9. Experimental

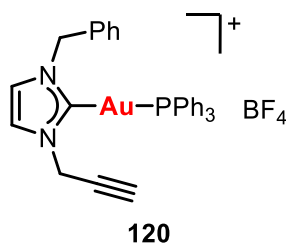
---



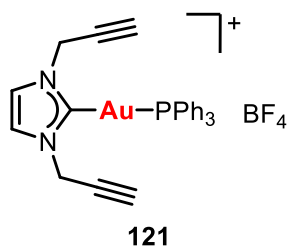
1-Pyridyl-3-(2-propyn-1-yl)-1*H*-imidazol-3-ium bromide (0.2641 g, 1.0 mmol) and NaBF<sub>4</sub> (0.1098 g, 2.0 mmol) were dissolved in MeOH (10 ml) and the mixture stirred for 3 h. Solvent was removed under reduced pressure and the solid residue stirred in acetonitrile (20 ml) for 24 h. The solution was filtered through celite, the filtrate concentrated under reduced pressure to approximately 1 ml and Et<sub>2</sub>O added to precipitate a white solid which was collected and vacuum dried to give the product (0.2683 g, 99%).



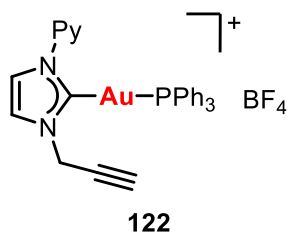
1-Methyl-3-(2-propyn-1-yl)-1*H*-imidazol-3-ium tetrafluoroborate (0.0208 g, 0.1 mmol) and [Au(acac)(PPh<sub>3</sub>)] (0.0559 g, 0.1 mmol) were mixed in CH<sub>2</sub>Cl<sub>2</sub> (10 ml) and stirred for 2 h. The solution was filtered through celite, the filtrate concentrated under reduced pressure to approximately 1 ml and Et<sub>2</sub>O added to precipitate a white solid which was collected and vacuum dried to give the product.



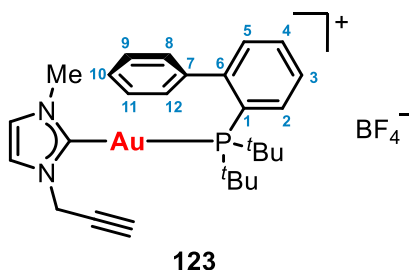
1-Benzyl-3-(2-propyn-1-yl)-1*H*-imidazol-3-ium tetrafluoroborate (0.0568 g, 0.2 mmol) and [Au(acac)(PPh<sub>3</sub>)] (0.1118 g, 0.2 mmol) were mixed in CH<sub>2</sub>Cl<sub>2</sub> (10 ml) and stirred for 2 h. The solution was filtered through celite, the filtrate concentrated under reduced pressure to approximately 1 ml and Et<sub>2</sub>O added to precipitate a white solid which was collected and vacuum dried to give the product.



1,3-bis(2-propyn-1-yl)-1*H*-imidazol-3-ium tetrafluoroborate (0.0463 g, 0.2 mmol) and [Au(acac)(PPh<sub>3</sub>)] (0.1118 g, 0.2 mmol) were mixed in CH<sub>2</sub>Cl<sub>2</sub> (10 ml) and stirred for 2 h. The solution was filtered through celite, the filtrate concentrated under reduced pressure to approximately 1 ml and Et<sub>2</sub>O added to precipitate a white solid which was collected and vacuum dried to give the product.



1-Pyridyl-3-(2-propyn-1-yl)-1*H*-imidazol-3-ium tetrafluoroborate (0.0542 g, 0.2 mmol) and [Au(acac)(PPh<sub>3</sub>)] (0.1118 g, 0.2 mmol) were mixed in CH<sub>2</sub>Cl<sub>2</sub> (10 ml) and stirred for 2 h. The solution was filtered through celite, the filtrate concentrated under reduced pressure to approximately 1 ml and Et<sub>2</sub>O added to precipitate a white solid which was collected and vacuum dried to give the product.



To a solution of 1-methyl-3-(2-propyn-1-yl)-1*H*-imidazol-3-ium tetrafluoroborate (0.0832 g, 0.4 mmol) and [AuCl(JohnPhos)] (0.2123 g, 0.4 mmol) in CH<sub>2</sub>Cl<sub>2</sub> (10 ml) was added NBu<sub>4</sub>(acac) (0.1366 g, 0.4 mmol) and the mixture stirred for 2 h. The solution washed with H<sub>2</sub>O (3 x 25 ml), dried over Na<sub>2</sub>SO<sub>4</sub> and then concentrated under reduced pressure to

## 4.9. Experimental

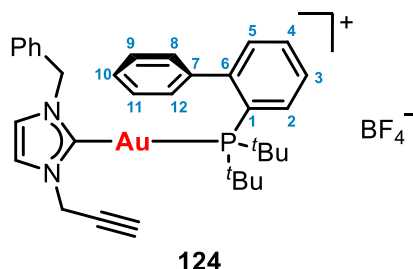
approximately 1 ml. Et<sub>2</sub>O (10 ml) was added to precipitate a white product which was collected and vacuum dried to give the product (0.1941 g, 69%).

**HRMS (ESI/QTOF) m/z:** [M]<sup>+</sup> Calcd for C<sub>27</sub>H<sub>35</sub>AuN<sub>2</sub>P 615.2198; Found 615.2213.

**<sup>1</sup>H NMR (300 MHz, CD<sub>2</sub>Cl<sub>2</sub>)** δ 7.97 – 7.91 (m, 1H, JohnPhos), 7.68 – 7.47 (m, 2H, JohnPhos), 7.40 – 7.21 (m, 6H, JohnPhos + CH imidazole), 7.15 (s, 1H, CH imidazole), 6.90 – 6.85 (m, 1H, Johnphos), 4.71 (d, <sup>4</sup>J<sub>HH</sub> = 2.6 Hz, 2H, CH<sub>2</sub>), 3.65 (s, 3H, Me), 2.66 (t, <sup>4</sup>J<sub>HH</sub> = 2.6 Hz, 1H, C≡CH), 1.46 (d, <sup>3</sup>J<sub>HP</sub> = 15.4 Hz, 18H, <sup>t</sup>Bu).

**<sup>31</sup>P{<sup>1</sup>H} NMR (121 MHz, CD<sub>2</sub>Cl<sub>2</sub>)** δ 63.66 (s, JohnPhos).

**<sup>13</sup>C APT (75 MHz, CD<sub>2</sub>Cl<sub>2</sub>)** δ 187.7 (N-C-N, observed by HMBC), 149.68 (d, <sup>2</sup>J<sub>CP</sub> = 14.1 Hz, C6 JohnPhos), 144.04 (d, <sup>3</sup>J<sub>CP</sub> = 6.3 Hz, C7 JohnPhos), 135.01 (d, <sup>4</sup>J<sub>CP</sub> = 2.1 Hz, C4 JohnPhos), 133.66 (d, <sup>2</sup>J<sub>CP</sub> = 7.4 Hz, C2 JohnPhos), 131.68 (d, <sup>3</sup>J<sub>CP</sub> = 2.3 Hz, C5 JohnPhos), 130.03 (s, C9/C11 JohnPhos), 129.19 (s, C8/C12 JohnPhos), 128.13 (d, <sup>3</sup>J<sub>CP</sub> = 6.6 Hz, C3 JohnPhos), 127.80 (s, C10 JohnPhos), 125.97 (d, <sup>1</sup>J<sub>CP</sub> = 43.5 Hz, C1 JohnPhos), 123.64 (d, <sup>4</sup>J<sub>CP</sub> = 3.1 Hz, CH imidazole), 121.66 (d, <sup>4</sup>J<sub>CP</sub> = 2.9 Hz, CH imidazole), 76.30 (s, C≡C-H), 40.85 (s, CH<sub>2</sub>), 38.68 (s, Me), 38.45 (d, <sup>1</sup>J<sub>CP</sub> = 23.4 Hz, C-CH<sub>3</sub> (<sup>t</sup>Bu)), 31.41 (d, <sup>2</sup>J<sub>CP</sub> = 6.4 Hz, CH<sub>3</sub> (<sup>t</sup>Bu)).



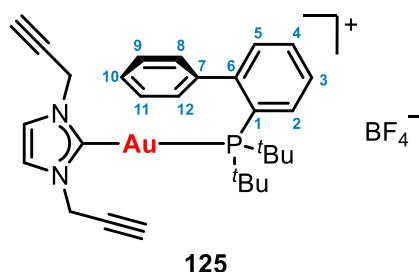
To a solution of 1-benzyl-3-(2-propyn-1-yl)-1*H*-imidazol-3-ium tetrafluoroborate (0.1136 g, 0.4 mmol) and [AuCl(JohnPhos)] (0.2123 g, 0.4 mmol) in CH<sub>2</sub>Cl<sub>2</sub> (10 ml) was added NBu<sub>4</sub>(acac) (0.1366 g, 0.4 mmol) and the mixture stirred for 2 h. The solution washed with H<sub>2</sub>O (3 x 25 ml), dried over Na<sub>2</sub>SO<sub>4</sub> and then concentrated under reduced pressure to approximately 1 ml. Et<sub>2</sub>O (10 ml) was added to precipitate a white product which was collected and vacuum dried to give the product (0.2369 g, 76%).

**HRMS (ESI/QTOF) m/z:** [M]<sup>+</sup> Calcd for C<sub>33</sub>H<sub>39</sub>AuN<sub>2</sub>P 691.2511; Found 691.2520.

**<sup>1</sup>H NMR (300 MHz, CD<sub>2</sub>Cl<sub>2</sub>)** δ 7.98 – 7.84 (m, 1H, JohnPhos), 7.65 – 7.49 (m, 2H, JohnPhos), 7.44 – 7.04 (m, 12H, JohnPhos + Ph + CH imidazole), 7.00 – 6.94 (m, 1H, JohnPhos), 5.14 (s, 2H, CH<sub>2</sub>Ph), 4.75 (d, <sup>4</sup>J<sub>HH</sub> = 2.6 Hz, 2H, CH<sub>2</sub>C≡CH), 2.69 (t, <sup>4</sup>J<sub>HH</sub> = 2.6 Hz, 1H, C≡CH), 1.39 (d, <sup>3</sup>J<sub>HP</sub> = 15.5 Hz, 18H, <sup>t</sup>Bu).

**$^{31}\text{P}\{^1\text{H}\}$  NMR (121 MHz,  $\text{CD}_2\text{Cl}_2$ )**  $\delta$  63.76 (s, JohnPhos).

**$^{13}\text{C}$  APT (75 MHz,  $\text{CD}_2\text{Cl}_2$ )**  $\delta$  143.99 (d,  $^3J_{\text{CP}} = 6.1$  Hz, C7 JohnPhos), 135.44 (s, *i*-Ph), 134.98 (d,  $^4J_{\text{CP}} = 2.1$  Hz, C4 JohnPhos), 133.71 (d,  $^2J_{\text{CP}} = 7.4$  Hz, C2 JohnPhos), 131.73 (d,  $^3J_{\text{CP}} = 2.2$  Hz, C5 JohnPhos), 130.12 (s, C9/C11 JohnPhos), 129.67 (s, Ph), 129.38 (s, C8/C12 JohnPhos), 129.32 (s, Ph), 128.15 (d,  $^3J_{\text{CP}} = 6.6$  Hz, C3 JohnPhos), 127.90 (s, Ph), 127.81 (s, JohnPhos), 122.79 (d,  $^4J_{\text{CP}} = 3.3$  Hz, CH imidazole), 122.12 (d,  $^4J_{\text{CP}} = 2.7$  Hz, CH imidazole), 76.57 (s,  $\text{C}\equiv\text{C-H}$ ), 55.44 (s,  $\text{CH}_2\text{Ph}$ ), 41.18 (s,  $\text{CH}_2$ ), 38.38 (d,  $^1J_{\text{CP}} = 23.3$  Hz,  $\text{C-CH}_3$  ( $t\text{Bu}$ )), 31.35 (d,  $^2J_{\text{CP}} = 6.2$  Hz,  $\text{CH}_3$  ( $t\text{Bu}$ )).



To a solution of 1,3-bis(2-propyn-1-yl)-1*H*-imidazol-3-ium tetrafluoroborate (0.0928 g, 0.4 mmol) and  $[\text{AuCl}(\text{JohnPhos})]$  (0.2123 g, 0.4 mmol) in  $\text{CH}_2\text{Cl}_2$  (10 ml) was added  $\text{NBu}_4(\text{acac})$  (0.1366 g, 0.4 mmol) and the mixture stirred for 2 h. The solution washed with  $\text{H}_2\text{O}$  (3 x 25 ml), dried over  $\text{Na}_2\text{SO}_4$  and then concentrated under reduced pressure to approximately 1 ml.  $\text{Et}_2\text{O}$  (10 ml) was added to precipitate a white product which was collected and vacuum dried to give the product (0.1830 g, 63%).

**HRMS (ESI/QTOF)  $m/z$ :**  $[\text{M}]^+$  Calcd for  $\text{C}_{29}\text{H}_{35}\text{AuN}_2\text{P}$  639.2179; Found 639.2198.

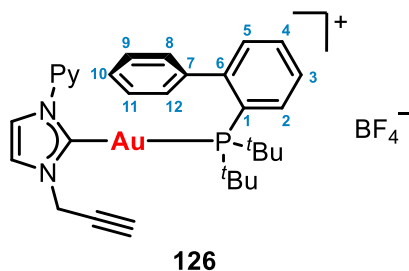
**$^1\text{H}$  NMR (300 MHz,  $\text{CD}_2\text{Cl}_2$ )**  $\delta$  7.97 – 7.90 (m, 1H, JohnPhos), 7.64 – 7.56 (m, 2H, JohnPhos), 7.42 – 7.19 (m, 7H, JohnPhos + CH imidazole), 6.94 – 6.89 (m, 1H, JohnPhos), 4.73 (d,  $^4J_{\text{HH}} = 2.7$  Hz, 4H,  $\text{CH}_2$ ), 2.69 (t,  $^4J_{\text{HH}} = 2.7$  Hz, 2H,  $\text{C}\equiv\text{CH}$ ), 1.47 (d,  $^3J_{\text{HP}} = 15.5$  Hz, 18H,  $t\text{Bu}$ ).

**$^{31}\text{P}\{^1\text{H}\}$  NMR (121 MHz,  $\text{CD}_2\text{Cl}_2$ )**  $\delta$  63.58 (s, JohnPhos).

**$^{13}\text{C}$  APT (75 MHz,  $\text{CD}_2\text{Cl}_2$ )**  $\delta$  188.25 (d,  $^2J_{\text{CP}} = 113.6$  Hz, N-C-N), 149.62 (d,  $^2J_{\text{CP}} = 14.2$  Hz, C6 JohnPhos), 143.99 (d,  $^3J_{\text{CP}} = 6.2$  Hz, C7 JohnPhos), 134.99 (d,  $^4J_{\text{CP}} = 2.2$  Hz, C4 JohnPhos), 133.67 (d,  $^2J_{\text{CP}} = 7.5$  Hz, C2 JohnPhos), 131.72 (d,  $^3J_{\text{CP}} = 2.4$  Hz, C5 JohnPhos), 130.11 (s, C9/C11 JohnPhos), 129.36 (s, C8/C12 JohnPhos), 128.16 (d,  $^3J_{\text{CP}} = 6.7$  Hz, C3 JohnPhos), 127.88 (s, C10 JohnPhos), 125.84 (d,  $^1J_{\text{CP}} = 43.9$  Hz, C1 JohnPhos), 122.14 (d,  $^4J_{\text{CP}} = 2.9$  Hz, CH imidazole), 76.59 (s,  $\text{C}\equiv\text{C-H}$ ), 41.22 (s,  $\text{CH}_2$ ), 38.46 (d,  $^1J_{\text{CP}} = 23.5$  Hz,  $\text{C-CH}_3$  ( $t\text{Bu}$ )), 31.42 (d,  $^2J_{\text{CP}} = 6.4$  Hz,  $\text{CH}_3$  ( $t\text{Bu}$ )).



## 4.9. Experimental



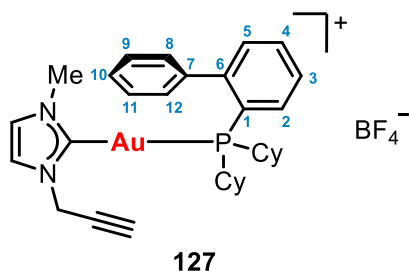
To a solution of 1-pyridyl-3-(2-propyn-1-yl)-1*H*-imidazol-3-ium tetrafluoroborate (0.1084 g, 0.4 mmol) and [AuCl(JohnPhos)] (0.2123 g, 0.4 mmol) in CH<sub>2</sub>Cl<sub>2</sub> (10 ml) was added NBU<sub>4</sub>(acac) (0.1366 g, 0.4 mmol) and the mixture stirred for 2 h. The solution washed with H<sub>2</sub>O (3 x 25 ml), dried over Na<sub>2</sub>SO<sub>4</sub> and then concentrated under reduced pressure to approximately 1 ml. Et<sub>2</sub>O (10 ml) was added to precipitate a white product which was collected and vacuum dried to give the product (0.199 g, 65%).

**HRMS (ESI/QTOF) m/z:** [M]<sup>+</sup> Calcd for C<sub>31</sub>H<sub>36</sub>AuN<sub>3</sub>P 678.2307; Found 678.2306.

**<sup>1</sup>H NMR (300 MHz, CD<sub>2</sub>Cl<sub>2</sub>)** δ 8.57-8.55 (m, 1H, Py), 8.01 – 7.87 (m, 2H, JohnPhos + Py), 7.83 – 7.73 (m, 2H, Py + *CH* imidazole), 7.64 – 7.44 (m, 4H, JohnPhos), 7.30 – 7.13 (m, 1H, Py), 7.11 – 6.91 (m, 4H, JohnPhos + *CH* imidazole), 6.88 – 6.75 (m, 1H, JohnPhos), 4.87 (d, <sup>4</sup>*J*<sub>HH</sub> = 2.6 Hz, 2H, *CH*<sub>2</sub>), 2.72 (t, <sup>4</sup>*J*<sub>HH</sub> = 2.6 Hz, 1H, C≡*CH*), 1.45 (d, <sup>3</sup>*J*<sub>CP</sub> = 15.4 Hz, 18H, <sup>*t*</sup>Bu).

**<sup>31</sup>P{<sup>1</sup>H} NMR (121 MHz, CD<sub>2</sub>Cl<sub>2</sub>)** δ 63.42 (s, JohnPhos).

**<sup>13</sup>C APT (75 MHz, CD<sub>2</sub>Cl<sub>2</sub>)** δ 187.78 (d, <sup>2</sup>*J*<sub>CP</sub> = 113.3 Hz, N-*C*-N), 150.68 (s, Py), 149.64 (d, <sup>2</sup>*J*<sub>CP</sub> = 14.2 Hz, C6 JohnPhos), 149.61 (s, Py), 143.74 (d, <sup>3</sup>*J*<sub>CP</sub> = 6.2 Hz, C7 JohnPhos), 139.87 (s, Py), 134.81 (d, <sup>4</sup>*J*<sub>CP</sub> = 2.2 Hz, C4 JohnPhos), 133.58 (d, <sup>2</sup>*J*<sub>CP</sub> = 7.5 Hz, C2 JohnPhos), 131.56 (d, <sup>3</sup>*J*<sub>CP</sub> = 2.3 Hz, C5 JohnPhos), 129.83 (s, C9/C11 JohnPhos), 129.05 (s, C8/C12 JohnPhos), 128.04 (d, <sup>3</sup>*J*<sub>CP</sub> = 6.6 Hz, C3 JohnPhos), 127.55 (s, C10 JohnPhos), 126.04 (d, <sup>1</sup>*J*<sub>CP</sub> = 43.7 Hz, C1 JohnPhos), 122.61 (d, <sup>4</sup>*J*<sub>CP</sub> = 2.9 Hz, *CH* imidazole), 121.31 (d, <sup>4</sup>*J*<sub>CP</sub> = 2.8 Hz, *CH* imidazole), 117.34 (s, Py), 76.71 (s, C≡*C*-H), 41.95 (s, *CH*<sub>2</sub>), 38.23 (d, <sup>1</sup>*J*<sub>CP</sub> = 23.5 Hz, *C*-CH<sub>3</sub> (<sup>*t*</sup>Bu)), 31.20 (d, <sup>2</sup>*J*<sub>CP</sub> = 6.5 Hz, CH<sub>3</sub> (<sup>*t*</sup>Bu)).



To a solution of 1-methyl-3-(2-propyn-1-yl)-1*H*-imidazol-3-ium tetrafluoroborate (0.0416 g, 0.2 mmol) and [AuCl(CyJohnPhos)] (0.1166 g, 0.2 mmol) in CH<sub>2</sub>Cl<sub>2</sub> (10 ml) was added NBu<sub>4</sub>(acac) (0.0683 g, 0.2 mmol) and the mixture stirred for 2 h. The solution washed with H<sub>2</sub>O (3 x 25 ml), dried over Na<sub>2</sub>SO<sub>4</sub> and then concentrated under reduced pressure to approximately 1 ml. Et<sub>2</sub>O (10 ml) was added to precipitate a white product which was collected and vacuum dried to give the product (0.1054 g, 69%).

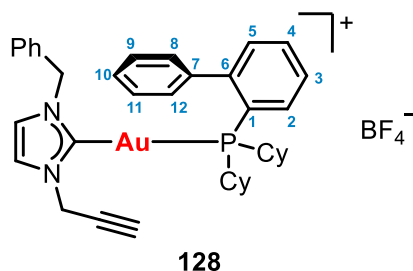
**HRMS (ESI/QTOF) m/z:** [M]<sup>+</sup> Calcd for C<sub>31</sub>H<sub>39</sub>AuN<sub>2</sub>P 667.2511; Found 667.2546.

**<sup>1</sup>H NMR (300 MHz, CD<sub>2</sub>Cl<sub>2</sub>)** δ 7.72 – 7.54 (m, 3H, CyJohnPhos), 7.40 – 7.23 (m, 6H, CyJohnPhos + CH imidazole), 7.17 – 7.16 (m, 1H, CyJohnPhos), 7.07 – 6.98 (m, 1H, CyJohnPhos), 4.72 (d, <sup>4</sup>J<sub>HH</sub> = 2.6 Hz, 2H, CH<sub>2</sub>), 2.66 (t, <sup>4</sup>J<sub>HH</sub> = 2.6 Hz, 1H, C≡CH), 2.53 – 2.29 (m, 2H, Cy), 2.12 – 2.05 (m, 2H, Cy), 1.97 – 1.66 (m, 8H, Cy), 1.55 – 1.08 (m, 10H, Cy).

**<sup>31</sup>P{<sup>1</sup>H} NMR (121 MHz, CD<sub>2</sub>Cl<sub>2</sub>)** δ 43.75 (s, CyJohnPhos).

**<sup>13</sup>C APT (75 MHz, CD<sub>2</sub>Cl<sub>2</sub>)** δ 188.84 (d, <sup>2</sup>J<sub>CP</sub> = 119.2 Hz, N-C-N), 149.54 (d, <sup>2</sup>J<sub>CP</sub> = 13.6 Hz, C6 CyJohnPhos), 143.12 (d, <sup>3</sup>J<sub>CP</sub> = 6.0 Hz, C7 CyJohnPhos), 133.63 (d, <sup>4</sup>J<sub>CP</sub> = 3.3 Hz, C4 CyJohnPhos), 132.97 (d, <sup>2</sup>J<sub>CP</sub> = 7.5 Hz, C2 CyJohnPhos), 131.62 (d, <sup>3</sup>J<sub>CP</sub> = 2.3 Hz, C5 JohnPhos), 130.19 (s, C9/C11 CyJohnPhos), 129.23 (s, C8/C12 CyJohnPhos), 128.72 (d, <sup>3</sup>J<sub>CP</sub> = 7.2 Hz, C3 CyJohnPhos), 128.08 (s, C10 CyJohnPhos), 124.85 (d, <sup>1</sup>J<sub>CP</sub> = 49.2 Hz, C1 CyJohnPhos), 123.72 (d, <sup>4</sup>J<sub>CP</sub> = 3.3 Hz, CH imidazole), 121.81 (d, <sup>4</sup>J<sub>CP</sub> = 3.1 Hz, CH imidazole), 76.77 (s, C≡C-H), 76.11 (s, C≡C-H), 40.81 (s, CH<sub>2</sub>), 38.65 (s, Me), 36.86 (d, <sup>1</sup>J<sub>CP</sub> = 31.2 Hz, CH Cy), 31.66 (d, J<sub>CP</sub> = 4.2 Hz, CH<sub>2</sub> Cy), 30.31 (s, CH<sub>2</sub>, Cy), 27.19 (d, J<sub>CP</sub> = 6.5 Hz, CH<sub>2</sub>, Cy), 27.02 (d, J<sub>CP</sub> = 8.4 Hz, CH<sub>2</sub> Cy), 26.38 (d, J<sub>CP</sub> = 1.5 Hz, CH<sub>2</sub> Cy).

## 4.9. Experimental



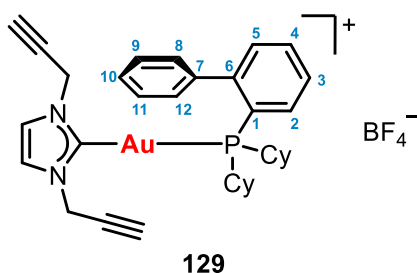
To a solution of 1-benzyl-3-(2-propyn-1-yl)-1*H*-imidazol-3-ium tetrafluoroborate (0.0568 g, 0.2 mmol) and [AuCl(CyJohnPhos)] (0.1166 g, 0.2 mmol) in CH<sub>2</sub>Cl<sub>2</sub> (10 ml) was added NBU<sub>4</sub>(acac) (0.0683 g, 0.2 mmol) and the mixture stirred for 2 h. The solution washed with H<sub>2</sub>O (3 x 25 ml), dried over Na<sub>2</sub>SO<sub>4</sub> and then concentrated under reduced pressure to approximately 1 ml. Et<sub>2</sub>O (10 ml) was added to precipitate a white product which was collected and vacuum dried to give the product (0.1163 g, 70%).

**HRMS (ESI/QTOF) m/z:** [M]<sup>+</sup> Calcd for C<sub>37</sub>H<sub>43</sub>AuN<sub>2</sub>P 743.2824; Found 743.2858.

**<sup>1</sup>H NMR (300 MHz, CD<sub>2</sub>Cl<sub>2</sub>)** δ 7.84 – 6.85 (m, 17H, CyJohnPhos + Ph + CH imidazole), 5.17 (s, 2H, CH<sub>2</sub>Ph), 4.76 (d, <sup>4</sup>J<sub>HH</sub> = 2.6 Hz, 2H, CH<sub>2</sub>), 2.70 (t, <sup>4</sup>J<sub>HH</sub> = 2.6 Hz, 1H, C≡CH), 2.52 – 1.56 (m, 12H, Cy), 1.55 – 0.98 (m, 8H, Cy).

**<sup>31</sup>P{<sup>1</sup>H} NMR (121 MHz, CD<sub>2</sub>Cl<sub>2</sub>)** δ 43.97 (s, CyJohnPhos).

**<sup>13</sup>C APT (75 MHz, CD<sub>2</sub>Cl<sub>2</sub>)** δ 188.75 (d, <sup>2</sup>J<sub>CP</sub> = 118.8 Hz, N-C-N), 149.46 (d, <sup>2</sup>J<sub>CP</sub> = 13.4 Hz, C6 CyJohnPhos), 142.97 (d, <sup>3</sup>J<sub>CP</sub> = 6.0 Hz, C7 CyJohnPhos), 135.76 (s, *i*-Ph), 133.70 (d, <sup>4</sup>J<sub>CP</sub> = 3.7 Hz, C4 CyJohnPhos), 132.99 (d, <sup>2</sup>J<sub>CP</sub> = 7.6 Hz, C2 CyJohnPhos), 131.66 (d, <sup>3</sup>J<sub>CP</sub> = 2.3 Hz, C5 CyJohnPhos), 130.22 (s, C9/C11 CyJohnPhos), 129.57 (s, Ph), 129.38 (s, C8/C12 CyJohnPhos), 129.24 (s, Ph), 128.73 (d, <sup>3</sup>J<sub>CP</sub> = 7.4 Hz, C3 CyJohnPhos), 128.23 (s, Ph), 127.77 (s, C10 CyJohnPhos), 124.73 (d, <sup>1</sup>J<sub>CP</sub> = 49.3 Hz, C1 CyJohnPhos), 122.88 (d, <sup>4</sup>J<sub>CP</sub> = 3.2 Hz, CH imidazole), 122.30 (d, <sup>4</sup>J<sub>CP</sub> = 3.0 Hz, CH imidazole), 76.67 (s, C≡C-H), 76.34 (s, C≡C-H), 55.35 (s, CH<sub>2</sub>Ph), 41.11 (s, CH<sub>2</sub>), 36.89 (d, <sup>1</sup>J<sub>CP</sub> = 31.2 Hz, CH Cy), 31.65 (d, J<sub>CP</sub> = 4.1 Hz, CH<sub>2</sub>, Cy), 30.27 (s, CH<sub>2</sub>, Cy), 27.14 (d, J<sub>CP</sub> = 5.1 Hz, CH<sub>2</sub>, Cy), 26.97 (d, J<sub>CP</sub> = 7.1 Hz, CH<sub>2</sub>, Cy), 26.27 (d, J<sub>CP</sub> = 1.5 Hz, CH<sub>2</sub>, Cy).



To a solution of 1,3-bis(2-propyn-1-yl)-1*H*-imidazol-3-ium tetrafluoroborate (0.0464 g, 0.2 mmol) and [AuCl(CyJohnPhos)] (0.1166 g, 0.2 mmol) in CH<sub>2</sub>Cl<sub>2</sub> (10 ml) was added NBu<sub>4</sub>(acac) (0.0683 g, 0.2 mmol) and the mixture stirred for 2 h. The solution washed with H<sub>2</sub>O (3 x 25 ml), dried over Na<sub>2</sub>SO<sub>4</sub> and then concentrated under reduced pressure to approximately 1 ml. Et<sub>2</sub>O (10 ml) was added to precipitate a white product which was collected and vacuum dried to give the product (0.1199 g, 77%).

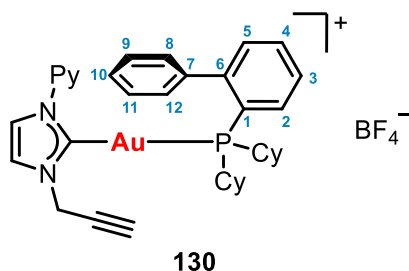
**HRMS (ESI/QTOF) m/z:** [M]<sup>+</sup> Calcd for C<sub>33</sub>H<sub>39</sub>AuN<sub>2</sub>P 691.2511; Found 691.2487.

**<sup>1</sup>H NMR (300 MHz, CD<sub>2</sub>Cl<sub>2</sub>)** δ 7.71 – 7.55 (m, 3H, CyJohnPhos), 7.42 – 7.21 (m, 7H, CyJohnPhos + CH imidazole), 7.10 – 7.02 (m, 1H, CyJohnPhos), 4.74 (d, <sup>4</sup>J<sub>HH</sub> = 2.6 Hz, 4H, CH<sub>2</sub>), 2.69 (t, <sup>4</sup>J<sub>HH</sub> = 2.6 Hz, 1H, C≡CH), 2.49 – 2.38 (m, 2H, Cy), 2.15 – 2.02 (m, 2H, Cy), 1.95 – 1.67 (m, 10H, Cy), 1.56 – 1.09 (m, 8H, Cy).

**<sup>31</sup>P{<sup>1</sup>H} NMR (121 MHz, CD<sub>2</sub>Cl<sub>2</sub>)** δ 43.62 (s, CyJohnPhos).

**<sup>13</sup>C APT (75 MHz, CD<sub>2</sub>Cl<sub>2</sub>)** δ 188.92 (d, <sup>2</sup>J<sub>CP</sub> = 118.3 Hz, N-C-N), 149.51 (d, <sup>2</sup>J<sub>CP</sub> = 13.4 Hz, C6 CyJohnPhos), 143.08 (d, <sup>3</sup>J<sub>CP</sub> = 6.1 Hz, C7 CyJohnPhos), 133.62 (d, <sup>4</sup>J<sub>CP</sub> = 3.4 Hz, C4 CyJohnPhos), 132.99 (d, <sup>2</sup>J<sub>CP</sub> = 7.5 Hz, C2 CyJohnPhos), 131.68 (d, <sup>3</sup>J<sub>CP</sub> = 2.3 Hz, C5 CyJohnPhos), 130.28 (s, C9/C11 CyJohnPhos), 129.37 (s, C8/C12 CyJohnPhos), 128.76 (d, <sup>3</sup>J<sub>CP</sub> = 7.3 Hz, C3 CyJohnPhos), 128.17 (s, C10 CyJohnPhos), 124.69 (d, <sup>1</sup>J<sub>CP</sub> = 49.6 Hz, C1 CyJohnPhos), 122.25 (d, <sup>4</sup>J<sub>CP</sub> = 3.1 Hz, CH imidazole), 76.53 (s, C≡C-H), 76.43 (s, C≡C-H), 41.23 (s, CH<sub>2</sub>), 36.86 (d, <sup>1</sup>J<sub>CP</sub> = 31.4 Hz, CH Cy), 31.65 (d, J<sub>CP</sub> = 4.1 Hz, CH<sub>2</sub>, Cy), 30.28 (s, CH<sub>2</sub>, Cy), 27.20 (d, J<sub>CP</sub> = 5.9 Hz, CH<sub>2</sub>, Cy), 27.02 (d, J<sub>CP</sub> = 7.8 Hz, CH<sub>2</sub>, Cy), 26.35 (d, J<sub>CP</sub> = 1.4 Hz, CH<sub>2</sub>, Cy).

## 4.9. Experimental



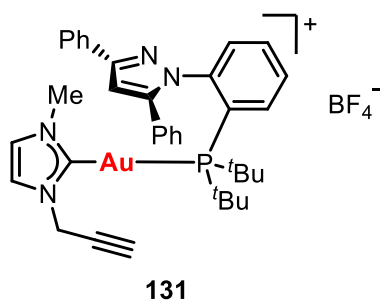
To a solution of 1-pyridyl-3-(2-propyn-1-yl)-1*H*-imidazol-3-ium tetrafluoroborate (0.0542 g, 0.2 mmol) and [AuCl(CyJohnPhos)] (0.1166 g, 0.2 mmol) in CH<sub>2</sub>Cl<sub>2</sub> (10 ml) was added NBu<sub>4</sub>(acac) (0.0683 g, 0.2 mmol) and the mixture stirred for 2 h. The solution washed with H<sub>2</sub>O (3 x 25 ml), dried over Na<sub>2</sub>SO<sub>4</sub> and then concentrated under reduced pressure to approximately 1 ml. Et<sub>2</sub>O (10 ml) was added to precipitate a white product which was collected and vacuum dried to give the product (0.1161 g, 71%).

**HRMS (ESI/QTOF) m/z:** [M]<sup>+</sup> Calcd for C<sub>35</sub>H<sub>40</sub>AuN<sub>3</sub>P 730.2620; Found 730.2599.

**<sup>1</sup>H NMR (300 MHz, CD<sub>2</sub>Cl<sub>2</sub>)** δ 8.58 – 8.55 (m, 1H, Py), 7.98 – 7.87 (m, 1H, Py), 7.85 – 7.75 (m, 2H, Py + *CH* imidazole), 7.69 – 7.45 (m, 5H, CyJohnPhos), 7.30 – 7.23 (m, 1H, CyJohnPhos), 7.15 – 6.98 (m, 4H, CyJohnPhos + Py + *CH* imidazole), 6.96 – 6.83 (m, 1H, CyJohnPhos), 4.90 (d, <sup>4</sup>*J*<sub>HH</sub> = 2.6 Hz, 2H, CH<sub>2</sub>), 2.72 (t, <sup>4</sup>*J*<sub>HH</sub> = 2.6 Hz, 1H, C≡CH), 2.44 – 2.33 (m, 2H, Cy), 2.17 – 0.89 (m, 20H, Cy).

**<sup>31</sup>P{<sup>1</sup>H} NMR (121 MHz, CD<sub>2</sub>Cl<sub>2</sub>)** δ 43.16 (s, CyJohnPhos).

**<sup>13</sup>C APT (75 MHz, CD<sub>2</sub>Cl<sub>2</sub>)** δ 188.27 (d, <sup>2</sup>*J*<sub>CP</sub> = 117.5 Hz, N-C-N), 149.68 (s, Py), 149.55 (d, <sup>2</sup>*J*<sub>CP</sub> = 13.3 Hz, C6 CyJohnPhos), 142.92 (d, <sup>3</sup>*J*<sub>CP</sub> = 6.0 Hz, C7 CyJohnPhos), 139.60 (s, Py), 133.57 (d, <sup>4</sup>*J*<sub>CP</sub> = 3.6 Hz, C4 CyJohnPhos), 132.94 (d, <sup>2</sup>*J*<sub>CP</sub> = 7.6 Hz, C2 CyJohnPhos), 131.59 (d, <sup>3</sup>*J*<sub>CP</sub> = 2.3 Hz, C5 CyJohnPhos), 129.99 (s, C9/C11 CyJohnPhos), 129.07 (s, C8/C12 CyJohnPhos), 128.69 (d, <sup>3</sup>*J*<sub>CP</sub> = 7.4 Hz, C3 CyJohnPhos), 127.89 (s, C10 CyJohnPhos), 125.08 (s, Py), 124.42 (s, Py), 122.69 (d, <sup>4</sup>*J*<sub>CP</sub> = 2.8 Hz, *CH* imidazole), 121.39 (d, <sup>4</sup>*J*<sub>CP</sub> = 3.0 Hz, *CH* imidazole), 117.32 (s, Py), 76.55 (s, C≡C-H), 76.43 (s, C≡C-H), 41.99 (s, CH<sub>2</sub>), 36.68 (d, <sup>1</sup>*J*<sub>CP</sub> = 31.5 Hz, *CH* Cy), 31.60 (d, *J*<sub>CP</sub> = 4.3 Hz, CH<sub>2</sub>, Cy), 30.03 (s, CH<sub>2</sub>, Cy), 27.17 (d, *J*<sub>CP</sub> = 3.4 Hz, CH<sub>2</sub>, Cy), 26.99 (d, *J*<sub>CP</sub> = 5.4 H, CH<sub>2</sub>, Cy), 26.42 (d, *J*<sub>CP</sub> = 1.4 Hz, CH<sub>2</sub>, Cy).



To a solution of 1-methyl-3-(2-propyn-1-yl)-1*H*-imidazol-3-ium tetrafluoroborate (0.0416 g, 0.2 mmol) and [AuCl(TrippyPhos)] (0.1346 g, 0.2 mmol) in CH<sub>2</sub>Cl<sub>2</sub> (10 ml) was added NBu<sub>4</sub>(acac) (0.0683 g, 0.2 mmol) and the mixture stirred for 2 h. The solution washed with H<sub>2</sub>O (3 x 25 ml), dried over Na<sub>2</sub>SO<sub>4</sub> and then concentrated under reduced pressure to approximately 1 ml. Et<sub>2</sub>O (10 ml) was added to precipitate a white product which was collected and vacuum dried to give the product (0.0548 g, 67%).

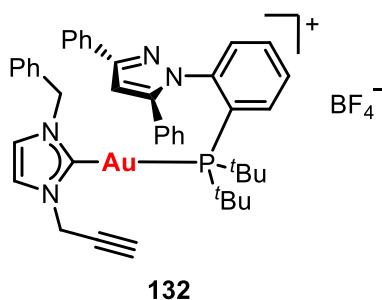
**HRMS (ESI/QTOF) m/z:** [M]<sup>+</sup> Calcd for C<sub>36</sub>H<sub>41</sub>AuN<sub>4</sub>P 757.2729; Found 757.2658.

**<sup>1</sup>H NMR (300 MHz, CD<sub>2</sub>Cl<sub>2</sub>)** δ 8.13 – 8.07 (m, 1H, TrippyPhos), 7.74 – 7.53 (m, 4H, TrippyPhos), 7.47 – 7.25 (m, 8H, TrippyPhos), 7.24 – 7.14 (m, 1H, TrippyPhos), 7.10 (s, 1H, *CH* imidazole), 6.93 (s, 1H, *CH* imidazole), 6.81 (s, 1H, TrippyPhos), 4.20 (ABX-system, 2H, Δδ = 0.38, *J*<sub>AB</sub> = 17.5 Hz, *J*<sub>AX</sub> = 2.6 Hz, *J*<sub>BX</sub> = 2.6 Hz, CH<sub>2</sub>), 3.16 (s, 3H, Me), 2.46 (t, <sup>4</sup>*J*<sub>HH</sub> = 2.6 Hz, 1H, C≡CH), 1.62 (d, <sup>3</sup>*J*<sub>HP</sub> = 15.8 Hz, 9H, <sup>*t*</sup>Bu), 1.51 (d, <sup>3</sup>*J*<sub>HP</sub> = 15.7 Hz, 9H, <sup>*t*</sup>Bu).

**<sup>31</sup>P{<sup>1</sup>H} NMR (121 MHz, CD<sub>2</sub>Cl<sub>2</sub>)** δ 60.09 (s, TrippyPhos).

**<sup>13</sup>C APT (75 MHz, CD<sub>2</sub>Cl<sub>2</sub>)** δ 136.47 (s, TrippyPhos), 133.36 (d, *J* = 2.0 Hz, TrippyPhos), 132.35 (d, *J* = 5.1 Hz, TrippyPhos), 129.54 (s, TrippyPhos), 129.48 (s, TrippyPhos), 129.41 (s, TrippyPhos), 129.29 (s, TrippyPhos), 128.47 (s, TrippyPhos), 125.61 (s, TrippyPhos), 123.44 (d, <sup>4</sup>*J*<sub>CP</sub> = 3.2 Hz, *CH* imidazole), 121.58 (d, <sup>4</sup>*J*<sub>CP</sub> = 3.0 Hz, *CH* imidazole), 104.86, 76.10 (s, C≡C-H), 40.28 (s, CH<sub>2</sub>C≡CH), 37.98 (s, Me), 32.03 (d, <sup>2</sup>*J*<sub>CP</sub> = 6.0 Hz, CH<sub>3</sub> <sup>*t*</sup>Bu), 31.61 (d, <sup>2</sup>*J*<sub>CP</sub> = 6.0 Hz, CH<sub>3</sub> <sup>*t*</sup>Bu).

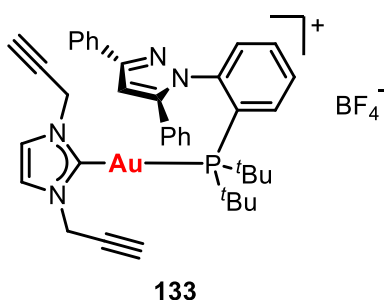
## 4.9. Experimental



To a solution of 1-benzyl-3-(2-propyn-1-yl)-1*H*-imidazol-3-ium tetrafluoroborate (0.0568 g, 0.2 mmol) and [AuCl(TrippyPhos)] (0.1346 g, 0.2 mmol) in CH<sub>2</sub>Cl<sub>2</sub> (10 ml) was added NBu<sub>4</sub>(acac) (0.0683 g, 0.2 mmol) and the mixture stirred for 2 h. The solution washed with H<sub>2</sub>O (3 x 25 ml), dried over Na<sub>2</sub>SO<sub>4</sub> and then concentrated under reduced pressure to approximately 1 ml. Et<sub>2</sub>O (10 ml) was added to precipitate a white product which was collected and vacuum dried to give the product (0.1381 g, 75%).

**HRMS (ESI/QTOF) m/z:** [M]<sup>+</sup> Calcd for C<sub>42</sub>H<sub>45</sub>AuN<sub>4</sub>P 833.3042; Found 833.3049.

**<sup>31</sup>P{<sup>1</sup>H} NMR (121 MHz, CD<sub>2</sub>Cl<sub>2</sub>)** δ 60.06 (s, TrippyPhos).



To a solution of 1,3-bis(2-propyn-1-yl)-1*H*-imidazol-3-ium tetrafluoroborate (0.0464 g, 0.2 mmol) and [AuCl(TrippyPhos)] (0.1346 g, 0.2 mmol) in CH<sub>2</sub>Cl<sub>2</sub> (10 ml) was added NBu<sub>4</sub>(acac) (0.0683 g, 0.2 mmol) and the mixture stirred for 2 h. The solution washed with H<sub>2</sub>O (3 x 25 ml), dried over Na<sub>2</sub>SO<sub>4</sub> and then concentrated under reduced pressure to approximately 1 ml. Et<sub>2</sub>O (10 ml) was added to precipitate a white product which was collected and vacuum dried to give the product (0.1285 g, 74%).

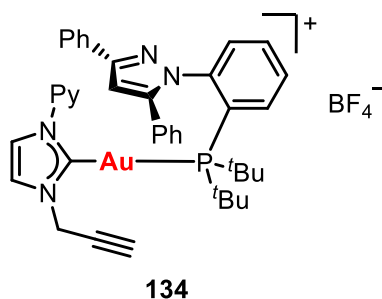
**HRMS (ESI/QTOF) m/z:** [M]<sup>+</sup> Calcd for C<sub>38</sub>H<sub>41</sub>AuN<sub>4</sub>P 781.2729; Found 781.2739.

**<sup>1</sup>H NMR (300 MHz, CD<sub>2</sub>Cl<sub>2</sub>)** δ 8.13 – 8.07 (m, 1H, TrippyPhos), 7.78 – 7.64 (m, 1H, TrippyPhos), 7.64 – 7.51 (m, 4H, TrippyPhos), 7.44 – 7.23 (m, 8H, TrippyPhos), 7.16 (s, 2H, CH imidazole), 6.85 (s, 1H, TrippyPhos), 4.20 (ABX-system, 2H, Δδ = 0.40, J<sub>AB</sub> = 17.5 Hz,

$J_{AX} = 2.6$  Hz,  $J_{BX} = 2.6$  Hz, CH<sub>2</sub>), 2.48 (t,  $^4J_{HH} = 2.6$  Hz, 1H, CH), 1.63 (d,  $^3J_{HH} = 15.9$  Hz, 9H, CH<sub>3</sub> <sup>*t*</sup>Bu), 1.51 (d,  $J = 15.7$  Hz, 9H, CH<sub>3</sub> <sup>*t*</sup>Bu).

**$^{31}\text{P}\{^1\text{H}\}$  NMR (121 MHz, CD<sub>2</sub>Cl<sub>2</sub>)**  $\delta$  59.97 (s, TrippyPhos).

**$^{13}\text{C}$  APT (75 MHz, CD<sub>2</sub>Cl<sub>2</sub>)**  $\delta$  136.46 (s, TrippyPhos), 133.41 (s, TrippyPhos), 132.35 (d,  $J = 5.1$  Hz, TrippyPhos), 129.64 (s, TrippyPhos), 129.59 (s, TrippyPhos), 129.54 (s, TrippyPhos), 129.51 (s, TrippyPhos), 129.46 (s, TrippyPhos), 129.40 (s, TrippyPhos), 128.53 (s, TrippyPhos), 125.60 (s, TrippyPhos), 121.98 (s, CH imidazole), 104.97 (s, TrippyPhos), 76.43 (s, C $\equiv$ C-H), 40.61 (s, CH<sub>2</sub>C $\equiv$ CH), 32.02 (d,  $^2J_{CP} = 6.8$  Hz, CH<sub>3</sub> <sup>*t*</sup>Bu), 31.63 (d,  $^2J_{CP} = 6.1$  Hz, CH<sub>3</sub> <sup>*t*</sup>Bu).



To a solution 1-pyridyl-3-(2-propyn-1-yl)-1H-imidazol-3-ium tetrafluoroborate (0.0542 g, 0.2 mmol) and [AuCl(TrippyPhos)] (0.1346 g, 0.2 mmol) in CH<sub>2</sub>Cl<sub>2</sub> (10 ml) was added NBu<sub>4</sub>(acac) (0.0683 g, 0.2 mmol) and the mixture stirred for 2 h. The solution washed with H<sub>2</sub>O (3 x 25 ml), dried over Na<sub>2</sub>SO<sub>4</sub> and then concentrated under reduced pressure to approximately 1 ml. Et<sub>2</sub>O (10 ml) was added to precipitate a white product which was collected and vacuum dried to give the product (0.1198 g, 66%).

**HRMS (ESI/QTOF) m/z:** [M]<sup>+</sup> Calcd for C<sub>40</sub>H<sub>42</sub>AuN<sub>5</sub>P 820.2838; Found 820.2802.

**$^1\text{H}$  NMR (300 MHz, CD<sub>2</sub>Cl<sub>2</sub>)**  $\delta$  8.23 – 8.20 (m, 1H, TrippyPhos), 8.13 – 8.07 (m, 1H, Py), 7.69 – 7.46 (m, 7H, TrippyPhos), 7.37 – 7.17 (m, 7H, TrippyPhos), 7.08 – 6.98 (m, 4H, TrippyPhos), 6.62 (s, 1H, TrippyPhos), 4.17 (ABX-system, 2H,  $\Delta\delta = 0.66$ ,  $J_{AB} = 17.6$  Hz,  $J_{AX} = 2.6$  Hz,  $J_{BX} = 2.6$  Hz, CH<sub>2</sub>), 2.53 (t,  $^4J_{HH} = 2.6$  Hz, 1H, CH), 1.61 (d,  $^3J_{HP} = 15.8$  Hz, 9H, CH<sub>3</sub> <sup>*t*</sup>Bu), 1.52 (d,  $^3J_{HP} = 15.7$  Hz, 9H, CH<sub>3</sub> <sup>*t*</sup>Bu).

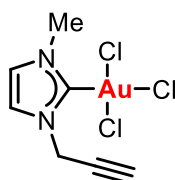
**$^{31}\text{P}\{^1\text{H}\}$  NMR (121 MHz, CD<sub>2</sub>Cl<sub>2</sub>)**  $\delta$  59.58 (s, TrippyPhos).

**$^{13}\text{C}$  APT (75 MHz, CD<sub>2</sub>Cl<sub>2</sub>)**  $\delta$  149.29 (s, Py), 139.40 (s, Py), 136.42 (s, TrippyPhos), 133.27 (d,  $J = 2.1$  Hz, TrippyPhos), 132.24 (d,  $J = 5.0$  Hz, TrippyPhos), 129.49 (s, TrippyPhos), 129.37 (s, TrippyPhos), 129.20 (s, TrippyPhos), 128.39 (s, TrippyPhos), 125.51 (s, TrippyPhos),



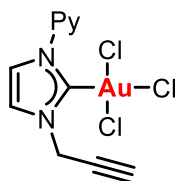
## 4.9. Experimental

124.61 (s, Py), 122.32 (d,  $^4J_{\text{CP}} = 2.8$  Hz, CH imidazole), 121.31 (d,  $^4J_{\text{CP}} = 2.9$  Hz, CH imidazole), 116.85, 104.61 (s, TrippyPhos), 76.51 (s, C≡C-H), 41.14 (s, CH<sub>2</sub>C≡CH), 39.30 (d,  $^1J_{\text{CP}} = 9.8$  Hz, C <sup>t</sup>Bu), 38.99 (d,  $^1J_{\text{CP}} = 10.4$  Hz, C <sup>t</sup>Bu), 31.91 (d,  $^2J_{\text{CP}} = 6.8$  Hz, CH<sub>3</sub> <sup>t</sup>Bu), 31.40 (d,  $^2J_{\text{CP}} = 6.2$  Hz, CH<sub>3</sub> <sup>t</sup>Bu).



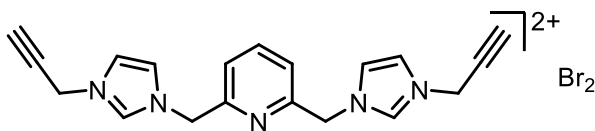
**135**

To a solution of **103** (10 mg) in CH<sub>2</sub>Cl<sub>2</sub> (1 ml) was added Cl<sub>2</sub> (20 μl, 0.5 M soln in CCl<sub>4</sub>). The solution was layered with pentane and yellow crystals formed which were analysed by single crystal X-ray diffraction.



**136**

To a solution of **106** (10 mg) in CH<sub>2</sub>Cl<sub>2</sub> (1 ml) was added Cl<sub>2</sub> (20 μl, 0.5 M soln in CCl<sub>4</sub>). The solution was layered with pentane and yellow crystals formed which were analysed by single crystal X-ray diffraction.

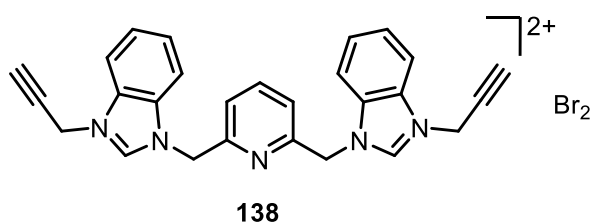


**137**

To a solution of imidazole (0.4034 g, 6.0 mmol) in acetonitrile (15 ml) was added NaOH (25% soln, 3 ml) and the solution stirred for 10 min. 2,6-Bis(bromomethyl)pyridine (0.7948 g, 3.0 mmol) was added and the solution stirred for 4 days. Solvent was removed under reduced pressure and the solid residue dissolved in chloroform (20 ml), washed with H<sub>2</sub>O (3 x 25 ml) and dried over Na<sub>2</sub>SO<sub>4</sub>. The solution was concentrated under reduced pressure to approximately 1 ml and Et<sub>2</sub>O (10 ml) added to precipitate a white solid (0.4067 g). The solid

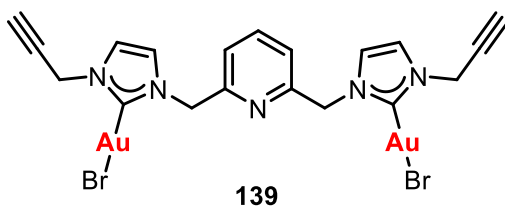
was dissolved in acetonitrile (30 ml), propargyl bromide (0.36 ml, 3.4 mmol) was added and the solution heated to reflux for 20 h. A white precipitate formed which was collected by filtration, washed with Et<sub>2</sub>O and vacuum dried to give the product (0.6368 g, 44%).

**<sup>1</sup>H NMR (400 MHz, DMSO)** δ 9.38 (s, 2H, N-CH-N imidazole), 7.98 (t, <sup>3</sup>J<sub>HH</sub> = 7.8 Hz, 1H, C4H pyridine), 7.85 (t, <sup>3</sup>J<sub>HH</sub> = 1.8 Hz, 2H, CH imidazole), 7.74 (t, <sup>3</sup>J<sub>HH</sub> = 1.8 Hz, 2H), CH imidazole, 7.50 (d, <sup>3</sup>J<sub>HH</sub> = 7.8 Hz, 2H, CH pyridine), 5.60 (s, 4H, CH<sub>2</sub>), 5.29 (d, <sup>4</sup>J<sub>HH</sub> = 2.6 Hz, 4H, CH<sub>2</sub>), 3.90 (t, <sup>4</sup>J<sub>HH</sub> = 2.6 Hz, 2H, C≡CH).



To a solution of benzimidazole (0.7088 g, 6.0 mmol) in acetonitrile (15 ml) was added NaOH (25% soln, 3 ml) and the solution stirred for 10 min. 2,6-Bis(bromomethyl)pyridine (0.7948 g, 3.0 mmol) was added and the solution stirred for 4 days. Solvent was removed under reduced pressure and the solid residue dissolved in chloroform (20 ml), washed with H<sub>2</sub>O (3 x 25 ml) and dried over Na<sub>2</sub>SO<sub>4</sub>. The solution was concentrated under reduced pressure to approximately 1 ml and Et<sub>2</sub>O (10 ml) added to precipitate a white solid (0.8472 g). The solid was dissolved in acetonitrile (30 ml), propargyl bromide (0.54 ml, 5.0 mmol) was added and the solution heated to reflux for 20 h. A white precipitate formed which was collected by filtration, washed with Et<sub>2</sub>O and vacuum dried to give the product (1.0350 g, 60%).

**<sup>1</sup>H NMR (400 MHz, DMSO)** δ 9.94 (s, 2H, N-CH-N), 8.04 – 7.95 (m, 3H), 7.71 – 7.64 (m, 4H, benzimidazole/Py), 7.62 – 7.54 (m, 2H, benzimidazole/Py), 7.47 – 7.43 (m, 2H, benzimidazole/Py), 5.87 (s, 4H, CH<sub>2</sub>), 5.52 (d, <sup>4</sup>J<sub>HH</sub> = 2.6 Hz, 4H, CH<sub>2</sub>), 3.92 (t, <sup>4</sup>J<sub>HH</sub> = 2.6 Hz, 2H, C≡CH).

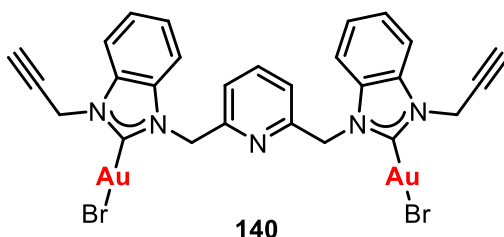


To a solution of **137** (0.0239 g, 0.05 mmol) in acetone (5 ml) was added [AuCl(tht)] (0.0321 g, 0.1 mmol) and excess Cs<sub>2</sub>CO<sub>3</sub> and the mixture stirred for 2 h. The solution was filtered

## 4.9. Experimental

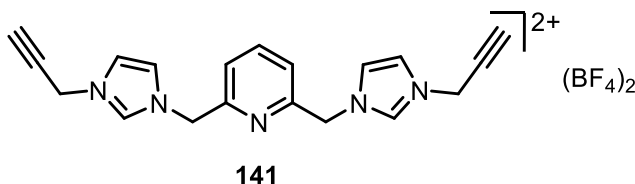
through celite, the filtrate concentrated under reduced pressure to approximately 1 ml and Et<sub>2</sub>O (10 ml) added to precipitate a white solid which was collected and vacuum dried to give the product (0.0174 g, 39%).

**<sup>1</sup>H NMR (400 MHz, DMSO)**  $\delta$  7.87 (t,  $^3J_{\text{HH}} = 7.8$  Hz, 1H, C4H pyridine), 7.56 (d,  $^3J_{\text{HH}} = 2.0$  Hz, 2H, CH imidazole), 7.51 (d,  $^3J_{\text{HH}} = 2.0$  Hz, 2H, CH imidazole), 7.25 (d,  $^3J_{\text{HH}} = 7.8$  Hz, 2H, CH pyridine), 5.44 (s, 4H, CH<sub>2</sub>), 5.05 (d,  $^4J_{\text{HH}} = 2.6$  Hz, 4H, CH<sub>2</sub>), 3.62 (t,  $^4J_{\text{HH}} = 2.5$  Hz, 2H, C $\equiv$ CH).



To a solution of **138** (0.0239 g, 0.05 mmol) in acetone (5 ml) was added [AuCl(tht)] (0.0321 g, 0.1 mmol) and excess Cs<sub>2</sub>CO<sub>3</sub> and the mixture stirred for 2 h. The solution was filtered through celite, concentrated under reduced pressure to approximately 1 ml and Et<sub>2</sub>O (10 ml) added to precipitate a white solid which was collected and vacuum dried to give the product (0.0165 g, 34%).

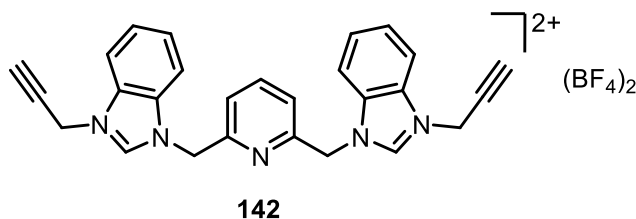
**<sup>1</sup>H NMR (400 MHz, DMSO)**  $\delta$  7.91 (t,  $^3J_{\text{HH}} = 7.7$  Hz, 1H, C4H pyridine), 7.79 (d,  $^3J_{\text{HH}} = 8.2$  Hz, 2H, benzimidazole), 7.53 (d,  $J = 7.7$  Hz, 2H, CH pyridine), 7.50 – 7.43 (m, 2H, benzimidazole), 7.38 (d,  $^3J_{\text{HH}} = 8.2$  Hz, 2H, benzimidazole), 7.29 – 7.25 (m, 2H, benzimidazole), 5.70 (s, 4H, CH<sub>2</sub>), 5.35 (d,  $^4J_{\text{HH}} = 2.6$  Hz, 4H, CH<sub>2</sub>), 3.57 (t,  $^4J_{\text{HH}} = 2.5$  Hz, 2H, C $\equiv$ CH).



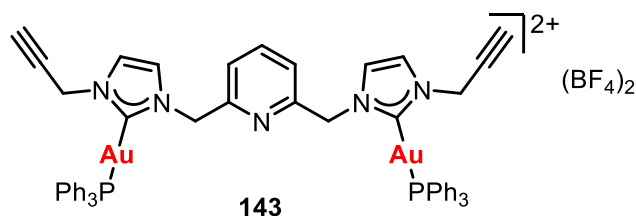
To a solution of **137** (0.7158 g, 1.5 mmol) was in MeOH (15 ml) was added NaBF<sub>4</sub> (0.3294 g, 3.0 mmol) and the solution stirred for 3 h. Solvent was removed under reduced pressure and the solid residue was dissolved in acetonitrile (50 ml), filtered through celite and the filtrate concentrated to dryness under reduced pressure to give a white solid which was washed with Et<sub>2</sub>O and vacuum dried to give the product (0.7193 g, 98%).

**$^1\text{H}$  NMR (400 MHz, DMSO)**  $\delta$  9.32 (s, 2H, N-CH-N), 7.98 (t,  $^3J_{\text{HH}} = 7.8$  Hz, 1H, C4H pyridine), 7.83 (t,  $^3J_{\text{HH}} = 1.8$  Hz, 2H, CH imidazole), 7.72 (t,  $^3J_{\text{HH}} = 1.8$  Hz, 2H, CH imidazole), 7.49 (d,  $^3J_{\text{HH}} = 7.8$  Hz, 2H, CH pyridine), 5.58 (s, 4H,  $\text{CH}_2$ ), 5.25 (d,  $^4J_{\text{HH}} = 2.6$  Hz, 4H,  $\text{CH}_2$ ), 3.88 (t,  $^4J_{\text{HH}} = 2.6$  Hz, 2H,  $\text{C}\equiv\text{CH}$ ).

**$^{19}\text{F}$  NMR (376 MHz, DMSO)**  $\delta$  -148.21 (s,  $\text{BF}_4$ )

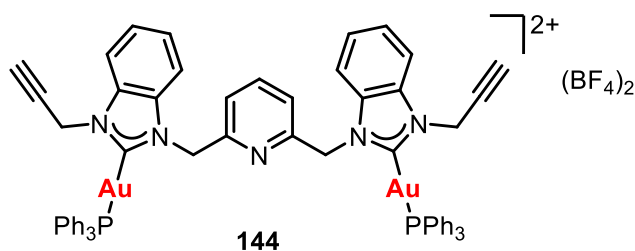


To a solution of **138** (1.1546 g, 2.0 mmol) was in MeOH (15 ml) was added  $\text{NaBF}_4$  (0.4392 g, 4.0 mmol) and the solution stirred for 3 h. Solvent was removed under reduced pressure and the solid residue was dissolved in acetonitrile (50 ml), filtered through celite and the filtrate concentrated to dryness under reduced pressure to give a white solid which was washed with  $\text{Et}_2\text{O}$  and vacuum dried to give the product (0.9835 g, 83%).

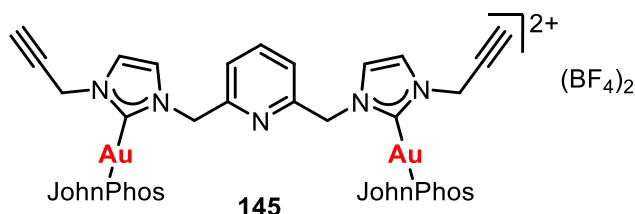


To a solution of **141** (0.0246 g, 0.5 mmol) in  $\text{CH}_2\text{Cl}_2$  (10 ml) was added  $[\text{Au}(\text{acac})(\text{PPh}_3)]$  (0.0559 g, 0.1 mmol) and the solution stirred for 2 h. The solution was filtered through celite, the filtrate concentrated under reduced pressure to approximately 1 ml and  $\text{Et}_2\text{O}$  (10 ml) added to precipitate a white solid which was collected and vacuum dried to give the product (0.0577 g, 82%).

## 4.9. Experimental



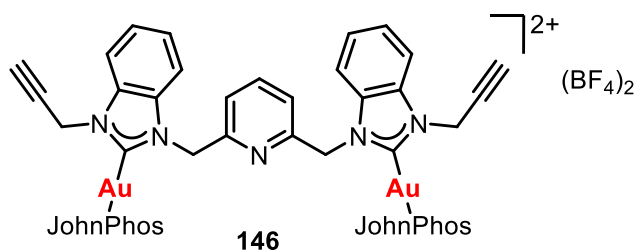
To a solution of **142** (0.0296 g, 0.05 mmol) in  $\text{CH}_2\text{Cl}_2$  (10 ml) was added  $[\text{Au}(\text{acac})(\text{PPh}_3)]$  (0.0559 g, 0.1 mmol) and the solution stirred for 2 h. The solution was filtered through celite, the filtrate concentrated under reduced pressure to approximately 1 ml and  $\text{Et}_2\text{O}$  (10 ml) added to precipitate a white solid which was collected and vacuum dried to give the product (0.0648 g, 86%).



To a solution of **141** (0.0491 g, 0.1 mmol) in  $\text{CH}_2\text{Cl}_2$  (10 ml) was added  $[\text{AuCl}(\text{JohnPhos})]$  (0.1062 g, 0.2 mmol) and  $\text{NBu}_4(\text{acac})$  (0.0683 g, 0.2 mmol) and the solution stirred for 2 h. The solution washed with  $\text{H}_2\text{O}$  (3 x 25 ml), dried over  $\text{Na}_2\text{SO}_4$  and then concentrated under reduced pressure to approximately 1 ml.  $\text{Et}_2\text{O}$  (10 ml) was added to precipitate a white product which was collected and vacuum dried to give the product (0.1898 g, 62%).

**$^1\text{H}$  NMR (300 MHz,  $\text{CD}_2\text{Cl}_2$ )**  $\delta$  7.97 – 6.99 (m, 23H, JohnPhos + Py + imidazole), 6.94 – 6.83 (m, 2H, JohnPhos), 5.21 (s, 4H,  $\text{CH}_2\text{Py}$ ), 4.75 (d,  $^4J_{\text{HH}} = 2.6$  Hz, 4H,  $\text{CH}_2\text{C}\equiv\text{C}$ ), 2.69 (t,  $^4J_{\text{HH}} = 2.6$  Hz, 2H,  $\text{C}\equiv\text{CH}$ ), 1.38 (d,  $^3J_{\text{HP}} = 15.5$  Hz, 36H).

**$^{31}\text{P}\{^1\text{H}\}$  NMR (121 MHz,  $\text{CD}_2\text{Cl}_2$ )**  $\delta$  63.85 (s, JohnPhos).

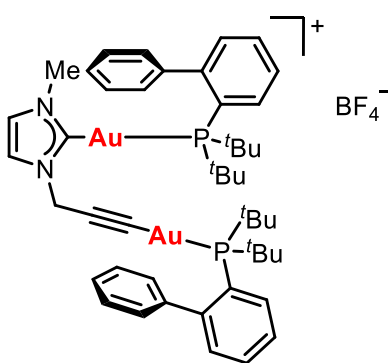


To a solution of **142** (0.0591 g, 0.1 mmol) in  $\text{CH}_2\text{Cl}_2$  (10 ml) was added  $[\text{AuCl}(\text{JohnPhos})]$  (0.1062 g, 0.2 mmol) and  $\text{NBu}_4(\text{acac})$  (0.0683 g, 0.2 mmol) and the solution stirred for 2 h.

The solution washed with H<sub>2</sub>O (3 x 25 ml), dried over Na<sub>2</sub>SO<sub>4</sub> and then concentrated under reduced pressure to approximately 1 ml. Et<sub>2</sub>O (10 ml) was added to precipitate a white product which was collected and vacuum dried to give the product (0.2055 g, 65%).

**<sup>1</sup>H NMR (300 MHz, CD<sub>2</sub>Cl<sub>2</sub>)** δ 7.96 – 7.48 (m, 6H, JohnPhos), 7.39 – 7.15 (m, 21H, JohnPhos + Py + Benzimidazole), 6.72 – 6.64 (m, 2H, JohnPhos), 5.46 (s, 4H, CH<sub>2</sub>Py), 4.99 (d, <sup>4</sup>J<sub>HH</sub> = 2.6 Hz, 4H, CH<sub>2</sub>C≡C), 2.65 (t, <sup>4</sup>J<sub>HH</sub> = 2.6 Hz, 2H, C≡CH), 1.39 (d, <sup>3</sup>J<sub>HP</sub> = 15.6 Hz, 36H, <sup>t</sup>Bu).

**<sup>31</sup>P{<sup>1</sup>H} NMR (121 MHz, CD<sub>2</sub>Cl<sub>2</sub>)** δ 63.68 (s, JohnPhos).



**147**

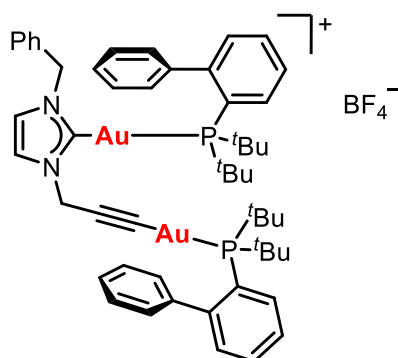
To a solution of **99** (0.0201 g, 0.1 mmol) in methanol (10 ml) was added [AuCl(JohnPhos)] (0.1062 g, 0.2 mmol) and excess potassium hydroxide and the solution stirred for 24 h. Solvent was removed under reduced pressure and the solid residue dissolved in CH<sub>2</sub>Cl<sub>2</sub> (15 ml). The solution was filtered through celite, the filtrate concentrated under reduced pressure to approximately 1 ml and Et<sub>2</sub>O (10 ml) added to precipitate a white solid which was collected and vacuum dried to give the product (0.0953 g, 80%).

**HRMS (ESI/QTOF) m/z:** [M]<sup>+</sup> Calcd for C<sub>47</sub>H<sub>61</sub>Au<sub>2</sub>N<sub>2</sub>P<sub>2</sub> 1109.3636; Found 1109.3650.

**<sup>1</sup>H NMR (400 MHz, CD<sub>2</sub>Cl<sub>2</sub>)** δ 7.96 – 7.84 (m, 4H, JohnPhos), 7.63 – 7.13 (m, 16H, JohnPhos + CH imidazole), 4.67 (d, <sup>5</sup>J<sub>HP</sub> = 1.6 Hz, 2H, CH<sub>2</sub>), 3.65 (s, 3H, Me), 1.46 (d, <sup>3</sup>J<sub>HP</sub> = 15.4 Hz, 18H, <sup>t</sup>Bu), 1.37 (d, <sup>3</sup>J<sub>HP</sub> = 15.0 Hz, 18H, <sup>t</sup>Bu).

**<sup>31</sup>P{<sup>1</sup>H} NMR (162 MHz, CD<sub>2</sub>Cl<sub>2</sub>)** δ 63.98 (s, JohnPhos), 63.86 (s, JohnPhos).

## 4.9. Experimental



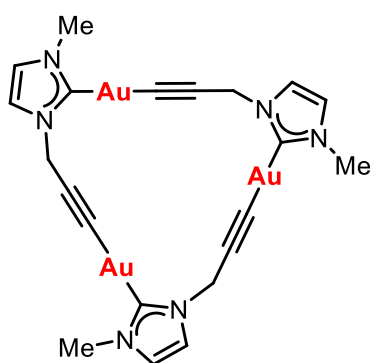
**148**

To a solution of **100** (0.0277 g, 0.1 mmol) in methanol (10 ml) was added [AuCl(JohnPhos)] (0.1062 g, 0.2 mmol) and excess potassium hydroxide and the solution stirred for 24 h. Solvent was removed under reduced pressure and the solid residue dissolved in CH<sub>2</sub>Cl<sub>2</sub> (15 ml). The solution was filtered through celite, the filtrate concentrated under reduced pressure to approximately 1 ml and Et<sub>2</sub>O (10 ml) added to precipitate a white solid which was collected and vacuum dried to give the product (0.0940 g, 74%).

**HRMS (ESI/QTOF) m/z:** [M]<sup>+</sup> Calcd for C<sub>53</sub>H<sub>65</sub>Au<sub>2</sub>N<sub>2</sub>P<sub>2</sub> 1185.3949; Found 1185.3899.

**<sup>1</sup>H NMR (400 MHz, CD<sub>2</sub>Cl<sub>2</sub>)** δ 7.94 – 7.86 (m, 2H, JohnPhos), 7.63 – 7.12 (m, 22H, JohnPhos + Ph + CH imidazole), 5.16 (s, 2H, CH<sub>2</sub>Ph), 4.72 (d, <sup>5</sup>J<sub>HP</sub> = 1.7 Hz, 2H, CH<sub>2</sub>C≡C), 1.39 (d, <sup>3</sup>J<sub>HP</sub> = 15.0 Hz, 18H, <sup>t</sup>Bu), 1.38 (d, <sup>3</sup>J<sub>HP</sub> = 15.0 Hz, 18H, <sup>t</sup>Bu).

**<sup>31</sup>P{<sup>1</sup>H} NMR (162 MHz, CD<sub>2</sub>Cl<sub>2</sub>)** δ 63.97 (s, JohnPhos), 63.96 (s, JohnPhos).



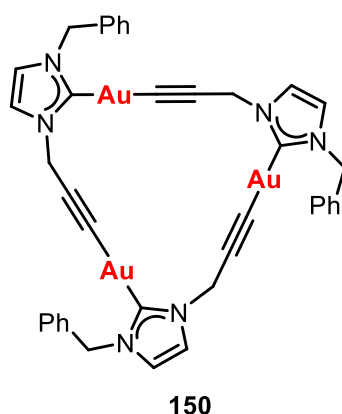
**149**

To a solution of **103** (0.0397 g, 0.1 mmol) in CH<sub>2</sub>Cl<sub>2</sub> (5 ml) was added diisopropylamine (0.0350 ml, 0.25 mmol) and CuI (2 mg) and the mixture stirred for 2 h. A pale yellow precipitate formed which was collected by vacuum filtration, washed with distilled water (20 ml) and acetone (20 ml) and vacuum dried to give the product (0.0242 g, 77%).

**HRMS (ESI-QTOF) m/z:**  $[M + 3\text{MeOH} + \text{Na}]^+$  Calcd for  $\text{C}_{24}\text{H}_{33}\text{Au}_3\text{N}_6\text{O}_3\text{Na}$  1067.1503; Found 1067.1523.

**$^1\text{H}$  NMR (400 MHz, DMSO)**  $\delta$  7.52 (s, 1H, CH), 7.45 (s, 1H, CH), 5.14 (s, 2H,  $\text{CH}_2$ ), 3.85 (s, 3H,  $\text{CH}_3$ ).

**$^{13}\text{C}$  APT (75 MHz, DMSO)**  $\delta$  182.74 (s, N-C-N), 122.45 (s, CH), 122.18 (s, CH), 102.90 (s,  $\text{C}\equiv\text{CH}$ ), 43.29 (s,  $\text{CH}_2$ ), 38.01 (s,  $\text{CH}_3$ ).



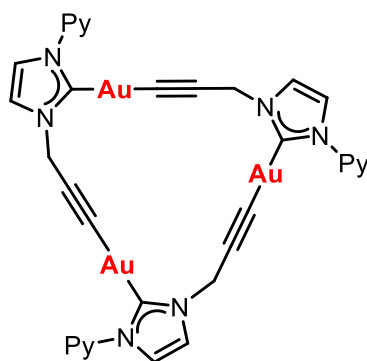
To a solution of **104** (0.0473 g, 0.1 mmol) in  $\text{CH}_2\text{Cl}_2$  (5 ml) was added diisopropylamine (0.0350 ml, 0.25 mmol) and CuI (2 mg) and the mixture stirred for 2 h. A white precipitate formed which was collected by vacuum filtration, washed with distilled water (20 ml) and acetone (20 ml) and vacuum dried to give the product (0.0255 g, 65%).

**HRMS (ESI-QTOF) m/z:**  $[M + \text{Na}]^+$  Calcd for  $\text{C}_{39}\text{H}_{33}\text{Au}_3\text{N}_6\text{Na}$  1199.1655; Found 1199.1721.

**$^1\text{H}$  NMR (400 MHz, DMSO)**  $\delta$  7.54-7.28 (m, 7H, 2CH + Ph), 5.30 (s, 2H,  $\text{CH}_2$ ), 5.17 (s, 2H,  $\text{CH}_2$ ).

Compound too insoluble to obtain  $^{13}\text{C}$  NMR spectrum.

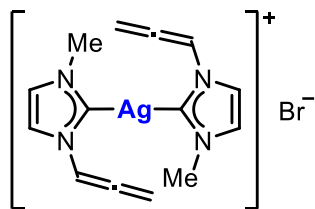


**151**

To a solution of **106** (0.0460 g, 0.1 mmol) in  $\text{CH}_2\text{Cl}_2$  (5 ml) was added diisopropylamine (0.0350 ml, 0.25 mmol) and CuI (2 mg) and the mixture stirred for 2 h. A white precipitate formed which was collected by vacuum filtration, washed with distilled water (20 ml) and acetone (20 ml) and vacuum dried to give the product (0.0311 g, 82%).

**HRMS (ESI-QTOF) m/z:**  $[\text{M} + \text{Na}]^+$  Calcd for  $\text{C}_{33}\text{H}_{24}\text{Au}_3\text{N}_9\text{Na}$  1160.1043; Found 1160.1031.

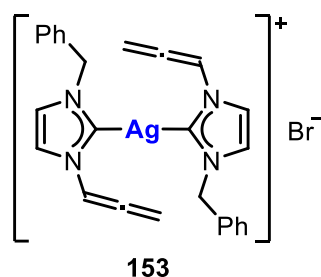
Compound too insoluble to obtain NMR spectra.

**152**

To a solution of **99** (0.0804 g, 0.4 mmol) in  $\text{CH}_2\text{Cl}_2/\text{MeOH}$  (5:1) (5 ml), was added  $\text{Ag}_2\text{O}$  (0.0534 g, 0.23 mmol) and the mixture was stirred for 5 h protected from light. The solution was filtered through celite, the filtrate concentrated under reduced pressure to approximately 1 ml and  $\text{Et}_2\text{O}$  (10 ml) added to precipitate a white solid which was collected and vacuum dried to give the product (0.0575 g, 67%).

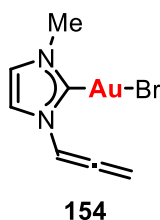
**$^1\text{H}$  NMR (300 MHz,  $\text{CD}_2\text{Cl}_2$ )**  $\delta$  7.35 (t,  $^4J_{\text{HH}} = 6.4$  Hz, 1H,  $\text{CH}=\text{C}$ ), 7.17 (d,  $^3J_{\text{HH}} = 1.9$  Hz, 1H,  $\text{CH}$  imidazole), 7.05 (d,  $^3J_{\text{HH}} = 1.9$  Hz, 1H,  $\text{CH}$  imidazole), 5.68 (d,  $^4J_{\text{HH}} = 6.4$  Hz, 2H,  $\text{CH}_2$ ), 3.87 (s, 3H, Me).

**$^{13}\text{C}$  APT (75 MHz,  $\text{CD}_2\text{Cl}_2$ )**  $\delta$  123.35 (s, CH imidazole), 119.67 (s, CH imidazole), 101.26 (s, CH), 90.08 (s,  $\text{CH}_2$ ), 39.76 (s, Me).



To a solution of **100** (0.0554 g, 0.2 mmol) in CH<sub>2</sub>Cl<sub>2</sub>/MeOH (5:1) (5 ml), was added Ag<sub>2</sub>O (0.0267 g, 0.12 mmol) and the mixture was stirred for 5 h protected from light. The solution was filtered through celite, the filtrate concentrated under reduced pressure to approximately 1 ml and Et<sub>2</sub>O (10 ml) added to precipitate a white solid which was collected and vacuum dried to give the product (0.0412 g, 71%).

**<sup>1</sup>H NMR (400 MHz, CDCl<sub>3</sub>)** δ 5.87 (t, <sup>4</sup>*J*<sub>HH</sub> = 6.4 Hz, 1H, CH), 5.59 – 5.26 (m, 5H, Ph), 5.19 (d, <sup>3</sup>*J*<sub>HH</sub> = 1.9 Hz, 1H, CH imidazole), 5.02 (d, <sup>3</sup>*J*<sub>HH</sub> = 1.9 Hz, 1H, CH imidazole), 3.72 (d, <sup>4</sup>*J*<sub>HH</sub> = 6.4 Hz, 2H, CH<sub>2</sub>=C), 3.38 (s, 2H, CH<sub>2</sub>Ph).

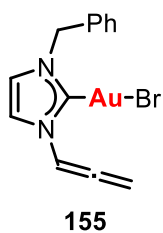


To a solution of **152** (0.0428 g, 0.1 mmol) in CH<sub>2</sub>Cl<sub>2</sub> (5 ml) was added [AuCl(tht)] (0.0641 g, 0.2 mmol) and the mixture stirred for 2 h. The solution was filtered through celite, the filtrate concentrated under reduced pressure to approximately 1 ml and Et<sub>2</sub>O (10 ml) added to precipitate a white solid which was collected and vacuum dried to give the product (0.0197 g, 99%).

**<sup>1</sup>H NMR (400 MHz, CDCl<sub>3</sub>)** δ 7.56 (t, <sup>4</sup>*J*<sub>HH</sub> = 6.4 Hz, 1H, CH=C), 7.13 (d, <sup>3</sup>*J*<sub>HH</sub> = 2.0 Hz, 1H, CH imidazole), 6.98 (d, <sup>3</sup>*J*<sub>HH</sub> = 2.0 Hz, 1H, CH imidazole), 5.64 (d, <sup>4</sup>*J*<sub>HH</sub> = 6.4 Hz, 2H, CH<sub>2</sub>), 3.86 (s, 3H, Me).

#### 4.9. Experimental

---



To a solution of **153** (0.0508 g, 0.1 mmol) in  $\text{CH}_2\text{Cl}_2$  (5 ml) was added  $[\text{AuCl}(\text{tht})]$  (0.0641 g, 0.2 mmol) and the mixture stirred for 2 h. The solution was filtered through celite, the filtrate concentrated under reduced pressure to approximately 1 ml and  $\text{Et}_2\text{O}$  (10 ml) added to precipitate a white solid which was collected and vacuum dried to give the product (0.0469 g, 99%).

**$^1\text{H}$  NMR (400 MHz,  $\text{CD}_2\text{Cl}_2$ )**  $\delta$  7.59 (t,  $^4J_{\text{HH}} = 6.4$  Hz, 1H,  $\text{CH}=\text{C}$ ), 7.49 – 7.31 (m, 5H, Ph), 7.16 (d,  $^3J_{\text{HH}} = 2.1$  Hz, 1H,  $\text{CH}$  imidazole), 6.97 (d,  $J = 2.1$  Hz, 1H,  $\text{CH}$  imidazole), 5.66 (d,  $^4J_{\text{HH}} = 6.4$  Hz, 2H,  $\text{CH}_2=\text{C}$ ), 5.39 (s, 2H,  $\text{CH}_2\text{Ph}$ ).



# Chapter 5 – Propargyl Gold Complexes

## 5.1. Introduction

Propargyl gold complexes are those in which the gold centre is coordinated by one or more alkynyl type ligands of the form  $R_nY-CH_2C\equiv C^-$  where Y is a heteroatom (Figure 5.1).

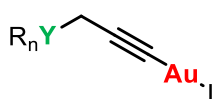


**Figure 5.1.** Propargyl gold complex general structure.

Alkynyl gold(I) complexes have been known for many years, in fact, gold acetylide was one of the earliest examples of a gold complex with a gold-carbon bond, reported by Berthelot in 1866,<sup>309</sup> although this is generally not considered an organogold complex since acetylide is isoelectronic with cyanide ( $N\equiv C^-$ ) or carbon monoxide (CO) and interpreted as a pseudohalide ligand. Later, in the 1960s and 70s, alkynyl gold(I) complexes bearing a phosphine ligand were prepared by the groups of Coates and Parkin<sup>34,45</sup> as well as by Mitchell and Stone.<sup>310</sup> Such complexes tend to exhibit remarkable stability due to the high bond dissociation energies around the gold centre. Alkynyl ligands are strong  $\sigma$ - and  $\pi$ - donors and recent studies combining photoelectron spectroscopy and theoretical calculations found the gold-carbon bond in alkynyl gold complexes to be one of the strongest gold-ligand bonds known.<sup>311</sup>

Alkynyl gold(I) complexes have been widely studied for their use in luminescence,<sup>312-316</sup> catalysis and materials science,<sup>317-321</sup> however only recently have their potential biological applications begun to be realised. The high stability of these complexes under physiological conditions overcomes one of the main issues in the development of new metallodrugs: their tendency to decompose due to reaction with biologically occurring reducing agents such as thiols. Initial studies show promising results for the antiproliferative activity of alkynyl gold(I) phosphine complexes in a variety of different cancer cell lines and hence they could make excellent chemotherapeutic agents. Propargyl gold(I) complexes show the same high stability as the simpler alkynyl gold(I) complexes but the introduction of a heteroatom provides the

possibility to make changes to the molecular scaffold to give improved properties such as luminescence, solubility or even an additional coordination site for the synthesis of di- or polynuclear propargyl gold(I) complexes. The relatively simple syntheses of the propargyl functionalised ligands and their corresponding gold(I) phosphine derivatives means that such complexes have huge potential in the development of new gold-based cancer treatments.

### 5.1.1. History of Gold in Medicine

The use of gold in medicine is not new. The earliest medicinal use of gold is generally attributed to the ancient Chinese around 2500 BC where elemental gold was reportedly used by physicians and surgeons to treat a variety of different ailments. In 8<sup>th</sup> century Europe the alchemists attempted to prepare elixirs of life containing metallic gold in the form of a powder or flakes, which they believed would cure all diseases and confer eternal youth. By the 13<sup>th</sup> century it was known that gold could be dissolved in aqua regia and it became possible to prepare drinkable gold or *aurum potabile*, a mixture of gold dissolved in aqua regia and diluted with oil of rosemary or other essential oils which was recommended for the treatment of leprosy. Seventeenth century pharmacopoeias describe the use of gold for treatment of ailments caused by a decrease in the ‘vital spirits’ such as melancholy, fainting and fever, and in the early 19<sup>th</sup> century a mixture of gold chloride and sodium chloride, Na[AuCl<sub>4</sub>], was used to treat syphilis.<sup>322</sup> Towards the end of the nineteenth century this same compound was prescribed as a treatment for chronic alcoholism. Despite the long history of the use of gold in medicine and the common belief that this metal possessed some form of healing properties, there was little or no biochemical basis for any of these historical treatments and it is unlikely that any of them were successful.

The breakthrough for the use of gold in modern medicine came in 1890 with the discovery by German bacteriologist, Robert Koch, that potassium dicyanoaurate, K[Au(CN)<sub>2</sub>] is bacteriostatic towards tubercle bacillus, *mycobacterium tuberculosis*, the microorganism responsible for tuberculosis. He described it as the most effective of all known antiseptics with an activity *in vitro* at a dilution of one part in two million.<sup>323</sup> The development of gold compounds for the treatment of tuberculosis soon followed. Although K[Au(CN)<sub>2</sub>] proved to some extent to be an effective treatment, there were many serious toxic side effects, leading scientists too look for alternatives. In 1913 Feldt confirmed that it was the gold, rather than the

## 5.1. Introduction

cyanide, which caused  $\text{K}[\text{Au}(\text{CN})_2]$  to be toxic to mycobacteria and he introduced sodium 4-amino-2-aurothiosalicylate (Krysolgan<sup>TM</sup>) as an alternative.<sup>324</sup> Gold(I) thiolates were found to be more stable in solution and far less toxic than  $\text{K}[\text{Au}(\text{CN})_2]$ . Other early examples include sodium aurothiosulfate (Sanocrysin<sup>TM</sup>), sodium aurothiomalate (Myocrysin<sup>TM</sup>), sodium aurothiopropanol sulfonate (Allocrysin<sup>TM</sup>) and aurothioglucose (Solganol-B-Oleosum<sup>TM</sup>) (Figure 5.2).

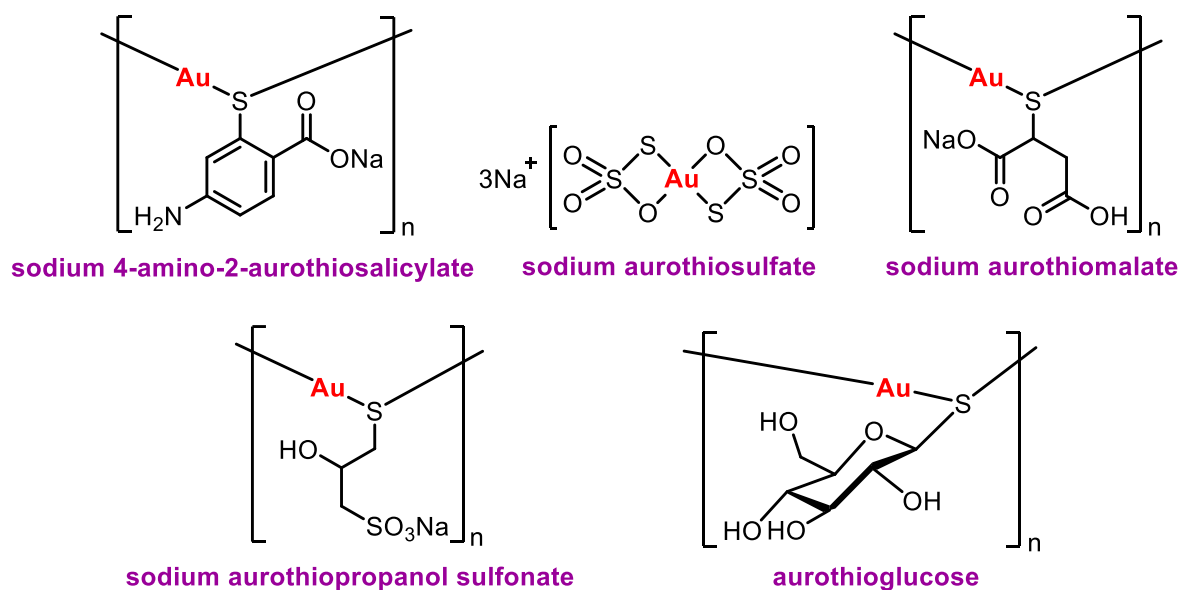


**Figure 5.2.** Early gold based treatments.

The incorrect but serendipitous assumption by Forestier in the early 1930s that tubercle bacillus was also linked to rheumatoid arthritis led to the administration of these gold-based treatments to patients with that disease. By the mid-1930s their use in the treatment of tuberculosis had stopped due to the lack of efficacy and numerous side effects, however, they were found to be very effective at slowing the progression of rheumatoid arthritis. Controlled trials by the Empire Rheumatism Council in 1960 confirmed these findings and since then, gold-based drugs have found use in both the treatment of rheumatoid arthritis as well as other rheumatic diseases such as juvenile rheumatoid arthritis and psoriatic arthritis.

The early gold(I) thiolates sodium 4-amino-2-aurothiosalicylate, sodium aurothiomalate, sodium aurothiopropanol sulfonate and aurothioglucose are coordination polymers formed by the thiolate group bridging two gold(I) ions. Despite their polymeric structure, the functional

groups present in these derivatives result in the compounds being water soluble. Sodium aurothiosulfate, while also bearing thiolate-type sulfur atoms bound to the gold(I) which could potentially participate in bridges, is found to have a monomeric structure. All of these water-soluble gold complexes have a low lipophilicity and are not well absorbed from the gut. Consequently, they have to be administered to patients by injection as an aqueous solution. In the 1970s and early 1980s Sutton and co-workers made another breakthrough with the development of auranofin, a gold phosphine compound, which could be administered orally to patients in the form of capsules and was approved for treatment in 1985.

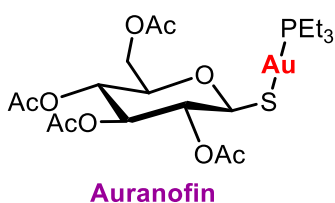


**Figure 5.3.** Structure of auranofin.

Auranofin or [2,3,4,6-tetra-O-acetyl-1-thio- $\beta$ -D-glucopyranosato-S-(triethylphosphine)gold] (Ridaura<sup>TM</sup>) (Figure 5.3) is a monomeric thiolate gold complex with limited water solubility but it has a high lipophilicity due to the triethylphosphine ligand. The possibility for the oral administration of this drug initially made it more popular than the traditional injectable gold(I) thiolate compounds and only mild side effects were observed. However, it was later found that auranofin was somewhat less effective than the injectable gold-based drugs for the treatment of rheumatoid arthritis and although it is still in clinical use today, alternative more effective and better tolerated rheumatoid arthritis treatments such as methotrexate have become more popular.

Rheumatoid arthritis is now known to be an autoimmune disorder which leads to an inflammation of the joints. Auranofin and other gold compounds halt or slow down the progression of this disease and reduce bone and cartilage damage by interfering with the body's immune system, although their exact mode of action is not well understood. Auranofin also exhibits anti-cancer activity and it is often cited that early studies into the cytotoxicity of auranofin and other gold complexes initiated following the success of cisplatin and as part of an ongoing investigation into alternative metal-based drugs. However, this is not the only



reason that led scientists to study the anti-cancer activity of the anti-arthritis drug. In the 1970s and 80s studies were also being carried out into the potential use of the known anti-cancer drugs, 6-mercaptopurine and cyclophosphamide, for the treatment of rheumatoid arthritis due to their known immunosuppressive and anti-inflammatory actions.<sup>325</sup> This work established an initial connection between the two diseases, and later, a long-term study into the mortality rates of patients suffering from rheumatoid arthritis and undergoing treatment with gold-based drugs found they had lower instances of malignant tumours than the rest of the population, leading scientists to believe there could be a connection between gold drugs and cancer.

Cell growth inhibition studies in 1979 unexpectedly found auranofin to show potent anti-cancer activity against HeLa cells *in vitro*,<sup>326</sup> prompting further studies with other cell lines. When compared to cisplatin, auranofin was found to show similar or greater cytotoxicity against a variety of different cell lines *in vitro*<sup>327,328</sup> and good *in vivo* efficacy against P388 lymphocytic leukaemia cells implanted in mice.<sup>329</sup> Subsequent screening of auranofin in various different cancer cell lines found a limited spectrum of anti-tumour activity but further studies into related gold-based anti-cancer treatments and their potential mode of action soon followed. In 1986 a comprehensive review of the anti-cancer properties of auranofin and structurally related analogues was published in which 62 different gold complexes were tested for *in vitro* cytotoxicity against B16 melanoma and P388 leukaemia cells, concluding that a wide variety of phosphine gold(I) thiolates display cytotoxicity.<sup>330</sup> Many promising classes of gold(I) compounds with anti-cancer activity have now been described including in addition to auranofin analogues (phosphine gold(I) thiolates), gold(I) complexes with multiple phosphine ligands, gold(I) phosphole compounds, gold(I) carbene complexes, gold(I) thiourea complexes and, more recently, alkynyl and propargyl gold(I) complexes (Figure 5.4).

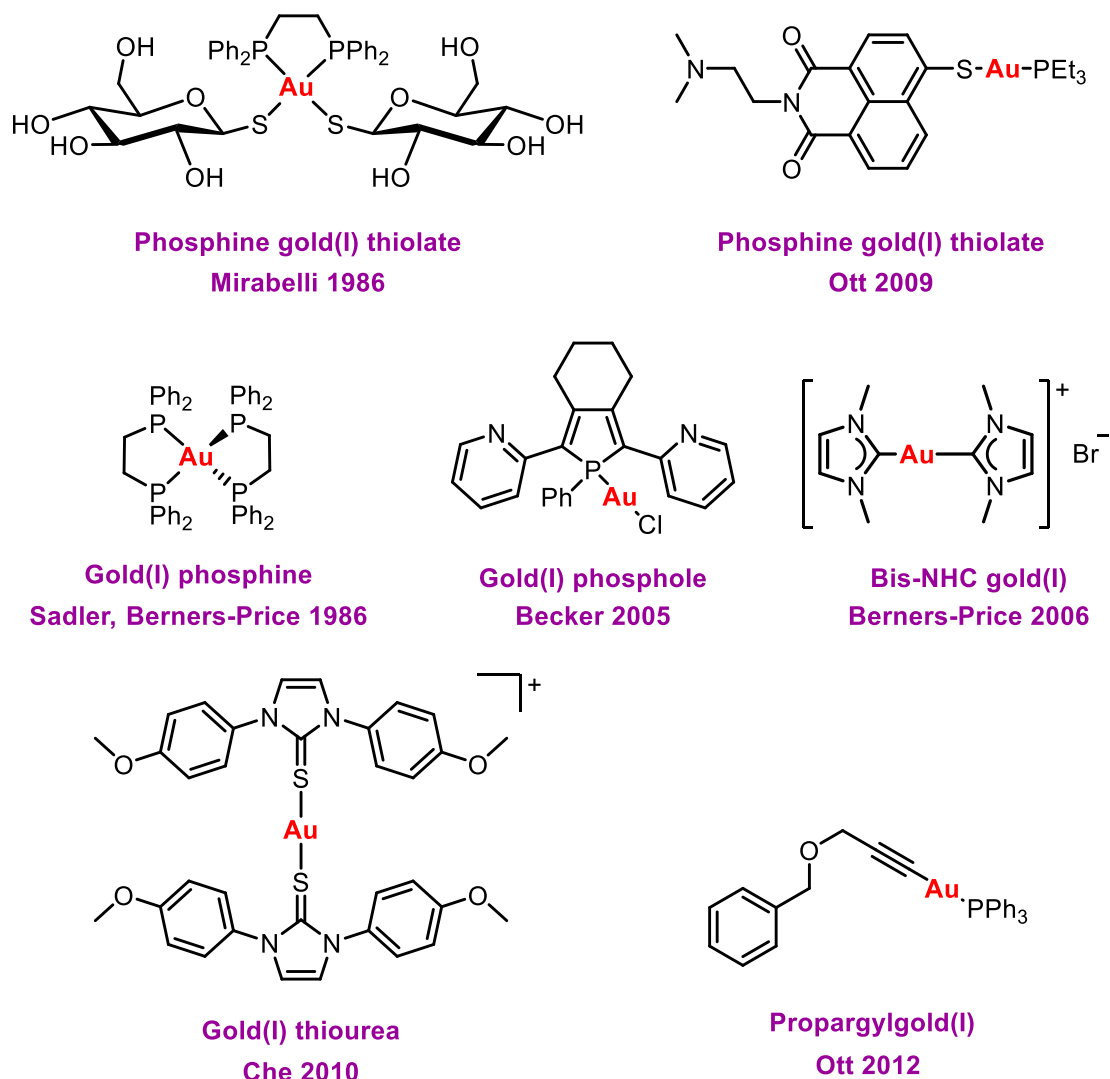


**Figure 5.4.** Gold(I) complexes with biological activity.

### 5.1.2. Mechanism of Action of Anti-Cancer Gold(I) Complexes

Many studies suggest that square planar anti-cancer metal complexes such as cis-platin and the iso-electronic gold(III) compounds exert cytotoxicity by targeting DNA, interfering with the transcription and replication processes and consequently leading to apoptosis of the cells. Gold(I) complexes, however, are believed to have a very different mode of action and their cytotoxicity most likely arises as a result of antimetochondrial action. Understanding the specific mode of action of auranofin and other antirheumatic and antitumoral gold(I) complexes has been of interest for many years, and while it is generally accepted that a single mode of action unlikely exists, the enzyme thioredoxin reductase (TrxR) does seem likely to be a main biological target.

## 5.1. Introduction

TrxR is a homodimeric flavoprotein which helps to regulate the redox state of the cell by redox homeostasis, maintaining the correct balance between oxidised and reduced forms of intracellular thiol containing compounds, mainly the NADPH dependent reduction of thioredoxin disulfide (Trx). The crystal structure of TrxR was determined in 2007, allowing the mode of action of this enzyme to be established. Each monomer of TrxR features an NADPH binding site, an FAD unit and an active site featuring a cysteine residue (Cys497) adjacent to a selenocysteine residue (Cys498) and in close proximity to two further cysteine residues (Cys59 and Cys64) (Figure 5.5). Electrons are transferred from NADPH via FAD to the active site of TrxR which can then reduce a substrate.

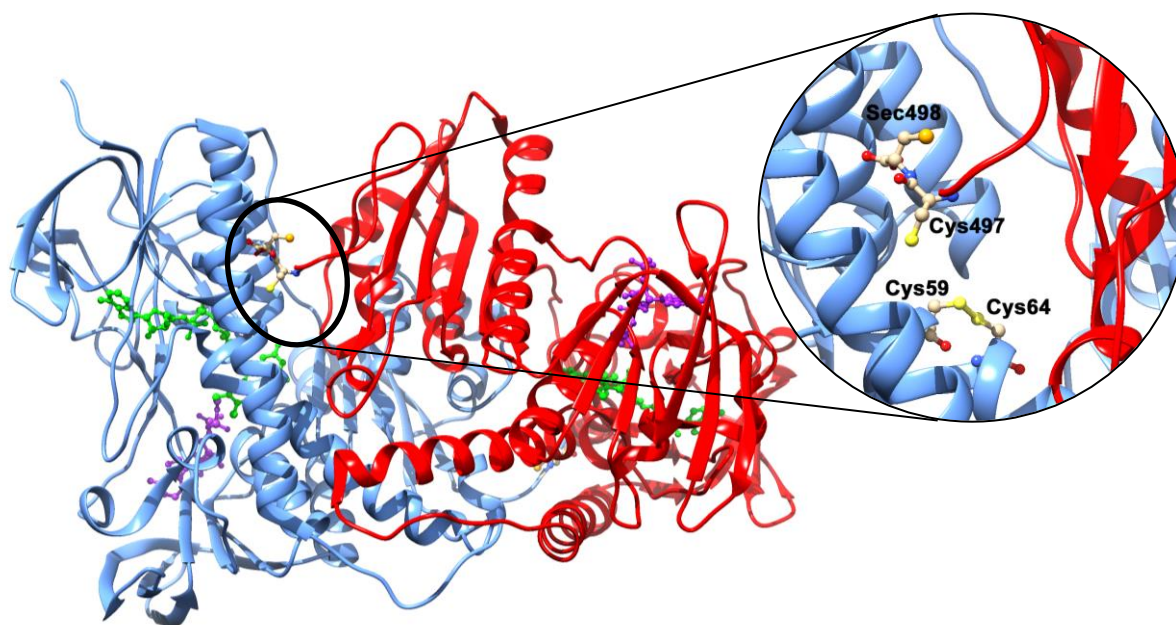


**Figure 5.5.** Ribbon representation of TrxR dimer (PDB entry 3ean) showing bound NADP<sup>+</sup> (purple) and FAD (green). The figure was obtained using Chimera software.

Cysteine is an amino acid bearing a thiol group and selenocysteine has the same structure but bears a more unusual selenol group (Figure 5.6).

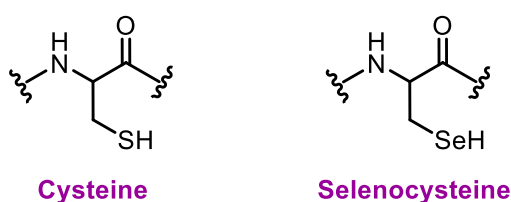
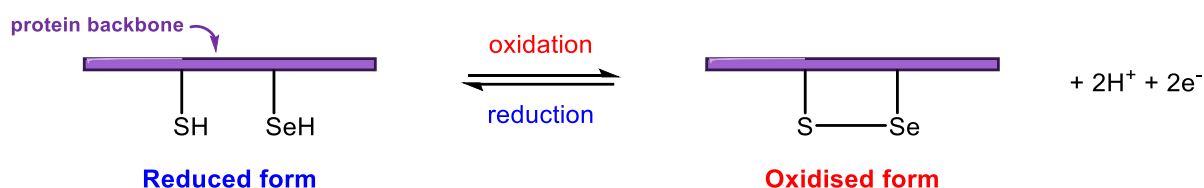


**Figure 5.6.** Structure of cysteine and selenocysteine residues.

The active site of TrxR maintains the redox homeostasis of the cell by changing its own oxidation state. In the fully reduced form, the residues Cys497 and Sec498 are in their thiol and selenol forms respectively, however, upon the reduction of a substrate, such as the oxidised form of Trx, these residues couple forming a selenylsulfide bond (Scheme 5.1). The reduction of Trx is a process essential for life in all mammals since the reduced form of Trx acts as an antioxidant and is known to be involved in several vital redox processes within the cell. Studies have even found that mice which overexpress this enzyme are more resistant to inflammation.

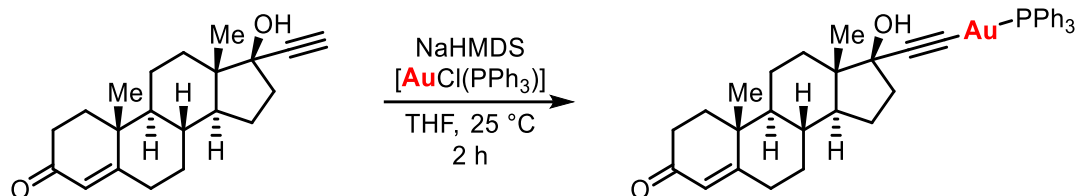


**Scheme 5.1.** Redox mechanism of TrxR active site.

The selenol group in the reduced form of TrxR will readily bind metal ions. Selenol is a soft base and therefore an excellent nucleophile for gold(I), the softest of all acids. The binding of gold to the selenocysteine residue would block the activity of TrxR, resulting in mitochondrial damage, impairing the ability of the enzyme to maintain redox homeostasis and ultimately leading to cell death. The preferred binding of the gold complexes to the selenol group, rather than the thiol group has been confirmed by studies comparing the inhibition of TrxR and glutathione reductase (GR), an enzyme which is structurally and functionally closely related to TrxR but lacks the selenocysteine residue in the active site, in which a much higher affinity was found for TrxR. An overexpression of TrxR has been observed in many tumour cell lines and hence complexes which target this protein specifically could make excellent anti-cancer drugs with selectivity for tumour cells over healthy cells. Research into gold(I) based anti-cancer compounds is therefore of interest.

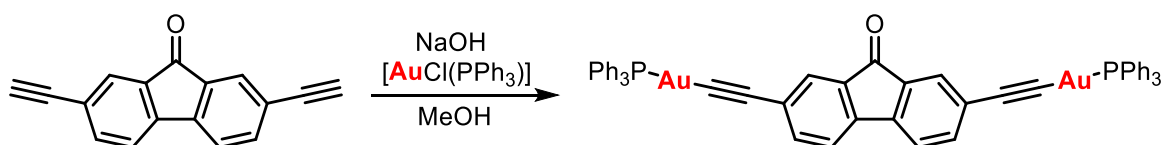
### 5.1.3. Alkynyl Gold(I) Phosphine Complexes with Anti-Cancer Activity

One of the first examples of alkynyl gold(I) phosphine complexes with biological activity was the synthesis of gold(I) triphenylphosphine complexes with ethynyl steroid ligands, reported in 2006. The complexes were prepared from the corresponding alkynyl steroids with NaHMDS and  $[\text{AuCl}(\text{PPh}_3)]$  in THF (Scheme 5.2), and initial reports found promising *in vitro* activities as potential cytostatics.<sup>331</sup>



**Scheme 5.2.** General method for the synthesis of ethynyl steroid gold(I) triphenylphosphine complexes.

A dinuclear diethynylfluorene derivative of gold(I) was found to show significant biological activity both *in vitro* and *in vivo*. The complex was prepared from the diethynyl fluorene by reaction with  $[\text{AuCl}(\text{PPh}_3)]$  in the presence of sodium hydroxide in methanol, resulting in the formation of an air-stable solid with high purity (Scheme 5.3). This complex showed excellent cytotoxicity against three different human cancer cell lines *in vitro* and good antitumour activity *in vivo* in a xenografted nude mice model. Limited adverse effects in vital organs were observed.<sup>332</sup>



**Scheme 5.3.** Synthesis of a dinuclear diethynylfluorene gold(I) triphenylphosphine complex.

In 2009 Mohr and co-workers prepared a series of propargyl gold(I) phosphine complexes from propargyl ethers and  $[\text{AuCl}(\text{PPh}_3)]$  in the presence of KOH. The mononuclear complexes (Figure 5.7) exhibited excellent cytotoxicity in ovarian cancer cell lines CH1 and SK-OV-3 as well as colon cancer cell line SW480 and HeLa cells. Some efficacy against malaria strains was also exhibited.<sup>333</sup>

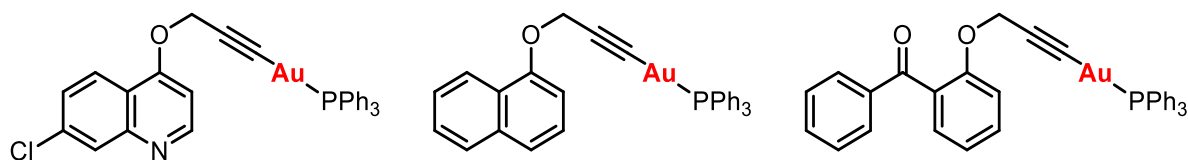


**Figure 5.7.** Gold(I) phosphine complexes with propargyl ether ligands.

Luminescent alkynyl gold(I) complexes containing the water-soluble PTA and DAPTA ligands (Figure 5.8) were reported in 2010. Cellular uptake of the complexes could be confirmed by

fluorescence microscopy. The complexes were found to show cytotoxicity to ovarian cancer cell lines while not showing any reactivity with DNA, as expected for gold(I) complexes.

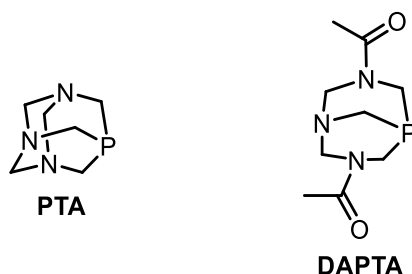
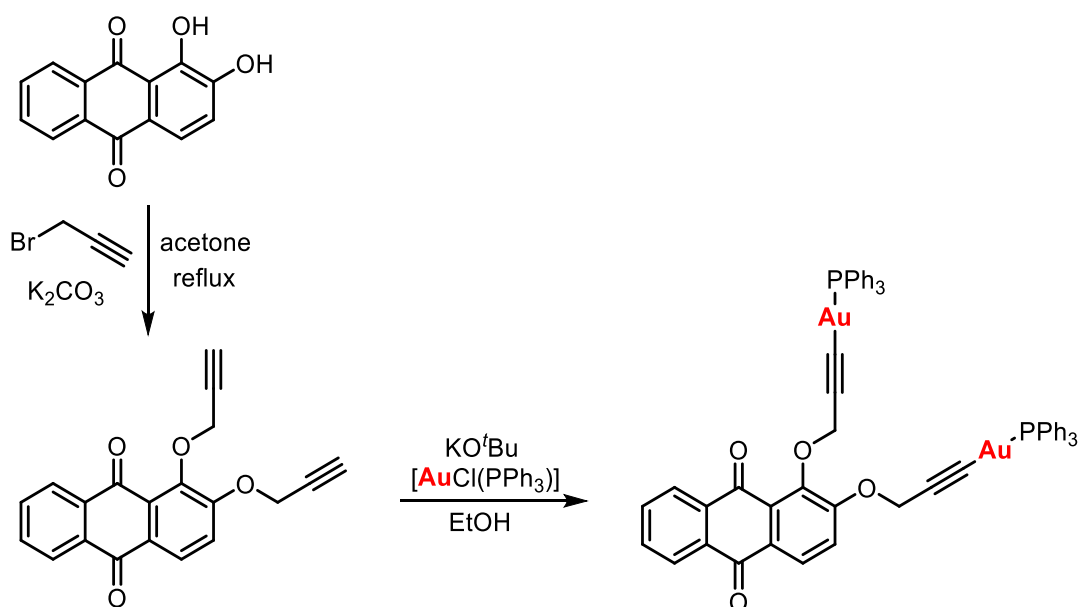


**Figure 5.8.** Structure of water soluble phosphines 1,3,5-triaza-7-phosphaadamantane (PTA) and 3,7-diacetyl-1,3,7-triaza-5-phosphabicyclo[3.3.1]nonane (DAPTA).

In 2012, complexes of gold(I) with propargyl functionalised anthraquinone fluorophores were prepared with a view to exploiting both the biological properties and the photophysical characteristics of the complexes. The ligands were prepared by reaction of the relevant hydroxyanthraquinones with propargyl bromide in the presence of potassium carbonate. The gold complexes were then prepared by reaction of the ligands with  $[\text{AuCl}(\text{PPh}_3)]$  and potassium tert-butoxide in ethanol (Scheme 5.4). Cytotoxicity studies found the complexes to be active against MCF7 cancer cells (breast adenocarcinoma) and cellular uptake could be confirmed by live cell imaging studies.<sup>334</sup>



**Scheme 5.4.** Synthesis of gold(I) triphenylphosphine complexes with propargyl functionalised anthraquinones.

In the same year Ott and co-workers reported six different alkynyl gold(I) triphenylphosphine complexes with anti-proliferative activity (Figure 5.9(a)) which were also found to be potent inhibitors of TrxR.<sup>335</sup> They went on to prepare a series of diphosphine derivatives (Figure 5.9(b)), however these showed little TrxR inhibition and had limited biological application due to their poor water solubility and weak luminescence.<sup>336</sup> Propynyloxycourmarin gold(I) derivatives with water soluble PTA and DAPTA phosphine ligands (Figure 5.9(c)) did show improved water solubility and very strong TrxR inhibition. They were also luminescent due to the chromophore unit; however only low cytotoxicity of the complexes was observed.<sup>337</sup>

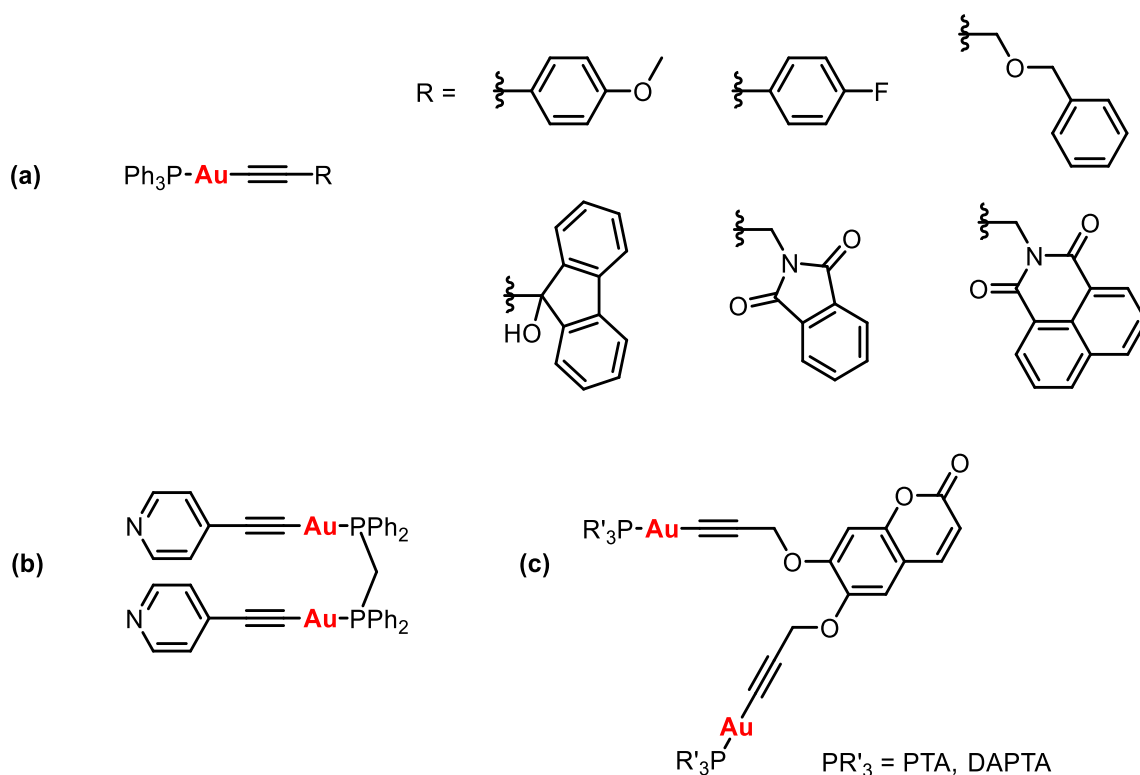
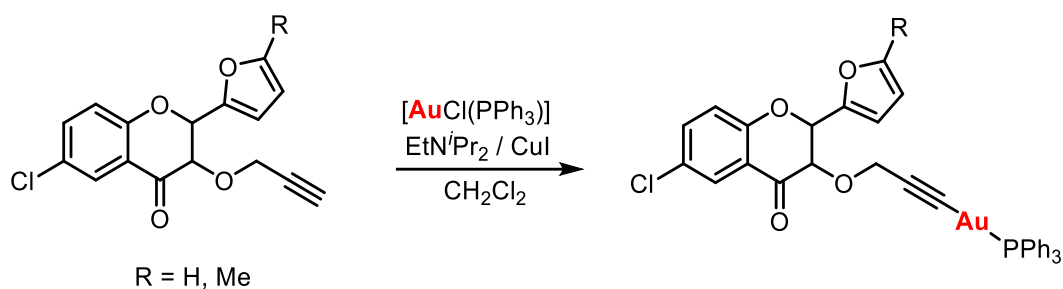


**Figure 5.9.** Alkynyl gold(I) triphenylphosphine derivatives with antiproliferative activity (a), diphosphine derivative (b) and propynyloxycourmarin gold(I) derivatives with water soluble phosphines (c).

In 2015 two complexes were reported in which a gold(I) triphenylphosphine moiety was bound to a flavonoid group via a propargyl ether (Scheme 5.5). The flavonoids themselves were already known to have both *in vitro* and *in vivo* anticancer activities and the addition of the propargyl gold(I) phosphine unit was found to increase the cytotoxicity against human prostate cancer cells.<sup>338</sup>



**Scheme 5.5.** Synthesis of gold(I) triphenylphosphine complexes with propargyl ether functionalised flavonoid ligands.

Very recently significant studies into 4-ethynylanisole gold(I) phosphine derivatives (Figure 5.10) revealed that the nature of the phosphine had no major effect on the observed cytotoxicity of the complex, however, complexes containing phosphines which did not bear a heteroatom appeared to have higher TrxR inhibition. Some solubility issues were encountered for *in vivo* experiments however nanoformulation of the complex in peanut oil resulted in a formulation suitable for injection into mice. Although the low dosages used did not have any significant effects on the tumours being studied, the complexes were all well tolerated.<sup>339</sup>

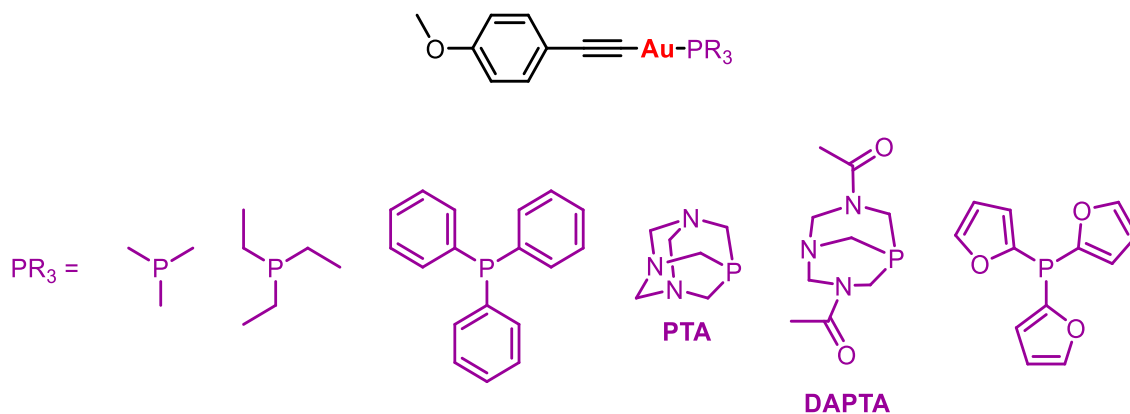


**Figure 5.10.** 4-Ethynylanisole gold(I) phosphine derivatives.

The alkynyl gold(I) phosphine moiety has proven to be a useful organometallic pharmacore which can readily be incorporated into different biologically active groups or chromophore structures to potentially give complexes with anticancer activities and the possibility for the study of the mechanism of action by fluorescence microscopy studies.



## 5.2. Synthesis of Propargyl Functionalised Ligands

Several different propargyl functionalised substrates with different heteroatoms were used for the preparation of the propargyl gold(I) phosphine complexes (Figure 5.11). Some of these were commercially available and others had to be prepared.

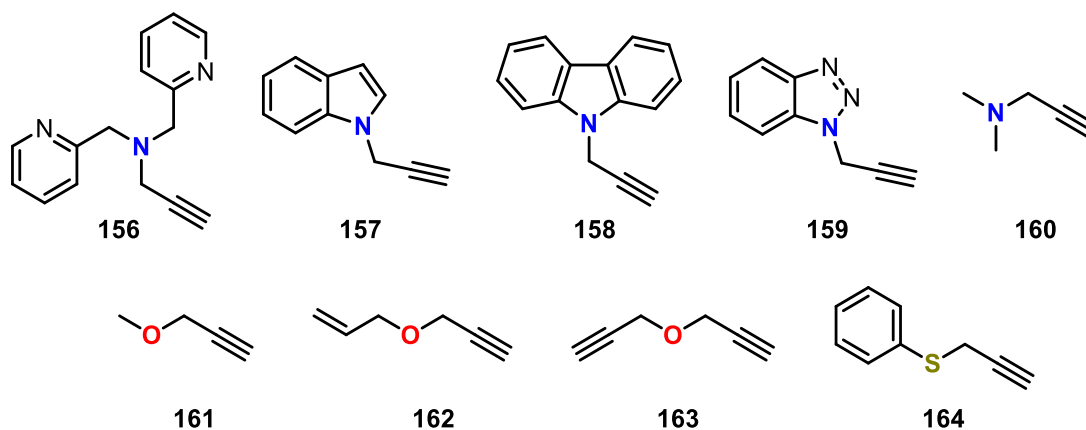
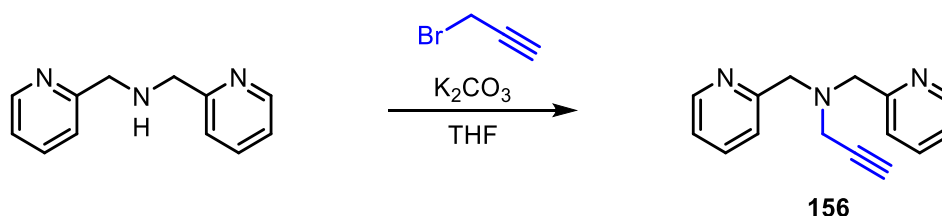


**Figure 5.11.** Propargyl functionalised substrates used for the preparation of gold complexes.

N-propargyl-di(2-picolyl)amine, **156**, was chosen as a suitable substrate since the pyridyl groups could provide an additional coordination site allowing the subsequent preparation of polynuclear complexes which would be likely to exhibit luminescence. This ligand was prepared following a previously reported procedure by reaction of di-(2-picolyl)amine and propargyl bromide in THF in the presence of excess potassium carbonate (Scheme 5.6).<sup>340,341</sup> After stirring overnight under argon the product was obtained in an excellent yield of 96%.



**Scheme 5.6.** Synthesis of N-propargyl-di(2-picolyl)amine

The successful formation of the product could be confirmed by <sup>1</sup>H NMR spectroscopy (Figure 5.12) in which the CH<sub>2</sub> and CH of the propargyl unit are observed as a doublet and a triplet, respectively. The lack of NH signal confirms the successful deprotonation of the amine.

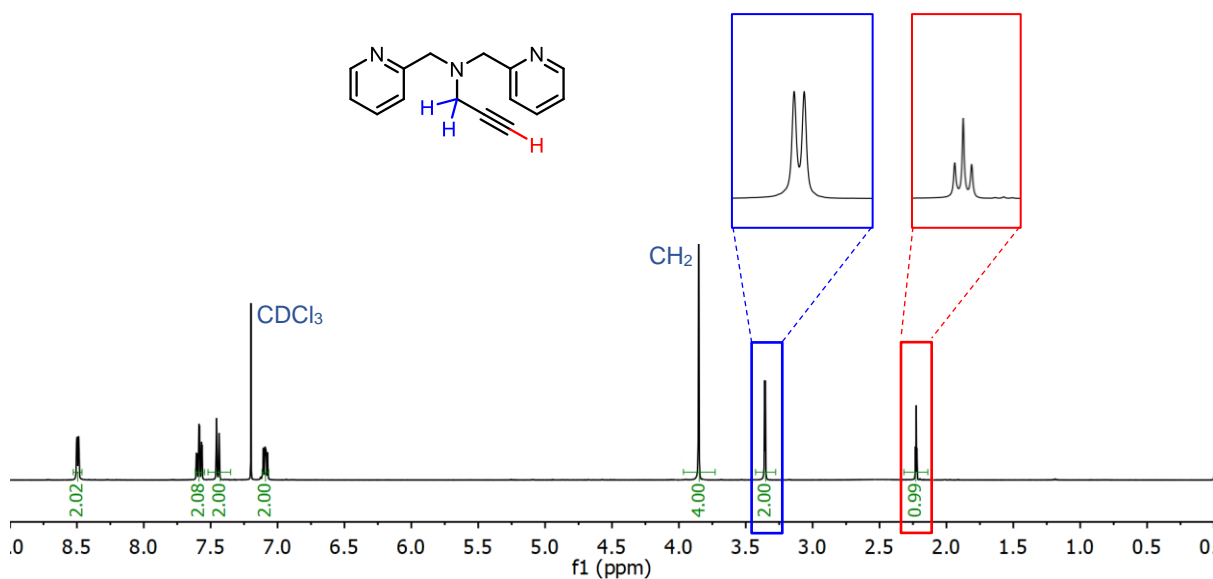
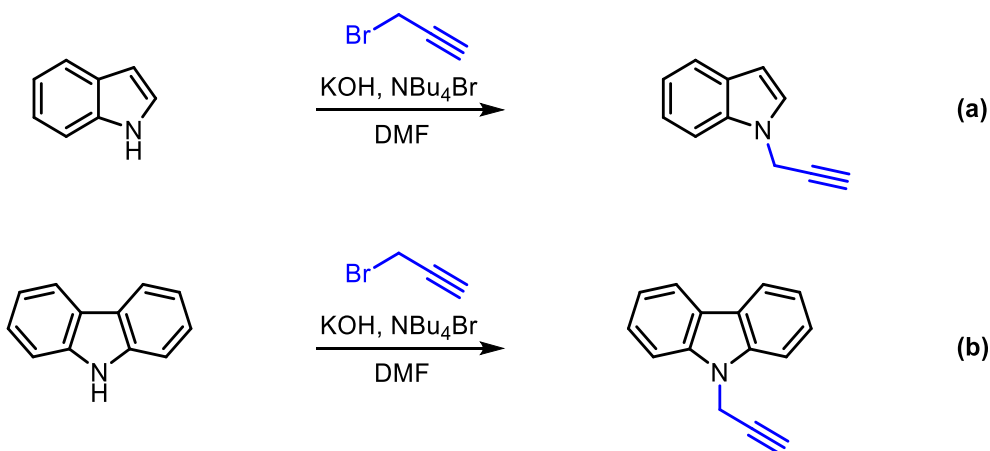


**Figure 5.12.**  $^1\text{H}$  NMR spectrum for N-propargyl-di-(2-picolyl)amine in  $\text{CDCl}_3$  at room temperature.

The propargyl derivatives of indole and carbazole, **157** and **158**, were again prepared by N-alkylation with propargyl bromide, but in these cases a stronger base was required to deprotonate the substrate. Potassium hydroxide in methanol was used and tetrabutylammonium bromide was employed as a phase transfer agent (Scheme 5.7). In both cases, following extraction into ethyl acetate and work-up the products were obtained cleanly and in good yields of 81% and 67%, respectively. The successful formation of the product could be confirmed by the lack of NH signal in the  $^1\text{H}$  NMR spectrum and the presence of a doublet and triplet corresponding to the  $\text{CH}_2$  and  $\text{CH}$  of the propargyl unit.



**Scheme 5.7.** Synthesis of N-propargyl indole (a) and N-propargyl carbazole (b).

## 5.2. Synthesis of Propargyl Functionalised Ligands

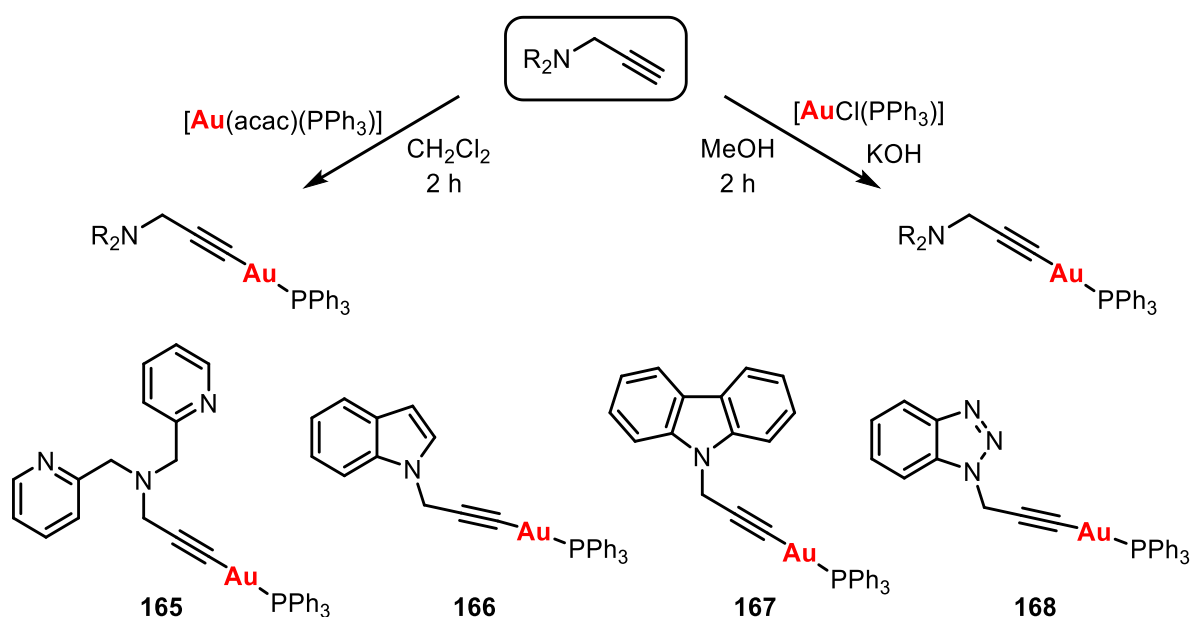
---

N-propargyl indole was selected as a suitable substrate for the preparation of biologically active gold(I) complexes since indole is a common structural motif in nature. Indole derivatives are found in many natural products and indole itself has been isolated from naturally occurring materials. Indole is also found in the liver, pancreas, brain and bile in the human body and hence derivatives of indole are likely to be biocompatible and potentially have some biological activity.<sup>342</sup> N-propargyl carbazole was chosen since carbazole is a known fluorophore and it was therefore hoped that corresponding gold(I) derivatives could exhibit both biological activity and photophysical properties. The other propargyl functionalised substrates, **159-164**, were commercially available and used as purchased

### 5.3. Synthesis of Propargyl Gold(I) Phosphine Complexes

#### 5.3.1. Derivatives with Nitrogen Substrates

Propargyl gold(I) triphenylphosphine derivatives could be prepared by two different methods (Scheme 5.8). Addition of  $[\text{Au}(\text{acac})(\text{PPh}_3)]$  to a solution of the propargyl substrate in dichloromethane led to the formation of the products **165-168**, which could be isolated by concentration of the reaction solution and precipitation with diethyl ether and were obtained in good yields (71-84%).



**Scheme 5.8.** Synthesis of propargyl gold(I) triphenylphosphine derivatives with nitrogen based substrates.

The products could also be prepared by the addition of  $[\text{AuCl}(\text{PPh}_3)]$  and potassium hydroxide to a solution of the substrate in methanol. This method avoids the need to prepare the acac gold(I) precursor and the products are obtained with high purity since they precipitate from the reaction solution. Again, the yields were good (62-81%) and in both methods the reaction times were similar. The second method is perhaps preferable for the due to the ease of isolation of the final products. All of the products were obtained as air-stable white solids.

Successful formation of products **165-168** could be confirmed by the disappearance of the propargyl C-H signal in the  $^1\text{H}$  NMR spectrum (e.g. Figure 5.13(a)). The propargyl  $\text{CH}_2$  signal is now observed as a singlet. In all cases the  $^{31}\text{P}\{^1\text{H}\}$  NMR spectrum showed a single sharp

### 5.3. Synthesis of Propargyl Gold Complexes

peak at around 42 ppm (e.g. Figure 5.13(b)), a typical value for a triphenylphosphine group bound to gold(I) with a *trans* carbon based ligand.

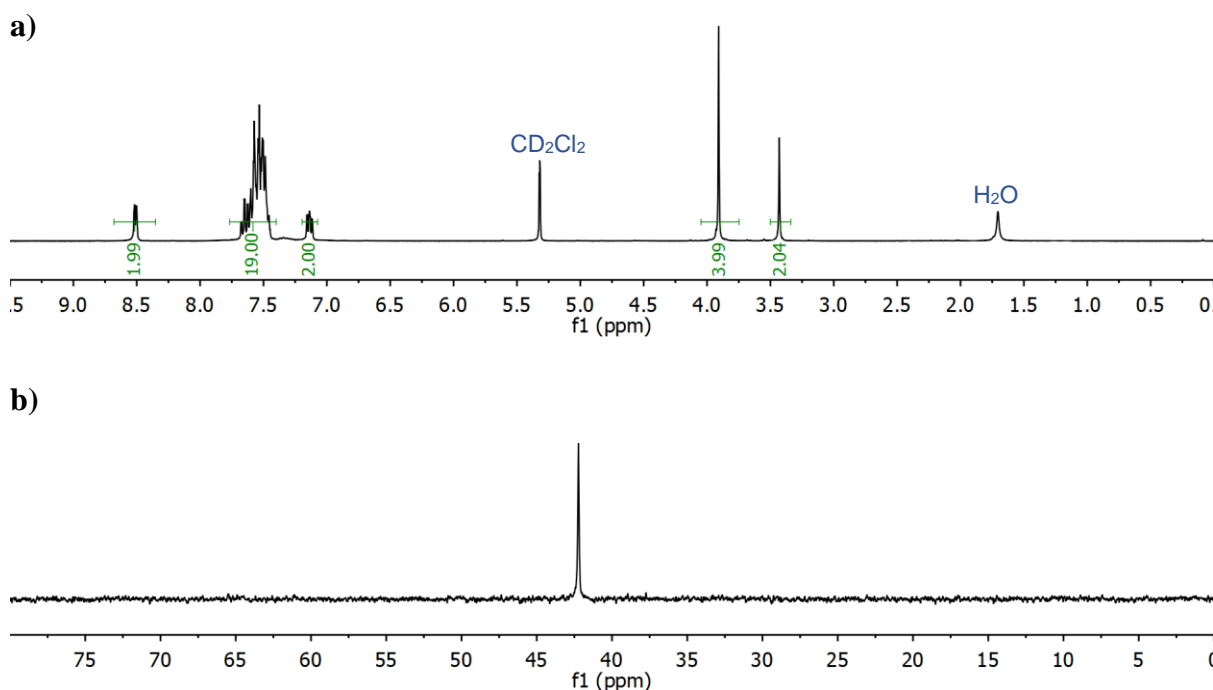


**Figure 5.13.**  $^1\text{H}$  NMR spectrum (a) and  $^{31}\text{P}\{^1\text{H}\}$  NMR spectrum of complex **165** in  $\text{CD}_2\text{Cl}_2$  at room temperature.

**Table 5.1.**  $^{31}\text{P}\{^1\text{H}\}$  NMR signals (162 MHz) in  $\text{CD}_2\text{Cl}_2$  at room temperature

Complex	$^{31}\text{P}\{^1\text{H}\}$ NMR (ppm)
<b>165</b>	42.23
<b>166</b>	42.14
<b>167</b>	42.11
<b>168</b>	41.74

The infrared absorption spectra of complexes **165-168** lack the  $\text{C}\equiv\text{C}-\text{H}$  stretch at around  $3300\text{ cm}^{-1}$  present in the substrates, hence confirming the deprotonation of the alkyne C-H. No Au-Cl absorption at around  $320\text{ cm}^{-1}$  is observed in any case, confirming the displacement of the chloride ligand from gold. The expected  $\text{C}\equiv\text{C}$  stretch at around  $2100\text{-}2260\text{ cm}^{-1}$  is too weak to be assigned in any case.

Complexes **165-168** were successfully characterised by high resolution mass spectrometry (ESI-TOF) and the results are shown in Table 5.2. In all cases the  $[\text{M}+\text{Na}]^+$  peak was observed.

**Table 5.2.** HRMS (ESI-TOF) Calculated and Found  $m/z$  Values

Complex	Peak	$m/z$ Calculated	$m/z$ Found
<b>165</b>	$[M]^+$	696.1837	696.1807
<b>166</b>	$[M+Na]^+$	636.1126	636.1134
<b>167</b>	$[M+Na]^+$	686.1282	686.1263
<b>168</b>	$[M+Na]^+$	638.1031	638.1041

Complexes **165**, **167** and **168** were characterised by single crystal X-ray diffraction. Suitable crystals were grown by the slow diffusion of pentane into a solution of the complex in dichloromethane. The molecular structures are shown in Figure 5.14.

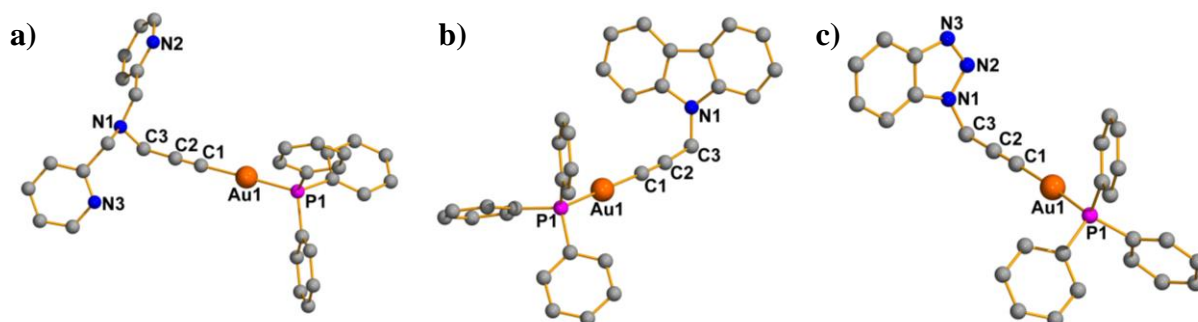


**Figure 5.14.** Molecular structures of complexes **165**, **167** and **168**. Selected bond lengths [Å] and angles [°] **165**: Au(1)-C(1) 2.024(5), Au(1)-P(1) 2.2709(13), C(1)-C(2) 1.169(7), C(2)-C(3) 1.492(7), C(1)-Au(1)-P(1) 178.84(14), C(1)-C(2)-C(3) 176.6(5); **167**: Au(1)-C(1) 2.002(2), Au(1)-P(1) 2.2693(9), C(1)-C(2) 1.196(3), C(2)-C(3) 1.471(3), C(1)-Au(1)-P(1) 175.55(5), C(1)-C(2)-C(3) 173.68(19); **168**: Au(1)-C(1) 1.998(3), Au(1)-P(1) 2.2780(8), C(1)-C(2) 1.194(5), C(2)-C(3) 1.474(4), N(1)-N(2) 1.355(4), N(2)-N(3) 1.296(4), C(1)-Au(1)-P(1) 175.26(9), C(1)-C(2)-C(3) 178.9(3).

In all cases a linear arrangement about the gold centre is observed with angles C(1)-Au(1)-P(1) of 178.84(14)° for **165**, 175.55(5)° for **167** and 175.26(9)° for **168**. The C-C bond distances in the propargyl unit are typical for those expected for a single and triple bond respectively with values C(1)-C(2) 1.169(7) Å and C(2)-C(3) 1.492(7) Å for **165**; C(1)-C(2) 1.196(3) Å and C(2)-C(3) 1.471(3) Å for **167**; and C(1)-C(2) 1.194(5) Å and C(2)-C(3) 1.474(4) Å for **168**.

In the crystal structure of complex **167**, the molecules are associated in dimers with intermolecular contacts observed between the carbazole units. The six-membered ring of one

molecule lies over the five-membered ring of another with a  $\pi$ -stacking-type interaction (Figure 5.15). Intermolecular distances centroid-centroid 3.551 Å and C(7)-N(1)' 3.546 Å are observed.

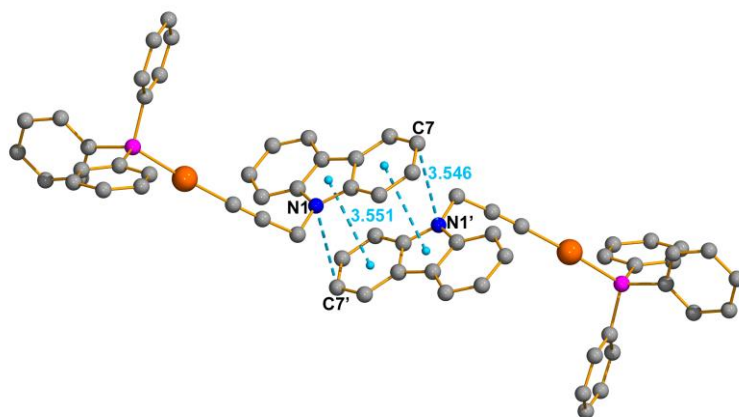


**Figure 5.15.** Intermolecular contacts for complex **167**.

Intermolecular contacts are also observed in the structure of complex **168** (Figure 5.16). In this case a slipped  $\pi$ -stacking interaction between the benzotriazole rings with a distance of 3.654 Å is observed.

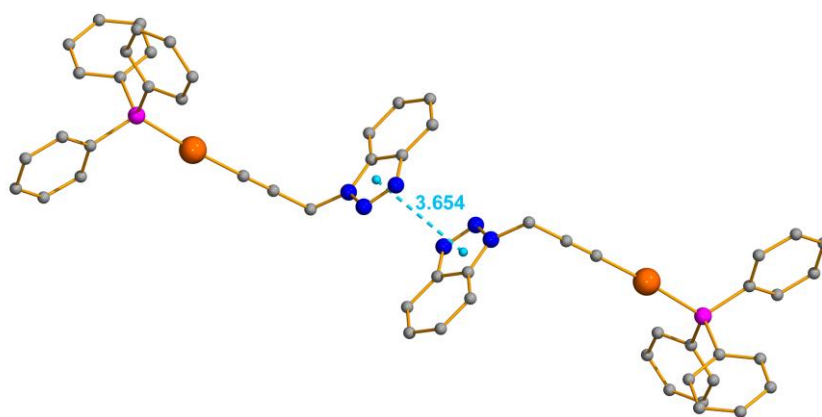
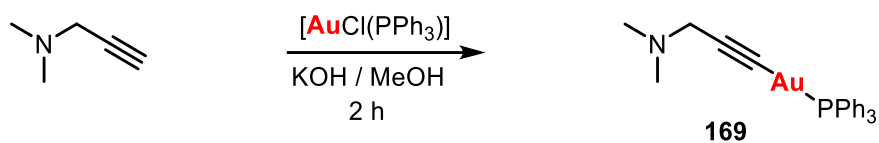


**Figure 5.16.** Intermolecular contacts for complex **168**.

Attempts were also made to prepare a gold(I) triphenylphosphine derivative from dimethylpropargylamine (Scheme 5.9). Reaction of the amine with [AuCl(PPh<sub>3</sub>)] and KOH in methanol did lead to the precipitation of a white solid and initial NMR studies show this to be the expected complex **169** (Figure 5.17(a), Figure 5.18(a)). However, after 12 hours in solution in dichloromethane, new peaks appear in the <sup>1</sup>H NMR spectrum (Figure 5.17(b)) and the <sup>31</sup>P{<sup>1</sup>H} spectrum becomes much broader (Figure 5.18(b)).



**Scheme 5.9.** Synthesis of complex **169**.

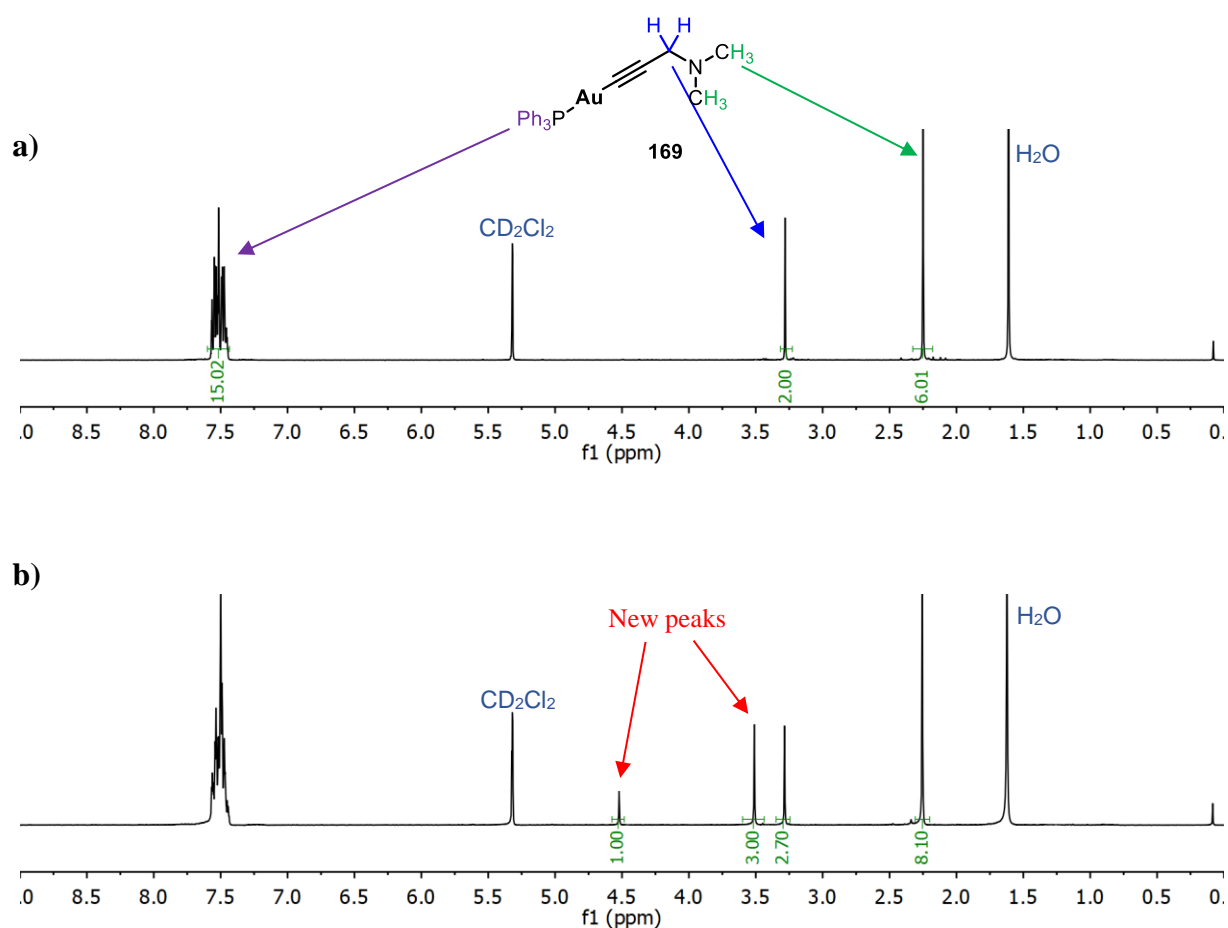


**Figure 5.17.**  $^1\text{H}$  NMR spectrum for complex **169** in  $\text{CD}_2\text{Cl}_2$  at room temperature after 5 min (a) and after 12 h (b).



### 5.3. Synthesis of Propargyl Gold Complexes

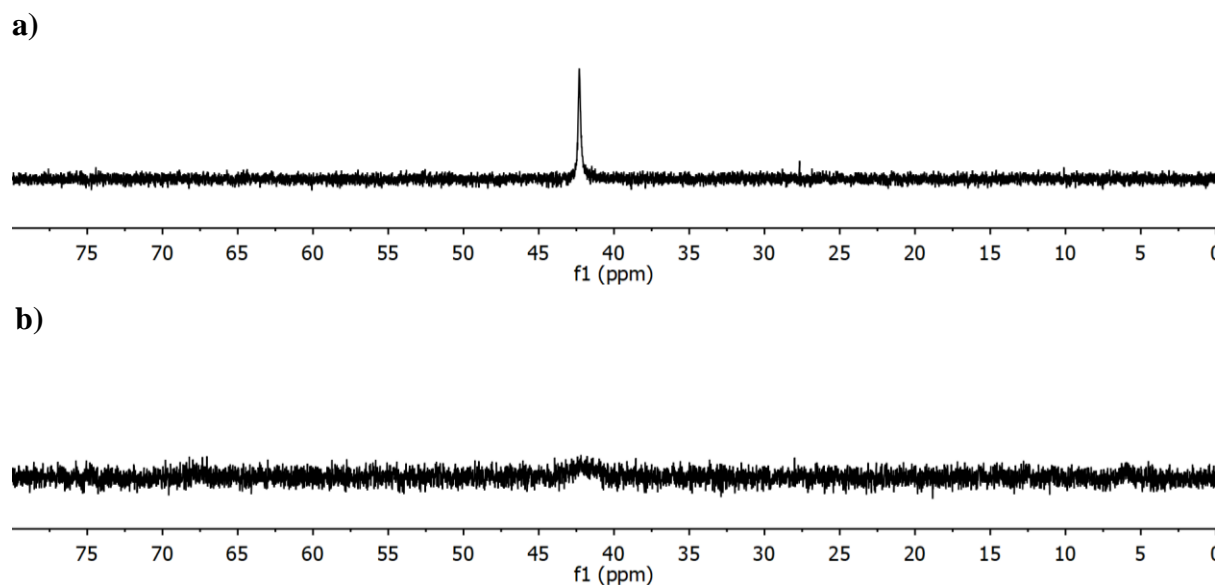
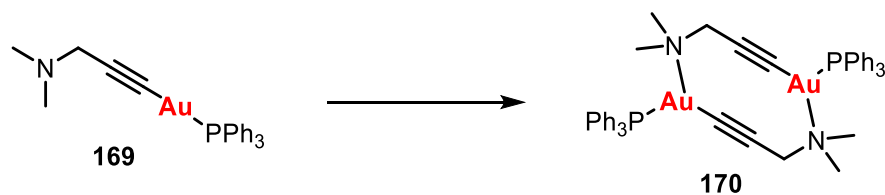


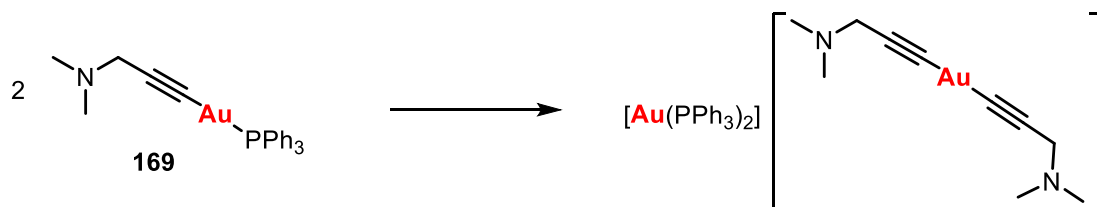
**Figure 5.18.**  $^{31}\text{P}$  NMR spectrum for complex **169** in  $\text{CD}_2\text{Cl}_2$  at room temperature after 5 min (a) and after 12 h (b).

One possible explanation could be the formation of a dimeric species **170** (Scheme 5.10).



**Scheme 5.10.** Proposed formation of dimeric complex **170**.

Another possibility could be the dissociation of the complex and the formation of the homoleptic species (Scheme 5.11). This could lead to a more complex supramolecular structure with stabilising aurophilic interactions (Figure 5.19).



**Scheme 5.11.** Possible formation of homoleptic species by dissociation of complex **169**.

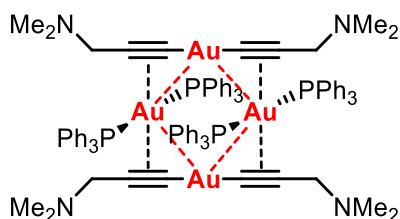
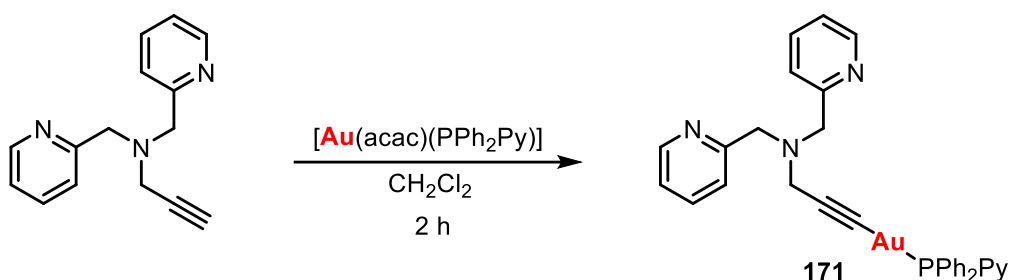


**Figure 5.19.** Possible supramolecular structure for homoleptic species derived from complex **169**.

Complex **171**, analogous to complex **165** but bearing diphenyl-2-pyridylphosphine rather than triphenylphosphine, was prepared by reaction of N-propargyl-di(2-picolyl)amine with  $[\text{Au}(\text{acac})(\text{PPh}_2\text{Py})]$  (Scheme 5.12). The product was obtained as a pale brown solid in a good yield, 84%. The pyridyl group in the phosphine could potentially provide an additional coordination site and changing the phosphine could also potentially affect the biological properties.



**Scheme 5.12.** Synthesis of complex **171**.

As with complex **165**, successful formation of the product could be confirmed by NMR studies (Figure 5.20). The  $^1\text{H}$  NMR spectrum lacks the alkyne CH signal, confirming deprotonation. The propargyl  $\text{CH}_2$  signal is observed as a singlet. A single sharp signal is observed in the  $^{31}\text{P}$  NMR spectrum at 41.41 ppm. The identity of the complex was also confirmed by high resolution mass spectrometry (ESI-TOF) with the molecular ion peak  $m/z$   $[\text{M}]^+$  calculated  $\text{C}_{32}\text{H}_{29}\text{AuN}_4\text{P}$  697.1790 and found 697.1795.

### 5.3. Synthesis of Propargyl Gold Complexes

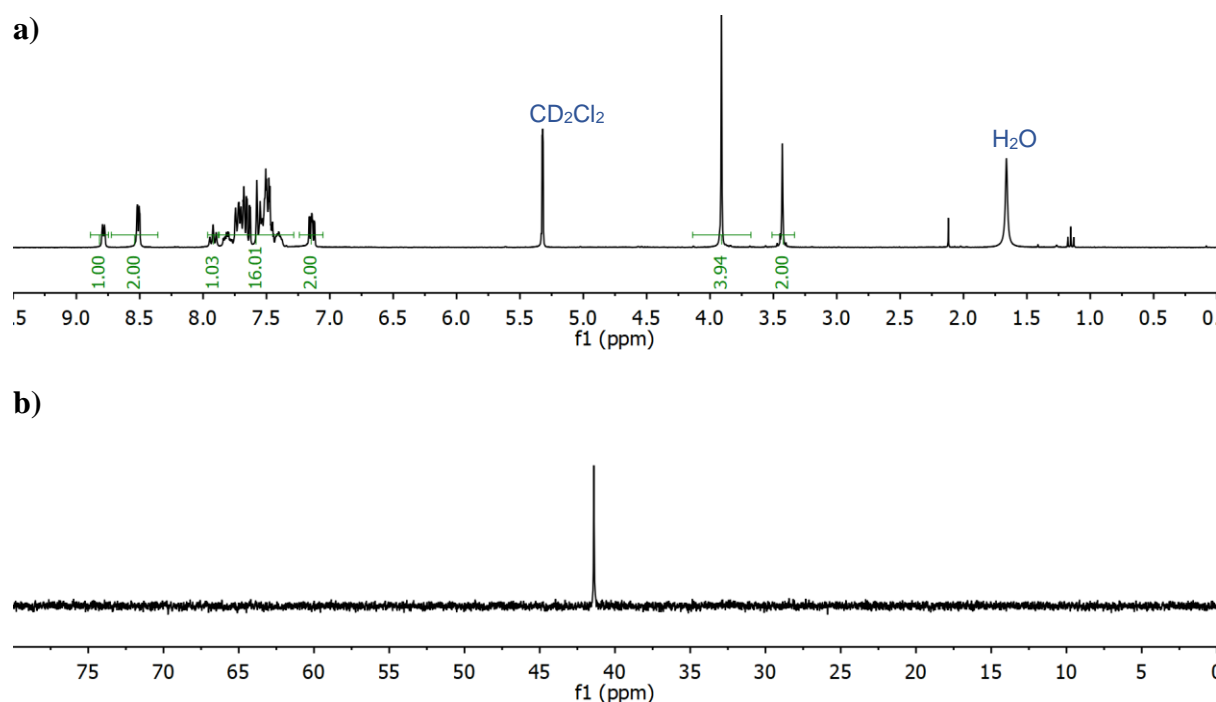
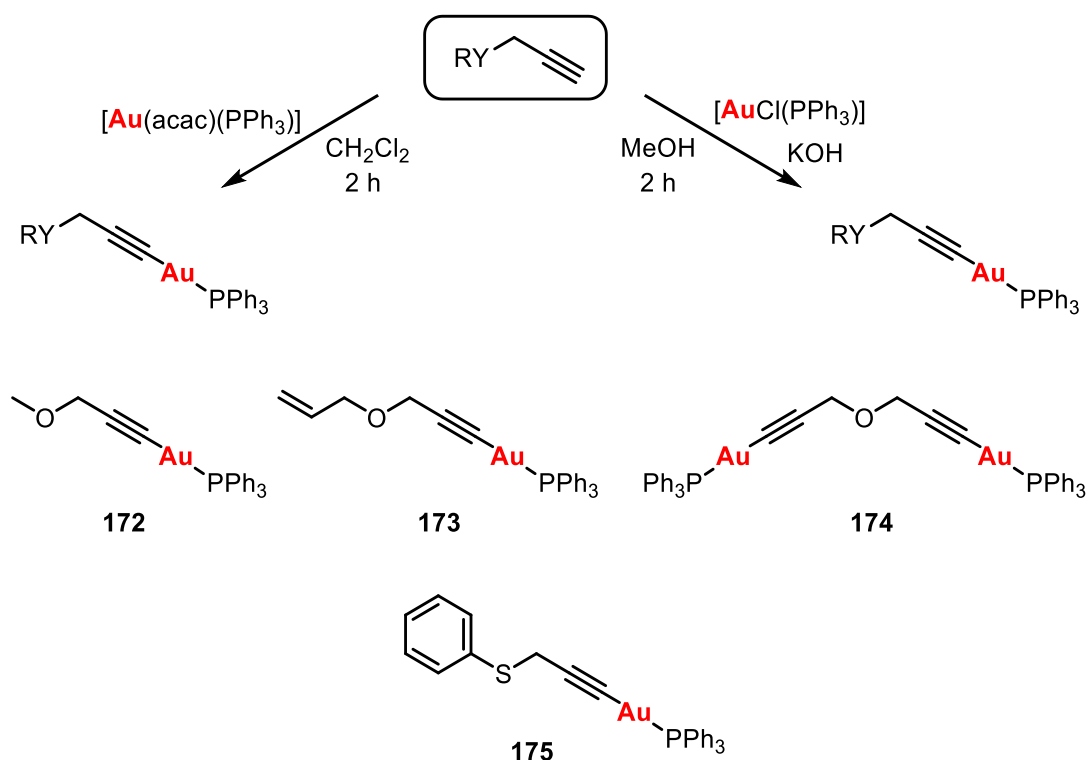


**Figure 5.20.**  $^1\text{H}$  NMR spectrum (a) and  $^{31}\text{P}\{^1\text{H}\}$  NMR spectrum (b) of complex **171** in  $\text{CD}_2\text{Cl}_2$  at room temperature.

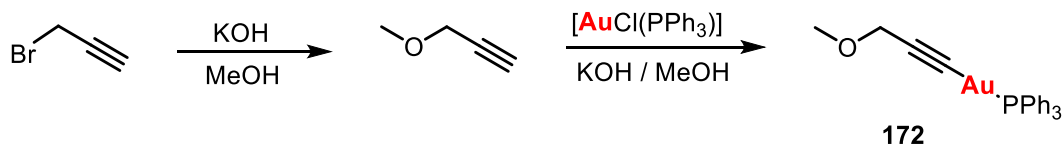
#### 5.3.2. Derivatives with Oxygen and Sulfur Substrates

Derivatives with propargyl ethers and propargyl thioethers were prepared analogously to those with the nitrogen based substrates, by either reaction with  $[\text{Au}(\text{acac})(\text{PPh}_3)]$  in dichloromethane or reaction with  $[\text{AuCl}(\text{PPh}_3)]$  and potassium hydroxide in methanol (Scheme 5.13). The products **172–175** were obtained in good yields as air-stable solids.

For complex **172**, the propargyl methyl ether was prepared *in situ* by reaction of propargyl bromide with potassium hydroxide and methanol, in a typical Williamson ether synthesis reaction. This ether was not isolated but reacted directly with  $[\text{AuCl}(\text{PPh}_3)]$  and potassium hydroxide to give the propargyl gold(I) complex **172** (Scheme 5.14).



**Scheme 5.13.** Synthesis of complexes **172-175**.



**Scheme 5.14.** Synthesis of complex **172** from propargyl bromide.

The successful formation of complex **172** could be confirmed by NMR spectroscopy. The  $^1\text{H}$  NMR spectrum shows a sharp singlet at 3.35 ppm which integrates as three protons corresponding to the methyl group (Figure 5.21(a)). A single sharp peak at 42.07 ppm is observed in the  $^{31}\text{P}\{^1\text{H}\}$  NMR spectrum (Figure 5.21(b)). In the  $^{13}\text{C}$  APT spectrum the *ipso*, *ortho*, *meta* and *para* carbon atoms are observed as doublets due to coupling with the phosphorus atom. The  $\text{CH}_2$  group of the propargyl unit is observed as a singlet at 61.17 ppm with negative phase. The methyl group is observed as a singlet with positive phase at 57.35 ppm. The other quaternary carbon atoms of the propargyl unit are not observed (Figure 5.21(c)).

### 5.3. Synthesis of Propargyl Gold Complexes

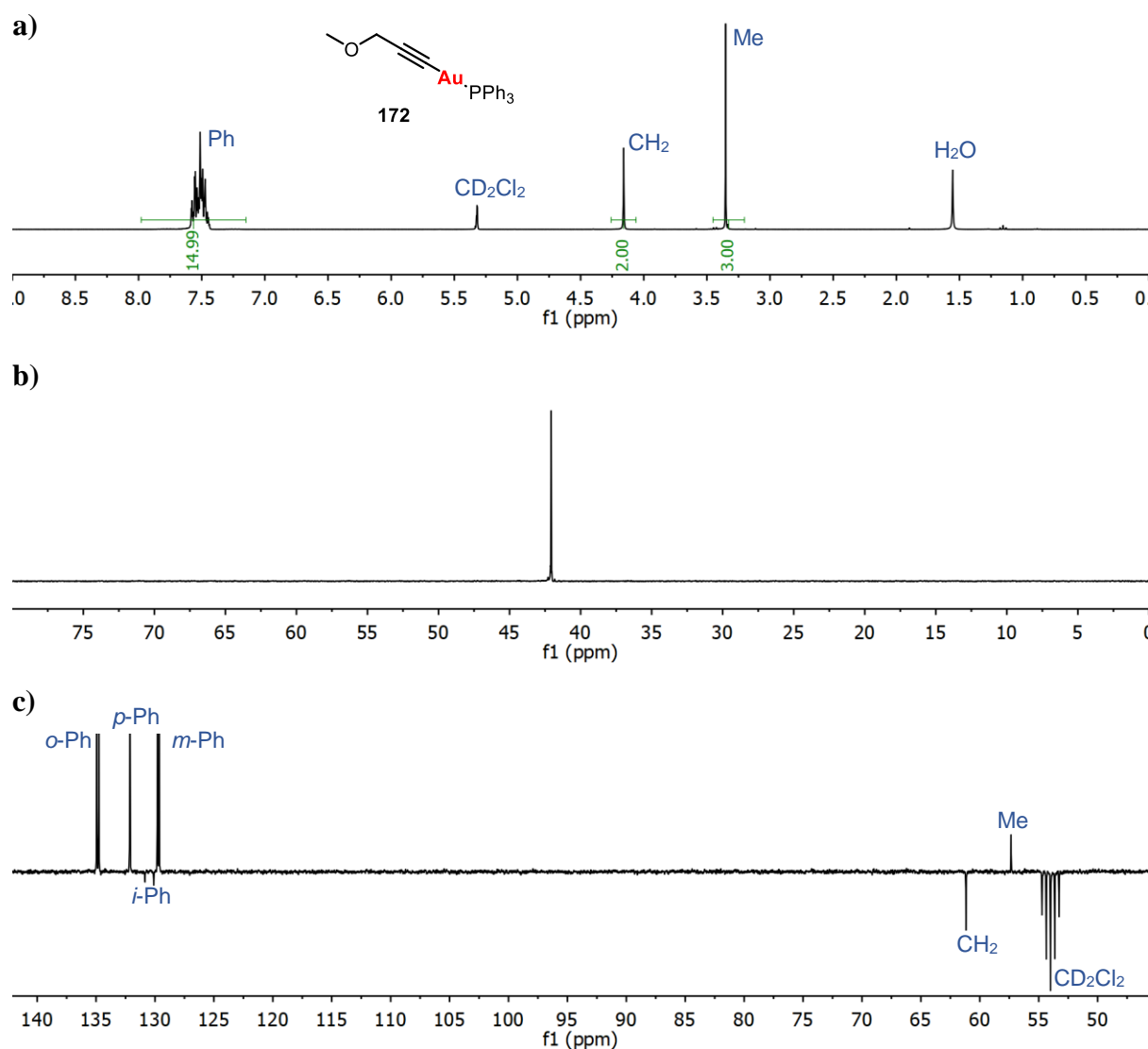


**Figure 5.21.**  $^1\text{H}$  NMR spectrum (a),  $^{31}\text{P}\{^1\text{H}\}$  NMR spectrum (b) and  $^{13}\text{C}$  APT spectrum (c) of complex **172** in  $\text{CD}_2\text{Cl}_2$  at room temperature.

The  $^1\text{H}$  NMR spectrum of complex **173** displays the typical splitting patterns expected for the allyl unit. The  $\text{CH}_2$  is observed as a doublet of doublet of doublets due to coupling with each of the other three protons. The terminal vinyl protons are each observed as doublet of doublet of triplets. The *trans* vinylic coupling is larger than the *cis*. The final vinylic CH is observed as a doublet of doublet of triplets due to coupling with both the *cis* and *trans* terminal vinylic CH protons and the  $\text{CH}_2$  group (Figure 5.22). The propargyl  $\text{CH}_2$  is again observed as a singlet and no propargyl CH signal is observed. The  $^{31}\text{P}\{^1\text{H}\}$  NMR spectrum shows a single sharp peak at 42.19 ppm.

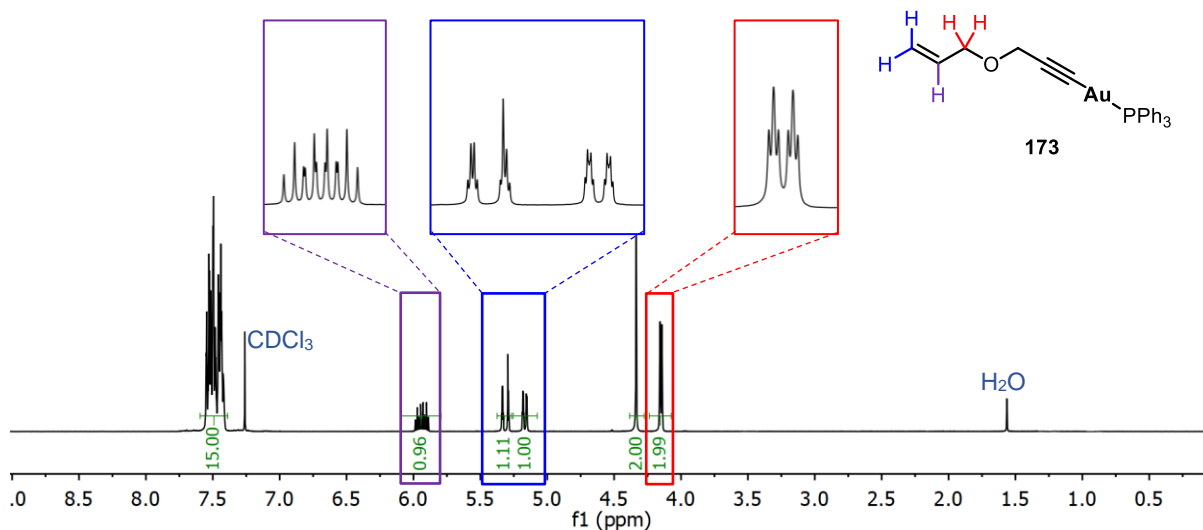


**Figure 5.22.**  $^1\text{H}$  NMR spectrum of complex **173** in  $\text{CDCl}_3$  at room temperature.

Complexes **172-175** were characterised by high resolution mass spectrometry with the molecular ion peak observed for complex **174** and the  $[\text{M}+\text{Na}]^+$  peaks observed for complexes **172**, **173** and **175**. The results are shown in Table 5.3.

**Table 5.3.** HRMS (ESI-TOF) Calculated and Found  $m/z$  Values

Complex	Peak	$m/z$ Calculated	$m/z$ Found
<b>172</b>	$[\text{M}+\text{Na}]^+$	551.0809	551.0831
<b>173</b>	$[\text{M}+\text{Na}]^+$	557.0966	557.0977
<b>174</b>	$[\text{M}]^+$	1011.1489	1011.1454
<b>175</b>	$[\text{M}+\text{Na}]^+$	629.0738	629.0744

Complexes **174** and **175** were characterised by single crystal X-ray diffraction. Suitable crystals were grown by the slow diffusion of pentane into a solution of the complex in dichloromethane. The molecular structures are shown in Figure 5.23. In both cases the triple and single carbon-carbon bonds of the propargyl unit can clearly be seen with distances  $\text{C}(1)\text{-C}(2)$  1.204(7) Å and  $\text{C}(2)\text{-C}(3)$  1.4519 Å for complex **174** and  $\text{C}(1)\text{-C}(2)$  1.204(5) Å and  $\text{C}(2)\text{-C}(3)$  1.468(5) Å for complex **175**. The propargyl unit has a linear geometry with angles  $\text{C}(1)\text{-C}(2)\text{-C}(3)$  177.5(7)° for complex **174** and  $\text{C}(1)\text{-C}(2)\text{-C}(3)$  175.3(4) for complex **175**. The geometry about the gold centre is slightly distorted from being linear, probably due to some steric hindrance

with the bulky triphenylphosphine groups, with angles C(1)-Au(1)-P(1)  $169.12(14)^\circ$  for complex **10** and C(1)-C(2)-C(3)  $175.3(4)^\circ$  for complex **175**.

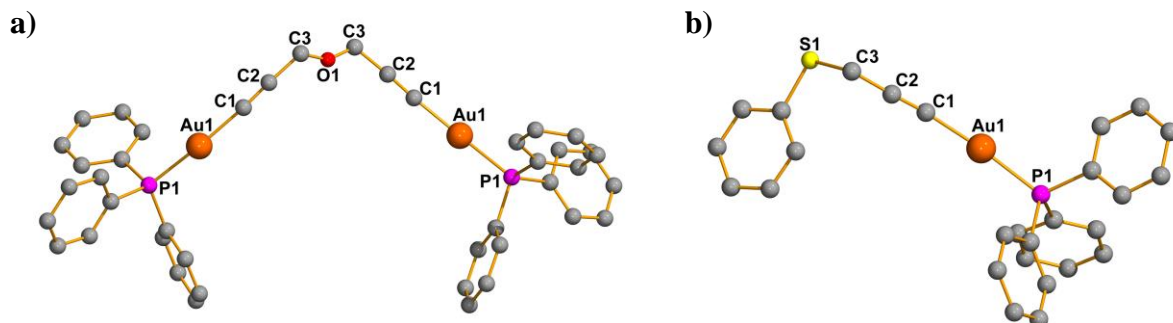


**Figure 5.23.** Molecular structures of complexes **174** (a) and **175** (b) (Hydrogen atoms are omitted for clarity). Selected bond lengths [Å] and angles [°] **174**: Au(1)-C(1) 2.001(5), Au(1)-P(1) 2.2744(13), C(1)-C(2) 1.204(7), C(2)-C(3) 1.451(9), C(1)-Au(1)-P(1)  $169.12(14)$ , C(1)-C(2)-C(3)  $177.5(7)$ ; **175**: Au(1)-C(1) 1.994(3), Au(1)-P(1) 2.2751(8), C(1)-C(2) 1.204(5), C(2)-C(3) 1.468(5), C(1)-Au(1)-P(1)  $173.60(9)$ , C(1)-C(2)-C(3)  $175.3(4)$ .

In the crystal structure of complex **174** the molecules are associated in chains due to intermolecular aurophilic interactions with an Au-Au distance of 3.291 Å (Figure 5.24).

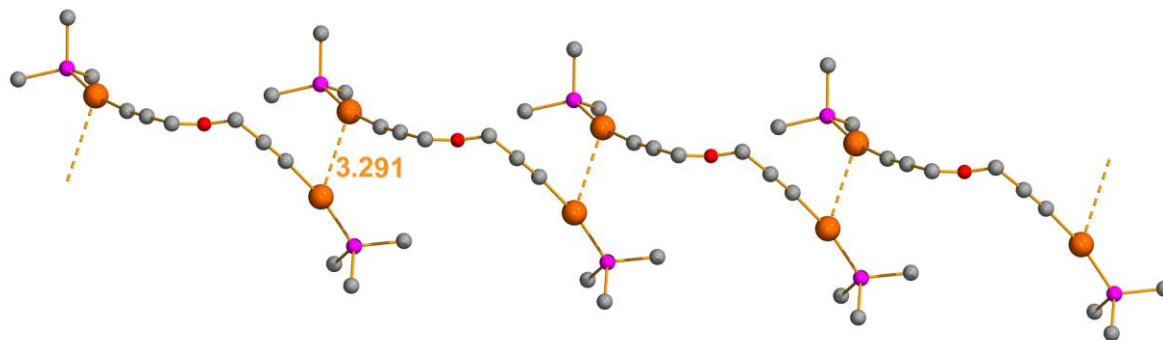
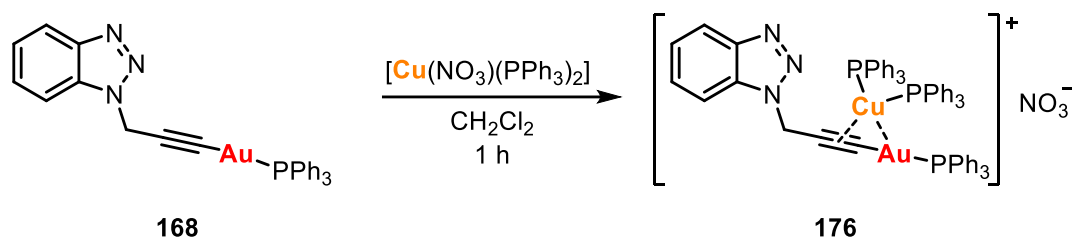


**Figure 5.24.** Intermolecular aurophilic interactions in the crystal structure of complex **174** (Phenyl rings and hydrogen atoms are omitted for clarity).

### 5.3.3. Synthesis of a Heterometallic Dinuclear Complex

Dinuclear complex **176** was prepared by reaction of complex **168** with  $[\text{Cu}(\text{NO}_3)(\text{PPh}_3)_2]$  in dichloromethane (Scheme 5.15). The product was obtained in a high yield (90%) as a yellow solid. The identity of the product can be confirmed by NMR studies. The  $^1\text{H}$  NMR spectrum is similar to that for complex **168** but 49 protons are now observed in the aromatic region, 4 from the benzotriazole group and 45 from the three triphenylphosphine groups (Figure 5.25(a)). The  $^{31}\text{P}\{^1\text{H}\}$  NMR spectrum at room temperature shows two broad peaks, one at around 40 ppm

corresponding to the phosphine coordinated to gold and one at 0 ppm corresponding to the two equivalent triphenylphosphine groups bounds to the copper (Figure 5.25(b)).



**Scheme 5.15.** Synthesis of complex **176**.

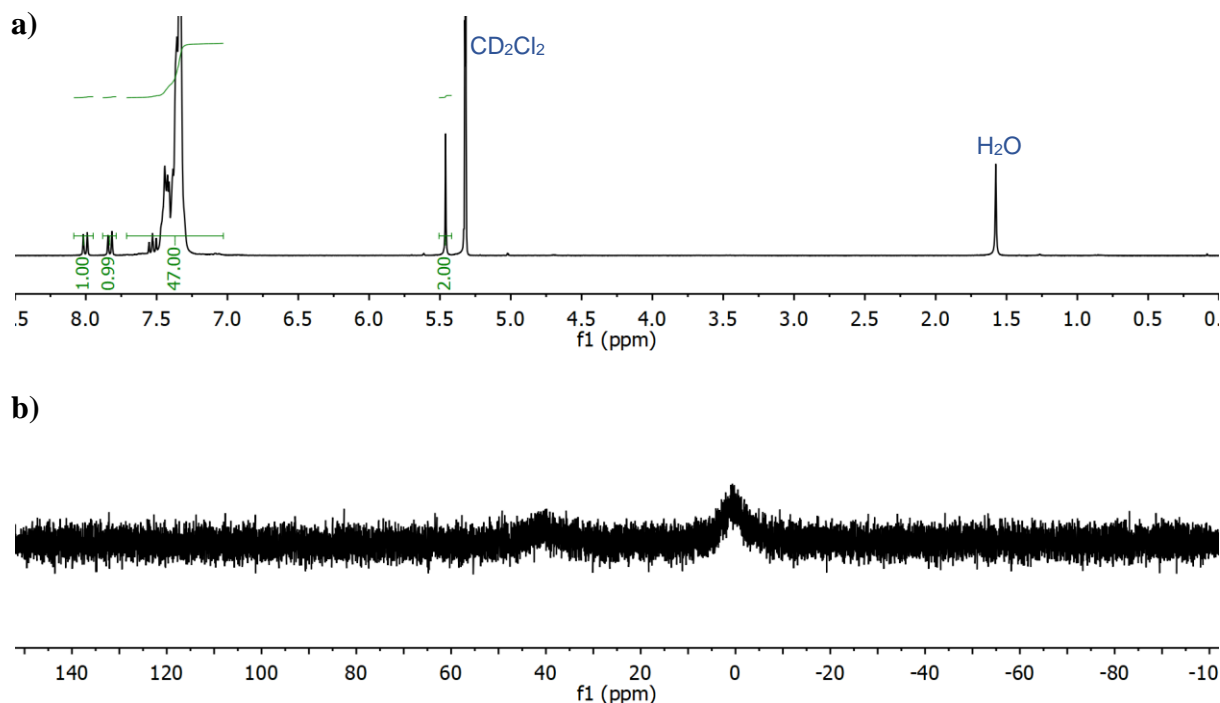


**Figure 5.25.**  $^1\text{H}$  NMR spectrum (a), and  $^{31}\text{P}\{^1\text{H}\}$  NMR spectrum (b) of complex **176** in  $\text{CD}_2\text{Cl}_2$  at room temperature.

Complex **176** was luminescent in the solid state both at room temperature and at 77 K. The excitation bands, emission bands and lifetimes are shown in Table 5.4. At room temperature three different excitation maxima are observed. Excitation at 390 nm results in an emission at 558 nm (Figure 5.26(a)) with a lifetime of 647  $\mu\text{s}$ , indicating phosphorescence. This band can be tentatively assigned to a  $^3\text{IL}(\pi\pi^*)$  transition where the metal is weakly involved. Additional excitation maxima are observed at 445 and 503 nm, both resulting in emission at 646 nm (Figure 5.26(b)). The emission as a result of excitation at 503 nm has a lifetime of 103  $\mu\text{s}$ , again



### 5.3. Synthesis of Propargyl Gold Complexes

indicating a phosphorescent emission. These bands are assigned to a MLCT transition involving the copper. At 77 K an excitation maximum at 353 nm is observed which gives a vibronic-structured emission band at around 499 nm (Figure 5.27(a)). This is assigned as an intraligand charge transfer transition in the phenyl rings of the triphenylphosphine ligand. This band was not observed at room temperature due to its low intensity. Three additional excitation maxima are observed: excitation at 380 nm which corresponds to an emission at 539 nm, excitation at 433 nm which corresponds to emission at 633 nm, and a weak excitation band at 488 nm which also leads to an emission at 633 nm (Figure 5.27(b)). As with at room temperature, the excitation at 380 nm and emission at 539 nm are assigned to a  $^3\text{IL}(\pi\pi^*)$  transition and the other bands are assigned to a MLCT transition involving the copper.

**Table 5.4.** Excitation and Emission Maxima for Complex **176**

Temperature (K)	Excitation $\lambda^{\text{max}}$ (nm)	Emission $\lambda^{\text{max}}$ (nm)	$\tau_0$ ( $\mu\text{s}$ )
298	390	558	647.8
	445	646	
	503	646	
77	352	499 (structured)	957.6
	380	539	
	433	633	
	488	633	

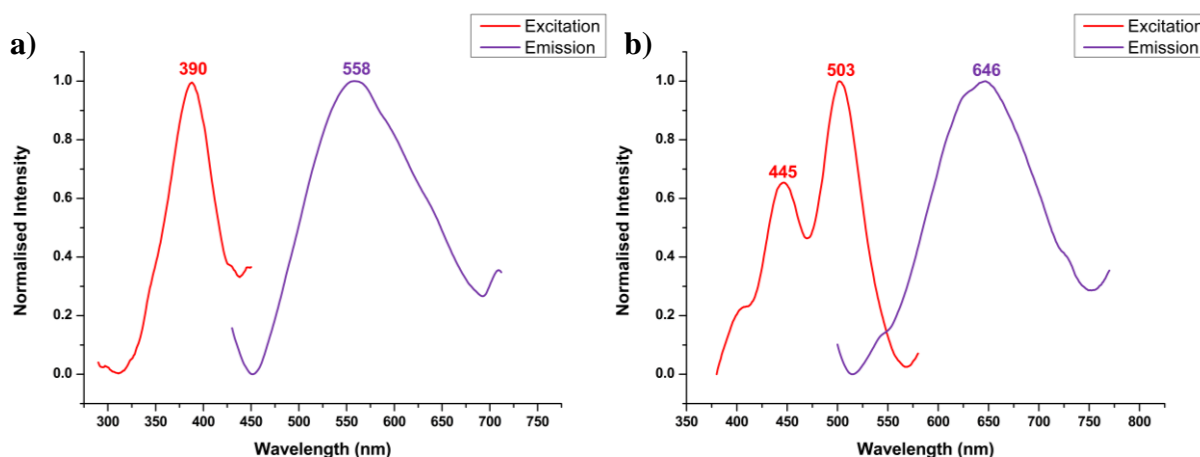


**Figure 5.26.** Excitation and emission maxima for complex **176** at room temperature.

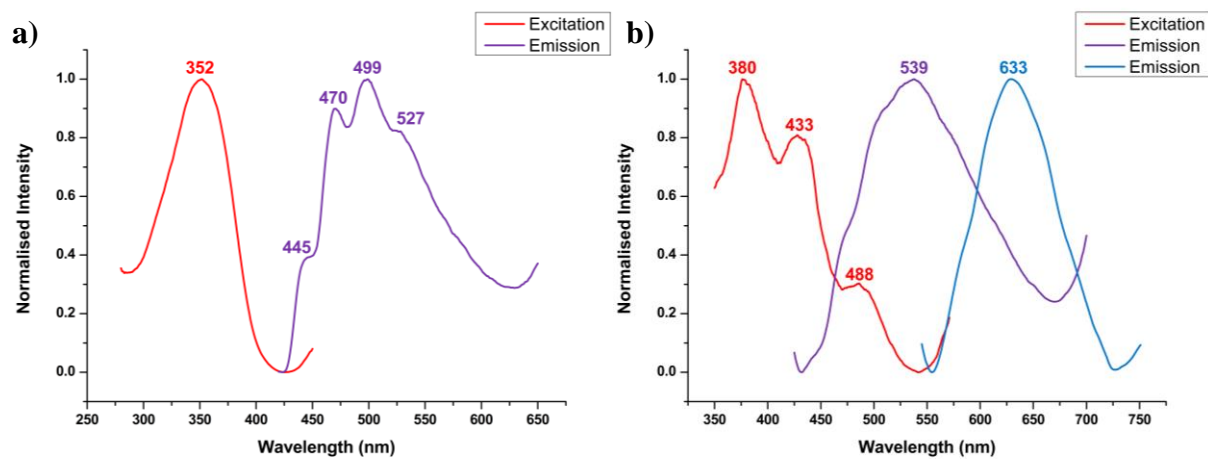


**Figure 5.27.** Excitation and emission maxima for complex **176** at 77 K.

---

## 5.4. Biological Activity

The biological activity of complexes **165-168** and **171-176** was studied by MTT assay for lung carcinoma cell line A549. The calculated  $IC_{50}$  values for the complexes after 24 h incubation time are shown in Table 5.5.

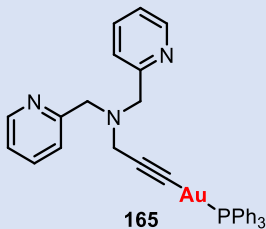
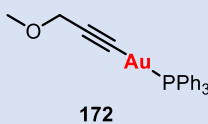
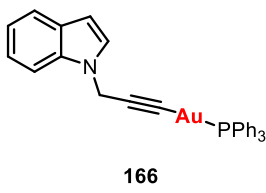
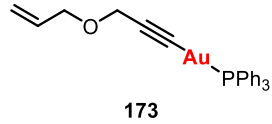
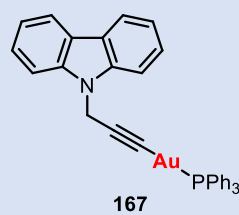
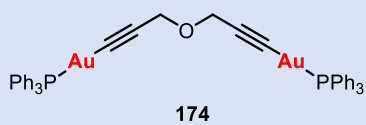
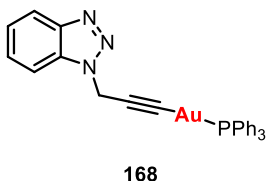
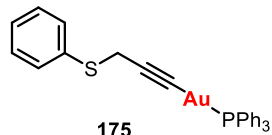
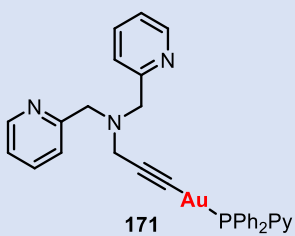
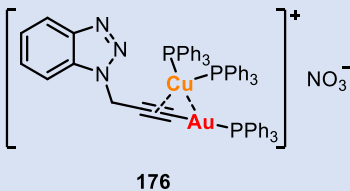
The carbazole derivative, complex **167**, was the only complex not to show any antiproliferative activity against A549 cells with an  $IC_{50}$  value of  $>100 \mu\text{M}$ . The other complexes showed excellent  $IC_{50}$  values for 24 h incubation with the cancer cells. No significant differences are observed upon changing the heteroatom of the propargyl substrate as all of the  $IC_{50}$  values are within a similar range  $9\text{--}13 \mu\text{M}$ , the sulfur derivative having the lowest  $IC_{50}$  value of the gold triphenylphosphine complexes at  $9.11 \pm 1.93 \mu\text{M}$ .

Changing the phosphine from triphenylphosphine to diphenyl-2-pyridylphosphine did give a slight improvement in activity with complex **165** having an  $IC_{50}$  of  $13.32 \pm 0.51 \mu\text{M}$  and complex **171** an  $IC_{50}$  of  $8.72 \pm 1.47 \mu\text{M}$ . This can be seen in the graph of cell viability against concentration (Figure 5.28).

Dinuclear gold triphenyl phosphine complex **174**, derivative of dipropargylether did not show a greater activity than the mononuclear propargylether derivatives **172** and **173**. There is therefore no correlation between the number of gold triphenylphosphine units in the complex and the overall activity.

The heterometallic complex **176** had the highest activity of the complexes measured with an  $IC_{50}$  of  $2.50 \pm 0.19 \mu\text{M}$  compared to the starting mononuclear gold complex **168** which has an  $IC_{50}$  of  $11.91 \pm 1.54 \mu\text{M}$ . Even at very low concentrations complex **176** is cytotoxic to the A549 cells (Figure 5.29).

**Table 5.5.** IC<sub>50</sub> Values for Complexes **1-4** and **7-12** after 24 h Incubation with A549 Cells

Complex	IC <sub>50</sub> (μM)	Complex	IC <sub>50</sub> (μM)
 165	13.32 ± 0.51	 172	10.27 ± 0.76
 166	12.73 ± 0.58	 173	10.61 ± 0.93
 167	>100	 174	12.28 ± 2.66
 168	11.91 ± 1.54	 175	9.11 ± 1.93
 171	8.72 ± 1.47	 176	2.50 ± 0.19

#### 5.4. Biological Activity

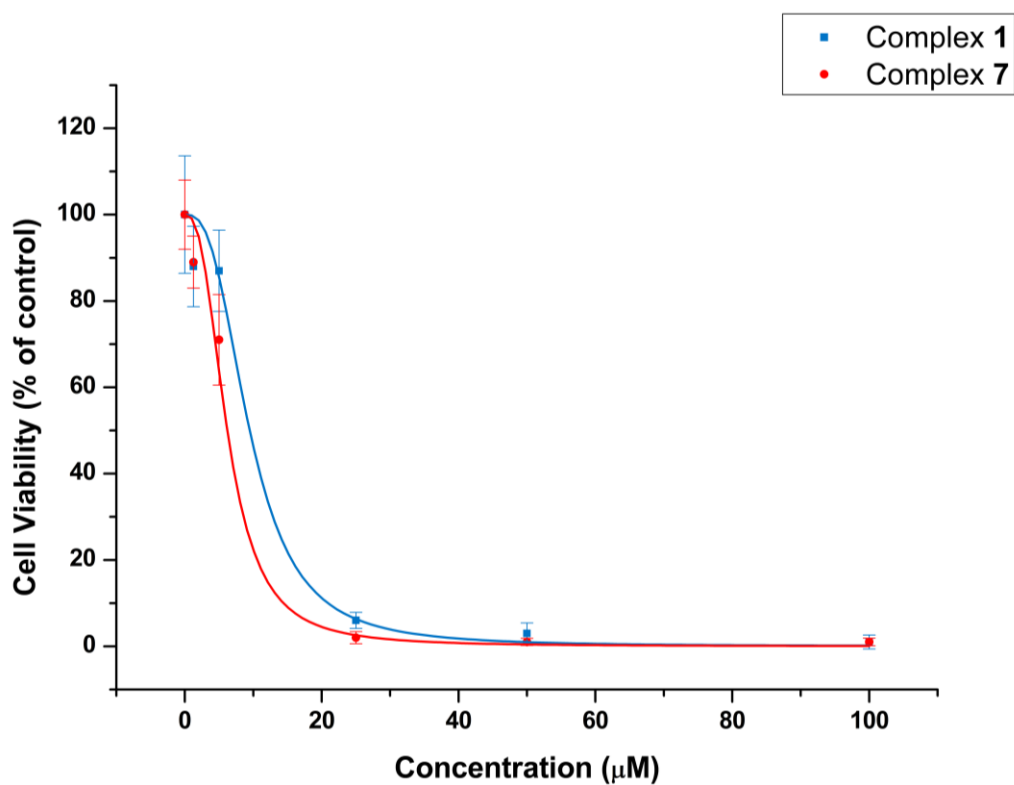


**Figure 5.28.** Cell viability (% of control) vs Concentration (μM) of complexes **1** and **7** for 24 h incubation with A549 cells.

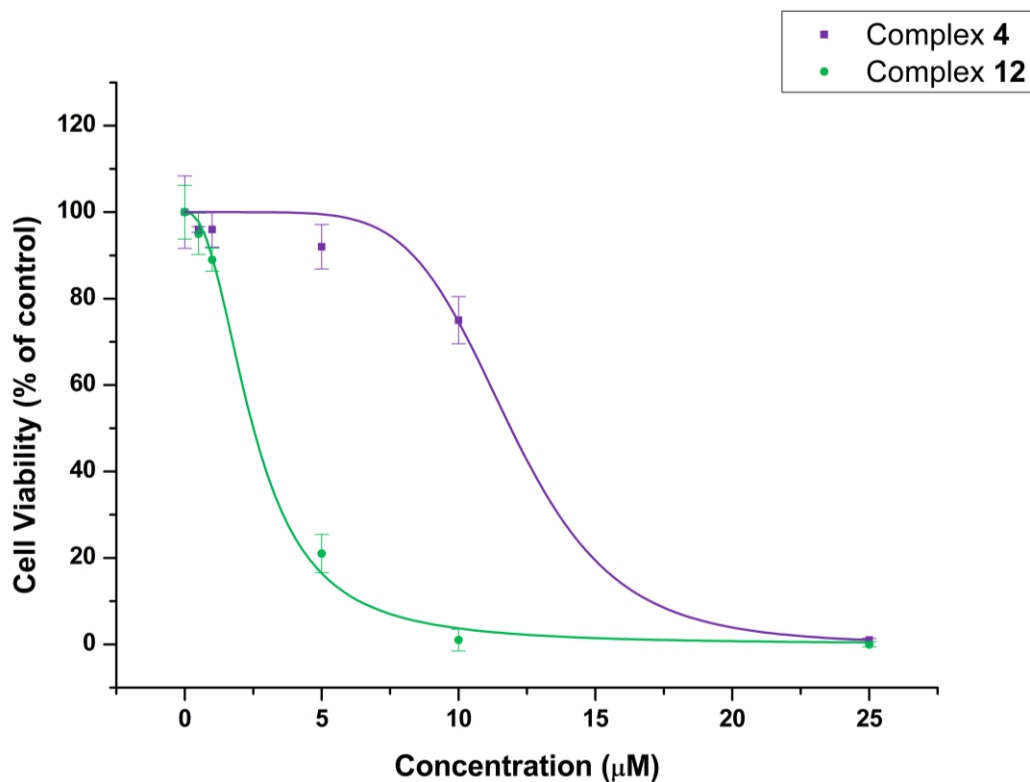


**Figure 5.29.** Cell viability (% of control) vs Concentration (μM) of complexes **4** and **12** for 24 h incubation with A549 cells.

## 5.5. Conclusions

A series biologically active of propargyl gold complexes have been prepared from propargyl amines, propargyl functionalised heterocyclic compounds, propargyl ethers and a propargyl sulfide.

The propargyl-di(2-picoly)amine ligand was readily prepared from di(2-picoly)amine and propargyl bromide in the presence of the weak base, potassium carbonate. The propargyl functionalised derivatives of the heterocyclic compounds, indole and carbazole, were prepared similarly by N-alkylation using propargyl bromide, however in these cases a stronger base was required to deprotonate the substrates and hence potassium hydroxide was used. The ligands were characterised by NMR spectroscopy.

The propargyl gold compounds could be prepared by two different methods: addition of [Au(acac)(PPh<sub>3</sub>)] to a solution of the substrate in dichloromethane, or reaction of the substrate with potassium hydroxide and [AuCl(PPh<sub>3</sub>)] in methanol. Similar yields were obtained in both cases. The complex derived from dimethylpropargylamine was unstable in solution, slowly converting into a different species. Based on NMR studies this was proposed to be either a dimer formed by association of the molecules or the homoleptic complex formed by dissociation of the ligands. All of the other complexes were highly stable and several examples were characterised by single crystal X-ray diffraction.

A heterometallic dinuclear complex with one gold and one copper centre derived from the propargyl functionalised benzotriazole substrate was prepared and characterised. This complex was found to be luminescent in the solid state, both at room temperature and at 77 K. The excitation and emission maxima were determined and assigned to <sup>3</sup>IL( $\pi\pi^*$ ) and MLCT transitions.

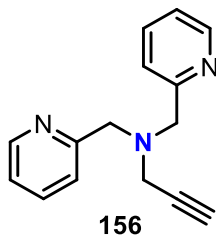
The antiproliferative activity of the complexes against lung cancer cell line A549 was tested by MTT assay. The carbazole derivative showed no antiproliferative activity at the concentrations tested, however all of the other complexes tested showed excellent activities with IC<sub>50</sub> values <14  $\mu$ M in all cases. Changing the heteroatom of the propargyl substrate did

## 5.5. Conclusions

---

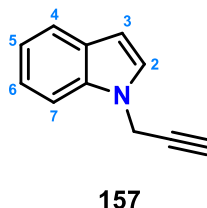
not make a significant difference to the anticancer activity of the complex, however the sulfur derivative was the most active of the gold triphenylphosphine complexes with an  $IC_{50}$  of  $9.11 \pm 1.93 \mu M$ . Changing the phosphine from triphenylphosphine to diphenyl-2-pyridyl phosphine did improve the activity slightly. The most active of the complexes was the cationic dinuclear complex bearing one copper and one gold centre which had an  $IC_{50}$  value of  $2.50 \pm 0.19 \mu M$ .

## 5.6. Experimental



Di(2-picolyl)amine (0.45 ml, 2.5 mmol) and propargyl bromide (0.32 ml, 80% in toluene, 2.93 mmol) were mixed in THF (15 ml) with excess  $K_2CO_3$  and stirred at room temperature under argon for 12 h. The reaction mixture was then diluted with ethyl acetate and filtered through a pad of  $K_2CO_3$ . The solution was concentrated to give **156** as a brown liquid.

**$^1H$  NMR (400 MHz,  $CDCl_3$ )**  $\delta$  8.55 (ddd,  $J = 4.9, 1.8, 0.9$  Hz, 2H, Py), 7.65 (td,  $J = 7.6, 1.9$  Hz, 2H, Py), 7.51 (dt,  $J = 7.8, 1.1$  Hz, 2H, Py), 7.15 (ddd,  $J = 7.5, 4.9, 1.2$  Hz, 2H, Py), 3.91 (s, 4H,  $CH_2$ Py), 3.42 (d,  $^4J_{HH} = 2.4$  Hz, 2H,  $CH_2C\equiv CH$ ), 2.29 (t,  $^4J_{HH} = 2.4$  Hz, 1H,  $C\equiv CH$ ).

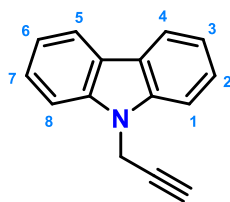


To a solution of indole (0.1171 g, 1.0 mmol) in DMF (15 ml) was added tetrabutylammonium bromide (0.0322 g, 0.1 mmol) and KOH (0.0561 g, 1.0 mmol) and the mixture stirred for 5 min. Propargyl bromide (0.13 ml, 80% in toluene, 1.2 mmol) and the mixture stirred for 12 h at room temperature. Ethyl acetate (20 ml) was added and the solution washed with  $H_2O$  (3 x 25 ml) and dried over  $Na_2SO_4$ . The solution was concentrated under reduced pressure to approximately 1 ml, and hexane added to precipitate a white solid which was collected and vacuum dried to give the product (0.1257 g, 81%).

**$^1H$  NMR (400 MHz,  $CDCl_3$ )**  $\delta$  7.65 (dt,  $J = 7.9, 1.0$  Hz, 1H, H7 indole), 7.45 – 7.38 (m, 1H, H4 indole), 7.30 – 7.23 (m, 2H, H6 indole), 7.22 (d,  $^3J_{HH} = 3.2$  Hz, 1H, H2 indole), 7.15 (ddd,  $^3J_{HH} = 8.0, ^3J_{HH} = 7.0, ^4J_{HH} = 1.0$  Hz, 1H, H5 indole), 6.55 (dd,  $^3J_{HH} = 3.2, ^4J_{HH} = 0.9$  Hz, 1H, H3 indole), 4.89 (d,  $^4J_{HH} = 2.6$  Hz, 2H,  $CH_2C\equiv CH$ ), 2.41 (t,  $^4J_{HH} = 2.5$  Hz, 1H,  $C\equiv CH$ ).



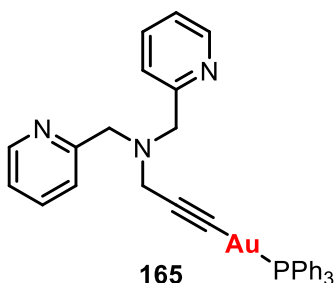
## 5.6. Experimental



**158**

To a solution of carbazole (0.1672 g, 1.0 mmol) in DMF (15 ml) was added tetrabutylammonium bromide (0.0322 g, 0.1 mmol) and KOH (0.0561 g, 1.0 mmol) and the mixture stirred for 5 min. Propargyl bromide (0.13 ml, 80% in toluene, 1.2 mmol) and the mixture stirred for 12 h at room temperature. Ethyl acetate (20 ml) was added and the solution washed with H<sub>2</sub>O (3 x 25 ml) and dried over Na<sub>2</sub>SO<sub>4</sub>. The solution was concentrated under reduced pressure to approximately 1 ml, and hexane added to precipitate a white solid which was collected and vacuum dried to give the product (0.1375 g, 67%).

**<sup>1</sup>H NMR (400 MHz, CDCl<sub>3</sub>)** δ 8.10 (dt, <sup>3</sup>J<sub>HH</sub> = 7.8, <sup>4</sup>J<sub>HH</sub> = 1.0 Hz, 2H, H4/H5 carbazole), 7.52 – 7.48 (m, 4H, H1/H2/H7/H8 carbazole), 7.30 – 7.27 (m, 2H, H3/H6 carbazole), 5.06 (d, <sup>4</sup>J<sub>HH</sub> = 2.5 Hz, 2H, CH<sub>2</sub>), 2.25 (t, <sup>4</sup>J<sub>HH</sub> = 2.5 Hz, 1H, C≡CH).



**165**

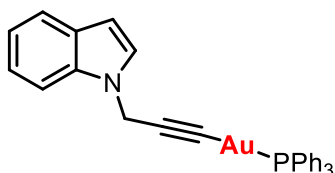
To a solution of **156** (0.0237 g, 0.1 mmol) in CH<sub>2</sub>Cl<sub>2</sub> (5 ml) was added [Au(acac)(PPh<sub>3</sub>)] (0.0559 g, 0.1 mmol) and the solution stirred for 2 h. The solution was filtered through celite, the filtrate concentrated under reduced pressure to approximately 1 ml and Et<sub>2</sub>O added to precipitate a pale yellow solid (0.0494 g, 71%).

**HRMS (ESI/QTOF) m/z:** [M]<sup>+</sup> Calcd for C<sub>33</sub>H<sub>30</sub>AuN<sub>3</sub>P 696.1837; Found 696.1807.

**<sup>1</sup>H NMR (300 MHz, CD<sub>2</sub>Cl<sub>2</sub>)** δ 8.51 (ddd, <sup>3</sup>J<sub>HH</sub> = 4.9, <sup>4</sup>J<sub>HH</sub> = 1.9, <sup>5</sup>J<sub>HH</sub> = 1.0 Hz, 2H, Py), 7.70 – 7.41 (m, 18H, PPh<sub>3</sub>/Py), 7.14 (ddd, <sup>3</sup>J<sub>HH</sub> = 7.4, <sup>4</sup>J<sub>HH</sub> = 4.9, <sup>5</sup>J<sub>HH</sub> = 1.4 Hz, 2H, Py), 3.91 (s, 4H, CH<sub>2</sub>Py), 3.42 (s, 2H, CH<sub>2</sub>C≡C).

**<sup>31</sup>P NMR (121 MHz, CD<sub>2</sub>Cl<sub>2</sub>)** δ 42.20 (s, PPh<sub>3</sub>).

**$^{13}\text{C}$  APT (75 MHz,  $\text{CD}_2\text{Cl}_2$ )**  $\delta$  160.35 (s, Py), 149.56 (s, Py), 136.74 (s, Py), 134.86 (d,  $^2J_{\text{CP}}$  = 13.9 Hz, *o*-PPh<sub>3</sub>), 132.08 (s, *p*-PPh<sub>3</sub>), 129.71 (d,  $^3J_{\text{CP}}$  = 11.2 Hz, *m*-PPh<sub>3</sub>), 123.58 (s, Py), 122.36 (s, Py), 97.68 (s,  $\text{CH}_2\text{C}\equiv\text{CAu}$ ), 60.00 (s,  $\text{CH}_2\text{Py}$ ), 44.15 (s,  $\text{CH}_2\text{C}\equiv\text{CAu}$ ).

**166**

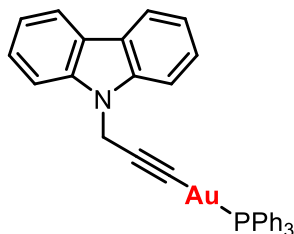
To a solution of **157** (0.0310 g, 0.2 mmol) in MeOH (15 ml) was added [AuCl(PPh<sub>3</sub>)] (0.0989 g, 0.2 mmol) and KOH (0.0168 g, 0.3 mmol) and the mixture stirred for 12 h. A white precipitate formed which was collected, washed with Et<sub>2</sub>O and vacuum dried to give the product (0.0761 g, 62%).

**HRMS (ESI/QTOF) m/z:** [M+Na]<sup>+</sup> Calcd for C<sub>29</sub>H<sub>23</sub>AuNNaP 636.1126; Found 636.1134.

**$^1\text{H}$  NMR (400 MHz,  $\text{CDCl}_3$ )**  $\delta$  7.61 (dt,  $J$  = 7.8, 1.0 Hz, 1H, H7 indole), 7.55 – 7.40 (m, 17H, PPh<sub>3</sub>/H2+H4 indole), 7.21 (ddd,  $^3J_{\text{HH}}$  = 8.3,  $^3J_{\text{HH}}$  = 7.0,  $^4J_{\text{HH}}$  = 1.2 Hz, 1H, H6 indole), 7.09 (ddd,  $^3J_{\text{HH}}$  = 7.9,  $^3J_{\text{HH}}$  = 7.0,  $^4J_{\text{HH}}$  = 1.0 Hz, 1H, H5 indole), 6.49 (dd,  $^3J_{\text{HH}}$  = 3.2 Hz,  $^4J_{\text{HH}}$  = 0.9 Hz, 1H, H3 indole), 5.04 (d,  $^5J_{\text{HP}}$  = 1.5 Hz, 2H,  $\text{CH}_2\text{C}\equiv\text{C}$ ).

**$^{31}\text{P}$  NMR (162 MHz,  $\text{CDCl}_3$ )**  $\delta$  42.14 (s, PPh<sub>3</sub>).

**$^{13}\text{C}$  APT (101 MHz,  $\text{CDCl}_3$ )**  $\delta$  134.41 (d,  $^2J_{\text{CP}}$  = 13.8 Hz, *o*-PPh<sub>3</sub>), 131.72 (s, *p*-PPh<sub>3</sub>), 130.05 (s, C7a indole), 129.49 (s, C3a indole), 129.29 (d,  $^3J_{\text{CP}}$  = 11.3 Hz, *m*-PPh<sub>3</sub>), 127.74 (s, indole), 126.66 (d,  $^1J_{\text{CP}}$  = 142.1 Hz, *i*-PPh<sub>3</sub>), 121.46 (s, indole), 120.92 (s, indole), 119.43 (C7 indole), 109.74 (s, C5 indole), 101.22 (s, C4 indole), 97.06 (d,  $^2J_{\text{CP}}$  = 26.8 Hz,  $\text{CH}_2\text{C}\equiv\text{CAu}$ ), 37.01 (s,  $\text{CH}_2\text{C}\equiv\text{CAu}$ ).

**167**

To a solution of **158** (0.0410 g, 0.2 mmol) in MeOH (15 ml) was added [AuCl(PPh<sub>3</sub>)] (0.0989 g, 0.2 mmol) and KOH (0.0168 g, 0.3 mmol) and the mixture stirred for 12 h. A white

## 5.6. Experimental

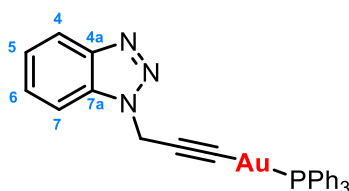
precipitate formed which was collected, washed with Et<sub>2</sub>O and vacuum dried to give the product (

**HRMS (ESI/QTOF) m/z:** [M+Na]<sup>+</sup> Calcd for C<sub>33</sub>H<sub>25</sub>AuNNaP 686.1282; Found 686.1263.

**<sup>1</sup>H NMR (300 MHz, CDCl<sub>3</sub>)** δ 8.07 (d, <sup>3</sup>J<sub>HH</sub> = 7.6 Hz, 2H, H4/H5 carbazole), 7.61 (dt, <sup>3</sup>J<sub>HH</sub> = 8.2 Hz, <sup>4</sup>J<sub>HH</sub> = 0.9 Hz, 2H, H1/H8, carbazole), 7.52 – 7.36 (m, 17H, PPh<sub>3</sub> + H2/H7 carbazole), 7.21 (ddd, <sup>3</sup>J<sub>HH</sub> = 7.9 Hz, <sup>3</sup>J<sub>HH</sub> = 7.1 Hz, <sup>4</sup>J<sub>HH</sub> = 1.0 Hz, 2H, H3/H6 carbazole), 5.21 (d, <sup>5</sup>J<sub>HP</sub> = 1.4 Hz, 2H, CH<sub>2</sub>C≡CAu).

**<sup>31</sup>P NMR (162 MHz, CDCl<sub>3</sub>)** δ 42.11 (s, PPh<sub>3</sub>).

**<sup>13</sup>C APT (75 MHz, CDCl<sub>3</sub>)** δ 134.39 (d, <sup>2</sup>J<sub>CP</sub> = 13.8 Hz, *o*-PPh<sub>3</sub>), 131.65 (d, <sup>4</sup>J<sub>CP</sub> = 2.4 Hz, *p*-PPh<sub>3</sub>), 129.24 (d, <sup>3</sup>J<sub>CP</sub> = 11.3 Hz, *m*-PPh<sub>3</sub>), 125.77 (s, C2/C7 carbazole), 120.29 (s, C4/C5 carbazole), 119.06 (s, C3/C6 carbazole), 109.38 (s, C1/C8 carbazole), 33.55 (s, CH<sub>2</sub>C≡CAu).



**168**

Method 1: To a solution of **159** (0.0157 g, 0.1 mmol) in CH<sub>2</sub>Cl<sub>2</sub> (5 ml) was added [Au(acac)(PPh<sub>3</sub>)] (0.0559 g, 0.1 mmol) and the solution stirred for 2 h. The solution was filtered through celite, the filtrate concentrated under reduced pressure to approximately 1 ml and Et<sub>2</sub>O (10 ml) added to precipitate a white solid which was collected and vacuum dried to give the product (0.0455 g, 74%).

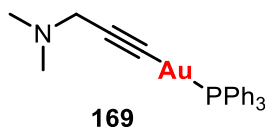
Method 2: To a solution of **159** (0.0315 g, 0.2 mmol) in MeOH (15 ml) was added [AuCl(PPh<sub>3</sub>)] (0.0989 g, 0.2 mmol) and KOH (0.0168 g, 0.3 mmol) and the mixture stirred for 12 h. A white precipitate formed which was collected, washed with Et<sub>2</sub>O and vacuum dried to give the product (0.0895 g, 73%).

**HRMS (ESI/QTOF) m/z:** [M+Na]<sup>+</sup> Calcd for C<sub>27</sub>H<sub>21</sub>AuN<sub>3</sub>NaP 638.1031; Found 638.1041.

**<sup>1</sup>H NMR (300 MHz, CD<sub>2</sub>Cl<sub>2</sub>)** δ 8.02 (d, <sup>3</sup>J<sub>HH</sub> = 8.4 Hz, 1H, H4), 7.90 (d, <sup>3</sup>J<sub>HH</sub> = 8.3 Hz, 1H, H7), 7.59 – 7.42 (m, 16H, PPh<sub>3</sub>/H5), 7.38 (ddd, <sup>3</sup>J<sub>HH</sub> = 8.1 Hz, <sup>3</sup>J<sub>HH</sub> = 6.9 Hz, <sup>4</sup>J<sub>HH</sub> = 1.1 Hz, 1H, H5), 5.54 (s, 2H, CH<sub>2</sub>C≡CAu).

**<sup>31</sup>P NMR (121 MHz, CD<sub>2</sub>Cl<sub>2</sub>)** δ 41.67 (s, PPh<sub>3</sub>).

**$^{13}\text{C}$  APT (75 MHz,  $\text{CD}_2\text{Cl}_2$ )**  $\delta$  146.23 (s, C7a), 134.20 (d,  $^2J_{\text{CP}} = 13.8$  Hz, *o*-PPh<sub>3</sub>), 132.60 (s, C4a), 131.58 (d,  $^4J_{\text{CP}} = 2.5$  Hz, *p*-PPh<sub>3</sub>), 129.13 (d,  $^3J_{\text{CP}} = 11.3$  Hz, *m*-PPh<sub>3</sub>), 127.00 (s, C6), 123.69 (s, C5), 119.54 (s, C4), 110.66 (C7), 93.46 (s,  $\text{CH}_2\text{C}\equiv\text{CAu}$ ), 39.34 (s,  $\text{CH}_2\text{C}\equiv\text{CAu}$ ).

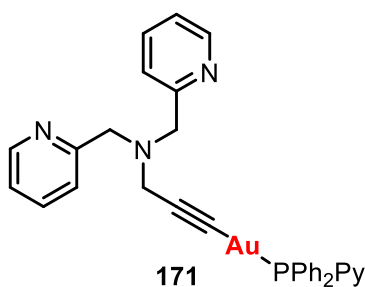


Method 1: To a solution of **160** (16.3  $\mu\text{l}$ , 0.1 mmol) in  $\text{CH}_2\text{Cl}_2$  (5 ml) was added  $[\text{Au}(\text{acac})(\text{PPh}_3)]$  (0.0559 g, 0.1 mmol) and the solution stirred for 2 h. The solution was filtered through celite, the filtrate concentrated under reduced pressure to approximately 1 ml and  $\text{Et}_2\text{O}$  (10 ml) added to precipitate a white solid which was collected and vacuum dried to give the product (0.0540 g, 99%).

Method 2: To a solution of **160** (32.6  $\mu\text{l}$ , 0.2 mmol) in MeOH (15 ml) was added  $[\text{AuCl}(\text{PPh}_3)]$  (0.0989 g, 0.2 mmol) and KOH (0.0168 g, 0.3 mmol) and the mixture stirred for 12 h. A white precipitate formed which was collected, washed with  $\text{Et}_2\text{O}$  and vacuum dried to give the product (0.0129 g, 12%).

**$^1\text{H}$  NMR (400 MHz,  $\text{CD}_2\text{Cl}_2$ )**  $\delta$  7.62 – 7.38 (m, 15H, PPh<sub>3</sub>), 3.28 (s, 2H,  $\text{CH}_2$ ), 2.25 (s, 6H, Me).

**$^{31}\text{P}$  NMR (162 MHz,  $\text{CD}_2\text{Cl}_2$ )**  $\delta$  42.30 (s, PPh<sub>3</sub>).



To a solution of **156** (0.0237 g, 0.1 mmol) in  $\text{CH}_2\text{Cl}_2$  (5 ml) was added  $[\text{Au}(\text{acac})(\text{PPh}_2\text{Py})]$  (0.0560 g, 0.1 mmol) and the solution stirred for 2 h. The solution was filtered through celite, the filtrate concentrated under reduced pressure to approximately 1 ml and  $\text{Et}_2\text{O}$  added to precipitate a pale yellow solid (0.0585 g, 84%).

**HRMS (ESI/QTOF) m/z:**  $[\text{M}]^+$  Calcd for  $\text{C}_{32}\text{H}_{29}\text{AuN}_4\text{P}$  697.1790; Found 697.1795.

## 5.6. Experimental

**$^1\text{H}$  NMR (300 MHz,  $\text{CD}_2\text{Cl}_2$ )**  $\delta$  8.79 (ddd,  $J = 4.8, 1.8, 0.9$  Hz, 1H, Py), 8.51 (ddd,  $J = 4.9, 1.9, 1.0$  Hz, 2H, Py), 7.92 (t,  $J = 7.5$  Hz, 2H, Py), 7.87 – 7.36 (m, 15H,  $\text{PPh}_2\text{Py} + \text{Py}$ ), 7.14 (ddd,  $J = 7.4, 4.9, 1.4$  Hz, 2H, Py), 3.91 (s, 4H,  $\text{CH}_2\text{Py}$ ), 3.43 (s, 2H,  $\text{CH}_2\text{C}\equiv\text{C}$ ).

**$^{31}\text{P}$  NMR (121 MHz,  $\text{CD}_2\text{Cl}_2$ )**  $\delta$  41.40 (s,  $\text{PPh}_2\text{Py}$ ).

**$^{13}\text{C}$  APT (75 MHz,  $\text{CD}_2\text{Cl}_2$ )**  $\delta$  160.39 (s, C2 Py), 151.79 (d,  $^2J_{\text{CP}} = 15.2$  Hz, C3 Py ( $\text{PPh}_2\text{Py}$ )), 149.56 (s, Py), 137.11 (d,  $^3J_{\text{CP}} = 10.6$  Hz, C4 Py ( $\text{PPh}_2\text{Py}$ )), 136.73 (s, Py), 135.25 (d,  $^2J_{\text{CP}} = 13.7$  Hz, *o*-Ph), 132.15 (s, *p*-Ph), 131.74 (s, C5 Py ( $\text{PPh}_2\text{Py}$ )), 129.54 (d,  $^3J_{\text{CP}} = 11.4$  Hz, *m*-Ph), 125.69 (d,  $^3J_{\text{PP}} = 2.3$  Hz, C6 Py ( $\text{PPh}_2\text{Py}$ )), 123.57 (s, Py), 122.35 (s, Py), 60.03 (s,  $\text{CH}_2\text{Py}$ ), 44.18 (s,  $\text{CH}_2\text{C}\equiv\text{CAu}$ ).



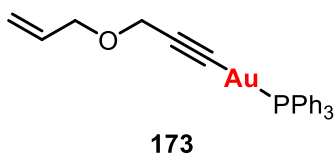
To a solution of propargyl bromide (10.8  $\mu\text{l}$ , 0.1 mmol) in MeOH (15 ml) was added  $[\text{AuCl}(\text{PPh}_3)]$  (0.0495 g, 0.1 mmol) and KOH (0.0168 g, 0.3 mmol) and the mixture stirred for 12 h. A white precipitate formed which was collected, washed with  $\text{Et}_2\text{O}$  and vacuum dried to give the product (0.0388 g, 73%).

**HRMS (ESI/QTOF)  $m/z$ :**  $[\text{M}+\text{Na}]^+$  Calcd for  $\text{C}_{22}\text{H}_{20}\text{AuNaOP}$  551.0809; Found 551.0831.

**$^1\text{H}$  NMR (300 MHz,  $\text{CD}_2\text{Cl}_2$ )**  $\delta$  7.69 – 7.36 (m, 15H,  $\text{PPh}_3$ ), 4.16 (s, 2H,  $\text{CH}_2$ ), 3.35 (s, 3H, Me).

**$^{31}\text{P}$  NMR (121 MHz,  $\text{CD}_2\text{Cl}_2$ )**  $\delta$  42.07 (s,  $\text{PPh}_3$ ).

**$^{13}\text{C}$  APT (75 MHz,  $\text{CD}_2\text{Cl}_2$ )**  $\delta$  134.86 (d,  $^2J_{\text{CP}} = 13.9$  Hz, *o*- $\text{PPh}_3$ ), 132.13 (d,  $^4J_{\text{CP}} = 2.5$  Hz, *p*- $\text{PPh}_3$ ), 130.48 (d,  $^1J_{\text{CP}} = 55.6$  Hz, *i*- $\text{PPh}_3$ ), 129.72 (d,  $^3J_{\text{CP}} = 11.2$  Hz, *m*- $\text{PPh}_3$ ), 61.17 (s,  $\text{CH}_2$ ), 57.35 (s, Me).



To a solution of **162** (16.7  $\mu\text{l}$ , 0.1 mmol) in  $\text{CH}_2\text{Cl}_2$  (5 ml) was added  $[\text{Au}(\text{acac})(\text{PPh}_3)]$  (0.0559 g, 0.1 mmol) and the solution stirred for 2 h. The solution was filtered through celite, the filtrate concentrated under reduced pressure to approximately 1 ml and  $\text{Et}_2\text{O}$  (10 ml) added

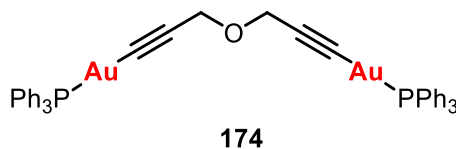
to precipitate a white solid which was collected and vacuum dried to give the product (0.0484 g, 87%).

**HRMS (ESI/QTOF) m/z:**  $[M+Na]^+$  Calcd for  $C_{24}H_{22}AuNaOP$  557.0966; Found 557.0977.

**$^1H$  NMR (300 MHz,  $CD_2Cl_2$ )**  $\delta$  7.66 – 7.39 (m, 15H,  $PPh_3$ ), 5.92 (ddt,  $^3J_{HH} = 17.3$  Hz,  $^3J_{HH} = 10.4$  Hz,  $^3J_{HH} = 5.5$  Hz, 1H), 5.27 (m, 1H, *trans* H), 5.15 (ddt,  $^3J_{HH} = 10.4$  Hz,  $^2J_{HH} = 2.0$  Hz,  $^4J_{HH} = 1.3$  Hz, 1H, *cis* H), 4.23 (s, 2H,  $CH_2C\equiv C$ ), 4.07 (ddd,  $^3J_{HH} = 5.5$  Hz,  $^4J_{HH} = 1.5$  Hz, 2H,  $CH_2CHC=CH_2$ ).

**$^{31}P$  NMR (121 MHz,  $CD_2Cl_2$ )**  $\delta$  42.05 (s,  $PPh_3$ ).

**$^{13}C$  APT (75 MHz,  $CD_2Cl_2$ )**  $\delta$  135.63 (s,  $CH_2CH=CH_2$ ), 134.85 (d,  $^2J_{CP} = 13.8$  Hz, *o*- $PPh_3$ ), 132.12 (d,  $^4J_{CP} = 2.4$  Hz, *p*- $PPh_3$ ), 130.45 (d,  $^1J_{CP} = 55.8$  Hz, *i*- $PPh_3$ ), 129.71 (d,  $^3J_{CP} = 11.2$  Hz, *m*- $PPh_3$ ), 116.86 (s,  $CH_2CH=CH_2$ ), 99.16 (d,  $^2J_{CP} = 26.4$  Hz,  $CH_2C\equiv CAu$ ), 70.45 (s,  $CH_2CH=CH_2$ ), 58.89 (s,  $CH_2C\equiv C$ ).



Method 1: To a solution of **163** (7.7  $\mu$ l, 0.05 mmol) in  $CH_2Cl_2$  (5 ml) was added  $[Au(acac)(PPh_3)]$  (0.0559 g, 0.1 mmol) and the solution stirred for 2 h. The solution was filtered through celite, the filtrate concentrated under reduced pressure to approximately 1 ml and  $Et_2O$  (10 ml) added to precipitate a white solid which was collected and vacuum dried to give the product (0.0242 g, 48%).

Method 2: To a solution of **163** (15.4  $\mu$ l, 0.1 mmol) in MeOH (15 ml) was added  $[AuCl(PPh_3)]$  (0.0989 g, 0.2 mmol) and KOH (0.0168 g, 0.3 mmol) and the mixture stirred for 12 h. A white precipitate formed which was collected, washed with  $Et_2O$  and vacuum dried to give the product (0.0534 g, 53%).

**HRMS (ESI/QTOF) m/z:**  $[M]^+$  Calcd for  $C_{42}H_{35}Au_2OP_2$  1011.1489; Found 1011.1454.

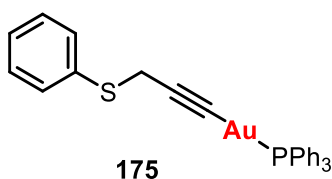
**$^1H$  NMR (300 MHz,  $CD_2Cl_2$ )**  $\delta$  7.66 – 7.43 (m, 30H,  $PPh_3$ ), 4.34 (s, 4H,  $CH_2$ ).

**$^{31}P$  NMR (121 MHz,  $CD_2Cl_2$ )**  $\delta$  42.07 (s,  $PPh_3$ ).

**$^{13}C$  APT (75 MHz,  $CD_2Cl_2$ )**  $\delta$  134.89 (d,  $^2J_{CP} = 13.9$  Hz, *o*- $PPh_3$ ), 132.08 (d,  $^4J_{HH} = 2.4$  Hz, *p*- $PPh_3$ ), 130.54 (d,  $^1J_{CP} = 55.5$  Hz, *i*- $PPh_3$ ), 129.70 (d,  $^3J_{CP} = 11.3$  Hz, *m*- $PPh_3$ ), 98.99 (d,  $^2J_{CP} = 26.5$  Hz,  $CH_2C\equiv CAu$ ), 57.33 (s,  $CH_2C\equiv C$ ).

## 5.6. Experimental

---



Method 1: To a solution of **164** (20.6  $\mu$ l, 0.1 mmol) in  $\text{CH}_2\text{Cl}_2$  (5 ml) was added  $[\text{Au}(\text{acac})(\text{PPh}_3)]$  (0.0559 g, 0.1 mmol) and the solution stirred for 2 h. The solution was filtered through celite, the filtrate concentrated under reduced pressure to approximately 1 ml and  $\text{Et}_2\text{O}$  (10 ml) added to precipitate a white solid which was collected and vacuum dried to give the product (0.0606 g, 99%).

Method 2: To a solution of **164** (20.6  $\mu$ l, 0.1 mmol) in MeOH (15 ml) was added  $[\text{AuCl}(\text{PPh}_3)]$  (0.0495 g, 0.1 mmol) and KOH (0.0168 g, 0.3 mmol) and the mixture stirred for 12 h. A white precipitate formed which was collected, washed with  $\text{Et}_2\text{O}$  and vacuum dried to give the product (0.0551 g, 91%).

**HRMS (ESI/QTOF) m/z:**  $[\text{M}+\text{Na}]^+$  Calcd for  $\text{C}_{27}\text{H}_{22}\text{AuNaPS}$  629.0738; Found 629.0744.

**$^1\text{H}$  NMR (300 MHz,  $\text{CD}_2\text{Cl}_2$ )**  $\delta$  7.62 – 7.13 (m, 20H,  $\text{PPh}_3$  + Ph), 3.78 (s, 2H,  $\text{CH}_2$ ).

**$^{31}\text{P}$  NMR (121 MHz,  $\text{CD}_2\text{Cl}_2$ )**  $\delta$  41.97 (s,  $\text{PPh}_3$ ).

**$^{13}\text{C}$  APT (75 MHz,  $\text{CD}_2\text{Cl}_2$ )**  $\delta$  136.86 (s, Ph), 134.23 (d,  $^2J_{\text{CP}} = 13.9$  Hz, *o*- $\text{PPh}_3$ ), 131.50 (d,  $^4J_{\text{HH}} = 2.4$  Hz, *p*- $\text{PPh}_3$ ), 129.84 (d,  $^1J_{\text{CP}} = 55.6$  Hz, *i*- $\text{PPh}_3$ ), 129.09 (d,  $^3J_{\text{CP}} = 11.4$  Hz, *m*- $\text{PPh}_3$ ), 128.75 (s, Ph), 128.50 (s, Ph), 125.78 (s, Ph), 23.34 (s,  $\text{CH}_2$ ).





# General Conclusions

Gold has a rich organometallic chemistry due to the huge number of possible coordination complexes and the exceptional ability of gold to form intra or intermolecular *aurophilic* interactions. Gold complexes can also exhibit properties such as luminescence or biological activity, giving them a variety of potential applications such as OLEDs, bioimaging or as anticancer agents. In this PhD thesis the coordination chemistry of gold with ylide, allenyl, NHC and propargyl ligands has been explored. Several new organogold complexes have been synthesised and the luminescence and biological properties have been studied.

In Chapter 2 the synthesis of several gold(I) and gold(III) derivatives of cyanomethyltriphenylphosphonium chloride is described. These include complexes in which the phosphonium salt is deprotonated once to give the ylide, which can bind to one metal centre; and complexes in which the phosphonium salt is deprotonated twice to give the yldiide unit which can bridge two metal centres to give dinuclear or polynuclear derivatives. Silver(I) and copper(I) derivatives were also prepared and structurally characterised. The tendency of these metals to adopt a tetrahedral geometry results in complexes in which additional coordination of the nitrile nitrogen atom of another molecule to the metal centre occurs, giving oligomeric or polymeric structures. For the gold derivatives a linear coordination is observed in all cases with no additional coordination of the nitrile nitrogen to the gold centres. The nitrile group can also provide an additional coordination site allowing the synthesis of heterometallic polynuclear complexes. Two luminescent polynuclear derivatives were prepared which exhibit phosphorescent emissions at 77 K. Several of the complexes also exhibited antiproliferative activity against lung cancer cell line A549. The triphenylphosphine derivatives were the most active with  $IC_{50}$  values considerable lower than that of cisplatin.

In Chapter 3 the synthesis of gold derivatives of propargyl functionalised phosphonium, ammonium and sulfonium salts is described. Triphenylpropargylphosphonium bromide was found to readily tautomerise to the allenyl form in solution in all solvents except acetonitrile. This phosphonium salt was successfully used to prepare the first examples of allenyl gold complexes and an interesting regioselectivity was found depending on the oxidation state of

gold. The coordination of gold(III) to the  $\gamma$ -carbon atom of the allenyl group resulted in the formation of axially chiral allenyl gold(III) derivatives. An analogous tautomerism was not observed in propargyl functionalised ammonium salts in solution and consequently gold(I) derivatives were prepared in which the coordination to gold occurs only through the terminal alkyne carbon of the propargyl unit. The antiproliferative activity of these complexes against A549 cells was studied with low IC<sub>50</sub> values found in all cases and increased activity observed for the dinuclear complex compared to the mononuclear derivatives. A propargyl functionalised sulfonium salt was also prepared and was found to only partially tautomerise to the allenyl derivative under forcing conditions (1 week at reflux in acetonitrile). Reaction of this salt with [Au(acac)(PPh<sub>3</sub>)] led to a mixture of the propargyl and allenyl gold derivatives.

A new method for the synthesis of NHC gold complexes is described in Chapter 4. This method has several advantages over previously reported methods in that the reactions can be carried out in air, reaction times are short and both bulky and small imidazolium salt precursors can be used. Moreover, the use of different gold precursors allows different groups to be incorporated into the complexes directly, without the need to first prepare the [AuCl(NHC)] complex and subsequently abstract the halide ligand. The new method was used to prepare a series of propargyl functionalised NHC gold complexes including bromo, pentafluorophenyl, bis-NHC and phosphine derivatives. It was found that a bulky phosphine is required for the formation of [Au(NHC)(PR<sub>3</sub>)]<sup>+</sup>, as equilibria were observed in solution for derivatives with smaller phosphines. Di- and trinuclear complexes were prepared by functionalisation of the propargyl side-arm of the NHC, with coordination of the terminal alkyne carbon to gold observed. Tautomerism of the propargyl unit to the allenyl form was only observed when the transmetallation method with silver oxide was used for the preparation of the NHC gold complexes. Both the silver complex and the corresponding gold derivative were characterised by single crystal X-ray diffraction, confirming the presence of the allenyl tautomer. Of all the complexes prepared, only the NHC gold phosphine derivatives were luminescent with phosphorescent emissions observed both at room temperature and at 77 K. These were assigned to ligand-to-metal-to-ligand charge transfer (LMLCT) transitions. While the imidazolium salt precursors showed no anticancer activity against A549 cells, the gold complexes were active. The best of these were the phosphine derivatives which showed antiproliferative activity far superior to that of cisplatin.

In the final chapter propargyl gold complexes were prepared and characterised. The gold(I) triphenylphosphine derivatives were synthesised by two different routes, however, in both cases similar yields were obtained. Several derivatives were structurally characterised by single crystal X-ray diffraction with intermolecular contacts observed. A heterometallic dinuclear gold(I) copper(I) complex was prepared which was luminescent at room temperature and at 77 K. Emission maxima were assigned to ligand-to-metal charge transfer (LMCT) and intraligand (IL)  $\pi\pi^*$  transitions. All of the complexes displayed antiproliferative activity against A549 cells with the exception of the carbazole derivative. Changing the heteroatom of the propargyl ligand did not significantly affect the activity. The cationic dinuclear gold copper complex, however, was considerably more active than the mononuclear complexes. Since this complex also displays luminescence it has the potential for future application in bioimaging studies.



# Conclusiones Generales

El oro tiene una rica química organometálica rica debido al gran número de complejos de coordinación que puede presentar y a su excepcional capacidad para formar interacciones aurofílicas intra o intermoleculares. Los complejos de oro además pueden presentar propiedades notables como la luminiscencia o la actividad biológica, dotándolos de una gran variedad de aplicaciones potenciales tales como por ejemplo OLEDs, estudios de bioimagen o como agentes anticancerígenos. En esta tesis doctoral se ha explorado la química de coordinación de oro con ligandos iluro, alenilo, NHC y propargilo. Se han sintetizado nuevos complejos organometálicos de oro y se ha estudiado su luminiscencia y sus propiedades biológicas.

En el capítulo 2 se ha descrito la síntesis de varios derivados de oro(I) y de oro(III) con cloruro de cianometiltrifenilfosfonio. Éstos incluyen complejos en los que la sal de fosfonio se desprotona una vez para dar el iluro, que se puede coordinar a un centro metálico, y complejos en los que la sal de fosfonio se desprotona dos veces para dar la unidad ildiuro, que puede actuar como puente entre dos centros metálicos para dar complejos dinucleares o polinucleares. Además, se han preparado y caracterizado derivados de plata(I) y cobre(I) obteniéndose también su estructura molecular por difracción de rayos-X de monocristal. Debido a la tendencia de estos metales a adoptar una geometría tetraédrica, los complejos resultantes presentan estructuras oligoméricas o poliméricas en las que existe una coordinación adicional del nitrógeno del grupo nitrilo de una molécula al centro metálico de otra. En todos los derivados de oro sintetizados se observa una coordinación linear sin ninguna coordinación adicional por parte del nitrógeno del grupo nitrilo a los centros áuricos. El grupo nitrilo, además, puede proporcionar un sitio de coordinación adicional, permitiendo así la síntesis de complejos polinucleares heterometálicos. Se han preparado dos derivados polinucleares luminiscentes que presentan emisiones fosforescentes a 77 K. Varios de los complejos además mostraron actividad antiproliferativa contra el cáncer del pulmón linear celular A549. Los derivados de trifenilfosfonio resultaron ser los más activos con valores de  $IC_{50}$  considerablemente más bajos que el cisplatino.

En el capítulo 3 se ha descrito la síntesis de derivados de sales de fosfonio, amonio y sulfonio funcionalizados con propargilo. Se ha observado que el bromuro de trifenilpropargilofosfonio tautomeriza fácilmente en disolución en todos los disolventes a excepción de acetonitrilo. Se ha utilizado esta sal de fosfonio para preparar los primeros ejemplos de complejos oro alenilo y se ha encontrado una regioselectividad interesante dependiendo del estado de oxidación del oro. La coordinación del carbono- $\gamma$  del grupo alenilo al oro(III) dio lugar a la formación de complejos oro(III) alenilo axialmente quirales. No se ha observado un tautomerismo análogo en las disoluciones de sales de amonio funcionalizadas con propargilo y por consiguiente se han preparado derivados de oro(I) en los que la coordinación al metal se produce únicamente a través del carbono terminal del alquino de la unidad propargilo. Se ha estudiado la actividad antiproliferativa de estos complejos en células A549, mostrando valores de  $IC_{50}$  bajos en todos los casos y se observó un aumento de actividad para el derivado dinuclear comparándolo con los derivados mononucleares. Además, se ha preparado una sal de sulfonio funcionalizada con propargilo y se observó que solo tautomeriza parcialmente al derivado alenilo bajo condiciones forzadas (una semana a reflujo en acetonitrilo). La reacción de esta sal con  $[Au(acac)(PPh_3)]$  dio lugar a una mezcla de los derivados de oro propargilo y alenilo.

Se ha descrito un nuevo método para la síntesis de complejos de oro NHC en el capítulo 4. Este método tiene varias ventajas con respecto a los métodos previamente descritos ya que las reacciones se pueden realizar al aire, los tiempos de reacción son menores y permite el uso de sales de imidazolio tanto pequeñas como voluminosas como precursores. Además, el uso de precursores diferentes de oro permite la incorporación directa de distintos grupos en el complejo sin la necesidad de preparar primero el complejo de  $[AuCl(NHC)]$  con la posterior abstracción del ligando halogenuro. Se ha utilizado este nuevo método para preparar una serie de complejos de oro NHC funcionalizados con propargilo, que incluyen bromuro, pentaflorofenilo, bis-NHC y fosfina. Se descubrió que para la formación de complejos  $[Au(NHC)(PR_3)]^+$  se requiere una fosfina voluminosa, ya que se observaron equilibrios en disolución al usar fosfinas pequeñas. Se han preparado derivados di- y trinucleares mediante la funcionalización del grupo propargilo del NHC, en los que se observa la coordinación del carbono alquino terminal al oro. Solo se ha observado tautomerismo de la unidad propargilo al alenilo al usar el método de transmetalación con óxido de plata para preparar los complejos oro NHC. Tanto el complejo de plata como el derivado de oro correspondiente se han caracterizado

por difracción de rayos-X de monocristal, confirmándose la presencia del tautomero alenilo. De todos los complejos preparados, solo los derivados fosfina oro NHC resultaron ser luminiscentes con emisiones fosforescentes a temperatura ambiente y a 77 K. Estas emisiones se han asignado a transiciones de transferencia de carga del ligando al metal al ligando (LMLCT). A pesar de que las sales de imidazolio no mostraron actividad anticancerígena en células A549, sí lo hicieron sus correspondientes complejos de oro. Los derivados de fosfinas mostraron una actividad antiproliferativa muy superior a la del cisplatino, siendo los compuestos con mayor actividad anticancerígena.

En el último capítulo se han preparado y caracterizado diversos complejos de oro propargilo. Se han sintetizado los derivados trifenilfosfina oro(I) mediante dos métodos diferentes. En los dos casos se obtuvieron rendimientos similares. Se han caracterizado estructuralmente varios derivados por difracción de rayos-X de monocristal y se han observado diversos contactos intermoleculares en varios casos. Se ha preparado un derivado dinuclear heterometálico de oro(I) y cobre(I) que mostró luminiscencia tanto a temperatura ambiente como a 77 K. Se han asignado bandas de emisión a transiciones de transferencia de carga del ligando al metal (LMCT) e intraligando (IL)  $\pi\pi^*$ . Todos los complejos mostraron actividad antiproliferativa en la línea celular A549 con la excepción del derivado de carbazol. No se observó ningún efecto significativo en la actividad al cambiar el heteroátomo del ligando propargilo. Sin embargo, el complejo catiónico dinuclear de oro y cobre fue considerablemente más activo que los complejos mononucleares, y al ser este complejo también luminiscente, presenta un gran potencial para futuras aplicaciones en estudios de bioimagen.

# References

1. B. Hammer and J. K. Norskov, *Nature*, 1995, **376**, 238-240.
2. H. Schmidbaur, *Gold: progress in chemistry, biochemistry, and technology*, Wiley, Chichester ; New York, 1999.
3. G. Morteani, in *Gold: progress in chemistry, biochemistry, and technology*, ed. H. Schmidbaur, Wiley, Chichester; New York, 1999, ch. 2, p. 40.
4. K. S. Pitzer, *Acc. Chem. Res.*, 1979, **12**, 271-276.
5. P. Pyykko and J. P. Desclaux, *Acc. Chem. Res.*, 1979, **12**, 276-281.
6. R. W. G. Wyckoff, *Crystal structures*, Interscience Publishers, New York., 2d edn., 1963.
7. L. Pauling, *The nature of the chemical bond and the structure of molecules and crystals; an introduction to modern structural chemistry*, Cornell University Press, Ithaca, N.Y., 3d edn., 1960.
8. A. Bayler, A. Schier, G. A. Bowmaker and H. Schmidbaur, *J. Am. Chem. Soc.*, 1996, **118**, 7006-7007.
9. S. Riedel and M. Kaupp, *Coord. Chem. Rev.*, 2009, **253**, 606-624.
10. M. Jansen, *Chem. Soc. Rev.*, 2008, **37**, 1826-1835.
11. J. E. Huheey, *Inorganic chemistry: principles of structure and reactivity*, Harper & Row, New York, SI units edn., 1975.
12. P. G. Jones, *Gold Bull.*, 1981, **14**, 102-118.
13. H. Schmidbaur, *Gold Bull.*, 1990, **23**, 11-21.
14. H. Schmidbaur, *Gold Bull.*, 2000, **33**, 3-10.
15. H. Schmidbaur and A. Schier, *Chem. Soc. Rev.*, 2008, **37**, 1931-1951.
16. H. Schmidbaur and A. Schier, *Chem. Soc. Rev.*, 2012, **41**, 370-412.
17. P. Pyykkö, N. Runeberg and F. Mendizabal, *Chem. Eur. J.*, 1997, **3**, 1451-1457.
18. P. Pyykkö, J. Li and N. Runeberg, *Chem. Phys. Lett.*, 1994, **218**, 133-138.
19. F. Scherbaum, A. Grohmann, B. Huber, C. Krüger and H. Schmidbaur, *Angew. Chem. Int. Ed. Engl.*, 1988, **27**, 1544-1546.
20. H. Schumann, C. Janiak, J. Pickardt and U. Börner, *Angew. Chem. Int. Ed. Engl.*, 1987, **26**, 789-790.
21. C. Janiak and R. Hoffmann, *J. Am. Chem. Soc.*, 1990, **112**, 5924-5946.



## References

---

22. K. Singh, J. R. Long and P. Stavropoulos, *J. Am. Chem. Soc.*, 1997, **119**, 2942-2943.
23. M. A. Bennett, M. Contel, D. C. R. Hockless and L. L. Welling, *Chem. Commun.*, 1998, 2401-2402.
24. V. J. Catalano, B. L. Bennett, S. Muratidis and B. C. Noll, *J. Am. Chem. Soc.*, 2001, **123**, 173-174.
25. T. G. H. James, *Gold Bull.*, 1972, **5**, 38-42.
26. A. Oddy, *Gold Bull.*, 1977, **10**, 79-87.
27. A. Oddy and S. La Niece, *Gold Bull.*, 1986, **19**, 19-27.
28. J. A. Donaldson, *Gold Bull.*, 1980, **13**, 117-124.
29. I. Freestone, N. Meeks, M. Sax and C. Higgitt, *Gold Bull.*, 2007, **40**, 270-277.
30. K. W. Scheele, *The chemical essays of Charles-William Scheele. Translated from the transactions of the Academy of Sciences at Stockholm. With additions [electronic resource]*, printed for J. Murray; W. Gordon and C. Elliot, Edinburgh, London, 1786.
31. E. Frankland and B. F. Duppa, *J. Chem. Soc.*, 1864, **17**, 29-36.
32. W. J. Pope and C. S. Gibson, *J. Chem. Soc., Trans.*, 1907, **91**, 2061-2066.
33. S. Gambarotta, C. Floriani, A. Chiesi-Villa and C. Guastini, *J. Chem. Soc., Chem. Commun.*, 1983, 1304-1306.
34. G. E. Coates and C. Parkin, *J. Chem. Soc.*, 1962, 3220-3226.
35. D. M. P. Mingos, J. Yau, S. Menzer and D. J. Williams, *Angew. Chem. Int. Ed. Engl.*, 1995, **34**, 1894-1895.
36. H. Lang, K. Kohler and L. Zsolnai, *Chem. Commun.*, 1996, 2043-2044.
37. H. V. R. Dias, M. Fianchini, T. R. Cundari and C. F. Campana, *Angew. Chem. Int. Ed.*, 2008, **47**, 556-559.
38. R. V. Parish, *Gold Bull.*, 1982, **15**, 51-63.
39. K. Moss, R. V. Parish, A. Laguna, M. Laguna and R. Uson, *J. Chem. Soc., Dalton Trans.*, 1983, 2071-2074.
40. F. G. A. Stone, *J. Fluorine Chem.*, 1999, **100**, 227-234.
41. J. Gil-Rubio and J. Vicente, *Dalton Trans.*, 2015, **44**, 19432-19442.
42. C. S. Gibson and J. L. Simonsen, *J. Chem. Soc.*, 1930, 2531-2536.
43. C. S. Gibson and W. M. Colles, *J. Chem. Soc.*, 1931, 2407-2416.
44. H. Gilman and L. A. Woods, *J. Am. Chem. Soc.*, 1948, **70**, 550-552.
45. G. E. Coates and C. Parkin, *J. Chem. Soc.*, 1963, 421-429.

## References

---

46. R. Uson, A. Laguna and J. Vicente, *J. Chem. Soc., Chem. Commun.*, 1976, 353-354.
47. S. Komiya, T. A. Albright, R. Hoffmann and J. K. Kochi, *J. Am. Chem. Soc.*, 1976, **98**, 7255-7265.
48. A. Tamaki and J. K. Kochi, *J. Organomet. Chem.*, 1973, **61**, 441-450.
49. A. N. Nesmeyanov, E. G. Perevalova, K. I. Grandberg, D. A. Lemenovskii, T. V. Baukova and O. B. Afanassova, *J. Organomet. Chem.*, 1974, **65**, 131-144.
50. H. Schmidbaur and O. Gasser, *Angew. Chem. Int. Ed. Engl.*, 1976, **15**, 502-503.
51. H. Schmidbaur, F. Scherbaum, B. Huber and G. Müller, *Angew. Chem. Int. Ed. Engl.*, 1988, **27**, 419-421.
52. F. Scherbaum, B. Huber, G. Müller and H. Schmidbaur, *Angew. Chem. Int. Ed. Engl.*, 1988, **27**, 1542-1544.
53. F. Scherbaum, A. Grohmann, G. Müller and H. Schmidbaur, *Angew. Chem. Int. Ed. Engl.*, 1989, **28**, 463-465.
54. K.-H. Wong, K.-K. Cheung, M. C.-W. Chan and C.-M. Che, *Organometallics*, 1998, **17**, 3505-3511.
55. L. S. Hollis and S. J. Lippard, *J. Am. Chem. Soc.*, 1983, **105**, 4293-4299.
56. C.-W. Chan, W.-T. Wong and C.-M. Che, *Inorg. Chem.*, 1994, **33**, 1266-1272.
57. H.-Q. Liu, T.-C. Cheung, S.-M. Peng and C.-M. Che, *J. Chem. Soc., Chem. Commun.*, 1995, 1787-1788.
58. C. Bronner and O. S. Wenger, *Dalton Trans.*, 2011, **40**, 12409-12420.
59. D.-A. Rosca, D. A. Smith and M. Bochmann, *Chem. Commun.*, 2012, **48**, 7247-7249.
60. B. Pitteri, G. Marangoni, F. Visentin, T. Bobbo, V. Bertolasi and P. Gilli, *J. Chem. Soc., Dalton Trans.*, 1999, 677-682.
61. M. A. Cinellu, G. Minghetti, M. V. Pinna, S. Stoccoro, A. Zucca and M. Manassero, *J. Chem. Soc., Dalton Trans.*, 2000, 1261-1265.
62. M. Bortoluzzi, E. De Faveri, S. Daniele and B. Pitteri, *Eur. J. Inorg. Chem.*, 2006, 3393-3399.
63. D.-A. Roşca, D. A. Smith, D. L. Hughes and M. Bochmann, *Angew. Chem. Int. Ed.*, 2012, **51**, 10643-10646.
64. D.-A. Roşca, J. A. Wright, D. L. Hughes and M. Bochmann, *Nat. Commun.*, 2013, **4**, 2167.

## References

---

65. N. Savjani, D.-A. Roşca, M. Schormann and M. Bochmann, *Angew. Chem. Int. Ed.*, 2013, **52**, 874-877.
66. W. C. Zeise, *Annalen der Physik*, 1827, **85**, 632-632.
67. X.-S. Xiao, W.-L. Kwong, X. Guan, C. Yang, W. Lu and C.-M. Che, *Chem. Eur. J.*, 2013, **19**, 9457-9462.
68. E. Langseth, M. L. Scheuermann, D. Balcells, W. Kaminsky, K. I. Goldberg, O. Eisenstein, R. H. Heyn and M. Tilset, *Angew. Chem. Int. Ed.*, 2013, **52**, 1660-1663.
69. F. R. Hartley, *Chem. Rev.*, 1969, **69**, 799-844.
70. F. Rekhroukh, C. Blons, L. Estevez, S. Mallet-Ladeira, K. Miqueu, A. Amgoune and D. Bourissou, *Chem. Sci.*, 2017, **8**, 4539-4545.
71. F. Bonati and G. Minghetti, *Synth. React. Inorg. Met.-Org. Chem.*, 1971, **1**, 299-302.
72. F. Bonati, A. Burini, B. R. Pietroni and B. Bovio, *J. Organomet. Chem.*, 1989, **375**, 147-160.
73. G. D. Frey, R. D. Dewhurst, S. Kousar, B. Donnadieu and G. Bertrand, *J. Organomet. Chem.*, 2008, **693**, 1674-1682.
74. G. Bertrand, M. Sioleilhavoup, M. Melaimi and R. Jazzar, *Angew. Chem. Int. Ed.*, 2017, n/a-n/a.
75. E. Y. Tsui, P. Müller and J. P. Sadighi, *Angew. Chem. Int. Ed.*, 2008, **47**, 8937-8940.
76. D. S. Laitar, P. Müller, T. G. Gray and J. P. Sadighi, *Organometallics*, 2005, **24**, 4503-4505.
77. P. Gassman, G. Meyer and F. Williams, *J. Am. Chem. Soc.*, 1972, **94**, 7741-7748.
78. J. A. Akana, K. X. Bhattacharyya, P. Müller and J. P. Sadighi, *J. Am. Chem. Soc.*, 2007, **129**, 7736-7737.
79. A. S. K. Hashmi, A. M. Schuster and F. Rominger, *Angew. Chem. Int. Ed.*, 2009, **48**, 8247-8249.
80. A. S. K. Hashmi, *Gold Bull.*, 2009, **42**, 275-279.
81. R. L. LaLonde, J. W. E. Brenzovich, D. Benitez, E. Tkatchouk, K. Kelley, I. I. I. W. A. Goddard and F. D. Toste, *Chem. Sci.*, 2010, **1**, 226-233.
82. P. H.-Y. Cheong, P. Morganelli, M. R. Luzung, K. N. Houk and F. D. Toste, *J. Am. Chem. Soc.*, 2008, **130**, 4517-4526.
83. D. Weber, M. A. Tarselli and M. R. Gagné, *Angew. Chem. Int. Ed.*, 2009, **48**, 5733-5736.

## References

---

84. D. Weber and M. R. Gagné, *Org. Lett.*, 2009, **11**, 4962-4965.
85. M. Contel, J. Jimenez, P. G. Jones, A. Laguna and M. Laguna, *J. Chem. Soc., Dalton Trans.*, 1994, 2515-2518.
86. D. Wang, R. Cai, S. Sharma, J. Jirak, S. K. Thummanapelli, N. G. Akhmedov, H. Zhang, X. Liu, J. L. Petersen and X. Shi, *J. Am. Chem. Soc.*, 2012, **134**, 9012-9019.
87. G. Seidel, C. W. Lehmann and A. Fürstner, *Angew. Chem. Int. Ed.*, 2010, **49**, 8466-8470.
88. J. E. Heckler, M. Zeller, A. D. Hunter and T. G. Gray, *Angew. Chem. Int. Ed.*, 2012, **51**, 5924-5928.
89. A. Gómez-Suárez, S. Dupuy, A. M. Z. Slawin and S. P. Nolan, *Angew. Chem. Int. Ed.*, 2013, **52**, 938-942.
90. H. Schmidbaur and A. Schier, *Organometallics*, 2010, **29**, 2-23.
91. T. J. Brown and R. A. Widenhoefer, *Organometallics*, 2011, **30**, 6003-6009.
92. A. Griprane, H. Garcia, A. Corma and E. Álvarez, *ACS Catal.*, 2011, **1**, 1647-1653.
93. V. López-Carrillo and A. M. Echavarren, *J. Am. Chem. Soc.*, 2010, **132**, 9292-9294.
94. M. C. Blanco, J. Cámara, M. C. Gimeno, P. G. Jones, A. Laguna, J. M. López-de-Luzuriaga, M. E. Olmos and M. D. Villacampa, *Organometallics*, 2012, **31**, 2597-2605.
95. A. S. K. Hashmi, *Acc. Chem. Res.*, 2014, **47**, 864-876.
96. F. Lazreg, S. Guidone, A. Gomez-Herrera, F. Nahra and C. S. J. Cazin, *Dalton Trans.*, 2017, **46**, 2439-2444.
97. L. Ye, Y. Wang, D. H. Aue and L. Zhang, *J. Am. Chem. Soc.*, 2012, **134**, 31-34.
98. M. M. Hansmann, F. Rominger and A. S. K. Hashmi, *Chem. Sci.*, 2013, **4**, 1552-1559.
99. R. J. Harris and R. A. Widenhoefer, *Angew. Chem. Int. Ed.*, 2015, **54**, 6867-6869.
100. W. Debrouwer and A. Fürstner, *Chem. Eur. J.*, 2017, **23**, 4271-4275.
101. A. M. Echavarren, *Nat. Chem.*, 2009, **1**, 431-433.
102. A. S. K. Hashmi, *Angew. Chem. Int. Ed.*, 2008, **47**, 6754-6756.
103. Y. Wang, M. E. Muratore and A. M. Echavarren, *Chem. Eur. J.*, 2015, **21**, 7332-7339.
104. G. Seidel and A. Fürstner, *Angew. Chem. Int. Ed.*, 2014, **53**, 4807-4811.
105. M. W. Hussong, F. Rominger, P. Krämer and B. F. Straub, *Angew. Chem. Int. Ed.*, 2014, **53**, 9372-9375.
106. M. Joost, L. Estévez, S. Mallet-Ladeira, K. Miqueu, A. Amgoune and D. Bourissou, *Angew. Chem. Int. Ed.*, 2014, **53**, 14512-14516.

## References

---

107. A. J. Chalk, *J. Am. Chem. Soc.*, 1964, **86**, 4733-4734.
108. D. Belli Dell'Amico, F. Calderazzo, R. Dantona, J. Straehle and H. Weiss, *Organometallics*, 1987, **6**, 1207-1210.
109. T. J. Brown, M. G. Dickens and R. A. Widenhoefer, *J. Am. Chem. Soc.*, 2009, **131**, 6350-6351.
110. T. J. Brown, M. G. Dickens and R. A. Widenhoefer, *Chem. Commun.*, 2009, 6451-6453.
111. R. E. M. Brooner, T. J. Brown and R. A. Widenhoefer, *Chem. Eur. J.*, 2013, **19**, 8276-8284.
112. T. J. Brown, A. Sugie, M. G. D. Leed and R. A. Widenhoefer, *Chem. Eur. J.*, 2012, **18**, 6959-6971.
113. M. García-Mota, N. Cabello, F. Maseras, A. M. Echavarren, J. Pérez-Ramírez and N. Lopez, *ChemPhysChem*, 2008, **9**, 1624-1629.
114. P. Schulte and U. Behrens, *Chem. Commun.*, 1998, 1633-1634.
115. T. N. Hooper, M. Green and C. A. Russell, *Chem. Commun.*, 2010, **46**, 2313-2315.
116. V. Lavallo, G. D. Frey, S. Kousar, B. Donnadiou and G. Bertrand, *Proc. Natl. Acad. Sci.*, 2007, **104**, 13569-13573.
117. J. Vicente, M. T. Chicote and M. C. Lagunas, *Helv. Chim. Acta*, 1999, **82**, 1202-1210.
118. E. E. Schweizer, S. D. Goff and W. P. Murray, *J. Org. Chem.*, 1977, **42**, 200-205.
119. G. B. Bagdasaryan, P. S. Pogosyan, G. A. Panosyan and M. G. Indzhikyan, *Russ. J. Gen. Chem.*, 2008, **78**, 1177-1183.
120. M. V. Baker, P. J. Barnard, S. J. Berners-Price, S. K. Brayshaw, J. L. Hickey, B. W. Skelton and A. H. White, *Dalton Trans.*, 2006, 3708-3715.
121. J. Carlos Lima and L. Rodriguez, *Chem. Soc. Rev.*, 2011, **40**, 5442-5456.
122. B. Bertrand and A. Casini, *Dalton Trans.*, 2014, **43**, 4209-4219.
123. M. A. Cinellu, I. Ott and A. Casini, in *Bioorganometallic Chemistry*, Wiley-VCH Verlag GmbH & Co. KGaA, 2014, pp. 117-140.
124. O. I. Kolodiaznyi, in *Phosphorus Ylides*, Wiley-VCH Verlag GmbH, 1999, pp. 1-8.
125. K. C. Nicolaou, M. W. Härter, J. L. Gunzner and A. Nadin, *Liebigs Annalen*, 1997, **1997**, 1283-1301.
126. A.-H. Li, L.-X. Dai and V. K. Aggarwal, *Chem. Rev.*, 1997, **97**, 2341-2372.
127. A. Michaelis and H. V. Gimborn, *Ber. Dtsch. Chem. Ges.*, 1894, **27**, 272-277.

## References

---

128. A. W. Johnson, *Ylides and imines of phosphorus*, John Wiley Sons Inc., New York, 1993.
129. H. Schmidbaur, *Acc. Chem. Res.*, 1975, **8**, 62-70.
130. H. Schmidbaur, R. Mandl Johann, A. Wohlleben and A. Fügner, *Zeitschrift für Naturforschung B*, 1978, **33**, 1325.
131. H. Schmidbaur, *Pure Appl. Chem.*, 1978, **50**, 19.
132. H. Schmidbaur, *Angew. Chem. Int. Ed. Engl.*, 1983, **22**, 907-927.
133. I. Zugrăvescu and M. Petrovanu, *N-ylid chemistry*, McGraw-Hill, New York, 1976.
134. W. K. Musker, *J. Chem. Educ.*, 1968, **45**, 200.
135. J. S. Clark, *Nitrogen, oxygen, and sulfur ylide chemistry : a practical approach in chemistry*, Oxford University Press, New York, 2002.
136. B. M. Trost and L. S. Melvin, *Sulfur ylides: emerging synthetic intermediates*, Academic Press, New York,, 1975.
137. D. Lloyd, I. Gosney and R. A. Ormiston, *Chem. Soc. Rev.*, 1987, **16**, 45-74.
138. A. O. Starzewski, in *Late Transition Metal Polymerization Catalysis*, Wiley-VCH Verlag GmbH & Co. KGaA, 2003, pp. 1-26.
139. B. E. Maryanoff and A. B. Reitz, *Chem. Rev.*, 1989, **89**, 863-927.
140. J. C. J. Bart, *Journal of the Chemical Society B: Physical Organic*, 1969, 350-365.
141. C. Zhu, A. Yoshimura, L. Ji, Y. Wei, V. N. Nemykin and V. V. Zhdankin, *Org. Lett.*, 2012, **14**, 3170-3173.
142. F. H. Allen, O. Kennard, D. G. Watson, L. Brammer, A. G. Orpen and R. Taylor, *Journal of the Chemical Society, Perkin Transactions 2*, 1987, S1-S19.
143. R. A. Eades, P. G. Gassman and D. A. Dixon, *J. Am. Chem. Soc.*, 1981, **103**, 1066-1068.
144. R. Hoffmann, D. B. Boyd and S. Z. Goldberg, *J. Am. Chem. Soc.*, 1970, **92**, 3929-3936.
145. D. L. Cooper, T. P. Cunningham, J. Gerratt, P. B. Karadakov and M. Raimondi, *J. Am. Chem. Soc.*, 1994, **116**, 4414-4426.
146. D. G. Gilheany, *Chem. Rev.*, 1994, **94**, 1339-1374.
147. F. Bernardi, H. B. Schlegel, M.-H. Whangbo and S. Wolfe, *J. Am. Chem. Soc.*, 1977, **99**, 5633-5636.
148. T. A. Albright, J. K. Burdett and M.-H. Whangbo, in *Orbital Interactions in Chemistry*, John Wiley & Sons, Inc., New York, 1985.

## References

---

149. D. J. Mitchell, S. Wolfe and H. B. Schlegel, *Can. J. Chem.*, 1981, **59**, 3280-3292.
150. A. Streitwieser, A. Rajca, R. S. McDowell and R. Glaser, *J. Am. Chem. Soc.*, 1987, **109**, 4184-4188.
151. H. J. Bestmann, A. J. Kos, K. Witzgall and P. V. R. Schleyer, *Chem. Ber.*, 1986, **119**, 1331-1349.
152. D. A. Dixon, T. H. Dunning, R. A. Eades and P. G. Gassman, *J. Am. Chem. Soc.*, 1983, **105**, 7011-7017.
153. H. Schmidbaur, in *Gmelin Handbuch der Anorganischen Chemie*, ed. H. Schmidbaur, Springer-Verlag, Berlin, 1980, ch. 1, pp. 29-30.
154. H. Schmidbaur, in *Gmelin Handbuch der Anorganischen Chemie*, ed. H. Schmidbaur, Springer-Verlag, Berlin, 1980, ch. 1, pp. 40-42.
155. J. Vicente, M. T. Chicote, C. MacBeath and P. G. Jones, *Organometallics*, 2003, **22**, 1843-1848.
156. G. Aksnes, *Acta Chem. Scand.*, 1961, **15**, 438-440.
157. F. Ramirez and S. Dershowitz, *J. Org. Chem.*, 1957, **22**, 41-45.
158. H. Staudinger and J. Meyer, *Helv. Chim. Acta*, 1919, **2**, 619-635.
159. G. Wittig and M. Rieber, *Justus Liebigs Ann. Chem.*, 1949, **562**, 187-192.
160. G. Wittig and G. Geissler, *Justus Liebigs Ann. Chem.*, 1953, **580**, 44-57.
161. D. Seyferth and S. O. Grim, *J. Am. Chem. Soc.*, 1961, **83**, 1610-1613.
162. B. L. Barnett and C. Krüger, *Journal of Crystal and Molecular Structure*, 1972, **2**, 271-279.
163. H. Schmidbaur and R. Franke, *Angew. Chem. Int. Ed. Engl.*, 1973, **12**, 416-417.
164. H. Schmidbaur, J. E. Mandl, W. Richter, V. Bejenke, A. Frank and G. Huttner, *Chem. Ber.*, 1977, **110**, 2236-2241.
165. J. Stein, J. P. Fackler, C. Pappas and H. W. Chen, *J. Am. Chem. Soc.*, 1981, **103**, 2192-2198.
166. H. Schmidbaur, J. R. Mandl, A. Frank and G. Huttner, *Chem. Ber.*, 1976, **109**, 466-472.
167. L. R. Falvello, S. Fernández, R. Navarro and E. P. Urriolabeitia, *Inorg. Chem.*, 1997, **36**, 1136-1142.
168. X. M. Zhang and F. G. Bordwell, *J. Am. Chem. Soc.*, 1994, **116**, 968-972.
169. J. Ammer, C. Nolte, K. Karaghiosoff, S. Thallmair, P. Mayer, R. de Vivie-Riedle and H. Mayr, *Chem. Eur. J.*, 2013, **19**, 14612-14630.

## References

---

170. M. Shafiq, M. N. Tahir, I. U. Khan, M. N. Arshad and N. Zaib un, *Acta Crystallogr. Sect. Sect. E: Struct. Rep. Online*, 2008, **64**, o2213-o2213.
171. S. Trippett and D. M. Walker, *J. Chem. Soc.*, 1959, 3874-3876.
172. A. Luquin, E. Cerrada and M. Laguna, in *Gold Chemistry*, Wiley-VCH Verlag GmbH & Co. KGaA, 2009, pp. 93-181.
173. T. Mosmann, *Journal of Immunological Methods*, 1983, **65**, 55-63.
174. S. Ma, *Chem. Rev.*, 2005, **105**, 2829-2872.
175. B. Alcaide, P. Almendros and C. Aragoncillo, *Chem. Soc. Rev.*, 2010, **39**, 783-816.
176. R. Zimmer, C. U. Dinesh, E. Nandan and F. A. Khan, *Chem. Rev.*, 2000, **100**, 3067-3126.
177. W. Yang and A. S. K. Hashmi, *Chem. Soc. Rev.*, 2014, **43**, 2941-2955.
178. K. M. Brummond and H. Chen, in *Modern Allene Chemistry*, Wiley-VCH Verlag GmbH, 2004, pp. 1041-1089.
179. N. Krause and A. Hoffmann-Röder, in *Modern Allene Chemistry*, Wiley-VCH Verlag GmbH, 2004, pp. 997-1040.
180. B. L. Shaw and A. J. Stringer, *Inorganica Chimica Acta Reviews*, 1973, **7**, 1-10.
181. J. A. Marshall, B. W. Gung and M. L. Grachan, in *Modern Allene Chemistry*, Wiley-VCH Verlag GmbH, 2004, pp. 493-592.
182. J. H. Van't Hoff, *La Chimie dans l'espace*, P.M. Bazendijk, Rotterdam, 1875.
183. B. S. Burton and H. von Pechmann, *Ber. Dtsch. Chem. Ges.*, 1887, **20**, 145-149.
184. E. R. H. Jones, G. H. Mansfield and M. C. Whiting, *J. Chem. Soc.*, 1954, 3208-3212.
185. F. W. Semmler, *Ber. Dtsch. Chem. Ges.*, 1906, **39**, 726-731.
186. H. Gilman, P. R. v. Ess and R. R. Burtner, *J. Am. Chem. Soc.*, 1933, **55**, 3461-3463.
187. H. Staudinger and L. Ruzicka, *Helv. Chim. Acta*, 1924, **7**, 212-235.
188. L. Crombie, S. H. Harper and D. Thompson, *J. Chem. Soc.*, 1951, 2906-2915.
189. F. Schütt, *Ber. Dtsch. Bot. Ges.*, 1890, **8**, 9-32.
190. H. Rapoport, H. H. Strain, W. A. Svec, K. Aitzetmueller, M. Grandolfo, J. J. Katz, H. Kjoesen, S. Norgard and S. Liaaen-Jensen, *J. Am. Chem. Soc.*, 1971, **93**, 1823-1825.
191. R. Ben-Shoshan and R. Pettit, *J. Am. Chem. Soc.*, 1967, **89**, 2231-2232.
192. K. Okamoto, Y. Kai, N. Yasuoka and N. Kasai, *J. Organomet. Chem.*, 1974, **65**, 427-441.



## References

---

193. T. J. Brown, A. Sugie, M. G. Dickens and R. A. Widenhoefer, *Organometallics*, 2010, **29**, 4207-4209.
194. M. Green, N. Mayne and F. G. A. Stone, *Chem. Commun. (London)*, 1966, 755-756.
195. R. J. Goodfellow, M. Green, N. Mayne, A. J. Rest and F. G. A. Stone, *J. Chem. Soc. A*, 1968, 177-180.
196. P. W. Jolly and R. Pettit, *J. Organomet. Chem.*, 1968, **12**, 491-495.
197. M. D. Johnson and C. Mayle, *J. Chem. Soc. D*, 1969, 192-192.
198. J. Barluenga, A. A. Trabanco, J. Flórez, S. García-Granda and M.-A. Llorca, *J. Am. Chem. Soc.*, 1998, **120**, 12129-12130.
199. B. Reichmann, M. Drexler, B. Weibert, N. Szesni, T. Strittmatter and H. Fischer, *Organometallics*, 2011, **30**, 1215-1223.
200. D. F. Schafer, P. T. Wolczanski and E. B. Lobkovsky, *Organometallics*, 2011, **30**, 6518-6538.
201. H. Matsuzaka, H. Koizumi, Y. Takagi, M. Nishio and M. Hidai, *J. Am. Chem. Soc.*, 1993, **115**, 10396-10397.
202. N. Carleton, J. F. Corrigan, S. Doherty, R. Pixner, Y. Sun, N. J. Taylor and A. J. Carty, *Organometallics*, 1994, **13**, 4179-4182.
203. P. Blenkiron, J. F. Corrigan, N. J. Taylor, A. J. Carty, S. Doherty, M. R. J. Elsegood and W. Clegg, *Organometallics*, 1997, **16**, 297-300.
204. P. Crochet, B. Demerseman, M. I. Vallejo, M. P. Gamasa, J. Gimeno, J. Borge and S. García-Granda, *Organometallics*, 1997, **16**, 5406-5415.
205. B. Buriez, D. J. Cook, K. J. Harlow, A. F. Hill, T. Welton, A. J. P. White, D. J. Williams and J. D. E. T. Wilton-Ely, *J. Organomet. Chem.*, 1999, **578**, 264-267.
206. H. D. Hansen and J. H. Nelson, *Organometallics*, 2000, **19**, 4740-4755.
207. M. Jiménez-Tenorio, M. D. Palacios, M. C. Puerta and P. Valerga, *J. Organomet. Chem.*, 2004, **689**, 2776-2785.
208. Y. Nishimura, Y. Arikawa, T. Inoue and M. Onishi, *Dalton Trans.*, 2005, 930-937.
209. Y. Arikawa, K. Ikeda, T. Asayama, Y. Nishimura and M. Onishi, *Chem. Eur. J.*, 2007, **13**, 4024-4036.
210. S. Bolaño, M. M. Rodríguez-Rocha, J. Bravo, J. Castro, E. Oñate and M. Peruzzini, *Organometallics*, 2009, **28**, 6020-6030.

## References

---

211. I. García de la Arada, J. Díez, M. P. Gamasa and E. Lastra, *Organometallics*, 2015, **34**, 1345-1353.
212. H. Werner, R. Fluegel, B. Windmueller, A. Michenfelder and J. Wolf, *Organometallics*, 1995, **14**, 612-618.
213. C. Bohanna, B. Callejas, A. J. Edwards, M. A. Esteruelas, F. J. Lahoz, L. A. Oro, N. Ruiz and C. Valero, *Organometallics*, 1998, **17**, 373-381.
214. R. P. Hughes, R. B. Larichev, L. N. Zakharov and A. L. Rheingold, *Organometallics*, 2006, **25**, 3943-3947.
215. J. M. A. Wouters, R. A. Klein, C. J. Elsevier, L. Haming and C. H. Stam, *Organometallics*, 1994, **13**, 4586-4593.
216. P. W. Blosser, M. Calligaris, D. G. Schimpff and A. Wojcicki, *Inorg. Chim. Acta*, 2001, **320**, 110-116.
217. H. Berke, P. Harter, G. Huttner and L. Zsolnai, *Z Naturforsch B*, 1981, **36**, 929-937.
218. A. Santiago, M. Gomez-Gallego, C. R. de Arellano and M. A. Sierra, *Chem. Commun.*, 2013, **49**, 1112-1114.
219. R. Wiedemann, P. Steinert, O. Gevert and H. Werner, *J. Am. Chem. Soc.*, 1996, **118**, 2495-2496.
220. H. Werner, F. Kukla and P. Steinert, *Eur. J. Inorg. Chem.*, 2002, 1377-1389.
221. H. Werner, R. Wiedemann, M. Laubender, B. Windmüller, P. Steinert, O. Gevert and J. Wolf, *J. Am. Chem. Soc.*, 2002, **124**, 6966-6980.
222. P.-M. Pellny, F. G. Kirchbauer, V. V. Burlakov, W. Baumann, A. Spannenberg and U. Rosenthal, *Chem. Eur. J.*, 2000, **6**, 81-90.
223. S. Zhang, W.-X. Zhang, J. Zhao and Z. Xi, *J. Am. Chem. Soc.*, 2010, **132**, 14042-14045.
224. S. Kumar Podiyanachari, G. Kehr, C. Mück-Lichtenfeld, C. G. Daniliuc and G. Erker, *J. Am. Chem. Soc.*, 2013, **135**, 17444-17456.
225. G. Fan, X. Xie, Y. Liu and Y. Li, *Organometallics*, 2013, **32**, 1636-1642.
226. G. Bender, C. G. Daniliuc, B. Wibbeling, G. Kehr and G. Erker, *Dalton Trans.*, 2014, **43**, 12210-12213.
227. T. Beweries, V. V. Burlakov, S. Peitz, M. A. Bach, P. Arndt, W. Baumann, A. Spannenberg and U. Rosenthal, *Organometallics*, 2007, **26**, 6827-6831.
228. J. Ugolotti, G. Dierker, G. Kehr, R. Fröhlich, S. Grimme and G. Erker, *Angew. Chem. Int. Ed.*, 2008, **47**, 2622-2625.

## References

---

229. S. P. Semproni and P. J. Chirik, *Organometallics*, 2014, **33**, 3727-3737.
230. Y. Takahashi, K. Tsutsumi, Y. Nakagai, T. Morimoto, K. Kakiuchi, S. Ogoshi and H. Kurosawa, *Organometallics*, 2008, **27**, 276-280.
231. Y.-J. Kim, H.-K. Kim, J.-H. Lee, Z. N. Zheng and S. W. Lee, *Inorg. Chim. Acta*, 2013, **398**, 54-63.
232. L. Canovese, F. Visentin, C. Biz, T. Scattolin, C. Santo and V. Bertolasi, *J. Organomet. Chem.*, 2015, **786**, 21-30.
233. H. Azami, T. Tsukada, R. Tanifuji, R. Seki and M. Iwasaki, *Chem. Lett.*, 2015, **44**, 1550-1551.
234. F. Théron, M. Verny and R. Vessière, in *The Carbon–Carbon Triple Bond (1978)*, John Wiley & Sons, Ltd., 1978, pp. 381-445.
235. A. S. K. Hashmi, in *Modern Allene Chemistry*, Wiley-VCH Verlag GmbH, 2004, pp. 2-50.
236. A. Wojcicki, *Inorg. Chem. Commun.*, 2002, **5**, 82-97.
237. R. S. Keng and Y. C. Lin, *Organometallics*, 1990, **9**, 289-291.
238. T.-W. Tseng, I.-Y. Wu, J.-H. Tsai, Y.-C. Lin, D.-J. Chen, G.-H. Lee, M.-C. Cheng and Y. Wang, *Organometallics*, 1994, **13**, 3963-3971.
239. M.-C. Chen, R.-S. Keng, Y.-C. Lin, Y. Wang, M.-C. Cheng and G.-H. Lee, *J. Chem. Soc., Chem. Commun.*, 1990, 1138-1140.
240. S. Ogoshi, Y. Fukunishi, K. Tsutsumi and H. Kurosawa, *J. Chem. Soc., Chem. Commun.*, 1995, 2485-2486.
241. S. Ogoshi, Y. Fukunishi, K. Tsutsumi and H. Kurosawa, *Inorg. Chim. Acta*, 1997, **265**, 9-15.
242. H. Kurosawa and S. Ogoshi, *Bull. Chem. Soc. Jpn.*, 1998, **71**, 973-984.
243. I. A. Cade, A. L. Colebatch, A. F. Hill and A. C. Willis, *Organometallics*, 2014, **33**, 3198-3204.
244. A. L. Colebatch, I. A. Cade, A. F. Hill and M. M. Bhadbhade, *Organometallics*, 2013, **32**, 4766-4774.
245. N. W. Alcock, J. Cartwright, A. F. Hill, M. Marcellin and H. M. Rawles, *J. Chem. Soc., Chem. Commun.*, 1995, 369-370.
246. J. P. Paolini, *J. Comput. Chem.*, 1990, **11**, 1160-1163.
247. M. N. Hopkinson, C. Richter, M. Schedler and F. Glorius, *Nature*, 2014, **510**, 485-496.

## References

---

248. A. J. Arduengo, R. L. Harlow and M. Kline, *J. Am. Chem. Soc.*, 1991, **113**, 361-363.
249. J. W. Runyon, O. Steinhof, H. V. R. Dias, J. C. Calabrese, W. J. Marshall and A. J. Arduengo, *Aust. J. Chem.*, 2011, **64**, 1165-1172.
250. F. Glorius, in *N-Heterocyclic Carbenes in Transition Metal Catalysis*, ed. F. Glorius, Springer Berlin Heidelberg, Berlin, Heidelberg, 2007, pp. 1-20.
251. A. C. Hillier, W. J. Sommer, B. S. Yong, J. L. Petersen, L. Cavallo and S. P. Nolan, *Organometallics*, 2003, **22**, 4322-4326.
252. R. Breslow, *J. Am. Chem. Soc.*, 1958, **80**, 3719-3726.
253. D. A. DiRocco, K. M. Oberg and T. Rovis, *J. Am. Chem. Soc.*, 2012, **134**, 6143-6145.
254. H. W. Wanzlick, *Angew. Chem. Int. Ed. Engl.*, 1962, **1**, 75-80.
255. H. W. Wanzlick and H. J. Schönherr, *Angew. Chem. Int. Ed. Engl.*, 1968, **7**, 141-142.
256. K. Öfele, *J. Organomet. Chem.*, 1968, **12**, P42-P43.
257. B. Cetinkaya, P. Dixneuf and M. F. Lappert, *J. Chem. Soc., Dalton Trans.*, 1974, 1827-1833.
258. H. V. Huynh, in *The Organometallic Chemistry of N-heterocyclic Carbenes*, John Wiley & Sons, Ltd, 2017, pp. 171-219.
259. F. E. Hahn and M. C. Jahnke, *Angew. Chem. Int. Ed.*, 2008, **47**, 3122-3172.
260. N. Kuhn and A. Al-Sheikh, *Coord. Chem. Rev.*, 2005, **249**, 829-857.
261. P. L. Arnold and I. J. Casely, *Chem. Rev.*, 2009, **109**, 3599-3611.
262. S. K. Schneider, W. A. Herrmann and E. Herdtweck, *Z. Anorg. Allg. Chem.*, 2003, **629**, 2363-2370.
263. S. López, E. Herrero-Gómez, P. Pérez-Galán, C. Nieto-Oberhuber and A. M. Echavarren, *Angew. Chem. Int. Ed.*, 2006, **45**, 6029-6032.
264. C. A. Witham, P. Mauleón, N. D. Shapiro, B. D. Sherry and F. D. Toste, *J. Am. Chem. Soc.*, 2007, **129**, 5838-5839.
265. R. Corberán, J. Ramírez, M. Poyatos, E. Peris and E. Fernández, *Tetrahedron: Asymmetry*, 2006, **17**, 1759-1762.
266. M. R. Fructos, P. de Frémont, S. P. Nolan, M. M. Díaz-Requejo and P. J. Pérez, *Organometallics*, 2006, **25**, 2237-2241.
267. A. Corma, C. González-Arellano, M. Iglesias, S. Pérez-Ferreras and F. Sánchez, *Synlett*, 2007, 1771-1774.

## References

268. A. S. K. Hashmi, T. D. Ramamurthi and F. Rominger, *Adv. Synth. Catal.*, 2010, **352**, 971-975.
269. L. Huang, F. Rominger, M. Rudolph and A. S. K. Hashmi, *Chem. Commun.*, 2016, **52**, 6435-6438.
270. J. Zhang, P. Gu, K. Chen and M. Shi, in *PATAI'S Chemistry of Functional Groups*, 2015, pp. 1-84.
271. İ. Özdemir, A. Denizci, H. T. Öztürk and B. Çetinkaya, *Appl. Organomet. Chem.*, 2004, **18**, 318-322.
272. İ. Özdemir, N. Temelli, S. Günal and S. Demir, *Molecules*, 2010, **15**, 2203-2210.
273. P. J. Barnard and S. J. Berners-Price, *Coord. Chem. Rev.*, 2007, **251**, 1889-1902.
274. M. V. Baker, P. J. Barnard, S. J. Berners-Price, S. K. Brayshaw, J. L. Hickey, B. W. Skelton and A. H. White, *J. Organomet. Chem.*, 2005, **690**, 5625-5635.
275. L. B. Chen, *Annual Review of Cell Biology*, 1988, **4**, 155-181.
276. J. L. Hickey, R. A. Ruhayel, P. J. Barnard, M. V. Baker, S. J. Berners-Price and A. Filipovska, *J. Am. Chem. Soc.*, 2008, **130**, 12570-12571.
277. R. Rubbiani, S. Can, I. Kitanovic, H. Alborzinia, M. Stefanopoulou, M. Kokoschka, S. Mönchgesang, W. S. Sheldrick, S. Wölfl and I. Ott, *J. Med. Chem.*, 2011, **54**, 8646-8657.
278. Y. Li, G.-F. Liu, C.-P. Tan, L.-N. Ji and Z.-W. Mao, *Metallomics*, 2014, **6**, 1460-1468.
279. R. V. Parish and S. M. Cottrill, *Gold Bull.*, 1987, **20**, 3-12.
280. C. F. Shaw, *Chem. Rev.*, 1999, **99**, 2589-2600.
281. P. N. Fonteh, F. K. Keter and D. Meyer, *BioMetals*, 2010, **23**, 185-196.
282. V. K.-M. Au, K. M.-C. Wong, N. Zhu and V. W.-W. Yam, *J. Am. Chem. Soc.*, 2009, **131**, 9076-9085.
283. J. J. Yan, A. L.-F. Chow, C.-H. Leung, R. W.-Y. Sun, D.-L. Ma and C.-M. Che, *Chem. Commun.*, 2010, **46**, 3893-3895.
284. S. K. Fung, T. Zou, B. Cao, P.-Y. Lee, Y. M. E. Fung, D. Hu, C.-N. Lok and C.-M. Che, *Angew. Chem. Int. Ed.*, 2017, **56**, 3892-3896.
285. H. M. J. Wang, C. Y. L. Chen and I. J. B. Lin, *Organometallics*, 1999, **18**, 1216-1223.
286. A. Citta, E. Schuh, F. Mohr, A. Folda, M. L. Massimino, A. Bindoli, A. Casini and M. P. Rigobello, *Metallomics*, 2013, **5**, 1006-1015.

## References

---

287. R. Visbal, I. Ospino, J. M. López-de-Luzuriaga, A. Laguna and M. C. Gimeno, *J. Am. Chem. Soc.*, 2013, **135**, 4712-4715.
288. P. de Frémont, N. M. Scott, E. D. Stevens and S. P. Nolan, *Organometallics*, 2005, **24**, 2411-2418.
289. S. Singh, S. S. Kumar, V. Jancik, H. W. Roesky, H.-G. Schmidt and M. Noltemeyer, *Eur. J. Inorg. Chem.*, 2005, **2005**, 3057-3062.
290. H. M. J. Wang and I. J. B. Lin, *Organometallics*, 1998, **17**, 972-975.
291. M. R. L. Furst and C. S. J. Cazin, *Chem. Commun.*, 2010, **46**, 6924-6925.
292. A. S. K. Hashmi, C. Lothschütz, C. Böhlting, T. Hengst, C. Hubbert and F. Rominger, *Adv. Synth. Catal.*, 2010, **352**, 3001-3012.
293. A. S. K. Hashmi, C. Lothschütz, K. Graf, T. Häffner, A. Schuster and F. Rominger, *Adv. Synth. Catal.*, 2011, **353**, 1407-1412.
294. A. S. K. Hashmi, D. Riedel, M. Rudolph, F. Rominger and T. Oeser, *Chem. Eur. J.*, 2012, **18**, 3827-3830.
295. D. Riedel, T. Wurm, K. Graf, M. Rudolph, F. Rominger and A. S. K. Hashmi, *Adv. Synth. Catal.*, 2015, **357**, 1515-1523.
296. S. Zhu, R. Liang, L. Chen, C. Wang, Y. Ren and H. Jiang, *Tetrahedron Lett.*, 2012, **53**, 815-818.
297. M. Fèvre, J. Pinaud, A. Leteneur, Y. Gnanou, J. Vignolle, D. Taton, K. Miqueu and J.-M. Sotiropoulos, *J. Am. Chem. Soc.*, 2012, **134**, 6776-6784.
298. A. Collado, A. Gomez-Suarez, A. R. Martin, A. M. Z. Slawin and S. P. Nolan, *Chem. Commun.*, 2013, **49**, 5541-5543.
299. R. Visbal, A. Laguna and M. C. Gimeno, *Chem. Commun.*, 2013, **49**, 5642-5644.
300. E. J. Fernandez, M. C. Gimeno, P. G. Jones, A. Laguna, M. Laguna and J. M. Lopez-de-Luzuriaga, *Organometallics*, 1995, **14**, 2918-2922.
301. J. Forniés, J. Gómez, E. Lalinde and M. T. Moreno, *Inorg. Chim. Acta*, 2003, **347**, 145-154.
302. N. Gonsior and H. Ritter, *Macromol. Chem. Phys.*, 2011, **212**, 2633-2640.
303. H. Li, L.-Y. Jin and R.-J. Tao, *Acta Crystallographica Section E*, 2008, **64**, o900.
304. M. C. Lukowiak, M. Meise and R. Haag, *Synlett*, 2014, **25**, 2161-2165.
305. M. Hollering, M. Albrecht and F. E. Kühn, *Organometallics*, 2016, **35**, 2980-2986.

## References

---

306. J. Wimberg, S. Meyer, S. Dechert and F. Meyer, *Organometallics*, 2012, **31**, 5025-5033.
307. S. Gaillard, P. Nun, A. M. Z. Slawin and S. P. Nolan, *Organometallics*, 2010, **29**, 5402-5408.
308. Gwan-Hong Min, Taeun Yim, Hyun Yeong Lee, Dal Ho Huh, Eunjoo Lee, Junyoung Mun, Seung M. Oh and Y. G. Kim, *Bull. Korean Chem. Soc.*, 2006, **27**, 847-853.
309. M. Berthelot, *Justus Liebigs Ann. Chem.*, 1866, **139**, 150-164.
310. C. M. Mitchell and F. G. A. Stone, *J. Chem. Soc., Dalton Trans.*, 1972, 102-107.
311. H.-T. Liu, X.-G. Xiong, P. Diem Dau, Y.-L. Wang, D.-L. Huang, J. Li and L.-S. Wang, *Nat. Commun.*, 2013, **4**, 2201.
312. K.-L. Cheung, S.-K. Yip and V. W.-W. Yam, *J. Organomet. Chem.*, 2004, **689**, 4451-4462.
313. W. Lu, H.-F. Xiang, N. Zhu and C.-M. Che, *Organometallics*, 2002, **21**, 2343-2346.
314. C.-M. Che, H.-Y. Chao, V. M. Miskowski, Y. Li and K.-K. Cheung, *J. Am. Chem. Soc.*, 2001, **123**, 4985-4991.
315. V. W.-W. Yam and S. W.-K. Choi, *J. Chem. Soc., Dalton Trans.*, 1996, 4227-4232.
316. D. Li, X. Hong, C.-M. Che, W.-C. Lo and S.-M. Peng, *J. Chem. Soc., Dalton Trans.*, 1993, 2929-2932.
317. N. J. Long and C. K. Williams, *Angew. Chem. Int. Ed.*, 2003, **42**, 2586-2617.
318. F. Paul and C. Lapinte, *Coord. Chem. Rev.*, 1998, **178**, 431-509.
319. I. R. Whittall, M. G. Humphrey, S. Houbrechts, A. Persoons and D. C. R. Hockless, *Organometallics*, 1996, **15**, 5738-5745.
320. I. R. Whittall, M. G. Humphrey, M. Samoc and B. Luther-Davies, *Angew. Chem. Int. Ed. Engl.*, 1997, **36**, 370-371.
321. W. Ian R, M. Andrew M, H. Mark G and M. Samoc, in *Adv. Organomet. Chem.*, eds. R. West and A. F. Hill, Academic Press, 1999, vol. 43, pp. 349-405.
322. J. G. Niel and J. A. Chrestien, *Recherches et Observations sur les Effets des Pre'parations d'or du Dr. Chrestien dans le Traitement de Plusieurs Maladies, et Notamment dans Celui des Maladies Syphilitiques*, Gabon, Paris, 1821.
323. R. Koch, 1890.
324. A. Feldt, *Zur Chemotherapie der Tuberkulose mit Gold*, *Deut. Med. Wochenschr.*, 1913, **39**, 549-551.

## References

---

325. I. Lorenzen, *Ann Clin Res*, 1975, **7**, 195-201.
326. T. M. Simon, D. H. Kunishima, G. J. Vibert and A. Lorber, *Cancer*, 1979, **44**, 1965-1975.
327. A. E. Finkelstein, O. R. Burrone, D. T. Walz and A. Misher, *J Rheumatol*, 1977, **4**, 245-251.
328. T. M. Simon, D. H. Kunishima, G. J. Vibert and A. Lorber, *J Rheumatol Suppl*, 1979, **5**, 91-97.
329. T. M. Simon, D. H. Kunishima, G. J. Vibert and A. Lorber, *Cancer Res*, 1981, **41**, 94-97.
330. C. K. Mirabelli, R. K. Johnson, D. T. Hill, L. F. Faucette, G. R. Girard, G. Y. Kuo, C. M. Sung and S. T. Crooke, *J. Med. Chem.*, 1986, **29**, 218-223.
331. R. A. Stockland, M. C. Kohler, I. A. Guzei, M. E. Kastner, J. A. Bawiec, D. C. Labaree and R. B. Hochberg, *Organometallics*, 2006, **25**, 2475-2485.
332. C.-H. Chui, R. S.-M. Wong, R. Gambari, G. Y.-M. Cheng, M. C.-W. Yuen, K.-W. Chan, S.-W. Tong, F.-Y. Lau, P. B.-S. Lai, K.-H. Lam, C.-L. Ho, C.-W. Kan, K. S.-Y. Leung and W.-Y. Wong, *Biorg. Med. Chem.*, 2009, **17**, 7872-7877.
333. E. Schuh, S. M. Valiahdi, M. A. Jakupec, B. K. Keppler, P. Chiba and F. Mohr, *Dalton Trans.*, 2009, 10841-10845.
334. R. G. Balasingham, C. F. Williams, H. J. Mottram, M. P. Coogan and S. J. A. Pope, *Organometallics*, 2012, **31**, 5835-5843.
335. A. Meyer, C. P. Bagowski, M. Kokoschka, M. Stefanopoulou, H. Alborzinia, S. Can, D. H. Vlecken, W. S. Sheldrick, S. Wölfl and I. Ott, *Angew. Chem. Int. Ed.*, 2012, **51**, 8895-8899.
336. A. Meyer, A. Gutiérrez, I. Ott and L. Rodríguez, *Inorg. Chim. Acta*, 2013, **398**, 72-76.
337. R. Gavara, E. Aguiló, J. Schur, J. Llorca, I. Ott and L. Rodríguez, *Inorg. Chim. Acta*, 2016, **446**, 189-197.
338. N. Mirzadeh, S. H. Privér, A. Abraham, R. Shukla, V. Bansal and S. K. Bhargava, *Eur. J. Inorg. Chem.*, 2015, **2015**, 4275-4279.
339. V. Andermark, K. Göke, M. Kokoschka, M. A. Abu el Maaty, C. T. Lum, T. Zou, R. W.-Y. Sun, E. Aguiló, L. Oehninger, L. Rodríguez, H. Bunjes, S. Wölfl, C.-M. Che and I. Ott, *J. Inorg. Biochem.*, 2016, **160**, 140-148.
340. S. Huang, R. J. Clark and L. Zhu, *Org. Lett.*, 2007, **9**, 4999-5002.



## References

---

- 341. J. T. Simmons, J. R. Allen, D. R. Morris, R. J. Clark, C. W. Levenson, M. W. Davidson and L. Zhu, *Inorg. Chem.*, 2013, **52**, 5838-5850.
- 342. W. G. Sumpter and F. M. Miller, in *Chemistry of Heterocyclic Compounds*, John Wiley & Sons, Inc., Hoboken, NJ, USA, 1954, vol. 8, ch. 1, pp. 1-69.